

Enclosure 4

Non-proprietary Reference Documents

and

Redacted Versions of Proprietary

Reference Documents

(Public Version)

(13 Attachments)

(903 Total Pages, including cover sheets)

Enclosure 4 Document List

Attachment 1 - LTR-REA-17-116-NP, Revision 0, Reactor Vessel Neutron Exposure Data in Support of the Turkey Point Unit 3 and Unit 4 Subsequent License Renewal (SLR) Time-Limited Aging Analysis (TLAA), December 1, 2017

Attachment 2 – Areva Topical Report ANP-3646NP Revision 0, Low Upper-Shelf Toughness Fracture Mechanics Analysis of Turkey Point Units 3 and 4 Reactor Vessels for Levels C & D Service Loads at 80 Years, January 5, 2018 (Non-Proprietary)

Attachment 3 – Areva Topical Report, ANP-3647NP Revision 0, Low Upper-Shelf Toughness Fracture Mechanics Analysis of Turkey Point Units 3 and 4 Reactor Vessels for Levels C & D Service Loads at 80 Years, January 5, 2018 (Non-Proprietary)

Attachment 4 – SIA Report No. 1700109.402P, Revision 3 – REDACTED, Evaluation of Fatigue of ASME Section III, Class 1 Components for Turkey Point Units 3 and 4 for Subsequent License Renewal, December 2017

Attachment 5 – SIA Report No. 1700109.401P, Revision 3 – REDACTED, Evaluation of Environmentally-Assisted Fatigue for Turkey Point Units 3 and 4 for Subsequent License Renewal, January 2018

Attachment 6 – SIA Environmentally Assisted Fatigue Calculations

Pressurizer Lower Head

1700804.316P – REDACTED, Revision 0, 3-D Finite Element Model of Pressurizer Bottom Head, Skirt Assembly and Heater Wells, September 28, 2017

1700804.317, Revision 0, Pressurizer Lower Head Green's Functions and Unit Pressure, October 5, 2017

1700804.318, Revision 0, Pressurizer Lower Head Loads, Fatigue and EAF Analysis, November 7, 2017

Pressurizer Spray Nozzle

1700804.313P – REDACTED, Revision 1, Pressurizer Spray Nozzle Loads, December 7, 2017

1700804.314P – REDACTED, Revision 1, Pressurizer Spray Nozzle Finite Element Model and Stress Analyses, December 7, 2017

1700804.315P – REDACTED, Revision 1, Pressurizer Spray Nozzle Fatigue Analysis, December 7, 2017

Turkey Point Units 3 and 4
Docket Nos. 50-250 and 50-251
L-2018-004 Enclosure 4

Attachment 7 – Westinghouse Environmentally Assisted Fatigue Calculations

LTR-SDA-II-17-13-NP, Rev. 2, Environmentally Assisted Fatigue Evaluation of the Turkey Point Unit 3 and Unit 4 Pressurizer Upper Head and Shell and Reactor Vessel Core Support Blocks, November 30, 2017

LTR-CECO-17-025-NP, Rev. 1, Environmentally Assisted Fatigue Evaluation of the Turkey Point Unit 3 and Unit 4 Replacement Steam Generators, November 30, 2017

Attachment 8 – Areva Environmentally Assisted Fatigue Calculations: Areva Letter No. AREVA-17-02742, date December 6, 2017, Final CUF_{EN} Results – Turkey Point 3 & 4 – SLR EAF Analyses

- I. 32-9280707, Rev. 0, Turkey Point -3 & 4 CRDM Nozzle to Adapter Weld Connection EAF Evaluation, December 15, 2017
- II. 32-9280708, Rev. 0, Turkey Point 3 & 4 Replacement RVCH J Groove, December 12, 2017
- III. 32-9280709, Rev. 0, 12/15/17, TP CRDM Latch Housing Environmentally Assisted Fatigue, December 15, 2017
- IV. 32-9280710, Rev. 0, TP Vent Nozzle Environmentally Assisted Fatigue, December 14, 2017
- V. 32-9280711, Rev. 0, Turkey Point SLR EAF Analysis for Reactor Vessel Flange, December 14, 2017
- VI. 32-9280712, Rev. 0, TP CRDM Lower Joint Environmentally Assisted Fatigue, December 15, 2017

Attachment 9 – PWROG-17031-NP, Rev. 0, Update for Subsequent License Renewal: WCAP-15338-A, A Review of Cracking Associated with Weld Deposited Cladding in Operating PWR Plants, August 2017

Attachment 10 – PWR Owners Group, PWROG-17011-NP, Rev. 0, Update for Subsequent License Renewal: WCAP-14535A, Topical Report on Reactor Coolant Pump Flywheel Inspection Elimination' and WCAP-15666-A, Extension of Reactor Coolant Pump Motor Flywheel Examination, November 2017

Attachment 11 – WCAP-15354-NP, Revision 1, Technical Justification for Eliminating Primary Loop Pipe Rupture as a Structural Design Basis for Turkey Point Units 3 and 4 Nuclear Power Plants for the Subsequent License Renewal Time-Limited Aging Analysis Program (80 Years) Leak-Before-Break Evaluation, August 2017

Attachment 12 – SIA Leak-Before-Break Evaluation for Auxiliary Lines

0901350.401, Revision 3, Leak-Before-Break Evaluation Accumulator, Pressurizer Surge and Residual Heat Removal Lines Turkey Point Units 3 and 4, September 2017

0901350.304, Revision 3, Fatigue Crack Growth Evaluation, September 18, 2017

Turkey Point Units 3 and 4
Docket Nos. 50-250 and 50-251
L-2018-004 Enclosure 4

Attachment 13 – PWROG-17033- NP, Revision 0, Update for Subsequent License
Renewal: WCAP-13045, Compliance to ASME Code Case N-481 of the Primary
Loop Pump Casings of Westinghouse Type Nuclear Steam Supply Systems,
October 2017

Enclosure 4
Non-proprietary Reference Documents
and
Redacted Versions of Proprietary
Reference Documents
(Public Version)
Attachment 1

LTR-REA-17-116-NP, Revision 0
Reactor Vessel Neutron Exposure Data in Support of the
Turkey Point Unit 3 and Unit 4 Subsequent License
Renewal (SLR) Time-Limited Aging Analysis (TLAA),
December 1, 2017

(59 Total Pages, including cover sheets)



To: John T. Ahearn

Date: December 1, 2017

cc: Amy E. Freed

Arzu Alpan

From: Radiation Engineering & Analysis

Phone: (412) 374-5851

Email: hawkae@westinghouse.com

Our Ref: **LTR-REA-17-116-NP, Revision 0**

Subject: **Reactor Vessel Neutron Exposure Data in Support of the Turkey Point Unit 3 and Unit 4
Subsequent License Renewal (SLR) Time-Limited Aging Analysis (TLAA)**

Attachment(s): 1. Reactor Vessel Neutron Exposure Data in Support of the Turkey Point Unit 3 and Unit 4
Subsequent License Renewal (SLR) Time-Limited Aging Analysis (TLAA) (56 pages)

Attachment 1 provides select neutron exposure data applicable to the Turkey Point Unit 3 and Unit 4 reactor vessels and in-vessel surveillance capsules. The neutron exposure data in Attachment 1 are intended to be provided to Florida Power & Light (FPL) in support of their SLR project.

Please contact the undersigned if there are any questions regarding this information.

Author: *(Electronically Approved)**
Andrew E. Hawk
LOCA Integrated Services II

Reviewer: *(Electronically Approved)**
Benjamin W. Amiri
Radiation Engineering & Analysis

Approver: *(Electronically Approved)**
Laurent P. Houssay
Radiation Engineering & Analysis

**Electronically approved records are authenticated in the Process, Records and Information Management Environment.*

Attachment 1

Reactor Vessel Neutron Exposure Data in Support of the Turkey Point Unit 3 and Unit 4 Subsequent License Renewal (SLR) Time-Limited Aging Analysis (TLAA)

1.0 Reactor Vessel Neutron Exposure Data – Turkey Point Unit 3

Select neutron exposure data applicable to the Turkey Point Unit 3 reactor vessel and in-vessel surveillance capsules are provided in Table 1-1 through Table 1-26. The data provided in Table 1-1 through Table 1-26 were generated using Version 3.2 of the DORT discrete ordinates code and the BUGLE-96 cross-section library. The BUGLE-96 library provides a coupled 47-neutron, 20-gamma-ray-group cross-section data set produced specifically for light water reactor (LWR) applications. Furthermore, the neutron transport methodology used to generate the data provided in Table 1-1 through Table 1-26 followed the guidance of Regulatory Guide 1.190 (Reference 1), and was consistent with the United States Nuclear Regulatory Commission (USNRC) approved methodology described in WCAP-14040-A (Reference 2).

The neutron exposure data provided in Table 1-1 through Table 1-24 are the maximum values at either the reactor pressure vessel clad/base metal interface or the reactor pressure vessel outer surface. Note that for regions and materials above and below the core (e.g., the inlet nozzle welds, outlet nozzle welds, and lower shell to lower head ring weld), the neutron exposure values at the reactor pressure vessel outer surface can be greater than those at the clad/base metal interface.

In addition, the neutron exposure data provided in Table 1-5 through Table 1-12 are based on the lowest elevations of the inlet and outlet nozzle forging attachment welds, with the lowest elevations of those welds being determined at the inner surface of the pressure vessel.

**Table 1-1: Fast ($E > 1.0$ MeV) Neutron Fluence Rate at the Pressure Vessel
Clad/Base Metal Interface – Unit 3**

Cycle	Cycle Length (EFPY)	Cumulative Operating Time (EFPY)	Fluence Rate (n/cm ² -s)			
			0°	15°	30°	45°
1	1.15	1.15	6.05E+10	2.77E+10	1.54E+10	1.01E+10
2	0.78	1.92	5.92E+10	2.69E+10	1.46E+10	9.28E+09
3	0.76	2.68	5.64E+10	2.93E+10	1.75E+10	1.17E+10
4	0.78	3.46	5.67E+10	2.75E+10	1.38E+10	1.03E+10
5	0.78	4.24	7.17E+10	3.13E+10	1.28E+10	7.97E+09
6	0.50	4.74	6.64E+10	2.90E+10	1.17E+10	7.72E+09
7	0.92	5.66	5.09E+10	2.40E+10	1.32E+10	8.85E+09
8	1.36	7.03	5.27E+10	2.40E+10	1.30E+10	8.54E+09
9	1.03	8.06	3.23E+10	1.87E+10	1.27E+10	9.18E+09
10	1.25	9.31	3.10E+10	1.86E+10	1.19E+10	8.02E+09
11	1.31	10.62	3.31E+10	1.86E+10	1.21E+10	7.96E+09
12	1.24	11.86	3.24E+10	1.85E+10	1.18E+10	7.90E+09
13	1.25	13.11	3.17E+10	1.77E+10	1.13E+10	8.12E+09
14	1.24	14.36	3.35E+10	1.92E+10	1.24E+10	8.92E+09
15	1.32	15.68	3.41E+10	1.88E+10	1.18E+10	8.07E+09
16	1.39	17.07	3.49E+10	2.12E+10	1.41E+10	8.21E+09
17	1.31	18.37	3.41E+10	1.79E+10	1.11E+10	7.43E+09
18	1.47	19.85	2.99E+10	1.85E+10	1.28E+10	8.34E+09
19	1.31	21.15	3.42E+10	1.85E+10	1.16E+10	7.82E+09
20	1.46	22.61	3.24E+10	1.66E+10	1.00E+10	7.04E+09
21	1.22	23.83	3.16E+10	1.81E+10	1.17E+10	7.55E+09
22	1.36	25.19	3.36E+10	1.74E+10	1.07E+10	7.56E+09
23	1.38	26.58	3.46E+10	1.88E+10	1.19E+10	7.98E+09
24	1.36	27.94	3.42E+10	1.79E+10	1.09E+10	7.61E+09
25	1.21	29.16	3.94E+10	1.97E+10	1.11E+10	7.56E+09
26	1.30	30.46	4.67E+10	2.25E+10	1.31E+10	9.61E+09
27	1.42	31.88	5.30E+10	2.53E+10	1.29E+10	8.98E+09
28	1.27	33.14	4.62E+10	2.33E+10	1.36E+10	9.24E+09
29 ^[1]	1.43	34.57	4.62E+10	2.49E+10	1.46E+10	9.76E+09
Future ^[2]	--	--	5.46E+10	2.95E+10	1.73E+10	1.16E+10
Note(s): 1. Cycle 29 is the most recently completed operating cycle. Values listed for this cycle are projections based on design end of Cycle 29 burnup data. 2. Values beyond Cycle 29 are based on the average core power distributions and reactor operating conditions of Cycle 29, but include a 1.2 bias on the peripheral and re-entrant corner assembly relative powers.						

Table 1-2: Fast ($E > 1.0$ MeV) Neutron Fluence at the Pressure Vessel Clad/Base Metal Interface – Unit 3

Cycle	Cycle Length (EFPY)	Cumulative Operating Time (EFPY)	Fluence (n/cm ²)			
			0°	15°	30°	45°
1	1.15	1.15	2.19E+18	1.00E+18	5.58E+17	3.65E+17
2	0.78	1.92	3.62E+18	1.65E+18	9.11E+17	5.89E+17
3	0.76	2.68	4.97E+18	2.36E+18	1.33E+18	8.69E+17
4	0.78	3.46	6.37E+18	3.04E+18	1.67E+18	1.12E+18
5	0.78	4.24	8.11E+18	3.79E+18	1.98E+18	1.32E+18
6	0.50	4.74	9.16E+18	4.25E+18	2.17E+18	1.44E+18
7	0.92	5.66	1.06E+19	4.95E+18	2.55E+18	1.70E+18
8	1.36	7.03	1.28E+19	5.95E+18	3.09E+18	2.05E+18
9	1.03	8.06	1.37E+19	6.51E+18	3.50E+18	2.35E+18
10	1.25	9.31	1.48E+19	7.20E+18	3.96E+18	2.66E+18
11	1.31	10.62	1.61E+19	7.92E+18	4.44E+18	2.98E+18
12	1.24	11.86	1.73E+19	8.61E+18	4.90E+18	3.29E+18
13	1.25	13.11	1.86E+19	9.30E+18	5.34E+18	3.61E+18
14	1.24	14.36	1.99E+19	1.01E+19	5.83E+18	3.95E+18
15	1.32	15.68	2.13E+19	1.08E+19	6.32E+18	4.29E+18
16	1.39	17.07	2.29E+19	1.18E+19	6.93E+18	4.65E+18
17	1.31	18.37	2.43E+19	1.25E+19	7.39E+18	4.95E+18
18	1.47	19.85	2.56E+19	1.34E+19	7.98E+18	5.34E+18
19	1.31	21.15	2.71E+19	1.41E+19	8.46E+18	5.66E+18
20	1.46	22.61	2.85E+19	1.49E+19	8.92E+18	5.99E+18
21	1.22	23.83	2.98E+19	1.56E+19	9.38E+18	6.28E+18
22	1.36	25.19	3.12E+19	1.63E+19	9.83E+18	6.60E+18
23	1.38	26.58	3.27E+19	1.72E+19	1.04E+19	6.95E+18
24	1.36	27.94	3.42E+19	1.79E+19	1.08E+19	7.28E+18
25	1.21	29.16	3.57E+19	1.87E+19	1.13E+19	7.57E+18
26	1.30	30.46	3.75E+19	1.96E+19	1.18E+19	7.96E+18
27	1.42	31.88	3.99E+19	2.07E+19	1.24E+19	8.35E+18
28	1.27	33.14	4.18E+19	2.16E+19	1.29E+19	8.72E+18
29 ^[1]	1.43	34.57	4.38E+19	2.28E+19	1.35E+19	9.16E+18
Future ^[2]	--	36.00	4.63E+19	2.41E+19	1.43E+19	9.68E+18
Future ^[2]	--	48.00	6.69E+19	3.53E+19	2.08E+19	1.40E+19
Future ^[2]	--	60.00	8.76E+19	4.64E+19	2.73E+19	1.84E+19
Future ^[2]	--	72.00	1.08E+20	5.76E+19	3.38E+19	2.27E+19
Note(s): 1. Cycle 29 is the most recently completed operating cycle. Values listed for this cycle are projections based on design end of Cycle 29 burnup data. 2. Values beyond Cycle 29 are based on the average core power distributions and reactor operating conditions of Cycle 29, but include a 1.2 bias on the peripheral and re-entrant corner assembly relative powers.						

Table 1-3: Iron Atom Displacement Rate at the Pressure Vessel Clad/Base Metal Interface – Unit 3

Cycle	Cycle Length (EFPY)	Cumulative Operating Time (EFPY)	Displacement Rate (dpa/s)			
			0°	15°	30°	45°
1	1.15	1.15	9.87E-11	4.57E-11	2.51E-11	1.64E-11
2	0.78	1.92	9.64E-11	4.43E-11	2.37E-11	1.51E-11
3	0.76	2.68	9.20E-11	4.82E-11	2.84E-11	1.90E-11
4	0.78	3.46	9.24E-11	4.53E-11	2.25E-11	1.67E-11
5	0.78	4.24	1.17E-10	5.15E-11	2.08E-11	1.30E-11
6	0.50	4.74	1.08E-10	4.78E-11	1.92E-11	1.26E-11
7	0.92	5.66	8.29E-11	3.95E-11	2.15E-11	1.44E-11
8	1.36	7.03	8.58E-11	3.95E-11	2.11E-11	1.39E-11
9	1.03	8.06	5.26E-11	3.06E-11	2.06E-11	1.49E-11
10	1.25	9.31	5.05E-11	3.04E-11	1.93E-11	1.30E-11
11	1.31	10.62	5.39E-11	3.04E-11	1.95E-11	1.29E-11
12	1.24	11.86	5.27E-11	3.03E-11	1.91E-11	1.28E-11
13	1.25	13.11	5.17E-11	2.90E-11	1.83E-11	1.32E-11
14	1.24	14.36	5.46E-11	3.13E-11	2.01E-11	1.45E-11
15	1.32	15.68	5.54E-11	3.08E-11	1.91E-11	1.31E-11
16	1.39	17.07	5.68E-11	3.46E-11	2.28E-11	1.34E-11
17	1.31	18.37	5.55E-11	2.93E-11	1.80E-11	1.21E-11
18	1.47	19.85	4.87E-11	3.02E-11	2.07E-11	1.35E-11
19	1.31	21.15	5.56E-11	3.02E-11	1.88E-11	1.27E-11
20	1.46	22.61	5.27E-11	2.72E-11	1.63E-11	1.14E-11
21	1.22	23.83	5.14E-11	2.96E-11	1.90E-11	1.23E-11
22	1.36	25.19	5.47E-11	2.85E-11	1.73E-11	1.23E-11
23	1.38	26.58	5.63E-11	3.08E-11	1.94E-11	1.30E-11
24	1.36	27.94	5.57E-11	2.93E-11	1.76E-11	1.24E-11
25	1.21	29.16	6.41E-11	3.24E-11	1.81E-11	1.23E-11
26	1.30	30.46	7.61E-11	3.69E-11	2.13E-11	1.56E-11
27	1.42	31.88	8.63E-11	4.15E-11	2.11E-11	1.46E-11
28	1.27	33.14	7.52E-11	3.82E-11	2.21E-11	1.50E-11
29 ^[1]	1.43	34.57	7.53E-11	4.09E-11	2.37E-11	1.59E-11
Future ^[2]	--	--	8.90E-11	4.84E-11	2.80E-11	1.88E-11
Note(s): 1. Cycle 29 is the most recently completed operating cycle. Values listed for this cycle are projections based on design end of Cycle 29 burnup data. 2. Values beyond Cycle 29 are based on the average core power distributions and reactor operating conditions of Cycle 29, but include a 1.2 bias on the peripheral and re-entrant corner assembly relative powers.						

Table 1-4: Iron Atom Displacements at the Pressure Vessel Clad/Base Metal Interface – Unit 3

Cycle	Cycle Length (EFPY)	Cumulative Operating Time (EFPY)	Displacements (dpa)			
			0°	15°	30°	45°
1	1.15	1.15	3.57E-03	1.65E-03	9.07E-04	5.94E-04
2	0.78	1.92	5.90E-03	2.72E-03	1.48E-03	9.59E-04
3	0.76	2.68	8.11E-03	3.88E-03	2.16E-03	1.42E-03
4	0.78	3.46	1.04E-02	4.99E-03	2.72E-03	1.83E-03
5	0.78	4.24	1.32E-02	6.24E-03	3.22E-03	2.14E-03
6	0.50	4.74	1.49E-02	7.00E-03	3.52E-03	2.34E-03
7	0.92	5.66	1.73E-02	8.15E-03	4.15E-03	2.76E-03
8	1.36	7.03	2.09E-02	9.79E-03	5.02E-03	3.34E-03
9	1.03	8.06	2.24E-02	1.07E-02	5.69E-03	3.82E-03
10	1.25	9.31	2.42E-02	1.18E-02	6.44E-03	4.33E-03
11	1.31	10.62	2.62E-02	1.30E-02	7.22E-03	4.84E-03
12	1.24	11.86	2.83E-02	1.41E-02	7.96E-03	5.34E-03
13	1.25	13.11	3.03E-02	1.53E-02	8.68E-03	5.86E-03
14	1.24	14.36	3.24E-02	1.65E-02	9.47E-03	6.42E-03
15	1.32	15.68	3.47E-02	1.78E-02	1.03E-02	6.97E-03
16	1.39	17.07	3.72E-02	1.93E-02	1.13E-02	7.55E-03
17	1.31	18.37	3.95E-02	2.05E-02	1.20E-02	8.05E-03
18	1.47	19.85	4.18E-02	2.19E-02	1.30E-02	8.68E-03
19	1.31	21.15	4.41E-02	2.32E-02	1.37E-02	9.20E-03
20	1.46	22.61	4.65E-02	2.44E-02	1.45E-02	9.73E-03
21	1.22	23.83	4.85E-02	2.56E-02	1.52E-02	1.02E-02
22	1.36	25.19	5.08E-02	2.68E-02	1.60E-02	1.07E-02
23	1.38	26.58	5.33E-02	2.81E-02	1.68E-02	1.13E-02
24	1.36	27.94	5.56E-02	2.94E-02	1.76E-02	1.18E-02
25	1.21	29.16	5.81E-02	3.06E-02	1.83E-02	1.23E-02
26	1.30	30.46	6.11E-02	3.21E-02	1.91E-02	1.29E-02
27	1.42	31.88	6.50E-02	3.39E-02	2.00E-02	1.36E-02
28	1.27	33.14	6.80E-02	3.55E-02	2.09E-02	1.42E-02
29 ^[1]	1.43	34.57	7.14E-02	3.73E-02	2.20E-02	1.49E-02
Future ^[2]	--	36.00	7.54E-02	3.95E-02	2.32E-02	1.57E-02
Future ^[2]	--	48.00	1.09E-01	5.78E-02	3.38E-02	2.28E-02
Future ^[2]	--	60.00	1.43E-01	7.61E-02	4.44E-02	2.99E-02
Future ^[2]	--	72.00	1.76E-01	9.44E-02	5.49E-02	3.70E-02
Note(s): 1. Cycle 29 is the most recently completed operating cycle. Values listed for this cycle are projections based on design end of Cycle 29 burnup data. 2. Values beyond Cycle 29 are based on the average core power distributions and reactor operating conditions of Cycle 29, but include a 1.2 bias on the peripheral and re-entrant corner assembly relative powers.						

Table 1-5: Fast (E > 1.0 MeV) Neutron Fluence Rate at the Inlet Nozzle Welds – Unit 3

Cycle	Cycle Length (EFPY)	Cumulative Operating Time (EFPY)	Fluence Rate (n/cm ² -s) ^[1]		
			10°	20°	40°
1	1.15	1.15	1.02E+08	5.75E+07	3.28E+07
2	0.78	1.92	1.53E+08 ^[2]	7.29E+07 ^[2]	3.81E+07
3	0.76	2.68	1.05E+08	6.40E+07	3.81E+07
4	0.78	3.46	1.12E+08 ^[2]	5.96E+07	3.51E+07
5	0.78	4.24	1.40E+08 ^[2]	6.59E+07	3.15E+07
6	0.50	4.74	1.43E+08 ^[2]	6.37E+07	3.12E+07
7	0.92	5.66	1.09E+08 ^[2]	5.68E+07	3.23E+07
8	1.36	7.03	9.98E+07 ^[2]	5.41E+07	3.02E+07
9	1.03	8.06	6.47E+07	5.54E+07 ^[2]	3.85E+07 ^[2]
10	1.25	9.31	6.53E+07	6.64E+07 ^[2]	4.17E+07 ^[2]
11	1.31	10.62	6.68E+07	6.22E+07 ^[2]	3.84E+07 ^[2]
12	1.24	11.86	6.45E+07	5.27E+07 ^[2]	3.30E+07 ^[2]
13	1.25	13.11	6.09E+07	4.31E+07	2.78E+07
14	1.24	14.36	6.30E+07	4.38E+07	2.79E+07
15	1.32	15.68	6.34E+07	4.33E+07	2.66E+07
16	1.39	17.07	6.83E+07	5.14E+07	2.91E+07
17	1.31	18.37	6.28E+07	4.16E+07	2.55E+07
18	1.47	19.85	5.91E+07	4.53E+07	2.78E+07
19	1.31	21.15	6.32E+07	4.24E+07	2.61E+07
20	1.46	22.61	6.01E+07	3.92E+07	2.46E+07
21	1.22	23.83	6.13E+07	4.39E+07	2.66E+07
22	1.36	25.19	6.25E+07	4.12E+07	2.63E+07
23	1.38	26.58	6.52E+07	4.51E+07	2.79E+07
24	1.36	27.94	6.74E+07	4.20E+07	2.60E+07
25	1.21	29.16	7.10E+07	4.26E+07	2.49E+07
26	1.30	30.46	9.41E+07 ^[2]	5.21E+07	3.25E+07
27	1.42	31.88	1.41E+08 ^[2]	6.89E+07 ^[2]	3.54E+07
28	1.27	33.14	1.21E+08 ^[2]	6.54E+07 ^[2]	3.51E+07
29 ^[3]	1.43	34.57	1.22E+08 ^[2]	7.12E+07 ^[2]	3.70E+07
Future ^[4]	--	--	1.38E+08 ^[2]	8.04E+07 ^[2]	4.36E+07
Note(s): 1. Unless otherwise noted, values listed were determined at the pressure vessel outer surface. 2. Value was determined at the pressure vessel clad/base metal interface. 3. Cycle 29 is the most recently completed operating cycle. Values listed for this cycle are projections based on design end of Cycle 29 burnup data. 4. Values beyond Cycle 29 are based on the average core power distributions and reactor operating conditions of Cycle 29, but include a 1.2 bias on the peripheral and re-entrant corner assembly relative powers.					

Table 1-6: Fast ($E > 1.0$ MeV) Neutron Fluence at the Inlet Nozzle Welds – Unit 3

Cycle	Cycle Length (EFPY)	Cumulative Operating Time (EFPY)	Fluence (n/cm ²) ^[1]		
			10°	20°	40°
1	1.15	1.15	3.67E+15	2.08E+15	1.19E+15
2	0.78	1.92	7.31E+15 ^[2]	3.76E+15	2.12E+15
3	0.76	2.68	9.57E+15 ^[2]	5.30E+15	3.03E+15
4	0.78	3.46	1.23E+16 ^[2]	6.76E+15	3.90E+15
5	0.78	4.24	1.57E+16 ^[2]	8.38E+15	4.67E+15
6	0.50	4.74	1.80E+16 ^[2]	9.39E+15	5.16E+15
7	0.92	5.66	2.12E+16 ^[2]	1.10E+16	6.10E+15
8	1.36	7.03	2.55E+16 ^[2]	1.34E+16	7.40E+15
9	1.03	8.06	2.69E+16 ^[2]	1.50E+16	8.46E+15
10	1.25	9.31	2.90E+16 ^[2]	1.69E+16	9.70E+15
11	1.31	10.62	3.15E+16	1.91E+16 ^[2]	1.10E+16
12	1.24	11.86	3.40E+16	2.12E+16 ^[2]	1.21E+16
13	1.25	13.11	3.64E+16	2.26E+16 ^[2]	1.32E+16
14	1.24	14.36	3.89E+16	2.42E+16	1.43E+16
15	1.32	15.68	4.15E+16	2.61E+16	1.54E+16
16	1.39	17.07	4.45E+16	2.83E+16	1.67E+16
17	1.31	18.37	4.71E+16	3.00E+16	1.77E+16
18	1.47	19.85	4.98E+16	3.21E+16	1.90E+16
19	1.31	21.15	5.24E+16	3.39E+16	2.01E+16
20	1.46	22.61	5.52E+16	3.57E+16	2.12E+16
21	1.22	23.83	5.76E+16	3.74E+16	2.23E+16
22	1.36	25.19	6.02E+16	3.91E+16	2.34E+16
23	1.38	26.58	6.31E+16	4.11E+16	2.46E+16
24	1.36	27.94	6.60E+16	4.29E+16	2.57E+16
25	1.21	29.16	6.87E+16	4.45E+16	2.67E+16
26	1.30	30.46	7.23E+16	4.67E+16	2.80E+16
27	1.42	31.88	7.73E+16	4.95E+16	2.96E+16
28	1.27	33.14	8.11E+16	5.19E+16	3.10E+16
29 ^[3]	1.43	34.57	8.56E+16	5.48E+16	3.27E+16
Future ^[4]	--	36.00	9.09E+16	5.82E+16	3.46E+16
Future ^[4]	--	48.00	1.35E+17	8.68E+16	5.11E+16
Future ^[4]	--	60.00	1.85E+17 ^[2]	1.16E+17 ^[2]	6.77E+16
Future ^[4]	--	72.00	2.37E+17 ^[2]	1.46E+17 ^[2]	8.42E+16
Note(s): 1. Unless otherwise noted, values listed were determined at the pressure vessel outer surface. 2. Value was determined at the pressure vessel clad/base metal interface. 3. Cycle 29 is the most recently completed operating cycle. Values listed for this cycle are projections based on design end of Cycle 29 burnup data. 4. Values beyond Cycle 29 are based on the average core power distributions and reactor operating conditions of Cycle 29, but include a 1.2 bias on the peripheral and re-entrant corner assembly relative powers.					

Table 1-7: Iron Atom Displacement Rate at the Inlet Nozzle Welds – Unit 3

Cycle	Cycle Length (EFPY)	Cumulative Operating Time (EFPY)	Displacement Rate (dpa/s) ^[1]		
			10°	20°	40°
1	1.15	1.15	6.48E-13	4.03E-13	2.51E-13
2	0.78	1.92	7.67E-13	4.72E-13	2.88E-13
3	0.76	2.68	6.72E-13	4.42E-13	2.85E-13
4	0.78	3.46	6.81E-13	4.15E-13	2.63E-13
5	0.78	4.24	8.27E-13	4.66E-13	2.56E-13
6	0.50	4.74	7.99E-13	4.49E-13	2.50E-13
7	0.92	5.66	6.13E-13	3.88E-13	2.42E-13
8	1.36	7.03	5.91E-13	3.71E-13	2.28E-13
9	1.03	8.06	4.17E-13	3.16E-13	2.23E-13
10	1.25	9.31	4.16E-13	3.20E-13	2.15E-13
11	1.31	10.62	4.27E-13	3.20E-13	2.11E-13
12	1.24	11.86	4.14E-13	3.08E-13	2.05E-13
13	1.25	13.11	3.93E-13	2.86E-13	1.96E-13
14	1.24	14.36	4.08E-13	2.94E-13	2.00E-13
15	1.32	15.68	4.10E-13	2.91E-13	1.92E-13
16	1.39	17.07	4.44E-13	3.40E-13	2.13E-13
17	1.31	18.37	4.05E-13	2.80E-13	1.85E-13
18	1.47	19.85	3.84E-13	2.98E-13	1.99E-13
19	1.31	21.15	4.09E-13	2.86E-13	1.89E-13
20	1.46	22.61	3.85E-13	2.63E-13	1.75E-13
21	1.22	23.83	3.94E-13	2.90E-13	1.90E-13
22	1.36	25.19	4.01E-13	2.77E-13	1.87E-13
23	1.38	26.58	4.20E-13	3.01E-13	2.00E-13
24	1.36	27.94	4.25E-13	2.85E-13	1.89E-13
25	1.21	29.16	4.52E-13	2.93E-13	1.86E-13
26	1.30	30.46	5.52E-13	3.55E-13	2.36E-13
27	1.42	31.88	6.87E-13	4.26E-13	2.63E-13
28	1.27	33.14	6.00E-13	3.96E-13	2.54E-13
29 ^[2]	1.43	34.57	6.20E-13	4.25E-13	2.68E-13
Future ^[3]	--	--	7.33E-13	5.03E-13	3.17E-13
Note(s): 1. Values listed were determined at the pressure vessel outer surface. 2. Cycle 29 is the most recently completed operating cycle. Values listed for this cycle are projections based on design end of Cycle 29 burnup data. 3. Values beyond Cycle 29 are based on the average core power distributions and reactor operating conditions of Cycle 29, but include a 1.2 bias on the peripheral and re-entrant corner assembly relative powers.					

Table 1-8: Iron Atom Displacements at the Inlet Nozzle Welds – Unit 3

Cycle	Cycle Length (EFPY)	Cumulative Operating Time (EFPY)	Displacements (dpa) ^[1]		
			10°	20°	40°
1	1.15	1.15	2.34E-05	1.46E-05	9.07E-06
2	0.78	1.92	4.22E-05	2.61E-05	1.61E-05
3	0.76	2.68	5.83E-05	3.67E-05	2.30E-05
4	0.78	3.46	7.51E-05	4.69E-05	2.94E-05
5	0.78	4.24	9.54E-05	5.84E-05	3.57E-05
6	0.50	4.74	1.08E-04	6.55E-05	3.97E-05
7	0.92	5.66	1.26E-04	7.68E-05	4.67E-05
8	1.36	7.03	1.51E-04	9.27E-05	5.65E-05
9	1.03	8.06	1.65E-04	1.03E-04	6.38E-05
10	1.25	9.31	1.81E-04	1.16E-04	7.23E-05
11	1.31	10.62	1.99E-04	1.29E-04	8.10E-05
12	1.24	11.86	2.15E-04	1.41E-04	8.90E-05
13	1.25	13.11	2.31E-04	1.52E-04	9.67E-05
14	1.24	14.36	2.47E-04	1.64E-04	1.05E-04
15	1.32	15.68	2.64E-04	1.76E-04	1.13E-04
16	1.39	17.07	2.83E-04	1.91E-04	1.22E-04
17	1.31	18.37	3.00E-04	2.02E-04	1.30E-04
18	1.47	19.85	3.18E-04	2.16E-04	1.39E-04
19	1.31	21.15	3.35E-04	2.28E-04	1.47E-04
20	1.46	22.61	3.52E-04	2.40E-04	1.55E-04
21	1.22	23.83	3.68E-04	2.51E-04	1.62E-04
22	1.36	25.19	3.85E-04	2.63E-04	1.70E-04
23	1.38	26.58	4.03E-04	2.76E-04	1.79E-04
24	1.36	27.94	4.21E-04	2.89E-04	1.87E-04
25	1.21	29.16	4.39E-04	3.00E-04	1.94E-04
26	1.30	30.46	4.61E-04	3.14E-04	2.04E-04
27	1.42	31.88	4.92E-04	3.34E-04	2.15E-04
28	1.27	33.14	5.16E-04	3.49E-04	2.26E-04
29 ^[2]	1.43	34.57	5.44E-04	3.69E-04	2.38E-04
Future ^[3]	--	36.00	5.77E-04	3.91E-04	2.52E-04
Future ^[3]	--	48.00	8.54E-04	5.81E-04	3.72E-04
Future ^[3]	--	60.00	1.13E-03	7.72E-04	4.92E-04
Future ^[3]	--	72.00	1.41E-03	9.62E-04	6.12E-04
Note(s): 1. Values listed were determined at the pressure vessel outer surface. 2. Cycle 29 is the most recently completed operating cycle. Values listed for this cycle are projections based on design end of Cycle 29 burnup data. 3. Values beyond Cycle 29 are based on the average core power distributions and reactor operating conditions of Cycle 29, but include a 1.2 bias on the peripheral and re-entrant corner assembly relative powers.					

Table 1-9: Fast (E > 1.0 MeV) Neutron Fluence Rate at the Outlet Nozzle Welds – Unit 3

Cycle	Cycle Length (EFPY)	Cumulative Operating Time (EFPY)	Fluence Rate (n/cm ² -s) ^[1]		
			10°	20°	40°
1	1.15	1.15	9.09E+07	5.15E+07	2.94E+07
2	0.78	1.92	1.09E+08	6.10E+07	3.39E+07
3	0.76	2.68	9.43E+07	5.74E+07	3.42E+07
4	0.78	3.46	9.67E+07	5.33E+07	3.14E+07
5	0.78	4.24	1.18E+08	5.89E+07	2.81E+07
6	0.50	4.74	1.14E+08	5.68E+07	2.78E+07
7	0.92	5.66	8.71E+07	5.06E+07	2.88E+07
8	1.36	7.03	8.38E+07	4.83E+07	2.69E+07
9	1.03	8.06	5.82E+07	4.32E+07	2.89E+07
10	1.25	9.31	5.85E+07	4.46E+07 ^[2]	2.81E+07 ^[2]
11	1.31	10.62	6.00E+07	4.40E+07	2.69E+07
12	1.24	11.86	5.80E+07	4.21E+07	2.60E+07
13	1.25	13.11	5.49E+07	3.87E+07	2.49E+07
14	1.24	14.36	5.69E+07	3.94E+07	2.51E+07
15	1.32	15.68	5.73E+07	3.90E+07	2.39E+07
16	1.39	17.07	6.17E+07	4.63E+07	2.62E+07
17	1.31	18.37	5.67E+07	3.74E+07	2.29E+07
18	1.47	19.85	5.34E+07	4.07E+07	2.50E+07
19	1.31	21.15	5.72E+07	3.82E+07	2.34E+07
20	1.46	22.61	5.41E+07	3.51E+07	2.20E+07
21	1.22	23.83	5.52E+07	3.94E+07	2.38E+07
22	1.36	25.19	5.63E+07	3.69E+07	2.35E+07
23	1.38	26.58	5.88E+07	4.05E+07	2.50E+07
24	1.36	27.94	6.05E+07	3.77E+07	2.33E+07
25	1.21	29.16	6.39E+07	3.84E+07	2.24E+07
26	1.30	30.46	7.85E+07	4.66E+07	2.91E+07
27	1.42	31.88	9.88E+07	5.60E+07	3.15E+07
28	1.27	33.14	8.60E+07	5.28E+07	3.12E+07
29 ^[3]	1.43	34.57	8.87E+07	5.73E+07	3.30E+07
Future ^[4]	--	--	1.05E+08	6.75E+07	3.89E+07
Note(s): 1. Unless otherwise noted, values listed were determined at the pressure vessel outer surface. 2. Value was determined at the pressure vessel clad/base metal interface. 3. Cycle 29 is the most recently completed operating cycle. Values listed for this cycle are projections based on design end of Cycle 29 burnup data. 4. Values beyond Cycle 29 are based on the average core power distributions and reactor operating conditions of Cycle 29, but include a 1.2 bias on the peripheral and re-entrant corner assembly relative powers.					

Table 1-10: Fast ($E > 1.0$ MeV) Neutron Fluence at the Outlet Nozzle Welds – Unit 3

Cycle	Cycle Length (EFPY)	Cumulative Operating Time (EFPY)	Fluence (n/cm ²) ^[1]		
			10°	20°	40°
1	1.15	1.15	3.28E+15	1.86E+15	1.06E+15
2	0.78	1.92	5.96E+15	3.35E+15	1.89E+15
3	0.76	2.68	8.22E+15	4.73E+15	2.71E+15
4	0.78	3.46	1.06E+16	6.05E+15	3.48E+15
5	0.78	4.24	1.35E+16	7.49E+15	4.17E+15
6	0.50	4.74	1.53E+16	8.39E+15	4.61E+15
7	0.92	5.66	1.78E+16	9.86E+15	5.45E+15
8	1.36	7.03	2.14E+16	1.19E+16	6.61E+15
9	1.03	8.06	2.33E+16	1.34E+16	7.55E+15
10	1.25	9.31	2.56E+16	1.51E+16	8.65E+15
11	1.31	10.62	2.81E+16	1.69E+16	9.76E+15
12	1.24	11.86	3.04E+16	1.86E+16	1.08E+16
13	1.25	13.11	3.26E+16	2.01E+16	1.18E+16
14	1.24	14.36	3.48E+16	2.16E+16	1.27E+16
15	1.32	15.68	3.72E+16	2.33E+16	1.37E+16
16	1.39	17.07	3.99E+16	2.53E+16	1.49E+16
17	1.31	18.37	4.22E+16	2.68E+16	1.58E+16
18	1.47	19.85	4.47E+16	2.87E+16	1.70E+16
19	1.31	21.15	4.71E+16	3.03E+16	1.80E+16
20	1.46	22.61	4.96E+16	3.19E+16	1.90E+16
21	1.22	23.83	5.17E+16	3.34E+16	1.99E+16
22	1.36	25.19	5.41E+16	3.50E+16	2.09E+16
23	1.38	26.58	5.67E+16	3.68E+16	2.20E+16
24	1.36	27.94	5.93E+16	3.84E+16	2.30E+16
25	1.21	29.16	6.17E+16	3.99E+16	2.39E+16
26	1.30	30.46	6.49E+16	4.18E+16	2.51E+16
27	1.42	31.88	6.94E+16	4.43E+16	2.65E+16
28	1.27	33.14	7.28E+16	4.64E+16	2.77E+16
29 ^[2]	1.43	34.57	7.68E+16	4.90E+16	2.92E+16
Future ^[3]	--	36.00	8.15E+16	5.20E+16	3.09E+16
Future ^[3]	--	48.00	1.21E+17	7.76E+16	4.57E+16
Future ^[3]	--	60.00	1.61E+17	1.03E+17	6.04E+16
Future ^[3]	--	72.00	2.00E+17	1.29E+17	7.51E+16
Note(s): 1. Values listed were determined at the pressure vessel outer surface. 2. Cycle 29 is the most recently completed operating cycle. Values listed for this cycle are projections based on design end of Cycle 29 burnup data. 3. Values beyond Cycle 29 are based on the average core power distributions and reactor operating conditions of Cycle 29, but include a 1.2 bias on the peripheral and re-entrant corner assembly relative powers.					

Table 1-11: Iron Atom Displacement Rate at the Outlet Nozzle Welds – Unit 3

Cycle	Cycle Length (EFPY)	Cumulative Operating Time (EFPY)	Displacement Rate (dpa/s) ^[1]		
			10°	20°	40°
1	1.15	1.15	5.83E-13	3.62E-13	2.26E-13
2	0.78	1.92	6.87E-13	4.23E-13	2.58E-13
3	0.76	2.68	6.05E-13	3.98E-13	2.57E-13
4	0.78	3.46	6.13E-13	3.73E-13	2.37E-13
5	0.78	4.24	7.43E-13	4.19E-13	2.30E-13
6	0.50	4.74	7.17E-13	4.03E-13	2.24E-13
7	0.92	5.66	5.51E-13	3.49E-13	2.17E-13
8	1.36	7.03	5.31E-13	3.34E-13	2.05E-13
9	1.03	8.06	3.75E-13	2.84E-13	2.00E-13
10	1.25	9.31	3.74E-13	2.86E-13	1.92E-13
11	1.31	10.62	3.84E-13	2.87E-13	1.89E-13
12	1.24	11.86	3.73E-13	2.77E-13	1.84E-13
13	1.25	13.11	3.54E-13	2.58E-13	1.77E-13
14	1.24	14.36	3.68E-13	2.65E-13	1.80E-13
15	1.32	15.68	3.70E-13	2.63E-13	1.73E-13
16	1.39	17.07	4.01E-13	3.06E-13	1.92E-13
17	1.31	18.37	3.65E-13	2.53E-13	1.66E-13
18	1.47	19.85	3.47E-13	2.69E-13	1.79E-13
19	1.31	21.15	3.69E-13	2.58E-13	1.70E-13
20	1.46	22.61	3.47E-13	2.37E-13	1.58E-13
21	1.22	23.83	3.56E-13	2.61E-13	1.71E-13
22	1.36	25.19	3.62E-13	2.49E-13	1.68E-13
23	1.38	26.58	3.79E-13	2.71E-13	1.80E-13
24	1.36	27.94	3.83E-13	2.56E-13	1.70E-13
25	1.21	29.16	4.08E-13	2.65E-13	1.68E-13
26	1.30	30.46	4.96E-13	3.20E-13	2.13E-13
27	1.42	31.88	6.16E-13	3.82E-13	2.36E-13
28	1.27	33.14	5.38E-13	3.56E-13	2.28E-13
29 ^[2]	1.43	34.57	5.56E-13	3.82E-13	2.41E-13
Future ^[3]	--	--	6.57E-13	4.51E-13	2.85E-13
Note(s): 1. Values listed were determined at the pressure vessel outer surface. 2. Cycle 29 is the most recently completed operating cycle. Values listed for this cycle are projections based on design end of Cycle 29 burnup data. 3. Values beyond Cycle 29 are based on the average core power distributions and reactor operating conditions of Cycle 29, but include a 1.2 bias on the peripheral and re-entrant corner assembly relative powers.					

Table 1-12: Iron Atom Displacements at the Outlet Nozzle Welds – Unit 3

Cycle	Cycle Length (EFPY)	Cumulative Operating Time (EFPY)	Displacements (dpa) ^[1]		
			10°	20°	40°
1	1.15	1.15	2.11E-05	1.31E-05	8.16E-06
2	0.78	1.92	3.79E-05	2.34E-05	1.45E-05
3	0.76	2.68	5.24E-05	3.30E-05	2.06E-05
4	0.78	3.46	6.75E-05	4.22E-05	2.65E-05
5	0.78	4.24	8.57E-05	5.25E-05	3.21E-05
6	0.50	4.74	9.71E-05	5.89E-05	3.57E-05
7	0.92	5.66	1.13E-04	6.90E-05	4.20E-05
8	1.36	7.03	1.36E-04	8.33E-05	5.08E-05
9	1.03	8.06	1.48E-04	9.26E-05	5.73E-05
10	1.25	9.31	1.63E-04	1.04E-04	6.49E-05
11	1.31	10.62	1.79E-04	1.16E-04	7.27E-05
12	1.24	11.86	1.93E-04	1.27E-04	7.99E-05
13	1.25	13.11	2.07E-04	1.37E-04	8.68E-05
14	1.24	14.36	2.22E-04	1.47E-04	9.39E-05
15	1.32	15.68	2.37E-04	1.58E-04	1.01E-04
16	1.39	17.07	2.55E-04	1.72E-04	1.10E-04
17	1.31	18.37	2.70E-04	1.82E-04	1.16E-04
18	1.47	19.85	2.86E-04	1.95E-04	1.25E-04
19	1.31	21.15	3.01E-04	2.05E-04	1.32E-04
20	1.46	22.61	3.17E-04	2.16E-04	1.39E-04
21	1.22	23.83	3.31E-04	2.26E-04	1.46E-04
22	1.36	25.19	3.47E-04	2.37E-04	1.53E-04
23	1.38	26.58	3.63E-04	2.49E-04	1.61E-04
24	1.36	27.94	3.80E-04	2.60E-04	1.68E-04
25	1.21	29.16	3.95E-04	2.70E-04	1.74E-04
26	1.30	30.46	4.16E-04	2.83E-04	1.83E-04
27	1.42	31.88	4.43E-04	3.00E-04	1.94E-04
28	1.27	33.14	4.65E-04	3.14E-04	2.03E-04
29 ^[2]	1.43	34.57	4.90E-04	3.32E-04	2.14E-04
Future ^[3]	--	36.00	5.19E-04	3.52E-04	2.27E-04
Future ^[3]	--	48.00	7.68E-04	5.22E-04	3.34E-04
Future ^[3]	--	60.00	1.02E-03	6.93E-04	4.42E-04
Future ^[3]	--	72.00	1.27E-03	8.64E-04	5.50E-04
Note(s): 1. Values listed were determined at the pressure vessel outer surface. 2. Cycle 29 is the most recently completed operating cycle. Values listed for this cycle are projections based on design end of Cycle 29 burnup data. 3. Values beyond Cycle 29 are based on the average core power distributions and reactor operating conditions of Cycle 29, but include a 1.2 bias on the peripheral and re-entrant corner assembly relative powers.					

Table 1-13: Fast ($E > 1.0$ MeV) Neutron Fluence Rate at the Upper Shell to Intermediate Shell Weld – Unit 3

Cycle	Cycle Length (EFPY)	Cumulative Operating Time (EFPY)	Fluence Rate (n/cm^2-s) ^[1]			
			0°	15°	30°	45°
1	1.15	1.15	5.25E+09	2.41E+09	1.34E+09	8.76E+08
2	0.78	1.92	7.91E+09	3.60E+09	1.95E+09	1.24E+09
3	0.76	2.68	4.83E+09	2.51E+09	1.50E+09	9.99E+08
4	0.78	3.46	5.48E+09	2.66E+09	1.34E+09	9.97E+08
5	0.78	4.24	7.40E+09	3.22E+09	1.32E+09	8.22E+08
6	0.50	4.74	7.44E+09	3.25E+09	1.31E+09	8.65E+08
7	0.92	5.66	5.47E+09	2.59E+09	1.42E+09	9.53E+08
8	1.36	7.03	5.14E+09	2.34E+09	1.26E+09	8.32E+08
9	1.03	8.06	2.48E+09	1.84E+09	1.54E+09	1.12E+09
10	1.25	9.31	2.56E+09	2.07E+09	1.70E+09	1.16E+09
11	1.31	10.62	2.67E+09	2.00E+09	1.62E+09	1.07E+09
12	1.24	11.86	2.47E+09	1.79E+09	1.40E+09	9.37E+08
13	1.25	13.11	2.26E+09	1.44E+09	1.05E+09	7.57E+08
14	1.24	14.36	2.26E+09	1.37E+09	9.40E+08	6.74E+08
15	1.32	15.68	2.32E+09	1.39E+09	9.43E+08	6.48E+08
16	1.39	17.07	2.39E+09	1.60E+09	1.15E+09	6.75E+08
17	1.31	18.37	2.37E+09	1.36E+09	9.41E+08	6.30E+08
18	1.47	19.85	2.05E+09	1.39E+09	1.03E+09	6.73E+08
19	1.31	21.15	2.32E+09	1.35E+09	9.09E+08	6.14E+08
20	1.46	22.61	2.41E+09	1.43E+09	1.01E+09	7.08E+08
21	1.22	23.83	2.32E+09	1.53E+09	1.12E+09	7.25E+08
22	1.36	25.19	2.48E+09	1.48E+09	1.06E+09	7.51E+08
23	1.38	26.58	2.49E+09	1.54E+09	1.11E+09	7.45E+08
24	1.36	27.94	2.96E+09	1.54E+09	9.37E+08	6.58E+08
25	1.21	29.16	2.73E+09	1.37E+09	7.72E+08	5.24E+08
26	1.30	30.46	4.31E+09	2.08E+09	1.21E+09	8.88E+08
27	1.42	31.88	6.38E+09	3.05E+09	1.56E+09	1.08E+09
28	1.27	33.14	5.31E+09	2.68E+09	1.56E+09	1.06E+09
29 ^[2]	1.43	34.57	5.34E+09	2.88E+09	1.68E+09	1.13E+09
Future ^[3]	--	--	6.22E+09	3.36E+09	1.97E+09	1.32E+09

Note(s):

1. Values listed were determined at the pressure vessel clad/base metal interface.
2. Cycle 29 is the most recently completed operating cycle. Values listed for this cycle are projections based on design end of Cycle 29 burnup data.
3. Values beyond Cycle 29 are based on the average core power distributions and reactor operating conditions of Cycle 29, but include a 1.2 bias on the peripheral and re-entrant corner assembly relative powers.

Table 1-14: Fast ($E > 1.0$ MeV) Neutron Fluence at the Upper Shell to Intermediate Shell Weld – Unit 3

Cycle	Cycle Length (EFPY)	Cumulative Operating Time (EFPY)	Fluence (n/cm^2) ^[1]			
			0°	15°	30°	45°
1	1.15	1.15	1.90E+17	8.70E+16	4.84E+16	3.17E+16
2	0.78	1.92	3.83E+17	1.75E+17	9.61E+16	6.20E+16
3	0.76	2.68	4.99E+17	2.35E+17	1.32E+17	8.60E+16
4	0.78	3.46	6.34E+17	3.01E+17	1.65E+17	1.11E+17
5	0.78	4.24	8.16E+17	3.80E+17	1.97E+17	1.31E+17
6	0.50	4.74	9.34E+17	4.31E+17	2.18E+17	1.44E+17
7	0.92	5.66	1.09E+18	5.07E+17	2.59E+17	1.72E+17
8	1.36	7.03	1.31E+18	6.07E+17	3.14E+17	2.08E+17
9	1.03	8.06	1.39E+18	6.67E+17	3.64E+17	2.44E+17
10	1.25	9.31	1.50E+18	7.49E+17	4.31E+17	2.90E+17
11	1.31	10.62	1.61E+18	8.32E+17	4.98E+17	3.34E+17
12	1.24	11.86	1.70E+18	9.02E+17	5.53E+17	3.71E+17
13	1.25	13.11	1.79E+18	9.59E+17	5.94E+17	4.01E+17
14	1.24	14.36	1.88E+18	1.01E+18	6.31E+17	4.27E+17
15	1.32	15.68	1.98E+18	1.07E+18	6.70E+17	4.54E+17
16	1.39	17.07	2.08E+18	1.14E+18	7.21E+17	4.84E+17
17	1.31	18.37	2.18E+18	1.20E+18	7.59E+17	5.10E+17
18	1.47	19.85	2.27E+18	1.26E+18	8.07E+17	5.41E+17
19	1.31	21.15	2.37E+18	1.32E+18	8.45E+17	5.66E+17
20	1.46	22.61	2.48E+18	1.38E+18	8.91E+17	5.99E+17
21	1.22	23.83	2.57E+18	1.44E+18	9.34E+17	6.27E+17
22	1.36	25.19	2.68E+18	1.51E+18	9.80E+17	6.59E+17
23	1.38	26.58	2.79E+18	1.57E+18	1.03E+18	6.92E+17
24	1.36	27.94	2.91E+18	1.64E+18	1.07E+18	7.20E+17
25	1.21	29.16	3.02E+18	1.69E+18	1.10E+18	7.40E+17
26	1.30	30.46	3.20E+18	1.78E+18	1.15E+18	7.77E+17
27	1.42	31.88	3.48E+18	1.91E+18	1.22E+18	8.25E+17
28	1.27	33.14	3.69E+18	2.02E+18	1.28E+18	8.67E+17
29 ^[2]	1.43	34.57	3.93E+18	2.15E+18	1.36E+18	9.18E+17
Future ^[3]	--	36.00	4.21E+18	2.30E+18	1.44E+18	9.78E+17
Future ^[3]	--	48.00	6.57E+18	3.57E+18	2.19E+18	1.48E+18
Future ^[3]	--	60.00	8.92E+18	4.85E+18	2.93E+18	1.97E+18
Future ^[3]	--	72.00	1.13E+19	6.12E+18	3.68E+18	2.47E+18

Note(s):

1. Values listed were determined at the pressure vessel clad/base metal interface.
2. Cycle 29 is the most recently completed operating cycle. Values listed for this cycle are projections based on design end of Cycle 29 burnup data.
3. Values beyond Cycle 29 are based on the average core power distributions and reactor operating conditions of Cycle 29, but include a 1.2 bias on the peripheral and re-entrant corner assembly relative powers.

Table 1-15: Iron Atom Displacement Rate at the Upper Shell to Intermediate Shell Weld – Unit 3

Cycle	Cycle Length (EFPY)	Cumulative Operating Time (EFPY)	Displacement Rate (dpa/s) ^[1]			
			0°	15°	30°	45°
1	1.15	1.15	8.95E-12	4.14E-12	2.28E-12	1.49E-12
2	0.78	1.92	1.34E-11	6.16E-12	3.29E-12	2.10E-12
3	0.76	2.68	8.26E-12	4.33E-12	2.55E-12	1.70E-12
4	0.78	3.46	9.34E-12	4.57E-12	2.27E-12	1.69E-12
5	0.78	4.24	1.26E-11	5.55E-12	2.24E-12	1.40E-12
6	0.50	4.74	1.26E-11	5.58E-12	2.24E-12	1.47E-12
7	0.92	5.66	9.30E-12	4.43E-12	2.41E-12	1.62E-12
8	1.36	7.03	8.73E-12	4.02E-12	2.15E-12	1.41E-12
9	1.03	8.06	4.29E-12	3.15E-12	2.59E-12	1.88E-12
10	1.25	9.31	4.41E-12	3.52E-12	2.84E-12	1.94E-12
11	1.31	10.62	4.60E-12	3.40E-12	2.71E-12	1.80E-12
12	1.24	11.86	4.28E-12	3.05E-12	2.35E-12	1.58E-12
13	1.25	13.11	3.92E-12	2.49E-12	1.78E-12	1.29E-12
14	1.24	14.36	3.93E-12	2.38E-12	1.61E-12	1.15E-12
15	1.32	15.68	4.03E-12	2.41E-12	1.61E-12	1.11E-12
16	1.39	17.07	4.16E-12	2.76E-12	1.97E-12	1.16E-12
17	1.31	18.37	4.10E-12	2.36E-12	1.60E-12	1.08E-12
18	1.47	19.85	3.56E-12	2.40E-12	1.76E-12	1.15E-12
19	1.31	21.15	4.03E-12	2.34E-12	1.55E-12	1.05E-12
20	1.46	22.61	4.17E-12	2.45E-12	1.70E-12	1.20E-12
21	1.22	23.83	4.01E-12	2.63E-12	1.90E-12	1.23E-12
22	1.36	25.19	4.29E-12	2.54E-12	1.79E-12	1.27E-12
23	1.38	26.58	4.32E-12	2.65E-12	1.88E-12	1.27E-12
24	1.36	27.94	5.06E-12	2.66E-12	1.60E-12	1.12E-12
25	1.21	29.16	4.70E-12	2.38E-12	1.33E-12	9.02E-13
26	1.30	30.46	7.35E-12	3.57E-12	2.06E-12	1.51E-12
27	1.42	31.88	1.08E-11	5.21E-12	2.64E-12	1.83E-12
28	1.27	33.14	9.00E-12	4.57E-12	2.64E-12	1.80E-12
29 ^[2]	1.43	34.57	9.06E-12	4.91E-12	2.84E-12	1.91E-12
Future ^[3]	--	--	1.06E-11	5.74E-12	3.33E-12	2.23E-12
Note(s): 1. Values listed were determined at the pressure vessel clad/base metal interface. 2. Cycle 29 is the most recently completed operating cycle. Values listed for this cycle are projections based on design end of Cycle 29 burnup data. 3. Values beyond Cycle 29 are based on the average core power distributions and reactor operating conditions of Cycle 29, but include a 1.2 bias on the peripheral and re-entrant corner assembly relative powers.						

Table 1-16: Iron Atom Displacements at the Upper Shell to Intermediate Shell Weld – Unit 3

Cycle	Cycle Length (EFPY)	Cumulative Operating Time (EFPY)	Displacements (dpa) ^[1]			
			0°	15°	30°	45°
1	1.15	1.15	3.24E-04	1.50E-04	8.23E-05	5.39E-05
2	0.78	1.92	6.51E-04	3.00E-04	1.63E-04	1.05E-04
3	0.76	2.68	8.50E-04	4.05E-04	2.24E-04	1.46E-04
4	0.78	3.46	1.08E-03	5.17E-04	2.80E-04	1.88E-04
5	0.78	4.24	1.39E-03	6.53E-04	3.35E-04	2.22E-04
6	0.50	4.74	1.59E-03	7.42E-04	3.71E-04	2.46E-04
7	0.92	5.66	1.86E-03	8.70E-04	4.40E-04	2.92E-04
8	1.36	7.03	2.23E-03	1.04E-03	5.33E-04	3.53E-04
9	1.03	8.06	2.37E-03	1.15E-03	6.17E-04	4.15E-04
10	1.25	9.31	2.55E-03	1.29E-03	7.30E-04	4.91E-04
11	1.31	10.62	2.74E-03	1.43E-03	8.41E-04	5.65E-04
12	1.24	11.86	2.91E-03	1.55E-03	9.33E-04	6.27E-04
13	1.25	13.11	3.06E-03	1.64E-03	1.00E-03	6.78E-04
14	1.24	14.36	3.22E-03	1.74E-03	1.07E-03	7.23E-04
15	1.32	15.68	3.38E-03	1.84E-03	1.13E-03	7.69E-04
16	1.39	17.07	3.57E-03	1.96E-03	1.22E-03	8.20E-04
17	1.31	18.37	3.73E-03	2.06E-03	1.29E-03	8.64E-04
18	1.47	19.85	3.90E-03	2.17E-03	1.37E-03	9.18E-04
19	1.31	21.15	4.07E-03	2.26E-03	1.43E-03	9.61E-04
20	1.46	22.61	4.26E-03	2.38E-03	1.51E-03	1.02E-03
21	1.22	23.83	4.41E-03	2.48E-03	1.58E-03	1.06E-03
22	1.36	25.19	4.60E-03	2.59E-03	1.66E-03	1.12E-03
23	1.38	26.58	4.79E-03	2.70E-03	1.74E-03	1.17E-03
24	1.36	27.94	5.00E-03	2.82E-03	1.81E-03	1.22E-03
25	1.21	29.16	5.18E-03	2.91E-03	1.86E-03	1.26E-03
26	1.30	30.46	5.49E-03	3.05E-03	1.95E-03	1.32E-03
27	1.42	31.88	5.97E-03	3.29E-03	2.06E-03	1.40E-03
28	1.27	33.14	6.33E-03	3.47E-03	2.17E-03	1.47E-03
29 ^[2]	1.43	34.57	6.74E-03	3.69E-03	2.30E-03	1.56E-03
Future ^[3]	--	36.00	7.21E-03	3.95E-03	2.45E-03	1.66E-03
Future ^[3]	--	48.00	1.12E-02	6.13E-03	3.71E-03	2.50E-03
Future ^[3]	--	60.00	1.52E-02	8.30E-03	4.97E-03	3.35E-03
Future ^[3]	--	72.00	1.92E-02	1.05E-02	6.23E-03	4.19E-03

Note(s):

1. Values listed were determined at the pressure vessel clad/base metal interface.
2. Cycle 29 is the most recently completed operating cycle. Values listed for this cycle are projections based on design end of Cycle 29 burnup data.
3. Values beyond Cycle 29 are based on the average core power distributions and reactor operating conditions of Cycle 29, but include a 1.2 bias on the peripheral and re-entrant corner assembly relative powers.

Table 1-17: Fast ($E > 1.0$ MeV) Neutron Fluence Rate at the Intermediate Shell to Lower Shell Weld – Unit 3

Cycle	Cycle Length (EFPY)	Cumulative Operating Time (EFPY)	Fluence Rate (n/cm ² -s) ^[1]			
			0°	15°	30°	45°
1	1.15	1.15	5.89E+10	2.70E+10	1.50E+10	9.82E+09
2	0.78	1.92	5.74E+10	2.61E+10	1.42E+10	9.00E+09
3	0.76	2.68	5.44E+10	2.83E+10	1.69E+10	1.13E+10
4	0.78	3.46	5.51E+10	2.67E+10	1.34E+10	1.00E+10
5	0.78	4.24	6.82E+10	2.97E+10	1.22E+10	7.58E+09
6	0.50	4.74	6.43E+10	2.81E+10	1.14E+10	7.48E+09
7	0.92	5.66	4.96E+10	2.34E+10	1.29E+10	8.63E+09
8	1.36	7.03	4.86E+10	2.21E+10	1.20E+10	7.87E+09
9	1.03	8.06	2.08E+10	1.50E+10	1.22E+10	8.86E+09
10	1.25	9.31	1.99E+10	1.46E+10	1.12E+10	7.57E+09
11	1.31	10.62	2.14E+10	1.50E+10	1.15E+10	7.58E+09
12	1.24	11.86	2.09E+10	1.48E+10	1.15E+10	7.69E+09
13	1.25	13.11	2.06E+10	1.41E+10	1.08E+10	7.85E+09
14	1.24	14.36	2.17E+10	1.52E+10	1.17E+10	8.43E+09
15	1.32	15.68	2.19E+10	1.48E+10	1.11E+10	7.66E+09
16	1.39	17.07	2.24E+10	1.69E+10	1.33E+10	7.82E+09
17	1.31	18.37	2.21E+10	1.40E+10	1.06E+10	7.12E+09
18	1.47	19.85	1.94E+10	1.51E+10	1.23E+10	8.04E+09
19	1.31	21.15	2.21E+10	1.45E+10	1.10E+10	7.47E+09
20	1.46	22.61	2.10E+10	1.30E+10	9.58E+09	6.75E+09
21	1.22	23.83	2.05E+10	1.44E+10	1.12E+10	7.22E+09
22	1.36	25.19	2.17E+10	1.36E+10	1.02E+10	7.25E+09
23	1.38	26.58	2.22E+10	1.48E+10	1.14E+10	7.66E+09
24	1.36	27.94	3.32E+10	1.73E+10	1.05E+10	7.38E+09
25	1.21	29.16	3.72E+10	1.87E+10	1.05E+10	7.15E+09
26	1.30	30.46	4.55E+10	2.19E+10	1.28E+10	9.37E+09
27	1.42	31.88	5.11E+10	2.44E+10	1.25E+10	8.67E+09
28	1.27	33.14	4.44E+10	2.24E+10	1.31E+10	8.89E+09
29 ^[2]	1.43	34.57	4.46E+10	2.41E+10	1.41E+10	9.42E+09
Future ^[3]	--	--	5.27E+10	2.85E+10	1.67E+10	1.12E+10
Note(s): 1. Values listed were determined at the pressure vessel clad/base metal interface. 2. Cycle 29 is the most recently completed operating cycle. Values listed for this cycle are projections based on design end of Cycle 29 burnup data. 3. Values beyond Cycle 29 are based on the average core power distributions and reactor operating conditions of Cycle 29, but include a 1.2 bias on the peripheral and re-entrant corner assembly relative powers.						

Table 1-18: Fast ($E > 1.0$ MeV) Neutron Fluence at the Intermediate Shell to Lower Shell Weld – Unit 3

Cycle	Cycle Length (EFPY)	Cumulative Operating Time (EFPY)	Fluence (n/cm^2) ^[1]			
			0°	15°	30°	45°
1	1.15	1.15	2.13E+18	9.76E+17	5.43E+17	3.55E+17
2	0.78	1.92	3.54E+18	1.62E+18	8.90E+17	5.75E+17
3	0.76	2.68	4.84E+18	2.30E+18	1.30E+18	8.46E+17
4	0.78	3.46	6.20E+18	2.95E+18	1.63E+18	1.09E+18
5	0.78	4.24	7.87E+18	3.68E+18	1.92E+18	1.28E+18
6	0.50	4.74	8.89E+18	4.13E+18	2.10E+18	1.40E+18
7	0.92	5.66	1.03E+19	4.81E+18	2.48E+18	1.65E+18
8	1.36	7.03	1.24E+19	5.76E+18	2.99E+18	1.99E+18
9	1.03	8.06	1.31E+19	6.25E+18	3.39E+18	2.28E+18
10	1.25	9.31	1.39E+19	6.83E+18	3.83E+18	2.58E+18
11	1.31	10.62	1.48E+19	7.44E+18	4.31E+18	2.89E+18
12	1.24	11.86	1.56E+19	8.02E+18	4.75E+18	3.19E+18
13	1.25	13.11	1.64E+19	8.58E+18	5.18E+18	3.50E+18
14	1.24	14.36	1.73E+19	9.18E+18	5.64E+18	3.83E+18
15	1.32	15.68	1.82E+19	9.79E+18	6.11E+18	4.15E+18
16	1.39	17.07	1.92E+19	1.05E+19	6.69E+18	4.49E+18
17	1.31	18.37	2.01E+19	1.11E+19	7.13E+18	4.79E+18
18	1.47	19.85	2.10E+19	1.18E+19	7.70E+18	5.16E+18
19	1.31	21.15	2.19E+19	1.24E+19	8.15E+18	5.47E+18
20	1.46	22.61	2.28E+19	1.30E+19	8.59E+18	5.78E+18
21	1.22	23.83	2.36E+19	1.36E+19	9.02E+18	6.06E+18
22	1.36	25.19	2.46E+19	1.42E+19	9.46E+18	6.37E+18
23	1.38	26.58	2.55E+19	1.48E+19	9.96E+18	6.70E+18
24	1.36	27.94	2.70E+19	1.55E+19	1.04E+19	7.02E+18
25	1.21	29.16	2.84E+19	1.63E+19	1.08E+19	7.29E+18
26	1.30	30.46	3.03E+19	1.72E+19	1.13E+19	7.68E+18
27	1.42	31.88	3.26E+19	1.82E+19	1.19E+19	8.07E+18
28	1.27	33.14	3.43E+19	1.91E+19	1.24E+19	8.42E+18
29 ^[2]	1.43	34.57	3.63E+19	2.02E+19	1.31E+19	8.85E+18
Future ^[3]	--	36.00	3.87E+19	2.15E+19	1.38E+19	9.35E+18
Future ^[3]	--	48.00	5.87E+19	3.23E+19	2.01E+19	1.36E+19
Future ^[3]	--	60.00	7.86E+19	4.31E+19	2.64E+19	1.78E+19
Future ^[3]	--	72.00	9.86E+19	5.39E+19	3.27E+19	2.20E+19

Note(s):

1. Values listed were determined at the pressure vessel clad/base metal interface.
2. Cycle 29 is the most recently completed operating cycle. Values listed for this cycle are projections based on design end of Cycle 29 burnup data.
3. Values beyond Cycle 29 are based on the average core power distributions and reactor operating conditions of Cycle 29, but include a 1.2 bias on the peripheral and re-entrant corner assembly relative powers.

Table 1-19: Iron Atom Displacement Rate at the Intermediate Shell to Lower Shell Weld – Unit 3

Cycle	Cycle Length (EFPY)	Cumulative Operating Time (EFPY)	Displacement Rate (dpa/s) ^[1]			
			0°	15°	30°	45°
1	1.15	1.15	9.64E-11	4.46E-11	2.45E-11	1.60E-11
2	0.78	1.92	9.39E-11	4.32E-11	2.31E-11	1.47E-11
3	0.76	2.68	8.91E-11	4.67E-11	2.75E-11	1.84E-11
4	0.78	3.46	9.01E-11	4.41E-11	2.19E-11	1.63E-11
5	0.78	4.24	1.12E-10	4.92E-11	1.99E-11	1.24E-11
6	0.50	4.74	1.05E-10	4.65E-11	1.86E-11	1.23E-11
7	0.92	5.66	8.11E-11	3.87E-11	2.10E-11	1.41E-11
8	1.36	7.03	7.94E-11	3.65E-11	1.95E-11	1.29E-11
9	1.03	8.06	3.41E-11	2.45E-11	1.98E-11	1.44E-11
10	1.25	9.31	3.27E-11	2.39E-11	1.81E-11	1.23E-11
11	1.31	10.62	3.52E-11	2.45E-11	1.86E-11	1.23E-11
12	1.24	11.86	3.43E-11	2.43E-11	1.86E-11	1.25E-11
13	1.25	13.11	3.37E-11	2.31E-11	1.76E-11	1.28E-11
14	1.24	14.36	3.56E-11	2.48E-11	1.90E-11	1.37E-11
15	1.32	15.68	3.59E-11	2.42E-11	1.81E-11	1.25E-11
16	1.39	17.07	3.68E-11	2.76E-11	2.16E-11	1.28E-11
17	1.31	18.37	3.62E-11	2.30E-11	1.72E-11	1.16E-11
18	1.47	19.85	3.19E-11	2.46E-11	1.99E-11	1.31E-11
19	1.31	21.15	3.63E-11	2.38E-11	1.79E-11	1.22E-11
20	1.46	22.61	3.45E-11	2.14E-11	1.56E-11	1.10E-11
21	1.22	23.83	3.36E-11	2.36E-11	1.81E-11	1.18E-11
22	1.36	25.19	3.56E-11	2.23E-11	1.65E-11	1.18E-11
23	1.38	26.58	3.64E-11	2.42E-11	1.85E-11	1.25E-11
24	1.36	27.94	5.42E-11	2.85E-11	1.71E-11	1.20E-11
25	1.21	29.16	6.08E-11	3.07E-11	1.72E-11	1.17E-11
26	1.30	30.46	7.44E-11	3.61E-11	2.08E-11	1.53E-11
27	1.42	31.88	8.36E-11	4.03E-11	2.04E-11	1.42E-11
28	1.27	33.14	7.26E-11	3.69E-11	2.13E-11	1.45E-11
29 ^[2]	1.43	34.57	7.30E-11	3.96E-11	2.29E-11	1.54E-11
Future ^[3]	--	--	8.62E-11	4.69E-11	2.72E-11	1.82E-11
Note(s): 1. Values listed were determined at the pressure vessel clad/base metal interface. 2. Cycle 29 is the most recently completed operating cycle. Values listed for this cycle are projections based on design end of Cycle 29 burnup data. 3. Values beyond Cycle 29 are based on the average core power distributions and reactor operating conditions of Cycle 29, but include a 1.2 bias on the peripheral and re-entrant corner assembly relative powers.						

Table 1-20: Iron Atom Displacements at the Intermediate Shell to Lower Shell Weld – Unit 3

Cycle	Cycle Length (EFPY)	Cumulative Operating Time (EFPY)	Displacements (dpa) ^[1]			
			0°	15°	30°	45°
1	1.15	1.15	3.48E-03	1.61E-03	8.86E-04	5.80E-04
2	0.78	1.92	5.78E-03	2.67E-03	1.45E-03	9.40E-04
3	0.76	2.68	7.92E-03	3.79E-03	2.11E-03	1.38E-03
4	0.78	3.46	1.01E-02	4.88E-03	2.65E-03	1.78E-03
5	0.78	4.24	1.29E-02	6.08E-03	3.14E-03	2.09E-03
6	0.50	4.74	1.46E-02	6.82E-03	3.44E-03	2.28E-03
7	0.92	5.66	1.69E-02	7.94E-03	4.04E-03	2.69E-03
8	1.36	7.03	2.03E-02	9.52E-03	4.88E-03	3.25E-03
9	1.03	8.06	2.14E-02	1.03E-02	5.53E-03	3.72E-03
10	1.25	9.31	2.27E-02	1.13E-02	6.25E-03	4.20E-03
11	1.31	10.62	2.42E-02	1.23E-02	7.02E-03	4.71E-03
12	1.24	11.86	2.55E-02	1.32E-02	7.74E-03	5.20E-03
13	1.25	13.11	2.69E-02	1.41E-02	8.44E-03	5.70E-03
14	1.24	14.36	2.83E-02	1.51E-02	9.19E-03	6.24E-03
15	1.32	15.68	2.98E-02	1.61E-02	9.94E-03	6.76E-03
16	1.39	17.07	3.14E-02	1.73E-02	1.09E-02	7.32E-03
17	1.31	18.37	3.29E-02	1.83E-02	1.16E-02	7.80E-03
18	1.47	19.85	3.43E-02	1.94E-02	1.25E-02	8.41E-03
19	1.31	21.15	3.58E-02	2.04E-02	1.33E-02	8.91E-03
20	1.46	22.61	3.74E-02	2.14E-02	1.40E-02	9.41E-03
21	1.22	23.83	3.87E-02	2.23E-02	1.47E-02	9.87E-03
22	1.36	25.19	4.02E-02	2.33E-02	1.54E-02	1.04E-02
23	1.38	26.58	4.18E-02	2.43E-02	1.62E-02	1.09E-02
24	1.36	27.94	4.42E-02	2.55E-02	1.69E-02	1.14E-02
25	1.21	29.16	4.65E-02	2.67E-02	1.76E-02	1.19E-02
26	1.30	30.46	4.96E-02	2.82E-02	1.84E-02	1.25E-02
27	1.42	31.88	5.33E-02	3.00E-02	1.94E-02	1.31E-02
28	1.27	33.14	5.62E-02	3.15E-02	2.02E-02	1.37E-02
29 ^[2]	1.43	34.57	5.95E-02	3.33E-02	2.12E-02	1.44E-02
Future ^[3]	--	36.00	6.34E-02	3.54E-02	2.25E-02	1.52E-02
Future ^[3]	--	48.00	9.60E-02	5.31E-02	3.28E-02	2.21E-02
Future ^[3]	--	60.00	1.29E-01	7.09E-02	4.30E-02	2.90E-02
Future ^[3]	--	72.00	1.61E-01	8.86E-02	5.33E-02	3.59E-02

Note(s):

1. Values listed were determined at the pressure vessel clad/base metal interface.
2. Cycle 29 is the most recently completed operating cycle. Values listed for this cycle are projections based on design end of Cycle 29 burnup data.
3. Values beyond Cycle 29 are based on the average core power distributions and reactor operating conditions of Cycle 29, but include a 1.2 bias on the peripheral and re-entrant corner assembly relative powers.

Table 1-21: Fast ($E > 1.0$ MeV) Neutron Fluence Rate at the Lower Shell to Lower Head Ring Weld – Unit 3

Cycle	Cycle Length (EFPY)	Cumulative Operating Time (EFPY)	Fluence Rate (n/cm^2-s) ^[1]			
			0°	15°	30°	45°
1	1.15	1.15	7.11E+07	3.85E+07	2.26E+07	1.64E+07
2	0.78	1.92	7.90E+07	4.25E+07	2.44E+07	1.75E+07
3	0.76	2.68	6.99E+07	4.16E+07	2.60E+07	1.92E+07
4	0.78	3.46	7.12E+07	4.00E+07	2.20E+07	1.73E+07
5	0.78	4.24	8.67E+07	4.47E+07	2.09E+07	1.47E+07
6	0.50	4.74	8.45E+07	4.36E+07	2.03E+07	1.47E+07
7	0.92	5.66	6.50E+07	3.61E+07	2.11E+07	1.56E+07
8	1.36	7.03	6.07E+07	3.27E+07	1.89E+07	1.38E+07
9	1.03	8.06	3.66E+07	2.55E+07	1.90E+07	1.48E+07
10	1.25	9.31	3.47E+07	2.41E+07	1.69E+07	1.26E+07
11	1.31	10.62	3.85E+07	2.68E+07	1.94E+07	1.42E+07
12	1.24	11.86	3.67E+07	2.52E+07	1.79E+07	1.32E+07
13	1.25	13.11	3.57E+07	2.39E+07	1.69E+07	1.31E+07
14	1.24	14.36	3.68E+07	2.44E+07	1.69E+07	1.31E+07
15	1.32	15.68	3.75E+07	2.44E+07	1.66E+07	1.25E+07
16	1.39	17.07	3.92E+07	2.78E+07	2.00E+07	1.35E+07
17	1.31	18.37	3.77E+07	2.38E+07	1.62E+07	1.20E+07
18	1.47	19.85	3.38E+07	2.45E+07	1.82E+07	1.32E+07
19	1.31	21.15	3.78E+07	2.43E+07	1.66E+07	1.24E+07
20	1.46	22.61	3.59E+07	2.22E+07	1.48E+07	1.13E+07
21	1.22	23.83	3.53E+07	2.38E+07	1.67E+07	1.20E+07
22	1.36	25.19	3.72E+07	2.32E+07	1.57E+07	1.20E+07
23	1.38	26.58	3.85E+07	2.51E+07	1.75E+07	1.30E+07
24	1.36	27.94	4.24E+07	2.54E+07	1.61E+07	1.23E+07
25	1.21	29.16	4.51E+07	2.61E+07	1.57E+07	1.17E+07
26	1.30	30.46	5.76E+07	3.24E+07	1.99E+07	1.56E+07
27	1.42	31.88	6.93E+07	3.85E+07	2.15E+07	1.62E+07
28	1.27	33.14	5.92E+07	3.45E+07	2.13E+07	1.59E+07
29 ^[2]	1.43	34.57	6.00E+07	3.68E+07	2.28E+07	1.68E+07
Future ^[3]	--	--	7.08E+07	4.35E+07	2.70E+07	1.99E+07

Note(s):

1. Values listed were determined at the pressure vessel outer surface.
2. Cycle 29 is the most recently completed operating cycle. Values listed for this cycle are projections based on design end of Cycle 29 burnup data.
3. Values beyond Cycle 29 are based on the average core power distributions and reactor operating conditions of Cycle 29, but include a 1.2 bias on the peripheral and re-entrant corner assembly relative powers.

Table 1-22: Fast ($E > 1.0$ MeV) Neutron Fluence at the Lower Shell to Lower Head Ring Weld – Unit 3

Cycle	Cycle Length (EFPY)	Cumulative Operating Time (EFPY)	Fluence (n/cm^2) ^[1]			
			0°	15°	30°	45°
1	1.15	1.15	2.57E+15	1.39E+15	8.17E+14	5.94E+14
2	0.78	1.92	4.50E+15	2.43E+15	1.41E+15	1.02E+15
3	0.76	2.68	6.18E+15	3.43E+15	2.04E+15	1.48E+15
4	0.78	3.46	7.94E+15	4.42E+15	2.58E+15	1.91E+15
5	0.78	4.24	1.01E+16	5.51E+15	3.09E+15	2.27E+15
6	0.50	4.74	1.14E+16	6.20E+15	3.41E+15	2.50E+15
7	0.92	5.66	1.33E+16	7.25E+15	4.02E+15	2.95E+15
8	1.36	7.03	1.59E+16	8.66E+15	4.84E+15	3.54E+15
9	1.03	8.06	1.71E+16	9.49E+15	5.46E+15	4.03E+15
10	1.25	9.31	1.85E+16	1.04E+16	6.13E+15	4.52E+15
11	1.31	10.62	2.01E+16	1.16E+16	6.93E+15	5.11E+15
12	1.24	11.86	2.15E+16	1.25E+16	7.62E+15	5.62E+15
13	1.25	13.11	2.29E+16	1.35E+16	8.29E+15	6.14E+15
14	1.24	14.36	2.44E+16	1.44E+16	8.96E+15	6.66E+15
15	1.32	15.68	2.59E+16	1.55E+16	9.65E+15	7.18E+15
16	1.39	17.07	2.76E+16	1.67E+16	1.05E+16	7.77E+15
17	1.31	18.37	2.92E+16	1.77E+16	1.12E+16	8.26E+15
18	1.47	19.85	3.08E+16	1.88E+16	1.20E+16	8.88E+15
19	1.31	21.15	3.23E+16	1.98E+16	1.27E+16	9.39E+15
20	1.46	22.61	3.40E+16	2.08E+16	1.34E+16	9.91E+15
21	1.22	23.83	3.53E+16	2.17E+16	1.41E+16	1.04E+16
22	1.36	25.19	3.69E+16	2.27E+16	1.47E+16	1.09E+16
23	1.38	26.58	3.86E+16	2.38E+16	1.55E+16	1.15E+16
24	1.36	27.94	4.04E+16	2.49E+16	1.62E+16	1.20E+16
25	1.21	29.16	4.22E+16	2.59E+16	1.68E+16	1.24E+16
26	1.30	30.46	4.45E+16	2.72E+16	1.76E+16	1.31E+16
27	1.42	31.88	4.76E+16	2.90E+16	1.86E+16	1.38E+16
28	1.27	33.14	5.00E+16	3.04E+16	1.94E+16	1.44E+16
29 ^[2]	1.43	34.57	5.27E+16	3.20E+16	2.04E+16	1.52E+16
Future ^[3]	--	36.00	5.59E+16	3.40E+16	2.17E+16	1.61E+16
Future ^[3]	--	48.00	8.27E+16	5.04E+16	3.19E+16	2.36E+16
Future ^[3]	--	60.00	1.10E+17	6.69E+16	4.21E+16	3.12E+16
Future ^[3]	--	72.00	1.36E+17	8.34E+16	5.24E+16	3.87E+16

Note(s):

1. Values listed were determined at the pressure vessel outer surface.
2. Cycle 29 is the most recently completed operating cycle. Values listed for this cycle are projections based on design end of Cycle 29 burnup data.
3. Values beyond Cycle 29 are based on the average core power distributions and reactor operating conditions of Cycle 29, but include a 1.2 bias on the peripheral and re-entrant corner assembly relative powers.

Table 1-23: Iron Atom Displacement Rate at the Lower Shell to Lower Head Ring Weld – Unit 3

Cycle	Cycle Length (EFPY)	Cumulative Operating Time (EFPY)	Displacement Rate (dpa/s) ^[1]			
			0°	15°	30°	45°
1	1.15	1.15	4.71E-13	2.85E-13	1.78E-13	1.39E-13
2	0.78	1.92	5.19E-13	3.12E-13	1.92E-13	1.48E-13
3	0.76	2.68	4.67E-13	3.05E-13	2.00E-13	1.57E-13
4	0.78	3.46	4.71E-13	2.92E-13	1.74E-13	1.43E-13
5	0.78	4.24	5.68E-13	3.28E-13	1.73E-13	1.32E-13
6	0.50	4.74	5.53E-13	3.20E-13	1.68E-13	1.31E-13
7	0.92	5.66	4.28E-13	2.63E-13	1.64E-13	1.29E-13
8	1.36	7.03	3.98E-13	2.39E-13	1.48E-13	1.15E-13
9	1.03	8.06	2.47E-13	1.82E-13	1.38E-13	1.13E-13
10	1.25	9.31	2.33E-13	1.72E-13	1.24E-13	9.80E-14
11	1.31	10.62	2.58E-13	1.90E-13	1.41E-13	1.10E-13
12	1.24	11.86	2.46E-13	1.79E-13	1.31E-13	1.03E-13
13	1.25	13.11	2.39E-13	1.70E-13	1.24E-13	1.01E-13
14	1.24	14.36	2.46E-13	1.75E-13	1.25E-13	1.02E-13
15	1.32	15.68	2.50E-13	1.75E-13	1.23E-13	9.81E-14
16	1.39	17.07	2.64E-13	1.98E-13	1.46E-13	1.08E-13
17	1.31	18.37	2.50E-13	1.70E-13	1.20E-13	9.45E-14
18	1.47	19.85	2.29E-13	1.74E-13	1.32E-13	1.03E-13
19	1.31	21.15	2.52E-13	1.74E-13	1.23E-13	9.75E-14
20	1.46	22.61	2.38E-13	1.59E-13	1.10E-13	8.86E-14
21	1.22	23.83	2.36E-13	1.69E-13	1.22E-13	9.48E-14
22	1.36	25.19	2.47E-13	1.67E-13	1.16E-13	9.42E-14
23	1.38	26.58	2.57E-13	1.79E-13	1.29E-13	1.02E-13
24	1.36	27.94	2.79E-13	1.83E-13	1.22E-13	9.82E-14
25	1.21	29.16	2.97E-13	1.89E-13	1.20E-13	9.53E-14
26	1.30	30.46	3.78E-13	2.36E-13	1.53E-13	1.25E-13
27	1.42	31.88	4.53E-13	2.79E-13	1.68E-13	1.34E-13
28	1.27	33.14	3.89E-13	2.49E-13	1.62E-13	1.29E-13
29 ^[2]	1.43	34.57	3.96E-13	2.64E-13	1.73E-13	1.36E-13
Future ^[3]	--	--	4.68E-13	3.12E-13	2.05E-13	1.61E-13
Note(s): 1. Values listed were determined at the pressure vessel outer surface. 2. Cycle 29 is the most recently completed operating cycle. Values listed for this cycle are projections based on design end of Cycle 29 burnup data. 3. Values beyond Cycle 29 are based on the average core power distributions and reactor operating conditions of Cycle 29, but include a 1.2 bias on the peripheral and re-entrant corner assembly relative powers.						

Table 1-24: Iron Atom Displacements at the Lower Shell to Lower Head Ring Weld – Unit 3

Cycle	Cycle Length (EFPY)	Cumulative Operating Time (EFPY)	Displacements (dpa) ^[1]			
			0°	15°	30°	45°
1	1.15	1.15	1.70E-05	1.03E-05	6.43E-06	5.01E-06
2	0.78	1.92	2.97E-05	1.79E-05	1.11E-05	8.63E-06
3	0.76	2.68	4.09E-05	2.53E-05	1.59E-05	1.24E-05
4	0.78	3.46	5.25E-05	3.24E-05	2.02E-05	1.59E-05
5	0.78	4.24	6.65E-05	4.05E-05	2.45E-05	1.92E-05
6	0.50	4.74	7.52E-05	4.56E-05	2.71E-05	2.12E-05
7	0.92	5.66	8.76E-05	5.32E-05	3.19E-05	2.50E-05
8	1.36	7.03	1.05E-04	6.35E-05	3.82E-05	2.99E-05
9	1.03	8.06	1.13E-04	6.94E-05	4.27E-05	3.36E-05
10	1.25	9.31	1.22E-04	7.62E-05	4.76E-05	3.75E-05
11	1.31	10.62	1.33E-04	8.40E-05	5.35E-05	4.20E-05
12	1.24	11.86	1.42E-04	9.10E-05	5.86E-05	4.61E-05
13	1.25	13.11	1.52E-04	9.78E-05	6.35E-05	5.01E-05
14	1.24	14.36	1.61E-04	1.05E-04	6.84E-05	5.41E-05
15	1.32	15.68	1.72E-04	1.12E-04	7.35E-05	5.82E-05
16	1.39	17.07	1.83E-04	1.21E-04	7.99E-05	6.29E-05
17	1.31	18.37	1.94E-04	1.28E-04	8.49E-05	6.68E-05
18	1.47	19.85	2.04E-04	1.36E-04	9.10E-05	7.16E-05
19	1.31	21.15	2.15E-04	1.43E-04	9.61E-05	7.56E-05
20	1.46	22.61	2.26E-04	1.50E-04	1.01E-04	7.97E-05
21	1.22	23.83	2.35E-04	1.57E-04	1.06E-04	8.33E-05
22	1.36	25.19	2.45E-04	1.64E-04	1.11E-04	8.74E-05
23	1.38	26.58	2.57E-04	1.72E-04	1.17E-04	9.18E-05
24	1.36	27.94	2.69E-04	1.80E-04	1.22E-04	9.60E-05
25	1.21	29.16	2.80E-04	1.87E-04	1.26E-04	9.97E-05
26	1.30	30.46	2.95E-04	1.97E-04	1.33E-04	1.05E-04
27	1.42	31.88	3.16E-04	2.09E-04	1.40E-04	1.11E-04
28	1.27	33.14	3.31E-04	2.19E-04	1.47E-04	1.16E-04
29 ^[2]	1.43	34.57	3.49E-04	2.31E-04	1.55E-04	1.22E-04
Future ^[3]	--	36.00	3.70E-04	2.45E-04	1.64E-04	1.29E-04
Future ^[3]	--	48.00	5.48E-04	3.63E-04	2.41E-04	1.90E-04
Future ^[3]	--	60.00	7.25E-04	4.81E-04	3.19E-04	2.51E-04
Future ^[3]	--	72.00	9.02E-04	6.00E-04	3.97E-04	3.12E-04

Note(s):

1. Values listed were determined at the pressure vessel outer surface.
2. Cycle 29 is the most recently completed operating cycle. Values listed for this cycle are projections based on design end of Cycle 29 burnup data.
3. Values beyond Cycle 29 are based on the average core power distributions and reactor operating conditions of Cycle 29, but include a 1.2 bias on the peripheral and re-entrant corner assembly relative powers.

Table 1-25: Fast ($E > 1.0$ MeV) Neutron Fluence Rate at the Geometric Center of the Surveillance Capsules – Unit 3

Cycle	Cycle Length (EFPY)	Cumulative Operating Time (EFPY)	Fluence Rate (n/cm ² -s)				
			0°	10°	20°	30°	40°
1	1.15	1.15	1.66E+11	1.16E+11	5.14E+10	3.90E+10	2.59E+10
2	0.78	1.92	1.61E+11	1.13E+11	4.88E+10	3.66E+10	2.37E+10
3	0.76	2.68	1.54E+11	1.19E+11	5.73E+10	4.48E+10	3.03E+10
4	0.78	3.46	1.56E+11	1.17E+11	4.91E+10	3.49E+10	2.64E+10
5	0.78	4.24	2.00E+11	1.41E+11	5.20E+10	3.23E+10	2.07E+10
6	0.50	4.74	1.85E+11	1.31E+11	4.81E+10	2.96E+10	1.99E+10
7	0.92	5.66	1.40E+11	9.88E+10	4.55E+10	3.34E+10	2.27E+10
8	1.36	7.03	1.47E+11	9.89E+10	4.56E+10	3.29E+10	2.20E+10
9	1.03	8.06	7.15E+10	5.72E+10	3.90E+10	3.23E+10	2.35E+10
10	1.25	9.31	6.84E+10	5.61E+10	3.80E+10	2.99E+10	2.05E+10
11	1.31	10.62	7.33E+10	5.76E+10	3.75E+10	2.96E+10	1.98E+10
12	1.24	11.86	7.16E+10	5.71E+10	3.77E+10	3.00E+10	2.04E+10
13	1.25	13.11	7.02E+10	5.47E+10	3.53E+10	2.81E+10	2.05E+10
14	1.24	14.36	7.45E+10	5.91E+10	3.90E+10	3.14E+10	2.27E+10
15	1.32	15.68	7.55E+10	5.88E+10	3.75E+10	2.97E+10	2.07E+10
16	1.39	17.07	7.70E+10	6.24E+10	4.53E+10	3.57E+10	2.15E+10
17	1.31	18.37	7.58E+10	5.79E+10	3.47E+10	2.82E+10	1.92E+10
18	1.47	19.85	6.64E+10	5.41E+10	4.04E+10	3.25E+10	2.16E+10
19	1.31	21.15	7.60E+10	5.89E+10	3.64E+10	2.93E+10	2.02E+10
20	1.46	22.61	7.22E+10	5.45E+10	3.15E+10	2.53E+10	1.81E+10
21	1.22	23.83	7.00E+10	5.56E+10	3.71E+10	2.97E+10	1.96E+10
22	1.36	25.19	7.47E+10	5.66E+10	3.32E+10	2.69E+10	1.93E+10
23	1.38	26.58	7.65E+10	5.90E+10	3.73E+10	3.02E+10	2.06E+10
24	1.36	27.94	9.37E+10	7.03E+10	3.52E+10	2.75E+10	1.96E+10
25	1.21	29.16	1.08E+11	7.87E+10	3.78E+10	2.81E+10	1.94E+10
26	1.30	30.46	1.28E+11	9.02E+10	4.26E+10	3.29E+10	2.43E+10
27	1.42	31.88	1.44E+11	1.03E+11	4.56E+10	3.21E+10	2.26E+10
28	1.27	33.14	1.25E+11	9.08E+10	4.52E+10	3.41E+10	2.36E+10
29 ^[1]	1.43	34.57	1.26E+11	9.35E+10	5.03E+10	3.66E+10	2.49E+10
Future ^[2]	--	--	1.49E+11	1.11E+11	5.96E+10	4.34E+10	2.95E+10
Note(s): 1. Cycle 29 is the most recently completed operating cycle. Values listed for this cycle are projections based on design end of Cycle 29 burnup data. 2. Values beyond Cycle 29 are based on the average core power distributions and reactor operating conditions of Cycle 29, but include a 1.2 bias on the peripheral and re-entrant corner assembly relative powers.							

Table 1-26: Fast (E > 1.0 MeV) Neutron Fluence at the Geometric Center of the Surveillance Capsules – Unit 3

Cycle	Cycle Length (EFPY)	Cumulative Operating Time (EFPY)	Fluence (n/cm ²)				
			0°	10°	20°	30°	40°
1	1.15	1.15	5.99E+18	4.21E+18	1.86E+18	1.41E+18	9.36E+17
2	0.78	1.92	9.92E+18	6.97E+18	3.05E+18	2.31E+18	1.52E+18
3	0.76	2.68	1.36E+19	9.84E+18	4.43E+18	3.38E+18	2.24E+18
4	0.78	3.46	1.75E+19	1.27E+19	5.64E+18	4.24E+18	2.89E+18
5	0.78	4.24	2.24E+19	1.62E+19	6.91E+18	5.03E+18	3.40E+18
6	0.50	4.74	2.53E+19	1.83E+19	7.68E+18	5.50E+18	3.72E+18
7	0.92	5.66	2.94E+19	2.11E+19	9.00E+18	6.47E+18	4.38E+18
8	1.36	7.03	3.57E+19	2.54E+19	1.10E+19	7.89E+18	5.32E+18
9	1.03	8.06	3.80E+19	2.73E+19	1.22E+19	8.94E+18	6.09E+18
10	1.25	9.31	4.07E+19	2.95E+19	1.37E+19	1.01E+19	6.90E+18
11	1.31	10.62	4.38E+19	3.19E+19	1.53E+19	1.14E+19	7.72E+18
12	1.24	11.86	4.66E+19	3.41E+19	1.68E+19	1.25E+19	8.51E+18
13	1.25	13.11	4.93E+19	3.63E+19	1.82E+19	1.36E+19	9.32E+18
14	1.24	14.36	5.23E+19	3.86E+19	1.97E+19	1.49E+19	1.02E+19
15	1.32	15.68	5.54E+19	4.10E+19	2.13E+19	1.61E+19	1.11E+19
16	1.39	17.07	5.88E+19	4.38E+19	2.32E+19	1.77E+19	1.20E+19
17	1.31	18.37	6.19E+19	4.61E+19	2.47E+19	1.88E+19	1.28E+19
18	1.47	19.85	6.50E+19	4.87E+19	2.65E+19	2.03E+19	1.38E+19
19	1.31	21.15	6.81E+19	5.11E+19	2.80E+19	2.16E+19	1.47E+19
20	1.46	22.61	7.14E+19	5.36E+19	2.95E+19	2.27E+19	1.55E+19
21	1.22	23.83	7.41E+19	5.57E+19	3.09E+19	2.39E+19	1.62E+19
22	1.36	25.19	7.74E+19	5.82E+19	3.23E+19	2.50E+19	1.71E+19
23	1.38	26.58	8.07E+19	6.08E+19	3.40E+19	2.63E+19	1.80E+19
24	1.36	27.94	8.47E+19	6.38E+19	3.55E+19	2.75E+19	1.88E+19
25	1.21	29.16	8.88E+19	6.68E+19	3.69E+19	2.86E+19	1.96E+19
26	1.30	30.46	9.41E+19	7.05E+19	3.87E+19	2.99E+19	2.06E+19
27	1.42	31.88	1.01E+20	7.51E+19	4.07E+19	3.14E+19	2.16E+19
28	1.27	33.14	1.06E+20	7.87E+19	4.25E+19	3.27E+19	2.25E+19
29 ^[1]	1.43	34.57	1.11E+20	8.30E+19	4.48E+19	3.44E+19	2.36E+19
Future ^[2]	--	36.00	1.18E+20	8.79E+19	4.75E+19	3.63E+19	2.50E+19
Future ^[2]	--	48.00	1.74E+20	1.30E+20	7.01E+19	5.28E+19	3.61E+19
Future ^[2]	--	60.00	2.30E+20	1.72E+20	9.26E+19	6.92E+19	4.73E+19
Future ^[2]	--	72.00	2.87E+20	2.14E+20	1.15E+20	8.56E+19	5.85E+19

Note(s):

1. Cycle 29 is the most recently completed operating cycle. Values listed for this cycle are projections based on design end of Cycle 29 burnup data.
2. Values beyond Cycle 29 are based on the average core power distributions and reactor operating conditions of Cycle 29, but include a 1.2 bias on the peripheral and re-entrant corner assembly relative powers.

2.0 Reactor Vessel Neutron Exposure Data – Turkey Point Unit 4

Select neutron exposure data applicable to the Turkey Point Unit 4 reactor vessel and in-vessel surveillance capsules are provided in Table 2-1 through Table 2-26. The data provided in Table 2-1 through Table 2-26 were generated using Version 3.2 of the DORT discrete ordinates code and the BUGLE-96 cross-section library. The BUGLE-96 library provides a coupled 47-neutron, 20-gamma-ray-group cross-section data set produced specifically for LWR applications. Furthermore, the neutron transport methodology used to generate the data provided in Table 2-1 through Table 2-26 followed the guidance of Reference 1, and was consistent with the USNRC approved methodology described in Reference 2.

The neutron exposure data provided in Table 2-1 through Table 2-24 are the maximum values at either the reactor pressure vessel clad/base metal interface or the reactor pressure vessel outer surface. Note that for regions and materials above and below the core (e.g., the inlet nozzle welds, outlet nozzle welds, and lower shell to lower head ring weld), the neutron exposure values at the reactor pressure vessel outer surface can be greater than those at the clad/base metal interface.

In addition, the neutron exposure data provided in Table 2-5 through Table 2-12 are based on the lowest elevations of the inlet and outlet nozzle forging attachment welds, with the lowest elevations of those welds being determined at the inner surface of the pressure vessel.

**Table 2-1: Fast ($E > 1.0$ MeV) Neutron Fluence Rate at the Pressure Vessel
Clad/Base Metal Interface – Unit 4**

Cycle	Cycle Length (EFPY)	Cumulative Operating Time (EFPY)	Fluence Rate (n/cm ² -s)			
			0°	15°	30°	45°
1	1.21	1.21	6.43E+10	2.94E+10	1.63E+10	1.05E+10
2	0.76	1.97	6.00E+10	2.79E+10	1.52E+10	9.66E+09
3	0.68	2.66	5.88E+10	3.05E+10	1.75E+10	1.14E+10
4	0.84	3.49	5.31E+10	2.73E+10	1.44E+10	1.13E+10
5	0.35	3.85	3.57E+10	1.97E+10	1.45E+10	9.15E+09
6	1.12	4.96	6.00E+10	2.71E+10	1.32E+10	8.56E+09
7	0.71	5.68	5.47E+10	2.53E+10	1.25E+10	7.84E+09
8	0.71	6.39	5.30E+10	2.39E+10	1.20E+10	9.10E+09
9	0.66	7.05	3.19E+10	1.95E+10	1.29E+10	8.49E+09
10	1.28	8.33	3.19E+10	1.88E+10	1.25E+10	8.37E+09
11	1.28	9.60	3.20E+10	1.87E+10	1.21E+10	7.81E+09
12	1.12	10.72	3.29E+10	1.76E+10	1.14E+10	8.16E+09
13	1.19	11.91	3.26E+10	1.85E+10	1.21E+10	8.18E+09
14	1.24	13.15	3.14E+10	1.81E+10	1.14E+10	7.55E+09
15	1.25	14.40	3.54E+10	1.97E+10	1.26E+10	7.99E+09
16	1.37	15.76	3.32E+10	1.82E+10	1.19E+10	8.73E+09
17	1.40	17.16	3.36E+10	1.81E+10	1.19E+10	8.11E+09
18	1.44	18.60	3.28E+10	1.71E+10	1.10E+10	8.42E+09
19	1.38	19.98	3.32E+10	1.84E+10	1.14E+10	7.43E+09
20	1.46	21.44	3.28E+10	1.82E+10	1.19E+10	8.15E+09
21	1.22	22.66	4.16E+10	2.28E+10	1.44E+10	9.69E+09
22	1.36	24.02	3.38E+10	1.88E+10	1.21E+10	8.23E+09
23	1.26	25.28	3.25E+10	1.88E+10	1.24E+10	8.55E+09
24	1.41	26.68	3.45E+10	1.83E+10	1.14E+10	7.48E+09
25	1.24	27.92	3.83E+10	1.93E+10	1.12E+10	7.78E+09
26	1.44	29.36	4.19E+10	1.98E+10	1.13E+10	7.90E+09
27	1.36	30.72	4.92E+10	2.31E+10	1.27E+10	9.20E+09
28	1.39	32.11	4.70E+10	2.28E+10	1.23E+10	9.40E+09
29	1.43	33.53	4.97E+10	2.38E+10	1.37E+10	9.92E+09
30 ^[1]	1.40	33.50	4.99E+10	2.34E+10	1.31E+10	9.36E+09
Future ^[2]	--	--	5.46E+10	2.95E+10	1.73E+10	1.16E+10
Note(s): 1. Cycle 30 is the current operating cycle. Values listed for this cycle are projections based on design end of Cycle 30 burnup data. 2. Values beyond Cycle 30 are based on the average core power distributions and reactor operating conditions of Turkey Point Unit 3 Cycle 29, but include a 1.2 bias on the peripheral and re-entrant corner assembly relative powers.						

Table 2-2: Fast (E > 1.0 MeV) Neutron Fluence at the Pressure Vessel Clad/Base Metal Interface – Unit 4

Cycle	Cycle Length (EFPY)	Cumulative Operating Time (EFPY)	Fluence (n/cm ²)			
			0°	15°	30°	45°
1	1.21	1.21	2.46E+18	1.13E+18	6.23E+17	4.01E+17
2	0.76	1.97	3.89E+18	1.79E+18	9.84E+17	6.31E+17
3	0.68	2.66	5.15E+18	2.44E+18	1.36E+18	8.76E+17
4	0.84	3.49	6.55E+18	3.16E+18	1.74E+18	1.17E+18
5	0.35	3.85	6.95E+18	3.38E+18	1.90E+18	1.27E+18
6	1.12	4.96	9.06E+18	4.34E+18	2.36E+18	1.58E+18
7	0.71	5.68	1.03E+19	4.90E+18	2.64E+18	1.75E+18
8	0.71	6.39	1.15E+19	5.44E+18	2.91E+18	1.96E+18
9	0.66	7.05	1.21E+19	5.84E+18	3.18E+18	2.13E+18
10	1.28	8.33	1.32E+19	6.51E+18	3.68E+18	2.47E+18
11	1.28	9.60	1.43E+19	7.21E+18	4.17E+18	2.78E+18
12	1.12	10.72	1.54E+19	7.78E+18	4.55E+18	3.06E+18
13	1.19	11.91	1.66E+19	8.44E+18	4.99E+18	3.35E+18
14	1.24	13.15	1.79E+19	9.15E+18	5.43E+18	3.65E+18
15	1.25	14.40	1.92E+19	9.93E+18	5.91E+18	3.96E+18
16	1.37	15.76	2.07E+19	1.07E+19	6.43E+18	4.33E+18
17	1.40	17.16	2.22E+19	1.15E+19	6.95E+18	4.68E+18
18	1.44	18.60	2.36E+19	1.23E+19	7.44E+18	5.07E+18
19	1.38	19.98	2.51E+19	1.31E+19	7.94E+18	5.39E+18
20	1.46	21.44	2.66E+19	1.39E+19	8.49E+18	5.76E+18
21	1.22	22.66	2.80E+19	1.47E+19	8.94E+18	6.07E+18
22	1.36	24.02	2.95E+19	1.55E+19	9.46E+18	6.42E+18
23	1.26	25.28	3.08E+19	1.63E+19	9.95E+18	6.76E+18
24	1.41	26.68	3.23E+19	1.71E+19	1.05E+19	7.09E+18
25	1.24	27.92	3.38E+19	1.78E+19	1.09E+19	7.39E+18
26	1.44	29.36	3.57E+19	1.87E+19	1.14E+19	7.75E+18
27	1.36	30.72	3.77E+19	1.97E+19	1.19E+19	8.14E+18
28	1.39	32.11	3.98E+19	2.07E+19	1.25E+19	8.55E+18
29	1.40	33.50	4.20E+19	2.17E+19	1.31E+19	8.98E+18
30 ^[1]	1.36	34.86	4.41E+19	2.27E+19	1.36E+19	9.38E+18
Future ^[2]	--	36.00	4.61E+19	2.38E+19	1.43E+19	9.80E+18
Future ^[2]	--	48.00	6.67E+19	3.50E+19	2.08E+19	1.42E+19
Future ^[2]	--	60.00	8.74E+19	4.61E+19	2.73E+19	1.85E+19
Future ^[2]	--	72.00	1.08E+20	5.73E+19	3.38E+19	2.29E+19
Note(s): 1. Cycle 30 is the current operating cycle. Values listed for this cycle are projections based on design end of Cycle 30 burnup data. 2. Values beyond Cycle 30 are based on the average core power distributions and reactor operating conditions of Turkey Point Unit 3 Cycle 29, but include a 1.2 bias on the peripheral and re-entrant corner assembly relative powers.						

Table 2-3: Iron Atom Displacement Rate at the Pressure Vessel Clad/Base Metal Interface – Unit 4

Cycle	Cycle Length (EFPY)	Cumulative Operating Time (EFPY)	Displacement Rate (dpa/s)			
			0°	15°	30°	45°
1	1.21	1.21	1.05E-10	4.84E-11	2.64E-11	1.71E-11
2	0.76	1.97	9.78E-11	4.58E-11	2.47E-11	1.57E-11
3	0.68	2.66	9.60E-11	5.02E-11	2.85E-11	1.85E-11
4	0.84	3.49	8.66E-11	4.50E-11	2.34E-11	1.83E-11
5	0.35	3.85	5.82E-11	3.22E-11	2.34E-11	1.49E-11
6	1.12	4.96	9.78E-11	4.46E-11	2.14E-11	1.40E-11
7	0.71	5.68	8.92E-11	4.16E-11	2.04E-11	1.28E-11
8	0.71	6.39	8.63E-11	3.93E-11	1.95E-11	1.48E-11
9	0.66	7.05	5.20E-11	3.19E-11	2.10E-11	1.38E-11
10	1.28	8.33	5.19E-11	3.07E-11	2.03E-11	1.36E-11
11	1.28	9.60	5.21E-11	3.05E-11	1.96E-11	1.27E-11
12	1.12	10.72	5.36E-11	2.89E-11	1.85E-11	1.32E-11
13	1.19	11.91	5.31E-11	3.03E-11	1.97E-11	1.33E-11
14	1.24	13.15	5.11E-11	2.96E-11	1.85E-11	1.23E-11
15	1.25	14.40	5.77E-11	3.23E-11	2.05E-11	1.30E-11
16	1.37	15.76	5.41E-11	2.98E-11	1.92E-11	1.41E-11
17	1.40	17.16	5.46E-11	2.96E-11	1.92E-11	1.32E-11
18	1.44	18.60	5.34E-11	2.80E-11	1.77E-11	1.36E-11
19	1.38	19.98	5.40E-11	3.01E-11	1.84E-11	1.21E-11
20	1.46	21.44	5.34E-11	2.98E-11	1.93E-11	1.32E-11
21	1.22	22.66	6.75E-11	3.73E-11	2.33E-11	1.57E-11
22	1.36	24.02	5.50E-11	3.08E-11	1.95E-11	1.34E-11
23	1.26	25.28	5.30E-11	3.08E-11	2.01E-11	1.39E-11
24	1.41	26.68	5.61E-11	3.00E-11	1.85E-11	1.22E-11
25	1.24	27.92	6.23E-11	3.16E-11	1.82E-11	1.27E-11
26	1.44	29.36	6.82E-11	3.25E-11	1.84E-11	1.28E-11
27	1.36	30.72	8.00E-11	3.79E-11	2.06E-11	1.49E-11
28	1.39	32.11	7.65E-11	3.74E-11	2.00E-11	1.52E-11
29	1.40	33.50	8.10E-11	3.91E-11	2.23E-11	1.61E-11
30 ^[1]	1.36	34.86	8.12E-11	3.84E-11	2.13E-11	1.52E-11
Future ^[2]	--	--	8.90E-11	4.84E-11	2.80E-11	1.88E-11
Note(s): 1. Cycle 30 is the current operating cycle. Values listed for this cycle are projections based on design end of Cycle 30 burnup data. 2. Values beyond Cycle 30 are based on the average core power distributions and reactor operating conditions of Turkey Point Unit 3 Cycle 29, but include a 1.2 bias on the peripheral and re-entrant corner assembly relative powers.						

Table 2-4: Iron Atom Displacements at the Pressure Vessel Clad/Base Metal Interface – Unit 4

Cycle	Cycle Length (EFPY)	Cumulative Operating Time (EFPY)	Displacements (dpa)			
			0°	15°	30°	45°
1	1.21	1.21	4.01E-03	1.85E-03	1.01E-03	6.53E-04
2	0.76	1.97	6.33E-03	2.94E-03	1.60E-03	1.03E-03
3	0.68	2.66	8.40E-03	4.02E-03	2.21E-03	1.43E-03
4	0.84	3.49	1.07E-02	5.21E-03	2.83E-03	1.91E-03
5	0.35	3.85	1.13E-02	5.57E-03	3.09E-03	2.07E-03
6	1.12	4.96	1.48E-02	7.13E-03	3.84E-03	2.56E-03
7	0.71	5.68	1.68E-02	8.07E-03	4.30E-03	2.85E-03
8	0.71	6.39	1.87E-02	8.95E-03	4.74E-03	3.18E-03
9	0.66	7.05	1.98E-02	9.61E-03	5.17E-03	3.47E-03
10	1.28	8.33	2.15E-02	1.07E-02	5.98E-03	4.01E-03
11	1.28	9.60	2.33E-02	1.19E-02	6.77E-03	4.52E-03
12	1.12	10.72	2.51E-02	1.28E-02	7.39E-03	4.97E-03
13	1.19	11.91	2.71E-02	1.39E-02	8.10E-03	5.45E-03
14	1.24	13.15	2.91E-02	1.50E-02	8.80E-03	5.92E-03
15	1.25	14.40	3.14E-02	1.63E-02	9.60E-03	6.42E-03
16	1.37	15.76	3.37E-02	1.76E-02	1.04E-02	7.03E-03
17	1.40	17.16	3.61E-02	1.89E-02	1.13E-02	7.61E-03
18	1.44	18.60	3.85E-02	2.02E-02	1.21E-02	8.23E-03
19	1.38	19.98	4.09E-02	2.15E-02	1.29E-02	8.75E-03
20	1.46	21.44	4.33E-02	2.28E-02	1.38E-02	9.36E-03
21	1.22	22.66	4.57E-02	2.42E-02	1.45E-02	9.85E-03
22	1.36	24.02	4.80E-02	2.55E-02	1.53E-02	1.04E-02
23	1.26	25.28	5.01E-02	2.67E-02	1.61E-02	1.10E-02
24	1.41	26.68	5.26E-02	2.80E-02	1.70E-02	1.15E-02
25	1.24	27.92	5.50E-02	2.92E-02	1.77E-02	1.20E-02
26	1.44	29.36	5.81E-02	3.07E-02	1.85E-02	1.26E-02
27	1.36	30.72	6.14E-02	3.23E-02	1.94E-02	1.32E-02
28	1.39	32.11	6.47E-02	3.39E-02	2.02E-02	1.39E-02
29	1.40	33.50	6.83E-02	3.56E-02	2.12E-02	1.46E-02
30 ^[1]	1.36	34.86	7.18E-02	3.73E-02	2.21E-02	1.52E-02
Future ^[2]	--	36.00	7.50E-02	3.90E-02	2.31E-02	1.59E-02
Future ^[2]	--	48.00	1.09E-01	5.73E-02	3.37E-02	2.30E-02
Future ^[2]	--	60.00	1.42E-01	7.56E-02	4.43E-02	3.01E-02
Future ^[2]	--	72.00	1.76E-01	9.40E-02	5.49E-02	3.72E-02
Note(s): 1. Cycle 30 is the current operating cycle. Values listed for this cycle are projections based on design end of Cycle 30 burnup data. 2. Values beyond Cycle 30 are based on the average core power distributions and reactor operating conditions of Turkey Point Unit 3 Cycle 29, but include a 1.2 bias on the peripheral and re-entrant corner assembly relative powers.						

Table 2-5: Fast (E > 1.0 MeV) Neutron Fluence Rate at the Inlet Nozzle Welds – Unit 4

Cycle	Cycle Length (EFPY)	Cumulative Operating Time (EFPY)	Fluence Rate (n/cm ² -s) ^[1]		
			10°	20°	40°
1	1.21	1.21	1.08E+08	6.09E+07	3.44E+07
2	0.76	1.97	1.62E+08 ^[2]	7.83E+07 ^[2]	3.96E+07
3	0.68	2.66	1.16E+08	6.96E+07	3.99E+07
4	0.84	3.49	1.37E+08 ^[2]	6.57E+07 ^[2]	3.91E+07
5	0.35	3.85	9.93E+07 ^[2]	6.29E+07 ^[2]	3.60E+07 ^[2]
6	1.12	4.96	1.20E+08 ^[2]	5.92E+07	3.14E+07
7	0.71	5.68	1.39E+08 ^[2]	6.66E+07 ^[2]	3.24E+07
8	0.71	6.39	1.37E+08 ^[2]	5.92E+07 ^[2]	3.40E+07
9	0.66	7.05	9.22E+07 ^[2]	6.13E+07 ^[2]	3.27E+07 ^[2]
10	1.28	8.33	6.58E+07	5.98E+07 ^[2]	3.67E+07 ^[2]
11	1.28	9.60	6.83E+07	6.98E+07 ^[2]	4.26E+07 ^[2]
12	1.12	10.72	6.80E+07	7.01E+07 ^[2]	4.89E+07 ^[2]
13	1.19	11.91	6.66E+07	5.00E+07 ^[2]	3.15E+07 ^[2]
14	1.24	13.15	6.26E+07	4.41E+07 ^[2]	2.65E+07 ^[2]
15	1.25	14.40	6.87E+07	4.76E+07	2.81E+07
16	1.37	15.76	6.14E+07	4.21E+07	2.78E+07
17	1.40	17.16	6.26E+07	4.31E+07	2.74E+07
18	1.44	18.60	6.10E+07	4.00E+07	2.73E+07
19	1.38	19.98	6.27E+07	4.29E+07	2.55E+07
20	1.46	21.44	6.22E+07	4.31E+07	2.71E+07
21	1.22	22.66	7.64E+07	5.30E+07	3.29E+07
22	1.36	24.02	6.31E+07	4.38E+07	2.74E+07
23	1.26	25.28	6.28E+07	4.48E+07	2.87E+07
24	1.41	26.68	6.29E+07	4.24E+07	2.58E+07
25	1.24	27.92	7.25E+07	4.40E+07	2.65E+07
26	1.44	29.36	7.06E+07	4.14E+07	2.49E+07
27	1.36	30.72	9.19E+07 ^[2]	5.24E+07	3.14E+07
28	1.39	32.11	1.31E+08 ^[2]	6.58E+07 ^[2]	3.73E+07 ^[2]
29	1.40	33.50	1.31E+08 ^[2]	6.69E+07 ^[2]	3.82E+07 ^[2]
30 ^[3]	1.36	34.86	1.33E+08 ^[2]	6.76E+07 ^[2]	3.72E+07 ^[2]
Future ^[4]	--	--	1.45E+08 ^[2]	8.43E+07 ^[2]	4.39E+07
Note(s): 1. Unless otherwise noted, values listed were determined at the pressure vessel outer surface. 2. Value was determined at the pressure vessel clad/base metal interface. 3. Cycle 30 is the current operating cycle. Values listed for this cycle are projections based on design end of Cycle 30 burnup data. 4. Values beyond Cycle 30 are based on the average core power distributions and reactor operating conditions of Turkey Point Unit 3 Cycle 29, but include a 1.2 bias on the peripheral and re-entrant corner assembly relative powers.					

Table 2-6: Fast ($E > 1.0$ MeV) Neutron Fluence at the Inlet Nozzle Welds – Unit 4

Cycle	Cycle Length (EFPY)	Cumulative Operating Time (EFPY)	Fluence (n/cm ²) ^[1]		
			10°	20°	40°
1	1.21	1.21	4.14E+15	2.33E+15	1.32E+15
2	0.76	1.97	8.02E+15 ^[2]	4.04E+15	2.27E+15
3	0.68	2.66	1.05E+16 ^[2]	5.54E+15	3.13E+15
4	0.84	3.49	1.41E+16 ^[2]	7.20E+15	4.16E+15
5	0.35	3.85	1.52E+16 ^[2]	7.79E+15	4.54E+15
6	1.12	4.96	1.94E+16 ^[2]	9.88E+15	5.64E+15
7	0.71	5.68	2.26E+16 ^[2]	1.13E+16	6.37E+15
8	0.71	6.39	2.57E+16 ^[2]	1.26E+16	7.14E+15
9	0.66	7.05	2.76E+16 ^[2]	1.36E+16 ^[2]	7.78E+15
10	1.28	8.33	2.97E+16 ^[2]	1.60E+16 ^[2]	8.98E+15
11	1.28	9.60	3.20E+16 ^[2]	1.88E+16 ^[2]	1.03E+16
12	1.12	10.72	3.42E+16 ^[2]	2.13E+16 ^[2]	1.20E+16 ^[2]
13	1.19	11.91	3.59E+16 ^[2]	2.32E+16 ^[2]	1.31E+16 ^[2]
14	1.24	13.15	3.75E+16 ^[2]	2.48E+16 ^[2]	1.41E+16 ^[2]
15	1.25	14.40	3.92E+16 ^[2]	2.64E+16 ^[2]	1.50E+16 ^[2]
16	1.37	15.76	4.18E+16	2.78E+16 ^[2]	1.60E+16 ^[2]
17	1.40	17.16	4.46E+16	2.93E+16 ^[2]	1.71E+16 ^[2]
18	1.44	18.60	4.74E+16	3.08E+16 ^[2]	1.84E+16 ^[2]
19	1.38	19.98	5.01E+16	3.23E+16 ^[2]	1.95E+16
20	1.46	21.44	5.30E+16	3.42E+16 ^[2]	2.07E+16
21	1.22	22.66	5.59E+16	3.62E+16 ^[2]	2.20E+16
22	1.36	24.02	5.86E+16	3.81E+16	2.32E+16
23	1.26	25.28	6.11E+16	3.99E+16	2.43E+16
24	1.41	26.68	6.39E+16	4.18E+16	2.54E+16
25	1.24	27.92	6.67E+16	4.35E+16	2.65E+16
26	1.44	29.36	6.99E+16	4.54E+16	2.76E+16
27	1.36	30.72	7.38E+16	4.76E+16	2.89E+16
28	1.39	32.11	7.81E+16	5.01E+16	3.05E+16
29	1.40	33.50	8.26E+16	5.27E+16	3.21E+16
30 ^[3]	1.36	34.86	8.69E+16	5.53E+16	3.36E+16
Future ^[4]	--	36.00	9.11E+16	5.80E+16	3.52E+16
Future ^[4]	--	48.00	1.39E+17 ^[2]	8.87E+16 ^[2]	5.18E+16
Future ^[4]	--	60.00	1.94E+17 ^[2]	1.21E+17 ^[2]	6.84E+16
Future ^[4]	--	72.00	2.49E+17 ^[2]	1.53E+17 ^[2]	8.50E+16
Note(s): 1. Unless otherwise noted, values listed were determined at the pressure vessel outer surface. 2. Value was determined at the pressure vessel clad/base metal interface. 3. Cycle 30 is the current operating cycle. Values listed for this cycle are projections based on design end of Cycle 30 burnup data. 4. Values beyond Cycle 30 are based on the average core power distributions and reactor operating conditions of Turkey Point Unit 3 Cycle 29, but include a 1.2 bias on the peripheral and re-entrant corner assembly relative powers.					

Table 2-7: Iron Atom Displacement Rate at the Inlet Nozzle Welds – Unit 4

Cycle	Cycle Length (EFPY)	Cumulative Operating Time (EFPY)	Displacement Rate (dpa/s) ^[1]		
			10°	20°	40°
1	1.21	1.21	6.90E-13	4.27E-13	2.64E-13
2	0.76	1.97	7.87E-13	4.88E-13	2.99E-13
3	0.68	2.66	7.39E-13	4.80E-13	3.01E-13
4	0.84	3.49	6.90E-13	4.30E-13	2.84E-13
5	0.35	3.85	4.84E-13	3.53E-13	2.40E-13
6	1.12	4.96	6.89E-13	4.13E-13	2.43E-13
7	0.71	5.68	6.96E-13	4.26E-13	2.48E-13
8	0.71	6.39	6.65E-13	3.90E-13	2.51E-13
9	0.66	7.05	4.46E-13	3.32E-13	2.18E-13
10	1.28	8.33	4.19E-13	3.14E-13	2.09E-13
11	1.28	9.60	4.35E-13	3.31E-13	2.19E-13
12	1.12	10.72	4.31E-13	3.16E-13	2.22E-13
13	1.19	11.91	4.26E-13	3.18E-13	2.14E-13
14	1.24	13.15	4.01E-13	2.92E-13	1.90E-13
15	1.25	14.40	4.41E-13	3.17E-13	2.04E-13
16	1.37	15.76	3.98E-13	2.84E-13	1.98E-13
17	1.40	17.16	4.05E-13	2.89E-13	1.96E-13
18	1.44	18.60	3.93E-13	2.70E-13	1.92E-13
19	1.38	19.98	4.03E-13	2.87E-13	1.84E-13
20	1.46	21.44	4.02E-13	2.88E-13	1.93E-13
21	1.22	22.66	4.87E-13	3.49E-13	2.32E-13
22	1.36	24.02	4.08E-13	2.93E-13	1.96E-13
23	1.26	25.28	4.06E-13	2.98E-13	2.03E-13
24	1.41	26.68	4.06E-13	2.85E-13	1.86E-13
25	1.24	27.92	4.58E-13	3.00E-13	1.95E-13
26	1.44	29.36	4.52E-13	2.88E-13	1.87E-13
27	1.36	30.72	5.69E-13	3.60E-13	2.32E-13
28	1.39	32.11	6.07E-13	3.84E-13	2.51E-13
29	1.40	33.50	6.31E-13	4.04E-13	2.66E-13
30 ^[2]	1.36	34.86	6.28E-13	3.99E-13	2.58E-13
Future ^[3]	--	--	7.36E-13	5.05E-13	3.19E-13
Note(s): 1. Values listed were determined at the pressure vessel outer surface. 2. Cycle 30 is the current operating cycle. Values listed for this cycle are projections based on design end of Cycle 30 burnup data. 3. Values beyond Cycle 30 are based on the average core power distributions and reactor operating conditions of Turkey Point Unit 3 Cycle 29, but include a 1.2 bias on the peripheral and re-entrant corner assembly relative powers.					

Table 2-8: Iron Atom Displacements at the Inlet Nozzle Welds – Unit 4

Cycle	Cycle Length (EFPY)	Cumulative Operating Time (EFPY)	Displacements (dpa) ^[1]		
			10°	20°	40°
1	1.21	1.21	2.64E-05	1.64E-05	1.01E-05
2	0.76	1.97	4.53E-05	2.81E-05	1.73E-05
3	0.68	2.66	6.12E-05	3.84E-05	2.38E-05
4	0.84	3.49	7.94E-05	4.98E-05	3.13E-05
5	0.35	3.85	8.48E-05	5.37E-05	3.39E-05
6	1.12	4.96	1.09E-04	6.82E-05	4.25E-05
7	0.71	5.68	1.25E-04	7.78E-05	4.81E-05
8	0.71	6.39	1.40E-04	8.66E-05	5.38E-05
9	0.66	7.05	1.49E-04	9.35E-05	5.83E-05
10	1.28	8.33	1.66E-04	1.06E-04	6.67E-05
11	1.28	9.60	1.83E-04	1.20E-04	7.55E-05
12	1.12	10.72	1.99E-04	1.31E-04	8.33E-05
13	1.19	11.91	2.15E-04	1.43E-04	9.14E-05
14	1.24	13.15	2.30E-04	1.54E-04	9.88E-05
15	1.25	14.40	2.48E-04	1.67E-04	1.07E-04
16	1.37	15.76	2.65E-04	1.79E-04	1.15E-04
17	1.40	17.16	2.83E-04	1.92E-04	1.24E-04
18	1.44	18.60	3.01E-04	2.04E-04	1.33E-04
19	1.38	19.98	3.18E-04	2.16E-04	1.41E-04
20	1.46	21.44	3.37E-04	2.30E-04	1.50E-04
21	1.22	22.66	3.55E-04	2.43E-04	1.59E-04
22	1.36	24.02	3.73E-04	2.56E-04	1.67E-04
23	1.26	25.28	3.89E-04	2.67E-04	1.75E-04
24	1.41	26.68	4.07E-04	2.80E-04	1.83E-04
25	1.24	27.92	4.25E-04	2.92E-04	1.91E-04
26	1.44	29.36	4.45E-04	3.05E-04	1.99E-04
27	1.36	30.72	4.70E-04	3.20E-04	2.09E-04
28	1.39	32.11	4.96E-04	3.37E-04	2.20E-04
29	1.40	33.50	5.24E-04	3.55E-04	2.32E-04
30 ^[2]	1.36	34.86	5.51E-04	3.72E-04	2.43E-04
Future ^[3]	--	36.00	5.78E-04	3.90E-04	2.55E-04
Future ^[3]	--	48.00	8.56E-04	5.81E-04	3.75E-04
Future ^[3]	--	60.00	1.14E-03	7.72E-04	4.96E-04
Future ^[3]	--	72.00	1.41E-03	9.63E-04	6.16E-04
Note(s): 1. Values listed were determined at the pressure vessel outer surface. 2. Cycle 30 is the current operating cycle. Values listed for this cycle are projections based on design end of Cycle 30 burnup data. 3. Values beyond Cycle 30 are based on the average core power distributions and reactor operating conditions of Turkey Point Unit 3 Cycle 29, but include a 1.2 bias on the peripheral and re-entrant corner assembly relative powers.					

Table 2-9: Fast (E > 1.0 MeV) Neutron Fluence Rate at the Outlet Nozzle Welds – Unit 4

Cycle	Cycle Length (EFPY)	Cumulative Operating Time (EFPY)	Fluence Rate (n/cm ² -s) ^[1]		
			10°	20°	40°
1	1.21	1.21	9.68E+07	5.45E+07	3.08E+07
2	0.76	1.97	1.12E+08	6.33E+07	3.52E+07
3	0.68	2.66	1.04E+08	6.24E+07	3.57E+07
4	0.84	3.49	9.85E+07	5.58E+07	3.48E+07
5	0.35	3.85	6.87E+07	4.77E+07	3.02E+07
6	1.12	4.96	9.80E+07	5.30E+07	2.81E+07
7	0.71	5.68	9.96E+07	5.55E+07	2.88E+07
8	0.71	6.39	9.55E+07	5.00E+07	3.02E+07
9	0.66	7.05	6.36E+07	4.56E+07	2.75E+07
10	1.28	8.33	5.90E+07	4.32E+07	2.65E+07
11	1.28	9.60	6.11E+07	4.77E+07 ^[2]	2.93E+07 ^[2]
12	1.12	10.72	6.08E+07	4.81E+07 ^[2]	3.37E+07 ^[2]
13	1.19	11.91	5.98E+07	4.34E+07	2.73E+07
14	1.24	13.15	5.63E+07	3.96E+07	2.37E+07
15	1.25	14.40	6.18E+07	4.28E+07	2.52E+07
16	1.37	15.76	5.55E+07	3.79E+07	2.50E+07
17	1.40	17.16	5.66E+07	3.88E+07	2.46E+07
18	1.44	18.60	5.51E+07	3.59E+07	2.45E+07
19	1.38	19.98	5.66E+07	3.86E+07	2.29E+07
20	1.46	21.44	5.62E+07	3.87E+07	2.43E+07
21	1.22	22.66	6.87E+07	4.74E+07	2.94E+07
22	1.36	24.02	5.70E+07	3.94E+07	2.46E+07
23	1.26	25.28	5.67E+07	4.03E+07	2.57E+07
24	1.41	26.68	5.68E+07	3.81E+07	2.31E+07
25	1.24	27.92	6.51E+07	3.95E+07	2.38E+07
26	1.44	29.36	6.38E+07	3.74E+07	2.25E+07
27	1.36	30.72	8.09E+07	4.70E+07	2.82E+07
28	1.39	32.11	8.99E+07 ^[2]	5.08E+07	3.10E+07
29	1.40	33.50	9.04E+07	5.32E+07	3.28E+07
30 ^[3]	1.36	34.86	9.14E+07 ^[2]	5.26E+07	3.16E+07
Future ^[4]	--	--	1.05E+08	6.79E+07	3.91E+07
Note(s): 1. Unless otherwise noted, values listed were determined at the pressure vessel outer surface. 2. Value was determined at the pressure vessel clad/base metal interface. 3. Cycle 30 is the current operating cycle. Values listed for this cycle are projections based on design end of Cycle 30 burnup data. 4. Values beyond Cycle 30 are based on the average core power distributions and reactor operating conditions of Turkey Point Unit 3 Cycle 29, but include a 1.2 bias on the peripheral and re-entrant corner assembly relative powers.					

Table 2-10: Fast (E > 1.0 MeV) Neutron Fluence at the Outlet Nozzle Welds – Unit 4

Cycle	Cycle Length (EFPY)	Cumulative Operating Time (EFPY)	Fluence (n/cm ²) ^[1]		
			10°	20°	40°
1	1.21	1.21	3.71E+15	2.09E+15	1.18E+15
2	0.76	1.97	6.40E+15	3.61E+15	2.03E+15
3	0.68	2.66	8.64E+15	4.95E+15	2.80E+15
4	0.84	3.49	1.12E+16	6.43E+15	3.71E+15
5	0.35	3.85	1.20E+16	6.96E+15	4.05E+15
6	1.12	4.96	1.55E+16	8.82E+15	5.04E+15
7	0.71	5.68	1.77E+16	1.01E+16	5.69E+15
8	0.71	6.39	1.99E+16	1.12E+16	6.37E+15
9	0.66	7.05	2.12E+16	1.22E+16	6.94E+15
10	1.28	8.33	2.36E+16	1.39E+16	8.01E+15
11	1.28	9.60	2.60E+16	1.57E+16	9.14E+15
12	1.12	10.72	2.82E+16	1.73E+16	1.02E+16
13	1.19	11.91	3.04E+16	1.89E+16	1.12E+16
14	1.24	13.15	3.26E+16	2.04E+16	1.21E+16
15	1.25	14.40	3.50E+16	2.21E+16	1.31E+16
16	1.37	15.76	3.74E+16	2.38E+16	1.42E+16
17	1.40	17.16	3.99E+16	2.55E+16	1.53E+16
18	1.44	18.60	4.24E+16	2.71E+16	1.64E+16
19	1.38	19.98	4.49E+16	2.88E+16	1.74E+16
20	1.46	21.44	4.75E+16	3.06E+16	1.85E+16
21	1.22	22.66	5.01E+16	3.24E+16	1.96E+16
22	1.36	24.02	5.26E+16	3.41E+16	2.07E+16
23	1.26	25.28	5.48E+16	3.57E+16	2.17E+16
24	1.41	26.68	5.74E+16	3.74E+16	2.27E+16
25	1.24	27.92	5.99E+16	3.89E+16	2.37E+16
26	1.44	29.36	6.28E+16	4.06E+16	2.47E+16
27	1.36	30.72	6.63E+16	4.26E+16	2.59E+16
28	1.39	32.11	7.01E+16	4.49E+16	2.73E+16
29	1.40	33.50	7.41E+16	4.72E+16	2.87E+16
30 ^[2]	1.36	34.86	7.79E+16	4.95E+16	3.01E+16
Future ^[3]	--	36.00	8.17E+16	5.19E+16	3.15E+16
Future ^[3]	--	48.00	1.22E+17	7.76E+16	4.63E+16
Future ^[3]	--	60.00	1.61E+17	1.03E+17	6.11E+16
Future ^[3]	--	72.00	2.01E+17	1.29E+17	7.59E+16
Note(s): 1. Values listed were determined at the pressure vessel outer surface. 2. Cycle 30 is the current operating cycle. Values listed for this cycle are projections based on design end of Cycle 30 burnup data. 3. Values beyond Cycle 30 are based on the average core power distributions and reactor operating conditions of Turkey Point Unit 3 Cycle 29, but include a 1.2 bias on the peripheral and re-entrant corner assembly relative powers.					

Table 2-11: Iron Atom Displacement Rate at the Outlet Nozzle Welds – Unit 4

Cycle	Cycle Length (EFPY)	Cumulative Operating Time (EFPY)	Displacement Rate (dpa/s) ^[1]		
			10°	20°	40°
1	1.21	1.21	6.21E-13	3.84E-13	2.38E-13
2	0.76	1.97	7.05E-13	4.37E-13	2.68E-13
3	0.68	2.66	6.65E-13	4.32E-13	2.71E-13
4	0.84	3.49	6.19E-13	3.86E-13	2.55E-13
5	0.35	3.85	4.34E-13	3.16E-13	2.15E-13
6	1.12	4.96	6.20E-13	3.71E-13	2.19E-13
7	0.71	5.68	6.24E-13	3.82E-13	2.23E-13
8	0.71	6.39	5.96E-13	3.50E-13	2.25E-13
9	0.66	7.05	4.00E-13	2.98E-13	1.95E-13
10	1.28	8.33	3.77E-13	2.82E-13	1.87E-13
11	1.28	9.60	3.91E-13	2.96E-13	1.96E-13
12	1.12	10.72	3.87E-13	2.83E-13	1.98E-13
13	1.19	11.91	3.84E-13	2.85E-13	1.92E-13
14	1.24	13.15	3.61E-13	2.62E-13	1.71E-13
15	1.25	14.40	3.98E-13	2.86E-13	1.84E-13
16	1.37	15.76	3.60E-13	2.56E-13	1.78E-13
17	1.40	17.16	3.66E-13	2.61E-13	1.77E-13
18	1.44	18.60	3.54E-13	2.44E-13	1.73E-13
19	1.38	19.98	3.64E-13	2.58E-13	1.66E-13
20	1.46	21.44	3.63E-13	2.60E-13	1.74E-13
21	1.22	22.66	4.38E-13	3.14E-13	2.09E-13
22	1.36	24.02	3.68E-13	2.64E-13	1.77E-13
23	1.26	25.28	3.67E-13	2.69E-13	1.83E-13
24	1.41	26.68	3.66E-13	2.57E-13	1.68E-13
25	1.24	27.92	4.12E-13	2.70E-13	1.75E-13
26	1.44	29.36	4.08E-13	2.60E-13	1.69E-13
27	1.36	30.72	5.12E-13	3.24E-13	2.09E-13
28	1.39	32.11	5.44E-13	3.45E-13	2.25E-13
29	1.40	33.50	5.66E-13	3.62E-13	2.39E-13
30 ^[2]	1.36	34.86	5.63E-13	3.58E-13	2.31E-13
Future ^[3]	--	--	6.60E-13	4.53E-13	2.86E-13
Note(s): 1. Values listed were determined at the pressure vessel outer surface. 2. Cycle 30 is the current operating cycle. Values listed for this cycle are projections based on design end of Cycle 30 burnup data. 3. Values beyond Cycle 30 are based on the average core power distributions and reactor operating conditions of Turkey Point Unit 3 Cycle 29, but include a 1.2 bias on the peripheral and re-entrant corner assembly relative powers.					

Table 2-12: Iron Atom Displacements at the Outlet Nozzle Welds – Unit 4

Cycle	Cycle Length (EFPY)	Cumulative Operating Time (EFPY)	Displacements (dpa) ^[1]		
			10°	20°	40°
1	1.21	1.21	2.38E-05	1.47E-05	9.10E-06
2	0.76	1.97	4.07E-05	2.52E-05	1.55E-05
3	0.68	2.66	5.50E-05	3.45E-05	2.14E-05
4	0.84	3.49	7.14E-05	4.47E-05	2.81E-05
5	0.35	3.85	7.62E-05	4.82E-05	3.05E-05
6	1.12	4.96	9.80E-05	6.13E-05	3.82E-05
7	0.71	5.68	1.12E-04	6.99E-05	4.32E-05
8	0.71	6.39	1.26E-04	7.78E-05	4.83E-05
9	0.66	7.05	1.34E-04	8.40E-05	5.23E-05
10	1.28	8.33	1.49E-04	9.53E-05	5.99E-05
11	1.28	9.60	1.65E-04	1.07E-04	6.78E-05
12	1.12	10.72	1.78E-04	1.17E-04	7.48E-05
13	1.19	11.91	1.93E-04	1.28E-04	8.20E-05
14	1.24	13.15	2.07E-04	1.38E-04	8.87E-05
15	1.25	14.40	2.23E-04	1.50E-04	9.59E-05
16	1.37	15.76	2.38E-04	1.61E-04	1.04E-04
17	1.40	17.16	2.54E-04	1.72E-04	1.11E-04
18	1.44	18.60	2.70E-04	1.83E-04	1.19E-04
19	1.38	19.98	2.86E-04	1.94E-04	1.26E-04
20	1.46	21.44	3.03E-04	2.06E-04	1.35E-04
21	1.22	22.66	3.20E-04	2.18E-04	1.43E-04
22	1.36	24.02	3.36E-04	2.30E-04	1.50E-04
23	1.26	25.28	3.50E-04	2.41E-04	1.57E-04
24	1.41	26.68	3.66E-04	2.52E-04	1.65E-04
25	1.24	27.92	3.83E-04	2.62E-04	1.72E-04
26	1.44	29.36	4.01E-04	2.74E-04	1.79E-04
27	1.36	30.72	4.23E-04	2.88E-04	1.88E-04
28	1.39	32.11	4.47E-04	3.03E-04	1.98E-04
29	1.40	33.50	4.72E-04	3.19E-04	2.09E-04
30 ^[2]	1.36	34.86	4.96E-04	3.35E-04	2.19E-04
Future ^[3]	--	36.00	5.20E-04	3.51E-04	2.29E-04
Future ^[3]	--	48.00	7.70E-04	5.22E-04	3.37E-04
Future ^[3]	--	60.00	1.02E-03	6.94E-04	4.45E-04
Future ^[3]	--	72.00	1.27E-03	8.65E-04	5.54E-04
Note(s): 1. Values listed were determined at the pressure vessel outer surface. 2. Cycle 30 is the current operating cycle. Values listed for this cycle are projections based on design end of Cycle 30 burnup data. 3. Values beyond Cycle 30 are based on the average core power distributions and reactor operating conditions of Turkey Point Unit 3 Cycle 29, but include a 1.2 bias on the peripheral and re-entrant corner assembly relative powers.					

Table 2-13: Fast ($E > 1.0$ MeV) Neutron Fluence Rate at the Upper Shell to Intermediate Shell Weld – Unit 4

Cycle	Cycle Length (EFPY)	Cumulative Operating Time (EFPY)	Fluence Rate (n/cm^2-s) ^[1]			
			0°	15°	30°	45°
1	1.21	1.21	5.61E+09	2.57E+09	1.42E+09	9.15E+08
2	0.76	1.97	8.08E+09	3.75E+09	2.05E+09	1.30E+09
3	0.68	2.66	5.75E+09	2.99E+09	1.71E+09	1.11E+09
4	0.84	3.49	6.09E+09	3.14E+09	1.65E+09	1.29E+09
5	0.35	3.85	4.30E+09	2.37E+09	1.74E+09	1.10E+09
6	1.12	4.96	5.99E+09	2.70E+09	1.31E+09	8.55E+08
7	0.71	5.68	6.78E+09	3.13E+09	1.55E+09	9.70E+08
8	0.71	6.39	6.38E+09	2.88E+09	1.45E+09	1.10E+09
9	0.66	7.05	3.72E+09	2.28E+09	1.51E+09	9.91E+08
10	1.28	8.33	3.04E+09	2.02E+09	1.48E+09	9.88E+08
11	1.28	9.60	3.16E+09	2.25E+09	1.76E+09	1.14E+09
12	1.12	10.72	3.34E+09	2.23E+09	1.79E+09	1.28E+09
13	1.19	11.91	3.05E+09	1.92E+09	1.39E+09	9.44E+08
14	1.24	13.15	2.79E+09	1.66E+09	1.08E+09	7.13E+08
15	1.25	14.40	3.12E+09	1.75E+09	1.14E+09	7.20E+08
16	1.37	15.76	2.21E+09	1.32E+09	9.35E+08	6.89E+08
17	1.40	17.16	2.36E+09	1.39E+09	9.93E+08	6.81E+08
18	1.44	18.60	2.39E+09	1.37E+09	9.75E+08	7.51E+08
19	1.38	19.98	2.36E+09	1.43E+09	9.63E+08	6.31E+08
20	1.46	21.44	2.24E+09	1.39E+09	1.01E+09	6.88E+08
21	1.22	22.66	3.15E+09	1.98E+09	1.43E+09	9.66E+08
22	1.36	24.02	2.20E+09	1.38E+09	9.99E+08	6.84E+08
23	1.26	25.28	2.19E+09	1.43E+09	1.06E+09	7.35E+08
24	1.41	26.68	2.30E+09	1.38E+09	9.86E+08	6.47E+08
25	1.24	27.92	3.17E+09	1.60E+09	9.31E+08	6.45E+08
26	1.44	29.36	2.68E+09	1.26E+09	7.22E+08	5.04E+08
27	1.36	30.72	4.27E+09	2.00E+09	1.10E+09	7.98E+08
28	1.39	32.11	5.57E+09	2.71E+09	1.46E+09	1.12E+09
29	1.40	33.50	5.72E+09	2.73E+09	1.58E+09	1.14E+09
30 ^[2]	1.36	34.86	5.87E+09	2.75E+09	1.54E+09	1.10E+09
Future ^[3]	--	--	6.32E+09	3.42E+09	2.00E+09	1.34E+09
Note(s): 1. Values listed were determined at the pressure vessel clad/base metal interface. 2. Cycle 30 is the current operating cycle. Values listed for this cycle are projections based on design end of Cycle 30 burnup data. 3. Values beyond Cycle 30 are based on the average core power distributions and reactor operating conditions of Turkey Point Unit 3 Cycle 29, but include a 1.2 bias on the peripheral and re-entrant corner assembly relative powers.						

Table 2-14: Fast ($E > 1.0$ MeV) Neutron Fluence at the Upper Shell to Intermediate Shell Weld – Unit 4

Cycle	Cycle Length (EFPY)	Cumulative Operating Time (EFPY)	Fluence (n/cm^2) ^[1]			
			0°	15°	30°	45°
1	1.21	1.21	2.15E+17	9.82E+16	5.43E+16	3.50E+16
2	0.76	1.97	4.09E+17	1.88E+17	1.04E+17	6.63E+16
3	0.68	2.66	5.33E+17	2.53E+17	1.41E+17	9.03E+16
4	0.84	3.49	6.93E+17	3.35E+17	1.84E+17	1.24E+17
5	0.35	3.85	7.41E+17	3.62E+17	2.03E+17	1.37E+17
6	1.12	4.96	9.53E+17	4.57E+17	2.50E+17	1.67E+17
7	0.71	5.68	1.11E+18	5.28E+17	2.85E+17	1.89E+17
8	0.71	6.39	1.25E+18	5.92E+17	3.17E+17	2.13E+17
9	0.66	7.05	1.33E+18	6.39E+17	3.48E+17	2.34E+17
10	1.28	8.33	1.45E+18	7.21E+17	4.08E+17	2.74E+17
11	1.28	9.60	1.58E+18	8.12E+17	4.79E+17	3.20E+17
12	1.12	10.72	1.69E+18	8.90E+17	5.42E+17	3.65E+17
13	1.19	11.91	1.81E+18	9.63E+17	5.94E+17	4.00E+17
14	1.24	13.15	1.92E+18	1.03E+18	6.36E+17	4.28E+17
15	1.25	14.40	2.04E+18	1.10E+18	6.81E+17	4.57E+17
16	1.37	15.76	2.14E+18	1.15E+18	7.22E+17	4.86E+17
17	1.40	17.16	2.24E+18	1.21E+18	7.65E+17	5.16E+17
18	1.44	18.60	2.35E+18	1.28E+18	8.10E+17	5.50E+17
19	1.38	19.98	2.45E+18	1.34E+18	8.52E+17	5.78E+17
20	1.46	21.44	2.55E+18	1.40E+18	8.98E+17	6.09E+17
21	1.22	22.66	2.68E+18	1.48E+18	9.53E+17	6.47E+17
22	1.36	24.02	2.77E+18	1.54E+18	9.96E+17	6.76E+17
23	1.26	25.28	2.86E+18	1.60E+18	1.04E+18	7.05E+17
24	1.41	26.68	2.96E+18	1.66E+18	1.08E+18	7.34E+17
25	1.24	27.92	3.08E+18	1.72E+18	1.12E+18	7.59E+17
26	1.44	29.36	3.21E+18	1.78E+18	1.15E+18	7.82E+17
27	1.36	30.72	3.39E+18	1.86E+18	1.20E+18	8.16E+17
28	1.39	32.11	3.63E+18	1.98E+18	1.26E+18	8.65E+17
29	1.40	33.50	3.88E+18	2.10E+18	1.33E+18	9.15E+17
30 ^[2]	1.36	34.86	4.14E+18	2.22E+18	1.40E+18	9.63E+17
Future ^[3]	--	36.00	4.36E+18	2.34E+18	1.47E+18	1.01E+18
Future ^[3]	--	48.00	6.76E+18	3.64E+18	2.23E+18	1.52E+18
Future ^[3]	--	60.00	9.15E+18	4.93E+18	2.98E+18	2.02E+18
Future ^[3]	--	72.00	1.15E+19	6.23E+18	3.74E+18	2.53E+18
Note(s): 1. Values listed were determined at the pressure vessel clad/base metal interface. 2. Cycle 30 is the current operating cycle. Values listed for this cycle are projections based on design end of Cycle 30 burnup data. 3. Values beyond Cycle 30 are based on the average core power distributions and reactor operating conditions of Turkey Point Unit 3 Cycle 29, but include a 1.2 bias on the peripheral and re-entrant corner assembly relative powers.						

Table 2-15: Iron Atom Displacement Rate at the Upper Shell to Intermediate Shell Weld – Unit 4

Cycle	Cycle Length (EFPY)	Cumulative Operating Time (EFPY)	Displacement Rate (dpa/s) ^[1]			
			0°	15°	30°	45°
1	1.21	1.21	9.56E-12	4.42E-12	2.41E-12	1.56E-12
2	0.76	1.97	1.37E-11	6.42E-12	3.46E-12	2.20E-12
3	0.68	2.66	9.83E-12	5.14E-12	2.91E-12	1.90E-12
4	0.84	3.49	1.03E-11	5.37E-12	2.79E-12	2.18E-12
5	0.35	3.85	7.28E-12	4.04E-12	2.93E-12	1.86E-12
6	1.12	4.96	1.02E-11	4.65E-12	2.23E-12	1.46E-12
7	0.71	5.68	1.15E-11	5.35E-12	2.63E-12	1.65E-12
8	0.71	6.39	1.08E-11	4.93E-12	2.45E-12	1.85E-12
9	0.66	7.05	6.30E-12	3.87E-12	2.55E-12	1.67E-12
10	1.28	8.33	5.20E-12	3.44E-12	2.49E-12	1.66E-12
11	1.28	9.60	5.41E-12	3.83E-12	2.95E-12	1.91E-12
12	1.12	10.72	5.71E-12	3.78E-12	2.99E-12	2.15E-12
13	1.19	11.91	5.23E-12	3.29E-12	2.36E-12	1.60E-12
14	1.24	13.15	4.80E-12	2.86E-12	1.83E-12	1.21E-12
15	1.25	14.40	5.35E-12	3.02E-12	1.94E-12	1.23E-12
16	1.37	15.76	3.84E-12	2.29E-12	1.60E-12	1.18E-12
17	1.40	17.16	4.10E-12	2.40E-12	1.69E-12	1.16E-12
18	1.44	18.60	4.15E-12	2.37E-12	1.66E-12	1.28E-12
19	1.38	19.98	4.09E-12	2.48E-12	1.64E-12	1.08E-12
20	1.46	21.44	3.89E-12	2.40E-12	1.71E-12	1.17E-12
21	1.22	22.66	5.45E-12	3.40E-12	2.43E-12	1.64E-12
22	1.36	24.02	3.83E-12	2.39E-12	1.70E-12	1.17E-12
23	1.26	25.28	3.81E-12	2.47E-12	1.80E-12	1.25E-12
24	1.41	26.68	3.99E-12	2.39E-12	1.68E-12	1.10E-12
25	1.24	27.92	5.43E-12	2.76E-12	1.59E-12	1.10E-12
26	1.44	29.36	4.62E-12	2.20E-12	1.24E-12	8.69E-13
27	1.36	30.72	7.29E-12	3.45E-12	1.88E-12	1.36E-12
28	1.39	32.11	9.45E-12	4.62E-12	2.47E-12	1.88E-12
29	1.40	33.50	9.70E-12	4.68E-12	2.67E-12	1.93E-12
30 ^[2]	1.36	34.86	9.94E-12	4.71E-12	2.61E-12	1.86E-12
Future ^[3]	--	--	1.07E-11	5.84E-12	3.38E-12	2.27E-12
Note(s): 1. Values listed were determined at the pressure vessel clad/base metal interface. 2. Cycle 30 is the current operating cycle. Values listed for this cycle are projections based on design end of Cycle 30 burnup data. 3. Values beyond Cycle 30 are based on the average core power distributions and reactor operating conditions of Turkey Point Unit 3 Cycle 29, but include a 1.2 bias on the peripheral and re-entrant corner assembly relative powers.						

Table 2-16: Iron Atom Displacements at the Upper Shell to Intermediate Shell Weld – Unit 4

Cycle	Cycle Length (EFPY)	Cumulative Operating Time (EFPY)	Displacements (dpa) ^[1]			
			0°	15°	30°	45°
1	1.21	1.21	3.66E-04	1.69E-04	9.24E-05	5.96E-05
2	0.76	1.97	6.95E-04	3.23E-04	1.76E-04	1.13E-04
3	0.68	2.66	9.07E-04	4.34E-04	2.38E-04	1.53E-04
4	0.84	3.49	1.18E-03	5.76E-04	3.12E-04	2.11E-04
5	0.35	3.85	1.26E-03	6.21E-04	3.45E-04	2.32E-04
6	1.12	4.96	1.62E-03	7.85E-04	4.23E-04	2.83E-04
7	0.71	5.68	1.88E-03	9.05E-04	4.82E-04	3.20E-04
8	0.71	6.39	2.12E-03	1.02E-03	5.38E-04	3.62E-04
9	0.66	7.05	2.25E-03	1.10E-03	5.90E-04	3.97E-04
10	1.28	8.33	2.46E-03	1.24E-03	6.91E-04	4.64E-04
11	1.28	9.60	2.68E-03	1.39E-03	8.09E-04	5.41E-04
12	1.12	10.72	2.88E-03	1.52E-03	9.14E-04	6.16E-04
13	1.19	11.91	3.08E-03	1.65E-03	1.00E-03	6.76E-04
14	1.24	13.15	3.27E-03	1.76E-03	1.07E-03	7.24E-04
15	1.25	14.40	3.48E-03	1.88E-03	1.15E-03	7.72E-04
16	1.37	15.76	3.64E-03	1.98E-03	1.22E-03	8.23E-04
17	1.40	17.16	3.82E-03	2.08E-03	1.29E-03	8.74E-04
18	1.44	18.60	4.01E-03	2.19E-03	1.37E-03	9.32E-04
19	1.38	19.98	4.19E-03	2.30E-03	1.44E-03	9.79E-04
20	1.46	21.44	4.37E-03	2.41E-03	1.52E-03	1.03E-03
21	1.22	22.66	4.58E-03	2.54E-03	1.61E-03	1.10E-03
22	1.36	24.02	4.74E-03	2.64E-03	1.69E-03	1.15E-03
23	1.26	25.28	4.90E-03	2.74E-03	1.76E-03	1.20E-03
24	1.41	26.68	5.07E-03	2.85E-03	1.83E-03	1.25E-03
25	1.24	27.92	5.28E-03	2.95E-03	1.89E-03	1.29E-03
26	1.44	29.36	5.49E-03	3.05E-03	1.95E-03	1.33E-03
27	1.36	30.72	5.81E-03	3.20E-03	2.03E-03	1.39E-03
28	1.39	32.11	6.22E-03	3.40E-03	2.14E-03	1.47E-03
29	1.40	33.50	6.65E-03	3.61E-03	2.26E-03	1.55E-03
30 ^[2]	1.36	34.86	7.08E-03	3.81E-03	2.37E-03	1.63E-03
Future ^[3]	--	36.00	7.46E-03	4.02E-03	2.49E-03	1.71E-03
Future ^[3]	--	48.00	1.15E-02	6.23E-03	3.77E-03	2.57E-03
Future ^[3]	--	60.00	1.56E-02	8.44E-03	5.05E-03	3.43E-03
Future ^[3]	--	72.00	1.97E-02	1.07E-02	6.33E-03	4.29E-03

Note(s):

1. Values listed were determined at the pressure vessel clad/base metal interface.
2. Cycle 30 is the current operating cycle. Values listed for this cycle are projections based on design end of Cycle 30 burnup data.
3. Values beyond Cycle 30 are based on the average core power distributions and reactor operating conditions of Turkey Point Unit 3 Cycle 29, but include a 1.2 bias on the peripheral and re-entrant corner assembly relative powers.

Table 2-17: Fast (E > 1.0 MeV) Neutron Fluence Rate at the Intermediate Shell to Lower Shell Weld – Unit 4

Cycle	Cycle Length (EFPY)	Cumulative Operating Time (EFPY)	Fluence Rate (n/cm ² -s) ^[1]			
			0°	15°	30°	45°
1	1.21	1.21	6.26E+10	2.86E+10	1.58E+10	1.02E+10
2	0.76	1.97	5.82E+10	2.70E+10	1.48E+10	9.37E+09
3	0.68	2.66	5.72E+10	2.97E+10	1.71E+10	1.11E+10
4	0.84	3.49	5.13E+10	2.65E+10	1.39E+10	1.09E+10
5	0.35	3.85	3.47E+10	1.91E+10	1.41E+10	8.88E+09
6	1.12	4.96	5.81E+10	2.62E+10	1.27E+10	8.28E+09
7	0.71	5.68	5.31E+10	2.45E+10	1.22E+10	7.60E+09
8	0.71	6.39	5.16E+10	2.32E+10	1.17E+10	8.86E+09
9	0.66	7.05	3.10E+10	1.90E+10	1.26E+10	8.26E+09
10	1.28	8.33	2.08E+10	1.52E+10	1.20E+10	8.01E+09
11	1.28	9.60	2.03E+10	1.48E+10	1.18E+10	7.62E+09
12	1.12	10.72	2.07E+10	1.35E+10	1.06E+10	7.63E+09
13	1.19	11.91	2.08E+10	1.45E+10	1.14E+10	7.70E+09
14	1.24	13.15	2.01E+10	1.43E+10	1.08E+10	7.22E+09
15	1.25	14.40	2.27E+10	1.55E+10	1.20E+10	7.63E+09
16	1.37	15.76	2.13E+10	1.43E+10	1.13E+10	8.36E+09
17	1.40	17.16	2.11E+10	1.40E+10	1.13E+10	7.74E+09
18	1.44	18.60	2.11E+10	1.34E+10	1.05E+10	8.08E+09
19	1.38	19.98	2.17E+10	1.47E+10	1.08E+10	7.12E+09
20	1.46	21.44	2.20E+10	1.48E+10	1.15E+10	7.87E+09
21	1.22	22.66	1.85E+10	1.26E+10	9.73E+09	6.58E+09
22	1.36	24.02	2.20E+10	1.49E+10	1.15E+10	7.91E+09
23	1.26	25.28	2.05E+10	1.47E+10	1.18E+10	8.17E+09
24	1.41	26.68	2.17E+10	1.41E+10	1.07E+10	7.05E+09
25	1.24	27.92	3.71E+10	1.87E+10	1.09E+10	7.54E+09
26	1.44	29.36	4.02E+10	1.90E+10	1.09E+10	7.58E+09
27	1.36	30.72	4.79E+10	2.25E+10	1.24E+10	8.96E+09
28	1.39	32.11	4.52E+10	2.20E+10	1.18E+10	9.05E+09
29	1.40	33.50	4.81E+10	2.30E+10	1.33E+10	9.59E+09
30 ^[2]	1.36	34.86	4.80E+10	2.25E+10	1.26E+10	9.01E+09
Future ^[3]	--	--	5.27E+10	2.85E+10	1.67E+10	1.12E+10
Note(s): 1. Values listed were determined at the pressure vessel clad/base metal interface. 2. Cycle 30 is the current operating cycle. Values listed for this cycle are projections based on design end of Cycle 30 burnup data. 3. Values beyond Cycle 30 are based on the average core power distributions and reactor operating conditions of Turkey Point Unit 3 Cycle 29, but include a 1.2 bias on the peripheral and re-entrant corner assembly relative powers.						

Table 2-18: Fast ($E > 1.0$ MeV) Neutron Fluence at the Intermediate Shell to Lower Shell Weld – Unit 4

Cycle	Cycle Length (EFPY)	Cumulative Operating Time (EFPY)	Fluence (n/cm^2) ^[1]			
			0°	15°	30°	45°
1	1.21	1.21	2.40E+18	1.10E+18	6.06E+17	3.91E+17
2	0.76	1.97	3.79E+18	1.74E+18	9.61E+17	6.16E+17
3	0.68	2.66	5.03E+18	2.39E+18	1.33E+18	8.55E+17
4	0.84	3.49	6.38E+18	3.08E+18	1.69E+18	1.14E+18
5	0.35	3.85	6.77E+18	3.30E+18	1.85E+18	1.24E+18
6	1.12	4.96	8.81E+18	4.22E+18	2.30E+18	1.53E+18
7	0.71	5.68	1.00E+19	4.77E+18	2.57E+18	1.70E+18
8	0.71	6.39	1.12E+19	5.29E+18	2.84E+18	1.90E+18
9	0.66	7.05	1.18E+19	5.69E+18	3.10E+18	2.08E+18
10	1.28	8.33	1.27E+19	6.30E+18	3.58E+18	2.40E+18
11	1.28	9.60	1.35E+19	6.90E+18	4.05E+18	2.71E+18
12	1.12	10.72	1.42E+19	7.37E+18	4.43E+18	2.97E+18
13	1.19	11.91	1.50E+19	7.92E+18	4.86E+18	3.26E+18
14	1.24	13.15	1.58E+19	8.48E+18	5.28E+18	3.55E+18
15	1.25	14.40	1.67E+19	9.09E+18	5.75E+18	3.85E+18
16	1.37	15.76	1.76E+19	9.70E+18	6.24E+18	4.21E+18
17	1.40	17.16	1.85E+19	1.03E+19	6.74E+18	4.55E+18
18	1.44	18.60	1.95E+19	1.09E+19	7.21E+18	4.92E+18
19	1.38	19.98	2.04E+19	1.16E+19	7.68E+18	5.23E+18
20	1.46	21.44	2.14E+19	1.23E+19	8.21E+18	5.59E+18
21	1.22	22.66	2.21E+19	1.27E+19	8.59E+18	5.84E+18
22	1.36	24.02	2.31E+19	1.34E+19	9.08E+18	6.18E+18
23	1.26	25.28	2.39E+19	1.40E+19	9.55E+18	6.51E+18
24	1.41	26.68	2.49E+19	1.46E+19	1.00E+19	6.82E+18
25	1.24	27.92	2.63E+19	1.53E+19	1.05E+19	7.11E+18
26	1.44	29.36	2.81E+19	1.62E+19	1.09E+19	7.46E+18
27	1.36	30.72	3.02E+19	1.71E+19	1.15E+19	7.84E+18
28	1.39	32.11	3.22E+19	1.81E+19	1.20E+19	8.24E+18
29	1.40	33.50	3.43E+19	1.91E+19	1.26E+19	8.66E+18
30 ^[2]	1.36	34.86	3.64E+19	2.01E+19	1.31E+19	9.05E+18
Future ^[3]	--	36.00	3.82E+19	2.11E+19	1.37E+19	9.45E+18
Future ^[3]	--	48.00	5.82E+19	3.19E+19	2.00E+19	1.37E+19
Future ^[3]	--	60.00	7.82E+19	4.27E+19	2.63E+19	1.79E+19
Future ^[3]	--	72.00	9.81E+19	5.35E+19	3.27E+19	2.21E+19
Note(s): 1. Values listed were determined at the pressure vessel clad/base metal interface. 2. Cycle 30 is the current operating cycle. Values listed for this cycle are projections based on design end of Cycle 30 burnup data. 3. Values beyond Cycle 30 are based on the average core power distributions and reactor operating conditions of Turkey Point Unit 3 Cycle 29, but include a 1.2 bias on the peripheral and re-entrant corner assembly relative powers.						

Table 2-19: Iron Atom Displacement Rate at the Intermediate Shell to Lower Shell Weld – Unit 4

Cycle	Cycle Length (EFPY)	Cumulative Operating Time (EFPY)	Displacement Rate (dpa/s) ^[1]			
			0°	15°	30°	45°
1	1.21	1.21	1.02E-10	4.73E-11	2.58E-11	1.67E-11
2	0.76	1.97	9.52E-11	4.46E-11	2.41E-11	1.53E-11
3	0.68	2.66	9.37E-11	4.90E-11	2.78E-11	1.81E-11
4	0.84	3.49	8.41E-11	4.37E-11	2.27E-11	1.78E-11
5	0.35	3.85	5.67E-11	3.14E-11	2.29E-11	1.45E-11
6	1.12	4.96	9.49E-11	4.33E-11	2.08E-11	1.35E-11
7	0.71	5.68	8.68E-11	4.04E-11	1.98E-11	1.24E-11
8	0.71	6.39	8.43E-11	3.84E-11	1.91E-11	1.44E-11
9	0.66	7.05	5.07E-11	3.11E-11	2.05E-11	1.35E-11
10	1.28	8.33	3.41E-11	2.49E-11	1.94E-11	1.30E-11
11	1.28	9.60	3.34E-11	2.43E-11	1.91E-11	1.24E-11
12	1.12	10.72	3.40E-11	2.22E-11	1.73E-11	1.24E-11
13	1.19	11.91	3.41E-11	2.37E-11	1.84E-11	1.25E-11
14	1.24	13.15	3.31E-11	2.35E-11	1.76E-11	1.18E-11
15	1.25	14.40	3.72E-11	2.54E-11	1.95E-11	1.24E-11
16	1.37	15.76	3.50E-11	2.35E-11	1.84E-11	1.36E-11
17	1.40	17.16	3.46E-11	2.30E-11	1.83E-11	1.26E-11
18	1.44	18.60	3.45E-11	2.19E-11	1.70E-11	1.31E-11
19	1.38	19.98	3.55E-11	2.41E-11	1.76E-11	1.16E-11
20	1.46	21.44	3.62E-11	2.43E-11	1.87E-11	1.28E-11
21	1.22	22.66	3.04E-11	2.06E-11	1.58E-11	1.07E-11
22	1.36	24.02	3.61E-11	2.45E-11	1.87E-11	1.29E-11
23	1.26	25.28	3.37E-11	2.41E-11	1.91E-11	1.33E-11
24	1.41	26.68	3.56E-11	2.31E-11	1.74E-11	1.15E-11
25	1.24	27.92	6.05E-11	3.07E-11	1.77E-11	1.23E-11
26	1.44	29.36	6.57E-11	3.13E-11	1.77E-11	1.24E-11
27	1.36	30.72	7.83E-11	3.71E-11	2.02E-11	1.46E-11
28	1.39	32.11	7.40E-11	3.62E-11	1.93E-11	1.47E-11
29	1.40	33.50	7.85E-11	3.79E-11	2.16E-11	1.56E-11
30 ^[2]	1.36	34.86	7.85E-11	3.71E-11	2.06E-11	1.47E-11
Future ^[3]	1.21	1.21	1.02E-10	4.73E-11	2.58E-11	1.67E-11
Note(s): 1. Values listed were determined at the pressure vessel clad/base metal interface. 2. Cycle 30 is the current operating cycle. Values listed for this cycle are projections based on design end of Cycle 30 burnup data. 3. Values beyond Cycle 30 are based on the average core power distributions and reactor operating conditions of Turkey Point Unit 3 Cycle 29, but include a 1.2 bias on the peripheral and re-entrant corner assembly relative powers.						

Table 2-20: Iron Atom Displacements at the Intermediate Shell to Lower Shell Weld – Unit 4

Cycle	Cycle Length (EFPY)	Cumulative Operating Time (EFPY)	Displacements (dpa) ^[1]			
			0°	15°	30°	45°
1	1.21	1.21	3.92E-03	1.81E-03	9.89E-04	6.38E-04
2	0.76	1.97	6.21E-03	2.88E-03	1.57E-03	1.01E-03
3	0.68	2.66	8.23E-03	3.94E-03	2.17E-03	1.40E-03
4	0.84	3.49	1.04E-02	5.09E-03	2.76E-03	1.86E-03
5	0.35	3.85	1.11E-02	5.44E-03	3.02E-03	2.03E-03
6	1.12	4.96	1.44E-02	6.97E-03	3.75E-03	2.50E-03
7	0.71	5.68	1.64E-02	7.88E-03	4.20E-03	2.78E-03
8	0.71	6.39	1.83E-02	8.74E-03	4.63E-03	3.11E-03
9	0.66	7.05	1.93E-02	9.39E-03	5.05E-03	3.39E-03
10	1.28	8.33	2.07E-02	1.04E-02	5.83E-03	3.91E-03
11	1.28	9.60	2.21E-02	1.14E-02	6.61E-03	4.41E-03
12	1.12	10.72	2.32E-02	1.22E-02	7.21E-03	4.85E-03
13	1.19	11.91	2.45E-02	1.30E-02	7.91E-03	5.32E-03
14	1.24	13.15	2.58E-02	1.40E-02	8.59E-03	5.78E-03
15	1.25	14.40	2.73E-02	1.50E-02	9.36E-03	6.27E-03
16	1.37	15.76	2.88E-02	1.60E-02	1.02E-02	6.86E-03
17	1.40	17.16	3.03E-02	1.70E-02	1.10E-02	7.41E-03
18	1.44	18.60	3.19E-02	1.80E-02	1.17E-02	8.01E-03
19	1.38	19.98	3.34E-02	1.90E-02	1.25E-02	8.51E-03
20	1.46	21.44	3.51E-02	2.01E-02	1.34E-02	9.10E-03
21	1.22	22.66	3.63E-02	2.09E-02	1.40E-02	9.51E-03
22	1.36	24.02	3.78E-02	2.20E-02	1.48E-02	1.01E-02
23	1.26	25.28	3.92E-02	2.30E-02	1.55E-02	1.06E-02
24	1.41	26.68	4.07E-02	2.40E-02	1.63E-02	1.11E-02
25	1.24	27.92	4.31E-02	2.52E-02	1.70E-02	1.16E-02
26	1.44	29.36	4.61E-02	2.66E-02	1.78E-02	1.21E-02
27	1.36	30.72	4.94E-02	2.82E-02	1.87E-02	1.28E-02
28	1.39	32.11	5.27E-02	2.98E-02	1.95E-02	1.34E-02
29	1.40	33.50	5.61E-02	3.14E-02	2.05E-02	1.41E-02
30 ^[2]	1.36	34.86	5.95E-02	3.30E-02	2.13E-02	1.47E-02
Future ^[3]	--	36.00	6.26E-02	3.47E-02	2.23E-02	1.54E-02
Future ^[3]	--	48.00	9.53E-02	5.25E-02	3.26E-02	2.23E-02
Future ^[3]	--	60.00	1.28E-01	7.02E-02	4.29E-02	2.92E-02
Future ^[3]	--	72.00	1.61E-01	8.80E-02	5.32E-02	3.61E-02

Note(s):

1. Values listed were determined at the pressure vessel clad/base metal interface.
2. Cycle 30 is the current operating cycle. Values listed for this cycle are projections based on design end of Cycle 30 burnup data.
3. Values beyond Cycle 30 are based on the average core power distributions and reactor operating conditions of Turkey Point Unit 3 Cycle 29, but include a 1.2 bias on the peripheral and re-entrant corner assembly relative powers.

Table 2-21: Fast ($E > 1.0$ MeV) Neutron Fluence Rate at the Lower Shell to Lower Head Ring Weld – Unit 4

Cycle	Cycle Length (EFPY)	Cumulative Operating Time (EFPY)	Fluence Rate ($\text{n/cm}^2\text{-s}$) ^[1]			
			0°	15°	30°	45°
1	1.21	1.21	7.57E+07	4.10E+07	2.39E+07	1.72E+07
2	0.76	1.97	7.72E+07	4.22E+07	2.44E+07	1.74E+07
3	0.68	2.66	7.52E+07	4.46E+07	2.70E+07	1.96E+07
4	0.84	3.49	6.55E+07	3.85E+07	2.20E+07	1.79E+07
5	0.35	3.85	4.86E+07	3.06E+07	2.25E+07	1.61E+07
6	1.12	4.96	7.21E+07	3.84E+07	2.04E+07	1.47E+07
7	0.71	5.68	7.22E+07	3.91E+07	2.11E+07	1.49E+07
8	0.71	6.39	6.94E+07	3.69E+07	2.01E+07	1.61E+07
9	0.66	7.05	4.24E+07	2.87E+07	1.98E+07	1.44E+07
10	1.28	8.33	3.72E+07	2.57E+07	1.83E+07	1.35E+07
11	1.28	9.60	3.78E+07	2.66E+07	1.93E+07	1.39E+07
12	1.12	10.72	3.86E+07	2.54E+07	1.84E+07	1.42E+07
13	1.19	11.91	3.81E+07	2.58E+07	1.86E+07	1.38E+07
14	1.24	13.15	3.61E+07	2.43E+07	1.67E+07	1.22E+07
15	1.25	14.40	4.05E+07	2.65E+07	1.83E+07	1.31E+07
16	1.37	15.76	3.66E+07	2.39E+07	1.69E+07	1.34E+07
17	1.40	17.16	3.71E+07	2.40E+07	1.71E+07	1.29E+07
18	1.44	18.60	3.66E+07	2.29E+07	1.60E+07	1.30E+07
19	1.38	19.98	3.71E+07	2.44E+07	1.65E+07	1.20E+07
20	1.46	21.44	3.73E+07	2.46E+07	1.73E+07	1.30E+07
21	1.22	22.66	3.26E+07	2.15E+07	1.51E+07	1.12E+07
22	1.36	24.02	3.70E+07	2.46E+07	1.73E+07	1.30E+07
23	1.26	25.28	3.56E+07	2.44E+07	1.76E+07	1.33E+07
24	1.41	26.68	3.70E+07	2.37E+07	1.63E+07	1.19E+07
25	1.24	27.92	4.63E+07	2.70E+07	1.66E+07	1.25E+07
26	1.44	29.36	4.77E+07	2.64E+07	1.60E+07	1.21E+07
27	1.36	30.72	6.19E+07	3.41E+07	2.01E+07	1.56E+07
28	1.39	32.11	6.07E+07	3.43E+07	1.99E+07	1.60E+07
29	1.40	33.50	6.35E+07	3.55E+07	2.17E+07	1.68E+07
30 ^[2]	1.36	34.86	6.38E+07	3.52E+07	2.10E+07	1.61E+07
Future ^[3]	--	--	7.11E+07	4.37E+07	2.72E+07	2.00E+07
Note(s): 1. Values listed were determined at the pressure vessel outer surface. 2. Cycle 30 is the current operating cycle. Values listed for this cycle are projections based on design end of Cycle 30 burnup data. 3. Values beyond Cycle 30 are based on the average core power distributions and reactor operating conditions of Turkey Point Unit 3 Cycle 29, but include a 1.2 bias on the peripheral and re-entrant corner assembly relative powers.						

Table 2-22: Fast (E > 1.0 MeV) Neutron Fluence at the Lower Shell to Lower Head Ring Weld – Unit 4

Cycle	Cycle Length (EFPY)	Cumulative Operating Time (EFPY)	Fluence (n/cm ²) ^[1]			
			0°	15°	30°	45°
1	1.21	1.21	2.90E+15	1.57E+15	9.15E+14	6.59E+14
2	0.76	1.97	4.75E+15	2.58E+15	1.50E+15	1.08E+15
3	0.68	2.66	6.37E+15	3.54E+15	2.08E+15	1.50E+15
4	0.84	3.49	8.10E+15	4.56E+15	2.66E+15	1.97E+15
5	0.35	3.85	8.64E+15	4.90E+15	2.91E+15	2.15E+15
6	1.12	4.96	1.12E+16	6.25E+15	3.63E+15	2.67E+15
7	0.71	5.68	1.28E+16	7.13E+15	4.11E+15	3.01E+15
8	0.71	6.39	1.44E+16	7.96E+15	4.56E+15	3.37E+15
9	0.66	7.05	1.53E+16	8.56E+15	4.97E+15	3.67E+15
10	1.28	8.33	1.68E+16	9.59E+15	5.71E+15	4.21E+15
11	1.28	9.60	1.83E+16	1.07E+16	6.49E+15	4.77E+15
12	1.12	10.72	1.96E+16	1.16E+16	7.14E+15	5.27E+15
13	1.19	11.91	2.11E+16	1.25E+16	7.84E+15	5.79E+15
14	1.24	13.15	2.25E+16	1.35E+16	8.49E+15	6.27E+15
15	1.25	14.40	2.41E+16	1.45E+16	9.21E+15	6.79E+15
16	1.37	15.76	2.57E+16	1.56E+16	9.94E+15	7.36E+15
17	1.40	17.16	2.73E+16	1.66E+16	1.07E+16	7.93E+15
18	1.44	18.60	2.90E+16	1.77E+16	1.14E+16	8.52E+15
19	1.38	19.98	3.06E+16	1.87E+16	1.21E+16	9.04E+15
20	1.46	21.44	3.23E+16	1.99E+16	1.29E+16	9.64E+15
21	1.22	22.66	3.35E+16	2.07E+16	1.35E+16	1.01E+16
22	1.36	24.02	3.51E+16	2.17E+16	1.43E+16	1.06E+16
23	1.26	25.28	3.65E+16	2.27E+16	1.50E+16	1.12E+16
24	1.41	26.68	3.82E+16	2.38E+16	1.57E+16	1.17E+16
25	1.24	27.92	4.00E+16	2.48E+16	1.63E+16	1.22E+16
26	1.44	29.36	4.22E+16	2.60E+16	1.71E+16	1.27E+16
27	1.36	30.72	4.48E+16	2.75E+16	1.79E+16	1.34E+16
28	1.39	32.11	4.75E+16	2.90E+16	1.88E+16	1.41E+16
29	1.40	33.50	5.03E+16	3.05E+16	1.98E+16	1.48E+16
30 ^[2]	1.36	34.86	5.30E+16	3.20E+16	2.07E+16	1.55E+16
Future ^[3]	--	36.00	5.56E+16	3.36E+16	2.16E+16	1.62E+16
Future ^[3]	--	48.00	8.25E+16	5.02E+16	3.19E+16	2.38E+16
Future ^[3]	--	60.00	1.09E+17	6.67E+16	4.22E+16	3.14E+16
Future ^[3]	--	72.00	1.36E+17	8.33E+16	5.25E+16	3.89E+16
Note(s): 1. Values listed were determined at the pressure vessel outer surface. 2. Cycle 30 is the current operating cycle. Values listed for this cycle are projections based on design end of Cycle 30 burnup data. 3. Values beyond Cycle 30 are based on the average core power distributions and reactor operating conditions of Turkey Point Unit 3 Cycle 29, but include a 1.2 bias on the peripheral and re-entrant corner assembly relative powers.						

Table 2-23: Iron Atom Displacement Rate at the Lower Shell to Lower Head Ring Weld – Unit 4

Cycle	Cycle Length (EFPY)	Cumulative Operating Time (EFPY)	Displacement Rate (dpa/s) ^[1]			
			0°	15°	30°	45°
1	1.21	1.21	5.02E-13	3.03E-13	1.88E-13	1.46E-13
2	0.76	1.97	5.09E-13	3.10E-13	1.91E-13	1.47E-13
3	0.68	2.66	5.02E-13	3.27E-13	2.09E-13	1.63E-13
4	0.84	3.49	4.36E-13	2.80E-13	1.72E-13	1.45E-13
5	0.35	3.85	3.23E-13	2.21E-13	1.65E-13	1.28E-13
6	1.12	4.96	4.74E-13	2.82E-13	1.63E-13	1.27E-13
7	0.71	5.68	4.72E-13	2.85E-13	1.67E-13	1.28E-13
8	0.71	6.39	4.54E-13	2.70E-13	1.60E-13	1.32E-13
9	0.66	7.05	2.83E-13	2.05E-13	1.46E-13	1.14E-13
10	1.28	8.33	2.49E-13	1.83E-13	1.34E-13	1.05E-13
11	1.28	9.60	2.55E-13	1.89E-13	1.41E-13	1.09E-13
12	1.12	10.72	2.57E-13	1.81E-13	1.34E-13	1.09E-13
13	1.19	11.91	2.55E-13	1.84E-13	1.36E-13	1.07E-13
14	1.24	13.15	2.41E-13	1.73E-13	1.23E-13	9.62E-14
15	1.25	14.40	2.70E-13	1.89E-13	1.35E-13	1.04E-13
16	1.37	15.76	2.45E-13	1.72E-13	1.25E-13	1.03E-13
17	1.40	17.16	2.47E-13	1.72E-13	1.26E-13	1.00E-13
18	1.44	18.60	2.43E-13	1.65E-13	1.18E-13	9.96E-14
19	1.38	19.98	2.47E-13	1.74E-13	1.22E-13	9.50E-14
20	1.46	21.44	2.49E-13	1.76E-13	1.27E-13	1.01E-13
21	1.22	22.66	2.17E-13	1.53E-13	1.11E-13	8.76E-14
22	1.36	24.02	2.48E-13	1.76E-13	1.27E-13	1.01E-13
23	1.26	25.28	2.39E-13	1.74E-13	1.29E-13	1.03E-13
24	1.41	26.68	2.46E-13	1.70E-13	1.21E-13	9.42E-14
25	1.24	27.92	3.04E-13	1.95E-13	1.27E-13	1.01E-13
26	1.44	29.36	3.13E-13	1.92E-13	1.23E-13	9.88E-14
27	1.36	30.72	4.04E-13	2.48E-13	1.56E-13	1.26E-13
28	1.39	32.11	3.97E-13	2.48E-13	1.55E-13	1.28E-13
29	1.40	33.50	4.16E-13	2.58E-13	1.66E-13	1.35E-13
30 ^[2]	1.36	34.86	4.16E-13	2.55E-13	1.62E-13	1.31E-13
Future ^[3]	--	--	4.70E-13	3.14E-13	2.06E-13	1.62E-13
Note(s): 1. Values listed were determined at the pressure vessel outer surface. 2. Cycle 30 is the current operating cycle. Values listed for this cycle are projections based on design end of Cycle 30 burnup data. 3. Values beyond Cycle 30 are based on the average core power distributions and reactor operating conditions of Turkey Point Unit 3 Cycle 29, but include a 1.2 bias on the peripheral and re-entrant corner assembly relative powers.						

Table 2-24: Iron Atom Displacements at the Lower Shell to Lower Head Ring Weld – Unit 4

Cycle	Cycle Length (EFPY)	Cumulative Operating Time (EFPY)	Displacements (dpa) ^[1]			
			0°	15°	30°	45°
1	1.21	1.21	1.92E-05	1.16E-05	7.21E-06	5.59E-06
2	0.76	1.97	3.14E-05	1.90E-05	1.18E-05	9.13E-06
3	0.68	2.66	4.23E-05	2.61E-05	1.63E-05	1.26E-05
4	0.84	3.49	5.38E-05	3.35E-05	2.09E-05	1.65E-05
5	0.35	3.85	5.74E-05	3.59E-05	2.27E-05	1.79E-05
6	1.12	4.96	7.41E-05	4.59E-05	2.85E-05	2.23E-05
7	0.71	5.68	8.47E-05	5.23E-05	3.22E-05	2.52E-05
8	0.71	6.39	9.49E-05	5.84E-05	3.58E-05	2.82E-05
9	0.66	7.05	1.01E-04	6.26E-05	3.89E-05	3.06E-05
10	1.28	8.33	1.11E-04	7.00E-05	4.43E-05	3.48E-05
11	1.28	9.60	1.21E-04	7.76E-05	4.99E-05	3.92E-05
12	1.12	10.72	1.30E-04	8.40E-05	5.46E-05	4.30E-05
13	1.19	11.91	1.40E-04	9.09E-05	5.97E-05	4.71E-05
14	1.24	13.15	1.49E-04	9.76E-05	6.45E-05	5.08E-05
15	1.25	14.40	1.60E-04	1.05E-04	6.99E-05	5.49E-05
16	1.37	15.76	1.70E-04	1.13E-04	7.52E-05	5.94E-05
17	1.40	17.16	1.81E-04	1.20E-04	8.08E-05	6.38E-05
18	1.44	18.60	1.92E-04	1.28E-04	8.62E-05	6.83E-05
19	1.38	19.98	2.03E-04	1.35E-04	9.15E-05	7.24E-05
20	1.46	21.44	2.14E-04	1.43E-04	9.73E-05	7.71E-05
21	1.22	22.66	2.23E-04	1.49E-04	1.02E-04	8.05E-05
22	1.36	24.02	2.33E-04	1.57E-04	1.07E-04	8.48E-05
23	1.26	25.28	2.43E-04	1.64E-04	1.12E-04	8.89E-05
24	1.41	26.68	2.54E-04	1.71E-04	1.18E-04	9.31E-05
25	1.24	27.92	2.66E-04	1.79E-04	1.22E-04	9.70E-05
26	1.44	29.36	2.80E-04	1.87E-04	1.28E-04	1.02E-04
27	1.36	30.72	2.97E-04	1.98E-04	1.35E-04	1.07E-04
28	1.39	32.11	3.15E-04	2.09E-04	1.42E-04	1.13E-04
29	1.40	33.50	3.33E-04	2.20E-04	1.49E-04	1.19E-04
30 ^[2]	1.36	34.86	3.51E-04	2.31E-04	1.56E-04	1.24E-04
Future ^[3]	--	36.00	3.68E-04	2.43E-04	1.63E-04	1.30E-04
Future ^[3]	--	48.00	5.46E-04	3.61E-04	2.41E-04	1.91E-04
Future ^[3]	--	60.00	7.24E-04	4.80E-04	3.19E-04	2.53E-04
Future ^[3]	--	72.00	9.02E-04	5.99E-04	3.97E-04	3.14E-04

Note(s):

1. Values listed were determined at the pressure vessel outer surface.
2. Cycle 30 is the current operating cycle. Values listed for this cycle are projections based on design end of Cycle 30 burnup data.
3. Values beyond Cycle 30 are based on the average core power distributions and reactor operating conditions of Turkey Point Unit 3 Cycle 29, but include a 1.2 bias on the peripheral and re-entrant corner assembly relative powers.

Table 2-25: Fast (E > 1.0 MeV) Neutron Fluence Rate at the Geometric Center of the Surveillance Capsules – Unit 4

Cycle	Cycle Length (EFPY)	Cumulative Operating Time (EFPY)	Fluence Rate (n/cm ² -s)				
			0°	10°	20°	30°	40°
1	1.21	1.21	1.76E+11	1.24E+11	5.42E+10	4.11E+10	2.70E+10
2	0.76	1.97	1.63E+11	1.16E+11	5.08E+10	3.82E+10	2.47E+10
3	0.68	2.66	1.61E+11	1.25E+11	5.89E+10	4.49E+10	2.96E+10
4	0.84	3.49	1.46E+11	1.15E+11	4.94E+10	3.64E+10	2.88E+10
5	0.35	3.85	9.60E+10	7.22E+10	4.23E+10	3.66E+10	2.35E+10
6	1.12	4.96	1.67E+11	1.17E+11	4.86E+10	3.35E+10	2.22E+10
7	0.71	5.68	1.52E+11	1.07E+11	4.65E+10	3.18E+10	2.03E+10
8	0.71	6.39	1.45E+11	1.06E+11	4.07E+10	3.02E+10	2.31E+10
9	0.66	7.05	8.68E+10	6.89E+10	4.27E+10	3.30E+10	2.20E+10
10	1.28	8.33	7.09E+10	5.72E+10	3.99E+10	3.19E+10	2.16E+10
11	1.28	9.60	7.00E+10	5.69E+10	3.83E+10	3.08E+10	2.02E+10
12	1.12	10.72	7.17E+10	5.51E+10	3.33E+10	2.76E+10	1.99E+10
13	1.19	11.91	7.16E+10	5.64E+10	3.73E+10	3.02E+10	2.07E+10
14	1.24	13.15	6.92E+10	5.54E+10	3.68E+10	2.88E+10	1.95E+10
15	1.25	14.40	7.82E+10	6.08E+10	4.00E+10	3.20E+10	2.07E+10
16	1.37	15.76	7.35E+10	5.73E+10	3.63E+10	3.00E+10	2.22E+10
17	1.40	17.16	7.32E+10	5.61E+10	3.61E+10	3.00E+10	2.08E+10
18	1.44	18.60	7.26E+10	5.55E+10	3.28E+10	2.76E+10	2.14E+10
19	1.38	19.98	7.40E+10	5.79E+10	3.68E+10	2.87E+10	1.92E+10
20	1.46	21.44	7.44E+10	5.83E+10	3.71E+10	3.03E+10	2.10E+10
21	1.22	22.66	7.16E+10	5.61E+10	3.56E+10	2.88E+10	1.98E+10
22	1.36	24.02	7.50E+10	5.90E+10	3.77E+10	3.05E+10	2.12E+10
23	1.26	25.28	7.09E+10	5.73E+10	3.80E+10	3.12E+10	2.19E+10
24	1.41	26.68	7.61E+10	5.84E+10	3.57E+10	2.89E+10	1.93E+10
25	1.24	27.92	1.05E+11	7.68E+10	3.74E+10	2.85E+10	2.00E+10
26	1.44	29.36	1.16E+11	8.07E+10	3.76E+10	2.87E+10	2.03E+10
27	1.36	30.72	1.34E+11	9.26E+10	4.29E+10	3.16E+10	2.31E+10
28	1.39	32.11	1.28E+11	9.16E+10	4.21E+10	3.06E+10	2.35E+10
29	1.40	33.50	1.36E+11	9.64E+10	4.51E+10	3.45E+10	2.52E+10
30 ^[1]	1.36	34.86	1.36E+11	9.44E+10	4.39E+10	3.28E+10	2.37E+10
Future ^[2]	--	--	1.49E+11	1.11E+11	5.96E+10	4.34E+10	2.95E+10
Note(s): 1. Cycle 30 is the current operating cycle. Values listed for this cycle are projections based on design end of Cycle 30 burnup data. 2. Values beyond Cycle 30 are based on the average core power distributions and reactor operating conditions of Turkey Point Unit 3 Cycle 29, but include a 1.2 bias on the peripheral and re-entrant corner assembly relative powers.							

Table 2-26: Fast (E > 1.0 MeV) Neutron Fluence at the Geometric Center of the Surveillance Capsules – Unit 4

Cycle	Cycle Length (EFPY)	Cumulative Operating Time (EFPY)	Fluence (n/cm ²)				
			0°	10°	20°	30°	40°
1	1.21	1.21	6.73E+18	4.74E+18	2.07E+18	1.58E+18	1.03E+18
2	0.76	1.97	1.06E+19	7.53E+18	3.30E+18	2.49E+18	1.63E+18
3	0.68	2.66	1.41E+19	1.02E+19	4.56E+18	3.46E+18	2.26E+18
4	0.84	3.49	1.80E+19	1.33E+19	5.87E+18	4.42E+18	3.02E+18
5	0.35	3.85	1.90E+19	1.41E+19	6.34E+18	4.83E+18	3.28E+18
6	1.12	4.96	2.49E+19	1.82E+19	8.05E+18	6.01E+18	4.07E+18
7	0.71	5.68	2.83E+19	2.06E+19	9.10E+18	6.72E+18	4.52E+18
8	0.71	6.39	3.16E+19	2.30E+19	1.00E+19	7.40E+18	5.04E+18
9	0.66	7.05	3.34E+19	2.44E+19	1.09E+19	8.08E+18	5.50E+18
10	1.28	8.33	3.63E+19	2.67E+19	1.25E+19	9.37E+18	6.37E+18
11	1.28	9.60	3.91E+19	2.90E+19	1.41E+19	1.06E+19	7.18E+18
12	1.12	10.72	4.16E+19	3.10E+19	1.52E+19	1.16E+19	7.88E+18
13	1.19	11.91	4.43E+19	3.31E+19	1.66E+19	1.27E+19	8.66E+18
14	1.24	13.15	4.70E+19	3.52E+19	1.81E+19	1.38E+19	9.42E+18
15	1.25	14.40	5.01E+19	3.76E+19	1.96E+19	1.51E+19	1.02E+19
16	1.37	15.76	5.33E+19	4.01E+19	2.12E+19	1.64E+19	1.12E+19
17	1.40	17.16	5.65E+19	4.26E+19	2.28E+19	1.77E+19	1.21E+19
18	1.44	18.60	5.98E+19	4.51E+19	2.43E+19	1.90E+19	1.31E+19
19	1.38	19.98	6.30E+19	4.76E+19	2.59E+19	2.02E+19	1.39E+19
20	1.46	21.44	6.64E+19	5.03E+19	2.76E+19	2.16E+19	1.49E+19
21	1.22	22.66	6.92E+19	5.25E+19	2.90E+19	2.27E+19	1.57E+19
22	1.36	24.02	7.24E+19	5.50E+19	3.06E+19	2.40E+19	1.66E+19
23	1.26	25.28	7.52E+19	5.73E+19	3.21E+19	2.53E+19	1.74E+19
24	1.41	26.68	7.86E+19	5.99E+19	3.37E+19	2.66E+19	1.83E+19
25	1.24	27.92	8.27E+19	6.29E+19	3.51E+19	2.77E+19	1.91E+19
26	1.44	29.36	8.80E+19	6.65E+19	3.68E+19	2.90E+19	2.00E+19
27	1.36	30.72	9.37E+19	7.05E+19	3.87E+19	3.03E+19	2.10E+19
28	1.39	32.11	9.93E+19	7.45E+19	4.05E+19	3.17E+19	2.20E+19
29	1.40	33.50	1.05E+20	7.88E+19	4.25E+19	3.32E+19	2.31E+19
30 ^[1]	1.36	34.86	1.11E+20	8.28E+19	4.44E+19	3.46E+19	2.41E+19
Future ^[2]	--	36.00	1.16E+20	8.68E+19	4.65E+19	3.62E+19	2.52E+19
Future ^[2]	--	48.00	1.73E+20	1.29E+20	6.91E+19	5.26E+19	3.64E+19
Future ^[2]	--	60.00	2.29E+20	1.71E+20	9.17E+19	6.90E+19	4.75E+19
Future ^[2]	--	72.00	2.85E+20	2.13E+20	1.14E+20	8.55E+19	5.87E+19
Note(s): 1. Cycle 30 is the current operating cycle. Values listed for this cycle are projections based on design end of Cycle 30 burnup data. 2. Values beyond Cycle 30 are based on the average core power distributions and reactor operating conditions of Turkey Point Unit 3 Cycle 29, but include a 1.2 bias on the peripheral and re-entrant corner assembly relative powers.							

3.0 References

1. USNRC Regulatory Guide 1.190, "Calculational and Dosimetry Methods for Determining Pressure Vessel Neutron Fluence," Office of Nuclear Regulatory Research, March 2001.
2. Westinghouse Report WCAP-14040-A, Revision 4, "Methodology Used to Develop Cold Overpressure Mitigating System Setpoints and RCS Heatup and Cooldown Limit Curves," May 2004.

This page was added to the quality record by the PRIME system upon its validation and shall not be considered in the page numbering of this document.

Approval Information

Author Approval Hawk Andrew E Dec-01-2017 11:38:28

Reviewer Approval Amiri Benjamin W Dec-04-2017 16:35:52

Manager Approval Houssay Laurent Dec-04-2017 17:09:03

Files approved on Dec-04-2017

*** This record was final approved on 12/4/2017 5:09:03 PM. (This statement was added by the PRIME system upon its validation)

Enclosure 4
Non-proprietary Reference Documents
and
Redacted Versions of Proprietary
Reference Documents
(Public Version)
Attachment 2

**Areva Topical Report ANP-3646NP Revision 0
Low Upper-Shelf Toughness Fracture Mechanics Analysis of
Turkey Point Units 3 and 4 Reactor Vessels for Levels A & B
Service Loads at 80 Years, January 5, 2018 (Non-proprietary)**

(67 Total Pages, including cover sheets)



Low Upper-Shelf Toughness Fracture Mechanics Analysis of Turkey Point Units 3 and 4 Reactor Vessels for Levels A & B Service Loads at 80-Years

ANP-3646NP
Revision 0

Topical Report

January 2018

AREVA Inc.

(c) 2018 AREVA Inc.

Copyright © 2018

**AREVA Inc.
All Rights Reserved**

Nature of Changes

Item	Section(s) or Page(s)	Description and Justification
1	All	Initial Issue

Contents

	<u>Page</u>
1.0 INTRODUCTION	1-1
1.1 Equivalent Margins Analysis—Analysis of Record	1-3
2.0 REGULATORY REQUIREMENTS	2-1
2.1 Regulatory Requirements	2-1
2.2 Compliance with 10 CFR 50 Appendix G and Acceptance Criteria	2-2
2.2.1 Acceptance Criteria Levels A and B	2-3
3.0 DESCRIPTION OF TURKEY POINT REACTOR VESSELS	3-1
4.0 MATERIAL PROPERTIES	4-1
4.1 J-Integral Resistance Model	4-1
4.2 Mechanical Properties of Weld Metals	4-4
4.2.1 Mechanical Properties for the Turkey Point Reactor Vessels	4-4
5.0 FRACTURE MECHANICS ANALYSIS	5-1
5.1 Methodology	5-1
5.2 Procedure for Evaluating Levels A and B Service Loadings	5-2
5.3 Evaluation for Flaw Extension	5-6
5.3.1 Reactor Vessel Shell Welds	5-7
5.3.2 Reactor Vessel Transition Welds and RV Nozzle Welds	5-7
5.4 Evaluation for Flaw Stability	5-8
5.4.1 Reactor Vessel Shell Welds	5-9
5.4.2 Reactor Vessel Transition Welds and RV Nozzle Welds	5-9
6.0 SUMMARY AND CONCLUSIONS	6-1
6.1 Reactor Vessel Shell Welds	6-1
6.2 Reactor Vessel Transition Welds and RV Nozzle Welds	6-1
7.0 REFERENCES	7-1
8.0 CERTIFICATION	8-1
APPENDIX A B&WOG J-R MODEL-DATA ANALYSIS AND EMPIRICAL MODEL DEVELOPMENT	A-1

List of Tables

Table 3—1 Reactor Vessel Weld Locations--Copper Content and 80-Year Fluence Projections	3-2
Table 4—1 Parameters in Jd Model 4B	4-3
Table 4—2 Mechanical Properties of Turkey Point RV Shell Materials	4-5
Table 5—1 Reactor Vessel Shell Dimensions and Operating Conditions	5-10
Table 5—2 Plant Specific Flaw Evaluation Summary for RV Shell Regions	5-11
Table 5—3 Reactor Vessel Nozzle Belt Dimensions	5-12
Table 5—4 Flaw Evaluation Summary of Turkey Point Upper Transition and RV Nozzle-to-Shell Welds	5-13
Table 5—5 Flaw Evaluation Summary of Turkey Point Lower Transition Welds.....	5-13
Table 5—6 Applied J-Integral versus Flaw Extensions of Turkey Point Controlling RV Shell Weld (SA-1101)	5-14
Table 5—7 Mean & Lower Bound J-R Curve Values for Turkey Point Controlling RV Shell Weld (SA-1101)	5-15
Table A—1 Model 4B, Range of Test Data	A-3
Table A—2 New B&WOG Specimen Data for Model Assessment.....	A-5
Table A—3 Jd Model Coefficients (Models 4B, 5B, and 6B)	A-10
Table A—4 EMA Reconciliation for Limiting RV Shell Welds—Models 4B and 6B	A-18

List of Figures

Figure 3—1	Reactor Vessel—Turkey Point Unit 3	3-3
Figure 3—2	Reactor Vessel—Turkey Point Unit 4	3-4
Figure 5—1	J-Integral Flaw Extension for Turkey Point Controlling Reactor Vessel Shell weld (SA-1101)	5-16
Figure 5—2	J-Integral versus Flaw Extension for Turkey Point Inlet Nozzle	5-17
Figure A—1	BAW-2251A, Appendix B, Figure 3-1	A-4
Figure A—2	Jd (0.1) vs Fluence B&WOG J-R Model 4B and New Test Data (Normalized to Standard Conditions).....	A-7
Figure A—3	Original and New Data and Model Fit Normalized at Standardized Conditions vs Δa	A-11
Figure A—4	Original and New Data and Model Fit Normalized at Standard Conditions vs Fluence	A-12
Figure A—5	Model 6B Residuals vs Fitted Values	A-13
Figure A—6	Model 6B Standardized Residuals vs Fitted Values	A-14
Figure A—7	Normal Q-Q Plot of Standardized Residuals	A-15
Figure A—8	Comparison of Models 4B, 5B, and 6B at Standard Conditions	A-17

Nomenclature

Acronym	Definition
B&W	Babcock and Wilcox
B&WOG	Babcock and Wilcox Owners Group
CvUSE	Charpy Upper Shelf Energy
EFPY	Effective Full Power Years
EMA	Equivalent Margins Analysis
INF	Inlet Nozzle Forging
Jd	J deformation
J-R	J-integral Resistance
LAR	License Amendment Request
ONF	Outlet Nozzle Forging
PTN	Turkey Point Plant
PWROG	Pressurized Water Reactor Owners Group
RV	Reactor Vessel
RVWG	Reactor Vessel Working Group
SLR	Subsequent License Renewal
SRP	Standard Review Plan
Sy	Yield Strength
TSs	Technical Specifications
USE	Upper Shelf Energy

ABSTRACT

This topical report presents the results of an equivalent margins analysis (EMA) considering Levels A and B service loads for high copper Linde 80 weld metals using fluence values expected at 80-years (subsequent license renewal--SLR). This report applies to the following Westinghouse-designed reactor vessels fabricated by B&W: Turkey Point Plant (PTN) Units 3 and 4. Note that the Turkey Point EMA reported herein is technically identical to the Turkey Point EMA reported in BAW-2192P, Supplement 1, Revision 0, which was submitted to the NRC by the PWROG on December 15, 2017. That is, Sections 1.0 through 7.0 of ANP-3646P were generated by extracting Turkey Point 3 and 4-specific results from Sections 1.0 through 7.0 of BAW-2192, Supplement 1, Revision 0. Appendix A to ANP-3646P, B&WOG J-R Model-Data Analysis and Empirical Model Development, is identical to Appendix A of BAW-2192, Supplement 1, Revision 0, with the exception that references to plants other than Turkey Point 3 and 4 were removed from Sections A.1, A.2, and A.4.

The analytical procedure used in this topical report is in accordance with ASME Section XI, Appendix K, Subarticle K-1200. EMA results are reported for all reactor vessel weld locations with 80-year fluence projections that exceed $1.0 \text{ E}+17 \text{ n/cm}^2$ ($E > 1.0 \text{ MeV}$). The ASME Section XI, acceptance criteria for Levels A & B Service Loads for all reactor vessel shell welds are satisfied. The acceptance criteria for Levels A & B Service Loads for RV transition welds and RV nozzle welds are also satisfied. Consistent with BAW-2192PA, Revision 00, the B&WOG J-R Model 4B is used for Linde 80 welds.

Model 4B was developed based on fracture toughness test data obtained through approximately 1990, with specimen fluence that ranges from 0.0 to $8.45\text{E}+18 \text{ n/cm}^2$. Eighty-year fluence estimates for Turkey Point Units 3 and 4 exceeds $8.45\text{E}+18 \text{ n/cm}^2$ (e.g., maximum 80-year 1/4 T fluence is estimated at $6.53\text{E}+19 \text{ n/cm}^2$) and use of Model 4B to estimate J-integral resistance values, including the associated model uncertainty, for 80-years is made by extrapolation of the model. To assess the model extrapolation uncertainty, Model 4B is compared to new fracture toughness test data

(1990 to 2017) irradiated to fluence ranging from approximately $8.0\text{E}+18$ n/cm² to $5.8\text{E}+19$ n/cm². The majority of test data fell above the Model 4B mean and all of the test data fell above the Model 4B mean minus 2 standard error band. Therefore, use of Model 4B and associated uncertainty to extrapolate J-integral resistance for 80-year fluence applications was determined to be appropriate. This assessment is reported in Appendix A herein.

To further substantiate the use of Model 4B, all of the original fracture toughness data used to develop Model 4B was combined with new fracture toughness data, using the same model form, and a new Model 6B was generated. Model 6B was found to be essentially equivalent to Model 4B with respect to model mean and 2 standard errors. The EMA results reported herein using Model 4B were reconciled to Model 6B, with little or no change to the EMA results. Model 6B development and the EMA reconciliation to Model 4B are reported in Appendix A.

1.0 INTRODUCTION

The purpose of this topical report is to present the results of an equivalent margins analysis (EMA) considering Levels A and B service loads for high copper Linde 80 weld metals and applicable non-Linde 80 welds using fluence values expected at 80-years (subsequent license renewal--SLR). This topical report applies to the following Westinghouse-designed reactor vessels: Turkey Point Plant (PTN) Units 3 and 4, also referred to as Turkey Point Units 3 and 4. Note that the Turkey Point EMA reported herein is technically identical to the Turkey Point EMA reported in BAW-2192P, Supplement 1, Revision 0 [3], which was submitted to the NRC by the PWROG on December 15, 2017. That is, Sections 1.0 through 7.0 of ANP-3646P were generated by extracting Turkey Point 3 and 4-specific results from Sections 1.0 through 7.0 of BAW-2192, Supplement 1, Revision 0. Appendix A to ANP-3646P, B&WOG J-R Model-Data Analysis and Empirical Model Development, is identical to Appendix A of BAW-2192, Supplement 1, Revision 0, with the exception that references to plants other than Turkey Point 3 and 4 were removed from Sections A.1, A.2, and A.4.

Equivalent margins analyses for Turkey Point Units 3 and 4 are reported for all reactor vessel weld locations with 80-year fluence projections that exceed $1.0 \text{ E}+17 \text{ n/cm}^2$ ($E > 1.0 \text{ MeV}$) [2]. Upper shelf energy evaluations at reactor vessel base metal locations with 80-year fluence projections greater than $1.0 \text{ E}+17 \text{ n/cm}^2$, if needed, will be addressed separately in the Turkey Point Units 3 and 4 subsequent license renewal application. The EMA utilizes the B&WOG J-integral resistance (J-R) Model 4B reported in BAW-2192PA, Appendix B, [1]. The following groups are used for the welds within the scope of this report:

- Reactor Vessel Shell Welds—circumferential welds for Turkey Point Units 3 and 4 (also referred to as Turkey Point reactor vessels). There are no geometric discontinuities at these weld locations and all reactor vessel shell welds surround the effective height of the active core. These locations have historically been considered “beltline” or “beltline region” as defined by 10 CFR 50, Appendix G. All reactor vessel shell welds are Linde 80 welds.
- Transition Welds and RV Nozzle Welds—welds that are located above and below the reactor vessel shell welds that may experience 80-year fluence greater than $1.0 \text{ E}+17 \text{ n/cm}^2$ [2] and, must consider the effects of neutron irradiation embrittlement. In addition, the transition welds are located at geometric discontinuities (e.g., lower shell to lower head and upper shell to nozzle belt forging). These locations may or may not have been included as part of the 10 CFR 50 Appendix G [4] “beltline” definition for 60-years for the participating plants. All transition welds and RV nozzle welds (also referred to as RV nozzle-to-shell welds) are Linde 80 welds.

The EMA evaluations in this report are for all weld locations expected to receive fluence $> 1.0\text{E}+17 \text{ n/cm}^2$ [2] at 80 years. The use of the terms “beltline” and/or “extended beltline” are not used in this report.

The 60-year EMA summary report for Turkey Point Units 3 and 4 are reported in Section 1.1. Section 2.0 provides the current NRC regulatory requirements for the EMA. Section 3.0 provides a description of the reactor vessels within the scope of this report, with illustrations of reactor vessel welds that are evaluated for equivalent margins in Figures 3-1 through 3-2. Section 4.0 provides the material properties that are required for the EMA, and Section 5.0 presents the results of the EMA. Section 6.0 provides the summary and conclusions, Section 7.0 lists all references and Appendix A provides the technical basis for the use of B&WOG J-R Model 4B for the EMA reported herein.

1.1 ***Equivalent Margins Analysis—Analysis of Record***

The summary reports for the PTN EMA analyses of record are as follows:

Turkey Point Units 3 and 4

The Turkey Point Units 3 and 4 current licensing basis equivalent margins analysis at 48 EFPY is summarized in Section 2.1.2 of NRC document “TURKEY POINT UNITS 3 AND 4 - ISSUANCE OF AMENDMENTS REGARDING EXTENDED POWER UPRATE (TAC NOS. ME4907 AND ME4908),” Adams Accession number ML11293A365 [11]. NRC acceptance of the Turkey Point EMA at 48 EFPY for EPU is based on the following documentation:

- LICENSE AMENDMENT REQUEST FOR EXTENDED POWER UPRATE, ATTACHMENT 4, L-2010-113, Attachment 4 ADAMS--ML103560177 [12]
- Supplemental Response to NRC Request for Additional Information (RAI) Regarding Extended Power Uprate (EPU) License Amendment Request (LAR) No. 205 and Equivalent Margin Analysis (EMA), L-2010-303, ADAMS-ML103610321 [13]. Reference [13] contains AREVA document 77-2312-03 (P), LOW UPPER-SHELF TOUGHNESS FRACTURE MECHANICS ANALYSIS OF REACTOR VESSELS OF TURKEY POINT UNITS 3 AND 4 FOR EXTENDED LIFE THROUGH 48 EFFECTIVE FULL POWER YEARS
- Response to NRC Request for Additional Information Regarding Extended Power Uprate License Amendment Request No. 205 and Reactor Materials Issues – Round 1, L-2011-029, ADAMS--ML110700068 [14]. Reference [14] provides a response to RAI CVIB-1.2 regarding the code year used to perform the equivalent margins analysis (i.e., 1998 Edition vs 2004 Edition). The NRC SER for the Turkey Point Extended Power Uprate, Section 2.1.2, contains the evaluation of upper shelf energy--ADAMS-ML 11293A365 [11]

2.0 REGULATORY REQUIREMENTS

2.1 *Regulatory Requirements*

In accordance with 10 CFR 50 Appendix G [4], IV, A, 1, Reactor Vessel Upper Shelf Energy Requirements are as follows:

- a. Reactor vessel beltline materials must have Charpy upper-shelf energy in the transverse direction for base material and along the weld for weld material according to the ASME Code, of no less than 75 ft-lb (102 J) initially and must maintain Charpy upper-shelf energy throughout the life of the vessel of no less than 50 ft-lb (68 J), unless it is demonstrated in a manner approved by the Director, Office of Nuclear Reactor Regulation or Director, Office of New Reactors, as appropriate, that lower values of Charpy upper-shelf energy will provide margins of safety against fracture equivalent to those required by Appendix G of Section XI of the ASME Code. This analysis must use the latest edition and addenda of the ASME Code incorporated by reference into 10 CFR 50.55a (b) (2) at the time the analysis is submitted.
- b. Additional evidence of the fracture toughness of the beltline materials after exposure to neutron irradiation may be obtained from results of supplemental fracture toughness tests for use in the analysis specified in section IV.A.1.a.
- c. The analysis for satisfying the requirements of section IV.A.1 of this appendix must be submitted, as specified in § 50.4, for review and approval on an individual case basis at least three years prior to the date when the predicted Charpy upper-shelf energy will no longer satisfy the requirements of section IV.A.1 of this appendix, or on a schedule approved by the Director, Office of Nuclear Reactor Regulation or Director, Office of New Reactors, as appropriate.

When the reactor vessels within the scope of this report were fabricated, Charpy V-notch testing of the reactor vessel welds was in accordance with the original construction code, which did not specifically require Charpy V-notch tests on the upper shelf.

The construction code is as follows:

- Turkey Point--ASME B&PV Code, Section III, 1965 Edition through Summer 1966 Addenda

In accordance with NRC Regulatory Guide 1.161 [15], the NRC has determined that the analytical methods described in ASME Section XI, Appendix K, provide acceptable guidance for evaluating reactor pressure vessels when the Charpy upper-shelf energy falls below the 50 ft-lb limit of Appendix G to 10 CFR Part 50. However, the staff noted that Appendix K does not provide information on the selection of transients and gives very little detail on the selection of material properties. Selection of the limiting design transient (i.e., cooldown at 100 F/h) is consistent with BAW-2192PA [1], Section 5.3. Section 4.1 of this report includes a summary of the B&WOG J-integral resistance model, and Section 4.2 provides mechanical properties of weld metals.

The Linde 80 weld locations that are included within the scope of this report (i.e., weld locations with 80-year projected fluence $> 1.0\text{E}+17 \text{ n/cm}^2$) are all assumed to have upper shelf energy values below 50 ft-lb and thus require an equivalent margins analysis.

2.2 Compliance with 10 CFR 50 Appendix G and Acceptance Criteria

The analyses reported herein are performed in accordance with the 2007 Edition with 2008 Addenda [16] of Section XI of the ASME Code, Appendix K. The current edition of ASME Section XI listed in 10 CFR 50.55a is the 2013 Edition [17]. With regard to Appendix K, there are no differences between the 2007 Edition with 2008 Addenda and the 2013 Edition of ASME Section XI, and hence these ASME Section XI, Appendix K analyses are equally applicable to the 2013 Edition of the ASME Code.

The material properties used in this analysis are based on ASME Section II, Part D, 2007 Edition with 2008 Addenda. The only change in the material properties listed in the 2013 Edition of ASME Section II for the applicable properties is the coefficient of thermal expansion for stainless steel at 600°F; this value was changed from 9.8E-6 in/in/°F to 9.9E-6 in/in/°F. This does not impact the Levels A and B evaluation reported herein.

2.2.1 Acceptance Criteria Levels A and B

ASME Section XI [17], Subarticle K-2200, provides the following acceptance criteria for Levels A and B Service Conditions:

- a) When evaluating adequacy of the upper shelf toughness for the weld material for Levels A and B Service Loadings, an interior semi-elliptical surface flaw with a depth one-quarter of the wall thickness and a length six times the depth shall be postulated, with the flaw's major axis oriented along the weld of concern, and the flaw plane oriented in the radial direction. When evaluating adequacy of the upper shelf toughness for the base material, both interior axial and circumferential flaws with depths one quarter of the wall thickness and lengths six times the depth shall be postulated, and toughness properties for the corresponding orientation shall be used. Smaller flaw sizes may be used when justified. Two criteria shall be satisfied:
 1. The applied J-integral evaluated at a pressure 1.15 times the accumulation pressure as defined in the plant specific Overpressure Protection Report, with a structural factor of 1 on thermal loading for the plant specific heatup and cooldown conditions, shall be less than the J-integral of the material at a ductile flaw extension of 0.1 in. (2.5 mm).
 2. Flaw extensions at pressures up to 1.25 times the accumulation pressure of K-2200(a)(1) shall be ductile and stable, using a structural factor of 1 on thermal loading for the plant specific heatup and cooldown conditions.

- b) The J-integral resistance versus flaw extension curve shall be a conservative representation for the vessel material under evaluation.

3.0 DESCRIPTION OF TURKEY POINT REACTOR VESSELS

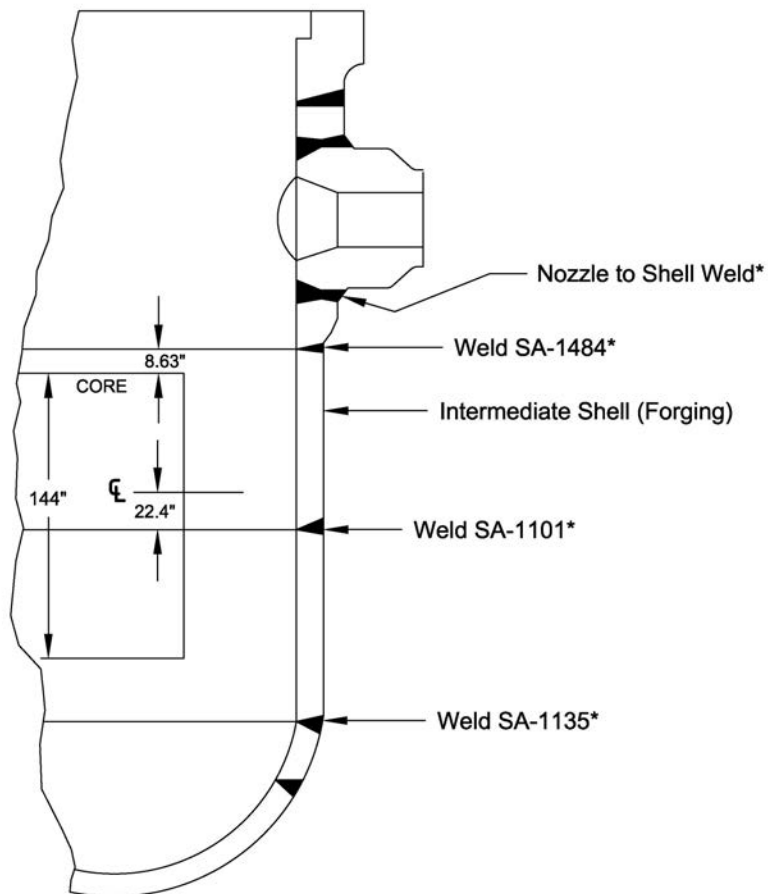
The Turkey Point reactor vessels and applicable weld locations are shown in Figures 3-1 through 3-2. All weld locations evaluated for equivalent margins in this report are identified by an asterisk (*) in each Figure. Plant-specific weld copper and nickel content and 80-year fluence projections data needed for the equivalent margins analysis are provided in Table 3—1. The fluence projections are reported for all reactor vessel weld locations that are expected to exceed $1.0\text{E}+17$ n/cm² at 80-years. The 80-year fluence projections are conservative estimates based on detailed transport calculations completed by Westinghouse Electric Corporation using a methodology that is in compliance with Regulatory Guide 1.190 (i.e., Westinghouse Report WCAP-14040-A, Revision 4, “Methodology Used to Develop Cold Overpressure Mitigating System Setpoints and RCS Heatup and Cooldown Limit Curves,” May 2004.)

Copper and nickel content of the reactor vessel shell welds is consistent with EMA analyses of record reported in Section 1.1; the copper and nickel content for transition welds and RV nozzle-to-nozzle belt forging welds reported in Table 3-1 were obtained from either the EMA analysis of record or Turkey Point reactor vessel fabrication reports.

Table 3—1
Reactor Vessel Weld Locations--Copper Content and 80-Year Fluence Projections

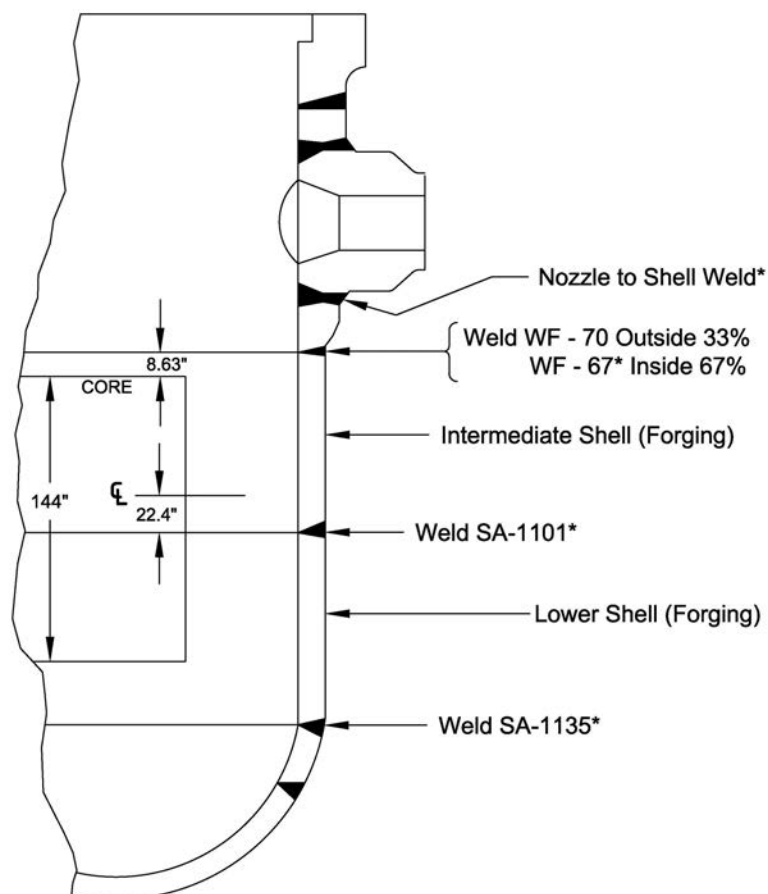
Reactor Vessel Material	Material ID and/or Heat Number	Cu, wt%	Ni, wt%	(IS) Inside Wetted Surface Fluence or (*) clad/base metal n/cm ² E> 1.0 MeV)
Turkey Point Unit 3, 80-Year Fluence (E > 1.0 MeV)				
US Forging to INF Welds	Heat 8T1762	0.19	0.57	(IS) 1.50E+18
	Heat 8T1554B	0.16	0.57	(IS) 1.50E+18
	Heat 71249	0.23	0.59	(IS) 1.50E+18
US Forging to ONF Welds	Heat 8T1762	0.19	0.57	(IS) 1.50E+18
US to IS Circ. Weld	SA-1484 Heat 72442	0.26	0.60	(*) 1.19E+19
IS to LS Circ. Weld	SA-1101 Heat 71249	0.23	0.59	(*) 1.04E+20
LS to Dutchman Circ. Weld	SA-1135 Heat 61782	0.23	0.52	(IS) 1.5E+18
Turkey Point Unit 4, 80-Year Fluence (E > 1.0 MeV)				
US to INF Welds	Heat 8T1762	0.19	0.57	(IS) 1.50E+18
	Heat 8T1554B	0.16	0.57	(IS) 1.50E+18
	Heat 299L44	0.34	0.68	(IS) 1.50E+18
US to ONF Welds	Heat 8T1554B	0.16	0.57	(IS) 1.50E+18
	Heat 299L44	0.34	0.68	(IS) 1.50E+18
US to IS Circ. Weld (ID 67%)	WF-67 Heat 72442	0.26	0.60	(*) 1.21E+19
IS to LS Circ. Weld	SA-1101 Heat 71249	0.23	0.59	(*) 1.03E+20
LS to Dutchman Circ. Weld	SA-1135 Heat 61782	0.23	0.52	(IS) 1.5E+18

Figure 3—1
Reactor Vessel—Turkey Point Unit 3



* Equivalent Margins Analysis
performed for these Linde 80 Welds.

Figure 3—2
Reactor Vessel—Turkey Point Unit 4



* Equivalent Margins Analysis
performed for these Linde 80 Welds.

4.0 MATERIAL PROPERTIES

4.1 *J-Integral Resistance Model*

The J-integral resistance model for Mn-Mo-Ni/Linde 80 welds in the reactor vessels of the B&WOG RVWG plants were developed using a large J-resistance data base. A detailed description of this model is provided in Appendix B of BAW-2192PA [1], Revision 00. This model was developed using specimens irradiated to $8.45\text{E}+18 \text{ n/cm}^2$, and the range of applicability of the model was extended (qualitatively) to approximately $1.90 \text{ E}+19 \text{ n/cm}^2$ in Appendix B, Figure 3-1, to BAW-2251A [5]. See Appendix A of this report for a discussion of the extension of the range of applicability of the B&WOG J-R model to fluence values expected at 80 years for Turkey Point Units 3 and 4.

The coefficients a , d , and C_4 are provided in Table 4-1. As required by ASME Section XI, ASME K-3300, when evaluating the vessel for Levels A, B, and C Service Loadings, the J-integral resistance versus crack-extension curve (J-R curve) shall be a conservative representation of the toughness of the controlling beltline material at upper shelf temperatures in the operating range. As such, the J_d correlation minus 2 standard errors is used for evaluation of Levels A & B service loadings (i.e., equation (1) multiplied by $\left[\frac{1}{1.65} \right]$).

As discussed in Appendix B to BAW-2192PA, the J-R curve was generated from a J-integral database obtained from the same class of material with the same orientation as the applicable reactor vessel materials using correlations for the effects of temperature, chemical composition, and fluence level. Crack extension was by ductile tearing with no cleavage. This complies with the ASME Code, Section XI, K-3300.

Table 4—1
Parameters in Jd Model 4B

--	--

4.2 *Mechanical Properties of Weld Metals*

The following subsections provide representative properties for the Turkey Point reactor vessels. The temperature dependent mechanical properties are developed from the 2007 Edition with 2008 Addenda of the ASME Code (Section II, Part D) for the reactor base metal and cladding (the ASME Code does not provide separate mechanical properties for base and weld metal). Both ASME Code minimum and representative irradiated yield strengths are also provided. The mechanical properties such as weld metal yield strengths typically used were the irradiated properties but in some cases the ASME Code minimum properties were conservatively considered. The irradiated material properties used herein are consistent with the PTN 60-year license renewal low upper shelf toughness analysis submittal (See Section 1.1 above).

4.2.1 Mechanical Properties for the Turkey Point Reactor Vessels

The Turkey Point reactor vessels are fabricated using A-508 Grade 2 Class 1 (3/4Ni-1/2Mo-1/3Cr-V) Low Alloy Steel (LAS) and stainless steel (18Cr-8Ni) cladding materials. Table 4-2 provides the Young's modulus (E), the mean coefficient of thermal expansion (α), and the yield strength (S_y) for the RV shell regions.

Table 4—2
Mechanical Properties of Turkey Point RV Shell Materials

	RV Base Metal			Weld Metals	
Temp. (°F)	E (ksi)	α (in/in/°F)	Sy (ksi)	SA-1101 (ksi)	SA-1135 (ksi)
70	27800	6.40E-06	50.0	[]	[]
200	27100	6.70E-06	47.0	[]	[]
300	26700	6.90E-06	45.5	[]	[]
400	26200	7.10E-06	44.2	[]	[]
500	25700	7.30E-06	43.2	[]	[]
600	25100	7.40E-06	42.1	[]	[]

For the Turkey Point reactor vessel shell and RV nozzle regions, the normal operating steady state condition cold leg temperature value is [] (Table 5-1).

Both the Turkey Point Units have SA-1101 and SA-1135 Linde 80 welds in the RV shell regions. The yield strength values for these weld metals at [], respectively.

5.0 FRACTURE MECHANICS ANALYSIS

5.1 *Methodology*

In accordance with ASME Section XI, Appendix K [16], Subarticle K-1200, the following analytical procedure was used for Levels A & B Service Loads.

- a. The postulated flaws in the reactor vessel shell welds, the transition welds as well as RV nozzle-to-shell welds were postulated in accordance with the acceptance criteria of Subarticle K-2200.
- b. Loading conditions at the locations of the postulated flaws were determined for Levels A and B Service Loadings. For Levels A and B Service loadings the equations to calculate the stress intensity factor (SIF) due to pressure and thermal gradients for a given pressure and cooldown rate are given in Article K-4210. Consistent with Section 5 of BAW-2192PA [1], the accumulation pressure is taken as ten percent above the design pressure and the maximum cooldown rate is 100°F/hr. In the area of the nozzle-to-shell weld, applied loadings consist of pressure, thermal, and attached piping reactions.
- c. Material properties, including E , α , σ_y , and the J-integral resistance curve (J-R curve), were determined at the locations of the postulated flaws. Young's modulus, mean coefficient of thermal expansion and yield strength are addressed in Section 4.2. The J-R curve is discussed in Section 4.1.

- d. The postulated flaws were evaluated in accordance with the acceptance criteria of Article K-2000. Requirements for evaluating the applied J-integral are provided in Subarticle K-3200, and for determining flaw stability in Subarticle K-3400. Subarticle K-3500(a) invokes the procedure provided in Subarticle K-4200 (K-4220) for evaluating the applied J-integral for a specified amount of ductile flaw extension. Three permissible evaluation methods to address flaw stability are described in Subarticle K-3500(b). The evaluation method selected herein is the J-R curve crack driving force diagram procedure described in Subarticle K-4310.

5.2 *Procedure for Evaluating Levels A and B Service Loadings*

For RV shell regions remote from structural discontinuities, the applied J -integral is calculated in accordance with Appendix K, Subsubarticle K-4210, using an effective flaw depth to account for small scale yielding at the crack tip, and evaluated per K-4220 for upper-shelf toughness and per K-4310 for flaw stability, as outlined below. The generic equations provided below are provided for both axially and circumferentially oriented flaws. Since all the Linde 80 welds for Turkey Point Units 3 and 4 are circumferential welds, only the equations for circumferential oriented flaws are applicable and used in the analysis.

- (1) For an axial flaw of depth a , the stress intensity factor due to internal pressure is calculated with a structural factor (SF) on pressure using the following:

$$K_{I_p} = (SF)p \left(1 + \frac{R_i}{t} \right) (\pi a)^{0.5} F_1$$

where

$$F_1 = 0.982 + 1.006 \left(\frac{a}{t} \right)^2, \quad 0.20 \leq \left(\frac{a}{t} \right) \leq 0.50$$

- (2) For a circumferential flaw of depth a , the stress intensity factor due to internal pressure is calculated with a structural factor (SF) on pressure using the following:

$$K_{Ip} = (SF)p \left(1 + \frac{R_i}{2t} \right) (\pi a)^{0.5} F_2$$

where

$$F_2 = 0.885 + 0.233 \left(\frac{a}{t} \right) + 0.345 \left(\frac{a}{t} \right)^2, \quad 0.20 \leq \left(\frac{a}{t} \right) \leq 0.50$$

- (3) For an axial or circumferential flaw of depth a , the stress intensity factor due to radial thermal gradients is calculated using the following:

$$K_{It} = C_m (CR) t^{2.5} F_3, \quad 0 \leq (CR) \leq 100^\circ\text{F/hr}$$

where for SA-508, Class 2 or SA-533, Grade B, Class1 steels the material coefficient C_m is defined as:

$$C_m = \frac{E\alpha}{(1-\nu)d} = 0.0051,$$

CR = cooldown rate ($^\circ\text{F/hr}$), and

$$F_3 = 0.1181 + 0.5353 \left(\frac{a}{t} \right) - 1.273 \left(\frac{a}{t} \right)^2 + 0.6046 \left(\frac{a}{t} \right)^3, \quad 0.20 \leq \left(\frac{a}{t} \right) \leq 0.50$$

- (4) The effective flaw depth for small scale yielding, a_e , is calculated using the following:

$$a_e = a + \left(\frac{1}{6\pi} \right) \left[\frac{K_{Ip} + K_{It}}{\sigma_y} \right]^2$$

- (5) For an axial flaw of depth a_e , the stress intensity factor due to internal pressure is:

$$K'_{lp} = (SF)p \left(1 + \frac{R_i}{t} \right) (\pi a_e)^{0.5} F'_1$$

where

$$F'_1 = 0.982 + 1.006 \left(\frac{a_e}{t} \right)^2, \quad 0.20 \leq \left(\frac{a_e}{t} \right) \leq 0.50$$

- (6) For a circumferential flaw of depth a_e , the stress intensity factor due to internal pressure is:

$$K'_{lp} = (SF)p \left(1 + \frac{R_i}{2t} \right) (\pi a_e)^{0.5} F'_2$$

where

$$F'_2 = 0.885 + 0.233 \left(\frac{a_e}{t} \right) + 0.345 \left(\frac{a_e}{t} \right)^2, \quad 0.20 \leq \left(\frac{a_e}{t} \right) \leq 0.50$$

- (7) For an axial or circumferential flaw of depth a_e , the stress intensity factor due to radial thermal gradients is:

$$K'_H = C_m (CR) t^{2.5} F'_3, \quad 0 \leq (CR) \leq 100^\circ \text{F/hr}$$

where

$$F'_3 = 0.1181 + 0.5353 \left(\frac{a_e}{t} \right) - 1.273 \left(\frac{a_e}{t} \right)^2 + 0.6046 \left(\frac{a_e}{t} \right)^3, \quad 0.20 \leq \left(\frac{a_e}{t} \right) \leq 0.50$$

- (8) The J -integral due to applied loads for small scale yielding is calculated using the following:

$$J_1 = 1000 \frac{(K'_{Ip} + K'_{It})^2}{E'}$$

where

$$E' = \frac{E}{1 - \nu^2}$$

- (9) Evaluation of upper-shelf toughness at a flaw extension of 0.10 in. is performed for a flaw depth,

$$a = 0.25t + 0.10 \text{ in.},$$

using

$$SF = 1.15$$

$$p = P_a$$

where P_a is the accumulation pressure for Levels A and B Service Loadings, such that

$$J_1 < J_{0.1}$$

where

J_1 = the applied J -integral for a safety factor of 1.15 on pressure,
and a safety factor of 1.0 on thermal loading

$J_{0.1}$ = the lower bound J -integral resistance at a ductile
flaw extension of 0.10 inches

- (10) Evaluation of flaw stability is performed through use of a crack driving force diagram procedure, by comparing the slopes of the applied J -integral curve and the lower bound J - R curve. The applied J -integral is calculated for a series of flaw depths corresponding to increasing amounts of ductile flaw extension. The applied pressure is the accumulation pressure for Levels A and B Service Loadings, P_a , and the safety factor (SF) on pressure is 1.25. Flaw stability at a given applied load is verified when the slope of the applied J -integral curve is less than the slope of the J - R curve at the point on the J - R curve where the two curves intersect.

For the Turkey Point reactor vessels, the applied J -integrals at the nozzle-to-shell welds and the upper transition welds were determined using stresses from a detailed three-dimensional finite element analysis. Path line stresses were used to determine applied J -integrals that included a plastic zone correction to account for small scale yielding. Based on the results of analysis performed for similar B&W fabricated reactor vessels it was deemed that the effects of structural discontinuities at the lower transition welds need not be explicitly addressed.

5.3 *Evaluation for Flaw Extension*

The applied J -integrals for the RV shell welds, the RV transition welds, and the RV nozzle welds are calculated as discussed in Section 5.2.

5.3.1 Reactor Vessel Shell Welds

The basic reactor vessel shell geometry and design pressure along with operating condition temperature information for the Turkey Point reactor vessels is provided in Table 5-1. Initial flaw depths equal to $\frac{1}{4}$ of the vessel wall thickness are analyzed for Levels A and B service loadings following the procedure outlined in Section 5.2 and evaluated for acceptance based on values for the J-integral resistance of the material from the Linde 80 J-R model discussed in Section 4.1. Calculations are initially carried out to identify the controlling weld such that subsequent detailed low upper shelf toughness flaw evaluations can be performed using the controlling weld.

The results of the evaluations for each of the RV shell welds are presented in Table 5-2. From the results of the evaluation in Table 5-2, the controlling RV shell welds can be observed. The controlling welds are determined by noting the minimum ratio of the material J-resistance ($J_{0.1}$) to the applied J-integral (J_1) (also referred to as “margin”).

For the Turkey Point reactor vessels, the controlling RV shell weld is the circumferential weld SA-1101 which is located between the intermediate and lower shell courses of both Units 3 and 4 reactor vessels. The minimum ratio of material J-resistance to applied J-integral ($J_{0.1}/J_1$) is [], which is significantly higher than the minimum acceptable value of 1.0.

5.3.2 Reactor Vessel Transition Welds and RV Nozzle Welds

The reactor vessel nozzle welds are located in the substantially thicker cylindrical shell section (reinforced to account for the inlet/outlet RV nozzle openings and typically referred to as the nozzle belt), located above the reactor vessel shell welds. The reactor vessel nozzle belt dimensions are reported in Table 5-3.

For the Turkey Point reactor vessels upper RV transition and RV nozzle weld regions, the J-applied results with the safety factor of 1.15 on applied pressure is compared against the lower bound J-integral resistance at a ductile flaw extension of 0.1 inches ($J_{0.1}$) in Table 5-4. The limiting item in this case is the inlet nozzle with a margin of [], which is significantly higher than the minimum acceptable value of 1.0. For the lower transition weld SA-1135, it is noted that this circumferential weld is located at the thickness transition between the cylindrical shell and the thinner lower head. This location was additionally evaluated using the dimensions applicable to the lower head [] since this will result in higher pressure stresses but lower thermal stresses when compared against the thicker RV cylindrical shell. For evaluation of the SA-1135 weld, the margin reduces from [] (considering the thicker RV shell as shown in Table 5-2) to [] (as given in Table 5-5) when considering the thinner lower head. Since the reduced margin is still significantly larger than 1.0, this simplified analytical approach is deemed to be an acceptable means of addressing the structural discontinuity at the lower transition weld.

5.4 *Evaluation for Flaw Stability*

The flaw stability analysis is performed by calculating the applied J-integrals for various amounts of flaw extension with a safety factor (on pressure) of 1.25. The resulting applied J-integral curve can then be compared against the lower bound J-R curve for the weld metal. It is noted that applied J-integrals are also calculated with a safety factor on pressure of 1.15 for illustration of the $J_{0.1}/J_1$ margin with respect to the lower bound J-R curve at a flaw extension of 0.1 inch.

5.4.1 Reactor Vessel Shell Welds

For the controlling SA-1101 weld material of Turkey Point Units 3 and 4, the applied J-integral values are calculated and shown in Table 5-6 with the corresponding mean and lower bound J - R curve values shown in Table 5-7. The resulting J-applied curves are then compared against the lower bound J- R curve for this material in Figure 5-1. An evaluation line at a flaw extension of 0.1 inch is included to confirm the results of Table 5-2 by showing the margin between the applied J-integral with the safety factor of 1.15 and the lower bound J-integral resistance of the material. The requirement for ductile and stable crack growth is demonstrated by Figure 5-1 since the slope of the applied J-integral curve for a safety factor of 1.25 is less than slope of the lower bound J - R curve at the point where the two curves intersect.

5.4.2 Reactor Vessel Transition Welds and RV Nozzle Welds

As discussed in Section 5.3.2 and shown in Table 5-4, the limiting location for the Turkey Point reactor vessels is the inlet nozzle with a margin of []. The applied J-integral for the inlet nozzle with a safety factor of 1.25 on pressure at various flaw extensions is plotted with the lower bound J-resistance curve in Figure 5-2. The slope of the applied J-integral is less than the slope of the lower bound J-resistance curve at the point of intersection, which demonstrates that the flaw is stable as required by ASME Section XI, Appendix K.



Table 5—2 Plant Specific Flaw Evaluation Summary for RV Shell Regions

--	--

Table 5—3 Reactor Vessel Nozzle Belt Dimensions

--	--

Table 5—4
Flaw Evaluation Summary of Turkey Point Upper Transition and RV Nozzle-to-Shell Welds

--	--

Table 5—5
Flaw Evaluation Summary of Turkey Point Lower Transition Welds

--	--

Table 5—6
Applied J-Integral versus Flaw Extensions of Turkey Point Controlling RV Shell Weld (SA-1101)

--	--

Table 5—7
Mean & Lower Bound J-R Curve Values for Turkey Point Controlling RV Shell Weld
(SA-1101)

--	--

Figure 5—1
J-Integral Flaw Extension for Turkey Point Controlling Reactor
Vessel Shell weld (SA-1101)

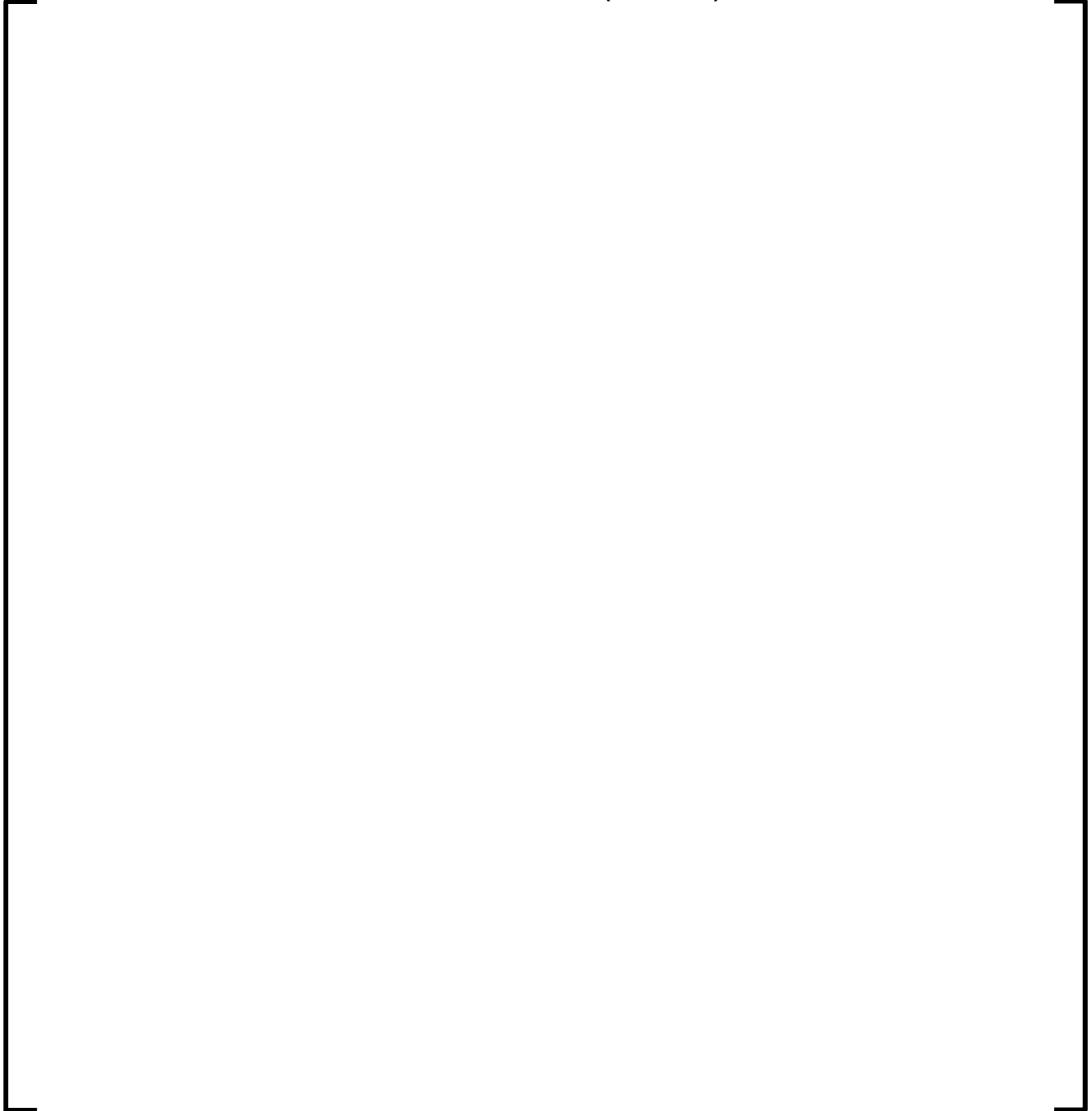


Figure 5—2
J-Integral versus Flaw Extension for Turkey Point Inlet Nozzle



6.0 SUMMARY AND CONCLUSIONS

6.1 *Reactor Vessel Shell Welds*

The ASME Section XI, acceptance criteria for Levels A & B Service Loads for all reactor vessel shell welds are satisfied. The results of the limiting welds for Turkey Point Units 3 and 4 are reported below.

- The limiting RV shell weld is TP 3 and 4 circumferential weld SA-1101. With factors of safety of 1.15 on pressure and 1.0 on thermal loading, the applied J-integral (J_1) is less than the J-integral of the material at a ductile flaw extension of 0.10 in. ($J_{0.1}$)—(Figure 5-1). The ratio $J_{0.1}/J_1 = [\quad]$ is significantly greater than the required value of 1.0.
- With a factor of safety of 1.25 on pressure and 1.0 on thermal loading, flaw extensions are ductile and stable since the slope of the applied J-integral curve is less than the slope of the lower bound J-R curve at the point where the two curves intersect (Figure 5-1).

6.2 *Reactor Vessel Transition Welds and RV Nozzle Welds*

The acceptance criteria for Levels A & B Service Loads for RV transition welds and RV nozzle welds are satisfied. The results of the limiting weld considering transition welds and RV nozzle welds (inlet and outlet) for Turkey Point are reported below.

- The limiting weld for the Turkey Point Units 3 and 4 RV transition welds (upper and lower) and the RV nozzle welds is the RV inlet nozzle-to-shell weld. With factors of safety of 1.15 on pressure and 1.0 on thermal loading, the applied J-integral (J_1) is less than the J-integral of the material at a ductile flaw extension of 0.10 in. ($J_{0.1}$) (Figure 5-2). The ratio $J_{0.1}/J_1 = [\quad]$ is significantly greater than the required value of 1.0.

- With a factor of safety of 1.25 on pressure and 1.0 on thermal loading, flaw extensions are ductile and stable since the slope of the applied J-integral curve is less than the slope of the lower bound J-R curve at the point where the two curves intersect (Figure 5-2).

7.0 REFERENCES

1. BAW-2192PA, Revision 00, "Low Upper Shelf Toughness Fracture Analysis of Reactor Vessels of B&W Owners Group Reactor Vessel Working Group for Levels A and B Conditions," April 1994, ADAMS Accession (Legacy) 9406240261 (P), 9312220294 (NP)
2. NRC Regulatory Issue Summary 2014-11, Information on Licensing Applications for Fracture Toughness Requirements for Ferritic Reactor Coolant Pressure Boundary Components
3. BAW-2192P, Supplement 1, Revision 00, "Low Upper Shelf Toughness Fracture Analysis of Reactor Vessels of B&W Owners Group Reactor Vessel Working Group for Levels A and B Conditions, December 2017
4. Code of Federal Regulations, Title 10, Part 50 – Domestic Licensing of Production and Utilization Facilities, Appendix G – Fracture Toughness Requirements, Federal Register Vol. 60. No. 243, December 19, 1995.
5. BAW-2251A, "Demonstration of the Management of Aging Effects for the Reactor Vessel, The B&W Owners Group Generic License Renewal Program," August 1999, ADAMS Accession Number 9909300150
6. Not used
7. Not used
8. Not used
9. Not used
10. Not used
11. TURKEY POINT UNITS 3 AND 4 - ISSUANCE OF AMENDMENTS REGARDING EXTENDED POWER UPRATE (TAC NOS. ME4907 AND ME4908)," Adams Accession number ML11293A365

12. LICENSE AMENDMENT REQUEST FOR EXTENDED POWER UPRATE, ATTACHMENT 4, L-2010-113, Attachment 4 ADAMS --ML103560177
13. Supplemental Response to NRC Request for Additional Information (RAI) Regarding Extended Power Uprate (EPU) License Amendment Request (LAR) No. 205 and Equivalent Margin Analysis (EMA), L-2010-303, ADAMS-ML103610321
14. Response to NRC Request for Additional Information Regarding Extended Power Uprate License Amendment Request No. 205 and Reactor Materials Issues – Round 1, L-2011-029, ADAMS--ML110700068
15. NRC Regulatory Guide 1.161, Evaluation of Reactor Pressure Vessels With Charpy Upper Shelf Energy Less Than 50 ft-lb
16. 2007 Edition (with 2008 Addenda) ASME & Boiler Pressure Vessel Code, Section XI, Rules for Inservice Inspection of Nuclear power Plant Components, Appendix K
17. 2013 Edition ASME & Boiler Pressure Vessel Code, Section XI, Rules for Inservice Inspection of Nuclear power Plant Components, Appendix K
18. BAW-1975, Applicability of the HSST Program Second and Third Irradiation Series Data to the Integrity of Nuclear Reactor Vessels, A.L. Lowe, June 1987
19. Not used
20. Not used
21. BAW-1543, Revision 4, Supplement 6-A, Supplement to the Master Integrated Reactor Vessel Surveillance Program, June 2007
22. ANP-3647P-000, Low Upper-Shelf Toughness Fracture Mechanics Analysis of Turkey Point Units 3 and 4 Reactor Vessels for Levels C & D Service Loads at 80-Years, January 2018

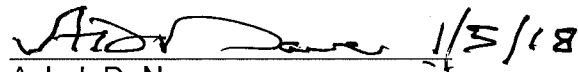
8.0 CERTIFICATION

This report is an accurate description of the low upper-shelf toughness fracture analysis of Turkey Point Units 3 and 4 reactor vessels.

 1/5/18


Mark A. Rinckel
Nuclear Analysis Unit

This report has been reviewed and is an accurate description of the low upper-shelf toughness fracture analysis of reactor vessels of Turkey Point Units 3 and 4.

 1/5/18

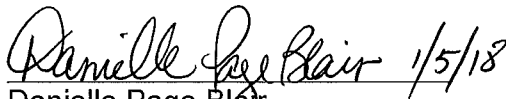
Ashok D. Nana
Component Analysis and Fracture
Mechanics Unit

Verification of independent review.

 1/5/18

David R. Cofflin
Component Analysis and Fracture
Mechanics Unit

This report is approved for release.

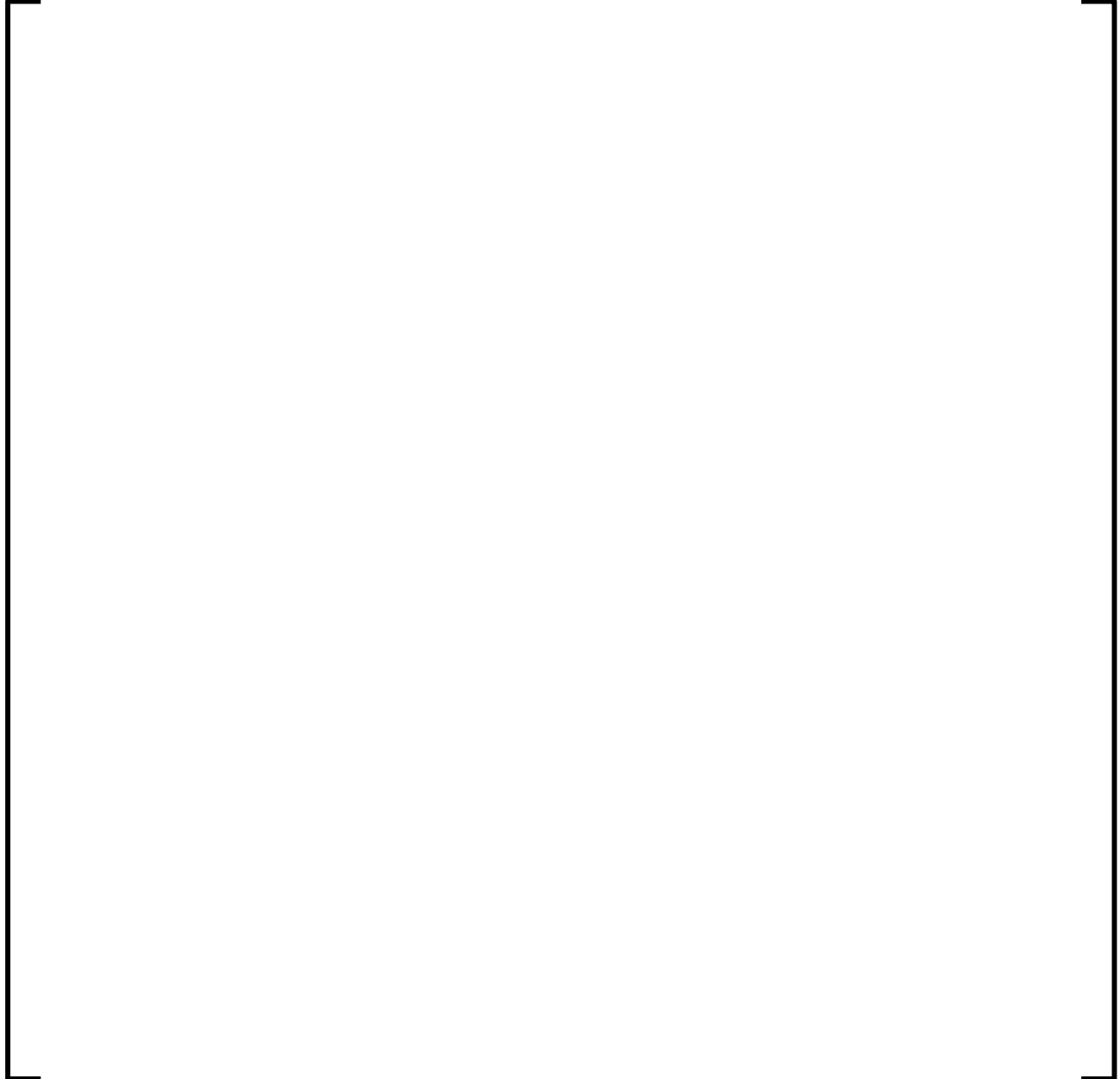
 1/5/18

Danielle Page Blair
NSSS Project Management

APPENDIX A

B&WOG J-R MODEL-DATA ANALYSIS AND EMPIRICAL MODEL DEVELOPMENT

A.1 *Background*



Low Upper-Shelf Toughness Fracture Mechanics Analysis of Turkey Point Units 3 and 4
Reactor Vessels for Levels A & B Service Loads at 80-Years
Topical Report

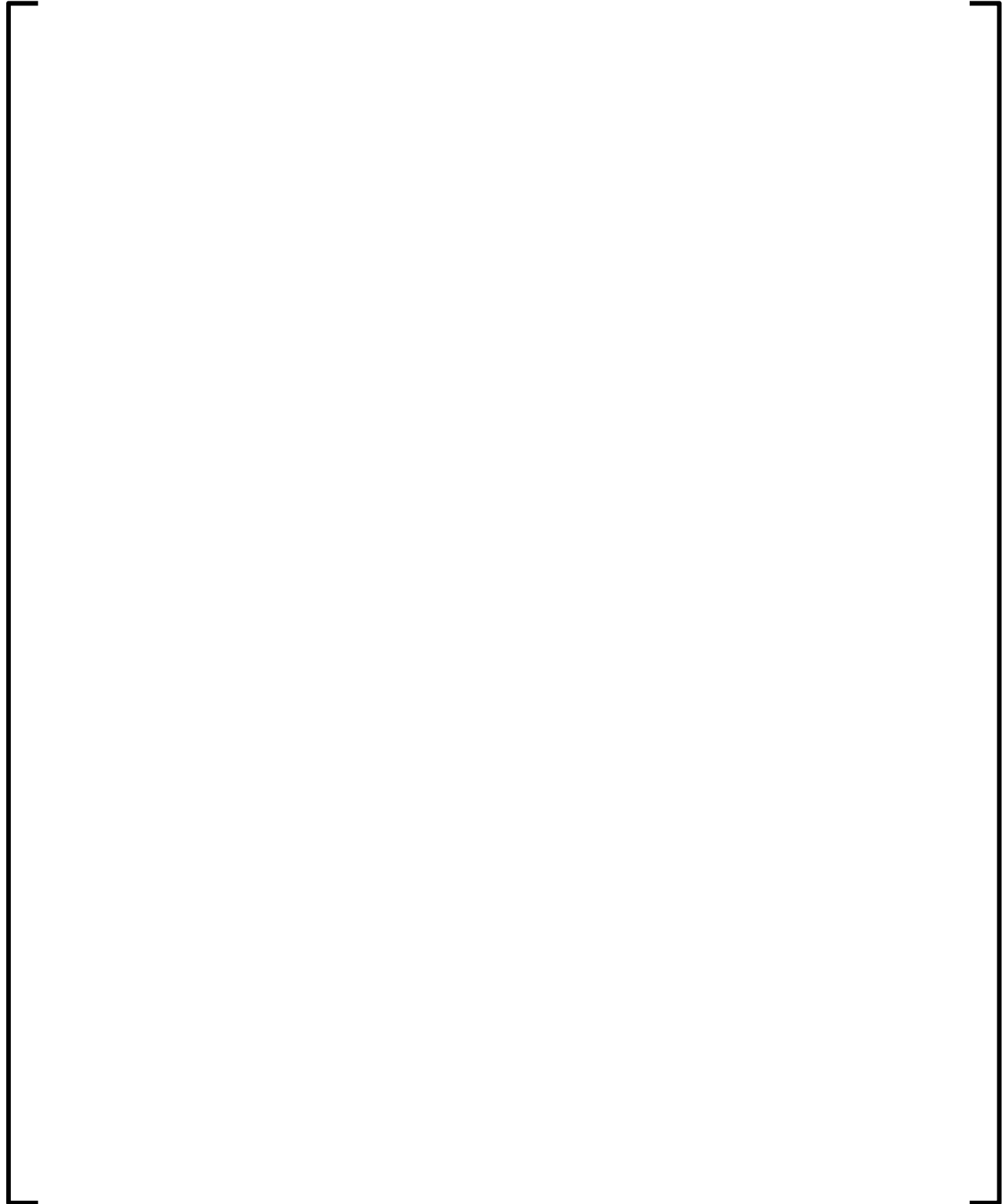


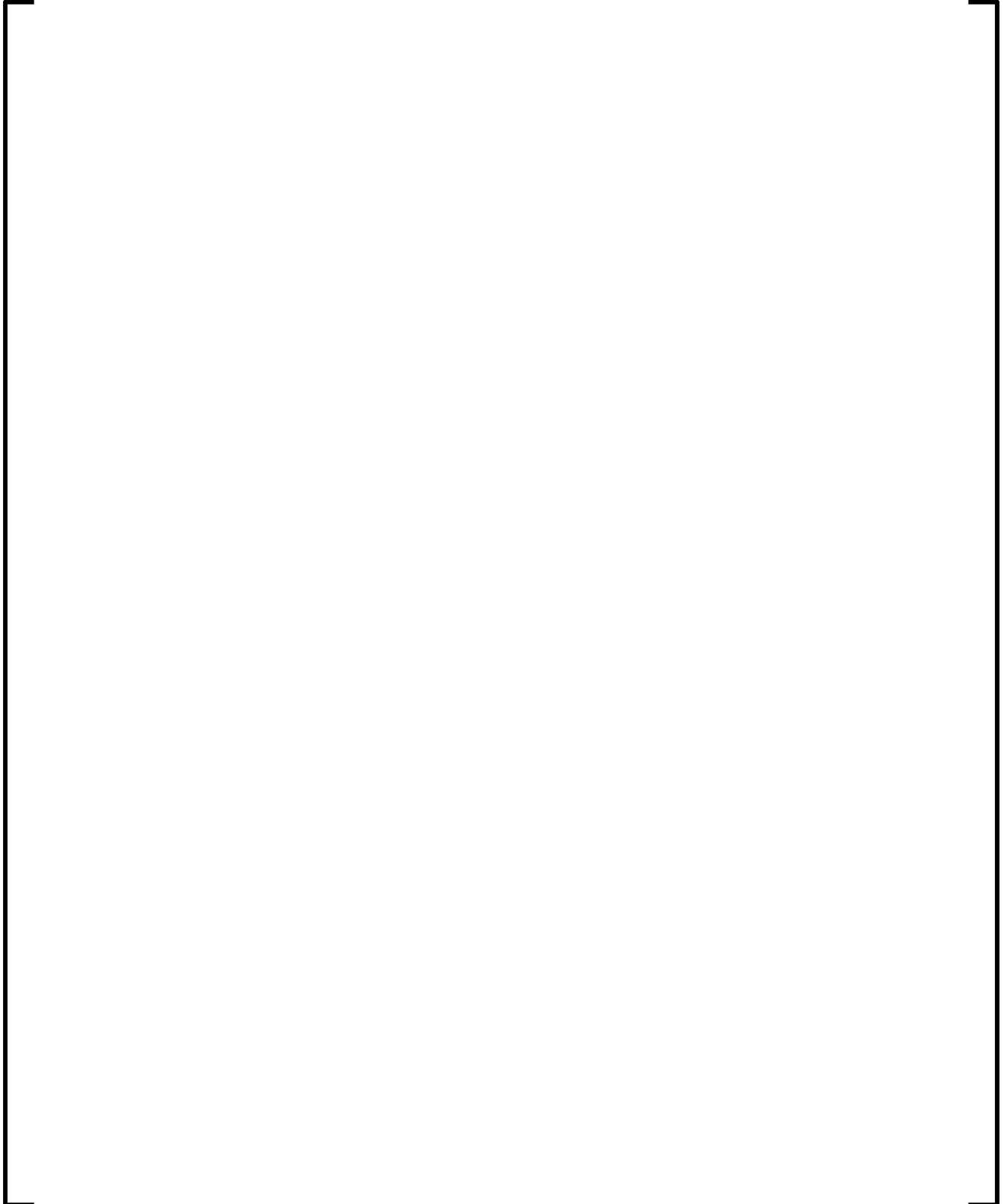
Table A—1 Model 4B, Range of Test Data

--

Figure A—1 BAW-2251A, Appendix B, Figure 3-1



A.2 *New B&WOG J- Δa Data and Comparison to B&WOG J-R Model*



Low Upper-Shelf Toughness Fracture Mechanics Analysis of Turkey Point Units 3 and 4
Reactor Vessels for Levels A & B Service Loads at 80-Years
Topical Report

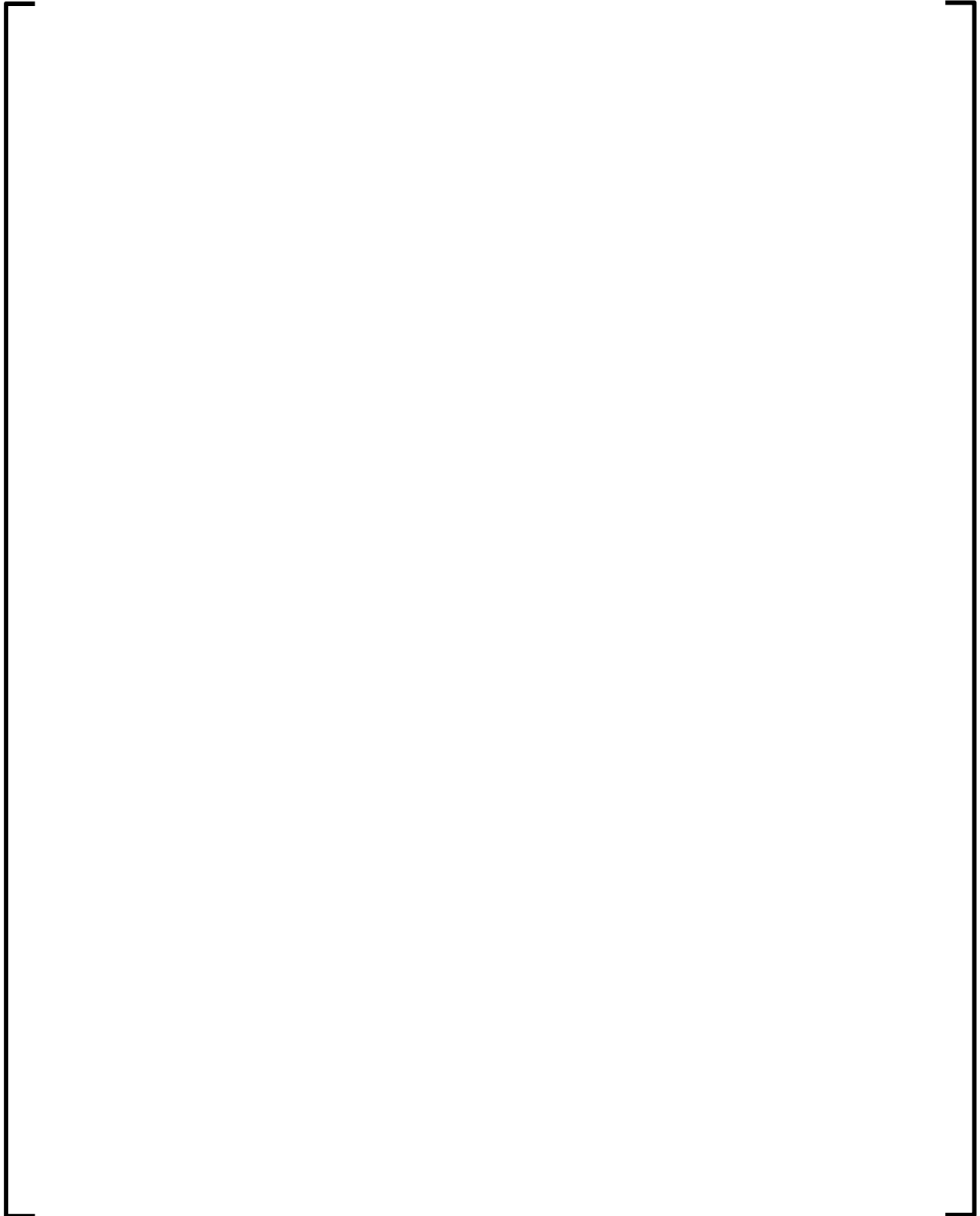
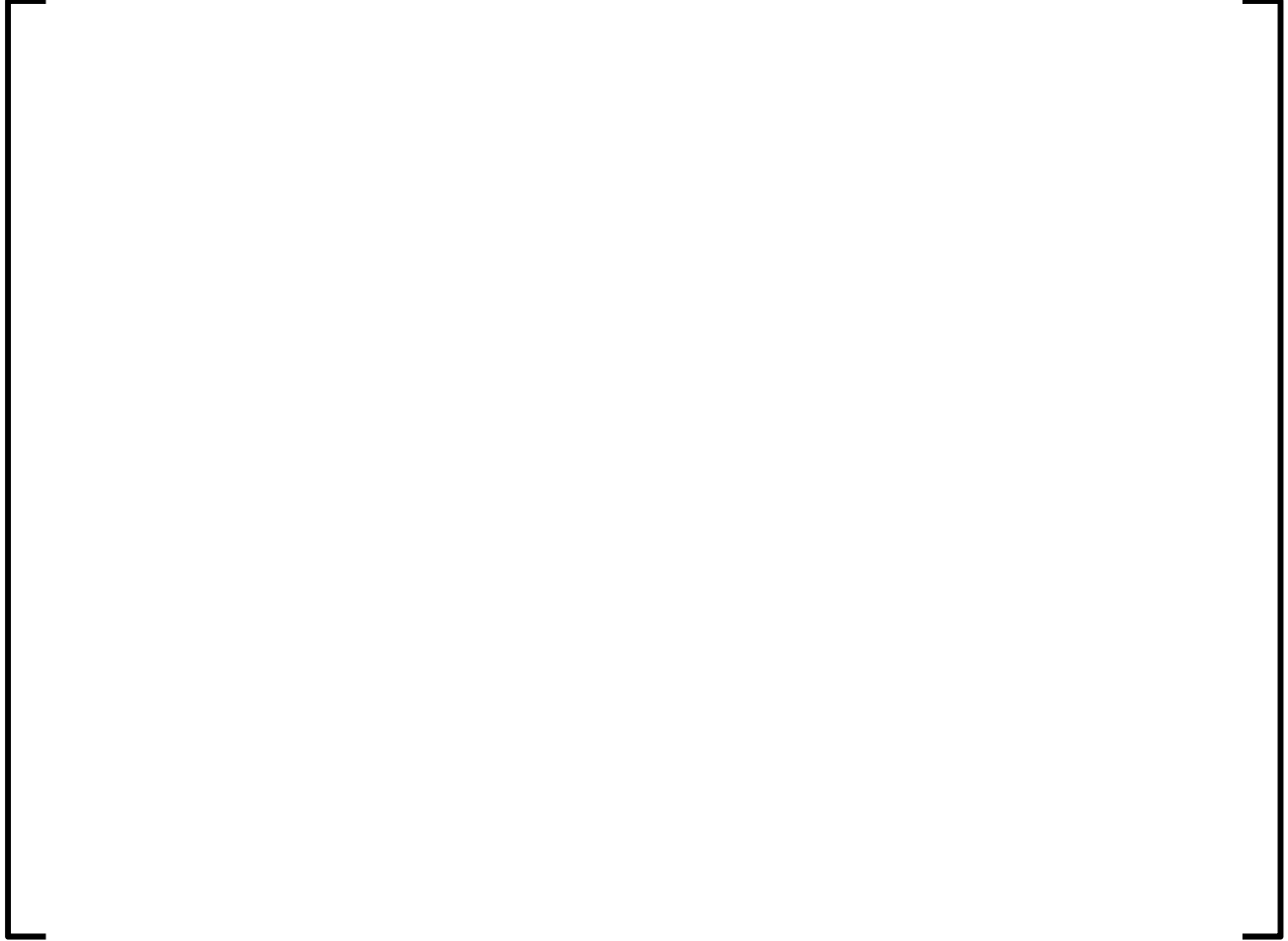
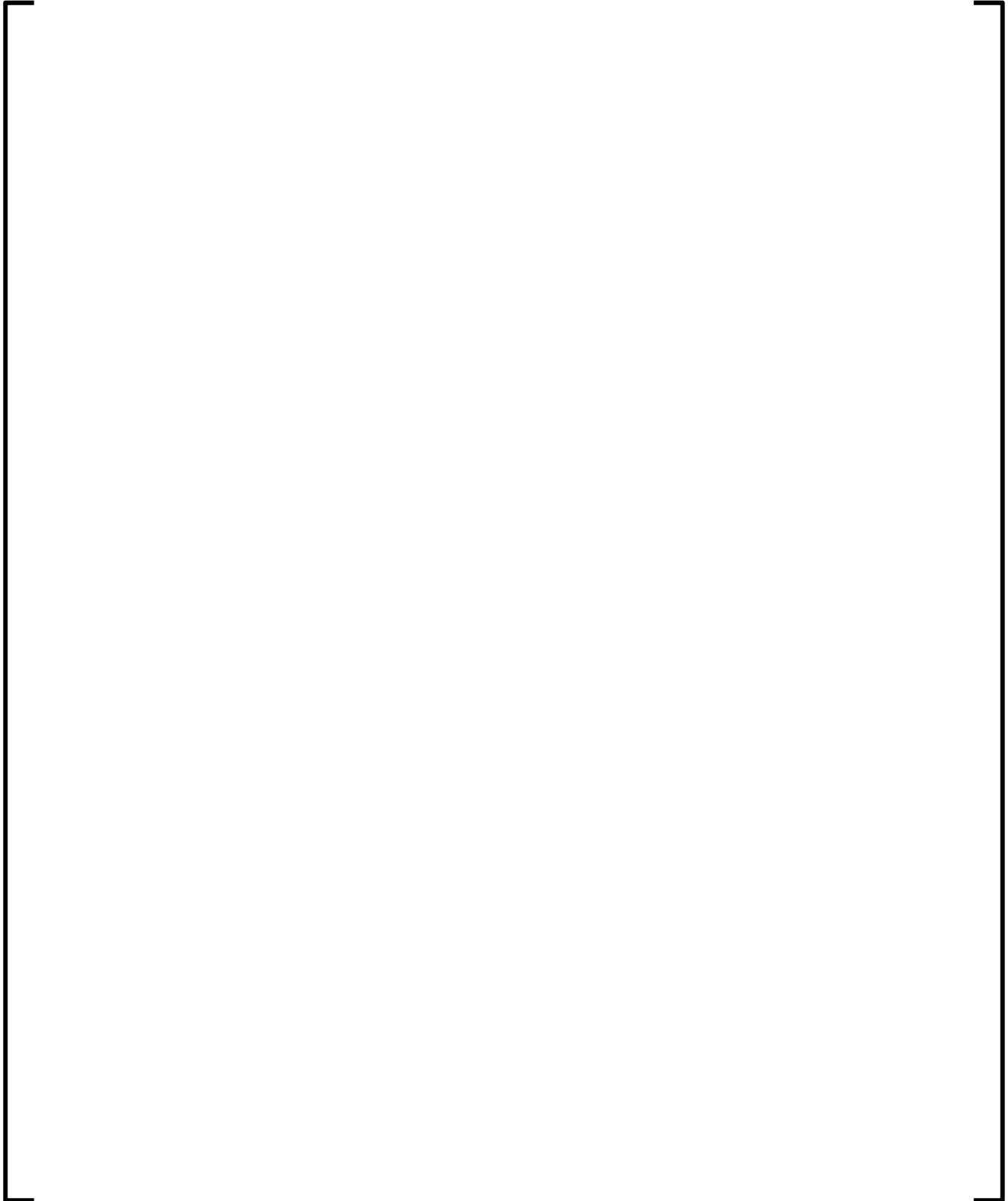


**Figure A—2 Jd (0.1) vs Fluence B&WOG J-R Model 4B and New
Test Data (Normalized to Standard Conditions)**



A.3 *New B&WOG J-R Model*



Low Upper-Shelf Toughness Fracture Mechanics Analysis of Turkey Point Units 3 and 4
Reactor Vessels for Levels A & B Service Loads at 80-Years
Topical Report

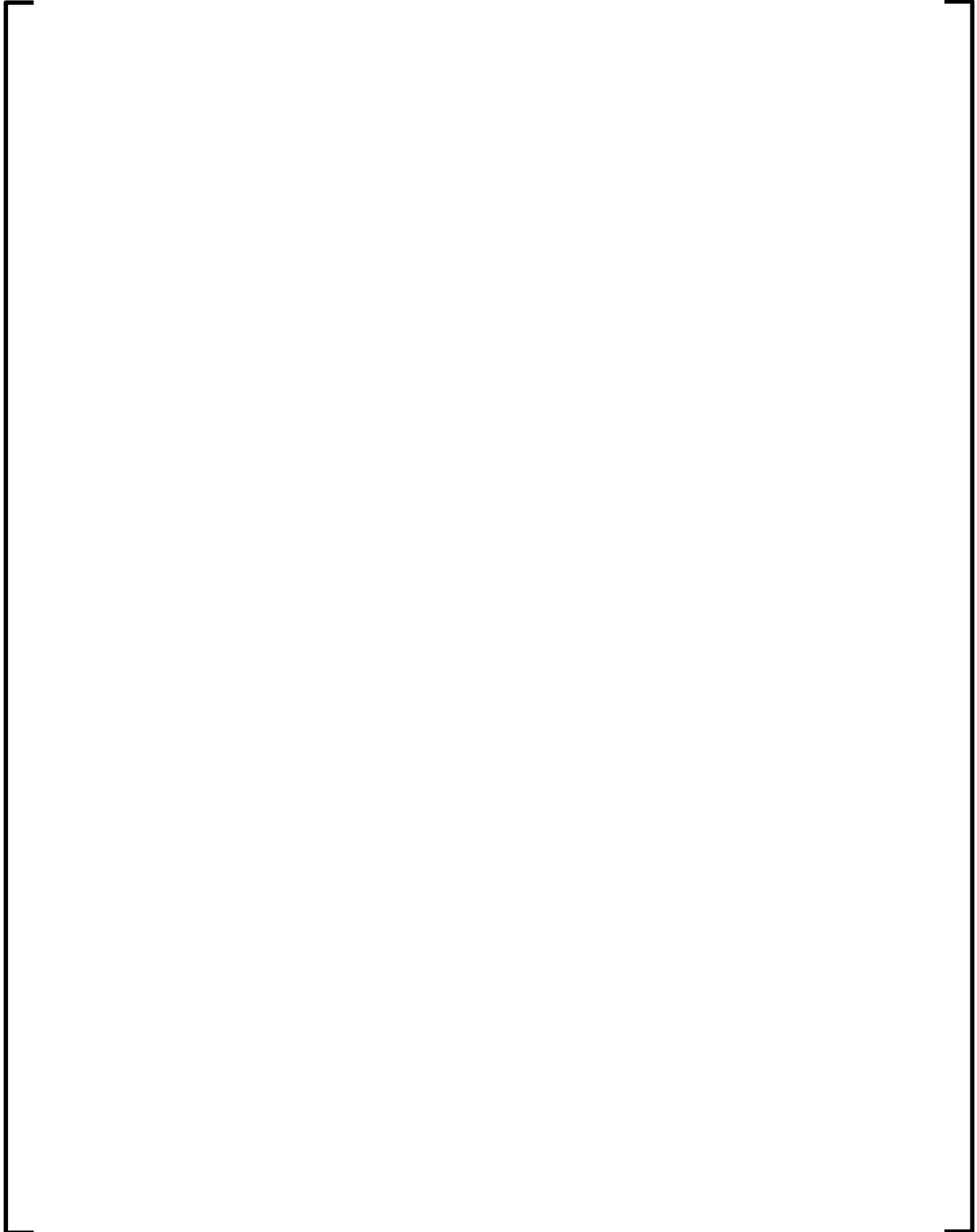


Table A—3 Jd Model Coefficients (Models 4B, 5B, and 6B)

--	--

**Figure A—3 Original and New Data and Model Fit Normalized at
Standardized Conditions vs Δa**



**Figure A—4 Original and New Data and Model Fit Normalized at
Standard Conditions vs Fluence**

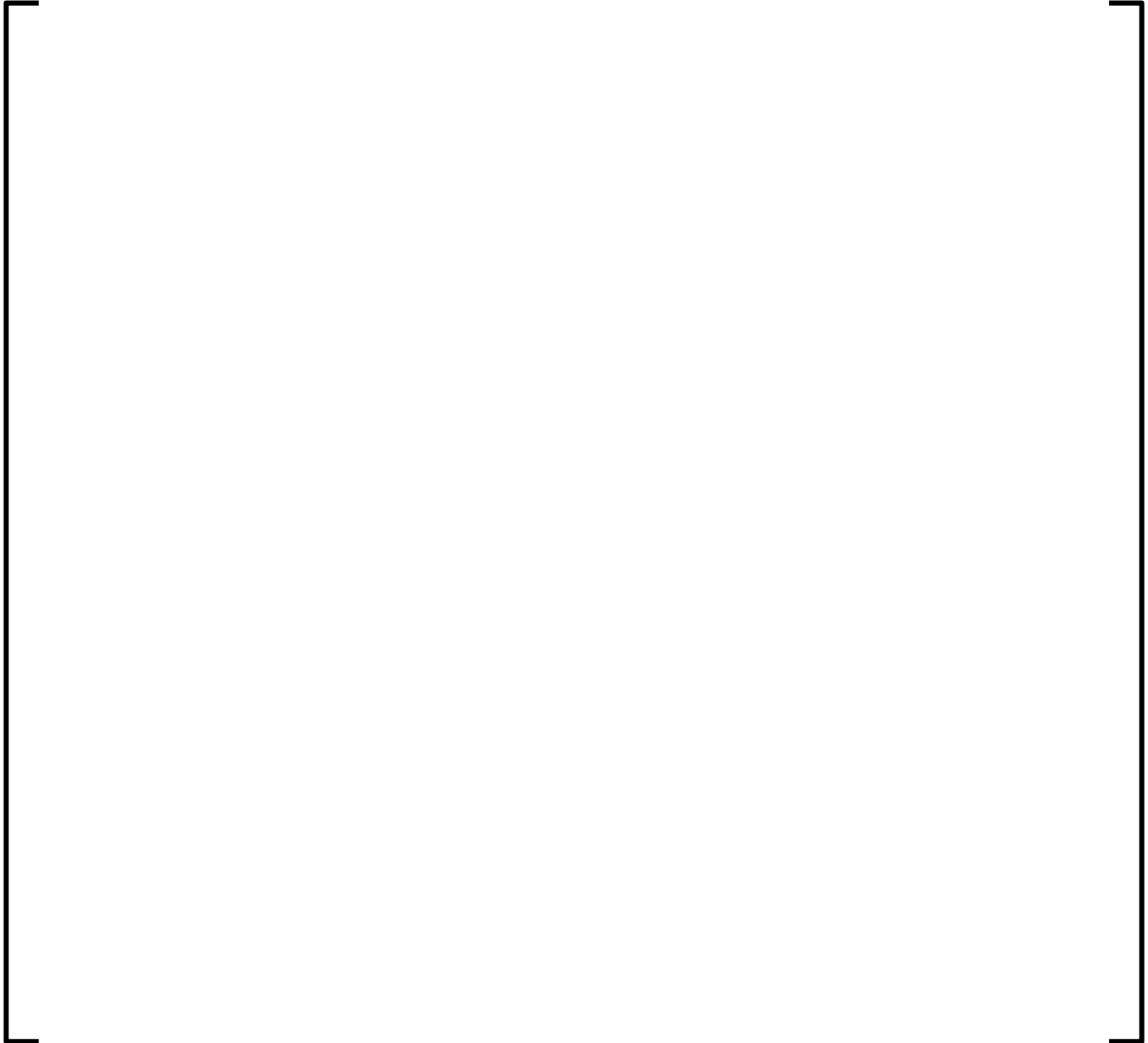


Figure A—5 Model 6B Residuals vs Fitted Values



Figure A—6 Model 6B Standardized Residuals vs Fitted Values



Figure A—7 Normal Q-Q Plot of Standardized Residuals



A.4 *Model 6B Reconciliation to EMA Results Presented in Section 6.0*

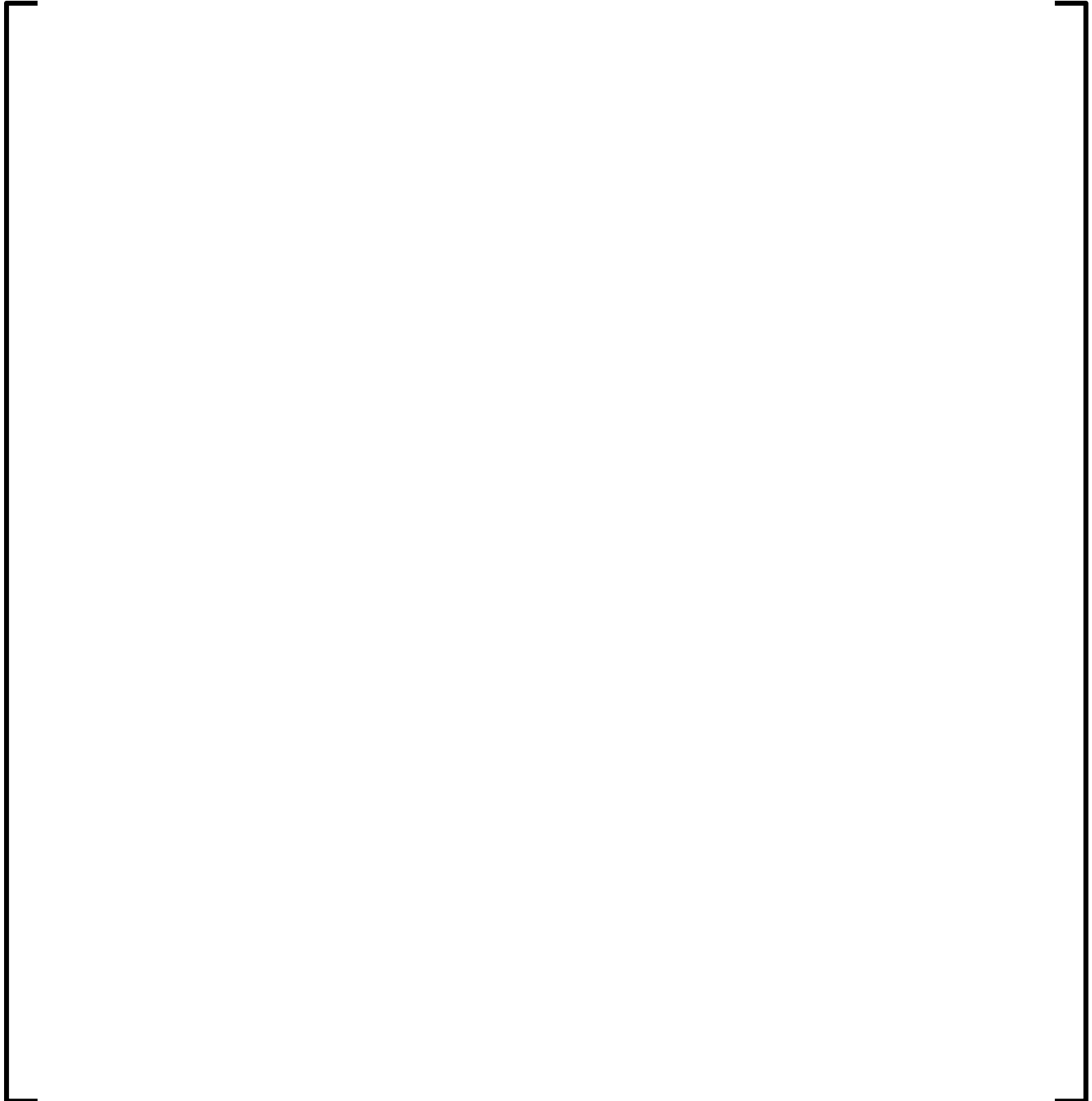


**Figure A—8 Comparison of Models 4B, 5B, and 6B at Standard
Conditions**



**Table A—4 EMA Reconciliation for Limiting RV Shell Welds—
Models 4B and 6B**

A.5 Summary and Conclusions



Enclosure 4
Non-proprietary Reference Documents
and
Redacted Versions of Proprietary
Reference Documents
(Public Version)
Attachment 3

**Areva Topical Report, ANP-3647NP Revision 0,
Low Upper-Shelf Toughness Fracture Mechanics Analysis of
Turkey Point Units 3 and 4 Reactor Vessels for Levels C & D
Service Loads at 80 Years January 5, 2018 (Non-proprietary)**

(53 Total Pages, including cover sheets)



Low Upper-Shelf Toughness Fracture Mechanics Analysis of Turkey Point Units 3 and 4 Reactor Vessels for Levels C & D Service Loads at 80-Years

ANP-3647NP
Revision 0

Topical Report

January 2018

AREVA Inc.

(c) 2018 AREVA Inc.

Copyright © 2018

**AREVA Inc.
All Rights Reserved**

Nature of Changes

Item	Section(s) or Page(s)	Description and Justification
1	All	Initial Issue

Contents

	<u>Page</u>
1.0 INTRODUCTION	1-1
1.1 Equivalent Margins Analysis—Analysis of Record	1-3
2.0 REGULATORY REQUIREMENTS	2-1
2.1 Regulatory Requirements	2-1
2.2 Compliance with 10 CFR 50 Appendix G and Acceptance Criteria	2-2
2.2.1 Acceptance Criteria Levels C and D	2-3
3.0 DESCRIPTION OF TURKEY POINT REACTOR VESSELS	3-1
4.0 MATERIAL PROPERTIES AND LEVELS C&D SERVICE LOADINGS	4-1
4.1 J-Integral Resistance Model	4-1
4.2 Mechanical Properties of Weld Metals	4-3
4.2.1 Mechanical Properties for the Turkey Point Reactor Vessels	4-4
4.3 Levels C and D Service Loadings	4-5
4.3.1 Turkey Point	4-5
5.0 FRACTURE MECHANICS ANALYSIS	5-1
5.1 Methodology	5-1
5.2 Procedure for Evaluating Levels C and D Service Loadings	5-2
5.2.1 Processing of Transient Time-History Data	5-3
5.2.2 Temperature Range for Upper Shelf Fracture Toughness Evaluations	5-3
5.2.3 Cladding Effects	5-4
5.3 Evaluation for Levels C and D Service Loadings	5-7
5.3.1 Reactor Vessel Shell Welds	5-8
5.3.2 Reactor Vessel Transition Welds and RV Nozzle Welds	5-10
6.0 SUMMARY AND CONCLUSIONS	6-1
6.1 Reactor Vessel Shell Welds	6-1
6.2 Reactor Vessel Transition Welds and RV Nozzle Welds	6-2
7.0 REFERENCES	7-1
8.0 CERTIFICATION	8-1

List of Tables

Table 3—1 Reactor Vessel Weld Locations--Copper Content and 80-Year Fluence Projections	3-2
Table 3—2 Reactor Vessel Shell Dimensions.....	3-3
Table 3—3 Reactor Vessel Nozzle Belt Dimensions	3-4
Table 4—1 Parameters in Jd Model 4B	4-3
Table 4—2 Mechanical Properties of Turkey Point RV Materials.....	4-4
Table 5—1 Turkey Point J-Integral versus Flaw Extension for Levels C & D Service Loadings	5-12
Table 5—2 Turkey Point-J-R Curves for Evaluation of Levels C & D Service Loadings	5-13
Table 5—3 Turkey Point-Levels C & D Results for Nozzle to Shell and Upper Transition Welds.....	5-14

List of Figures

Figure 3—1	Reactor Vessel—Turkey Point Unit 3	3-5
Figure 3—2	Reactor Vessel—Turkey Point Unit 4	3-6
Figure 4—1	Turkey Point Steam Line Break Transients	4-6
Figure 5—1	Turkey Point-KI versus Crack Tip Temperature for Levels C & D Service Loadings	5-15
Figure 5—2	Turkey Point-J-Integral versus Flaw Extension for Levels C & D Service Loadings	5-16
Figure 5—3	Turkey Point- Levels C & D Applied J Integral vs Crack Tip Temperature for the Outlet Nozzle to Shell Weld.....	5-17
Figure 5—4	Turkey Point- Levels C & D Applied J Integral vs Crack Extension for the Outlet Nozzle to Shell Weld	5-18

Nomenclature

Acronym**Definition**

B&W	Babcock and Wilcox
B&WOG	Babcock and Wilcox Owners Group
CvUSE	Charpy Upper Shelf Energy
EPFY	Effective Full Power Years
EMA	Equivalent Margins Analysis
INF	Inlet Nozzle Forging
Jd	J deformation
J-R	J-integral Resistance
ONF	Outlet Nozzle Forging
PTN	Turkey Point Plant
RV	Reactor Vessel
RVWG	Reactor Vessel Working Group
SLR	Subsequent License Renewal
Sy	Yield Strength
TSs	Technical Specifications
USE	Upper Shelf Energy

ABSTRACT

This topical report presents the results of an equivalent margins analysis (EMA) considering Levels C and D service loads for high copper Linde 80 weld metals and applicable non-Linde 80 welds using fluence values expected at 80-years (subsequent license renewal--SLR). This topical report applies to the following Westinghouse-designed reactor vessels fabricated by B&W: Turkey Point Plant (PTN) Units 3 and 4. Note that the Turkey Point EMA reported herein is technically identical to the Turkey Point EMA reported in BAW-2178P, Supplement 1, Revision 0, which was submitted to the NRC by the PWROG on December 15, 2017. That is, Sections 1.0 through 7.0 of ANP-3647P were generated by extracting Turkey Point 3 and 4-specific results from Sections 1.0 through 7.0 of BAW-2178, Supplement 1, Revision 0. The B&WOG J-integral resistance model is discussed in Appendix A to ANP-3646P, which is identical to Appendix A of BAW-2192, Supplement 1, Revision 0, with the exception that references to plants other than Turkey Point 3 and 4 were removed from Sections A.1, A.2, and A.4.

The analytical procedure used in this supplement is in accordance with ASME Section XI, Appendix K, Subarticle K-1200, with selection of design transients based on the guidance in Regulatory Guide 1.161, Section 4.0. EMA results are reported for all reactor vessel weld locations with 80-year fluence projections that exceed $1.0 \text{ E}+17 \text{ n/cm}^2$ ($E > 1.0 \text{ MeV}$). The ASME Section XI, acceptance criteria for Levels C & D Service Loads for all reactor vessel shell welds are satisfied. The acceptance criteria for Levels C & D Service Loads for RV transition welds and RV nozzle welds are also satisfied. Consistent with BAW-2178PA, Revision 0, B&WOG J-R Model 4B is used for the Linde 80 welds.

The EMA utilizes the B&WOG J-integral resistance (J-R) Model 4B reported in BAW-2192PA, Appendix B. Model 4B was developed based on fracture toughness test data obtained through approximately 1990, with specimen fluence that ranges from 0.0 to $8.45\text{E}+18 \text{ n/cm}^2$. Eighty-year fluence estimates for Turkey Point Units 3 and 4 exceeds $8.45\text{E}+18 \text{ n/cm}^2$ (e.g., maximum 80-year 1/4 T fluence at a crack extension of 0.1 inches is estimated at $6.38\text{E}+19 \text{ n/cm}^2$) and use of Model 4B to estimate J-integral resistance values, including the associated model uncertainty, for 80-years is made by extrapolation of the model. To assess the model extrapolation uncertainty, Model 4B is compared to new fracture toughness test data (1990 to 2017) irradiated to fluence ranging from $8.0\text{E}+18 \text{ n/cm}^2$ to $5.8\text{E}+19 \text{ n/cm}^2$. The majority of test data fell above the Model 4B mean and all of the test data fell above the Model 4B mean minus 2 standard error band. Therefore, use of Model 4B and associated uncertainty to extrapolate J-integral resistance for 80-year fluence applications was determined to be appropriate. This assessment is reported in ANP-3646P, Rev. 0, Appendix A.

To further substantiate the use of Model 4B, all of the original fracture toughness data used to develop Model 4B was combined with new fracture toughness data, using the same model form, and a new Model 6B was generated. Model 6B was found to be essentially equivalent to Model 4B with respect to model mean and 2 standard errors. The EMA results reported herein using Model 4B were reconciled to Model 6B, with little or no change to the EMA results. Model 6B development and the EMA reconciliation to Model 4B are reported in ANP-3646P, Rev. 0, Appendix A.

1.0 INTRODUCTION

The purpose of this topical report is to present an equivalent margins analysis (EMA) considering Levels C and D service loads for high copper Linde 80 weld metals and applicable non-Linde 80 welds using fluence values expected at 80-years (subsequent license renewal--SLR). This topical report applies to the following Westinghouse-designed reactor vessels fabricated by B&W: Turkey Point Plant (PTN) Units 3 and 4 (also referred to as Turkey Point Units 3 and 4). Note that the Turkey Point EMA reported herein is technically identical to the Turkey Point EMA reported in BAW-2178P, Supplement 1, Revision 0 [4], which was submitted to the NRC by the PWROG on December 15, 2017. That is, Sections 1.0 through 7.0 of ANP-3647P were generated by extracting Turkey Point 3 and 4-specific results from Sections 1.0 through 7.0 of BAW-2178, Supplement 1, Revision 0. The B&WOG J-integral resistance model is discussed in Appendix A to ANP-3646P, which is identical to Appendix A of BAW-2192, Supplement 1, Revision 0 [6], with the exception that references to plants other than Turkey Point 3 and 4 were removed from Sections A.1, A.2, and A.4.

The EMA reported herein utilizes the B&WOG J-integral resistance (J-R) Model 4B reported in BAW-2192PA, Appendix B. Justification for use of Model 4B for 80-year fluence is addressed in ANP-3646P, Rev. 0, Appendix A [3].

Equivalent margins analyses are reported for all reactor vessel weld locations with 80-year fluence projections that exceed $1.0 \text{ E}+17 \text{ n/cm}^2$ ($E > 1.0 \text{ MeV}$). Upper shelf energy evaluations at reactor vessel base metal locations with 80-year fluence projections greater than $1.0 \text{ E}+17 \text{ n/cm}^2$, if needed, will be addressed separately in the Turkey Point Units 3 and 4 subsequent license renewal application.

The following groups are used for the welds within the scope of this report.

- Reactor Vessel Shell Welds—circumferential welds for Turkey Point Units 3 and 4 (also referred to as Turkey Point reactor vessels). There are no geometric discontinuities at these weld locations and all reactor vessel shell welds surround the effective height of the active core. These locations have historically been considered “beltline” or “beltline region” as defined by 10 CFR 50, Appendix G. All reactor vessel shell welds are Linde 80 welds.
- Transition Welds and RV Nozzle Welds—welds that are located above and below the reactor vessel shell welds that may experience 80-year fluence greater than $1.0 \text{ E}+17 \text{ n/cm}^2$ and must consider the effects of neutron irradiation embrittlement. In addition, the transition welds are located at geometric discontinuities (e.g., lower shell to lower head and upper shell to nozzle belt forging). These locations may or may not have been included as part of the 10 CFR 50 Appendix G [5] “beltline” definition for 60-years for the participating plants. All transition welds and RV nozzle welds (also referred to as RV nozzle-to-shell welds) are Linde 80.

The EMA evaluations in this report are for all weld locations expected to receive fluence $> 1.0\text{E}+17 \text{ n/cm}^2$ [19] at 80 years. The use of the terms “beltline” and/or “extended beltline” are not used in this report.

The 60-year EMA summary reports for Turkey Point Units 3 and 4 are reported in Section 1.1. Section 2.0 provides the current NRC regulatory requirements for the EMA. Section 3.0 provides a description of all reactor vessels within the scope of this report, with illustrations of applicable reactor vessel welds in Figures 3-1 and 3-2. Section 4.0 provides the material properties that are required for the EMA, and Section 5.0 presents the results of the EMA. Section 6.0 provides the summary and conclusions, and Section 7.0 lists all references. ANP-3646P, Rev. 0, Appendix A [3] provides the technical justification for the use of B&WOG J-R Model 4B for the EMA reported herein.

1.1 *Equivalent Margins Analysis—Analysis of Record*

BAW-2178PA, Revision 00 [1] provided the EMA analysis of record for Levels C and D service loads for Turkey Point Units 3 and 4 for 40 years. For 60 years, Turkey Point Units 3 and 4 reported plant-specific evaluations. The summary reports for EMA analyses of record are as follows.

Turkey Point Units 3 and 4

The Turkey Point Units 3 and 4 current licensing basis equivalent margins analysis at 48 EFPY is summarized in Section 2.1.2 of NRC document “TURKEY POINT UNITS 3 AND 4 - ISSUANCE OF AMENDMENTS REGARDING EXTENDED POWER UPRATE (TAC NOS. ME4907 AND ME4908),” Adams Accession number ML11293A365 [12]. NRC acceptance of the Turkey Point EMA at 48 EFPY for EPU is based on the following documentation.

- LICENSE AMENDMENT REQUEST FOR EXTENDED POWER UPRATE, ATTACHMENT 4, L-2010-113, Attachment 4 ADAMS --ML103560177 [13]
- Supplemental Response to NRC Request for Additional Information (RAI) Regarding Extended Power Uprate (EPU) License Amendment Request (LAR) No. 205 and Equivalent Margin Analysis (EMA), L-2010-303, ADAMS-ML103610321 [14]. Reference [14] contains AREVA document 77-2312-03 (P), LOW UPPER-SHELF TOUGHNESS FRACTURE MECHANICS ANALYSIS OF REACTOR VESSELS OF TURKEY POINT UNITS 3 AND 4 FOR EXTENDED LIFE THROUGH 48 EFFECTIVE FULL POWER YEARS

- Response to NRC Request for Additional Information Regarding Extended Power Uprate License Amendment Request No. 205 and Reactor Materials Issues – Round 1, L-2011-029, ADAMS--ML110700068 [15]. Reference [15] provides a response to RAI CVIB-1.2 regarding the code year used to perform the equivalent margins analysis (i.e., 1998 Edition vs 2004 Edition). The NRC SER for the Turkey Point Extended Power Uprate, Section 2.1.2, contains the evaluation of upper shelf energy--ADAMS-ML 11293A365.

2.0 REGULATORY REQUIREMENTS

2.1 *Regulatory Requirements*

In accordance with 10 CFR 50 Appendix G [5], IV, A, 1, Reactor vessel Upper Shelf Energy Requirements are as follows.

- a. Reactor vessel beltline materials must have Charpy upper-shelf energy in the transverse direction for base material and along the weld for weld material according to the ASME Code, of no less than 75 ft-lb (102 J) initially and must maintain Charpy upper-shelf energy throughout the life of the vessel of no less than 50 ft-lb (68 J), unless it is demonstrated in a manner approved by the Director, Office of Nuclear Reactor Regulation or Director, Office of New Reactors, as appropriate, that lower values of Charpy upper-shelf energy will provide margins of safety against fracture equivalent to those required by Appendix G of Section XI of the ASME Code. This analysis must use the latest edition and addenda of the ASME Code incorporated by reference into 10 CFR 50.55a (b)(2) at the time the analysis is submitted.
- b. Additional evidence of the fracture toughness of the beltline materials after exposure to neutron irradiation may be obtained from results of supplemental fracture toughness tests for use in the analysis specified in section IV.A.1.a.
- c. The analysis for satisfying the requirements of section IV.A.1 of this appendix must be submitted, as specified in § 50.4, for review and approval on an individual case basis at least three years prior to the date when the predicted Charpy upper-shelf energy will no longer satisfy the requirements of section IV.A.1 of this appendix, or on a schedule approved by the Director, Office of Nuclear Reactor Regulation or Director, Office of New Reactors, as appropriate.

When the reactor vessels within the scope of this report were fabricated, Charpy V-notch tests of the reactor vessel welds were in accordance with the original construction code, which did not specifically require Charpy v-notch tests on the upper shelf. The applicable construction code is as follows.

- Turkey Point—ASME B&PV Code, Section III, 1965 Edition through Summer 1966 Addenda

In accordance with NRC Regulatory Guide 1.161 [16], the NRC has determined that the analytical methods described in ASME Section XI, Appendix K, provide acceptable guidance for evaluating reactor pressure vessels when the Charpy upper-shelf energy falls below the 50 ft-lb limit of Appendix G to 10 CFR Part 50. However, the staff noted that Appendix K does not provide information on the selection of transients and gives very little detail on the selection of material properties. Selection of design transients and selection of material properties are addressed in Sections 3.0 and 4.0.

The Linde 80 weld locations that are included within the scope of this report (i.e., weld locations with 80-year projected fluence $> 1.0E+17$ n/cm²) are all assumed to have upper shelf energy values below 50 ft-lb and thus require an equivalent margins analysis.

2.2 Compliance with 10 CFR 50 Appendix G and Acceptance Criteria

The analyses reported herein are performed in accordance with the 2007 Edition with 2008 Addenda [17] of Section XI of the ASME Code, Appendix K. The current edition of ASME Section XI listed in 10 CFR 50.55a is the 2013 Edition [18]. With regard to Appendix K, there are no differences between the 2007 Edition with 2008 Addenda and the 2013 Edition of ASME Section XI, and hence these ASME Section XI, Appendix K analyses are equally applicable to the 2013 Edition of the ASME Code.

The material properties used in this analysis are based on ASME Section II, Part D, 2007 Edition with 2008 Addenda. The only change in the material properties listed in the 2013 Edition of ASME Section II for the applicable properties is the coefficient of thermal expansion for stainless steel at 600°F; this value was changed from 9.8E-6 in/in/°F to 9.9E-6 in/in/°F. At the limiting time points in the Level C & D analysis, where cladding effects are included, the temperature of the cladding is well below 600°F, and thus this change does not impact the low upper shelf toughness analysis reported herein.

2.2.1 Acceptance Criteria Levels C and D

ASME Section XI [17], Subarticles K-2300 and K-2400, provide acceptance criteria for Levels C and D Service Conditions. Consistent with BAW-2178PA [1], the evaluations reported herein will utilize acceptance criteria applicable to Level C Service Loadings as summarized below.

- a) When evaluating adequacy of the upper shelf toughness for the weld material for Level C Service Loadings, interior semi-elliptical surface flaws with depths up to $1/10^{\text{th}}$ of the base metal wall thickness, plus the cladding thickness, with total depths not exceeding 1 in. (25 mm), and a surface length 6 times the depth, shall be postulated, with the flaw's major axis oriented along the weld of concern, and the flaw plane oriented in the radial direction. When evaluating adequacy of the upper shelf toughness for the base material, both interior axial and circumferential flaws shall be postulated, and toughness properties for the corresponding orientation shall be used. Flaws of various depths, ranging up to the maximum postulated depth, shall be analyzed to determine the most limiting flaw depth. Smaller maximum flaw sizes may be used when justified. Two criteria shall be satisfied:

1. The applied J-integral shall be less than the J-integral of the material at a ductile flaw extension of 0.10 in. (2.5 mm), using a structural factor of 1 on loading.
 2. Flaw extensions shall be ductile and stable, using a structural factor of 1 on loading.
- b) The J-integral resistance versus flaw extension curve shall be a conservative representation for the vessel material under evaluation.

The above Level C acceptance criteria will be conservatively imposed on the Level D transients defined in Section 4.3.1. In addition, for information purposes only, the acceptance criteria applicable to the Level D Service Loadings as summarized below will be reported for Level D transients.

- a) When evaluating adequacy of the upper shelf toughness for Level D Service Loadings, flaws as specified for Level C Service Loadings shall be postulated, and toughness properties for the corresponding orientation shall be used. Flaws of various depths, ranging up to the maximum postulated depth, shall be analyzed to determine the most limiting flaw depth. Flaw extensions shall be ductile and stable, using a factor of safety of 1.0 on loading.
- b) The J-integral resistance versus flaw extension curve shall be a best estimate representation for the vessel material under evaluation.
- c) The extent of stable flaw extension shall be less than or equal to 75% of the vessel wall thickness, and the remaining ligament shall not be subject to tensile instability.

3.0 DESCRIPTION OF TURKEY POINT REACTOR VESSELS

The Turkey Point reactor vessels with applicable weld locations are shown in Figure 3-1 and Figure 3-2. All weld locations evaluated for equivalent margins in this report are identified by an asterisk (*) in each figure. The Linde 80 welds copper and nickel content and 80-year fluence projections data needed for the equivalent margins analysis are provided in Table 3—1. The fluence projections are reported for all reactor vessel weld locations that are expected to exceed $1.0\text{E}+17$ n/cm² at 80 years. The 80-year fluence projections are conservative estimates based on detailed transport calculations completed by Westinghouse Electric Corporation using a methodology that is in compliance with Regulatory Guide 1.190 (i.e., Westinghouse Report WCAP-14040-A, Revision 4, “Methodology Used to Develop Cold Overpressure Mitigating System Setpoints and RCS Heatup and Cooldown Limit Curves,” May 2004.)

Copper and nickel content of the reactor vessel shell welds is consistent with EMA analyses of record reported in Section 1.1; the copper and nickel content for transition welds and RV nozzle-to-nozzle belt forging welds reported in Table 3-1 were obtained from either the EMA analyses of record or a search of Turkey Point reactor vessel fabrication reports.

The dimensions of the reactor vessel shell geometry for the Turkey Point reactor vessels are provided in Table 3-2. Similarly, the dimensions for the reactor vessel nozzle belt region located above the reactor vessel shell course are given in Table 3-3.

Low Upper-Shelf Toughness Fracture Mechanics Analysis of Turkey Point Units 3 and 4
Reactor Vessels for Levels C & D Service Loads at 80-Years
Topical Report

**Table 3—1 Reactor Vessel Weld Locations--Copper Content and
80-Year Fluence Projections**

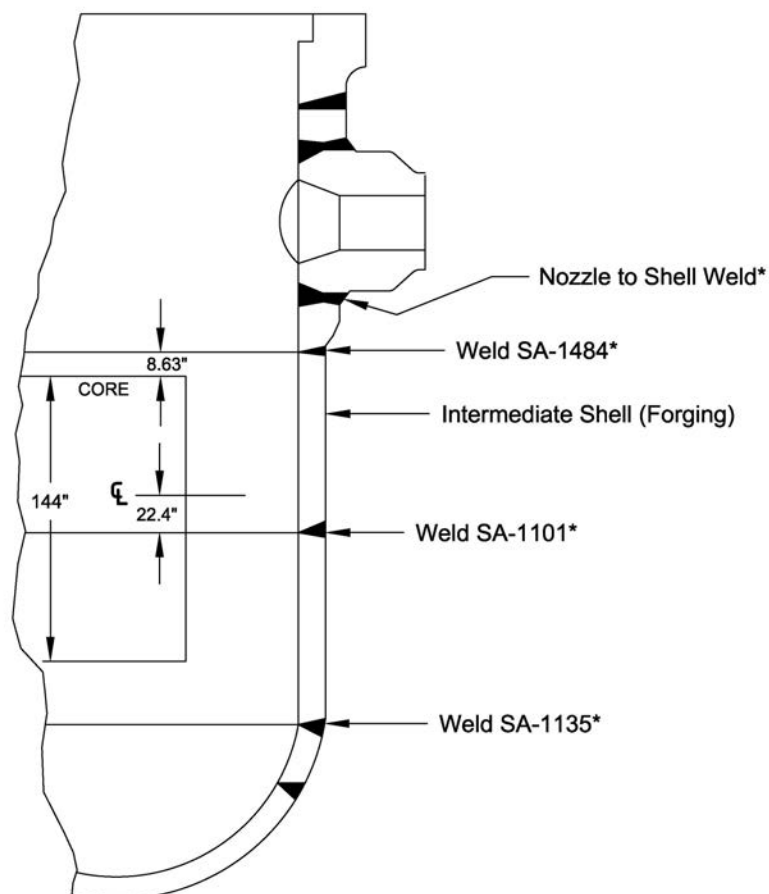
Reactor Vessel Material	Material ID and/or Heat Number	Cu, wt%	Ni, wt%	(IS) Inside Wetted Surface Fluence or (*) clad/base metal n/cm ² E> 1.0 MeV)
Turkey Point Unit 3, 80-Year Fluence (E > 1.0 MeV)				
US Forging to INF Welds	Heat 8T1762	0.19	0.57	(IS) 1.50E+18
	Heat 8T1554B	0.16	0.57	(IS) 1.50E+18
	Heat 71249	0.23	0.59	(IS) 1.50E+18
US Forging to ONF Welds	Heat 8T1762	0.19	0.57	(IS) 1.50E+18
US to IS Circ. Weld	SA-1484 Heat 72442	0.26	0.60	(*) 1.19E+19
IS to LS Circ. Weld	SA-1101 Heat 71249	0.23	0.59	(*) 1.04E+20
LS to Dutchman Circ. Weld	SA-1135 Heat 61782	0.23	0.52	(IS) 1.5E+18
Turkey Point Unit 4, 80-Year Fluence (E > 1.0 MeV)				
US to INF Welds	Heat 8T1762	0.19	0.57	(IS) 1.50E+18
	Heat 8T1554B	0.16	0.57	(IS) 1.50E+18
	Heat 299L44	0.34	0.68	(IS) 1.50E+18
US to ONF Welds	Heat 8T1554B	0.16	0.57	(IS) 1.50E+18
	Heat 299L44	0.34	0.68	(IS) 1.50E+18
US to IS Circ. Weld (ID 67%)	WF-67 Heat 72442	0.26	0.60	(*) 1.21E+19
IS to LS Circ. Weld	SA-1101 Heat 71249	0.23	0.59	(*) 1.03E+20
LS to Dutchman Circ. Weld	SA-1135 Heat 61782	0.23	0.52	(IS) 1.5E+18

Table 3—2 Reactor Vessel Shell Dimensions

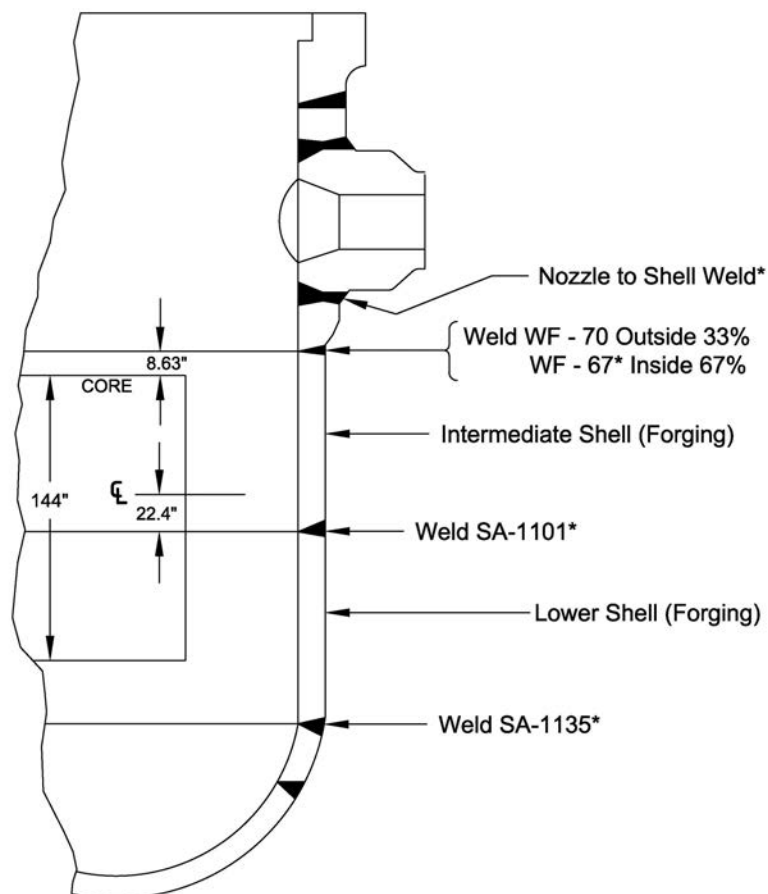
--	--

Table 3—3 Reactor Vessel Nozzle Belt Dimensions

--	--

Figure 3—1 Reactor Vessel—Turkey Point Unit 3

* Equivalent Margins Analysis
performed for these Linde 80 Welds.

Figure 3—2 Reactor Vessel—Turkey Point Unit 4

* Equivalent Margins Analysis
performed for these Linde 80 Welds.

4.0 MATERIAL PROPERTIES AND LEVELS C&D SERVICE LOADINGS

4.1 *J-Integral Resistance Model*

The J-integral resistance model for Mn-Mo-Ni/Linde 80 welds in the reactor vessels of the B&WOG RVWG plants were developed using a large J-resistance model (J-R model) data base. A detailed description of this model is provided in Appendix B of BAW-2192PA [2], Revision 0. This model was developed using specimens irradiated to $8.45\text{E}+18$ n/cm², and the range of applicability of the model was extended (qualitatively) to approximately $1.90\text{E}+19$ n/cm² in Appendix B, Figure 3-1, to BAW-2251A [6]. See Appendix A of ANP-3646P, Rev. 0 for a discussion of the extension of the range of applicability of the B&WOG J-R model to fluence values expected at 80 years for Turkey Point reactor vessels.

The coefficients, a , d , and C_4 are provided in Table 4-1. As required by ASME Section XI, ASME K-3300, when evaluating the vessel for Levels A, B, and C Service Loadings, the J-integral resistance versus crack-extension curve (J-R curve) shall be a conservative representation of the toughness of the controlling beltline material at upper shelf temperatures in the operating range. When evaluating the vessel for Level D Service Loadings, the J-R curve shall be a best estimate representation of the toughness of the controlling beltline material at upper shelf temperatures in the operating range. As such, the J_d correlation minus 2 standard errors is used for evaluation of Level C Service Loadings (i.e., equation (1) multiplied by []) while the unaltered J_d correlation would be used to evaluate Level D Service Loadings.

As discussed in Appendix B to BAW-2192PA, the J-R curve was generated from a J-integral database obtained from the same class of material with the same orientation using correlations for effects of temperature, chemical composition, and fluence level. Crack extension was by ductile tearing with no cleavage. This complies with ASME Section XI, K-3300.

Table 4—1 Parameters in Jd Model 4B**4.2 Mechanical Properties of Weld Metals**

The following subsections provide representative properties for the Turkey Point reactor vessels. The temperature dependent mechanical properties are developed from the 2007 Edition with 2008 Addenda of the ASME Code (Section III) for the reactor base metal and cladding (the ASME Code does not provide separate mechanical properties for base and weld metal). The only change in the material properties listed in the 2013 Edition of ASME Section II for the applicable properties is the coefficient of thermal expansion for stainless steel at 600°F; this value was changed from 9.8E-6 in/in/°F to 9.9E-6 in/in/°F. At the limiting time points in the Levels C & D analysis where cladding effects are included the temperature of the cladding is well below 600°F, and thus this change does not impact the EMA analyses summarized herein.

Both ASME Code minimum and representative irradiated yield strengths are also provided. The mechanical properties such as weld metal yield strengths typically used were the irradiated properties but in some cases the ASME Code minimum properties were conservatively considered. The irradiated material properties used herein are consistent with those used for the 60-year license renewal low upper shelf toughness analysis submittals created for the plants (See Section 1.1 above).

4.2.1 Mechanical Properties for the Turkey Point Reactor Vessels

The Turkey Point reactor vessels are fabricated using A-508 Grade 2 Class 1 (3/4Ni-1/2Mo-1/3Cr-V) Low Alloy Steel (LAS) and stainless steel (18Cr-8Ni) cladding materials. Table 4-2 provides the Young's modulus (E), the mean coefficient of thermal expansion (α), and the yield strength (Sy) for the RV base metal and weld material and the E and α properties for the RV cladding material.

Table 4—2
Mechanical Properties of Turkey Point RV Materials

Temp. (°F)	RV Base Metal			Weld Metals		Cladding	
	E (ksi)	α (in/in/°F)	Sy (ksi)	SA-1101 (ksi)	SA-1135 (ksi)	E (ksi)	α (in/in/°F)
70	27800	6.40E-06	50.0	[]	[]	28300	8.50E-06
200	27100	6.70E-06	47.0	[]	[]	27500	8.90E-06
300	26700	6.90E-06	45.5	[]	[]	27000	9.20E-06
400	26200	7.10E-06	44.2	[]	[]	26400	9.50E-06
500	25700	7.30E-06	43.2	[]	[]	25900	9.70E-06
600	25100	7.40E-06	42.1	[]	[]	25300	9.80E-06

4.3 *Levels C and D Service Loadings*

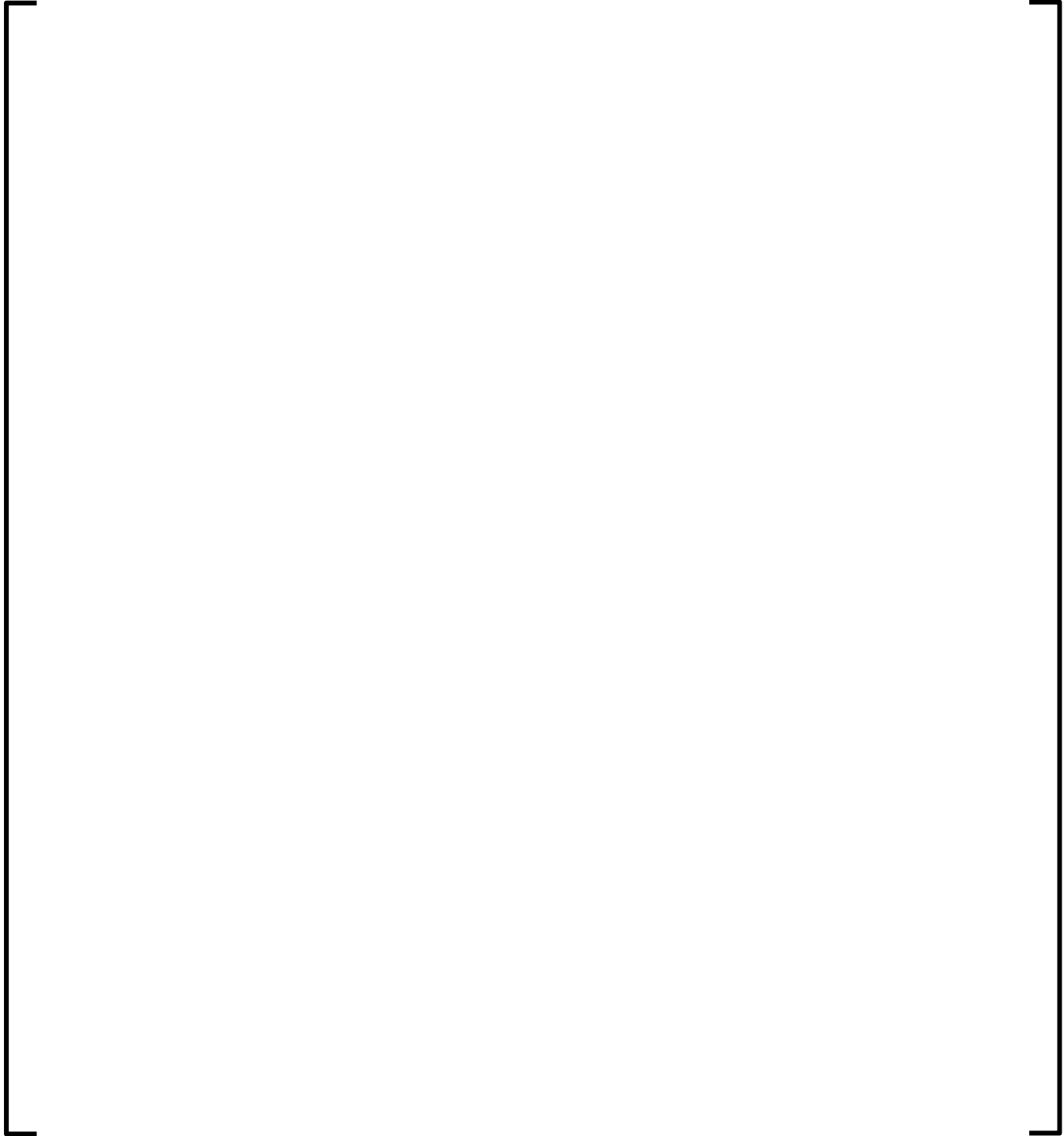
4.3.1 Turkey Point

Levels C and D Service Loadings were developed for the Turkey Point reactor vessels for the two steam line break transients listed below. The Turkey Point Safety Injection (SI) pump shutoff head will limit RCS pressure increase to 1660 psi.

Level D: Steam Line Break (SLB Without Offsite Power)
 Steam Line Break (SSDC 1.3 SLB)

The pressure and temperature steam line break transients for the Turkey Point reactor vessels are depicted in Figure 4-1.

Figure 4—1 Turkey Point Steam Line Break Transients



5.0 FRACTURE MECHANICS ANALYSIS

5.1 *Methodology*

In accordance with ASME Section XI, Appendix K [17], Subarticle K-1200, the following analytical procedure was used for Levels C & D Service Loadings:

- a) Flaws in the reactor vessel shell welds, the transition welds as well as RV nozzle-to-shell welds were postulated in accordance with the acceptance criteria of Subarticles K-2300 and K-2400.
- b) Loading conditions at the locations of the postulated flaws were determined for Levels C and D Service Loadings.
- c) Material properties, including E , α , σ_y , and the J-integral resistance curve (J-R curve), were determined at the locations of the postulated flaws. Young's modulus, mean coefficient of thermal expansion and yield strength are addressed in section 4.2. The J-R curve is discussed in section 4.1.
- d) The postulated flaws were evaluated in accordance with the acceptance criteria of Article K-2000 by calculating the applied J-integral according to the procedure provided by Subarticle K-5210. The applied J-integral was then evaluated to satisfy the criteria for flaw extension in Subarticle K-5220 and flaw stability in Subarticle K-5300.

5.2 Procedure for Evaluating Levels C and D Service Loadings

The evaluation for the Levels C and D service loadings is performed as follows:

- 1 For each transient described in Section 4.3, calculate stress intensity factors for a semi-elliptical flaw of depth up to $1/10^{\text{th}}$ of the base metal wall thickness, as a function of time, due to internal pressure and radial thermal gradients with a factor of safety of 1.0 on loading. The applied stress intensity factor, K_I , calculated for each of these transients is compared to the K_{Jc} upper-shelf toughness curve of the weld material. The transient for which the applied K_I most closely approaches the K_{Jc} curve is chosen as the limiting transient, and the critical time in the limiting transient selected for further evaluation occurs at the point where K_I most closely approaches the K_{Jc} curve.
- 2 At the critical transient time, develop a crack driving force diagram with the applied J -integral and J - R curves plotted as a function of flaw extension. The adequacy of the upper-shelf toughness is evaluated by comparing the applied J -integral with the J - R curve at a flaw extension of 0.10 in. Flaw stability is assessed by examining the slopes of the applied J -integral and J - R curves at the points of intersection.
- 3 Verify that the extent of stable flaw extension is no greater than 75% of the vessel wall thickness by determining when the applied J -integral curve intersects the mean J - R curve.
- 4 Verify that the remaining ligament is not subject to tensile instability. The internal pressure p shall be less than P_I , where P_I is the internal pressure at tensile instability of the remaining ligament. The pressure at instability, P_I , is given in K-5300, Appendix K of ASME Section XI for both axial and circumferential flaws.

5.2.1 Processing of Transient Time-History Data

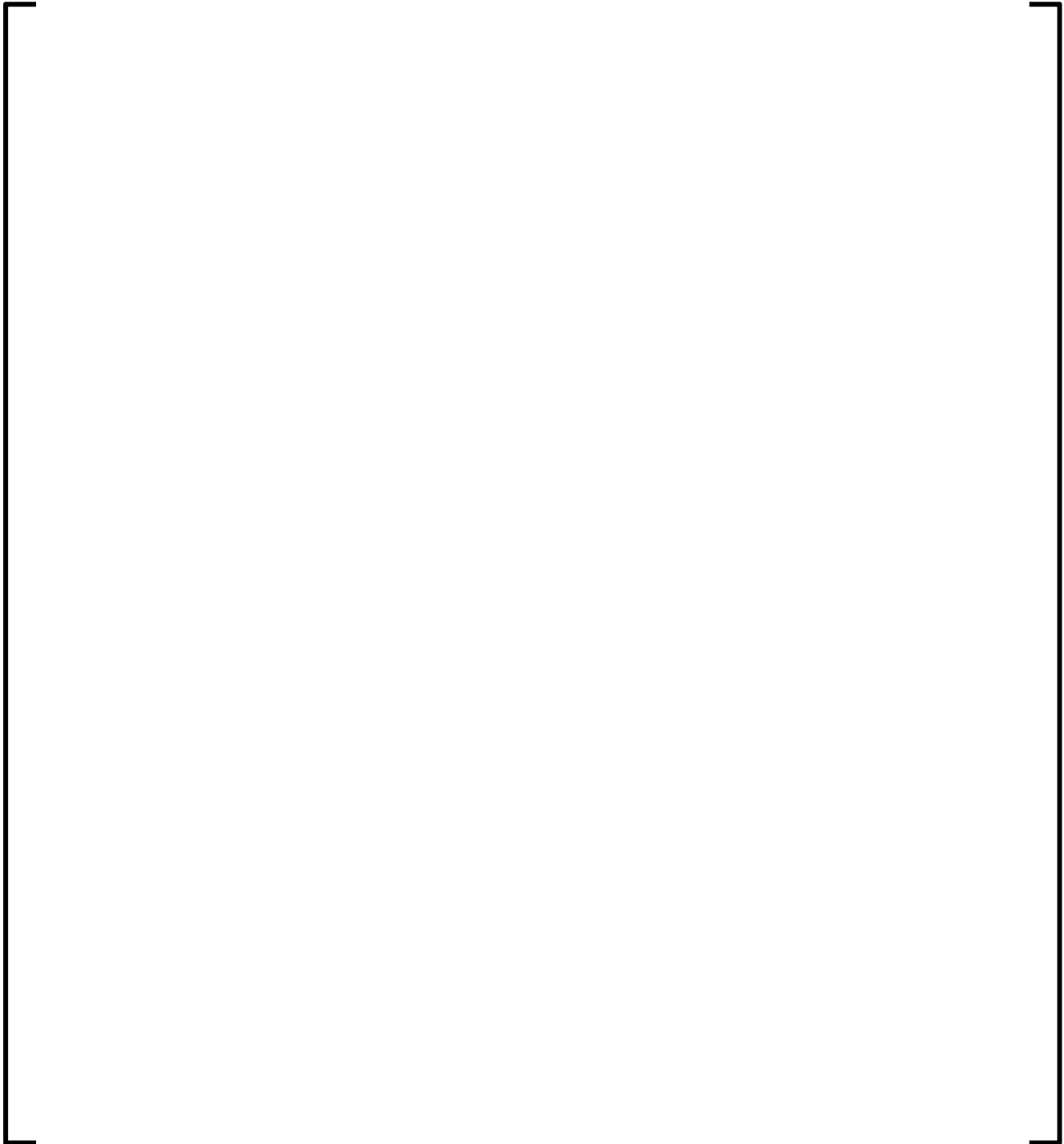
5.2.1.1 Turkey Point

For the Turkey Point reactor vessels, the applied J-integrals at the nozzle to shell welds and the upper transition weld were determined from three-dimensional finite element analysis. The through-thickness path line stresses were subsequently used to calculate stress intensity factors and the applied J-integrals were determined based on consideration of small scale yielding. For the controlling reactor vessel shell weld, stress intensity factors were calculated using the one-dimensional, finite element thermal and closed form stress models and linear elastic fracture mechanics methodology of the PCRIT computer code.

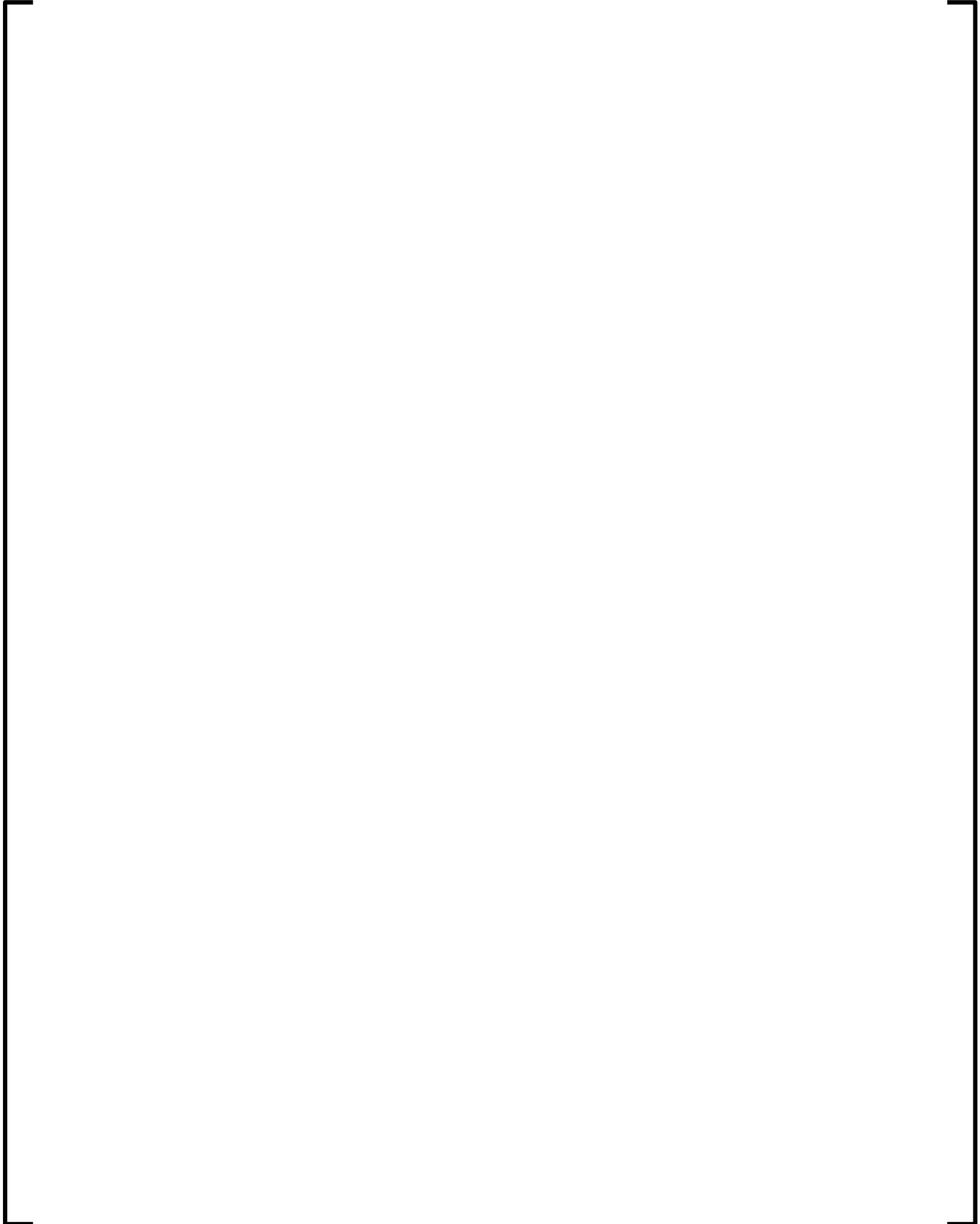
5.2.2 Temperature Range for Upper Shelf Fracture Toughness Evaluations

Upper-shelf fracture toughness is determined through use of Charpy V-notch impact energy versus temperature plots by noting the temperature above which the Charpy energy remains on a plateau, maintaining a relatively high constant energy level. Similarly, fracture toughness can be addressed in three different regions on the temperature scale, i.e., a lower-shelf toughness region, a transition region, and an upper-shelf toughness region. Fracture toughness of reactor vessel steel and associated weld metals are conservatively predicted by the ASME initiation toughness curve, K_{Ic} , in the lower-shelf and transition regions. In the upper-shelf region, the upper-shelf toughness curve, K_{Jc} , is derived from the upper-shelf J-integral resistance model described in Section 4.1. The upper-shelf toughness then becomes a function of fluence, copper content, temperature, and fracture specimen size. When upper-shelf toughness is plotted versus temperature, a plateau-like curve develops that decreases slightly with increasing temperature. Since the present analysis addresses the low upper-shelf fracture toughness issue, only the upper-shelf temperature range, which begins at the intersection of K_{Ic} and the upper-shelf toughness curves, K_{Jc} , is considered.

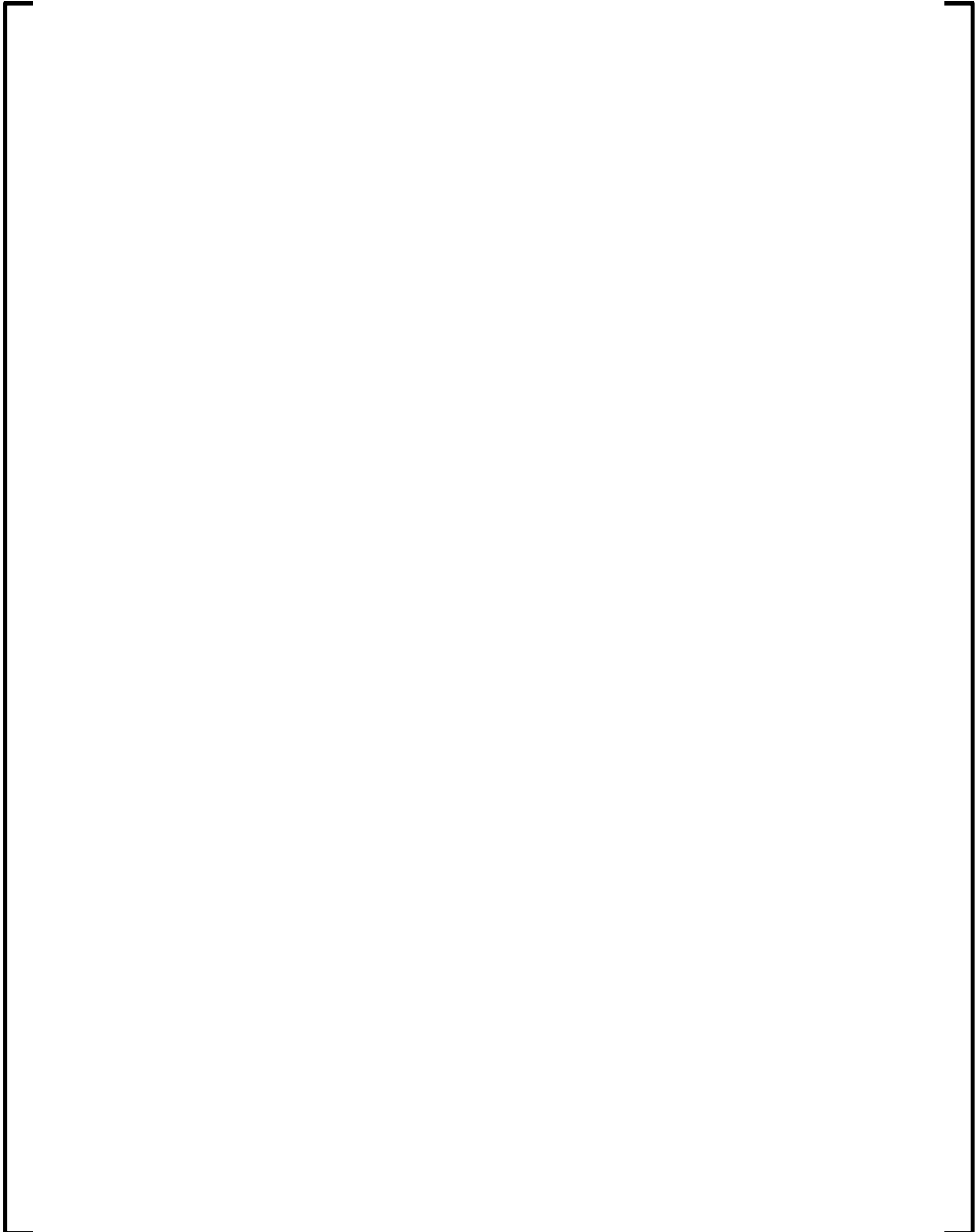
5.2.3 Cladding Effects



Low Upper-Shelf Toughness Fracture Mechanics Analysis of Turkey Point Units 3 and 4
Reactor Vessels for Levels C & D Service Loads at 80-Years
Topical Report



Low Upper-Shelf Toughness Fracture Mechanics Analysis of Turkey Point Units 3 and 4
Reactor Vessels for Levels C & D Service Loads at 80-Years
Topical Report



5.3 *Evaluation for Levels C and D Service Loadings*

The type of analysis models and computer code used to evaluate the RV shell welds, the RV transition welds and the RV nozzle welds for Levels C & D service loads are addressed in Sections 5.2.1.1. Section 4.3.1 addresses the specific types of transient events analyzed. The applied J-integral for the RV shell welds, the RV transition and nozzle welds, due to these Levels C & D transient events, is calculated and evaluated as discussed in Section 5.2.

The transition region toughness and upper shelf toughness are discussed in Section 5.2.2. Transition region toughness is obtained from the ASME Section XI equation for crack initiation,

$$K_{Ic} = 33.2 + 20.734 \exp[0.02(T - RT_{NDT})]$$

using the applicable RTNDT value for a flaw depth of 1/10th the wall thickness, where:

$$\begin{aligned} K_{Ic} &= \text{transition region toughness, ksi}\sqrt{\text{in}} \\ T &= \text{crack tip temperature, } ^\circ\text{F} \end{aligned}$$

Upper shelf toughness K_{Jc} is derived from the J-integral resistance model of Section 4.1 for a flaw depth of 1/10th the wall thickness, a crack extension of 0.10 inch, and the applicable fluence value at the crack tip:

$$K_{Jc} = \sqrt{\frac{J_{0.1} E}{1000(1 - \nu^2)}}$$

where

$$\begin{aligned} K_{Jc} &= \text{upper-shelf region toughness, ksi}\sqrt{\text{in}} \\ J_{0.1} &= \text{J-integral resistance at } \Delta a = 0.1 \text{ in.} \end{aligned}$$

Using the above equations, the transition and upper shelf toughness values as a function of temperature are determined for the controlling weld and Levels C and D service loading conditions.

5.3.1 Reactor Vessel Shell Welds

5.3.1.1 Turkey Point

For the Turkey Point reactor vessels, the controlling weld was identified to be the SA-1101 RV shell weld based on the results of Levels A and B Service Loadings. This controlling weld is therefore evaluated at a flaw depth of $1/10^{\text{th}}$ the base metal thickness for Levels C and D Service Loadings. The two main steam line break transients (SSDC 1.3 SLB & SLB without Offsite Power) identified in Section 4.3.1 and illustrated in Figure 4-1 are evaluated. The analysis is performed using the PCRIT Code.

Figure 5-1 shows the variation of the applied stress intensity factor, K_I , for these two transient cases as a function of the crack tip temperature. This figure also shows the transition region toughness K_{Ic} curve and the mean and lower bound upper-shelf toughness K_{Jc} curves with crack tip temperature. The K_{Ic} curve is determined using the Adjusted Reference Temperature (ART) value at $1/10^{\text{th}}$ of the wall thickness for the limiting weld SA-1101, which at 80-years is []. The symbols on the K_I curves for each of the two transient cases indicate points in time at which PCRIT solutions are available. The SSDC SLB is identified as the limiting transient since it most closely approaches the K_{Jc} limit of the weld. All subsequent analysis was therefore based on evaluation of this transient case. In the upper-shelf toughness range, the SSDC SLB K_I curve is closest to the lower bound K_{Jc} curve at 6.5 minutes into the transient. This time is selected as the critical time in the transient at which to perform the flaw evaluation for Levels C and D Service Loadings.

The additional stress intensity factor attributable to the cladding, $K_{I\text{clad}}$, at 6.5 minutes (limiting time point) into the SSDC SLB transient is determined to be [] at a flaw depth corresponding to $1/10^{\text{th}}$ of the wall thickness. Applied J-Integrals are calculated for the controlling weld for various flaw depths in Table 5-1 using stress intensity factors from PCRIT for the SSDC SLB (at 6.5 min.) and adding [] to account for cladding effects. Stress intensity factors are converted to J -integrals by the plane strain relationship,

$$J_{\text{applied}}(a) = 1000 \frac{K_{I\text{total}}^2(a)}{E} (1 - \nu^2)$$

Since the RV shell weld for the Turkey Point reactor vessels is [] inch thick as given in Table 3—2, the initial flaw depth of $1/10^{\text{th}}$ of the wall thickness is [] inches. The flaw extension is calculating by subtracting this depth from the built-in PCRIT flaw depths. The results along with the mean and lower bound J-R curves developed in Table 5-2 are plotted in Figure 5-2. An evaluation line is used at a flaw extension of 0.10 in. to show that the applied J -integral is less than the lower bound J -integral of the material, as required by Appendix K.

The applied J-integral at a flaw extension of 0.1 inch is determined to be [] as reported at the base of Table 5-1. The associated material J-resistance ($J_{0.1}$) to the applied J-integral (J_1) ratio can be determined using the lower bound and mean J-R curve values, from Table 5-2, for Levels C and D conditions, respectively. The margin for Level C Service Loading is [] and the margin for Level D Service Loading is []

The requirements for ductile and stable crack growth are demonstrated by Figure 5-2 since the slope of the applied J -integral curve is less than the slopes of both the lower bound and mean J -R curves at the points of intersection.

Referring to Figure 5-2, the Level D Service Loading requirement that the extent of stable flaw extension be no greater than 75% of the vessel wall thickness is easily satisfied since the applied J -integral curve intersects the mean J - R curve at a flaw extension that is only a small fraction of the wall thickness (less than 1%).

The last requirement for Level D Conditions is that the internal pressure p shall be less than P_I , the internal pressure at tensile instability of the remaining ligament. The calculations for P_I were determined for a circumferential flaw. An additional check is performed for circumferential flaws to ensure that internal pressure does not exceed the pressure at tensile instability caused by the applied hoop stress acting over the nominal wall thickness of the vessel. This validity limit on pressure is satisfied by

$$P_{\text{instability}} \leq 1.07 \sigma_o \frac{t}{R_i}.$$

To demonstrate that the remaining ligament does not exceed the pressure at instability a conservative flaw depth equal to $1/10^{\text{th}}$ of the wall thickness plus 0.1 inch is used. Although the internal pressure at tensile instability is calculated to be 12, 530 psi, the validity check on hoop stress requires that the internal pressure not exceed 6240 psi, which is still much greater than any anticipated accident condition pressure. Therefore, the remaining ligament is not subject to tensile instability.

5.3.2 Reactor Vessel Transition Welds and RV Nozzle Welds

The reactor vessel upper and lower transition welds are located above and below the reactor core, respectively (see Figures 3-1 and 3-2). The RV nozzle welds are located above the upper transition weld in the substantially thicker cylindrical section (reinforced to account for the inlet/outlet RV nozzle openings). The reactor vessel nozzle belt dimensions are reported in Table 3-3.

5.3.2.1 Turkey Point

For the Turkey Point reactor vessels the applied J-integrals for the nozzle to shell and upper transition welds were evaluated for Levels C and D Service Loadings. Both transients shown in Figure 4-1 are evaluated. For the SSDC transient the maximum pressure was capped at 1660 psi due to the shutoff head of the safety injection pumps. The bounding results with safety factor of 1.0 on the applied pressure are compared with the lower bound J-integral resistance at a ductile flaw extension of 0.1 inches in Table 5-3. The outlet nozzle is seen to be limiting and has a margin of []. The applied J-integral vs crack tip temperature for each transient, the SSDC SLB transient and SLB without offsite power transient (also referred to as AIS transient), is plotted in Figure 5-3 for the outlet nozzle, along with the temperature dependent mean and lower bound $J_{0.1}$ curves. As can be seen all points of the transient remain below the lower bound $J_{0.1}$. Additionally, Figure 5-3 shows the K_{Ic} fracture toughness using an RT_{NDT} of [], converted to an equivalent J using $K_{Ic}^2/(E/(1-\nu^2))$; the intersection of this curve with the $J_{0.1}$ curves establishes the upper shelf temperature range. The applied J-integral at the limiting time point at various flaw extensions is plotted with the lower bound J-resistance curve in Figure 5-4; the slope of the applied J-integral is less than the slope of the lower bound J-resistance curve at the point of intersection, which demonstrates that the flaw is stable as required by ASME Section XI, Appendix K.

**Table 5—1 Turkey Point J-Integral versus Flaw Extension for Levels
C & D Service Loadings**

--

**Table 5—2 Turkey Point-J-R Curves for Evaluation of Levels C & D
Service Loadings**

--

**Table 5—3 Turkey Point-Levels C & D Results for Nozzle to Shell and
Upper Transition Welds**

--	--

**Figure 5—1 Turkey Point-KI versus Crack Tip Temperature for
Levels C & D Service Loadings**

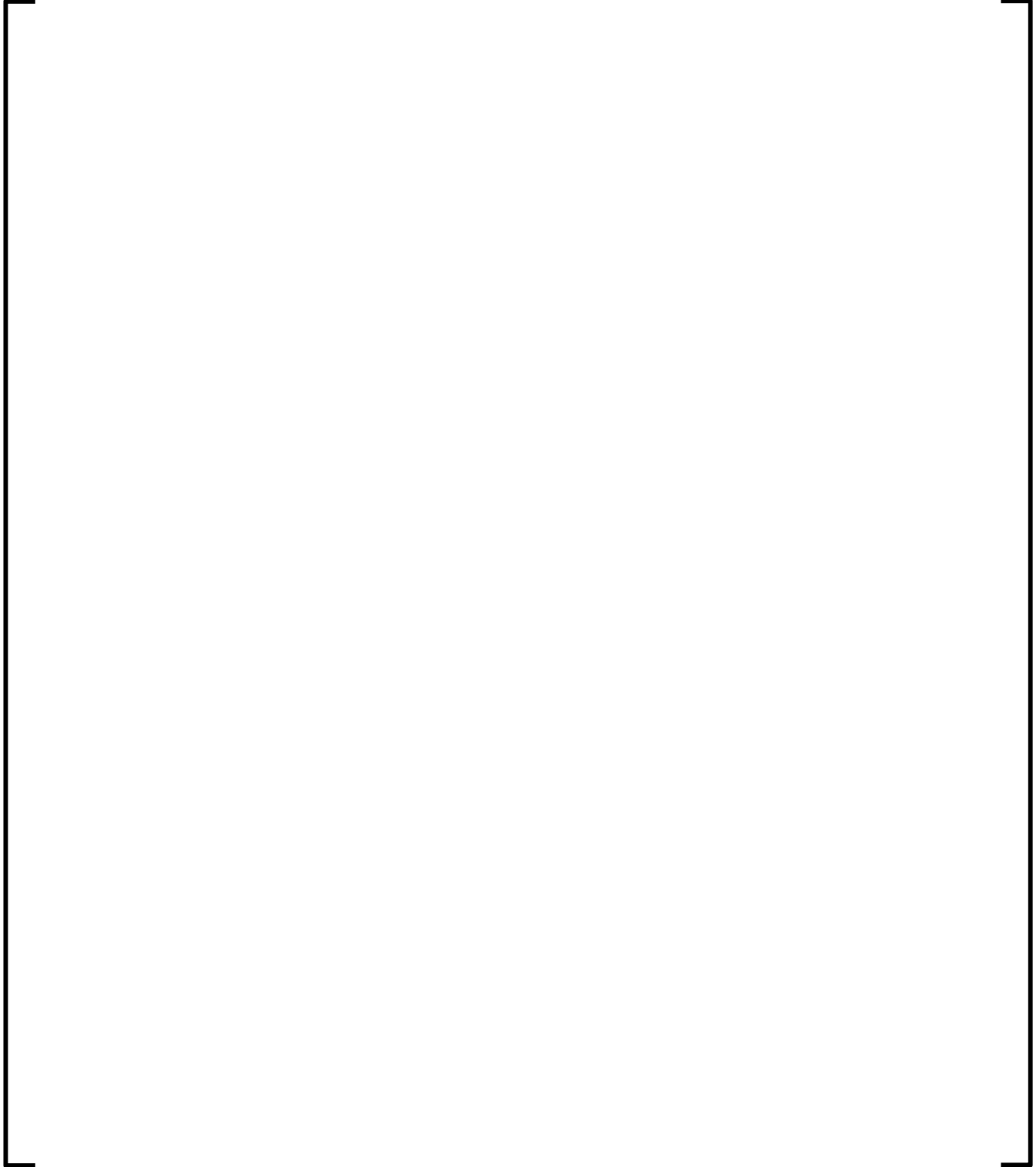


**Figure 5—2 Turkey Point-J-Integral versus Flaw Extension for
Levels C & D Service Loadings**

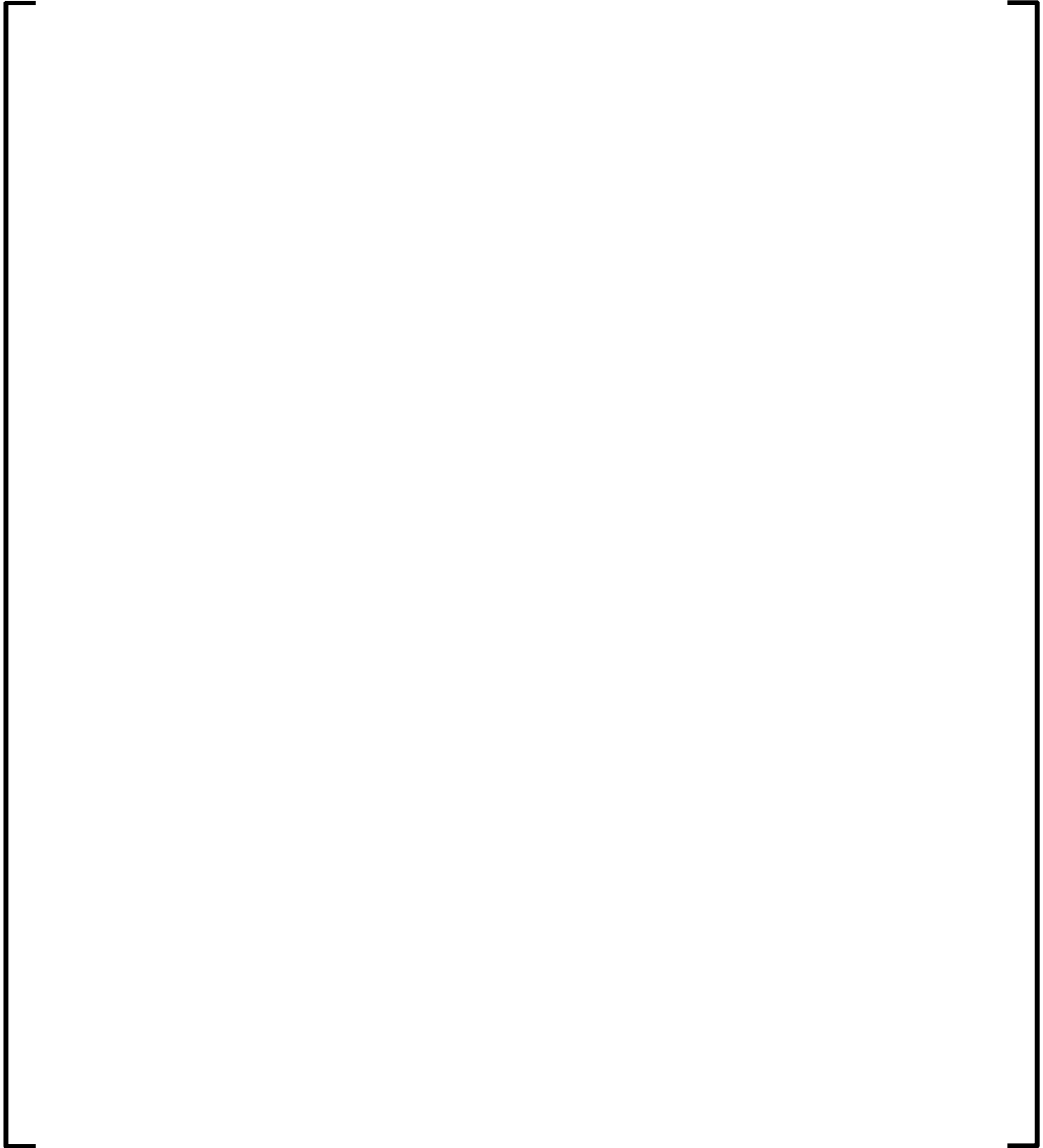


**Figure 5—3 Turkey Point- Levels C & D Applied J Integral vs Crack
Tip Temperature for the Outlet Nozzle to Shell Weld**



**Figure 5—4 Turkey Point- Levels C & D Applied J Integral vs Crack
Extension for the Outlet Nozzle to Shell Weld**



6.0 SUMMARY AND CONCLUSIONS

6.1 *Reactor Vessel Shell Welds*

The ASME Section XI, acceptance criteria for Levels C & D Service Loads for all reactor vessel shell welds are satisfied. ASME Section XI, Appendix K, Level C acceptance criteria (Subarticle K-2300), relative to the ratio of applied J-integral to J-integral of the material and use of the lower bound J-integral resistance curve, were conservatively imposed on the Level D transients evaluated in Section 5.0, although ASME Section XI, Subarticle K-2400(b) permits use of a best estimate J-integral resistance curve for Level D Service Loadings. The results of the limiting welds for Turkey Point Units 3 and 4 are reported below.

The limiting weld among the Turkey Point reactor vessel shell welds is Turkey Point Units 3 and 4 circumferential weld SA-1101. The limiting transient for Level C & D service loads is the SSDC 1.3 steam line break.

- With a factor of safety of 1.0 on loading, the applied J-integral (J_1) for the limiting reactor vessel shell weld (SA-1101) is less than the lower bound J-integral of the material at a ductile flaw extension of 0.10 inch ($J_{0.1}$) with a ratio $J_{0.1}/J_1 =$

$$\left[\frac{J_{0.1}}{J_1} \right] = \left[\frac{J_{0.1}}{J_1} \right]$$
, which is greater than the required value of 1.0. Using the mean J-R curve permitted by Subarticle K-2400 for this Service Level D transient, the ratio $J_{0.1}/J_1$ is $\left[\frac{J_{0.1}}{J_1} \right]$.
- With a factor of safety of 1.0 on loading, flaw extensions are ductile and stable for the limiting reactor vessel shell weld (SA-1101) since the slope of the applied J-integral curve is less than the slopes of both the lower bound and mean J-R curves at the points of intersection.
- For weld SA-1101 it was demonstrated that flaw growth is stable at much less than 75% of the vessel wall thickness. It has also been shown that the remaining ligament is sufficient to preclude tensile instability.

6.2 *Reactor Vessel Transition Welds and RV Nozzle Welds*

The ASME Section XI, acceptance criteria for Levels C & D Service Loads for all reactor vessel transition welds and reactor vessel nozzle welds are satisfied. ASME Section XI, Appendix K, Level C acceptance criteria (Subarticle K-2300), relative to the ratio of applied J-integral to J-integral of the material and use of the lower bound J-integral resistance curve, were conservatively imposed on the Level D transients evaluated in Section 5.0, although ASME Section XI, Subarticle K-2400(b) permits use of a best estimate J-integral resistance curve for Level D Service Loadings. The results of the limiting welds for Turkey Point Units 3 and 4 are reported below.

The upper transition weld and RV inlet and outlet nozzle-to-shell welds were evaluated for Levels C and D Service Loadings. The limiting transient for Level C & D service loads is the SSDC 1.3 steam line break.

- With a factor of safety of 1.0 on loading, the applied J-integral (J_1) for the RV nozzle-to-shell welds and upper transition weld are less than the lower bound J-integral of the material at a ductile flaw extension of 0.10 inch ($J_{0.1}$) with the following ratios for $J_{0.1}/J_1$: [] for the RV outlet nozzle-to-shell weld, [] for the RV inlet nozzle-to-shell weld, and [] for the upper transition weld. All 3 ratios are greater than the required value of 1.0.
- With a factor of safety of 1.0 on loading, flaw extensions are ductile and stable for the limiting RV outlet nozzle-to-shell weld (i.e., limiting location considering RV nozzle-to-shell welds and upper transition weld).
- For the RV outlet nozzle-to-shell weld it was demonstrated that flaw growth is stable at much less than 75% of the vessel wall thickness. Tensile instability was not explicitly calculated but because this section of the reactor vessel is thicker compared to the RV shell welds, it is considered to be bounded by the RV shell location.


7.0 REFERENCES

1. BAW-2178PA, Revision 00, "Low Upper Shelf Toughness Fracture Analysis of Reactor Vessels of B&W Owners Group Reactor Vessel Working Group for Level C and D Conditions," April 1994, ADAMS Accession (Legacy) 9406290288 (P)
2. BAW-2192PA, Revision 00, "Low Upper Shelf Toughness Fracture Analysis of Reactor Vessels of B&W Owners Group Reactor Vessel Working Group for Levels A and B Conditions," April 1994, ADAMS Accession (Legacy) 9406240261 (P), 9312220294 (NP)
3. ANP-3646P, Rev. 0, "Low Upper-Shelf Toughness Fracture Mechanics Analysis of Turkey Point Units 3 and 4 Reactor Vessels for Levels A & B Service Loads at 80-Years" (Proprietary), January 2018
4. 43-2178P, Supplement 1, Revision 0, Low Upper-Shelf Toughness Fracture Mechanics Analysis of Reactor Vessels of B&W Owners Reactor Vessel Working Group for Levels C & D Service Loads, December 2017
5. Code of Federal Regulations, Title 10, Part 50 – Domestic Licensing of Production and Utilization Facilities, Appendix G – Fracture Toughness Requirements, Federal Register Vol. 60. No. 243, December 19, 1995
6. 43-2192P, Supplement 1, Revision 0, Low Upper-Shelf Toughness Fracture Mechanics Analysis of Reactor Vessels of B&W Owners Reactor Vessel Working Group for Levels A & B Service Loads, December 2017
7. Not used
8. Not used
9. Not used
10. Not used
11. Not used

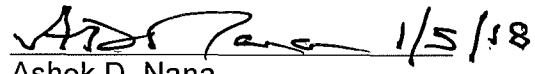
12. TURKEY POINT UNITS 3 AND 4 - ISSUANCE OF AMENDMENTS
REGARDING EXTENDED POWER UPRATE (TAC NOS. ME4907 AND
ME4908),” Adams Accession number ML11293A365
13. LICENSE AMENDMENT REQUEST FOR EXTENDED POWER UPRATE,
ATTACHMENT 4, L-2010-113, Attachment 4 ADAMS --ML103560177
14. Supplemental Response to NRC Request for Additional Information (RAI)
Regarding Extended Power Uprate (EPU) License Amendment Request
(LAR) No. 205 and Equivalent Margin Analysis (EMA), L-2010-303,
ADAMS-ML103610321
15. Response to NRC Request for Additional Information Regarding Extended
Power Uprate License Amendment Request No. 205 and Reactor
Materials Issues – Round 1, L-2011-029, ADAMS--ML110700068
16. NRC Regulatory Guide 1.161, Evaluation of Reactor Pressure Vessels
With Charpy Upper Shelf Energy Less Than 50 ft-lb
17. 2007 Edition (with 2008 Addenda) ASME & Boiler Pressure Vessel Code,
Section XI, Rules for Inservice Inspection of Nuclear power Plant
Components, Appendix K
18. 2013 Edition ASME & Boiler Pressure Vessel Code, Section XI, Rules for
Inservice Inspection of Nuclear power Plant Components, Appendix K
19. RIS-2014-11, NRC REGULATORY ISSUE SUMMARY 2014-11
INFORMATION ON LICENSING APPLICATIONS FOR FRACTURE
TOUGHNESS REQUIREMENTS FOR FERRITIC REACTOR COOLANT
PRESSURE BOUNDARY COMPONENTS

8.0 CERTIFICATION

This report is an accurate description of the low upper-shelf toughness fracture analysis of Turkey Point Units 3 and 4 vessels.


Mark A. Rinckel
Nuclear Analysis Unit

This report has been reviewed and is an accurate description of the low upper-shelf toughness fracture analysis of reactor vessels of Turkey Point Units 3 and 4.


Ashok D. Nana
Component Analysis & Fracture
Mechanics Unit

Verification of independent review.


David R. Cofflin
Component Analysis & Fracture
Mechanics Unit

This report is approved for release.


Danielle Page Blair
NSSS Project Management

Enclosure 4
Non-proprietary Reference Documents
and
Redacted Versions of Proprietary
Reference Documents
(Public Version)
Attachment 4

**SIA Report No. 1700109.402P, Revision 3 – REDACTED
Evaluation of Fatigue of ASME Section III, Class 1
Components for Turkey Point Units 3 and 4 for Subsequent
License Renewal, December 2017**

(44 Total Pages, including cover sheets)

THIS REPORT CONTAINS VENDOR PROPRIETARY INFORMATION

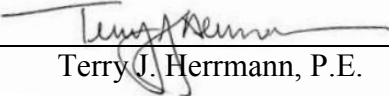
Report No. 1700109.402P
Revision 3 - REDACTED
Project No. 1700109
December 2017

**Evaluation of Fatigue of ASME Section III,
Class 1 Components for Turkey Point Units
3 and 4 for Subsequent License Renewal**

Prepared for:
Florida Power & Light Company
Juno Beach, FL
Purchase Order No. 2000230248 dated 02/16/2017

Prepared by:
Structural Integrity Associates, Inc.
San Jose, California

Prepared by:  *Date:* 12/17/2017
David A. Gerber, P.E.

Reviewed by:  *Date:* 12/17/2017
Terry J. Herrmann, P.E.

Approved by:  *Date:* 12/17/2017
David A. Gerber, P.E.

THIS REPORT CONTAINS VENDOR PROPRIETARY INFORMATION

REVISION CONTROL SHEET

Document Number: 1700109.402

Title: Evaluation of Fatigue of ASME Section III, Class 1 Components for
Turkey Point Units 3 and 4 for Subsequent License Renewal

Client: Florida Power & Light Company

SI Project Number: 1700109

Quality Program: ☒ Nuclear ☐ Commercial

Section	Pages	Revision	Date	Comments
1.0 2.0 3.0 4.0 5.0	1-1 – 1-6 2-1 – 2-11 3-1 – 3-14 4-1 5-1 – 5-4	0	10/2/2017	Formal Issue
1.0 2.0 3.0 5.0	1-9 – 1-11 2-3 – 2-6 2-11 – 2-12 3-1, 3-4 – 3-8 5-4	1	11/13/2017	Revision to tables and description of 10 CFR 54.21 dispositions
2.0	2-11, 2-12, 5-4	2	12/9/2017	Addition of CUF values for CRDM components and Reference [32].
2.0 5.0	2-11, 2-12, 5-4	3	12/17/2017	Removal of Reference [32] and addition of replacement Reference [27]. Reassignment of Footnote (1) in Table 2- 2. Update of two CRDM CUF values in Table 2-2.

Table of Contents

<u>Section</u>	<u>Page</u>
1.0 INTRODUCTION.....	1-6
1.1 Background.....	1-6
1.1.1 <i>History of Fatigue Analyses for Initial License Renewal</i>	1-7
1.1.2 <i>Current Licensing Bases for Fatigue</i>	1-7
1.1.3 <i>Develop 80-Year Fatigue Management TLAAs</i>	1-8
1.2 SRP-SLR Guidance for Metal Fatigue	1-8
1.3 Report Objectives.....	1-12
2.0 PLANT-SPECIFIC FATIGUE BACKGROUND FOR PTN.....	2-1
2.1 Existing Programs.....	2-1
2.1.1 <i>PTN Cycle Counting Program</i>	2-1
2.1.2 <i>PTN Fatigue Management Program</i>	2-7
2.2 PTN Fatigue Bases for 60-Years	2-8
2.2.1 <i>Class 1 Component Design-Codes of Construction</i>	2-8
2.2.2 <i>Design-Basis Transient Evaluation</i>	2-9
2.2.3 <i>Fatigue Design Bases</i>	2-10
3.0 PLANT-SPECIFIC ASSESSMENT OF FATIGUE EFFECTS FOR SUBSEQUENT LICENSE RENEWAL	3-1
3.1 PTN Cycle Counting Program.....	3-1
3.1.1 <i>Projection of 80-Year Cycles and Comparison to Administrative Limits</i>	3-1
3.2 PTN Fatigue Assessments.....	3-9
3.2.1 <i>Review of PTN Design-Basis Transient Severity</i>	3-9
3.2.2 <i>Review of PTN-ENG-LRAM-00-0044</i>	3-13
3.3 Evaluation of Metal Fatigue TLAAs for SLR	3-13
3.4 Conclusions.....	3-14
4.0 SUMMARY AND CONCLUSIONS	4-1
5.0 REFERENCES.....	5-1

List of Tables

<u>Table</u>	<u>Page</u>
Table 2-1: Actual Number of Transients Compared to Design-Basis Number of Transients – PTN Class 1 Components for 60 Years	2-3
Table 2-2: CLB CUF Values for Components Analyzed to ASME Section III, Class 1 Rules	2-11
Table 3-1: 80-Year Projections - PTN Unit 3	3-4
Table 3-2: 80-Year Projections - PTN Unit 4	3-6

List of Figures

<u>Figure</u>	<u>Page</u>
Figure 3-1. Unit 3 RCS Heatup Actual and Projected Cycles (for illustrative purposes)	3-8

PROPRIETARY INFORMATION NOTICE

*This report contains information that is proprietary to other vendors that is protected under one or more Non-Disclosure Agreements (NDAs). Such information is identified by red, bold-faced font surrounded by brackets. An example is {**this wording**}. Release of such information is not authorized without the express written permission of the authorized owner of the information.*

THIS REPORT CONTAINS VENDOR PROPRIETARY INFORMATION

1.0 INTRODUCTION

The original license renewal application (LRA) for Turkey Point Nuclear Plant Units 3 and 4 (PTN) had two objectives related to fatigue management for the 60-year operating period; first, to resolve the time limited aging analyses (TLAAs) on fatigue design confirming that the original transient design limits remain valid and second, to evaluate the environmentally-assisted fatigue (EAF) effects on specific components. This report supplements the first objective to demonstrate that the metal fatigue TLAAAs continue to confirm that the original transient design limits remain valid for the 80-year operating period.

This report presents an historical account of the work performed for the initial license renewal for the 60-year period for fatigue management of ASME Section III, Class 1 components, describes the activities planned for addressing the license renewal for the 80-year period (Subsequent License Renewal, SLR), and provides a disposition of the metal fatigue management TLAAAs for SLR.

1.1 Background

Florida Power & Light Company (FPL) is developing a SLR application (SLRA) to extend plant operations at PTN from 60 to 80 years. The PTN SLRA will build off the content from the original PTN license renewal application (LRA) submitted to the U.S. Nuclear Regulatory Commission (NRC) in 2000 [1], and adjust the content as necessary so that it follows the updated NRC guidance for SLR.

In response to FPL's original LRA submittal for PTN, the NRC issued renewed operating licenses in June 2002 to operate an additional 20 years beyond the original 40-year operating licenses. Structural Integrity Associates, Inc. (SI) provided support to FPL in 2000 and 2001 as a part of the LRA development and NRC approval for PTN. SI's support included the preparation of engineering documents, calculations, and evaluations associated with certain TLAAAs for PTN.

THIS REPORT CONTAINS VENDOR PROPRIETARY INFORMATION

This report addresses TLAAAs associated with metal fatigue for both PTN units to support operating license renewals from 60 to 80 years for PTN Units 3 and 4 that satisfy all the requirements specified by the NRC for SLR.

1.1.1 History of Fatigue Analyses for Initial License Renewal

For the LRA submitted in 2000, FPL evaluated plant cycles from the start of plant operation through June 1998 for both PTN units. The evaluation determined that 60-year projected quantities of each transient were less than the design numbers for each transient, thus demonstrating that the design number of transients will bound the expected cycles through the 60-year period of extended operation. FPL evaluated the severity of each transient accumulated through 1998 and determined that the design transient severities bounded the actual cycles to-date. A similar activity is performed in this report for the SLR period.

1.1.2 Current Licensing Bases for Fatigue

Because the 60-year projected cycles and the severities accumulated as of 1998 for all transients were bounded by the design number and severity of those transients, the fatigue design basis for ASME Section III, Class 1 components for the 60-year period was demonstrated to remain unchanged from the original design basis. Thus, FPL satisfied Part 54 to Title 10 of the U.S. Code of Federal Regulations (10 CFR 54) [23], specifically 10 CFR 54.21(c)(1)(i), for 60 years of operation, as indicated in Section 4.3.1 of the PTN LRA [1] and approved by the NRC in Section 4.3.4 of the PTN LRA Safety Evaluation Report (SER) [24]. With the NRC's issuance of the renewed licenses in 2002, this evaluation became a part of the current licensing bases (CLB) for the PTN units for 60 years of operation, and serves as the starting point for SLR evaluation of the fatigue TLAAAs.

1.1.3 Develop 80-Year Fatigue Management TLAs

A similar demonstration to that performed for the 60-year LRA for fatigue TLAs will be performed in this document for 80 years.

1.2 SRP-SLR Guidance for Metal Fatigue

This section summarizes the NRC's Standard Review Plan for SLR (SRP-SLR) [3] guidance that is applicable for Fatigue Management of ASME Section III, Class 1 Components.

The SRP-SLR provides guidance to NRC staff reviewers for SLRA content to ensure the quality and uniformity of NRC staff reviews, and to present a well-defined base from which to evaluate applicant programs and activities for SLR. The SRP-SLR is a companion document to the NRC's Generic Aging Lessons Learned Report for SLR (GALL-SLR) [2], which provides guidance for SLR applicants and contains the NRC staff's generic evaluation of plant aging management programs (AMPs) and establishes the technical basis for their adequacy.

Section 4.3, "Metal Fatigue," of the SRP-SLR specifies the areas of review to ensure that the metal component fatigue parameter evaluations are valid for SLR. The acceptance criteria for such calculations follow the requirements of 10 CFR 54 [23]. Specifically, pursuant to 10 CFR 54.21(c)(1)(i) through (iii), an applicant must demonstrate one of the following for each analysis:

- i. The analyses remain valid for the period of extended operation;
- ii. The analyses have been projected to the end of the period of extended operation; or
- iii. The effects of aging on the intended function(s) will be adequately managed for the period of extended operation.

In Section X.M1 of the GALL-SLR Report, the NRC staff evaluated a program for monitoring and tracking the number of occurrences and the severity of critical cyclic loadings for selected components. The GALL-SLR Report may be referenced in a SLRA and should be treated in the

THIS REPORT CONTAINS VENDOR PROPRIETARY INFORMATION

same manner as an approved topical report. In referencing the GALL-SLR Report, the applicant should indicate that the material referenced is applicable to their plant and should provide the information necessary to adopt the finding of program acceptability as described and evaluated in the report.

The scope of the X.M1 AMP includes those mechanical or structural components with fatigue TLAAAs or other analyses that depend on the number of occurrences and severity of transient cycles. The program monitors and tracks the number of occurrences and severity of thermal and pressure transients for the selected components, to ensure that they remain within the plant-specific limits. The program ensures that the fatigue analyses remain within their allowable limits, thus minimizing the likelihood of failures from fatigue-induced cracking of the components caused by cyclic strains in the component's material.

From the SRP-SLR, for components evaluated for metal fatigue three acceptance criteria are established dependent upon the validity of the fatigue analyses:

10 CFR 54.21(c)(1)(i): the fatigue calculations were not revised and remain valid for the 80-year period by demonstrating that the number of accumulated cycles and the assumed severity of each of the cycle loadings in the fatigue calculations are not projected to exceed the limits evaluated for those components. The projections must be shown to be consistent with historical plant operating characteristics and anticipated future operation. This criterion can be used for most ASME Section III, Class 1 components where there were no revised fatigue analyses since the 80-year projected cycles are shown to be less than the design set to which they were analyzed. This set of components do not require a metal fatigue AMP. Specific words from [2, para. 4.3.2.1.2.1] are provided:

The existing CUF_{en} calculations remain valid for the subsequent period of extended operation because the number of accumulated cycles, the assumed severity of the cyclic loadings, and the assumed water chemistry conditions evaluated in the calculations are not projected to exceed the limits evaluated for these parameters. The revised projections for the number of accumulated cycles are verified to be consistent with historical plant operating characteristics and anticipated future operation.

THIS REPORT CONTAINS VENDOR PROPRIETARY INFORMATION

A plant-specific justification can be provided to demonstrate that existing CUF_{en} calculations performed using guidance in Section 4.3.2.1.3 of NUREG-1800, Revision 2 will remain valid for the subsequent period of extended operation and are sufficiently conservative when compared to those CUF_{en} calculations that would be generated using the guidance in RG 1.207, Revision 1, or in NUREG/CR-6909, Revision 0 (with “average temperature” used consistent with the clarification that was added to NUREG/CR-6909, Revision 1).

10 CFR 54.21(c)(1)(ii): the fatigue calculations were revised using a projected number of cycles and assumed severity that will remain valid for the 80-year period. The projections must be shown to be consistent with historical plant operating characteristics and anticipated future operation. The resulting fatigue parameters must be verified to remain within the analyzed values for the 80-year period. This criterion can be used for the ASME Section III, Class 1 components that were successfully re-analyzed using projected cycles and the 80-year projected cycles are shown to be less than that set of cycles to which they were analyzed. This set of components requires a metal fatigue AMP to continually demonstrate that actual accumulated cycles remain within the analyzed projected cycles (cycle counting). Specific words from [2, para. 4.3.2.1.2.2] are provided:

The CUF_{en} calculations are revised and shown to remain acceptable throughout the subsequent period of extended operation based on a revised projection of the cumulative number of occurrences, the assumed severity of cyclic loadings, and the assumed water chemistry conditions to the end of the subsequent period of extended operation. The revised projections are verified to be consistent with historical plant operating characteristics and anticipated future operation. The resulting CUF_{en} values are verified to remain less than or equal to unity for the subsequent period of extended operation.

10 CFR 54.21(c)(1)(iii): the fatigue calculations having been revised using a projected number of cycles and assumed severity that will remain valid for the 80-year period did not result in acceptable 80-year projected fatigue usage values. In this case, the applicant uses a metal fatigue AMP as the basis for demonstrating that the effect or effects of aging on the intended function(s) of the structure(s) or component(s) in the fatigue parameter

THIS REPORT CONTAINS VENDOR PROPRIETARY INFORMATION

evaluations will be adequately managed during the subsequent period of extended operation. Guidance for this AMP is provided in Section X.M1, “Cyclic Load Monitoring,” of the GALL-SLR report provides one method that may be used to demonstrate compliance with the requirement in 10 CFR 54.21(c)(1)(iii). Specific words from [2, para. 4.3.2.1.2.3] are provided:

In Section X.M1 of the GALL-SLR Report, the NRC staff evaluated a program for monitoring and tracking the number of occurrences and the severity of critical cyclic loadings for selected components. In Section XI.M2 of the GALL-SLR Report, the NRC staff evaluated a program for monitoring and tracking water chemistry conditions. The NRC staff determined that these programs, when used together, are acceptable AMPs to address the effects of reactor water environment on component fatigue life according to 10 CFR 54.21(c)(1)(iii). The GALL-SLR Report may be referenced in a subsequent license renewal application and should be treated in the same manner as an approved topical report. In referencing the GALL-SLR Report, the applicant should indicate that the material referenced is applicable to the specific plant involved and should provide the information necessary to adopt the finding of program acceptability as described and evaluated in the report. The applicant also should verify that the approvals set forth in the GALL-SLR Report for the generic program apply to the applicant’s program.

Alternatively, the components could be replaced and the CUF_{en} values for the replacement components shown to be acceptable for the subsequent period of extended operation.

This type of Program requires monitoring and tracking the number of occurrences and severity of each of the thermal and pressure transients and requires corrective actions to ensure that applicable fatigue analyses remain within their allowable limits, including those in applicable cumulative usage factor (CUF) analyses. The program has two aspects, one to verify the continued acceptability of existing analyses through cycle counting and the other to provide periodically updated evaluations of the fatigue analyses to demonstrate that they continue to meet the appropriate limits.

This criterion can be used for the ASME Section III, Class 1 components for which the re-analysis using 80-year projected cycles did not result in acceptable fatigue life for the 80-year period. This set of components requires a metal fatigue AMP to continually demonstrate that actual accumulated cycles remain within the analyzed projected cycles (cycle counting) and that the CUF values remain below the acceptance level of 1.0. As stated in the GALL-SLR, actual plant operating conditions monitored by this program can be used to inform updated evaluations

THIS REPORT CONTAINS VENDOR PROPRIETARY INFORMATION

of the fatigue analyses to ensure they continue to meet the design or analysis-specific limit (fatigue monitoring).

1.3 Report Objectives

The objective of the report is to evaluate and document the plant-specific evaluation of the 80-year design basis for the ASME Section III, Class 1 components for PTN. This evaluation will form a part of the TLAAs on Metal Fatigue for the PTN SLRA.

This report includes a summary of the plant-specific evaluations previously performed for the 60-year period in Section 2 (i.e., the PTN CLB), and the evaluation performed for the 80-year SLR period in Section 3.

Based on the foregoing discussion, the objectives of this report are as follows:

- (i) To provide updated plant transient cycle projections for PTN for 80 years of operation for SLR.
- (ii) To evaluate transient severities for PTN for 80 years of operation for SLR.
- (iii) To demonstrate, based on (i) and (ii), that the PTN metal fatigue analyses will remain valid for 80 years in accordance with the requirements of 10 CFR 54.21(c)(1)(i).

This report serves as a replacement for SI Report No. SIR-00-089, Revision 0 (Attachment 8.1 to FPL Document No. PTN-ENG-LRAM-00-0055) [1] that reflects an updated PTN metal fatigue assessment for SLR.

THIS REPORT CONTAINS VENDOR PROPRIETARY INFORMATION

2.0 PLANT-SPECIFIC FATIGUE BACKGROUND FOR PTN

The plant-specific fatigue background for PTN was compiled and summarized for FPL's 60-year LRA in Section 2.0 of Attachment 8.1 to FPL Document No. PTN-ENG-LRAM-00-0055, Revision 1 (SI Report No. SIR-00-089) [1]. A summary of that information is provided in this section.

2.1 Existing Programs

PTN's TLAAs on fatigue were evaluated and resolved for 60 years of operation by fatigue monitoring of all relevant plant thermal transients to confirm that the original transient design limits remain valid for the 60-year operating period (i.e., the PTN Cycle Counting Program). The PTN Cycling Counting Program is summarized in the following section. This program forms the bases for the PTN-specific program described in Section 3.0 for SLR.

2.1.1 *PTN Cycle Counting Program*

Section 3.1 of Attachment 8.1 to FPL Document No. PTN-ENG-LRAM-00-0055, Revision 1 (SI Report No. SIR-00-089) [1] summarizes the PTN Cycle Counting Program implemented for 60 years of operation. FPL implemented a cycle counting procedure at PTN to ensure that the design-basis transient counts are not exceeded during 60 years of plant operation [7]. All significant plant events are captured and recorded via this procedure. The results from this program provide assurance that the structural design bases of the Class 1 plant components (both ASME Section III and ANSI B31.1 piping) are maintained for the 60-year operating period. In addition, a transient evaluation was performed for PTN that projected the actual transient counts established by the PTN Cycle Counting Program to 60 years of plant operation [5]. The results of the projection concluded that the original, 40-year primary system design transients are conservative with respect to quantities and severities for use as a basis for 60 years of operation. The evaluation included the reactor pressure vessel (RPV), the pressurizer, the reactor coolant system (RCS) pumps, the RCS loop piping, the control rod drive mechanisms and adapter cap

THIS REPORT CONTAINS VENDOR PROPRIETARY INFORMATION

seals, and the steam generators. The pressurizer lower head, pressurizer surge and spray nozzles, pressurizer surge and spray lines, charging lines and associated charging nozzles, and branch lines subject to NRC Bulletin 88-08 loading conditions were excluded from the evaluation. The pressurizer components were addressed through the surge line fatigue management program and the pressurizer spray lines and charging lines and nozzles were addressed as part of the B31.1 fatigue evaluation. The branch lines addressed by IEB 88-08 were determined not to be TLAA's.

EAF analysis was performed by scaling-up the NUREG/CR-6260 results for the older-vintage Westinghouse-design plants for PTN-specific conditions. Additional more refined analysis was performed for three of the locations to produce acceptable EAF results. Refined ANSYS analysis was performed for the RPV outlet nozzles, RPV core support pads and pressurizer spray nozzles to achieve CUF_{en} values < 1.0 (pressurizer spray nozzle employed a F_{en} multiplication factor of 4.0 in accordance with SER 1759, Section 4.3.2).

The results of the transient evaluation that form the CLB for PTN for 60 years of operation are summarized in Table 2-1 (from [1]). These results demonstrated that the original design basis (i.e., 40-year) transient definitions were adequate for 60 years of operation, thus satisfying §54.21(c)(1)(i) of the License Renewal Rule [23], as identified in Section 4.3.1 of the PTN LRA [1]. The PTN Fatigue Monitoring Program for license renewal is described in Section 3.2.7 of Appendix B of the PTN LRA.

THIS REPORT CONTAINS VENDOR PROPRIETARY INFORMATION

**Table 2-1: Actual Number of Transients Compared to Design-Basis Number of Transients –
PTN Class 1 Components for 60 Years**

Transient Number	Description	PTN Unit 3			PTN Unit 4		
		Projected Number of Cycles for 60 Years	40-Year Design-Basis Number of Cycles	% Used After 60 Years	Projected Number of Cycles for 60 Years	40-Year Design-Basis Number of Cycles	% Used After 60 Years
1	Station Heatup at 100°F/hour ⁽¹⁾	156 ⁽¹⁰⁾	200	78.0%	191 ⁽¹⁰⁾	200	95.5%
2	Station Cooldown at 100°F/hour ⁽¹⁾	155 ⁽¹⁰⁾	200	77.5%	190 ⁽¹⁰⁾	200	95.0%
3	Pressurizer Cooldown to 400 psia at 200°F/hr	142	200	71.0%	179	200	89.5%
4	Pressurizer Cooldown from 400 psia at 200°F/hr	142	200	71.0%	179	200	89.5%
5	Station Loading at 5% power per minute ⁽¹⁾	2,720 ⁽¹⁰⁾	14,500	18.8%	2,320 ⁽¹⁰⁾	14,500	16.0%
6	Station Unloading at 5% power per minute ⁽¹⁾	2,140 ⁽¹⁰⁾	14,500	14.8%	2,190 ⁽¹⁰⁾	14,500	15.1%
7	Step Load Increase of 10% of Full Power ⁽¹⁾	109 ⁽¹⁰⁾	2,000	5.5%	112 ⁽¹⁰⁾	2,000	5.6%
8	Step Load Decrease of 10% of Full Power ⁽¹⁾	220 ⁽¹⁰⁾	2,000	11.0%	123 ⁽¹⁰⁾	2,000	6.2%
9	Step Load Decrease of 50% of Full Power ⁽¹⁾	167 ⁽¹⁰⁾	200	83.5%	110 ⁽¹⁰⁾	200	55.0%
10	Steady State Fluctuations, +/- 100 psi, +/- 6°F ⁽¹⁾⁽²⁾	Exempted	Infinite	---	Exempted	Infinite	---
11	Feedwater Cycling at Hot Standby ⁽¹⁾⁽³⁾	Exempted	2,000	---	Exempted	2,000	---
12	Boron Concentration Equalization	6,358	36,600	17.4%	6,041	36,600	16.5%
13	Shipping, Handling, Refueling Events	---	---	---	---	---	---
14	Turbine Roll Test ⁽⁶⁾	0	10	0.0%	0	10	0.0%

Table continued on next page.

THIS REPORT CONTAINS VENDOR PROPRIETARY INFORMATION

**Table 2-1: Projected Number of Transients Compared to Design-Basis Number of Transients –
PTN Class 1 Components for 60 Years (continued)**

Transient Number	Description	PTN Unit 3			PTN Unit 4		
		Projected Number of Cycles for 60 Years	40-Year Design-Basis Number of Cycles	% Used After 60 Years	Projected Number of Cycles for 60 Years	40-Year Design-Basis Number of Cycles	% Used After 60 Years
15	Primary Side Hydrostatic Test a. Hydrostatic Test at 3107 psig Pressure, 100°F Temperature	1	1	100.0%	1	1	100.0%
16	b. Hydrostatic Test at 2485 psig Pressure and 400°F Temperature	3	5	60.0%	3	5	60.0%
17	Secondary Side Hydrostatic Test to 1356 psig						
	Steam Generator Loop A (pre- and post-1987)	21	35	60.0%	15	35	42.9%
	Steam Generator Loop B (pre- and post-1987)	17	35	48.6%	15	35	42.9%
	Steam Generator Loop C (pre- and post-1987)	17	35	48.6%	13	35	37.1%
18	Primary to Secondary Side Leak Test to 2,250	0	15	0.0%	0	15	0.0%
19	Secondary Leak Test to 1,085 psig						
	Steam Generator Loop A	4	50	8.0%	4	50	8.0%
	Steam Generator Loop B	7	50	14.0%	11	50	22.0%
	Steam Generator Loop C	4	50	8.0%	7	50	14.0%

THIS REPORT CONTAINS VENDOR PROPRIETARY INFORMATION

**Table 2-1: Projected Number of Transients Compared to Design-Basis Number of Transients –
PTN Class 1 Components for 60 Years (concluded)**

Transient Number	Description	PTN Unit 3			PTN Unit 4		
		Projected Number of Cycles for 60 Years	40-Year Design-Basis Number of Cycles	% Used After 60 Years	Projected Number of Cycles for 60 Years	40-Year Design-Basis Number of Cycles	% Used After 60 Years
20	Secondary to Primary Side Leak Test to 840 psig ⁽¹¹⁾ ,						
	Steam Generator Loop A	8	15	53.3%	14	15	93.3%
	Steam Generator Loop B	15	15	100.0%	15	15	100.0%
	Steam Generator Loop C	9	15	60.0%	15	15	100.0%
21	Loss of Load without Immediate Turbine Trip	43	80	53.8%	38	80	47.5%
22	Loss of AC Power	28	40	70.0%	29	40	72.5%
23	Partial Loss of Flow (Reverse Flow)	43	80	53.8%	43	80	53.8%
24	Loss of Secondary Pressure	2	6	33.3%	0	6	0.0%
25	Reactor Trip	291	400	72.8%	337 ⁽¹⁰⁾	400	84.3%
26	Inadvertent Auxiliary Spray	0	10	0.0%	0	10	0.0%
27	Operating Basis Earthquake (OBE)	0	50	0.0%	0	50	0.0%
28	Loss of Coolant Accident	0	1	0.0%	0	1	0.0%
29	Steam Line Break	0	1	0.0%	0	1	0.0%
30	Safe Shutdown Earthquake (SSE)	0	1	0.0%	0	1	0.0%

THIS REPORT CONTAINS VENDOR PROPRIETARY INFORMATION

Footnotes for Table 2-1:

- (1) Reported to the NRC as an Updated Final Safety Analysis Report (UFSAR) Table 4.1-8 [8] and Table 4.1-10 [28].
- (2) Not counted, not significant contributor to fatigue usage factor.
- (3) Not counted. Intermittent slug feeding at hot standby not performed.
- (4) Limited by Steam Generator Analysis. Represents pre-operational hydrostatic test.
- (5) Limited by Reactor Coolant Pump Analysis.
- (6) Pre-operational transient, performed once prior to initial startup.
- (7) NOT USED
- (8) Design allowable number was changed to 10 cycles (from original value of 35) for the RSG Specification and as presented in 0-ADM-553 [7].
This number was 35 cycles in Table 10.1-1, 10.3-1 and 10.3-2 of PTN-LR-00-0127 [5], and was reported in the LRA. This value of 35 cycles is retained for this table for historical accuracy. The current value of 10 cycles is reflected in Tables 3-1 and 3-2 for the 80-year projections.
- (9) Labelled as “hydrostatic pressure tests” in UFSAR Table 4.1-10 [28].
- (10) 60-Year Projected Cycles from response to RAI 4.3.1-1 [16]. Note that some transient description wording is slightly different.
- (11) Procedure cancelled per [30, Att. 4 page 2 of 6 and 5 of 6].

2.1.2 PTN Fatigue Management Program

The PTN Cycle Monitoring Program [6] provides the basis for the confirmatory management of fatigue-related effects identified in the License Renewal Aging Management Reviews (AMRs). These reviews address the RPVs, pressurizers, steam generators, RCS pump closure regions, and pressurizer surge lines.

A Cycle Monitoring Program is in place that tracks all thermal transients since the startup of both PTN units [7]. This program accounts for the fatigue-significant events by recording the actual cycles imposed on the RCS components and ensuring that the existing design frequency limits are not exceeded. Fatigue significant transient events are characterized as Technical Specification design cycles in the PTN Technical Specifications and Updated Final Safety Analysis Report [8]. Definitions and clarifications of these transient cycles are provided in Reference [7]. An independent review [5] concluded that this procedure accurately identifies and classifies plant transients and provides an effective and consistent method for categorizing, counting, and tracking the plant transients. The independent evaluation concluded that the program maintains in-depth information for each transient cycle counted, including consideration of both rate and magnitude in interpreting selected thermal events.

2.1.2.1 Review of the PTN Cycle Counting Program

The scope of PTN Cycle Counting Program contained in PTN-ENG-LRAM-00-0051 [6] includes the RPV, RPV internals, pressurizers, steam generators, reactor coolant pump (RCP) enclosures and pressurizer surge lines. As stated in PTN-ENG-LRAM-00-0051 [6], FPL Procedure 0-ADM-553 [7] directs PTN Operations to insure copies of all reactor operator logbooks and strip charts are sent to Reactor Engineering where knowledgeable plant personnel evaluate transient and cycle determination for recording in the procedure.

Other Class 1 components with ANSI B31.1 design bases are not within the scope of the PTN Cycle Counting Program. These components were evaluated as acceptable for 60 years through

a demonstration that the number of assumed equivalent full temperature thermal cycles would not be exceeded within the 60-year period of operation [10 - Section 4.3.4].

2.2 PTN Fatigue Bases for 60-Years

This section summarizes the relevant parts of FPL Document No. PTN-ENG-LRAM-00-0055 [4], and identifies what constitutes the CLB for PTN. As such, this CLB, which is applicable to 60 years of operation, forms the starting point for evaluation of Fatigue Management for the SLR period. A description of the design codes for construction used for the Class 1 components is provided.

2.2.1 Class 1 Component Design-Codes of Construction

The design code for the PTN RCS piping (loop and Class 1 attached piping) is the 1955 Edition of ANSI B31.1. This piping is reconciled to ANSI B31.1, 1973 Edition through the Winter 1976 Addenda, with one exception. The pressurizer surge line (including the hot leg surge nozzle) has been analyzed to the 1986 Edition of the ASME Boiler and Pressure Vessel Code, Section III, Subsection NB. Only this one exception involves explicitly defined design-basis transients. The implicit fatigue design basis for ANSI B31.1 components involves fatigue strength reduction factors applied to piping stress allowables that are measured in terms of design-basis numbers of equivalent full-range thermal cycles.

The regenerative heat exchangers were designed and fabricated in accordance with TEMA Class R and the ASME Boiler and Pressure Vessel Code, Section III, Class C (tube side) and Section VIII, Division 1 (shell side). The excess letdown heat exchangers were designed and fabricated in accordance with TEMA Class R and either the ASME Boiler and Pressure Vessel Code, Section III, Class C (tube side) or the ASME Boiler and Pressure Vessel Code, Section VIII, Division 1 (for the shell side). No explicit fatigue design requirements apply to these designs. The pressurizers were designed and fabricated in accordance with the requirements of the 1965 Edition of the ASME Boiler and Pressure Vessel Code, Section III, Subsection NB, which includes requirements for explicit fatigue design analysis.

The RPVs were manufactured by B&W, in accordance with the design and fabrication requirements of the 1965 Edition of the ASME Boiler and Pressure Vessel Code, Section III, Subsection NB, through the Summer 1966 Addenda. These requirements include an explicit fatigue design analysis.

The RCS pumps were designed in accordance with the ASME Boiler and Pressure Vessel Code, Section III, Article 4.

The original steam generator components were designed and analyzed to the 1965 Edition of the ASME Boiler and Pressure Vessel Code, through the Summer 1966 Addenda. The primary side of the steam generators with the exception of the channel heads were replaced at both PTN units in the 1980s. The secondary side of the steam generators were replaced with exception of the steam domes. The replacement steam generator components were constructed in accordance with the 1974 Edition of the ASME Boiler and Pressure Vessel Code, through the Summer 1976 Addenda.

2.2.2 Design-Basis Transient Evaluation

An evaluation performed for PTN for the 60-year LRA established that the existing NSSS primary system design transients bound the projected 60-year operation at both units [5]. The RCS component transient analyses were compared to the actual transients experienced at PTN. This comparison was accomplished by tracking actual plant transients and projecting them to 60 years of operation. The evaluation included an assessment of the transient severity for heatup and cooldown events, which demonstrated the design-basis transients bound the actual operating practices [5]. Thus, the actual transient severity was shown to be bounded by the design basis severity, and the 60-year projected number of cycles was shown to be less than the design frequency applicable to 40 years of operation. Based on this, the evaluation concluded that the existing NSSS primary system design transients, both in number and severity, are valid and conservative for use as a basis for a 60-year period of operation at both PTN units.

2.2.3 Fatigue Design Bases

The component fatigue values in the CLB analyzed to ASME B&PV Section III, Class 1 requirements are shown in Table 2-2 [16, 26, 27 and 31].

Table 2-2: CLB CUF Values for Components Analyzed to ASME Section III, Class 1 Rules

Component	EPU Cumulative Fatigue Usage	Allowable
Reactor Internals ⁽³⁾		
Upper Support Plate	{ }	1.0
Deep Beam	{ }	1.0
Upper Core Plate	{ }	1.0
Upper Core Plate Alignment Pins	{ }	1.0
Upper Support Columns	{ }	1.0
Lower Support Plate	{ }	1.0
Lower Support Plate to Core Barrel Weld	{ }	1.0
Lower Core Plate	{ }	1.0
Lower Support Columns	{ }	1.0
Core Barrel Flange	{ }	1.0
Core Barrel Outlet Nozzle	{ }	1.0
Radial Keys and Clevis Insert Assembly	{ }	1.0
CRDMs		
Latch Housing ⁽¹⁾	{ }	1.0
Rod Travel Housing ⁽⁷⁾	{ }	1.0
Cap ⁽⁷⁾	{ }	1.0
Lower Joint ⁽¹⁾	{ }	1.0
Middle Joint ⁽⁷⁾	{ }	1.0
Upper Joint ⁽⁷⁾	{ }	1.0
Steam Generator ⁽³⁾		
Divider Plate	{ }	1.0
Primary Chamber, Tubesheet and Stub Barrel Complex	{ }	1.0
Tube-to-Tubesheet Weld	{ }	1.0
Tubes	{ }	1.0
Upper Shell Drain	{ }	1.0
Feedwater Nozzle	{ }	1.0
Secondary Manway Bolts ⁽²⁾	{ }	1.0
Upper Shell Remnants	{ }	1.0
Secondary Hand-Hole and Inspection Port	{ }	1.0
Steam Outlet Nozzle Flow Limiters	{ }	1.0
Reactor Coolant Pump		
Reactor Coolant Pump Main Flange Studs ⁽⁵⁾	0.29	1.0
Main Flange ⁽⁵⁾	0.025	1.0
Casing ⁽⁶⁾	0.001	1.0

Table continued on next page.

**Table 2-2: CLB CUF Values for Components Analyzed to ASME Section III, Class 1 Rules
(concluded)**

Component	EPU Cumulative Fatigue Usage	Allowable
Pressurizer		
Spray Nozzle ⁽³⁾	{ }	1.0
Upper Head ⁽³⁾	{ }	1.0
Surge Nozzle ⁽³⁾	{ }	1.0
Safety and Relief Nozzle ⁽³⁾	{ }	1.0
Support Skirt and Flange ⁽⁴⁾	0.0165	1.0
Lower Head ⁽³⁾	{ }	1.0
Heater Well ⁽³⁾	{ }	1.0
Manway Pad ⁽³⁾	{ }	1.0
Manway Cover ⁽⁴⁾	0	1.0
Manway Bolts ⁽⁴⁾	0	1.0
Manway-Welded Diaphragm ⁽³⁾	{ }	1.0
Instrument Nozzle ⁽³⁾	{ }	1.0
Immersion Heater ⁽⁴⁾	0.0040	1.0
Reactor Pressure Vessel ⁽⁵⁾		
Vessel Flange	0.531	1.0
CRDM Housing J-Weld ⁽²⁾	0.73	1.0
CRDM Housing Bi-Metallic Weld	0.62	1.0
Vent Nozzle ⁽²⁾	0.49	1.0
Head Flange	0.083	1.0
Closure Studs ⁽²⁾	0.81	1.0
Shell-to-Shell Juncture	0.034	1.0
Bottom Head-to-Shell Juncture	0.023	1.0
Bottom Mounted Instrumentation Nozzles	0.002	1.0
Core Support Pads	0.020	1.0

Footnotes for Table 2-2:

- (1) CUF values from [27].
- (2) Location with recorded CUF is not wetted by reactor coolant.
- (3) CUF values from [26].
- (4) CUF values from FPL response to RAI 4.3.1-4 [16].
- (5) CUF values listed in EPU LAR L-2010-113 [31, Tables 2.2.2.3-1 and 2.2.2.6-1].
- (6) CUF values listed in UFSAR.

3.0 PLANT-SPECIFIC ASSESSMENT OF FATIGUE EFFECTS FOR SUBSEQUENT LICENSE RENEWAL

This section describes PTN-specific fatigue evaluations necessary to address fatigue-related TLAAs for the 80-year SLR period. The evaluations performed are as follows:

- (i) Evaluation of updated plant transient cycle projections for PTN for 80 years of operation for SLR.
- (ii) Evaluation of transient severities for PTN for 80 years of operation for SLR.
- (iii) Based on (i) and (ii), evaluation that the PTN metal fatigue analyses remain valid for 80 years in accordance with the requirements of 10 CFR 54.21(c)(1)(i).

3.1 PTN Cycle Counting Program

3.1.1 Projection of 80-Year Cycles and Comparison to Administrative Limits

A projection of the number of transients for both PTN units applicable to 80 years of operation is made using the average accumulation rate to-date and a shorter-term average accumulation rate. Because the accumulation behavior of more recent plant operations is expected to be a better predictor of future operation, it is weighted more heavily than earlier periods. In the projections shown in the tables that follow, the shorter-term weight is assumed to be a value of 3 for cycles that have occurred most recently (assumed to be the last 10 years), compared to a weighted value of 1 for the longer-term rate for cycles that occurred for the entire plant operating history prior to the last 10 years.

From past experience (as approved for the Callaway LRA [29]), SI has determined that a Short Term Rate factor of 3 over the most recent 10-year operating period aligns well with actual plant operation and is a bounding, but not overly conservative, estimation of future behavior. This approach is also more conservative compared to assuming a bi-linear method that applies the Short Term Rate to all future years in that it accounts for small deviations from the most recent operating experience. Further evidence of the appropriateness of the LTR and STR values is provided below and in Figure 3-1.

The future projected cycles to 80 years are added to the latest available cycle counts (last updated in July 2016). The projected cycle counts were determined using the following equations:

$$\begin{aligned}\text{LTR} &= \text{Long Term Rate of projected transient accumulation} \\ &= (\text{Cycles}_{\text{now}} - \text{Cycles}_{\text{initial}}) / (\text{Time}_{\text{now}} - \text{Time}_{\text{initial}})\end{aligned}\quad (3-1)$$

where:

$\text{Cycles}_{\text{now}}$ = the current number of cycles (as of the last available cycle counts)

$\text{Cycles}_{\text{initial}}$ = the initial number of cycles
= 0 cycles (both units)

Time_{now} = the time of the last available cycle counts (7/31/2016)

$\text{Time}_{\text{initial}}$ = the time of initial cycles (taken as start of power operations)
= 8/13/1972 (Unit 3)
= 5/30/1973 (Unit 4)

$$\begin{aligned}\text{STR} &= \text{Short Term Rate of projected transient accumulation} \\ &= (\text{Cycles}_{\text{now}} - \text{Cycles}_{\text{short term}}) / (\text{Time}_{\text{now}} - \text{Time}_{\text{short term}})\end{aligned}\quad (3-2)$$

where:

$\text{Cycles}_{\text{short term}}$ = the number of cycles accumulated in time period between Time_{now}
and $\text{Time}_{\text{short term}}$

$\text{Time}_{\text{short term}}$ = the time at ($\text{Time}_{\text{now}} - 10$ years)

$$\begin{aligned}\text{AR} &= \text{Average Rate of cycle accumulation for the } \text{Time}_{\text{now}} \text{ to } \text{Time}_{80} \text{ time period} \\ &= (\text{LTW} * \text{LTR} + \text{STW} * \text{STR}) / (\text{LTW} + \text{STW})\end{aligned}\quad (3-3)$$

where:

LTW = Long Term Weight Factor (weights cycles in the $\text{Time}_{\text{initial}}$ to
 Time_{now} time period)
= 1

STW = Short Term Weight Factor (weights cycles in the $\text{Time}_{\text{short term}}$ to
 Time_{now} time period)

$$= 3$$

$$\text{Cycles}_{80} = (\text{Cycles}_{\text{now}}) + \text{AR} * (\text{Time}_{80} - \text{Time}_{\text{now}}) \quad (3-4)$$

where:

$$\text{Cycles}_{80} = \text{projected number of cycles for 80 years}$$

The 80-year projections are presented in Tables 3-1 and 3-2, for Units 3 and 4, respectively. These tables are compiled for all plant transients monitored by 0-ADM-553. The previous 60-year projections are included in the tables for comparison purposes. They are generally higher values than the values projected for 80 years, most likely caused by the use of the conservative approach projecting the cycles from June 1998 out to 60 years, compared to the more detailed weighted approach described above that uses an additional 18 years of accumulated transients for both PTN units.

Figure 3-1 presents the results of the 80-Year Projection methodology applied to the PTN Unit 3 RCS Heatup cycles using $\text{LTW} = 1$ and $\text{STW} = 3$ for a 10-year short time span. It is evident from observation of the chart that the projection to 80 years conservatively bounds the trajectory of the actual cycles, and that the LTW and STW values are appropriate for use in the PTN transient projections.

THIS REPORT CONTAINS VENDOR PROPRIETARY INFORMATION

Table 3-1: 80-Year Projections - PTN Unit 3

PTN-3		Design Number	Through 2016		60 Year Projection ⁽⁹⁾	80-Year Projections			Source of Allowables			
Transient Number ⁽³⁾	Transient		Count through 2016	Percent of Design Number		80 Year Projection	Percent of Design Number	Weighted Projection Method ⁽¹⁾	UFSAR Table 4.1-8	UFSAR Table 4.1-10	0-ADM-553	Minimum
Normal												
1	Station Heatup at 100°F/hour	200	109	55%	156	164	82%	X	200	200	200	200
2	Station Cooldown at 100°F/hour	200	109	55%	155	164	82%	X	200	200	200	200
3	Pressurizer Cooldown at 200°F/hour ⁽⁵⁾⁽¹⁷⁾	200	95	48%	142	148	74%	X	---	200	200	200
5	Station Loading at 5% power per minute	14500	293	2%	2720	533	4%		14500 ⁽¹¹⁾	---	14500	2200 ⁽¹⁶⁾
6	Station Unloading at 5% power per minute	14500	242	2%	2140	440	3%		14500 ⁽¹¹⁾	---	14500	2200 ⁽¹⁶⁾
7	Step Load Increase of 10% of Full Power	2000	43	2%	109	79	4%		2000	---	2000	2000
8	Step Load Decrease of 10% of Full Power	2000	90	5%	220	164	8%		2000	---	2000	2000
9	Step Load Decrease of 50% of Full Power	200	68	34%	167	82	41%	X	200	---	200	200
	Steady State Fluctuations ⁽¹²⁾	0	Exempted						0			----
	Feedwater Cycling at Hot Standby ⁽¹⁵⁾	2000	Exempted						2000	---	---	2000
	Boron Concentration Equalization ⁽⁵⁾	36000	Not Counted						---	---	---	36600
Test												
14	Turbine Roll Test	10	1 ⁽⁴⁾⁽²⁰⁾	10%	1 ⁽²⁰⁾	1	10%		---	---	---	----
15	Hydrostatic Test at 3107 psig Pressure, 100°F Temperature ⁽⁶⁾⁽¹⁹⁾	1	1	100%	1	1	100%		1	---	5	1
16	Hydrostatic Test at 2485 psig Pressure and 400°F Temperature ⁽⁷⁾	5	1	20%	3	2	40%		5	5	---	5
17	Secondary Side Hydrostatic Test to 1356 psig	----	----	----	----	----	---	---	---	---	---	----
	Steam Generator Loop A ⁽¹⁰⁾	10	17 / 9 ⁽¹⁴⁾	90%	21	9	90%		---	10	35 ⁽²³⁾	10
	Steam Generator Loop B ⁽¹⁰⁾	10	13 / 7 ⁽¹⁴⁾	70%	17	7	70%		---	10	35 ⁽²³⁾	10
	Steam Generator Loop C ⁽¹⁰⁾	10	13 / 7 ⁽¹⁴⁾	70%	17	7	70%		---	10	35 ⁽²³⁾	10
	Primary to Secondary Side Leak Test to 2435 psig ⁽⁷⁾	150	1	1%	----	2	1%		---	150	150	150
18	Primary to Secondary Side Leak Test to 2250 psig ⁽⁶⁾	15	1	7%	0	2	13%		---	15	---	15
19	Secondary Side Leak Test ≥ 1085 psig ⁽²⁾	----	----	----	----	----	---	---	---	---	---	----
	Steam Generator Loop A ⁽¹³⁾	50	9	18%	4	21	42%		---	50	50	50
	Steam Generator Loop B ⁽¹³⁾	50	7	14%	7	16	32%		---	50	50	50
	Steam Generator Loop C ⁽¹³⁾	50	7	14%	4	16	32%		---	50	50	50
	Secondary to Primary Side Leak Test to 840 psig ⁽⁶⁾⁽⁸⁾	---	---	---	----	---	---	---	---	---	---	----
	Steam Generator Loop A	15	8	53%	8	8	53%		---	15	---	15
	Steam Generator Loop B	15	15	100%	15	15	100%		---	15	---	15
	Steam Generator Loop C	15	9	60%	9	9	60%		---	15	---	15

Table continued on next page.

Table 3-1: PTN 80-Year Projections - PTN Unit 3 (concluded)

PTN-3		Design Number	Through 2016		60 Year Projection (9)	80-Year Projections			Source of Allowables			
Transient Number (3)	Transient		Count through 2016	Percent of Design Number		80 Year Projection	Percent of Design Number	Weighted Projection Method (1)	UFSAR Table 4.1-8	UFSAR Table 4.1-10	O-ADM- 553	Minimum
Upset												
21	Loss of Load without Immediate Turbine Trip or Reactor Trip	80	15	19%	43	28	35%		---	80	80	80
22	Loss of Off-Site AC Electrical Power	40	6	15%	28	10	25%	X	---	40	40	40
23	Loss of Flow in One Reactor Coolant Loop	80	14	18%	43	26	33%		---	80	80	80
25	Reactor Trip	400	183	46%	291	272	68%	X	400	400	400	400
26	Inadvertent Auxiliary Spray (18)(21)	10	0	0%	0	1	10%		---	10	---	10
27	OBE (22)	50	0	0%	0	10	20%		---	---	---	20
	Loss of Secondary Pressure (Press Loss) (6)	6	1	17%	2	2	33%		---	---	6	6

Footnotes

- ✓ (1) Weighted projection method used for counted normal and upset transients in which 60-year projections for either unit are over 70% of design numbers in SIR-00-089 [1].
- ✓ (2) Labelled as "Secondary Leak Test" in O-ADM-553 [7]. Labelled as "Hydrostatic Pressure Test" in Table 4.1-10 [28].
- ✓ (3) Transient numbers from Table 3-1 of SIR-00-089 [1].
- ✓ (4) Not expected to have any additional cycles on RSGs.
- ✓ (5) Applies to Pressurizer only.
- ✓ (6) Applies to Steam Generator only. Labelled as "Secondary Leak Test" in O-ADM-553 [7].
- ✓ (7) Limited by Reactor Coolant Pump Analysis [16, Attachment 1, pages 44 and 45].
- ✓ (8) Leak Test Procedure cancelled per [30].
- ✓ (9) 60-year projections from [5, PTN-LR-00-0127 Table 10.3-1].
- ✓ (10) Not expected to have any additional cycles on RSGs.
- ✓ (11) Cycle limits for baffle-former bolts only is being lowered from 14,500 to 2,200 due EPU RCS conditions (Table 4.1-8 of UFSAR [8]).
- ✓ (12) Not counted, not significant contributor to fatigue usage factor.
- ✓ (13) 80-year plant life projected cycles computed using 65 years of life for the RSGs.
- ✓ (14) Values are [(pre-and post- 1987) / (post- 1987)] cycles [5, PTN-LR-00-0127 Table 10.3-1].
- ✓ (15) Not counted, intermittent slug feeding at hot standby not performed.
- ✓ (16) Limit of 2,200 cycles established for baffle former bolts only per UFSAR Table 4.1-8 [8].
- ✓ (17) Represents 200 cycles each of: (1) pressurizer cooldown cycles at $\leq 200^{\circ}\text{F/hr}$ from nominal pressure and (2) pressurizer cooldown cycles at $\leq 200^{\circ}\text{F/hr}$ from 400 psia [28].
- ✓ (18) Spray water temperature differential to 560°F .
- ✓ (19) Applies to Steam Generator only. Represents pre-operational test [16, Note 3 on Attachment 1, pages 44 and 45].
- ✓ (20) Adjustment in 60-year projection in [5, PTN-LR-00-0127 Table 10.3-1] - recorded as a value of 0 when 1 was assumed in pre-operational startup.
- ✓ (21) One cycle is projected for 80 years to remain within the analytical basis if that event occurs.
- ✓ (22) One cycle of 10 events is projected for 80 years to remain within the analytical basis if that event occurs.
- ✓ (23) Recommended revision O-ADM-553 to align with UFSAR Table 4.1-10.

THIS REPORT CONTAINS VENDOR PROPRIETARY INFORMATION

Table 3-2: 80-Year Projections - PTN Unit 4

PTN-4		Design Number	Through 2016		60 Year Projection ⁽⁹⁾	80-Year Projections			Source of Allowables			
Transient Number ⁽³⁾	Transient		Count through 2016	Percent of Design Number		80 Year Projection	Percent of Design Number	Weighted Projection Method ⁽¹⁾	UFSAR Table 4.1-8	UFSAR Table 4.1-10	O-ADM-553	Minimum
Normal												
1	Station Heatup at 100°F/hour	200	121	61%	191	181	91%	X	200	200	200	200
2	Station Cooldown at 100°F/hour	200	121	61%	190	181	91%	X	200	200	200	200
3	Pressurizer Cooldown at 200°F/hour ⁽⁵⁾⁽¹⁷⁾	200	104	52%	179	158	79%	X	---	200	200	200
5	Station Loading at 5% power per minute	14500	260	2%	2320	484	3%		14500 ⁽¹¹⁾	---	14500	2200 ⁽¹⁶⁾
6	Station Unloading at 5% power per minute	14500	242	2%	2190	451	3%		14500 ⁽¹¹⁾	---	14500	2200 ⁽¹⁶⁾
7	Step Load Increase of 10% of Full Power	2000	44	2%	112	82	4%		2000	---	2000	2000
8	Step Load Decrease of 10% of Full Power	2000	57	3%	123	107	5%		2000	---	2000	2000
9	Step Load Decrease of 50% of Full Power	200	42	21%	110	51	26%	X	200	---	200	200
	Steady State Fluctuations ⁽¹²⁾	0	Exempted						0			----
	Feedwater Cycling at Hot Standby ⁽¹⁵⁾	2000	Exempted						2000	---	---	2000
	Boron Concentration Equalization ⁽⁵⁾	36000	Not Counted						---	---	---	36600
Test												
14	Turbine Roll Test	10	1 ⁽⁴⁾⁽²⁰⁾	10%	1 ⁽²⁰⁾	1	10%		---	---	---	----
15	Hydrostatic Test at 3107 psig Pressure, 100°F Temperature ⁽⁶⁾⁽¹⁹⁾	1	1	100%	1	1	100%		1	---	5	1
16	Hydrostatic Test at 2485 psig Pressure and 400°F Temperature ⁽⁷⁾	5	1	20%	3	2	40%		5	5	---	5
17	Secondary Side Hydrostatic Test to 1356 psig	----	----	----	----	----	----	---	----	----	----	----
	Steam Generator Loop A ⁽¹⁰⁾	10	11 / 6 ⁽¹⁴⁾	60%	15	6	90%		---	10	35 ⁽²³⁾	10
	Steam Generator Loop B ⁽¹⁰⁾	10	11 / 6 ⁽¹⁴⁾	60%	15	6	70%		---	10	35 ⁽²³⁾	10
	Steam Generator Loop C ⁽¹⁰⁾	10	9 / 5 ⁽¹⁴⁾	50%	13	5	70%		---	10	35 ⁽²³⁾	10
	Primary to Secondary Side Leak Test to 2435 psig ⁽⁷⁾	150	1	1%	----	2	1%		---	150	150	150
18	Primary to Secondary Side Leak Test to 2250 psig ⁽⁶⁾	15	1	7%	0	2	13%		---	15	---	15
19	Secondary Side Leak Test ≥ 1085 psig ⁽²⁾	----	----	----	----	----	----	---	----	----	----	----
	Steam Generator Loop A ⁽¹³⁾	50	6	12%	4	14	28%		---	50	50	50
	Steam Generator Loop B ⁽¹³⁾	50	6	12%	11	14	28%		---	50	50	50
	Steam Generator Loop C ⁽¹³⁾	50	5	10%	7	12	24%		---	50	50	50
	Secondary to Primary Side Leak Test to 840 psig ⁽⁶⁾⁽⁸⁾				---	----	----	---	----	----	----	----
	Steam Generator Loop A	15	14	93%	14	14	93%		---	15	---	15
	Steam Generator Loop B	15	15	100%	15	15	100%		---	15	---	15
	Steam Generator Loop C	15	15	100%	15	15	100%		---	15	---	15

Table continued on next page.

Table 3-2: PTN 80-Year Projections - PTN Unit 4 (concluded)

PTN-4		Design Number	Through 2016		60 Year Projection (9)	80-Year Projections			Source of Allowables			
Transient Number (3)	Transient		Count through 2016	Percent of Design Number		80 Year Projection	Percent of Design Number	Weighted Projection Method (1)	UFSAR Table 4.1-8	UFSAR Table 4.1-10	O-ADM- 553	Minimum
Upset												
21	Loss of Load without Immediate Turbine Trip or Reactor Trip	80	14	18%	38	27	34%		---	80	80	80
22	Loss of Off-Site AC Electrical Power	40	13	33%	29	19	48%	X	---	40	40	40
23	Loss of Flow in One Reactor Coolant Loop	80	11	14%	43	21	26%		---	80	80	80
25	Reactor Trip	400	187	47%	337	292	73%	X	400	400	400	400
26	Inadvertent Auxiliary Spray (18)(21)	10	0	0%	0	1	10%		---	10	---	10
27	OBE (22)	50	0	0%	0	10	20%		---	---	---	20
	Loss of Secondary Pressure (Press Loss) (6)(21)	6	0	0%	0	1	17%		---	---	6	6

Footnotes

- ✓ (1) Weighted projection method used for counted normal and upset transients in which 60-year projections for either unit are over 70% of design numbers in SIR-00-089 [1].
- ✓ (2) Labelled as "Secondary Leak Test" in O-ADM-553 [7]. Labelled as "Hydrostatic Pressure Test" in Table 4.1-10 [28].
- ✓ (3) Transient numbers from Table 3-1 of SIR-00-089 [1].
- ✓ (4) Not expected to have any additional cycles on RSGs.
- ✓ (5) Applies to Pressurizer only.
- ✓ (6) Applies to Steam Generator only. Labelled as "Secondary Leak Test" in O-ADM-553 [7].
- ✓ (7) Limited by Reactor Coolant Pump Analysis [16, Attachment 1, pages 44 and 45].
- ✓ (8) Leak Test Procedure cancelled per [30].
- ✓ (9) 60-year projections from [5, PTN-LR-00-0127 Table 10.3-1].
- ✓ (10) Not expected to have any additional cycles on RSGs.
- ✓ (11) Cycle limits for baffle-former bolts only is being lowered from 14,500 to 2,200 due EPU RCS conditions (Table 4.1-8 of UFSAR [8]).
- ✓ (12) Not counted, not significant contributor to fatigue usage factor.
- ✓ (13) 80-year plant life projected cycles computed using 66 years of life for the RSGs.
- ✓ (14) Values are [(pre-and post- 1987) / (post- 1987)] cycles [5, PTN-LR-00-0127 Table 10.3-1].
- ✓ (15) Not counted, intermittent slug feeding at hot standby not performed.
- ✓ (16) Limit of 2,200 cycles established for baffle former bolts only per UFSAR Table 4.1-8 [8].
- ✓ (17) Represents 200 cycles each of: (1) pressurizer cooldown cycles at $\leq 200^{\circ}\text{F/hr}$ from nominal pressure and (2) pressurizer cooldown cycles at $\leq 200^{\circ}\text{F/hr}$ from 400 psia [28].
- ✓ (18) Spray water temperature differential to 560°F .
- ✓ (19) Applies to Steam Generator only. Represents pre-operational test [16, Note 3 on Attachment 1, pages 44 and 45].
- ✓ (20) Adjustment in 60-year projection in [5, PTN-LR-00-0127 Table 10.3-2] - recorded as a value of 0 when 1 was assumed in pre-operational startup.
- ✓ (21) One cycle is projected for 80 years to remain within the analytical basis if that event occurs.
- ✓ (22) One cycle of 10 events is projected for 80 years to remain within the analytical basis if that event occurs.
- ✓ (23) Recommended revision O-ADM-553 to align with UFSAR Table 4.1-10.

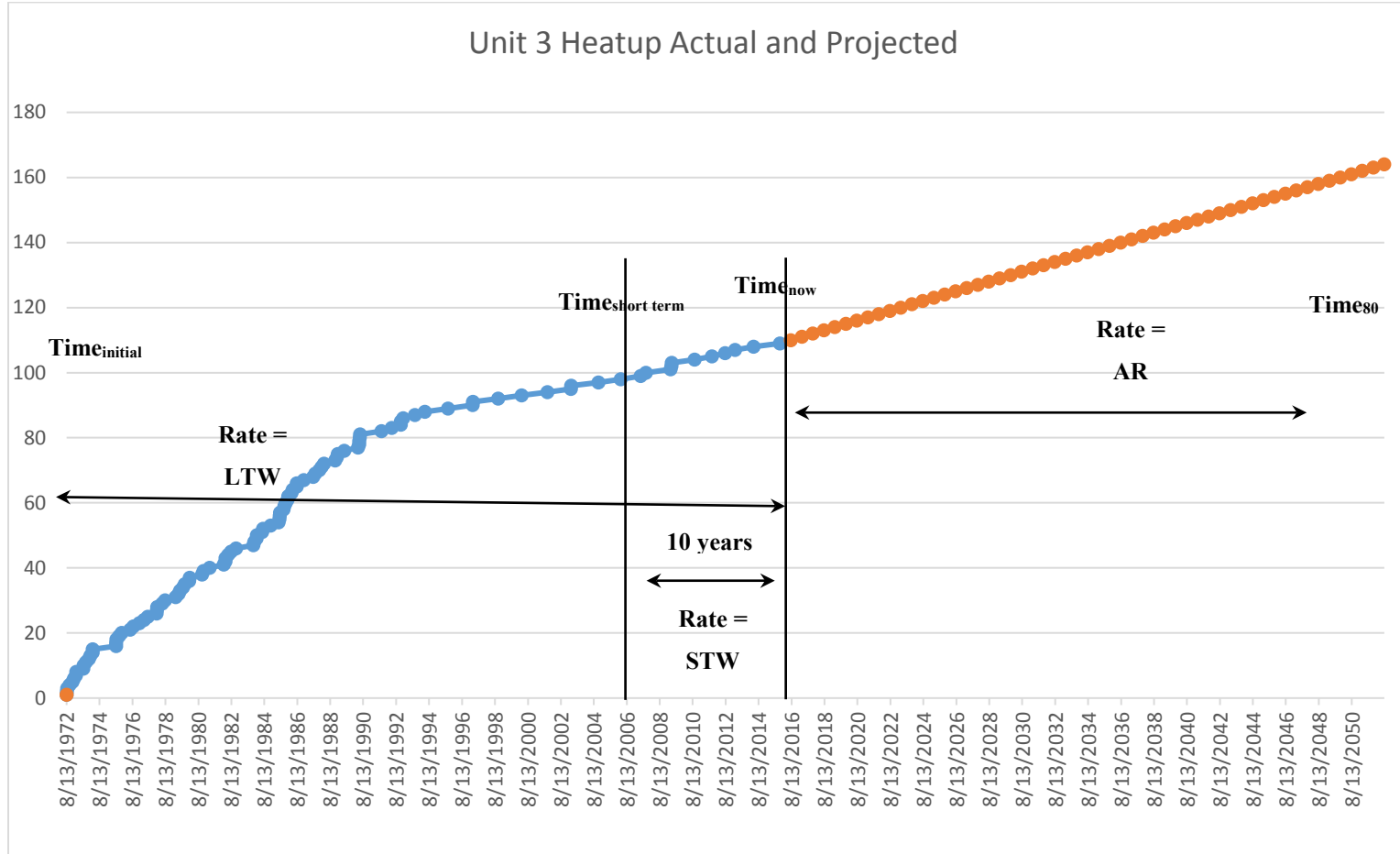


Figure 3-1. Unit 3 RCS Heatup Actual and Projected Cycles

3.2 PTN Fatigue Assessments

3.2.1 Review of PTN Design-Basis Transient Severity

This section describes and summarizes the review performed by FPL of all FSAR and auxiliary transient severities that are part of the ASME Code, Section III, Class 1 component fatigue analyses.

As stated in PTN-ENG-LRAM-00-0051, Procedure 0-ADM-553 directs Operations to insure copies of all reactor operator logbooks and strip charts are sent to Reactor Engineering where knowledgeable plant personnel evaluate transient and cycle determination for recording in the procedure. Thus, FPL's Reactor Engineering assessments performed under the direction of Procedure 0-ADM-553 form a key element in assessing actual transient severities.

Following is information provided by FPL response to RFI-FPL-SI-001 [25].

3.2.1.1 Actual PTN Plant Transients Less Severe than Design Basis Transients

Actual PTN plant transients are less severe than design basis transients based on the following:

Westinghouse performed a study in ~1998 that was part of the 60-year license renewal application that was reviewed and approved by the NRC in a letter dated August 17, 2001 from David B. Matthews, Director Division of Regulatory Program to Mr. J. A. Stall, Senior Vice President, Nuclear and Chief Operating Officer, FPL.

As part of the application review FPL submitted a response to an NRC Request for Additional Information, RAI 4.3.1-1 that addressed the issue of cycle severity (first paragraph on page 46 of 74). In addition, the NRC determined that the applicant's program for maintaining transient records satisfied the requirements of 10CFR54.21(c)(1).

The Conclusion statement in Section 4.3.4 of Turkey Point Unit 3 & 4, License Renewal Safety Evaluation Report (Accession Number: ML021280541)) documents this acceptance.

THIS REPORT CONTAINS VENDOR PROPRIETARY INFORMATION

A similar investigation was performed for Extended Power Uprate (EPU) and was documented in the NRC Safety Evaluation Report (SER) issued 6/15/12 and concluded that “EPU had no adverse impact,” as follows:

“2.2.2 Pressure-Retaining Components and Supports (p. 56 of SER)

The NRC staff’s review focused on the effects of the proposed EPU on the design input parameters and the design-basis loads and load combinations for normal operating, upset, emergency, and faulted conditions. The NRC staff’s review covered (1) the analyses of flow induced vibration and (2) the analytical methodologies, assumptions, ASME Code editions, and computer programs used for these analyses. The NRC staff’s review also included a comparison of the resulting stresses and, where applicable, fatigue cumulative usage factors (CUFs) against the code-allowable limits.

NRC Technical Evaluation of Technical Specification Changes (p. 424 of SER)

The licensee stated in Section 2.2.6.2 of Attachment 4 in its application dated October 21, 2010, that the TS Table 5.6-1 values conservatively estimated the magnitude and frequency of the temperature and pressure transients resulting from various plant conditions. These magnitudes and frequencies were evaluated within the component fatigue analysis discussed within Section 2.2.2 of the staff’s safety evaluation. Furthermore, the frequency of occurrence for the parameters within Table 5.6-1 are unchanged for EPU conditions.”

Source: “Safety Evaluation by the Office of Nuclear Reactor Regulation Related to Amendment No.249 to Renewed Facility Operating License No. DPR-31 and Amendment No. 245 to Renewed Facility Operating License No. DPR-41,” Florida Power and Light Company Turkey Point Plant, Unit Nos. 3 and 4, Docket Nos. 50-250 and 50-251, ADAMS Accession No. ML11293A365.

- The number of actual plant design transients fall well below the design transient projections developed over the past 20 years demonstrating that plant performance continues to improve and that the recent projections are conservative;
- Industry fatigue monitoring has shown for over 30 years that the design basis for the number and severity of design transients is conservative.

THIS REPORT CONTAINS VENDOR PROPRIETARY INFORMATION

3.2.1.2 Plant Procedures

Plant procedures require out of specification events to be evaluated under the Corrective Action Program with Licensee Event Reports (LERs) issued if necessary. FPL's procedures and Cycle Counting Program provide assurance that plant transients have remained within the design envelope in terms of parameter severity and numbers of transients or have been technically reconciled with the design and that this will continue into and throughout the SLR period of operation.

Any transient exceedances are identified and addressed through:

FPL Procedure No. 0-ADM-553, which states, in excerpted parts:

1.0 PURPOSE

The purpose of this procedure is to establish the requirement for recording the actual cycles imposed on various plant systems and to ensure that the design cycles are not exceeded.

- Subsection 5.6:

"The Reactor Engineering Supervisor shall ensure that a Condition report is issued in accordance with PI-AA-104-1000, corrective Action, if either the allowed rate of change or number of cycles, as described in Subsection 4.1 and 4.2 of this procedure, is exceeded. Record the Condition Report Number in the Comment Section of Attachment 1."

- Subsection 4.1:

Plant Cycle: Any plant evolution or transient as defined by this procedure that has the potential of being a Design Cycle

- Subsection 4.2:

Technical Specification Design Cycle (TSDC): Any plant evolution or transient that meets the Technical Specification criteria for a Design Cycle (UFSAR Section 4.1; Table 4.1-10)

THIS REPORT CONTAINS VENDOR PROPRIETARY INFORMATION

3.2.1.3 Results To-Date:

For PTN Unit 3:

See AR 02093849 Pressurizer Heat up Rate –Pressurizer Heat up Rate Exceeded Technical Specification 3.4.9.2 limit of 100⁰ F in one hour.

Event Summary

On 11/25/2015, the plant was being taken to a depressurized condition in order to repair the Reactor Vessel Level Monitoring System probe seals. This required taking the reactor coolant system (RCS) to a solid condition. Normally, the steps to raise the pressurizer to 70% are performed while the RCS is being cooled at the beginning of the outage. The plant conditions were different than what the operators normally experience. Normally, pressurizer fill evolutions are performed in parallel with RCS cooldown or when preparing to vent the RCS following refueling. The emergent repair to the Reactor Vessel Level Monitoring System required collapsing the bubble without an RCS cooldown in progress.

The operating crew and station personnel did not think that raising pressurizer level in Mode 5 with a bubble present would be different than normal pressurizer fill evolutions. This led the crew to have an incorrect mental model of when the system was susceptible to the temperature stratification. The operating crew applied an incorrect understanding of a procedural note, which was influenced by past experiences and thought the pressurizer fill rate limit only applied during bubble collapsing evolutions and that no limit applied while raising pressurizer level to 70%. Pressurizer heaters and spray flow were controlled to maintain the temperature of the water constant throughout pressurizer. The settings used allowed temperature stratification within the pressurizer to occur. During the pressurizer fill, pressurizer liquid temperature dropped from 440 °F to a low value of 315 °F. This cooldown was in excess of 100 °F/ hr, but was less than the cooldown rate Technical Specification limit of 200 °F/ hr. The rapid pressurizer heatup occurred during the out surge after the fill was completed as the hotter saturated water in the upper

THIS REPORT CONTAINS VENDOR PROPRIETARY INFORMATION

pressurizer lowered into the lower pressurizer and exited the surge nozzle. The subsequent heatup from 315 °F to 430 occurred over 15 minutes exceeding the heat up rate Technical Specification limit of 100 °F/ hr.

Operators stabilized pressurizer and reactor coolant system temperatures and entered a 30 hour action to be in cold shutdown for which existing plant conditions satisfied. In accordance with the technical specification, an engineering evaluation was performed to determine the effects of the limit violation on structural integrity of the pressurizer. The evaluation concluded that the thermal transient impact of fatigue on the pressurizer lower region is bounded by analysis and the structural integrity of the pressurizer is acceptable.

For Unit 4:

No reported events.

Thus, to-date FPL Procedure No. 0-ADM-553 procedure has not recorded any events where the design cycle was exceeded in terms of number or severity.

3.2.2 Review of PTN-ENG-LRAM-00-0044

Fatigue management of the pressurizer surge line for both units is accomplished through an NRC approved plant specific program utilizing IWB inspections per ASME Section XI [17]. The PTN-ENG-LRAM-0044 document [22] states that any new flaws discovered as part of this plant specific program will be evaluated for EAF effects [4].

3.3 Evaluation of Metal Fatigue TLAAAs for SLR

As discussed in Section 1.2, three acceptance criteria are available for evaluation of component metal fatigue TLAAAs that are dependent upon the validity of the fatigue analyses:

THIS REPORT CONTAINS VENDOR PROPRIETARY INFORMATION

10 CFR 54.21(c)(1)(i): This criterion can be used for most ASME Section III, Class 1 components where there were no revised fatigue analyses since the 80-year projected cycles are shown to be less than the design set to which they were analyzed. ***This set of components do not require a fatigue management AMP.***

10 CFR 54.21(c)(1)(ii): This criterion can be used for the ASME Section III, Class 1 components that were successfully re-analyzed using projected cycles and the 80-year projected cycles are shown to be less than that set of cycles to which they were analyzed. ***This set of components requires a fatigue management AMP to continually demonstrate that actual accumulated cycles remain within the analyzed projected cycles (cycle counting).***

10 CFR 54.21(c)(1)(iii): This criterion can be used for the ASME Section III, Class 1 components for which the re-analysis using 80-year projected cycles did not result in acceptable fatigue life for the 80-year period. ***This set of components requires a fatigue management AMP to continually demonstrate that actual accumulated cycles remain within the analyzed projected cycles (cycle counting) and that the CUF values remain below the acceptance level of 1.0.*** As stated in NUREG-2191, actual plant operating conditions monitored by this program can be used to inform updated evaluations of the fatigue analyses to ensure they continue to meet the design or analysis-specific limit ***(fatigue monitoring).***

3.4 Conclusions

The following conclusion were demonstrated in this section.

- (i) Evaluation of updated plant transient cycle projections for PTN for 80 years of operation for SLR is provided in 3.1.1.
- (ii) Evaluation of transient severities for PTN for 80 years of operation for SLR is provided in 3.2.1.
- (iii) Based on (i) and (ii), evaluation that the PTN metal fatigue analyses remain valid for 80 years in accordance with the requirements of 10 CFR 54.21(c)(1)(i).

4.0 SUMMARY AND CONCLUSIONS

This report addresses metal fatigue TLAAAs for both PTN units. As such, this report documents the metal fatigue TLAAAs necessary to support operating license renewals from 60 to 80 years for PTN that satisfy all the requirements specified by the NRC for SLR.

Section 2.0 summarizes PTN's TLAAAs on metal fatigue that were resolved for 60 years of operation through fatigue monitoring of all relevant plant thermal transients to confirm that the original transient design limits remain valid for the 60-year operating period (i.e., the PTN Cycle Counting Program).

Section 3.0 contains the plant-specific assessment of metal fatigue TLAAAs for PTN for SLR. The plant-specific assessment is separated into three parts, the PTN Cycle Counting Program which includes 80-year cycle projections, the PTN Fatigue Assessment including a review of transient severity, and a summary of how these two elements satisfy NRC requirements for SLR. Collectively, these parts serve as a replacement to the PTN 60-year fatigue assessment that reflects an updated assessment applicable to SLR. The PTN Cycle Counting Program should be used to verify the continued acceptability of all fatigue analyses through cycle counting and periodically updated evaluations, if necessary, to demonstrate that they continue to remain valid and meet the appropriate limits throughout the SLR period.

Based on the evaluation and results presented in this report, the TLAAAs for metal fatigue are adequately evaluated for PTN, as required by the GALL-SLR [3]. Therefore, the proposed approach described in this report is recommended for inclusion in FPL's SLRA for PTN to address metal fatigue.

THIS REPORT CONTAINS VENDOR PROPRIETARY INFORMATION

5.0 REFERENCES

1. Attachment 8.1 to FPL Document No. PTN-ENG-LRAM-00-0055, Revision 1, “Engineering Evaluation of Environmental Effects of Fatigue,” (SI Report No. SIR-00-089, Revision 0, “Position Document to Address GSI-190 Issues Related to Fatigue Evaluation for Turkey Point Units 3 and 4,” July 2000, SI File No. FPL-10Q-401).
2. NUREG-2192, Final Report, “Standard Review Plan for Review of Subsequent License Renewal Applications for Nuclear Power Plants,” U.S. Nuclear Regulatory Commission, Washington, DC, July 2017, ADAMS Accession No. ML17188A158.
3. NUREG-2191, Final Report, “Generic Aging Lessons Learned for Subsequent License Renewal (GALL-SLR) Report,” Volumes 1 and 2, U.S. Nuclear Regulatory Commission, Washington, DC, July 2017, Agencywide Documents Access and Management System (ADAMS) Accession Nos. ML17187A031 and ML17187A204 for Volumes 1 & 2, respectively.
4. FPL Document No. PTN-ENG-LRAM-00-0055. Revision 1, “Engineering Evaluation for Environmental Effects of Fatigue,” July 16, 2001, SI File No. 1700109.204.
5. FPL Letter No. PTN-LR-00-0127, “Florida Power & Light Company, Turkey Point Units 3 & 4, License Renewal Project, GSI-190 Position Paper,” July 12, 2000, SI File No. FPL-10Q-204.
6. FPL Document No. PTN-ENG-LRAM-00-0051, Revision 4, “Fatigue Monitoring Program – License Renewal Basis Document,” SI File No. 1700109.202.
7. FPL Procedure No. 0-ADM-553, Revision 5, “Maintaining Records for Design Cycles,” Units 3 and 4, 3/10/16, SI File No. 1700109.203.
8. PTN UFSAR, Table 4.1-8, (Design Thermal and Loading Cycles – 60 Years), SI File No. 1700109.208.

THIS REPORT CONTAINS VENDOR PROPRIETARY INFORMATION

9. SI Calculation No. 0900948.302, Revision 1, “Environmentally-Assisted Fatigue Evaluation of the RPV Shell Using 60-Year Projected Cycles and Enveloping Cycles,” April 22, 2010.
10. FPL Letter No. L-2000-177, “Application for Renewed Operating Licenses, Turkey Point Units 3 and 4,” September 8, 2000, ADAMS Accession No. ML003749654.
11. Attachment 8.2 to FPL Document No. PTN-ENG-LRAM-00-0055, Revision 1, “Engineering Evaluation of Environmental Effects of Fatigue,” (SI Report No. SIR-01-042, “Transmittal of Final RAI Responses on Fatigue,” April 13, 2001, SI File No. FPL-10Q-402).
12. SI Report SIR-01-042, Addendum 1, “Transmittal of Revised RAI Response,” September 14, 2001, SI File No. FPL-10Q-402.
13. SI Calculation Number FPL-09Q-307, “Pressurizer Insurge/Outsurge Fatigue Analysis,” August 1, 2000.
14. SI Calculation Number 1100768.304, “Pressurizer Spray Nozzle Fatigue Analysis,” Revision 0, February 7, 2012.
15. NUREG/CR-6260 (INEL-95/0045), “Application of NUREG/CR-5999 Interim Fatigue Curves to Selected Nuclear Power Plant Components,” U.S. Nuclear Regulatory Commission, Washington, DC, March 1995, ADAMS Accession No. ML031480219.
16. FPL Letter No. L-2001-75, “Response to Request for Additional Information for the Review of the Turkey Point Units 3 and 4 License Renewal Application,” April 19, 2001, ADAMS Accession No. ML011170195.
17. FPL Letter No. L-2012-214 from Michael Kiley to U.S. Nuclear Regulatory Commission, “Turkey Point Units 3 and 4, Docket Nos. 50-250 and 50-251, License Renewal Commitment, Submittal of Pressurizer Surge Line Welds Inspection Program,” May 16, 2012, ADAMS Accession No. ML12152A156.

THIS REPORT CONTAINS VENDOR PROPRIETARY INFORMATION

18. SI Calculation No.0900948.301, “Environmental Fatigue Evaluation of Reactor Coolant System Components/Nozzles and Connected Systems,” Revision 1, April 30, 2010.
19. SI Calculation No. 1100756.304, “Flaw Tolerance Evaluation of the Nozzle-to-Piping Welds of the Hot Leg Surge Nozzle and Pressurizer Surge Nozzle,” Revision 0, April 8, 2012.
20. SI Calculation No.1100756.401, “Flaw Tolerance Evaluation of Turkey Point Surge Line Welds Using ASME Code Section XI, Appendix L,” Revision 1, May 10, 2012.
21. Turkey Point, Units 3 and 4, “Submittal of Fifth 10 Year Interval Inservice Inspection (ISI) Program Plan,” ADAMS Accession No. ML13141A595.
22. FPL Letter PTN-ENG-LRAM-00-0044, Rev. 3, “ASME Section XI, Subsections IWB, IWC and IWD Inservice Inspection Program – License Renewal Program Basis Document,” SI File No. 1700109.201.
23. U.S. Code of Federal Regulations, Title 10, Chapter I -- Nuclear Regulatory Commission, Part 54, “Requirements for Renewal of Operating Licenses for Nuclear Power Plants.”.
24. NRC Extended Operating License Approval, including:
 - a. NRC Letter from Rajendar Auluck to J. A. Stall, “Issuance of Renewed Facility Operating Licenses Nos. DPR-31 and DPR-41 for Turkey Point Nuclear Generating Units Nos. 3 and 4,” U.S. Nuclear Regulatory Commission, Washington, DC, June 6, 2002, ADAMS Accession No. ML021550105.
 - b. NUREG-1759, “Safety Evaluation Report Related to the License Renewal of Turkey Point Nuclear Plant, Units 3 and 4,” U.S. Nuclear Regulatory Commission, Washington, DC, April 2002, ADAMS Accession No. ML021280541.
 - c. NUREG-1759, Supplement 1, “Safety Evaluation Report Related to the License Renewal of Turkey Point Nuclear Plant, Units 3 and 4,” U.S. Nuclear Regulatory Commission, Washington, DC, May 2002, ADAMS Accession No. ML021560094.
25. RFI-FPL-SI-001, *Severity Design Input*, SI File No. 1700109.209.

THIS REPORT CONTAINS VENDOR PROPRIETARY INFORMATION

26. Westinghouse letter reference LTR-MRCDA-17-81, Rev. 0, *Requested Cumulative Fatigue Usage Factors from Turkey Point Unit 3 and Unit 4 EPU Licensing Report*, included in Westinghouse letter reference NEXT-17-145, Transmittal of Westinghouse Proprietary Information to Structural Integrity Associates (SIA) per Purchase Order, **WESTINGHOUSE PROPRIETARY**, SI File No. 1700109.111P.
27. AREVA Letter AREVA-17-02801, Proprietary and Non-Proprietary Documents and Affidavits, **AREVA PROPRIETARY**, dated 12/15/2017, SI File No. 1700804.206P.
28. PTN UFSAR Table 4.1-10, (Component Cyclic or Transient Limits), SI File No. 1700109.208.
29. License Renewal Application, Callaway Unit 1, ML113530372 and NUREG-2172, Safety Evaluation Report Related to the License Renewal of Callaway Plant, Unit 1, ADAMS Accession No. ML15068A342.
30. FPL Letter PTN-LR-99-00127, "Florida Power & Light Company Turkey Point Units 3 & 4 License Renewal Project", September 22, 1999, SI File No. FPL-10Q-204.
31. Turkey Point Units 3 and 4, License Amendment Request for Extended Power Uprate, L-2010-113 Attachment 4, ADAMS Accession No. ML103560177, SI File No. 1700109.210.

Enclosure 4
Non-proprietary Reference Documents
and
Redacted Versions of Proprietary
Reference Documents
(Public Version)
Attachment 5

**SIA Report No. 1700109.401P, Revision 3 – REDACTED
Evaluation of Environmentally-Assisted Fatigue for Turkey
Point Units 3 and 4 for Subsequent License Renewal,
January 2018**

(62 Total Pages, including cover sheets)

Report No. 1700109.401P
Revision 3 - REDACTED
Project No. 1700109
January 2018

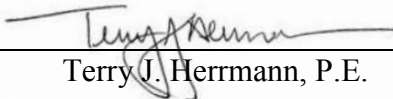
**Evaluation of Environmentally-Assisted
Fatigue for Turkey Point Units 3 and 4 for
Subsequent License Renewal**

Prepared for:
Florida Power & Light Company
Juno Beach, FL
Purchase Order No. 2000230248 dated 02/16/2017

Prepared by:
Structural Integrity Associates, Inc.
San Jose, California

Prepared by: 
David A. Gerber, P.E.

Date: 1/4/2018

Reviewed by: 
Terry J. Herrmann, P.E.

Date: 11/4/2018

Approved by: 
David A. Gerber, P.E.

Date: 1/4/2018

REVISION CONTROL SHEET

Document Number: **1700109.401P - REDACTED**

Title: Evaluation of Environmentally-Assisted Fatigue for Turkey Point Units 3 and 4 for
Subsequent License Renewal

Client: Florida Power & Light Company

SI Project Number: **1700109**

Quality Program: ☒ Nuclear ☐ Commercial

Section	Pages	Revision	Date	Comments
1.0 2.0 3.0 4.0 5.0 App. A	1-1 – 1-7 2-1 – 2-15 3-1 – 3-17 4-1 – 4-2 5-1 – 5-6 A-1 – A-7	0	11/13/2017	Initial Issue
2.0 3.0 5.0	2-12, 2-13, 3-7 – 3-9 3-11 – 3-14, 3-18 – 3-20, 5-5 – 5-7	1	12/9/2017	Insertion of 60-year CUF values for CRDM components and 80-year CUF, F_{en} and CUF_{en} values for CRDM and RPV components. Annotation of “P” on file names of vendor proprietary documents added. Added new references. Change highlighted text to bold italicized text.
3.0 5.0	3-11 – 3-14 5-5, 5-7	2	12/17/2017	Update of two CRDM CUF values and correction of the Vent Nozzle CUF value in Table 3-3, replacement of Reference [23] in Table 3-3, removal of References [41} and [43] from List of References, addition of three footnotes in Table 3-4, update of CUF_{en} of CRDM Upper Joint and update of revision number of Reference [29].
2.0 3.0 5.0	2-15, 3-2, 3-7, 3-8, 3-15, 5-5	3	1/4/2018	Remove GALL Rev. 2 references.

Table of Contents

<u>Section</u>	<u>Page</u>
1.0 INTRODUCTION.....	1-1
1.1 Background.....	1-1
1.2 GALL-SLR Guidance for EAF.....	1-1
1.2.1 Summary of the NRC's SLR Guidance for EAF.....	1-2
1.2.2 Summary of the EAF TLAA's Performed for PTN for 60 Years	1-5
1.3 Report Objectives.....	1-7
2.0 PLANT-SPECIFIC FATIGUE BACKGROUND FOR PTN.....	2-1
2.1 PTN Cycle Counting Program.....	2-2
2.2 PTN EAF Assessment.....	2-9
2.3 PTN Surge Line Inspection Program.....	2-14
3.0 PLANT-SPECIFIC ASSESSMENT OF ENVIRONMENTALLY-ASSISTED FATIGUE EFFECTS FOR SUBSEQUENT LICENSE RENEWAL.....	3-1
3.1 PTN Cycle Counting Program.....	3-2
3.2 PTN EAF Assessment.....	3-7
3.3 Plant-Specific Limiting Locations	3-14
3.4 Summary of PTN EAF Assessment.....	3-15
4.0 SUMMARY AND CONCLUSIONS	4-1
5.0 REFERENCES.....	5-1
APPENDIX A F_{EN} CALCULATIONS.....	A-1

List of Tables

<u>Table</u>	<u>Page</u>
Table 2-1: Projected Number of Transients Compared to Design-Basis Number of Transients – PTN Class 1 Components for 60 Years	2-4
Table 2-2: Summary of the PTN EAF Assessment for 60 Years of Operation	2-11
Table 3-1: Summary of Transient Projections for 80 Years of Operation (PTN Unit 3)	3-3
Table 3-2: Summary of Transient Projections for 80 Years of Operation (PTN Unit 4)	3-5
Table 3-3: Other Class 1 RCPB Components with a CUF Value ⁽¹⁾	3-9
Table 3-4: Summary of the PTN EAF Assessment for SLR (80 Years of Operation)	3-10
Table 3-5 Minimum Cycles Used in EAF Analyses	3-18

PROPRIETARY INFORMATION NOTICE

This report contains information that is proprietary to other vendors that is protected under one or more Non-Disclosure Agreements (NDAs). Such information is identified by red, bold-faced font surrounded by brackets. An example is {**this wording**}. Release of such information is not authorized without the express written permission of the authorized owner of the information.

1.0 INTRODUCTION

1.1 Background

Florida Power & Light Company (FPL) is developing a Subsequent License Renewal (SLR) application (SLRA) to extend plant operations at Turkey Point Nuclear Plant Units 3 and 4 (PTN) from 60 to 80 years. The PTN SLRA will build off the content from the original PTN license renewal application (LRA) submitted to the U.S. Nuclear Regulatory Commission (NRC) in 2000 [1], and adjust the content as necessary so that it follows the updated NRC guidance for SLR.

In response to FPL's original LRA submittal for PTN, the NRC issued renewed operating licenses on June 6, 2002 to operate an additional 20 years beyond the original 40-year operating licenses [2]. Structural Integrity Associates, Inc. (SI) provided support to FPL in 2000 and 2001 as a part of the LRA development and NRC approval for PTN. SI's support included the preparation of engineering documents, calculations, and evaluations associated with certain time limited aging analyses (TLAAs) for PTN.

This report addresses TLAAAs associated with environmentally-assisted fatigue (EAF) for both PTN units. As such, this report documents the EAF TLAAAs necessary to support operating license renewals from 60 to 80 years for PTN that satisfy all the requirements specified by the NRC for SLR.

1.2 GALL-SLR Guidance for EAF

Two of the NRC's applicable guidance documents for SLR were published in July 2017, and two others for EAF are still under development. Specifically, this guidance includes the following four documents:

- NUREG-2191, "Generic Aging Lessons Learned for Subsequent License Renewal (GALL-SLR) Report" [3].

- NUREG-2192, “Standard Review Plan for Review of Subsequent License Renewal Applications for Nuclear Power Plants” [4].
- Draft Regulatory Guide (RG) DG-1309 (Proposed Revision 1 of RG 1.207), “Guidelines for Evaluating the Effects of Light-Water Reactor Coolant Environments in Fatigue Analyses of Metal Components” [5].
- NUREG/CR-6909 (ANL 12/60), Revision 1 (Draft), “Effect of LWR Coolant Environments on Fatigue Life of Reactor Materials” [6].

Since some of the above documents are not yet published as final guidance, this report satisfies all applicable NRC requirements for the EAF TLAAs based on the NRC’s final guidance for SLR and current content of the draft guidance for EAF, plus any additional knowledge gained from ongoing interactions between the industry and NRC as the documents approach final publication.

The following two subsections provide an overview of the NRC’s draft guidance for EAF, and summarize the PTN EAF TLAAs prepared for FPL’s 60-year LRA. Section 1.3 describes the report objectives and identifies the updates needed to assess EAF for PTN for 80 years of operation based on the NRC’s SLR guidance.

1.2.1 Summary of the NRC’s SLR Guidance for EAF

The NRC’s Standard Review Plan for SLR (SRP-SLR) [4] provides guidance to NRC staff reviewers for SLRA content to ensure the quality and uniformity of NRC staff reviews, and to present a well-defined base from which to evaluate applicant programs and activities for SLR. The SRP-SLR is a companion document to the NRC’s Generic Aging Lessons Learned Report for SLR (GALL-SLR) [3], which provides guidance for SLR applicants and contains the NRC staff’s generic evaluation of plant aging management programs (AMPs) and establishes the technical basis for their adequacy.

Section 4.3, “Metal Fatigue,” of the SRP-SLR specifies the areas of review to ensure that the metal component fatigue parameter evaluations are valid for SLR. For EAF, these areas include

component fatigue life estimates based on cumulative usage factor (CUF) calculations, and CUF adjusted to account for the effects of the reactor water environment (CUF_{en}). The acceptance criteria for such calculations follow the requirements of Part 54 to Title 10 of the U.S. Code of Federal Regulations (10 CFR 54) [7]. Specifically, pursuant to 10 CFR 54.21(c)(1)(i) through (iii), an applicant must demonstrate one or more of the following for each analysis:

- i. The analyses remain valid for the period of extended operation;
- ii. The analyses have been projected to the end of the period of extended operation; or
- iii. The effects of aging on the intended function(s) will be adequately managed for the period of extended operation.

For components evaluated for CUF_{en}, the acceptance criteria depend on the applicant's choice of 10 CFR 54.21(c)(1)(i), (ii), or (iii). Applicants must also include CUF_{en} calculations for additional component locations if they are more limiting than those previously evaluated for 60 years of operation. Examples of critical components are identified in NUREG/CR-6260 [8]; however, plant-specific component locations in the reactor coolant pressure boundary (RCPB) may be more limiting than those considered in NUREG/CR-6260, and thus must also be considered. Plant-specific justification can be provided to demonstrate that calculations for the NUREG/CR-6260 locations do not need to be included.

Chapter X, "Aging Management Programs That May Be Used to Demonstrate Acceptability of Time-Limited Aging Analyses in Accordance with 10 CFR 54.21(c)(1)(iii)," of the GALL-SLR Report provides an AMP acceptable to the NRC for managing EAF. Specifically, Section X.M1, "Fatigue Monitoring," defines an acceptable basis for managing structures and components (SCs) that are the subject of metal fatigue or cycle-based TLAAAs or other analyses that assess fatigue or cyclical loading, in accordance with the 10 CFR 54.21(c)(1), including EAF assessments of CUF_{en}.

In Section X.M1 of the GALL-SLR Report, the NRC staff evaluated an AMP for monitoring and tracking the number of occurrences and the severity of critical cyclic loadings for selected components. The scope of the X.M1 AMP includes those mechanical or structural components

with fatigue TLAAAs or other analyses that depend on the number of occurrences and severity of transient cycles associated with the plant license renewal period. The X.M1 AMP has two aspects, one that verifies the continued acceptability of existing analyses through cycle counting, and the other that provides periodically updated evaluations of the fatigue analyses to demonstrate that they continue to meet the appropriate limits. In the former, the program assures that the number of occurrences and severity of each transient remains within the limits of the fatigue analyses, which in turn ensure that the analyses remain valid. For the latter, actual plant operating conditions monitored by this program can be used to inform updated evaluations of the fatigue analyses to ensure the analyses continue to meet the design or analysis-specific limit, thus minimizing the likelihood of failures from fatigue-induced cracking of the components caused by cyclic strains in the component's material.

EAF effects on fatigue are evaluated by assessing the specific set of sample critical components for the plant. The X.M1 AMP monitors and tracks the number of occurrences and severity of each of the critical thermal and pressure transients for the selected components to maintain the CUF_{en} below the design limit of 1.0. This program also relies on the GALL-SLR Report AMP XI.M2, "Water Chemistry," to provide monitoring of appropriate environmental parameters for calculating environmental fatigue multiplier (F_{en}) values, which are used to calculate CUF_{en} from CUF.

EAF effects on fatigue for the critical components can be evaluated using the positions described in RG 1.207, Revision 1 [5], NUREG/CR-6909, Revision 0 [10] (with "average temperature" used consistent with the clarification that was added to NUREG/CR-6909, Revision 1) [6], or other subsequent NRC-endorsed alternatives.

In some cases, flaw tolerance evaluations are used to establish inspection frequencies for components that, for example, exceed CUF or CUF_{en} fatigue limits. As an example, ASME Code, Section XI, Nonmandatory Appendix L [9] provides guidance on the performance of fatigue flaw tolerance evaluations to determine acceptability for continued service of RCPB components subjected to cyclic loadings. In flaw tolerance evaluations, the predicted size of a postulated fatigue flaw, whose initial size is typically based on the resolution of the inspection

method, is a computed parameter that is used to determine the appropriate inspection frequency. The X.M1 AMP monitors and tracks the number of occurrences and severity of critical thermal and pressure transients for the selected components that are used in the fatigue flaw tolerance evaluations to verify that the inspection frequencies remain appropriate.

Component locations within the scope of this program are updated based on operating experience (OE), plant modifications, and inspection findings.

The GALL-SLR Report may be referenced in a SLRA and should be treated in the same manner as an approved topical report. In referencing the GALL-SLR Report, the applicant should indicate that the material referenced is applicable to their plant and should provide the information necessary to support the finding of program acceptability as described and evaluated in the report.

1.2.2 Summary of the EAF TLAA's Performed for PTN for 60 Years

As part of the PTN LRA for 60 years of operation, a report was prepared to describe how the TLAA's on fatigue and the technical issue associated with EAF evaluation in response to Generic Safety Issue (GSI) 190 [11] were addressed for PTN [12]. That work was further enhanced through responses to NRC Requests for Additional Information (RAIs) [13]. Because the work pre-dated the initial revision of the GALL Report [14], guidance for EAF evaluation was still being developed and has continued to evolve based on industry experience. The recommended approach for PTN accomplished two objectives. First, the TLAA's on fatigue design were resolved by confirming that the original transient design limits remain valid for the 60-year operating period. Fatigue monitoring was used to ensure these transient limits would not be exceeded. Second, EAF effects on fatigue life were examined using the most recent data from laboratory simulation of the reactor coolant environment [15,16]. These two evaluations were kept separate, since fatigue design is a TLAA and part of the plant current licensing basis (CLB), while the consideration of reactor water environmental effects on fatigue life, as described in GSI-190, was not a part of the original PTN CLB.

The SIR-00-089 report [12] examined the PTN fatigue design basis as it applied to the resolution of fatigue design TLAAAs and described existing plant programs for managing fatigue crack initiation and growth that were to be used to continue to manage the effects of fatigue during the license renewal term. It also described the results from regulatory and industry studies on the effect of environmental fatigue that were used to address EAF effects in response to GSI-190 for PTN. The results from the PTN plant cycle monitoring program were shown to satisfy license renewal requirements for the fatigue TLAAAs, specifically paragraph 10 CFR 54.21(c)(1)(i), where the number of plant transient design cycles for 40 years of operation and transient severity were shown to remain valid for the period of extended operation.

With respect to EAF, the report addressed reactor water environmental effects on the fatigue life of selected fatigue-sensitive reactor coolant system (RCS) components, in accordance with the resolution of GSI-190. The method chosen for this EAF evaluation was based on existing industry evaluations that were pertinent to PTN. Principally, this information was obtained from NUREG/CR-6260, as well as generic industry environmental fatigue studies and additional laboratory data [15,16]. Existing plant programs were described for managing the effects of fatigue and any modifications or enhancements required for the renewal period. EAF effects were shown to be acceptable for all NUREG/CR-6260 components except for the pressurizer surge line. This remaining component was therefore addressed through inspection programs. Based on results of high calculated CUF_{en} values, the surge line was determined to be a candidate for additional inspection considerations during the license renewal period. All welds in the surge line were therefore included as a part of future ISI programs. The surge line inspection approach was submitted to the NRC for review in 2012 [17], and was subsequently approved by the NRC in 2013 [18].

Additional EAF evaluations were undertaken for the reactor pressure vessel (RPV) shell and the RCS components/nozzles and connected systems in 2010 as a part of an Extended Power Uprate (EPU) project for PTN [19]. In addition, the pressurizer spray nozzle was reevaluated for EAF using finite element methods in 2011/2012 [20]. Additional analyses were undertaken by Westinghouse [21, 22] and AREVA, NP [21, 23] for EPU. The results of all these evaluations supersede the applicable results from SIR-00-089.

Collectively, these analyses documented that the TLAAs for fatigue and EAF effects were properly evaluated for PTN for 60 years of operation, so the approach was included in FPL's LRA for PTN. The approach was subsequently approved by the NRC when the PTN renewed operating licenses were issued in 2002. As such, they form the CLB for PTN, and serve as the input for the EAF evaluation for SLR.

1.3 Report Objectives

Based on the summaries provided in Section 1.2, the objectives of this report are as follows:

- (i) To perform updated EAF screening for SLR for critical locations using all available CUF values for all PTN Class 1 RCPB components exposed to the water environment for 60 years of operation.
- (ii) To develop updated PTN environmental multipliers that adopt the latest F_{en} methods provided in RG 1.207, Revision 1.
- (iii) To calculate updated CUF_{en} values for all bounding PTN CUF locations using updated transient projections for 80 years and the updated F_{en} values.
- (iv) To demonstrate that the PTN EAF analyses will remain valid for 80 years in accordance with the requirements of 10 CFR 54.21(c)(1)(i).
- (v) To serve as a replacement for Attachments 8.1 and 8.2 to FPL Document No. PTN-ENG-LRAM-00-0055 that reflects an updated PTN EAF assessment for SLR.

The relevant plant-specific fatigue background for PTN, which established the CLB for 60 years of operation and serves as the starting point for assessing EAF for SLR, is described in Section 2.0. The plant-specific assessment of EAF effects for PTN for SLR is contained in Section 3.0.

A summary of the key results of this report and the conclusions relevant to SLR are provided in Section 4.0.

This report was prepared with information currently available. Analyses are in progress to supply values for the locations in the tables populated with TBD (To Be Determined) notations, at which time this report can be revised to incorporate updated information.

2.0 PLANT-SPECIFIC FATIGUE BACKGROUND FOR PTN

The plant-specific fatigue background for PTN was initially compiled and summarized for FPL's 60-year LRA in Section 2.0 of Attachment 8.1 to FPL Document No. PTN-ENG-LRAM-00-0055, Revision 1 (SI Report No. SIR-00-089) [12]. That summary is duplicated in this section, with appropriate updates from the NRC's review and approval of the LRA and EPU, as well as updates made for SLR.

With respect to EAF, as described in Section 1.2.2, there are six sets of previous analyses that form the CLB for PTN and serve as the input for the EAF evaluation for SLR, as follows:

1. Section 3.0 of Attachment 8.1 to FPL Document No. PTN-ENG-LRAM-00-0055, Revision 1 (SI Report No. SIR-00-089) [12], which describes how reactor water environmental effects on the fatigue life of selected fatigue-sensitive RCS components, in accordance with the resolution of GSI-190, were addressed for PTN.
2. Attachment 8.2 to FPL Document No. PTN-ENG-LRAM-00-0055, Revision 1 (SI Report No. SIR-01-042, Rev. 0) [13], which further enhanced the Item 1 report through responses to NRC RAIs¹.
3. Section 4.0 of Attachment 8.1 to FPL Document No. PTN-ENG-LRAM-00-0055, Revision 1 (SI Report No. SIR-00-089), which addressed EAF management of the PTN surge line weld locations through a PTN plant-specific program utilizing the ASME Code Section XI inspection program. The plant-specific surge line inspection program was approved by the NRC in 2013 [18].
4. SI Calculation No. 0900948.302, which performed an additional EAF evaluation for the RPV shell as a part of EPU implementation for PTN in 2010 [19.b]. SI Calculation No. 0900948.301 determined that EAF evaluations for RCS components/nozzles and connected systems were not impacted by EPU [19.a]. Some of the results of the EPU evaluations supersede the applicable results from Items 1 and 2 above.

¹ Throughout this section, reference is made to the RAI responses filed in the NRC's Agencywide Documents Access and Management System (ADAMS) as the source of any data rather than Attachment 8.1 to FPL Document No. PTN-ENG-LRAM-00-0055, Revision 1.

5. SI Calculation Nos. 1100768.301 through 1100768.304, which performed an updated finite element EAF evaluation for the pressurizer spray nozzle in response to license renewal commitments for PTN in 2011/2012 [20]. Those results supersede the applicable results from Items 1 and 2 above.
6. Westinghouse [21, 22] and AREVA evaluations [21, 23] for EPU.

PTN's TLAAAs on fatigue were resolved for 60 years of operation by the above analyses through a combination of three demonstrations: (i) fatigue monitoring of all relevant plant thermal transients to confirm that the original transient design limits remain valid for the 60-year operating period (i.e., the PTN Cycle Counting Program), (ii) reactor water environmental effects on fatigue life were examined using the most recent data from laboratory simulations of the reactor coolant environment (i.e., the PTN EAF Assessment), and (iii) inspection of the surge line welds under a plant-specific program utilizing the ASME Code Section XI inspection program to verify the absence of fatigue cracking (i.e., the PTN Surge Line Inspection Program). Each of these three demonstrations are summarized in the sections that follow and form the bases for the PTN-specific program described in Section 3.0 for addressing EAF effects for SLR.

2.1 PTN Cycle Counting Program

Section 3.1 of Attachment 8.1 to FPL Document No. PTN-ENG-LRAM-00-0055, Revision 1 (SI Report No. SIR-00-089) [12] summarizes the PTN cycle counting program implemented for 60 years of operation. FPL implemented a cycle counting procedure at PTN to ensure that the design-basis transient counts are not exceeded during 60 years of plant operation [2421]. All significant plant events are captured and recorded via this procedure. The results from this program provide assurance that the structural design bases of the Class 1 plant components (both ASME Section III and ANSI B31.1 piping) are maintained for the 60-year operating period. In addition, a transient evaluation was performed for PTN that extrapolated the actual transient counts established by the FPL cycle counting program to 60 years of plant operation [25]. The results of the extrapolation concluded that the existing primary system design transients are conservative for use as a basis for 60 years of operation.

THIS REPORT CONTAINS VENDOR PROPRIETARY INFORMATION

As stated in Section 4.3.1 of the PTN LRA [1] and discussed in Section 2.2 of this report, the evaluation verified the structural integrity of the RPV, RPV internals, pressurizer, steam generators (SGs), reactor coolant pumps (RCPs), and the pressurizer surge lines will remain valid for the period of extended operation. Similarly, Section 4.3.4 of the PTN LRA [1] stated similar results for the PTN piping designed in accordance with ANSI B31.1, “Power Piping.”

The results of the transient evaluation that form the CLB for PTN for 60 years of operation are summarized in Table 2-1 [29]. *[Footnotes for Table 2-2 in [29] are not included in Table 2-1].* These results demonstrated that the design basis (i.e., 40-year) transient definitions were adequate for 60 years of operation, thus satisfying §54.21(c)(1)(i) of the License Renewal Rule [7], as identified in Section 4.3.1 of the PTN LRA [1] and approved by the NRC in the LRA Safety Evaluation Report (SER) [2.b]. The PTN Fatigue Monitoring Program for license renewal is described in Section 16.2.7 of the PTN UFSAR.

THIS REPORT CONTAINS VENDOR PROPRIETARY INFORMATION

**Table 2-1: Projected Number of Transients Compared to Design-Basis Number of Transients –
PTN Class 1 Components for 60 Years**

Transient Number	Description	PTN Unit 3			PTN Unit 4		
		Projected Number of Cycles for 60 Years	40-Year Design-Basis Number of Cycles	% Used After 60 Years	Projected Number of Cycles for 60 Years	40-Year Design-Basis Number of Cycles	% Used After 60 Years
1	Station Heatup at 100°F/hour	156	200	78.0%	191 ⁽¹⁰⁾	200	95.5%
2	Station Cooldown at 100°F/hour	155	200	77.5%	190 ⁽¹⁰⁾	200	95.0%
3	Pressurizer Cooldown to 400 psia at 200°F/hr	142	200	71.0%	179	200	89.5%
4	Pressurizer Cooldown from 400 psia at 200°F/hr	142	200	71.0%	179	200	89.5%
5	Station Loading at 5% power per minute	2,720	14,500	18.8%	2,320	14,500	16.0%
6	Station Unloading at 5% power per minute	2,140	14,500	14.8%	2,190	14,500	15.1%
7	Step Load Increase of 10% of Full Power	109	2,000	5.5%	112	2,000	5.6%
8	Step Load Decrease of 10% of Full Power	220	2,000	11.0%	123	2,000	6.2%
9	Step Load Decrease of 50% of Full Power	167	200	83.5%	110	200	55.0%
10	Steady State Fluctuations, +/- 100 psi, +/- 6°F	Exempted	Infinite	---	Exempted	Infinite	---
11	Feedwater Cycling at Hot Standby	Exempted	2,000	---	Exempted	2,000	---
12	Boron Concentration Equalization	6,358	36,600	17.4%	6,041	36,600 ⁽⁷⁾	16.5%
13	Shipping, Handling, Refueling Events	---	---	---	---	---	---
14	Turbine Roll Test	0	10	0.0%	0	10	0.0%

**Table 2-1: Projected Number of Transients Compared to Design-Basis Number of Transients –
PTN Class 1 Components for 60 Years (continued)**

Transient Number	Description	PTN Unit 3			PTN Unit 4		
		Projected Number of Cycles for 60 Years	40-Year Design-Basis Number of Cycles	% Used After 60 Years	Projected Number of Cycles for 60 Years	40-Year Design-Basis Number of Cycles	% Used After 60 Years
15	Primary Side Hydrostatic Test a. Hydrostatic Test at 3107 psig Pressure, 100°F Temperature ⁽¹⁾⁽⁴⁾	1 ⁽¹⁰⁾	1	100.0%	1 ⁽¹⁰⁾	1	100.0%
16	b. Hydrostatic Test at 2485 psig Pressure and 400°F Temperature ⁽¹⁾⁽⁵⁾	3 ⁽¹⁰⁾	5	60.0%	3 ⁽¹⁰⁾	5	60.0%
17	Secondary Side Hydrostatic Test to 1356 psig ⁽⁸⁾⁽⁹⁾						
	Steam Generator Loop A (pre- and post-1987)	21	35	60.0%	15	35	42.9%
	Steam Generator Loop B (pre- and post-1987)	17	35	48.6%	15	35	42.9%
	Steam Generator Loop C (pre- and post-1987)	17	35	48.6%	13	35	37.1%
18	Primary to Secondary Side Leak Test to 2,250	0	15	0.0%	0	15	0.0%
19	Secondary Leak Test to 1,085 psig ⁽⁹⁾						
	Steam Generator Loop A	4	50	8.0%	4	50	8.0%
	Steam Generator Loop B	7	50	14.0%	11	50	22.0%
	Steam Generator Loop C	4	50	8.0%	7	50	14.0%
20	Secondary to Primary Side Leak Test to 840 psig ⁽¹¹⁾						
	Steam Generator Loop A	8	15	53.3%	14	15	93.3%
	Steam Generator Loop B	15	15	100.0%	15	15	100.0%
	Steam Generator Loop C	9	15	60.0%	15	15	100.0%

Table 2-1: (concluded)

Transient Number	Description	PTN Unit 3			PTN Unit 4		
		Projected Number of Cycles for 60 Years	40-Year Design-Basis Number of Cycles	% Used After 60 Years	Projected Number of Cycles for 60 Years	40-Year Design-Basis Number of Cycles	% Used After 60 Years
21	Loss of Load without Immediate Turbine Trip	43	80	53.8%	38	80	47.5%
22	Loss of AC Power	28	40	70.0%	29	40	72.5%
23	Partial Loss of Flow (Reverse Flow)	43	80	53.8%	43	80	53.8%
24	Loss of Secondary Pressure	2	6	33.3%	0	6	0.0%
25	Reactor Trip ⁽¹⁾	291 ⁽¹⁰⁾	400	72.8%	337 ⁽¹⁰⁾	400	84.3%
26	Inadvertent Auxiliary Spray	0	10	0.0%	0	10	0.0%
27	Operating Basis Earthquake (OBE)	0	50	0.0%	0	50	0.0%
28	Loss of Coolant Accident	0	1	0.0%	0	1	0.0%
29	Steam Line Break	0	1	0.0%	0	1	0.0%
30	Safe Shutdown Earthquake (SSE)	0	1	0.0%	0	1	0.0%

THIS REPORT CONTAINS VENDOR PROPRIETARY INFORMATION

Transient Number	Description	PTN Unit 3			PTN Unit 4		
		Projected Number of Cycles for 60 Years	40-Year Design-Basis Number of Cycles	% Used After 60 Years	Projected Number of Cycles for 60 Years	40-Year Design-Basis Number of Cycles	% Used After 60 Years
15	Primary Side Hydrostatic Test a. Hydrostatic Test at 3107 psig Pressure, 100°F Temperature	1	1	100.0%	1	1	100.0%
16	b. Hydrostatic Test at 2485 psig Pressure and 400°F Temperature	3	5	60.0%	3	5	60.0%
17	Secondary Side Hydrostatic Test to 1356 psig Steam Generator Loop A (pre- and post-1987)	21	35	60.0%	15	35	42.9%
	Steam Generator Loop B (pre- and post-1987)	17	35	48.6%	15	35	42.9%
	Steam Generator Loop C (pre- and post-1987)	17	35	48.6%	13	35	37.1%
18	Primary to Secondary Side Leak Test to 2,250	0	15	0.0%	0	15	0.0%
19	Secondary Leak Test to 1,085 psig Steam Generator Loop A	4	50	8.0%	4	50	8.0%
	Steam Generator Loop B	7	50	14.0%	11	50	22.0%
	Steam Generator Loop C	4	50	8.0%	7	50	14.0%
20	Secondary to Primary Side Leak Test to 840 psig Steam Generator Loop A	8	15	53.3%	14	15	93.3%
	Steam Generator Loop B	15	15	100.0%	15	15	100.0%
	Steam Generator Loop C	9	15	60.0%	15	15	100.0%

**Table 2-1: Projected Number of Transients Compared to Design-Basis Number of Transients –
PTN Class 1 Components for 60 Years (concluded)**

Transient Number	Description	PTN Unit 3			PTN Unit 4		
		Projected Number of Cycles for 60 Years	40-Year Design-Basis Number of Cycles	% Used After 60 Years	Projected Number of Cycles for 60 Years	40-Year Design-Basis Number of Cycles	% Used After 60 Years
21	Loss of Load without Immediate Turbine Trip	43	80	53.8%	38	80	47.5%
22	Loss of AC Power	28	40	70.0%	29	40	72.5%
23	Partial Loss of Flow (Reverse Flow)	43	80	53.8%	43	80	53.8%
24	Loss of Secondary Pressure	2	6	33.3%	0	6	0.0%
25	Reactor Trip	291	400	72.8%	337 ⁽¹⁰⁾	400	84.3%
26	Inadvertent Auxiliary Spray	0	10	0.0%	0	10	0.0%
27	Operating Basis Earthquake (OBE)	0	50	0.0%	0	50	0.0%
28	Loss of Coolant Accident	0	1	0.0%	0	1	0.0%
29	Steam Line Break	0	1	0.0%	0	1	0.0%
30	Safe Shutdown Earthquake (SSE)	0	1	0.0%	0	1	0.0%

2.2 PTN EAF Assessment

Section 3.2 of Attachment 8.1 to FPL Document No. PTN-ENG-LRAM-00-0055, Revision 1 (SI Report No. SIR-00-089) [12] summarizes the PTN evaluation of reactor water environmental effects for 60 years of operation. Attachment 8.2 to FPL Document No. PTN-ENG-LRAM-00-0055, Revision 1 (SI Report No. SIR-01-042, Rev. 0) [13] further enhanced the PTN EAF assessment through responses to NRC RAIs.

The PTN LRA pre-dated GALL requirements, so treatment of EAF effects was still being finalized by the NRC in the wake of the resolution of GSI 190. Based on this, FPL evaluated EAF effects using a combination of methods that included NUREG/CR-6260 [8], NUREG/CR-5704 [16], and NUREG/CR-6583 [15]. The use of NUREG/CR-6260 was directly relevant to PTN because the “Older Vintage Westinghouse Plant” evaluated in Section 5.5 of that document matched PTN in the design codes used, as well as the analytical approach and techniques used. In addition, the evaluated transient cycles matched or bounded PTN.

The PTN EAF assessment for 60 years was performed in five parts:

- First, Section 3.2.1 of Attachment 8.1 to FPL Document No. PTN-ENG-LRAM-00-0055, Revision 1 performed an evaluation of the selected components from NUREG/CR-6260. This included the RPV at the core support guide weld, the RPV inlet and outlet nozzles, the surge line hot leg nozzle safe end, the charging nozzle, the safety injection nozzle, and the RHR line tee.
- Second, Section 3.2.2 of Attachment 8.1 to FPL Document No. PTN-ENG-LRAM-00-0055, Revision 1 performed an evaluation of Class 1 components that FPL originally excluded from the transient evaluation to demonstrate long-term structural acceptability for continued operation beyond 40 years for PTN. This included the pressurizer lower head, pressurizer surge and spray nozzles, pressurizer surge and spray lines, charging lines and associated charging nozzles, and all branch lines subject to NRC Bulletin 88-08 loading conditions.

- Third, some of the above results were enhanced in responses to NRC RAIs.
- Fourth, some of the above results were updated as a part of EPU implementation at PTN in 2010 [21].
- Fifth, some of the above results were updated as a part of fulfilling license renewal commitments for PTN in 2011/2012.

A summary of the EAF assessments that form the CLB for PTN for 60 years of operation is provided in Table 2-2. These results demonstrated that the CUF_{en} values for all evaluated components except the surge line weld locations were within the allowable value of 1.0 for 60 years of plant operation, as identified in Section 4.3.5 of the PTN LRA [1].

Table 2-2: Summary of the PTN EAF Assessment for 60 Years of Operation

Component	60-Year CLB CUF	F_{en}	Material	Latest 60-Year CUF_{en}
RPV Shell at Core Support Pads ^(1,2)	0.478 ⁽²⁾ / 0.509 (UFSAR) ⁽²⁾	1.76 ⁽²⁾	Low Alloy/Carbon ⁽³⁾	0.8413 ⁽²⁾
RPV Inlet Nozzle ^(1,4) (inside surface)	0.073 ⁽⁴⁾ / 0.066 (UFSAR) ⁽⁴⁾	2.45 ⁽⁴⁾	Low Alloy/Carbon ⁽³⁴⁾	0.179 ⁽⁴⁾
RPV Outlet Nozzle ^(1,5) (inside surface)	0.056 ⁽⁵⁾ / 0.063 (UFSAR) ⁽⁵⁾	2.45 ⁽⁵⁾	Low Alloy/Carbon ⁽³⁾	0.137 ⁽⁵⁾
RCS Piping Surge Line Hot Leg Nozzle ^(1,6)	0.944 ⁽⁶⁾	4.5 ⁽⁶⁾	Stainless steel ⁽³⁾	4.248 ⁽⁶⁾
RCS Piping Safety Injection Nozzle ^(1,7)	0.046 ⁽⁷⁾	7.11 ⁽⁷⁾	Stainless steel ⁽³⁾	0.327 ⁽⁷⁾
RCS Piping Charging Nozzle ^(1,8)	0.030 ⁽⁸⁾	10.63 ⁽⁸⁾	Stainless steel ⁽³⁾	0.319 ⁽⁸⁾
RCS Piping Residual Heat Removal (RHR) Piping Tee ^(1,9)	0.022 ⁽⁹⁾	9.32 ⁽⁹⁾	Stainless steel ⁽³⁾	0.205 ⁽⁹⁾
Pressurizer Surge Nozzle ⁽¹⁰⁾	{ } ⁽¹⁰⁾	Addressed by inspection AMP (see Section 2.3)		
Pressurizer Spray Nozzle ⁽¹¹⁾	{ } / 0.24667 ⁽¹¹⁾	4.0 ⁽¹¹⁾	Not reported in [26]	< 1.0 ⁽¹¹⁾
Pressurizer Safety and Relief Nozzle ⁽¹²⁾	{ } ⁽¹²⁾	4.0 ⁽¹²⁾	Not reported in [26]	< 1.0 ⁽¹²⁾
Pressurizer Lower Head, Heater Well ⁽¹³⁾	0.461 / { } ⁽¹³⁾	4.2 ⁽¹³⁾	Stainless steel ⁽¹³⁾	1.94 ⁽¹³⁾
Pressurizer Lower Head/Perforation ⁽¹⁴⁾	{ } ⁽¹⁴⁾	4.0 ⁽¹⁴⁾	Not reported in [26]	< 1.0 ⁽¹⁴⁾
Pressurizer Upper Head and Shell ⁽¹⁵⁾	Negligible / { } ⁽¹⁵⁾	4.0 ⁽¹⁵⁾	Not reported in [26]	< 1.0 ⁽¹⁵⁾
Pressurizer Support Skirt/Flange ⁽¹⁶⁾	0.0165 ⁽¹⁶⁾	4.0 ⁽¹⁶⁾	Not reported in [26]	< 1.0 ⁽¹⁶⁾
Pressurizer Manway Pad ⁽¹⁷⁾	{ } ⁽¹⁷⁾	4.0 ⁽¹⁷⁾	Not reported in [26]	< 1.0 ⁽¹⁷⁾
Pressurizer Manway Cover ⁽¹⁸⁾	0.0 ⁽¹⁸⁾	4.0 ⁽¹⁸⁾	Not reported in [26]	< 1.0 ⁽¹⁸⁾
Pressurizer Manway Bolts ⁽¹⁸⁾	0.0 ⁽¹⁸⁾	4.0 ⁽¹⁸⁾	Not reported in [26]	< 1.0 ⁽¹⁸⁾
Pressurizer Welded Manway Diaphragm ⁽¹⁹⁾	{ } ⁽¹⁹⁾	4.0 ⁽¹⁹⁾	Not reported in [26]	< 1.0 ⁽¹⁹⁾
Pressurizer Support Lug ⁽²⁰⁾	Not Installed ⁽²⁰⁾	---	---	---
Pressurizer Instrument Nozzle ⁽²¹⁾	{ } ⁽²¹⁾	4.0 ⁽²¹⁾	Not reported in [26]	< 1.0 ⁽²¹⁾
Pressurizer Immersion Heater ⁽²²⁾	0.0040 ⁽²²⁾	4.0 ⁽²²⁾	Not reported in [26]	< 1.0 ⁽²²⁾
Pressurizer Valve Support Bracket ⁽²⁰⁾	Not Installed ⁽²⁰⁾	---	---	---

For notes, see next page.

Table 2-2: Summary of the PTN EAF Assessment for 60 Years of Operation (concluded)

Notes for Table 2-2:

1. NUREG/CR-6260 component location, per Table 1 in the response to RAI 4.3.5-1 [26].
2. For the RPV Shell at Core Support Pads location, a revised CUF value of 0.4030 and a CUF_{en} value of 0.9894 was obtained in Table 5 of SI Calculation No. 0900948.302, Revision 1 [19.b]. The value of 0.478 shown was reported for EPU [21, Table 2.2.2.3-1]. The F_{en} was calculated as $(0.8413/0.478) = 1.76$ for PTN-4. The CUF was reported in the UFSAR as 0.509 [22].
3. As identified in the response to RAI 4.3.5-1 [26].
4. For the RPV Inlet Nozzle, the value reported as U_{PTN} in Table 1 in the response to RAI 4.3.5-1 [26] was updated to the value shown as a part of EPU implementation [21]. The refined CUF_{en} value of 0.372 shown in Table 3 in the response to RAI 4.3.5-1 [26] was also revised, and the value of 0.073 shown was reported for EPU [21, Table 2.2.2.3-1]. The F_{en} was calculated as $(0.179/0.073) = 2.45$.
5. For the RPV Outlet Nozzle, the value reported as U_{PTN} in Table 1 in the response to RAI 4.3.5-1 [26] was updated to the value shown as a part of EPU implementation [21]. The CUF_{en} value was also revised, and the value of 0.056 shown was reported for EPU [21, Table 2.2.2.3-1]. The F_{en} was calculated as $(0.137/0.056) = 2.45$.
6. For the RCS Piping Surge Line Hot Leg Nozzle, the CUF value is U_{PTN} in Table 1 in the response to RAI 4.3.5-1 [26]. The CUF_{en} value is U_{6260} in Table 1 in the response to RAI 4.3.5-1 [26]. The F_{en} was calculated as $(4.248/0.944) = 4.5$.
7. For the RCS Piping Safety Injection Nozzle, the PTN location was evaluated to ANSI B31.1 rules and does not produce a fatigue usage value, so the NUREG/CR-6260 (U_{code}) value was used from Table 1 of the response to RAI 4.3.5-1 [26]. The value was not revised for EPU. The CUF_{en} value is U_{6260} from Table 1 in the response to RAI 4.3.5-1 [26]. The F_{en} was calculated as $(0.327/0.046) = 7.11$.
8. For the RCS Piping Charging Nozzle, the PTN location was evaluated to ANSI B31.1 rules and does not produce a fatigue usage value, so the NUREG/CR-6260 (U_{code}) value was used from Table 1 of the response to RAI 4.3.5-1 [26]. The value was not revised for EPU. The CUF_{en} value is U_{6260} from Table 1 in the response to RAI 4.3.5-1 [26]. The F_{en} was calculated as $(0.319/0.030) = 10.63$.
9. For the RCS Piping RHR Piping Tee Nozzle, the PTN location was evaluated to ANSI B31.1 rules and does not produce a fatigue usage value, so the NUREG/CR-6260 (U_{code}) value was used from Table 1 of the response to RAI 4.3.5-1 [26]. The value was not revised for EPU. The CUF_{en} value is U_{6260} from Table 1 in the response to RAI 4.3.5-1 [26]. The F_{en} was calculated as $(0.205/0.022) = 9.32$.
10. For the Pressurizer Surge Nozzle, the CUF value of 0.5202 from the table in the response to RAI 4.3.1-4 [26] was updated to { } as a part of EPU implementation [21, 22]. EAF for the PTN surge line components is satisfactorily addressed through a PTN plant-specific program utilizing the ASME Code Section XI inspection program, as discussed in Section 2.3.
11. For the Pressurizer Spray Nozzle, the CUF value of 0.8906 from the table in the response to RAI 4.3.1-4 [26] was updated to 0.24667 in Table 5 of SI Calculation No. 1100768.304, Revision 0 [20.d] in 2012. A value of { } was reported as a part of EPU implementation in 2010 [21, 22]. In the response to RAI 4.3.1-4 [26], a screening F_{en} of 4.0 was used to justify acceptability of all pressurizer locations with a CLB CUF less than 0.25.
12. For the Pressurizer Safety and Relief Nozzle, the CUF value of 0.148 from the table in the response to RAI 4.3.1-4 [26] was updated to { } as a part of EPU implementation [21, 22]. In the response to RAI 4.3.1-4 [26], a screening F_{en} of 4.0 was used to justify acceptability of all pressurizer locations with a CLB CUF less than 0.25.
13. For the Pressurizer Lower Head, Heater Well, the CUF value of 0.461 from the table in the response to RAI 4.3.1-4 [26] was updated to { } as a part of EPU implementation [21, 22]. In

the response to RAI 4.3.1-4 [26], an F_{en} of 4.2 was used to determine a maximum CUF_{en} value of 1.94, which was qualitatively dispositioned based on inherent margins in the calculational process, the low risk significance associated with these penetrations, current visual inspections performed on the penetrations as part of the ASME Section XI, Subsections IWB, IWC, and IWD Inservice Inspection Program, and the fact that the surge line is significantly more limiting from a fatigue perspective when considering reactor water environmental effects.

14. For the Pressurizer Lower Head/Perforation, the CUF value of 0.0165 from the table in the response to RAI 4.3.1-4 [26] was updated to { } as a part of EPU implementation [21, 22]. In the response to RAI 4.3.1-4 [26], a screening F_{en} of 4.0 was used to justify acceptability of all pressurizer locations with a CLB CUF less than 0.25.
15. For the Pressurizer Upper Head and Shell, the CUF value of 0.7737 from the table in the response to RAI 4.3.1-4 [26] was qualitatively revised to a negligible value in the RAI response. That value was updated to { } as a part of EPU implementation [21, 22]. In the response to RAI 4.3.1-4 [26], a screening F_{en} of 4.0 was used to justify acceptability of all pressurizer locations with a CLB CUF less than 0.25.
16. For the Pressurizer Support Skirt/Flange, the CUF value of 0.0165 from the table in the response to RAI 4.3.1-4 [26] was not revised as a part of EPU implementation [21, 22]. In the response to RAI 4.3.1-4 [26], a screening F_{en} of 4.0 was used to justify acceptability of all pressurizer locations with a CLB CUF less than 0.25.
17. For the Pressurizer Manway Pad, the CUF value of 0.0 from the table in the response to RAI 4.3.1-4 [26] was updated to { } as a part of EPU implementation [21, 22]. In the response to RAI 4.3.1-4 [26], a screening F_{en} of 4.0 was used to justify acceptability of all pressurizer locations with a CLB CUF less than 0.25.
18. For the Pressurizer Manway Cover and Bolts, the CUF values of 0.0 from the table in the response to RAI 4.3.1-4 [26] were not updated as a part of EPU implementation [21, 22]. In the response to RAI 4.3.1-4 [26], a screening F_{en} of 4.0 was used to justify acceptability of all pressurizer locations with a CLB CUF less than 0.25.
19. For the Pressurizer Manway Welded Diaphragm, the CUF value of 0.0321 from the table in the response to RAI 4.3.1-4 [26] was updated to { } as a part of EPU implementation [21, 22]. In the response to RAI 4.3.1-4 [26], a screening F_{en} of 4.0 was used to justify acceptability of all pressurizer locations with a CLB CUF less than 0.25.
20. For the Pressurizer Support Lug and Valve Support Bracket, there was no CUF value reported in the table in the response to RAI 4.3.1-4 [26] as these components are not installed at PTN.
21. For the Pressurizer Instrument Nozzle, the CUF value of 0.0627 from the table in the response to RAI 4.3.1-4 [26] was updated to { } as a part of EPU implementation [21, 22]. In the response to RAI 4.3.1-4 [26], a screening F_{en} of 4.0 was used to justify acceptability of all pressurizer locations with a CLB CUF less than 0.25.
22. For the Pressurizer Immersion Heater, the CUF value of 0.004 from the table in the response to RAI 4.3.1-4 [26]. In the response to RAI 4.3.1-4 [26], a screening F_{en} of 4.0 was used to justify acceptability of all pressurizer locations with a CLB CUF less than 0.25.

2.3 PTN Surge Line Inspection Program

As discussed in Section 3.2.2.2 of Attachment 8.1 to FPL Document No. PTN-ENG-LRAM-00-0055, Revision 1 (SI Report No. SIR-00-089) [12] and indicated by the results shown in Table 2-2, the CUF_{en} results for locations in the PTN surge line (the RCS Piping Surge Line Hot Leg Nozzle and the Pressurizer Surge Nozzle) could not be reduced to below the allowable value of 1.0. Therefore, FPL identified the surge line as a candidate for additional inspection considerations during the license renewal period. Thus, the entire surge line was included as a part of the ASME Code Section XI risk informed inservice inspection (RI-ISI) program, as described in Section 4.0 of Attachment 8.1 to FPL Document No. PTN-ENG-LRAM-00-0055, Revision 1.

In their response to RAI 4.3.5-2 [26], FPL committed to an inspection-based AMP to address fatigue of the PTN pressurizer surge lines during the period of extended operation using an approach like that documented in the ASME Code, Section XI, Nonmandatory Appendix L [9]. Because the NRC had not endorsed the Appendix L approach at the time of PTN's LRA submittal, FPL committed to inspection of all surge line welds on both PTN units during the fourth inservice inspection interval, prior to entering the extended period of operation, and using the inspection results to assess the appropriate approach for addressing EAF of the surge lines using one or more of the following:

1. Further refinement of the fatigue analysis to lower the $CUF(s)$ to below 1.0, or
2. Repair of the affected locations, or
3. Replacement of the affected locations, or
4. Manage the effects of fatigue by an inspection program that has been reviewed and approved by the NRC (e.g., periodic non-destructive examination of the affected locations at inspection intervals to be determined by a method accepted by the NRC).

If selected, the inspection details for Option 4, such as scope, qualification, method, and frequency, required submittal to the NRC for review and approval prior to entering the period of extended operation.

The surge line inspection program was developed and submitted to the NRC for review in 2012 [17]. This program was based on a flaw tolerance evaluation performed in accordance with ASME Code, Section XI, Appendix L using initial postulated flaw sizes consistent with sizes that are detectable by qualified nondestructive examination (NDE) techniques and fatigue crack growth rates that account for the effects of the reactor coolant environment. The results also determined that there was additional margin between the inspection frequency and the shortest allowable operating period for the most limiting flaw assumed in the evaluation. The analysis concluded that a 10-year inspection frequency was adequate for detecting cracking caused by EAF of the pressurizer surge line welds before there is a loss of intended function.

The surge line inspection program was approved by the NRC in 2013 [18]. Based on its review of the surge line inspection program, the NRC found the program acceptable because it satisfies the ten elements for an acceptable AMP, as described in Section A.1.2.3 of the SRP-SLR [4], and it adequately manages cracking caused by EAF in the pressurizer surge line welds. The NRC staff also found that FPL determined an appropriate approach for addressing EAF of the pressurizer surge lines and thus fulfilled their license renewal commitment.

Based on this, the PTN CLB for assessing EAF of the pressurizer surge line welds is inspection every ten years to verify the absence of fatigue cracking. Therefore, CUF_{en} analyses for surge line components are not necessary for SLR.

3.0 PLANT-SPECIFIC ASSESSMENT OF ENVIRONMENTALLY-ASSISTED FATIGUE EFFECTS FOR SUBSEQUENT LICENSE RENEWAL

The relevant plant-specific fatigue background for 60 years of operation summarized in Section 2.0 forms the CLB for PTN, and serves as the starting point for assessing EAF for SLR. The plant-specific assessment of EAF effects for PTN for SLR is contained in this section. The plant-specific assessment is separated into four parts, with the following objectives:

1. **PTN Cycle Counting Program**. Section 0 describes the latest results from the PTN Cycle Counting Program and provides a summary of the updated evaluation of transient counts and severities performed for SLR.
2. **PTN EAF Assessment**. Section 0 describes the PTN-specific EAF calculations for all limiting locations for SLR. The assessment incorporates the CUFs for all Class 1 RCPB components that are exposed to a water environment, revises the prior PTN environmental multipliers in Table 2-2 to adopt the latest F_{en} methods provided in RG 1.207, Revision 1, and calculates CUF_{en} values for all relevant PTN components listed in Table 2-2 using the updated transient projections for SLR and the updated F_{en} values.
3. **Plant-Specific Limiting Locations**. Section 3.3 provides the bases for why the plant-specific limiting locations evaluated for EAF in Section 0 are limiting locations per GALL-SLR Chapter X.M1 requirements for PTN.
4. **Summary of PTN EAF Assessment**. Section 3.4 summarizes the plant-specific EAF assessment results and the relevant changes to the PTN fatigue bases for SLR.

These four parts are addressed in the sections that follow, and collectively, they serve as a replacement to the PTN 60-year EAF assessment that reflects an updated PTN EAF assessment for SLR.

3.1 PTN Cycle Counting Program

The PTN Cycle Counting Program is addressed through FPL Procedure No. 0-ADM-553 [21]. For PTN's first license renewal for 60 years of operation, this program was investigated to project transient counts out to 60 years and evaluate transient severities. That investigation concluded that the original 40-year design basis transient counts and severities remained valid for 60 years of operation. Therefore, as discussed in Section 1.2.2, FPL concluded that the PTN Cycle Counting Program satisfied the license renewal requirements for fatigue TLAAs in 10 CFR 54.21(c)(1)(i).

For SLR, an updated investigation was performed to develop revised transient projections and evaluate transient severities for 80 years of operation [29]. That investigation concluded that the original 40-year design basis transient counts and severities, which are also the CLB for PTN for 60 years of operation, remain valid for SLR. A summary of the transient projections for 80 years of operation from the investigation are shown in Table 3-1 (Unit 3) and Table 3-2 (Unit 4), excerpted from [29] (*footnoted References for the tables are for [29]*).

Based on the 80-year evaluation performed for SLR, the same transients and transient counts used for the 60-year EAF assessment remain applicable for 80 years of operation, and were used in the updated EAF assessment for 80 years that is discussed in the following section.

THIS REPORT CONTAINS VENDOR PROPRIETARY INFORMATION

Table 3-1: Summary of Transient Projections for 80 Years of Operation (PTN Unit 3)

PTN-3		Design Number	Through 2016		60 Year Projection (9)	80-Year Projections			Source of Allowables			
Transient Number (3)	Transient		Count through 2016	Percent of Design Number		80 Year Projection	Percent of Design Number	Weighted Projection Method (1)	UFSAR Table 4.1-8	UFSAR Table 4.1-10	0-ADM- 553	Minimum
Normal												
1	Station Heatup at 100°F/hour	200	109	55%	156	164	82%	X	200	200	200	200
2	Station Cooldown at 100°F/hour	200	109	55%	155	164	82%	X	200	200	200	200
3	Pressurizer Cooldown at 200°F/hour (5)(17)	200	95	48%	142	148	74%	X	---	200	200	200
5	Station Loading at 5% power per minute	14500	293	2%	2720	533	4%		14500 (11)	---	14500	2200 (16)
6	Station Unloading at 5% power per minute	14500	242	2%	2140	440	3%		14500 (11)	---	14500	2200 (16)
7	Step Load Increase of 10% of Full Power	2000	43	2%	109	79	4%		2000	---	2000	2000
8	Step Load Decrease of 10% of Full Power	2000	90	5%	220	164	8%		2000	---	2000	2000
9	Step Load Decrease of 50% of Full Power	200	68	34%	167	82	41%	X	200	---	200	200
	Steady State Fluctuations (12)	0	Exempted						0			----
	Feedwater Cycling at Hot Standby (15)	2000	Exempted						2000	---	---	2000
	Boron Concentration Equalization (5)	36000	Not Counted						---	---	---	36600
Test												
14	Turbine Roll Test	10	1 (4)(20)	10%	1 (20)	1	10%		---	---	---	----
15	Hydrostatic Test at 3107 psig Pressure, 100°F Temperature (6)(19)	1	1	100%	1	1	100%		1	---	5	1
16	Hydrostatic Test at 2485 psig Pressure and 400°F Temperature (7)	5	1	20%	3	2	40%		5	5	---	5
17	Secondary Side Hydrostatic Test to 1356 psig	----	----	----	----	----	---	---	---	---	---	----
	Steam Generator Loop A (10)	10	17 / 9 (14)	90%	21	9	90%		---	10	35 (23)	10
	Steam Generator Loop B (10)	10	13 / 7 (14)	70%	17	7	70%		---	10	35 (23)	10
	Steam Generator Loop C (10)	10	13 / 7 (14)	70%	17	7	70%		---	10	35 (23)	10
	Primary to Secondary Side Leak Test to 2435 psig (7)	150	1	1%	----	2	1%		---	150	150	150
18	Primary to Secondary Side Leak Test to 2250 psig (6)	15	1	7%	0	2	13%		---	15	---	15
19	Secondary Side Leak Test ≥ 1085 psig (2)	----	----	----	----	----	---	---	---	---	---	----
	Steam Generator Loop A (13)	50	9	18%	4	21	42%		---	50	50	50
	Steam Generator Loop B (13)	50	7	14%	7	16	32%		---	50	50	50
	Steam Generator Loop C (13)	50	7	14%	4	16	32%		---	50	50	50
	Secondary to Primary Side Leak Test to 840 psig (6)(8)	---	---	---	----	---	---	---	---	---	---	----
	Steam Generator Loop A	15	8	53%	8	8	53%		---	15	---	15
	Steam Generator Loop B	15	15	100%	15	15	100%		---	15	---	15
	Steam Generator Loop C	15	9	60%	9	9	60%		---	15	---	15

Table continued on next page.

Table 3-1: Summary of Transient Projections for 80 Years of Operation (PTN Unit 3) (concluded)

PTN-3		Design Number	Through 2016		60 Year Projection (9)	80-Year Projections			Source of Allowables			
Transient Number (3)	Transient		Count through 2016	Percent of Design Number		80 Year Projection	Percent of Design Number	Weighted Projection Method (1)	UFSAR Table 4.1-8	UFSAR Table 4.1-10	O-ADM- 553	Minimum
Upset												
21	Loss of Load without Immediate Turbine Trip or Reactor Trip	80	15	19%	43	28	35%		---	80	80	80
22	Loss of Off-Site AC Electrical Power	40	6	15%	28	10	25%	X	---	40	40	40
23	Loss of Flow in One Reactor Coolant Loop	80	14	18%	43	26	33%		---	80	80	80
25	Reactor Trip	400	183	46%	291	272	68%	X	400	400	400	400
26	Inadvertent Auxiliary Spray (18)(21)	10	0	0%	0	1	10%		---	10	---	10
27	OBE (22)	50	0	0%	0	10	20%		---	---	---	20
	Loss of Secondary Pressure (Press Loss) (6)	6	1	17%	2	2	33%		---	---	6	6

Footnotes

- ✓ (1) Weighted projection method used for counted normal and upset transients in which 60-year projections for either unit are over 70% of design numbers in SIR-00-089 [1].
- ✓ (2) Labelled as "Secondary Leak Test" in O-ADM-553 [7]. Labelled as "Hydrostatic Pressure Test" in Table 4.1-10 [28].
- ✓ (3) Transient numbers from Table 3-1 of SIR-00-089 [1].
- ✓ (4) Not expected to have any additional cycles on RSGs.
- ✓ (5) Applies to Pressurizer only.
- ✓ (6) Applies to Steam Generator only. Labelled as "Secondary Leak Test" in O-ADM-553 [7].
- ✓ (7) Limited by Reactor Coolant Pump Analysis [16, Attachment 1, pages 44 and 45].
- ✓ (8) Leak Test Procedure cancelled per [30].
- ✓ (9) 60-year projections from [5, PTN-LR-00-0127 Table 10.3-1].
- ✓ (10) Not expected to have any additional cycles on RSGs.
- ✓ (11) Cycle limits for baffle-former bolts only is being lowered from 14,500 to 2,200 due EPU RCS conditions (Table 4.1-8 of UFSAR [8]).
- ✓ (12) Not counted, not significant contributor to fatigue usage factor.
- ✓ (13) 80-year plant life projected cycles computed using 65 years of life for the RSGs.
- ✓ (14) Values are [(pre-and post- 1987) / (post- 1987)] cycles [5, PTN-LR-00-0127 Table 10.3-1].
- ✓ (15) Not counted, intermittent slug feeding at hot standby not performed.
- ✓ (16) Limit of 2,200 cycles established for baffle former bolts only per UFSAR Table 4.1-8 [8].
- ✓ (17) Represents 200 cycles each of: (1) pressurizer cooldown cycles at ≤ 200°F/hr from nominal pressure and (2) pressurizer cooldown cycles at ≤ 200°F/hr from 400 psia [28].
- ✓ (18) Spray water temperature differential to 560°F.
- ✓ (19) Applies to Steam Generator only. Represents pre-operational test [16, Note 3 on Attachment 1, pages 44 and 45].
- ✓ (20) Adjustment in 60-year projection in [5, PTN-LR-00-0127 Table 10.3-1] - recorded as a value of 0 when 1 was assumed in pre-operational startup.
- ✓ (21) One cycle is projected for 80 years to remain within the analytical basis if that event occurs.
- ✓ (22) One cycle of 10 events is projected for 80 years to remain within the analytical basis if that event occurs.
- ✓ (23) Recommended revision O-ADM-553 to align with UFSAR Table 4.1-10.

THIS REPORT CONTAINS VENDOR PROPRIETARY INFORMATION

Table 3-2: Summary of Transient Projections for 80 Years of Operation (PTN Unit 4)

PTN-4		Design Number	Through 2016		60 Year Projection (9)	80-Year Projections			Source of Allowables			
Transient Number (3)	Transient		Count through 2016	Percent of Design Number		80 Year Projection	Percent of Design Number	Weighted Projection Method (1)	UFSAR Table 4.1-8	UFSAR Table 4.1-10	O-ADM- 553	Minimum
Normal												
1	Station Heatup at 100°F/hour	200	121	61%	191	181	91%	X	200	200	200	200
2	Station Cooldown at 100°F/hour	200	121	61%	190	181	91%	X	200	200	200	200
3	Pressurizer Cooldown at 200°F/hour (5)(17)	200	104	52%	179	158	79%	X	---	200	200	200
5	Station Loading at 5% power per minute	14500	260	2%	2320	484	3%		14500 (11)	---	14500	2200 (16)
6	Station Unloading at 5% power per minute	14500	242	2%	2190	451	3%		14500 (11)	---	14500	2200 (16)
7	Step Load Increase of 10% of Full Power	2000	44	2%	112	82	4%		2000	---	2000	2000
8	Step Load Decrease of 10% of Full Power	2000	57	3%	123	107	5%		2000	---	2000	2000
9	Step Load Decrease of 50% of Full Power	200	42	21%	110	51	26%	X	200	---	200	200
	Steady State Fluctuations (12)	0	Exempted						0			----
	Feedwater Cycling at Hot Standby (15)	2000	Exempted						2000	---	---	2000
	Boron Concentration Equalization (5)	36000	Not Counted						---	---	---	36600
Test												
14	Turbine Roll Test	10	1 (4)(20)	10%	1 (20)	1	10%		---	---	---	----
15	Hydrostatic Test at 3107 psig Pressure, 100°F Temperature (6)(19)	1	1	100%	1	1	100%		1	---	5	1
16	Hydrostatic Test at 2485 psig Pressure and 400°F Temperature (7)	5	1	20%	3	2	40%		5	5	---	5
17	Secondary Side Hydrostatic Test to 1356 psig	----	----	----	----	----	----	---	----	----	----	----
	Steam Generator Loop A (10)	10	11 / 6 (14)	60%	15	6	90%		---	10	35 (23)	10
	Steam Generator Loop B (10)	10	11 / 6 (14)	60%	15	6	70%		---	10	35 (23)	10
	Steam Generator Loop C (10)	10	9 / 5 (14)	50%	13	5	70%		---	10	35 (23)	10
	Primary to Secondary Side Leak Test to 2435 psig (7)	150	1	1%	----	2	1%		---	150	150	150
18	Primary to Secondary Side Leak Test to 2250 psig (6)	15	1	7%	0	2	13%		---	15	---	15
19	Secondary Side Leak Test ≥ 1085 psig (2)	----	----	----	----	----	----	---	----	----	----	----
	Steam Generator Loop A (13)	50	6	12%	4	14	28%		---	50	50	50
	Steam Generator Loop B (13)	50	6	12%	11	14	28%		---	50	50	50
	Steam Generator Loop C (13)	50	5	10%	7	12	24%		---	50	50	50
	Secondary to Primary Side Leak Test to 840 psig (6)(8)				----	----	----	---	----	----	----	----
	Steam Generator Loop A	15	14	93%	14	14	93%		---	15	---	15
	Steam Generator Loop B	15	15	100%	15	15	100%		---	15	---	15
	Steam Generator Loop C	15	15	100%	15	15	100%		---	15	---	15

Table continued on next page.

Table 3-2: Summary of Transient Projections for 80 Years of Operation (PTN Unit 4)

PTN-4		Design Number	Through 2016		60 Year Projection (9)	80-Year Projections			Source of Allowables			
Transient Number (3)	Transient		Count through 2016	Percent of Design Number		80 Year Projection	Percent of Design Number	Weighted Projection Method (1)	UFSAR Table 4.1-8	UFSAR Table 4.1-10	O-ADM- 553	Minimum
Upset												
21	Loss of Load without Immediate Turbine Trip or Reactor Trip	80	14	18%	38	27	34%		---	80	80	80
22	Loss of Off-Site AC Electrical Power	40	13	33%	29	19	48%	X	---	40	40	40
23	Loss of Flow in One Reactor Coolant Loop	80	11	14%	43	21	26%		---	80	80	80
25	Reactor Trip	400	187	47%	337	292	73%	X	400	400	400	400
26	Inadvertent Auxiliary Spray (18)(21)	10	0	0%	0	1	10%		---	10	---	10
27	OBE (22)	50	0	0%	0	10	20%		---	---	---	20
	Loss of Secondary Pressure (Press Loss) (6)(21)	6	0	0%	0	1	17%		---	---	6	6

Footnotes

- ✓ (1) Weighted projection method used for counted normal and upset transients in which 60-year projections for either unit are over 70% of design numbers in SIR-00-089 [1].
- ✓ (2) Labelled as "Secondary Leak Test" in O-ADM-553 [7]. Labelled as "Hydrostatic Pressure Test" in Table 4.1-10 [28].
- ✓ (3) Transient numbers from Table 3-1 of SIR-00-089 [1].
- ✓ (4) Not expected to have any additional cycles on RSGs.
- ✓ (5) Applies to Pressurizer only.
- ✓ (6) Applies to Steam Generator only. Labelled as "Secondary Leak Test" in O-ADM-553 [7].
- ✓ (7) Limited by Reactor Coolant Pump Analysis [16, Attachment 1, pages 44 and 45].
- ✓ (8) Leak Test Procedure cancelled per [30].
- ✓ (9) 60-year projections from [5, PTN-LR-00-0127 Table 10.3-1].
- ✓ (10) Not expected to have any additional cycles on RSGs.
- ✓ (11) Cycle limits for baffle-former bolts only is being lowered from 14,500 to 2,200 due EPU RCS conditions (Table 4.1-8 of UFSAR [8]).
- ✓ (12) Not counted, not significant contributor to fatigue usage factor.
- ✓ (13) 80-year plant life projected cycles computed using 66 years of life for the RSGs.
- ✓ (14) Values are [(pre-and post- 1987) / (post- 1987)] cycles [5, PTN-LR-00-0127 Table 10.3-1].
- ✓ (15) Not counted, intermittent slug feeding at hot standby not performed.
- ✓ (16) Limit of 2,200 cycles established for baffle former bolts only per UFSAR Table 4.1-8 [8].
- ✓ (17) Represents 200 cycles each of: (1) pressurizer cooldown cycles at ≤ 200°F/hr from nominal pressure and (2) pressurizer cooldown cycles at ≤ 200°F/hr from 400 psia [28].
- ✓ (18) Spray water temperature differential to 560°F.
- ✓ (19) Applies to Steam Generator only. Represents pre-operational test [16, Note 3 on Attachment 1, pages 44 and 45].
- ✓ (20) Adjustment in 60-year projection in [5, PTN-LR-00-0127 Table 10.3-2] - recorded as a value of 0 when 1 was assumed in pre-operational startup.
- ✓ (21) One cycle is projected for 80 years to remain within the analytical basis if that event occurs.
- ✓ (22) One cycle of 10 events is projected for 80 years to remain within the analytical basis if that event occurs.
- ✓ (23) Recommended revision O-ADM-553 to align with UFSAR Table 4.1-10.

3.2 PTN EAF Assessment

For SLR, PTN-specific EAF calculations were performed for the limiting PTN components. All components with CUF values were considered in the EAF assessment so that the plant-specific limiting locations were addressed by the assessment to be consistent with GALL-SLR guidance. The assessment serves as an update and replacement to the EAF assessment performed for 60 years that is summarized in Table 2-2.

The PTN EAF assessment for SLR was performed using the applicable guidance from the SRP-SLR [4]. Section 4.3.2.1.2, “Components Evaluated for CUF_{en} ,” of the SRP-SLR for components evaluated for CUF_{en} states the following:

Applicants should also include CUF_{en} calculations for additional component locations if they are considered to be more limiting than those previously evaluated. This sample set includes the locations identified in NUREG/CR-6260 and additional plant-specific component locations in the reactor coolant pressure boundary if they may be more limiting than those considered in NUREG/CR-6260. Plant-specific justification can be provided to demonstrate that calculations for the NUREG/CR-6260 locations do not need to be included. Environmental effects on fatigue for these critical components can be evaluated using the positions described in Regulatory Guide (RG) 1.207, Revision 14; NUREG/CR-6909, Revision 0 (with “average temperature” used consistent with the clarification that was added to NUREG/CR-6909, Revision 1); or other subsequent NRC-endorsed alternatives.

For PTN, the older-vintage Westinghouse PWR plant is applicable; in fact, the “Older Vintage Westinghouse Plant” evaluated in Section 5.5 of NUREG/CR-6260 is directly relevant to PTN because the design codes, analytical approach and techniques used for that plant matches those used for PTN. In addition, the evaluated transient cycles matched or bounded PTN. Therefore, the evaluation from NUREG/CR-6260 is directly applicable to PTN.

Based on the foregoing discussion, the updated SLR EAF assessment for PTN was performed as follows:

- The plant-specific NUREG/CR-6260 locations were reevaluated for SLR.
- To ensure that any locations that may be more limiting than the NUREG/CR- 6260 locations were addressed, the reactor coolant pressure boundary (RCPB) components with existing ASME Code fatigue analyses CUFs presented in Tables 2-2 and 3-3 were evaluated for EAF for SLR.
- Revised plant-specific EAF multipliers applicable for SLR were calculated based on the latest F_{en} methods using the guidance in NUREG/CR–6909, Revision 0 [10] (with “average temperature” used consistent with the clarification that was added to NUREG/CR–6909, Revision 1 [6]).

The SLR EAF assessment results from Appendix A are summarized in Table 3-3. These results are discussed in Section 3.4.

Table 3-3: Other Class 1 RCPB Components with a CUF Value ⁽¹⁾

Component	Location	60-Year CLB CUF
RPV	Head Flange	0.083
	Vessel Flange	0.531
	Closure Studs	0.81
	CRDM Housing -- J-weld	0.730
	CRDM Housing -- Bi-metallic Weld	0.620
	Vent Nozzle	0.620
	Shell-to-Shell Juncture	0.034
	Bottom Head-to-Shell Juncture	0.023
	Bottom Mounted Instrumentation Nozzles	0.002
	Core Support Pads	0.020
Control Rod Drive Mechanisms (CRDMs)	Latch Housing	{ }
	Rod Travel Housing	{ }
	Cap	{ }
	Lower Joint	{ }
	Middle Joint	{ }
	Upper Joint	{ }
Steam Generators (S/Gs) (Primary Side)	Divider Plate	{ }
	Primary Chamber, Tubesheet and Stub Barrel Complex	{ }
	Tube-to-Tubesheet Weld	{ }
	Tubes	{ }
Steam Generators (S/Gs) (Secondary Side)	Upper Shell Drain	{ }
	Feedwater Nozzle	{ }
	Secondary Manway Bolts	{ }
	Upper Shell Remnants	{ }
	Secondary Hand-Hole & Inspection Port	{ }
	Steam Outlet Nozzle Flow Limiters	{ }
		{ }
Reactor Coolant Pumps (RCPs)	Main Flange Studs	0.29
	Main Flange	0.025
	Casing	0.001
Reactor Internals	Upper Support Plate	{ }
	Deep Beam	{ }
	Upper Core Plate	{ }
	Upper Core Plate Alignment Pins	{ }
	Upper Support Columns	{ }
	Lower Support Plate	{ }
	Lower Support Plate to Core Barrel Weld	{ }
	Lower Core Plate	{ }
	Lower Support Columns	{ }
	Core Barrel Flange	{ }
	Core Barrel Outlet Nozzle	{ }
	Radial Keys and Clevis Insert Assembly	{ }

Footnote for Table 3-3:

1. From Table 2-2 of Reference [29].

Table 3-4: Summary of the PTN EAF Assessment for SLR (80 Years of Operation)

Component ⁽¹⁾	80-Year CUF ⁽²⁾	F_{en} ⁽³⁾	Material ⁽⁴⁾	80-Year CUF_{en} ⁽⁵⁾
RPV Shell at Core Support Pads	0.509 ⁽²⁴⁾ / NA ⁽²²⁾	N/A ⁽¹⁰⁾ / NA ⁽²²⁾	Low alloy steel	N/A ⁽¹⁰⁾ / 0.910 ⁽⁶⁾⁽⁸⁾
RPV Inlet Nozzle (inside surface)	0.073 ⁽²⁴⁾	2.45	Carbon steel with stainless steel clad and a stainless steel weld butter safe end	0.179
RPV Outlet Nozzle (inside surface)	0.056 ⁽²⁴⁾	2.45	Carbon steel with stainless steel clad and a stainless steel weld butter safe end	0.137
Head Flange	0.083 ⁽²⁵⁾	6.28	Low Alloy Steel ⁽²³⁾	0.521
Vessel Flange ⁽²⁰⁾	0.531 ⁽²⁵⁾ / { }	6.28 / { }	Low Alloy Steel ⁽²³⁾	3.333/ 0.373 ⁽²⁶⁾
CRDM Housing - J-Groove Weld ⁽¹⁴⁾⁽¹⁵⁾	0.73 ⁽²⁵⁾ / { }	Not wetted / { }	Inconel	N/A ⁽²¹⁾ / 0.274 ⁽²⁶⁾
CRDM Housing - Bi-Metallic (Nozzle-to-Adapter) Weld ⁽¹⁸⁾	0.62 ⁽²⁵⁾ / { }	3.75 / { }	Inconel	2.323 / 0.695 ⁽²⁶⁾
Vent Nozzle ⁽¹⁴⁾⁽¹⁶⁾	0.49 ⁽²⁵⁾ / { }	Not wetted / { }	Inconel	N/A ⁽²¹⁾ / 0.230 ⁽²⁶⁾
Shell-to-Shell Juncture	0.034 ⁽²⁵⁾	14.06	Unknown -- use maximum	0.478
Bottom Head-to-Shell Juncture	0.023 ⁽²⁵⁾	14.06	Unknown -- use maximum	0.323
Bottom Mounted Instrumentation Nozzles	0.002 ⁽²⁵⁾	14.06	Unknown -- use maximum	0.028
Core Support Pads	0.046 ⁽²⁴⁾	14.06	Unknown -- use maximum	0.281
RCS Piping Safety Injection Nozzle	0.030 ⁽²⁴⁾	14.06	Stainless steel	0.647
RCS Piping Charging Nozzle	0.022 ⁽²⁴⁾	14.06	Stainless steel	0.422
RCS Piping Residual Heat Removal (RHR) Piping	0.046 ⁽²⁴⁾	14.06	Stainless steel	0.200

Table continued on next page.

Table 3-4: Summary of the PTN EAF Assessment for SLR (80 Years of Operation)

(continued)

Component ⁽¹⁾	80-Year CUF ⁽²⁾	F_{en} ⁽³⁾	Material ⁽⁴⁾	80-Year CUF_{en} ⁽⁵⁾
Pressurizer Spray Nozzle	{ } ⁽²⁴⁾ / 0.0721 ⁽¹¹⁾	14.06 / 7.33	Carbon steel with stainless steel clad, stainless steel thermal sleeve, and a stainless steel safe end	{ } / 0.5289 ⁽⁶⁾⁽⁷⁾⁽¹¹⁾
Pressurizer Safety and Relief Nozzle	{ } ⁽²⁴⁾	14.06	Carbon steel with stainless steel clad and a stainless steel safe end	{ }
Pressurizer Lower Head, Heater Well	{ } ⁽²⁴⁾ / { } ⁽¹²⁾	14.06 / { }	Carbon steel with stainless steel clad and J-groove weld cover filet	{ } / 0.093 ⁽⁶⁾⁽¹²⁾
Pressurizer Lower Head/ Perforation	{ } ⁽²⁴⁾	14.06	Carbon steel with stainless steel clad	{ }
Pressurizer Upper Head and Shell	{ } ⁽²⁴⁾ / NA ⁽²²⁾	6.28 / NA ⁽²²⁾	Low alloy steel	{ } / 0.974 ⁽⁶⁾⁽⁸⁾
Pressurizer Support Skirt/Flange	0.0165 ⁽²⁴⁾	6.28	Carbon steel	0.104
Pressurizer Manway Pad	{ } ⁽²⁴⁾	6.28	Carbon steel	{ }
Pressurizer Manway Cover	0.0 ⁽²⁴⁾	6.28	Carbon steel	0.000
Pressurizer Manway Bolts	0.0 ⁽²⁴⁾	6.28	Low Alloy Steel	0.000
Pressurizer Welded Manway Diaphragm	{ } ⁽²⁴⁾	3.75	Nickel Alloy	{ }
Pressurizer Instrument Nozzle	{ } ⁽²⁴⁾	14.06	Stainless steel	{ }
Pressurizer Immersion Heater	0.0040 ⁽²⁴⁾	14.06	Stainless steel	0.056
CRDM Latch Housing ⁽¹⁹⁾	{ } ⁽²⁵⁾ / { }	14.06 / { }	Stainless Steel	{ } / 0.269 ⁽²⁶⁾
CRDM Rod Travel Housing	{ } ⁽²⁵⁾	14.06	TBD	0.675
CRDM Cap	{ } ⁽²⁵⁾	14.06	TBD	0.042
CRDM Lower Joint	{ } ⁽²⁵⁾ / { } ⁽¹⁷⁾	14.06 / { } ⁽¹⁷⁾	Stainless Steel	{ } / 0.749 ⁽²⁶⁾
CRDM Middle Joint	{ } ⁽²⁵⁾	14.06	TBD	{ }
CRDM Upper Joint	{ } ⁽²⁵⁾	14.06	TBD	{ }

Table continued on next page.

**Table 3-4: Summary of the PTN EAF Assessment for SLR (80 Years of Operation)
(concluded)**

Component ⁽¹⁾	80-Year CUF ⁽²⁾	F_{en} ⁽³⁾	Material ⁽⁴⁾	80-Year CUF_{en} ⁽⁵⁾
S/G Divider Plate	{ } ⁽²⁵⁾ / NA ⁽²²⁾	3.75 / NA ⁽²²⁾	Inconel	{ } / 0.881 ⁽⁶⁾⁽⁹⁾
S/G Primary Chamber, Tubesheet and Stub Barrel Complex	{ } ⁽²⁵⁾	6.28	Unknown -- use maximum	{ }
S/G Tube-to-Tubesheet Weld ⁽¹³⁾	{ } ⁽²⁵⁾	14.06	Unknown -- use maximum	{ }
S/G Tubes	{ } ⁽²⁵⁾ / NA ⁽²²⁾	3.75 / NA ⁽²²⁾	Inconel	{ } / 0.903 ⁽⁶⁾⁽⁹⁾
RCP Main Flange	0.025 ⁽²⁵⁾	14.06	Unknown -- use maximum	0.351
RCP Casing	0.001 ⁽²⁵⁾	14.06	Unknown -- use maximum	0.014

Footnotes for Table 3-4:

1. Components are those components in Table 2-2.
2. "CUF (for 80 Years)" from Table 2-2. Based on the transient counts and severities remaining valid for SLR (see Section 0), the 80-Year CUF value remains equal to the 60-Year CUF value unless noted otherwise.
3. The maximum F_{en} value for the material.
4. The component material corresponding to the maximum F_{en} value obtained from [28].
5. The allowable value for CUF_{en} is 1.0.
6. This value was determined through the use of the NUREG/CR-6909 DRAFT Revision 1 [6] rules.
7. The value of CUF_{en} shown results from evaluation of one (1) Inadvertent Auxiliary Spray (IAS) transient. Evaluation of four (4) IAS transients results in a $CUF_{en} = 0.9036$.
8. From [32].
9. From [33].
10. Not Applicable (N/A) due to mismatch of UFSAR-reported CUF with previously reported EPU [21, Table 2.2.2.3-1] CUF_{en} .
11. CUF and CUF_{en} values from [30.c]. Calculation contains vendor proprietary references.
12. CUF and CUF_{en} values from [31.c]. Calculation contains vendor proprietary references.
13. S/G Tube-to-Tubesheet Weld will be included in the S/G inspection program.
14. The location with the highest CUF_{en} that is wetted by reactor coolant will be identified and values provided in lieu of the locations currently listed.
15. { } [38].
16. { } [37].
17. From [40].
18. From [35].
19. From [36].
20. From [39].
21. Not Applicable (N/A) because the location reported is not wetted.
22. Not Available (NA).
23. Head Flange is SA-508 Class 2 material and Vessel Flange is SA-508 Class 3 material [34].
24. From Table 2-2.
25. From Table 3-3.
26. From [42].

3.3 Plant-Specific Limiting Locations

Consistent with the SRP-SLR requirements discussed in Section 0, Chapter X.M1 of the GALL-SLR Report [3] states, in part, the following:

CUF_{en} is CUF adjusted to account for the effects of the reactor water environment on component fatigue life. For a plant, the effects of reactor water environment on fatigue are evaluated by assessing a set of sample critical components for the plant. Examples of critical components are identified in NUREG/CR-6260; however, plant-specific component locations in the reactor coolant pressure boundary may be more limiting than those considered in NUREG/CR-6260, and thus should also be considered.

The locations evaluated for EAF in Section 3.2 for PTN represent the limiting locations from a CUF perspective per GALL-SLR Chapter X.M1 requirements for PTN based on the following:

- In the PTN 60-year LRA, the plant-specific NUREG/CR-6260 locations for the older-vintage Westinghouse plant were evaluated. The older-vintage Westinghouse plant evaluated in NUREG/CR-6260 is directly relevant to PTN because the design codes, analytical approach and techniques used match those used at PTN. In addition, the evaluated transient cycles matched or bounded PTN. In all the CUF calculations documented in Section 5.5, “Older Vintage Westinghouse Plant,” of NUREG/CR-6260, EAF evaluation was consistently performed for “the locations of highest design CUF.” Therefore, use of maximum plant-specific F_{en} values, coupled with these highest CUF values, ensures bounding CUF_{en} values for PTN.
- Based on the comprehensive review of the PTN fatigue bases that was recently performed for SLR [29], all Class 1 locations evaluated for CUF were evaluated in the EAF assessment in Appendix A except for those locations that are not part of the RCPB or those locations that are not exposed to a water environment such that EAF effects do not apply, as follows:
 - All surge line locations were excluded from CUF_{en} calculations because they were evaluated for EAF via inspection management, as discussed in Section 2.3. This

includes the RCS Piping Surge Line Hot Leg Nozzle and the Pressurizer Surge Nozzle.

- The following locations are not exposed to the environment so EAF assessment is not required: The RPV Closure Studs and the RCP Main Flange Studs.
- The following locations are not part of the RCPB: All S/G Secondary Side locations and all Reactor Internals locations. Only RCPB locations require EAF assessment per Section 4.3.2.1.2, “Components Evaluated for CUF_{en} ” of the SRP-SLR [4].
- For each CUF value evaluated for EAF, bounding F_{en} multipliers were used for the materials present in the component location. In cases where the materials were not known, F_{en} values for all three F_{en} material groupings (carbon and low alloy steels, stainless steels, and nickel alloys) were determined and the maximum multiplier was used.

Therefore, the SLR EAF assessment for PTN satisfies GALL Chapter X.M1 guidance for components selection as the PTN EAF assessment considers the NUREG/CR-6260 locations as well as all other plant-specific limiting locations.

3.4 Summary of PTN EAF Assessment

The following summarizes SLR EAF assessment for PTN:

- Based on an 80-year transient evaluation performed for SLR, the same transients, transient severity and transient counts used for the 60-year EAF assessment are bounding for 80 years of operation. Therefore, the 60-year CLB CUF values remain unchanged and were used in the updated EAF assessment for 80 years. These CUF values use design transients counts for all locations and reflect power uprate.
- The SLR EAF assessment for PTN considers the NUREG/CR-6260 locations, as well as all other plant-specific limiting locations with a CUF calculation that are exposed to a water environment and are part of the RCPB. Therefore, it satisfies GALL Chapter X.M1 and related SRP-SLR guidance for component selection.

- The PTN EAF assessment uses plant-specific F_{en} values, coupled with the highest CUF values, to determine bounding CUF_{en} values.
- Revised plant-specific EAF multipliers applicable for SLR were calculated that generally make use of the latest F_{en} methods provided in RG 1.207, Revision 1 [5]. As noted in Appendix A, the PTN CUF values still reflect the use of the fatigue curves from the applicable Section III used in each component's CUF calculation because detailed fatigue tables for each PTN component locations are not available. Therefore, the guidance of Section C.1.1 of RG 1.207, Revision 1 [5] (for carbon and low alloy steel), Section C.2.1 (for SS), and Section C.3.1 (for Ni-Cr-Fe alloys) could not be fully implemented in the calculations for all locations. This shortcoming should be addressed as part of the resolution of high CUF_{en} values discussed below.
- The CUF_{en} values calculated using the ASME Code fatigue curves of record for each location are above the allowable of 1.0 for 14 locations: the RPV Head Flange, the RPV Vessel Flange, the RPV CRDM Housing – J-Weld, the RPV CRDM Housing – Bi-Metallic Weld, the RPV Vent Nozzle, the Pressurizer Spray Nozzle, the Pressurizer Lower Head Heater Well, the Pressurizer Upper Head and Shell, the CRDM Latch Housing, the CRDM Lower Joint, the S/G Divider Plate, the S/G Primary Chamber Tubesheet and Stub Barrel Complex, the S/G Tube-to-Tubesheet Weld and the S/G Tubes. For these locations, FPL should satisfactorily assess EAF using one or more of the following options:
 - Further refinement of the EAF analysis to lower the CUF_{en} values to below 1.0, or
 - repair of the affected locations, or
 - replacement of the affected locations, or
 - management of EAF effects using an inspection program that has been reviewed and approved by the NRC.

To fully satisfy GALL-SLR AMP requirements, FPL should complete one of these options at least two years prior to the period of SLR operation. If the last option is selected, FPL should provide the NRC with the inspection details of the AMP requiring staff approval prior to the period of SLR operation.

THIS REPORT CONTAINS VENDOR PROPRIETARY INFORMATION

- The components shown in Table 3-3 with 80-year CUF_{en} values less than 1.0 are acceptable for 80 years of operation.
- Some of the EAF-analyzed components required refined analysis techniques and use 80-year projected cycles for selected transients to achieve a CUF_{en} value below 1.0. Table 3-5 provides which 80-year projected transients and their minimum values which have been used in the EAF analyses.
- The PTN EAF assessment should be coupled with the PTN Cycle Counting Program to verify the continued acceptability of all EAF analyses through cycle counting and periodically updated evaluations, if necessary, to demonstrate that they continue to meet the appropriate limits throughout the SLR period.

The PTN-specific EAF assessment and the above recommendations to use updated fatigue curves and resolve unacceptable CUF_{en} values serve as an acceptable AMP that satisfies GALL-SLR Report, Chapter X.M1 guidance to manage SCs that are the subject of fatigue TLAAs in accordance with the requirements in 10 CFR 54.21(c)(1)(iii).

Table 3-5: Minimum Cycles Used in EAF Analyses

Component	Design Number	Pressurizer Spray Nozzle	Pressurizer Lower Head	RSG Divider Plate	RSG Tubes	Pzr Upper Head and Shell	RV Core Support Blocks	CRDM Bi-Metallic (Nozzle-to-Adapter) Weld	CRDM Latch Housing	RVCH CRDM Nozzle and J-Groove Weld	Vessel Flange	Minimum Cycles	CRDM Lower Joint (from RVCH installation at 80 years for bounding Unit 4)
Station Heatup at 100°F/hour	200	181	181	181	181			181	181	181	181	181	92
Station Cooldown at 100°F/hour	200	181	181	181	181			181		181	181	181	
Station Loading at 5% power per minute	14500	484		533	533	533			533	533	533	484	
Station Unloading at 5% power per minute	14500	450		533	533	451				451	440	440	
Step Load Increase of 10% of Full Power	2000	82		164	164							82	82
Step Load Decrease of 10% of Full Power	2000	106		164	164							106	
Step Load Decrease of 50% of Full Power	200	51								82	82	51	82
Loss of Load without Immediate Turbine Trip or	80	27								28	28	27	13
Loss of Flow in One Reactor Coolant Loop	80	21								26	26	21	
Inadvertent Auxiliary Spray	10	2 ⁽¹⁾										0	
Hydrostatic Test at 2485 psig Pressure and 400°F	5	3					2					2	
Primary to Secondary Side Leak Test to 2435 psig	150	4										4	
Loss of AC Power	40									19	19	19	8
Reactor Trip	400							311		292	292	292	
OBE	50							10	10			10	
Rod Trips ⁽²⁾	2600								2000			2000	144

Footnotes for Table 3-5:

- (1) One (1) occurrence of the IAS transient is specified in Tables 3-1 and 3-2. Evaluation of the pressurizer spray nozzle shows that evaluation of two (2) IAS transients results in an acceptable $CUF_{en} \leq 1.0$ value [30.c].
- (2) Transient not counted.

4.0 SUMMARY AND CONCLUSIONS

This report addresses TLAAAs associated with EAF for both PTN units. As such, this report documents the EAF TLAAAs necessary to support operating license renewals from 60 to 80 years for both PTN units that satisfy all the requirements specified by the NRC for SLR.

Section 2.0 summarizes PTN's TLAAAs on fatigue that were resolved for 60 years of operation by analyses that used a combination of three demonstrations: (i) fatigue monitoring of all relevant plant thermal transients to confirm that the original transient design limits remain valid for the 60-year operating period (i.e., the PTN Cycle Counting Program), (ii) reactor water environmental effects on fatigue life using the most recent data from laboratory simulation of the reactor coolant environment (i.e., the PTN EAF Assessment), and (iii) inspection of the surge line welds under the ASME Code Section XI inspection program to verify the absence of fatigue cracking (i.e., the PTN Surge Line Inspection Program). Collectively, these three demonstrations form the EAF CLB for PTN and represent the inputs to the PTN-specific program for addressing EAF effects for SLR.

Section 3.0 contains the plant-specific assessment of EAF effects for PTN for SLR. The plant-specific assessment is separated into four parts, the PTN Cycle Counting Program, the PTN EAF Assessment, discussion of the plant-specific limiting locations evaluated in the PTN EAF Assessment, and a summary of the PTN EAF Assessment and how it satisfies NRC requirements for SLR. Collectively, these four parts serve as a replacement to the PTN 60-year EAF assessment that reflects an updated assessment applicable to SLR. The PTN EAF assessment should be coupled with the PTN Cycle Counting Program to verify the continued acceptability of all EAF analyses through cycle counting and periodically updated evaluations, if necessary, to demonstrate that they continue to remain valid and meet the appropriate limits throughout the SLR period. The PTN-specific EAF assessment and the associated recommended options for resolving unacceptable CUF_{en} values serve as an acceptable AMP that satisfies GALL-SLR Report, Chapter X.M1 guidance to manage SCs that are the subject of EAF TLAAAs in accordance with the requirements in 10 CFR 54.21(c)(1)(iii).

THIS REPORT CONTAINS VENDOR PROPRIETARY INFORMATION

Based on the evaluation and results presented in this report, the TLAAs for EAF are adequately evaluated for PTN, and the potential effects of the reactor water environment have been properly evaluated, as required by the GALL-SLR [3]. Therefore, the proposed approach described in this report is recommended for inclusion in FPL's SLRA for PTN to address EAF.

This report was prepared with information currently available. Several TBD (To Be Determined) notations populate the 80-Year CUF, F_{en} , Materials and 80-Year CUF_{en} columns in Table 3-4. Analyses are in progress to supply values for the locations in the tables populated with TBD notations.

5.0 REFERENCES

1. FPL Letter No. L-2000-177, “Application for Renewed Operating Licenses, Turkey Point Units 3 and 4,” September 8, 2000, ADAMS Accession No. ML003749654.
2. NRC Extended Operating License Approval, including:
 - a. NRC Letter from Rajendar Auluck to J. A. Stall, “Issuance of Renewed Facility Operating Licenses Nos. DPR-31 and DPR-41 for Turkey Point Nuclear Generating Units Nos. 3 and 4,” U.S. Nuclear Regulatory Commission, Washington, DC, June 6, 2002, ADAMS Accession No. ML021550105.
 - b. NUREG-1759, “Safety Evaluation Report Related to the License Renewal of Turkey Point Nuclear Plant, Units 3 and 4,” U.S. Nuclear Regulatory Commission, Washington, DC, April 2002, ADAMS Accession No. ML021280541.
 - c. NUREG-1759, Supplement 1, “Safety Evaluation Report Related to the License Renewal of Turkey Point Nuclear Plant, Units 3 and 4,” U.S. Nuclear Regulatory Commission, Washington, DC, May 2002, ADAMS Accession No. ML021560094.
3. NUREG-2191, Final Report, “Generic Aging Lessons Learned for Subsequent License Renewal (GALL-SLR) Report,” Volumes 1 and 2, U.S. Nuclear Regulatory Commission, Washington, DC, July 2017, Agencywide Documents Access and Management System (ADAMS) Accession Nos. ML17187A031 and ML17187A204.
4. NUREG-2192, Final Report, “Standard Review Plan for Review of Subsequent License Renewal Applications for Nuclear Power Plants,” U.S. Nuclear Regulatory Commission, Washington, DC, July 2017, ADAMS Accession No. ML17188A158.
5. NRC Draft Regulatory Guide DG-1309 (Proposed Revision 1 of Regulatory Guide 1.207), “Guidelines for Evaluating the Effects of Light-Water Reactor Coolant Environments in Fatigue Analyses of Metal Components,” U.S. Nuclear Regulatory Commission, Washington, DC, November 2014, ADAMS Accession No. ML14171A584.

6. NUREG/CR-6909 (ANL 12/60), Revision 1, Draft Report for Comment, “Effect of LWR Coolant Environments on Fatigue Life of Reactor Materials,” U.S. Nuclear Regulatory Commission, Washington, DC, March 2014, ADAMS Accession No. ML14087A068.
7. U.S. Code of Federal Regulations, Title 10, Chapter I -- Nuclear Regulatory Commission, Part 54, “Requirements for Renewal of Operating Licenses for Nuclear Power Plants.”
8. NUREG/CR-6260 (INEL-95/0045), “Application of NUREG/CR-5999 Interim Fatigue Curves to Selected Nuclear Power Plant Components,” U.S. Nuclear Regulatory Commission, Washington, DC, March 1995, ADAMS Accession No. ML031480219.
9. ASME Boiler and Pressure Vessel Code, Section XI, Rules for Inservice Inspection of Nuclear Power Plant Components, Nonmandatory Appendix L, “Operating Plant Fatigue Assessment,” American Society of Mechanical Engineers, New York, NY, 2013 Edition.
10. NUREG/CR-6909 (ANL-06/08), “Effect of LWR Coolant Environments on Fatigue Life of Reactor Materials,” U.S. Nuclear Regulatory Commission, Washington, DC, February 2007, ADAMS Accession No. ML070660620.
11. NUREG-0933, Supplement 24, “A Prioritization of Generic Safety Issues,” Section 3, “New Generic Issues,” Issue 190, “Fatigue Evaluation of Metal Components for 60-Year Plant Life (Rev. 2),” U. S. Nuclear Regulatory Commission, Washington, DC, June 30, 2000, ADAMS Accession No. ML020740117.
12. Attachment 8.1 to FPL Document No. PTN-ENG-LRAM-00-0055, Revision 1, “Engineering Evaluation of Environmental Effects of Fatigue,” (SI Report No. SIR-00-089, Revision 0, “Position Document to Address GSI-190 Issues Related to Fatigue Evaluation for Turkey Point Units 3 and 4,” July 2000, SI File No. FPL-10Q-401).
13. Attachment 8.2 to FPL Document No. PTN-ENG-LRAM-00-0055, Revision 1, “Engineering Evaluation of Environmental Effects of Fatigue,” (SI Report No. SIR-01-

042, “Transmittal of Final RAI Responses on Fatigue,” April 13, 2001, SI File No. FPL-10Q-402).

14. NUREG-1801, Revision 0, “Generic Aging Lessons Learned (GALL) Report,” U.S. Nuclear Regulatory Commission, Washington, DC, July 2001, ADAMS Accession Nos. ML012060392, ML012060514, ML012060539, and ML012060521.
15. NUREG/CR-6583 (ANL-97/18), “Effects of LWR Coolant Environments on Fatigue Design Curves of Carbon and Low-Alloy Steels,” U.S. Nuclear Regulatory Commission, Washington, DC, March 1998, ADAMS Accession No. ML031480391.
16. NUREG/CR-5704 (ANL-98/31), “Effects of LWR Coolant Environments on Fatigue Design Curves of Austenitic Stainless Steels,” U.S. Nuclear Regulatory Commission, Washington, DC, April 1999, ADAMS Accession No. ML031480394.
17. PTN Surge Line Appendix L Evaluation, including:
 - a. SI Calculation Nos. 1100756.301 through 1100756.306 (EC 276235) and SI Report No. 1100756.401 (EC 276242), “Turkey Point on the Pressurizer Surge Nozzle Flaw Tolerance Using Appendix L,” April 2012.
 - b. FPL Letter No. L-2012-214 from Michael Kiley to U.S. Nuclear Regulatory Commission, “Turkey Point Units 3 and 4, Docket Nos. 50-250 and 50-251, License Renewal Commitment, Submittal of Pressurizer Surge Line Welds Inspection Program,” May 16, 2012, ADAMS Accession No. ML12152A156.
18. Letter from Farideh E. Saba, Senior Project Manager (NRC) to Mr. Mano Nazar (NextEra Energy), “Turkey Point Nuclear Generating Units 3 and 4 - Review of License Renewal Commitment for Pressurizer Surge Line Welds Inspection Program (TAC Nos. ME8717 and ME8718),” U.S. Nuclear Regulatory Commission, Washington, DC, May 29, 2013, ADAMS Accession No. ML13141A595.
19. SI evaluations performed for Extended Power Uprate (EPU), including:

THIS REPORT CONTAINS VENDOR PROPRIETARY INFORMATION

- a. SI Calculation No. 0900948.301, Revision 1, “Environmental Fatigue Evaluation of Reactor Coolant System Components/Nozzles and Connected Systems,” April 30, 2010.
- b. SI Calculation No. 0900948.302, Revision 1, “Environmentally-Assisted Fatigue Evaluation of the RPV Shell Using 60-Year Projected Cycles and Enveloping Cycles,” April 22, 2010.
- 20. SI evaluations performed in response to License Renewal Commitments, including
 - a. SI Calculation No. 1100768.301, Revision 1, “Pressurizer Spray Nozzle Design Loads Calculation,” December 1, 2011.
 - b. SI Calculation No. 1100768.302, Revision 0, “Finite Element Model of the Pressurizer Spray Nozzles,” November 1, 2011.
 - c. SI Calculation No. 1100768.303, Revision 0, “Thermal and Mechanical Stress Analyses of Pressurizer Spray Nozzles,” February 7, 2012.
 - d. SI Calculation No. 1100768.304, Revision 0, “Pressurizer Spray Nozzle Fatigue Analysis,” February 7, 2012.
- 21. Turkey Point, Units 3 and 4 License Amendment Request for Extended Power Uprate (LAR No. 205), Attachment 4, ADAMS Accession No. ML103560177, SI File No. 1700109.210.
- 22. Westinghouse Letter No. LTR-MRCDA-17-81, Revision 1, “Requested Cumulative Fatigue Usage Factors from Turkey Point Unit 3 and Unit 4 EPU Licensing Report,” transmitted by Westinghouse Letter No. NEXT-17-145, **PROPRIETARY INFORMATION**, August 22, 2017, SI File No. 1700109.111P.
- 23. NOT USED
- 24. FPL Procedure No. 0-ADM-553, Revision 3, “Maintaining Records for Design Cycles,” 9/13/12, SI File No. 1700109.203.

THIS REPORT CONTAINS VENDOR PROPRIETARY INFORMATION

25. FPL Letter No. PTN-LR-00-0127, “Florida Power & Light Company, Turkey Point Units 3 & 4, License Renewal Project, GSI-190 Position Paper,” July 12, 2000, SI File No. FPL-10Q-204.
26. FPL Letter No. L-2001-75, “Response to Request for Additional Information for the Review of the Turkey Point Units 3 and 4 License Renewal Application,” April 19, 2001, ADAMS Accession No. ML011170195.
27. NOT USED
28. FPL Request for Input No. RFI-FPL-SI-004, “Turkey Point Units 3 and 4 Subsequent License Renewal (SLR) Time Limited Aging Analyses (TLAAs) Project,” approved 5/24/17, SI File No. 1700109.205.
29. SI Report No. 1700109.402P, Revision 3, “Evaluation of Fatigue of ASME Section III, Class 1 Components for Turkey Point Units 3 and 4 for Subsequent License Renewal,” December 2017. **Contains Vendor Proprietary Information.**
30. SI evaluations performed for the Pressurizer Spray Nozzle, including:
 - a. SI Calculation No. 1700804.313P, Revision 1, “Pressurizer Spray Nozzle Loads,” December 7, 2017. **Contains Vendor Proprietary Information**
 - b. SI Calculation No. 1700804.314P, Revision 1, “Pressurizer Spray Nozzle Finite Element Model and stress Analysis,” December 7, 2017. **Contains Vendor Proprietary Information.**
 - c. SI Calculation No. 1700804.315P, Revision 1, “Pressurizer Spray Nozzle Fatigue Analysis,” December 7, 2017. **Contains Vendor Proprietary Information.**
31. SI evaluations performed for the Pressurizer Lower Head, Heater Penetration:
 - a. SI Calculation No. 1700804.316P, Revision 0, “3-D Finite Element Model of Pressurizer Bottom Head, Skirt Assembly and Heater Wells,” September 28, 2017. **Contains Vendor Proprietary Information.**

THIS REPORT CONTAINS VENDOR PROPRIETARY INFORMATION

- b. SI Calculation No. 1700804.317, Revision 0, “Pressurizer Lower Head Green’s Functions and Unit Pressure,” October 5, 2017.
 - c. SI Calculation No. 1700804.318, Revision 0, “Pressurizer Lower Head Loads, Fatigue and EAF Analysis,” November 7, 2017.
- 32. Westinghouse Letter No. LTR-SDA-II-17-15, *Environmentally Assisted Fatigue Evaluation of the Turkey Point Unit 3 and 4 Pressurizer Upper Head and Reactor Vessel Core Support Blocks*, Rev. 0, dated October 16, 2017, SI File No. 1700804.204.
 - 33. Westinghouse Letter No. LTR-CECO-17-016, *Environmentally Assisted Fatigue Evaluation of the Turkey Point Unit 3 and 4 Replacement Steam Generators*, Rev. 0, dated October 25, 2017, SI File No. 1700804.205.
 - 34. FPL Drawing Number 5613-M-460-2, *Spec. Drawing for Replacement Reactor Vessel Closure Head*, Revision 0, SI File No. 1700109.212.
 - 35. AREVA Calculation No. 32-9279174-000, *Turkey Point – 3 & 4 CRDM Nozzle to Adapter Weld Connection EAF Evaluation*, SI File No. 1700804.206P.
- PROPRIETARY**
- 36. AREVA Calculation No. 32-9279367-000, *TP CRDM Latch Housing Environmentally Assisted Fatigue*, SI File No. 1700804.206P. **PROPRIETARY**
 - 37. AREVA Calculation No. 32-9279362-000, *TP Vent Nozzle Environmentally Assisted Fatigue*, SI File No. 1700804.206P. **PROPRIETARY**
 - 38. AREVA Calculation No. 32-9279212-000, *Turkey Point – 3 & 4 Replacement RVCH CRDM Nozzle EAF Analysis*, SI File No. 1700804.206P. **PROPRIETARY**
 - 39. AREVA Calculation No. 32-9279161-000, *Turkey Point SLR EAF Analysis for Reactor Vessel Flange*, SI File No. 1700804.206P. **PROPRIETARY**
 - 40. AREVA Calculation No. 32-9280202-000, *TP CRDM Lower Joint Environmentally Assisted Fatigue*, SI File No. 1700804.206P. **PROPRIETARY**

41. NOT USED
42. AREVA Letter No. AREVA-17-02742, Final CUFen Results – Turkey Point 3 & 4 –
SLR EAF Analyses, SI File No. 1700804.206.

APPENDIX A

F_{EN} CALCULATIONS

This appendix contains the details of the environmentally adjusted cumulative usage factor (CUF_{en}) calculations for Turkey Point Nuclear Plant, Units 3 and 4 (PTN) for Subsequent License Renewal (SLR) operation out to 80 years.

Chapter X.M1 of the GALL-SLR Report [3] states, in part, the following:

CUF_{en} is CUF adjusted to account for the effects of the reactor water environment on component fatigue life. For a plant, the effects of reactor water environment on fatigue are evaluated by assessing a set of sample critical components for the plant. Examples of critical components are identified in NUREG/CR-6260; however, plant-specific component locations in the reactor coolant pressure boundary may be more limiting than those considered in NUREG/CR-6260, and thus should also be considered.

Environmental effects on fatigue for these critical components may be evaluated using the guidance in Regulatory Guide (RG) 1.207, Revision 1; alternatively, the bases in NUREG/CR-6909, Revision 0 (with “average temperature” used consistent with the clarification that was added to NUREG/CR-6909, Revision 1); or other subsequent U.S. Nuclear Regulatory Commission (NRC)-endorsed alternatives.

Consistent with this guidance, environmental adjustment factor (F_{en}) calculations are performed in this appendix for PTN for SLR using the methods documented in the latest draft of RG 1.207, Revision 1 [5] (final publication of the RG is still pending).

Section C of the draft of RG 1.207, Revision 1 refers to the equations in Appendix A of NUREG/CR-6909, Revision 1 for calculating F_{en} values. Therefore, the F_{en} equations from Appendix A of the latest draft of NUREG/CR-6909, Revision 1 [6] are summarized here and used in updated PTN CUF_{en} calculations.

Carbon and Low Alloy Steels

The nominal environmental fatigue adjustment factor for both carbon and low-alloy steels, $F_{\text{en-CS-LAS}}$, is expressed as:

$$F_{\text{en-CS-LAS}} = \exp ((0.003 - 0.031 \epsilon^*) S^* T^* O^*) \quad (\text{Eqn. A-1})$$

where S^* , T^* , O^* , and ϵ^* are transformed sulfur (S) content, transformed material temperature (T), transformed dissolved oxygen (DO) level, and transformed strain rate (ϵ), respectively, defined as:

$$\begin{aligned} S^* &= 2.0 + 98 S & (S \leq 0.015 \text{ wt. \%}) \\ S^* &= 3.47 & (S > 0.015 \text{ wt. \%}) \end{aligned} \quad (\text{Eqn. A-2})$$

$$\begin{aligned} T^* &= 0.395 & (T < 150 \text{ }^\circ\text{C}) \\ T^* &= (T - 75)/190 & (150 \text{ }^\circ\text{C} \leq T \leq 325 \text{ }^\circ\text{C}) \end{aligned} \quad (\text{Eqn. A-3})$$

$$\begin{aligned} O^* &= 1.49 & (\text{DO} < 0.04 \text{ ppm}) \\ O^* &= \ln (\text{DO}/0.009) & (0.04 \text{ ppm} \leq \text{DO} \leq 0.5 \text{ ppm}) \\ O^* &= 4.02 & (\text{DO} > 0.5 \text{ ppm}) \end{aligned} \quad (\text{Eqn. A-4})$$

$$\begin{aligned} \epsilon^* &= 0 & (\dot{\epsilon} > 2.2\%/s) \\ \epsilon^* &= \ln (\dot{\epsilon}/2.2) & (0.0004\%/s \leq \dot{\epsilon} \leq 2.2\%/s) \\ \epsilon^* &= \ln (0.0004/2.2) & (\dot{\epsilon} < 0.0004\%/s) \end{aligned} \quad (\text{Eqn. A-5})$$

A threshold value of 0.07% for strain amplitude (one-half the strain range for the cycle, ϵ_a) is defined, below which environmental effects on the fatigue lives of these steels do not occur. Thus, $F_{\text{en-CS-LAS}}$ is equal to 1.0 when ϵ_a is less than or equal to 0.07%.

Section C.1.1 of RG 1.207, Revision 1 [5] states that the CUF for carbon and low alloy steel components should be computed using the design fatigue curves provided in Figures A.1 and A.2 and Table A.1 in Appendix A to NUREG/CR-6909, Revision 1, or, alternatively, using the fatigue design curve for carbon and low-alloy steel in Appendix I to Section III of the 2013 Edition of the ASME Code.

Stainless Steels

The nominal environmental fatigue adjustment factor for wrought and cast austenitic stainless steels (SSs), $F_{\text{en-SS}}$, is expressed as:

$$F_{\text{en-SS}} = \exp (-T^* O^* \dot{\epsilon}^*) \quad (\text{Eqn. A-6})$$

where T^* , O^* , and $\dot{\epsilon}^*$ are transformed material temperature (T), transformed dissolved oxygen (DO) level, and transformed strain rate ($\dot{\epsilon}$), respectively, defined as:

$$\begin{aligned} T^* &= 0 & (T \leq 100 \text{ }^\circ\text{C}) \\ T^* &= (T - 100)/250 & (100 \text{ }^\circ\text{C} \leq T \leq 325 \text{ }^\circ\text{C}) \end{aligned} \quad (\text{Eqn. A-7})$$

$$\begin{aligned} \dot{\epsilon}^* &= 0 & (\dot{\epsilon} > 10\%/s) \\ \dot{\epsilon}^* &= \ln (\dot{\epsilon}/10) & (0.0004\%/s \leq \dot{\epsilon} \leq 10\%/s) \\ \dot{\epsilon}^* &= \ln (0.0004/10) & (\dot{\epsilon} < 0.0004\%/s) \end{aligned} \quad (\text{Eqn. A-8})$$

For all wrought and cast SSs and heat treatments, SS weld metals, and sensitized high-carbon wrought and cast SSs:

$$O^* = 0.29 \quad (\text{for any DO level})$$

For all wrought SSs except sensitized high-carbon SSs:

$$O^* = 0.14 \quad (\text{DO} \geq 0.1 \text{ ppm}) \quad (\text{Eqn. A-9})$$

A threshold value of 0.10% for ϵ_a is defined, below which environmental effects on the fatigue lives of these steels do not occur. Thus, $F_{\text{en-SS}}$ is equal to 1.0 when ϵ_a is less than or equal to 0.10%.

Section C.2.1 of RG 1.207, Revision 1 [5] states that the CUF for SS components should be computed using the design fatigue curves provided in Figure A.3 and Table A.2 in Appendix A to NUREG/CR-6909, Revision 1.

Nickel Alloys

The nominal environmental fatigue adjustment factor for Ni-Cr-Fe steels, $F_{\text{en-Ni}}$, is expressed as:

$$F_{\text{en-Ni}} = \exp (-T^* O^* \dot{\epsilon}^*) \quad (\text{Eqn. A-10})$$

where T^* , O^* , and $\dot{\epsilon}^*$ are transformed material temperature (T), transformed dissolved oxygen (DO) level, and transformed strain rate ($\dot{\epsilon}$), respectively, defined as:

$$\begin{aligned} T^* &= 0 & (T \leq 50 \text{ }^\circ\text{C}) \\ T^* &= (T - 50)/275 & (50 \text{ }^\circ\text{C} \leq T \leq 325 \text{ }^\circ\text{C}) \end{aligned} \quad (\text{Eqn. A-11})$$

$$\begin{aligned} \dot{\epsilon}^* &= 0 & (\dot{\epsilon} > 5.0\%/s) \\ \dot{\epsilon}^* &= \ln (\dot{\epsilon}/5.0) & (0.0004\%/s \leq \dot{\epsilon} \leq 5.0\%/s) \\ \dot{\epsilon}^* &= \ln (0.0004/5.0) & (\dot{\epsilon} < 0.0004\%/s) \end{aligned} \quad (\text{Eqn. A-12})$$

$$\begin{aligned} O^* &= 0.06 & (\text{DO} \geq 0.1 \text{ ppm}) \\ O^* &= 0.14 & (\text{DO} < 0.1 \text{ ppm}) \end{aligned} \quad (\text{Eqn. A-13})$$

A threshold value of 0.10% for ϵ_a is defined, below which environmental effects on the fatigue lives of these steels do not occur. Thus, $F_{\text{en-Ni}}$ is equal to 1.0 when ϵ_a is less than or equal to 0.10%.

Section C.3.1 of RG 1.207, Revision 1 [5] states that the CUF for Ni-Cr-Fe alloy components should be computed using the design fatigue curves provided in Figure A.3 and Table A.2 in Appendix A to NUREG/CR-6909, Revision 1, or, alternatively, the fatigue design curve for Ni-Cr-Fe alloys in Section III of the 2013 Edition of the ASME Code may be used.

CUF_{en}

The environmentally adjusted cumulative usage factor for 80 years is computed as:

$$\text{CUF}_{\text{en-80}} = F_{\text{en}} \text{CUF}_{80} \quad (\text{Eqn. A-14})$$

where:

$\text{CUF}_{\text{en-80}}$ = environmentally adjusted cumulative usage factor for 80 years of operation

- F_{en} = environmental adjustment factor for the specific component material using Equation A-1 for carbon and low alloy steels, Equation A-6 for SSs, or Equation A-10 for Ni-Cr-Fe alloys.
- CUF_{80} = cumulative usage factor for 80 years of operation

PTN-Specific CUF_{en-80} Calculations

The following is considered with respect to the PTN-specific CUF_{en-80} calculations:

- In the absence of detailed fatigue tables for each PTN component locations, the following inputs were used for all calculations:
 - **Dissolved Oxygen, DO.** A DO value that bounds normal operating conditions and represents the controlled value of 5 parts per billion (ppb), or 0.005 parts per million (ppm), from the PTN Water Chemistry Program (FPL Procedure No. 0-ADM-651) [28, excerpted] is considered in the calculations to yield bounding F_{en} values. The threshold DO level of 0.040 ppm is used in the carbon and low alloy steel F_{en} calculations, the threshold DO level of 0.1 ppm is used in the Ni-Cr-Fe alloy F_{en} calculations, and the DO level does not affect the SS F_{en} calculations for pressurized water reactors (PWRs). Therefore, the PTN controlled value for the DO level is well removed from any levels that would affect the F_{en} calculations. In addition, PTN's FPL's procedure requires that a Condition Report be initiated to take remedial actions if this level is exceeded.
 - **Temperature, T.** A maximum temperature value of 617 °F (325 °C) was used to yield bounding F_{en} values, which represents the maximum RCS temperature that all components may be exposed to for plant operations.
 - **Sulfur Content, S.** In the absence of Certified Material Test Reports (CMTRs) for all carbon and low alloy steel components, the F_{en} upper bound S threshold of 0.015 wt. % for Equation A-2 is used to yield bounding F_{en} values.
 - **Strain Rate, $\dot{\epsilon}$.** In the absence of detailed transient load pair information, the bounding $\dot{\epsilon}$ of 0.004 %/sec is used in Equations A-5, A-8, and A-12 to yield bounding F_{en} values.

- F_{en} calculations are performed for each of the materials present in each component, and the maximum F_{en} for all materials in each component is used to compute bounding, component-specific CUF_{en-80} values. The F_{en} value is computed from the CUF_{en} and CUF values where they are available. In cases where the materials are not known, F_{en} values for all three F_{en} material groupings (carbon and low alloy steels, stainless steels, and nickel alloys) are determined and the maximum multiplier is used. The maximum F_{en} values used are:
 - Stainless Steel – 14.06
 - Ni-Cr-Fe – 3.75
 - Carbon / Low Alloy Steel – 6.28
- The PTN CUF values still reflect the use of the fatigue curves from the applicable Section III Code of record for each location because detailed fatigue tables for each PTN component locations are not available. Therefore, the guidance of Section C.1.1 of RG 1.207, Revision 1 [5] (for carbon and low alloy steel), Section C.2.1 (for SS), and Section C.3.1 (for Ni-Cr-Fe alloys) could not be fully implemented in the calculations.

Enclosure 4
Non-proprietary Reference Documents
and
Redacted Versions of Proprietary
Reference Documents
(Public Version)
Attachment 6

SIA Environmentally Assisted Fatigue Calculations

Pressurizer Lower Head

1700804.316P – REDACTED, Revision 0, 3-D Finite Element Model of Pressurizer Bottom Head, Skirt Assembly and Heater Wells, September 28, 2017

1700804.317, Revision 0, Pressurizer Lower Head Green's Functions and Unit Pressure, October 5, 2017

1700804.318, Revision 0, Pressurizer Lower Head Loads, Fatigue and EAF Analysis, November 7, 2017

Pressurizer Spray Nozzle

1700804.313P – REDACTED, Revision 1, Pressurizer Spray Nozzle Loads, December 7, 2017

1700804.314P – REDACTED, Revision 1, Pressurizer Spray Nozzle Finite Element Model and Stress Analyses, December 7, 2017

1700804.315P – REDACTED, Revision 1, Pressurizer Spray Nozzle Fatigue Analysis, December 7, 2017

(120 Total Pages, including cover sheets)



CALCULATION PACKAGE

File No.: 1700804.316P-REDACTED

Project No.: 1700804

Quality Program Type: ☒ Nuclear ☐ Commercial

PROJECT NAME:

Turkey Point TLAA's for SLR -Component EAF Analyses

CONTRACT NO.:

PO Number 2000243484

CLIENT:

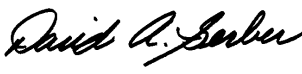



Florida Power & Light Company

PLANT:

Turkey Point Units 3 & 4

CALCULATION TITLE:

3-D Finite Element Model of Pressurizer Bottom Head, Skirt Assembly and Heater Wells

Document Revision	Affected Pages	Revision Description	Project Manager Approval Signature & Date	Preparer(s) & Checker(s) Signatures & Date
0	1 - 15 A-1 - A-2	Initial Issue.	 David A. Gerber DAG 09/28/2017	 Tyler D. Novotny TDN 09/27/2017  Chris S. Lohse CSL 09/28/2017  Jim Wu JW 09/28/2017
THIS DOCUMENT CONTAINS STRUCTURAL INTEGRITY; CLIENT; DESIGN OR SUPPLIER PROPRIETARY INFORMATION. THIS DOCUMENT MAY NOT BE DISCLOSED, WHOLLY OR IN PART, TO ANY THIRD PARTIES WITHOUT THE PRIOR WRITTEN CONSENT OF STRUCTURAL INTEGRITY ASSOCIATES, INC.				

PROPRIETARY INFORMATION NOTICE

THIS DOCUMENT CONTAINS PROPRIETARY INFORMATION THAT IS THE INTELLECTUAL PROPERTY OF STRUCTURAL INTEGRITY ASSOCIATES, INC. IN ACCORDANCE WITH THE TERMS OF THE CLIENT CONTRACT. THE CLIENT MAY USE THE INFORMATION CONTAINED IN THIS DOCUMENT SOLELY FOR THEIR PURPOSES. IF THE DOCUMENT IS SUBMITTED TO THE NUCLEAR REGULATORY COMMISSION (NRC), STRUCTURAL INTEGRITY ASSOCIATES, INC. WILL PROVIDE PROPRIETARY AND NON-PROPRIETARY VERSIONS OF THE DOCUMENT FOR NRC USE ALONG WITH THE REQUIRED LETTER STATING THE PERMITTED USE BY THE NRC. THIS DOCUMENT MAY NOT BE DISCLOSED, WHOLLY OR IN PART, TO ANY THIRD PARTIES WITHOUT THE PRIOR WRITTEN CONSENT OF STRUCTURAL INTEGRITY ASSOCIATES, INC.

Note: Proprietary References are identified with a "P" in the SI File Number.

This entire document is considered Proprietary or Proprietary information used in the document is "Bracketed" ({ }).

Table of Contents

1.0	OBJECTIVE	4
2.0	TECHNICAL APPROACH	4
3.0	ASSUMPTIONS / DESIGN INPUTS	4
4.0	FINITE ELEMENT MODEL	5
5.0	MATERIALS	5
6.0	RESULTS	5
7.0	REFERENCES	6
	APPENDIX A COMPUTER FILES	A-1

List of Tables

Table 1:	Component Materials	7
Table 2:	Mn-1/2Mo Steel Material Properties	8
Table 3:	Carbon Steel, C < 0.30%, Material Properties	8
Table 4:	Type 304 and Type 308 Stainless Steel Material Properties	9
Table 5:	Type 316 Stainless Steel Material Properties	9

List of Figures

Figure 1.	Pressurizer Bottom Head and Support Skirt Dimensions	10
Figure 2.	Header Well and Bottom Head Dimensions	11
Figure 3.	ANSYS Finite Element Model	12
Figure 4.	ANSYS Finite Element Model (normal to symmetry plane)	13
Figure 5.	ANSYS Finite Element Model (Top View)	14
Figure 6.	ANSYS Finite Element Model Heater Well Details	15

1.0 OBJECTIVE

The objective of this calculation is to develop a 3-D finite element model (FEM) of the pressurizer bottom head, skirt assembly and heater wells using the ANSYS software package [1]. The 3-D FEM model will be used in later thermal/mechanical stress analyses and subsequent ASME Code, Section III evaluations.

2.0 TECHNICAL APPROACH

A 3-D FEM will be developed using the ANSYS software package [1]. The model will include a portion of the pressurizer side shell, the bottom head of the pressurizer, the surge nozzle, the interior surface cladding on the surge nozzle and pressurizer, the heater wells and the associated attachment welds and the support skirt assembly. The structural material properties used in the 3-D FEM are based on the ASME Code, 2010 Edition [2]. The 2010 Edition is used as is an approved Section III Edition of the ASME Code in the latest version of 10CFR50.55a. This version also includes the latest fatigue curve for stainless steel which must be used for calculating environmental assisted fatigue.

This calculation pertains to geometry only. No stress evaluations are performed herein; therefore, items such as loads and boundary conditions are addressed in a separate calculation package. The model integrity is verified by applying an internal pressure. Note that this check is only for ensuring nodal connectivity and is not an official pressure evaluation. Note that a mesh sensitivity evaluation is not performed. The later evaluations will address the corner regions and factors to be applied to account for the modeling of the bottom head and heater penetrations.

3.0 ASSUMPTIONS / DESIGN INPUTS

The dimensions for the pressurizer side shell, bottom head and support skirt are provided in References [3] through [5]. The dimensions modeled are shown in Figure 1 and Figure 2.

- The heaters that pass through the heater wells are considered non-structural items and are not modeled. The attachment weld between the heater and the heater well is excluded.
- The counter bore at the outside surface of the heater well bore hole was not modeled and its exclusion is judged to have negligible impact in the stresses at the pressurizer bottom head. The small gap created by the counter bore is modeled as two independent cylinders so that each cylinder moves independent of one another. This modeling simplification has a negligible impact on the results.
- The internal heater support plate and support plate brackets were not modeled. The heater support plates & brackets are not the subject of the NB-3200 analysis and are remote from the region of interest; therefore not modeling them is judged as acceptable.
- The surge nozzle retaining basket was not modeled. The surge nozzle retaining brackets are located on the exterior of the nozzle and are remove from the region of interest; therefore not modeling them is judged as acceptable.
- The weld material at the bottom head-to-side shell weld is not modeled. The material changes instantaneously from the low alloy steel shell barrel to the carbon steel lower head material. Since

the material transition is remote from the area of interest; the instantaneous material transition is acceptable. .

- The heater well head was not specifically modeled as it lies external to the pressurizer shell and is remote from the area of interest. The full specified thermal well length of 11.5 inches was modeled but only as a constant thickness pipe, the exact length was kept constant for all penetrations.

4.0 FINITE ELEMENT MODEL

The entire model is developed using the 8-node brick element, SOLID45 (the thermal equivalent for thermal analyses is SOLID70). A 180° section of the pressurizer is modeled. The resulting finite element model is shown in Figure 3 through Figure 6. Detailed views of the heater well are provided in Figure 6.

The increased clad thickness in the bottom head, where the heater wells attach to the pressurizer, is modeled as 0.375 inches. A total of 39 heater wells are modeled in three concentric rings. The modeling of the penetrations includes the heater well and the associated attachment J-groove and cover fillet welds.

The modeled heater well bore hole outside diameter is 1.135 inches. The heater well head was not specifically modeled as it lies external to the pressurizer shell. The full specified thermal well length of 11.5 inches was modeled but only as a constant thickness pipe, the exact length was kept constant for all penetrations.

A detailed view of the heater well in the finite element model is shown in Figure 6.

5.0 MATERIALS

Table 1 provides a summary of the material properties. The structural material properties used in the 3-D FEM are based on the ASME Code, 2010 Edition [2], and are defined as a range of temperature-dependent properties as shown in Table 2 through Table 5.

6.0 RESULTS

A representative 3-D finite element model of the Turkey Point pressurizer bottom head region has been developed for future thermal and stress analyses. The model includes a portion of the pressurizer side shell, the bottom head of the pressurizer, the surge nozzle, the interior surface cladding on the surge nozzle and pressurizer, the heater sleeves and associated attachment J-groove/cover fillet welds and the support skirt assembly.

The relevant input files are included in the project computer files listed in Appendix A. No analyses are performed in this calculation.

7.0 REFERENCES

1. ANSYS Mechanical APDL, Release 14.5 (w/Service Pack 1 UP20120918), ANSYS, Inc., September 2012.
2. American Society of Mechanical Engineers, Boiler and Pressure Vessel Code, Section II, Part D, 2010 Edition.
3. Florida Power & Light Drawing 5610-M-410-6, Revision 9, “Turkey Point Units 3 & 4, Pressurizer Outline,”, SI File No. FPL-09Q-201.
4. Florida Power & Light Drawing 5610-M-410-108, Revision 3, “Turkey Point Units 3 & 4, Pressurizer General Assembly,”, SI File No. FPL-09Q-201.
5. SI Calculation 1100756.303P, Revision 2, “Finite Element Stress Analysis for Pressurizer Surge Nozzles,” CONTAINS VENDOR PROPRIETARY INFORMATION.

Table 1: Component Materials

Component	Material	Reference
Shell Barrel	SA-302 Gr. B Mn-1/2Mo Steel	[3]
Lower Head	{ }	[3]
Surge Nozzle	{ }	[3]
Surge Nozzle-to-Safe End Weld	{ }	[5]
Surge Nozzle Safe End	{ }	[3]
Surge Nozzle Safe End-to-Reducer Weld	Type 316 SS (16Cr-12Ni-2Mo)	[5]
Reducer (14" x 12")	{ }	[5]
Reducer-to-Piping Weld	Type 316 SS (16Cr-12Ni-2Mo)	[5]
Surge Line Piping	SA-376 Type 316 SS (16Cr-12Ni-2Mo)	[5]
Cladding	{ }	[5]
Thermal Sleeve	SA-240 Type 304 SS (18Cr-12Ni)	[5]
Support Skirt and Flange	SA-516 Gr 70 Carbon Steel $\leq 0.30\% C$	[3]
Heater Well	Type 316 SS (16Cr-12Ni-2Mo)	Assumed
Heater Well J-Groove/Fillet Welds	Type ER308 SS (20Cr-10Ni)	Assumed

Table 2: Mn-1/2Mo Steel Material Properties

	Temperature						
	70	200	300	400	500	600	700
Modulus of Elasticity ⁽¹⁾ , E, psi	2.90E+07	2.85E+07	2.80E+07	2.76E+07	2.70E+07	2.63E+07	2.53E+07
Mean Coefficient of Thermal Expansion ⁽²⁾ , α , in/in/°F	7.0E-06	7.3E-06	7.4E-06	7.6E-06	7.7E-06	7.8E-06	7.9E-06
Thermal Conductivity ⁽³⁾ , K, Btu/s-ft-°F	23.7	23.5	23.4	23.1	22.7	22.2	21.6
Specific Heat ⁽⁴⁾ , C _p , Btu/lb-°F	0.107	0.115	0.121	0.126	0.131	0.137	0.142
Density, ρ , lb/in ³	0.28						
Poisson's Ratio ν	0.30						

Notes

- Reference [2] Table TM-1, Material Group A, Mn-1/2Mo.
- Reference [2] Table TE-1, Material Group 2, Mn-1/2Mo.
- Reference [2] Table TCD, Material Group C, Mn-1/2Mo.
- Specific heat is calculated as described in Note 1 of Table TCD of the ASME Code [2].
- Poisson's Ratio (ν) = 0.3, and density, ρ , are assumed to be temperature independent.

Table 3: Carbon Steel, C < 0.30%, Material Properties

	Temperature						
	70	200	300	400	500	600	700
Modulus of Elasticity ⁽¹⁾ , E, psi	2.94E+07	2.88E+07	2.83E+07	2.79E+07	2.73E+07	2.65E+07	2.55E+07
Mean Coefficient of Thermal Expansion ⁽²⁾ , α , in/in/°F	6.4E-06	6.7E-06	6.9E-06	7.1E-06	7.3E-06	7.4E-06	7.6E-06
Thermal Conductivity ⁽³⁾ , K, Btu/s-ft-°F	34.9	33.7	32.3	30.9	29.4	28.0	26.6
Specific Heat ⁽⁴⁾ , C _p , Btu/lb-°F	0.103	0.114	0.119	0.124	0.128	0.134	0.140
Density, ρ , lb/in ³	0.28						
Poisson's Ratio ν	0.30						

Notes

- Reference [2] Table TM-1, Carbon Steels C ≤ 0.30%.
- Reference [2] Table TE-1, Material Group 1, "Carbon Steel."
- Reference [2] Table TCD, Material Group A, "Carbon Steel."
- Specific Heat, C_p, is calculated as described in Note 1 of Table TCD of the ASME Code [2].
- Poisson's Ratio (ν) = 0.3, and density, ρ , are assumed to be temperature independent.

Table 4: Type 304 and Type 308 Stainless Steel Material Properties

	Temperature						
	70	200	300	400	500	600	700
Modulus of Elasticity ⁽¹⁾ , E, psi	2.83E+07	2.75E+07	2.70E+07	2.64E+07	2.59E+07	2.53E+07	2.48E+07
Mean Coefficient of Thermal Expansion ⁽²⁾ , α , in/in/°F	8.5E-06	8.9E-06	9.2E-06	9.5E-06	9.7E-06	9.9E-06	10.0E-06
Thermal Conductivity ⁽³⁾ , K, Btu/s-ft-°F	8.6	9.3	9.8	10.4	10.9	11.3	11.8
Specific Heat ⁽⁴⁾ , C _p , Btu/lb-°F	0.114	0.119	0.122	0.126	0.129	0.130	0.132
Density, ρ , lb/in ³	0.29						
Poisson's Ratio ν	0.31						

Notes

- Reference [2] Table TM-1, Material Group G, for Type 304 18Cr-8Ni (Type 308 20Cr-10Ni is not specifically listed in the notes to Table TE-1 but is assumed to be part of Group 3).
- Reference [2] Table TE-1, Material Group 3, for Type 304 18Cr-8Ni (Type 308 20Cr-10Ni is not specifically listed in the notes to Table TE-1 but is assumed to be part of Group 3).
- Reference [2] Table TCD, Material Group J, for Type 304 18Cr-8Ni (Type 308 20Cr-10Ni is not specifically listed in the notes to Table TE-1 but is assumed to be part of Group 3).
- Specific Heat, C_p, is calculated as described in Note 1 of Table TCD of the ASME Code [2].
- Poisson's Ratio (ν) = 0.3, and density, ρ , are assumed to be temperature independent.

Table 5: Type 316 Stainless Steel Material Properties

	Temperature						
	70	200	300	400	500	600	700
Modulus of Elasticity ⁽¹⁾ , E, psi	2.83E+07	2.75E+07	2.70E+07	2.64E+07	2.59E+07	2.53E+07	2.48E+07
Mean Coefficient of Thermal Expansion ⁽²⁾ , α , in/in/°F	8.5E-06	8.9E-06	9.2E-06	9.5E-06	9.7E-06	9.9E-06	10.0E-06
Thermal Conductivity ⁽³⁾ , K, Btu/s-ft-°F	8.2	8.8	9.3	9.8	10.2	10.7	11.2
Specific Heat ⁽⁴⁾ , C _p , Btu/lb-°F	0.118	0.121	0.124	0.126	0.127	0.129	0.131
Density, ρ , lb/in ³	0.29						
Poisson's Ratio ν	0.31						

Notes

- Reference [2] Table TM-1, Material Group G, for 16Cr-12Ni-2Mo.
- Reference [2] Table TE-1, Material Group 3, for 16Cr-12Ni-2Mo.
- Reference [2] Table TCD, Material Group K, for 16Cr-12Ni-2Mo.
- Specific Heat, C_p, is calculated as described in Note 1 of Table TCD of the ASME Code [2].
- Poisson's Ratio and density, ρ , are assumed to be temperature independent.

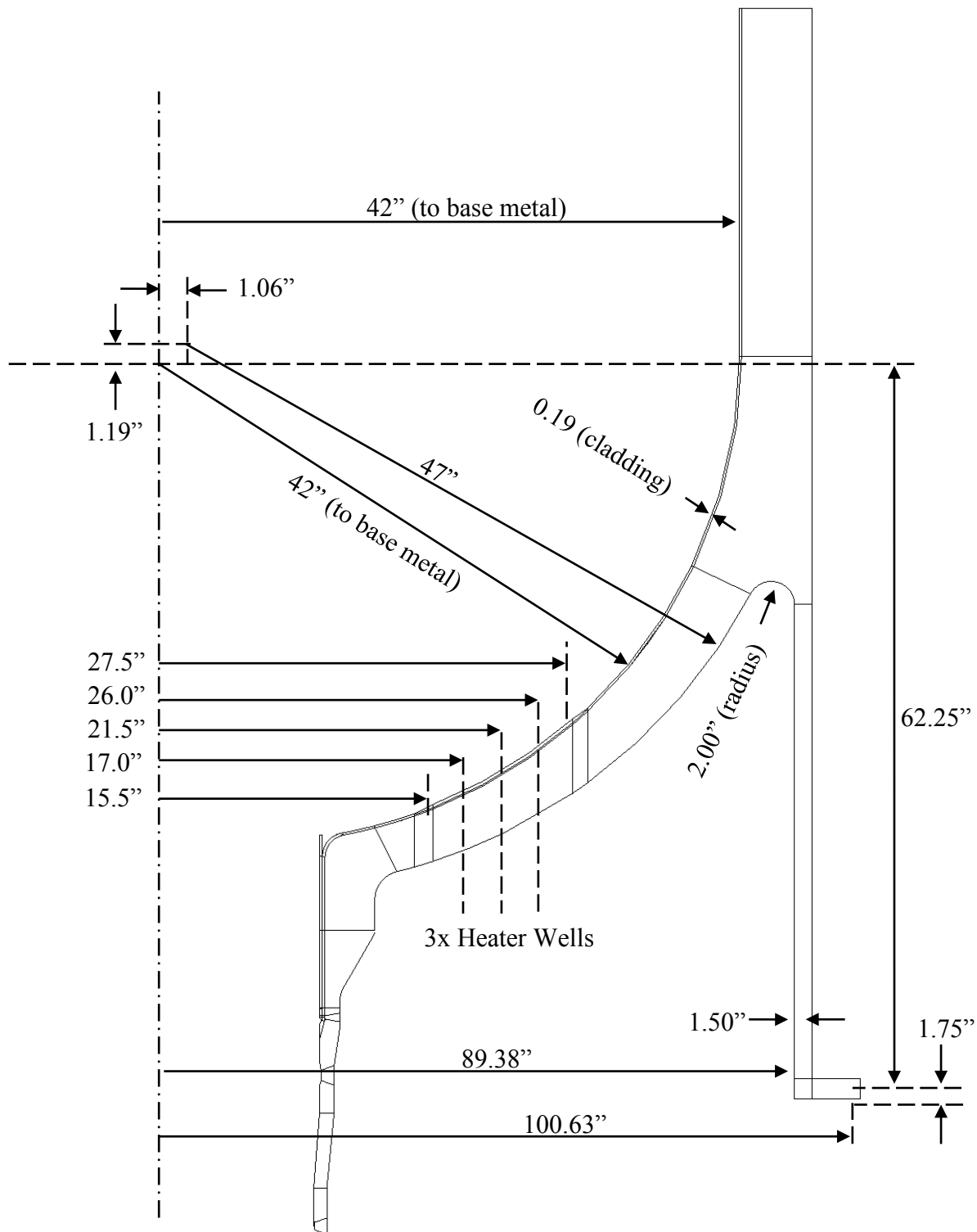


Figure 1. Pressurizer Bottom Head and Support Skirt Dimensions

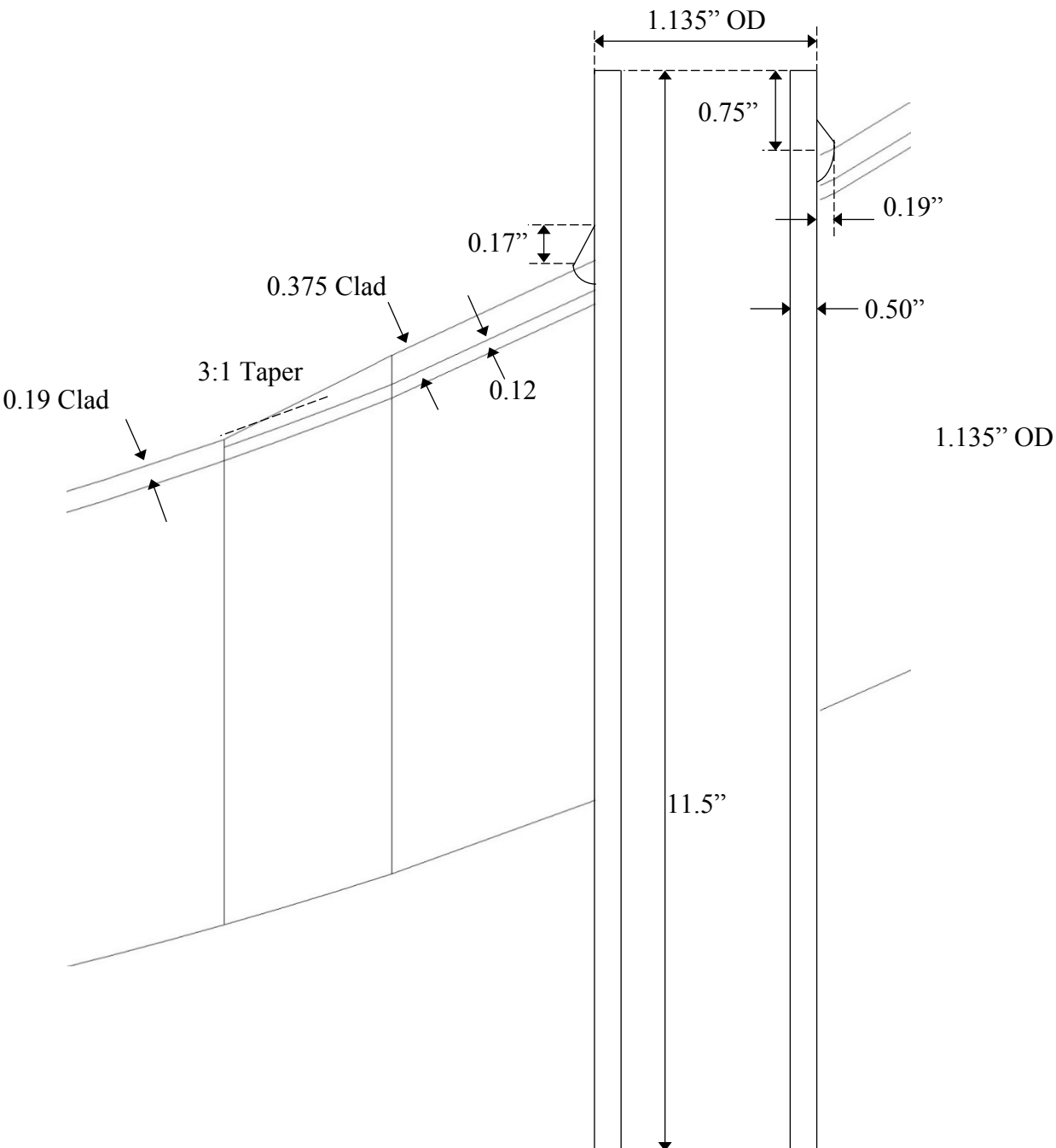


Figure 2. Header Well and Bottom Head Dimensions

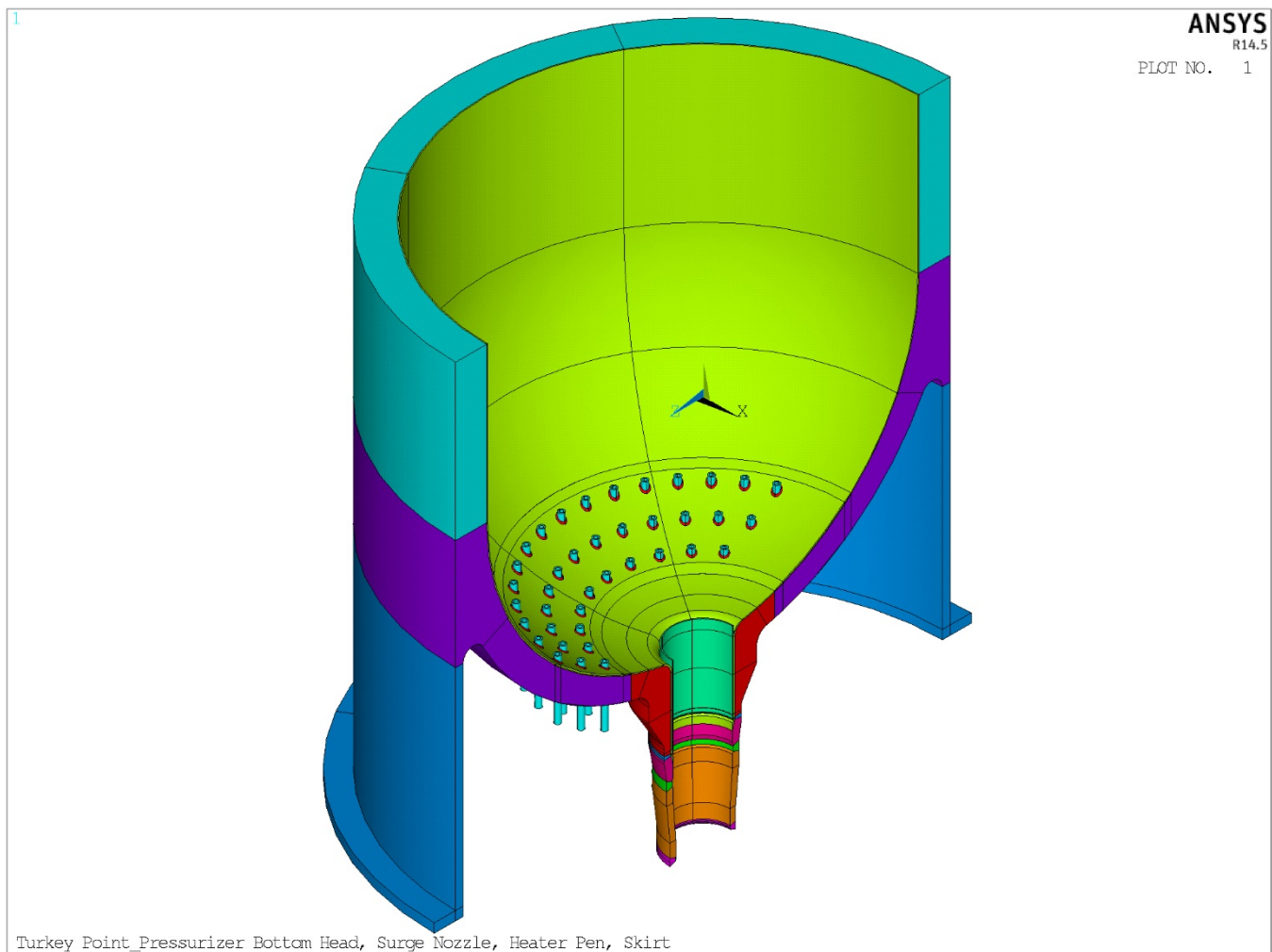


Figure 3. ANSYS Finite Element Model

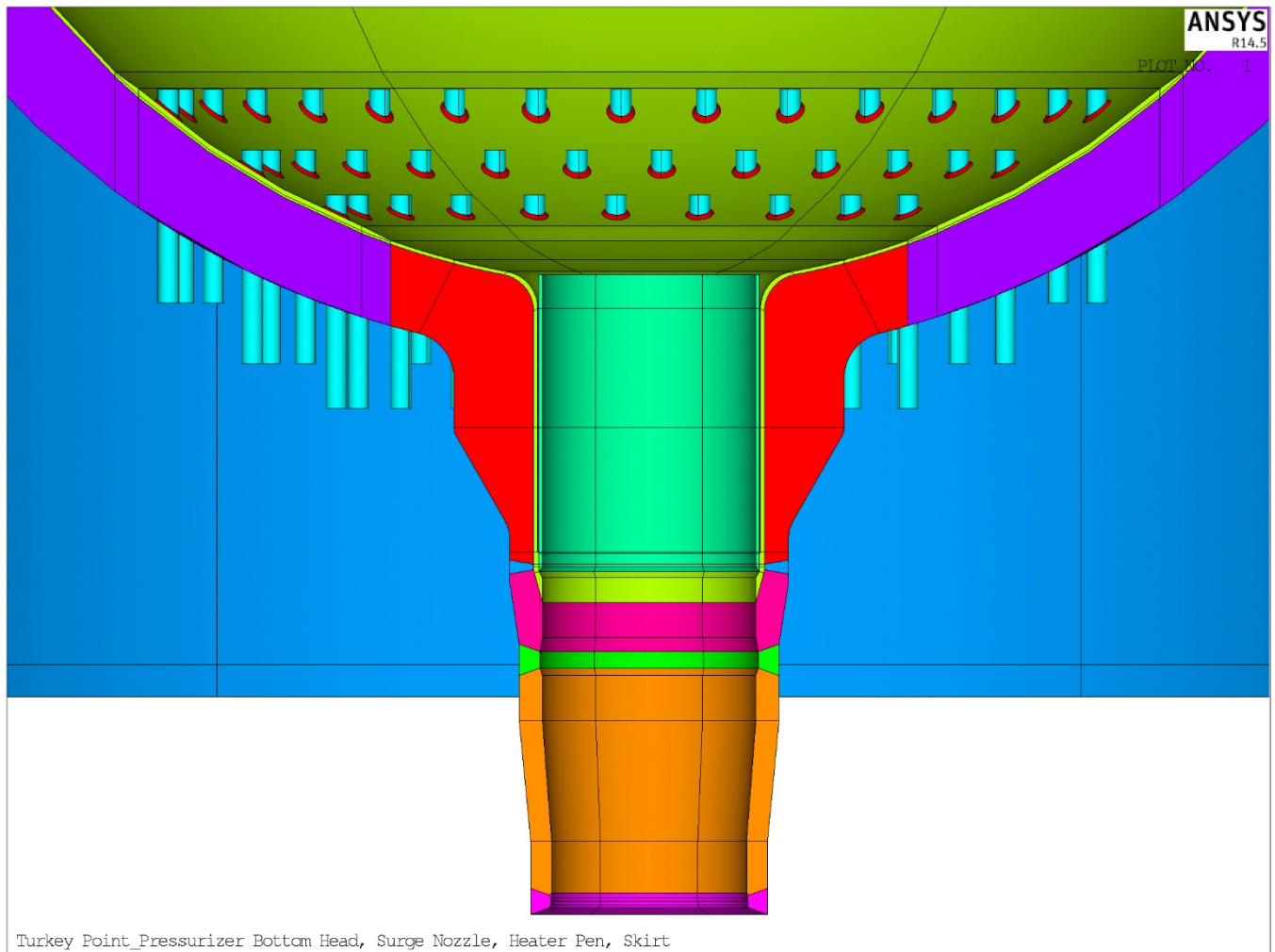


Figure 4. ANSYS Finite Element Model (normal to symmetry plane)

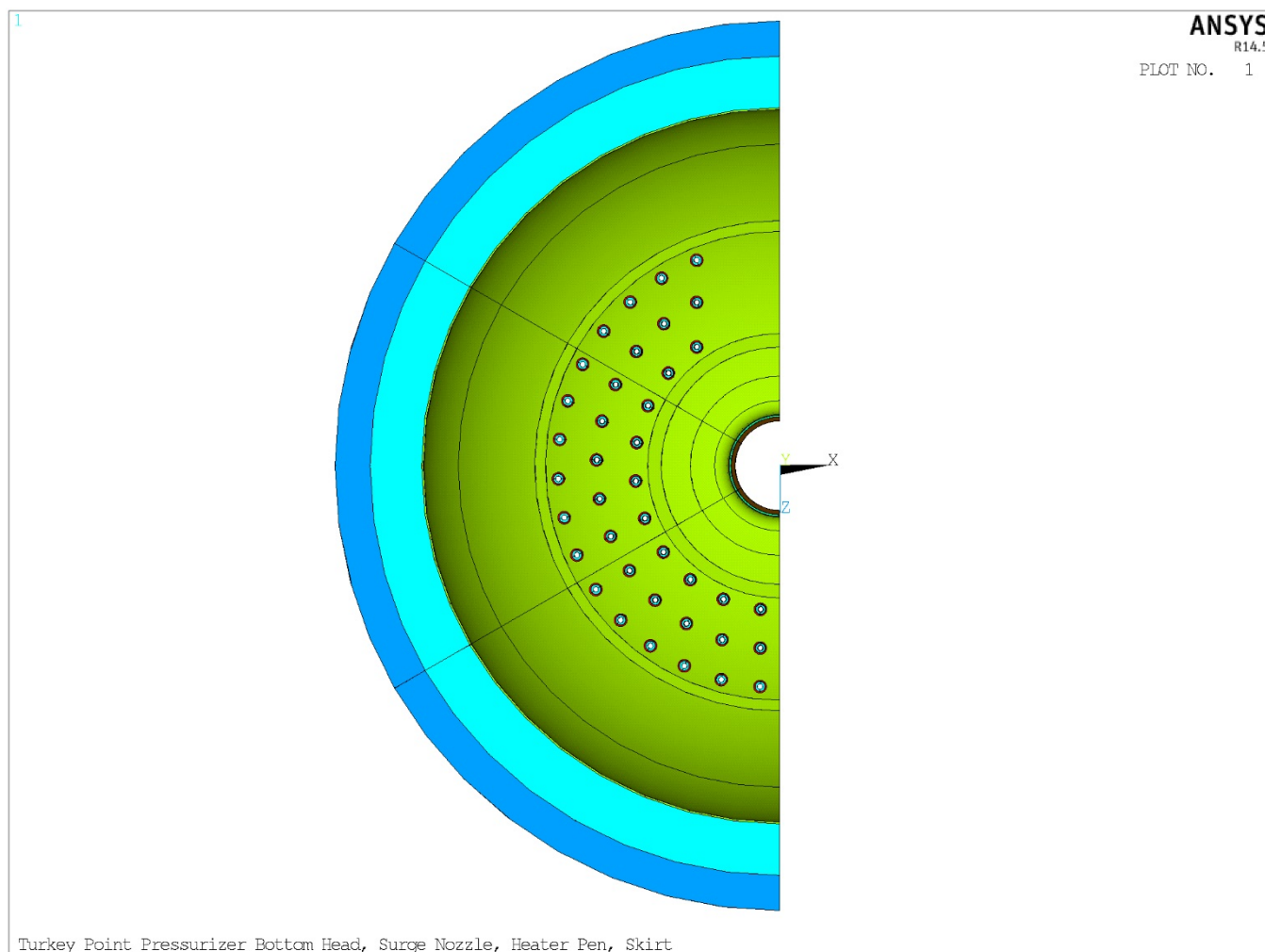


Figure 5. ANSYS Finite Element Model (Top View)

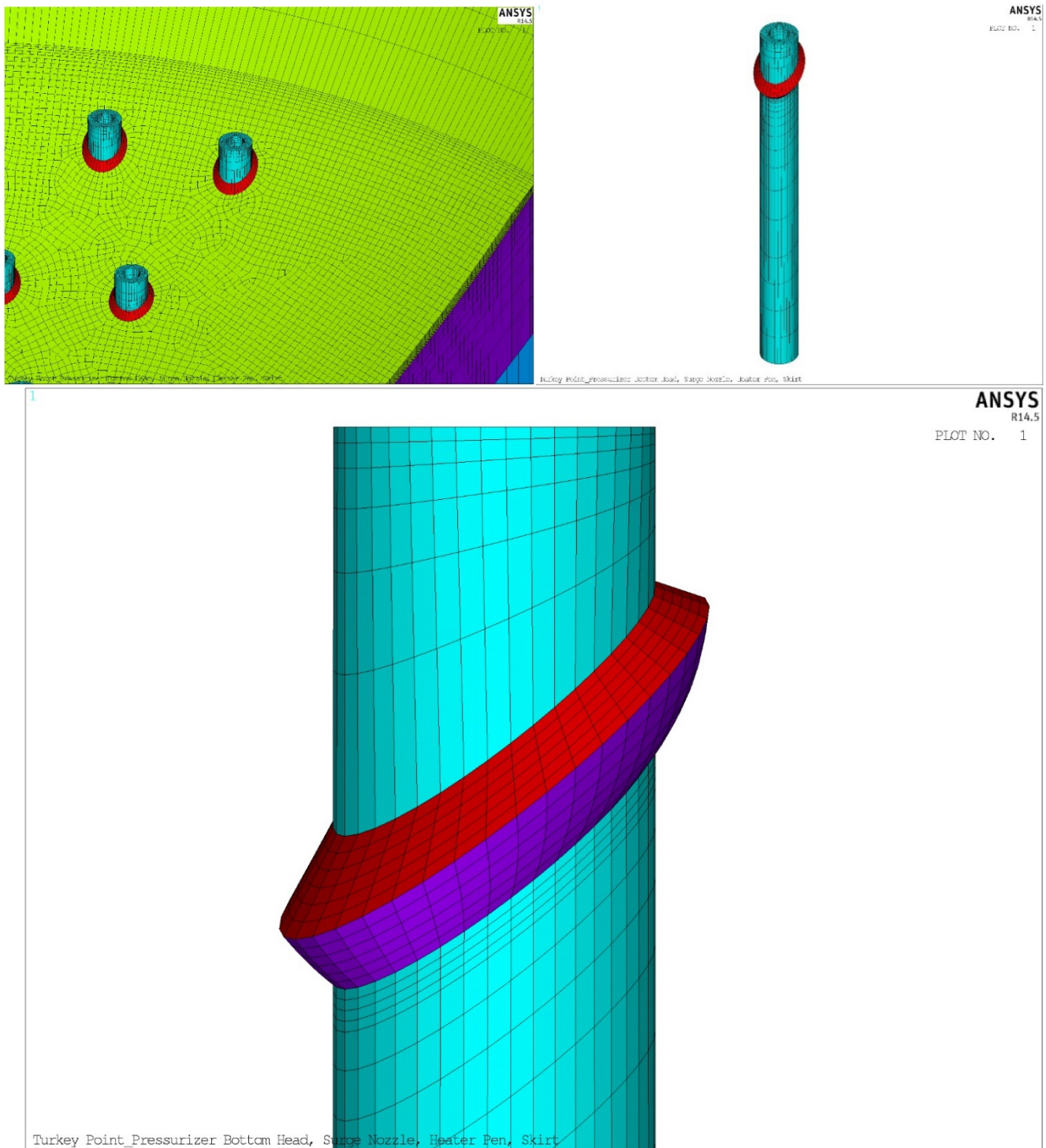


Figure 6. ANSYS Finite Element Model Heater Well Details

Appendix A

COMPUTER FILES

Computer Files

Filename	Description
BottomHead.inp	ANSYS geometry input file for stress analysis



CALCULATION PACKAGE

File No.: 1700804.317

Project No.: 1700804

Quality Program Type: ☒ Nuclear ☐ Commercial

PROJECT NAME:

Turkey Point TLAA's for SLR -- Component EAF Analyses

CONTRACT NO.:

2000243484, Rev. 1

CLIENT:

Florida Power & Light (FPL)

PLANT:

Turkey Point 3 and 4

CALCULATION TITLE:

Pressurizer Lower Head Green's Functions and Unit Pressure

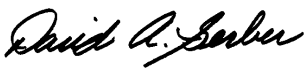
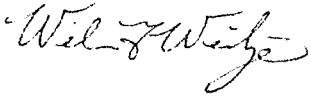

Document Revision	Affected Pages	Revision Description	Project Manager Approval Signature & Date	Preparer(s) & Checker(s) Signatures & Date
0	1 - 10 A-1 - A-1	Initial Issue	 D.A. Gerber, P.E. 10/5/2017	 W.F. Weitze, P.E. 10/2/2017  M. Fong 10/5/2017

Table of Contents

1.0	OBJECTIVE	3
2.0	METHODOLOGY	3
3.0	ASSUMPTIONS / DESIGN INPUTS	3
4.0	CALCULATIONS	8
5.0	RESULTS OF ANALYSIS	8
6.0	CONCLUSIONS AND DISCUSSION	9
7.0	REFERENCES	10
	Appendix A COMPUTER FILES	A-1

List of Tables

Table 1: Material Properties at 350°F	4
---	---

List of Figures

Figure 1: Thermal Zones	5
Figure 2: Common Structural Boundary Conditions, Green's Function and Pressure Runs ...	7
Figure 3: Pressure Boundary Conditions, Unit Pressure Run	8
Figure 4: Bounding Path for EAF	9

1.0 OBJECTIVE

The objective of this calculation package is to calculate the Green's function and unit pressure stresses for the bounding location on the pressurizer lower head at Turkey Point (PTN). These results will be used as input to an environmentally assisted fatigue (EAF) analysis of this location.

2.0 METHODOLOGY

A previous calculation package [1] documented the development of the three-dimensional (3D) finite element model (FEM) of the pressurizer lower head, including the surge nozzle and heater penetrations, using the ANSYS software package [2]. This model is modified to use constant material properties, as is required for Green's function analyses (see additional explanation in Section 3.0). Four thermal zones are defined based on a previous two-dimensional (2D) analysis of the PTN lower head [3]. For each thermal zone, a step temperature change is analyzed in ANSYS, resulting in calculated temperature as a function of location and time.

Then, for each thermal analysis, stress components are calculated as functions of location and time using linear elastic FEM methodology. In addition, a unit pressure stress analysis is performed, yielding stress components as functions of location only. The bounding location for EAF is determined based on a previous 3D analysis of a similar Westinghouse lower head [4]. Stress components for the thermal and pressure stress analyses are linearized at this location, and for the four thermal stress analyses, Green's functions are generated.

3.0 ASSUMPTIONS / DESIGN INPUTS

The following assumptions are introduced in this calculation package:

- All outside surfaces are assumed to be perfectly insulated, which means that a heat transfer coefficient of zero is applied. As a result, the outside surface temperature has no effect on the results.
- For the Green's function methodology, stress components are assumed to be linearly and directly proportional to the magnitude of the temperature change in a given time step. See additional explanation below.

Although material properties are in reality temperature-dependent, the Green's function (influence function) approach computes stress components as linearly proportional to the magnitude of the temperature change in a given time step. Therefore, these Green's functions are developed using constant material properties, judged to be appropriately representative for all conditions. Based on previous experience, the temperature dependence of the materials has a relatively negligible impact.

Table 1 shows the material properties used in the analysis [5, Section II, Part D].

Table 1: Material Properties at 350°F

Components	Description	Mat No.	EX, 10 ⁶ psi	ALPX, in/in/°F	KX, Btu/hr-ft-°F	TD, ft ² /hr	C, Btu/lbm-°F	DENS, lbm/in ³
Pressurizer shell barrel	Mn-1/2Mo steel	1	27.8	7.9	23.3	0.390	0.123	0.28
Lower head, surge nozzle, skirt	Carbon steel, C < 0.30%	2, 3, 15	28.1	7.5	31.6	0.537	0.122	0.28
Nozzle-SE weld, clad, sleeve, heater welds	308*, 304 stainless	4, 9, 11, 13, 14	26.7	10.1	10.1	0.162	0.124	0.29
Safe end (SE), reducer, welds, tubes	316 stainless	5 to 8, 12	26.7	10.1	9.5	0.152	0.125	0.29

General notes: EX = modulus of elasticity, ALPX = coefficient of thermal expansion (instantaneous value is conservatively used), KX = thermal conductivity, TD = thermal diffusivity, C = specific heat (calculated as KX/TD/DENS with appropriate unit conversion), DENS = density. Values used for Poisson's ratio (not shown in table) and density are the same as in the FEM calculation package [1].

* Type 304 properties are applied to type 308 as was done for FEM development [1, Table 4].

The inside surface is separated into four thermal zones based on a previous 2D analysis of the PTN lower head as shown in Figure 1 [3, Figure 10]. Boundaries between thermal zones are slightly different in the current analysis due to modeling differences.

Heat transfer coefficients (h) are also taken from the 2D analysis, and are as follows [3, Table 3]:

- Zone 1: 340 Btu/hr-ft²-°F (bounding value chosen)
- Zones 2, 3, and 4: 200 Btu/hr-ft²-°F

The FEM includes the thermal sleeve, but does not include water gap elements behind the thermal sleeve [1]. Therefore, to account for the insulating effect of the thermal sleeve, an overall heat transfer coefficient is calculated and applied to the surge nozzle surface behind the thermal sleeve. Using $h = 340 \text{ Btu/hr-ft}^2\text{-°F}$, thermal sleeve thickness (t) = 0.19" [3, Figure 3] = 0.015833', $KX = 10.1 \text{ Btu/hr-ft-°F}$, water gap width (δ) = 0.0625" [3, Appendix D] = 0.005208', and water gap equivalent conductivity (k_w) = 0.5 Btu/hr-ft²-°F [3, Appendix D], the overall heat transfer coefficient U becomes:

$$U = 1/(1/h + t/KX + \delta/k_w) = 67 \text{ Btu/hr-ft}^2\text{-°F}$$

For each of the four thermal zones, a thermal analysis is performed in which temperature in that zone is step-changed from 0 to 1000°F, and temperature in the other three zones is kept at 0°F. The step change is applied over a very short time interval of 0.099 second, based on starting and ending times of 0.001 and 0.1 second, respectively. The time-varying analysis is continued to 10000 seconds so that temperature changes over time are calculated. Then, a steady state analysis is performed to determine the final temperature state.

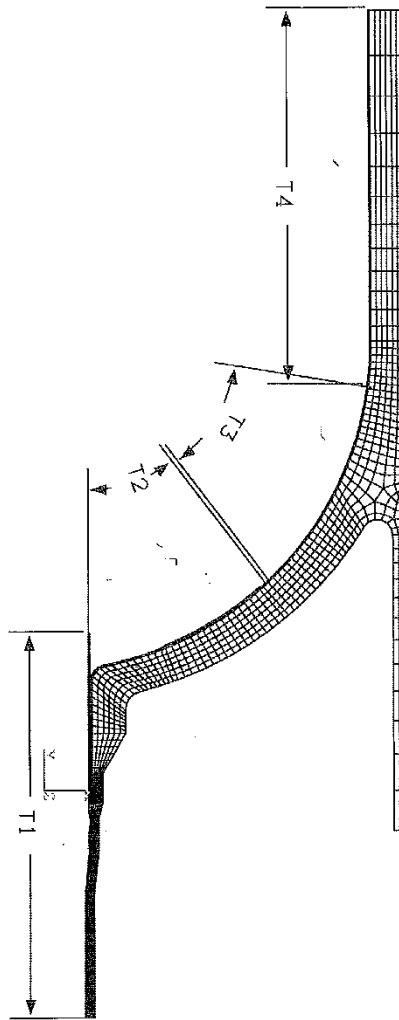


Figure 1: Thermal Zones

Note: element grid is from previous analysis and does not reflect current model.

The following boundary conditions are applied for the structural runs, that is the four Green's function stress passes and the unit pressure run:

- Symmetry boundary conditions are applied at the symmetry plane.
- Nodes at the top of the pressurizer and the bottom of the surge nozzle are coupled in the axial (vertical) direction.
- The bottom of the skirt is anchored.

In addition, for the pressure run only:

- Unit pressure of 1000 psi is applied to all inside surfaces.

- End cap loads are applied to the top of the pressurizer, the bottom of the surge nozzle, and the bottom of each heater penetration.

End cap loads are calculated as follows:

$$P_{\text{end-cap}} = -P r_{\text{inside}}^2 / (r_{\text{outside}}^2 - r_{\text{inside}}^2), \text{ where}$$

$P_{\text{end-cap}}$ = end cap load, psi

P = pressure = 1000 psi

r_{inside} = inside radius, in

r_{outside} = outside radius, in

Values of r_{inside} and r_{outside} are different for the pressurizer barrel, surge nozzle safe end, and heater penetrations, and are taken from the FEM calculation package [1, Figures 1 and 2 and supporting file *BottomHead.inp*].

Figure 2 shows the structural boundary conditions that are common to the Green's function runs and the unit pressure run. Figure 3 shows the applied pressures, including cap loads, for the unit pressure run.

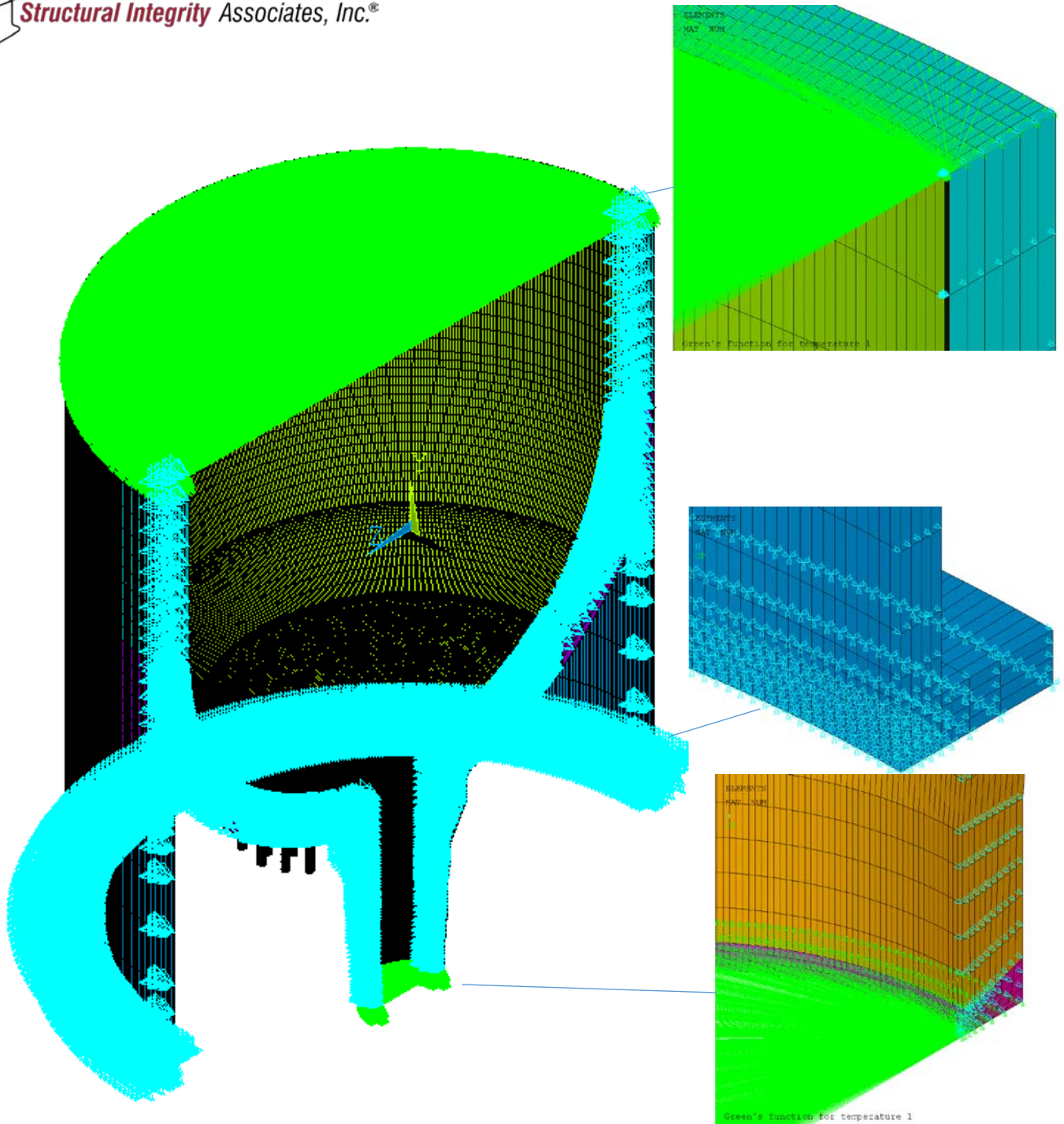


Figure 2: Common Structural Boundary Conditions, Green's Function and Pressure Runs

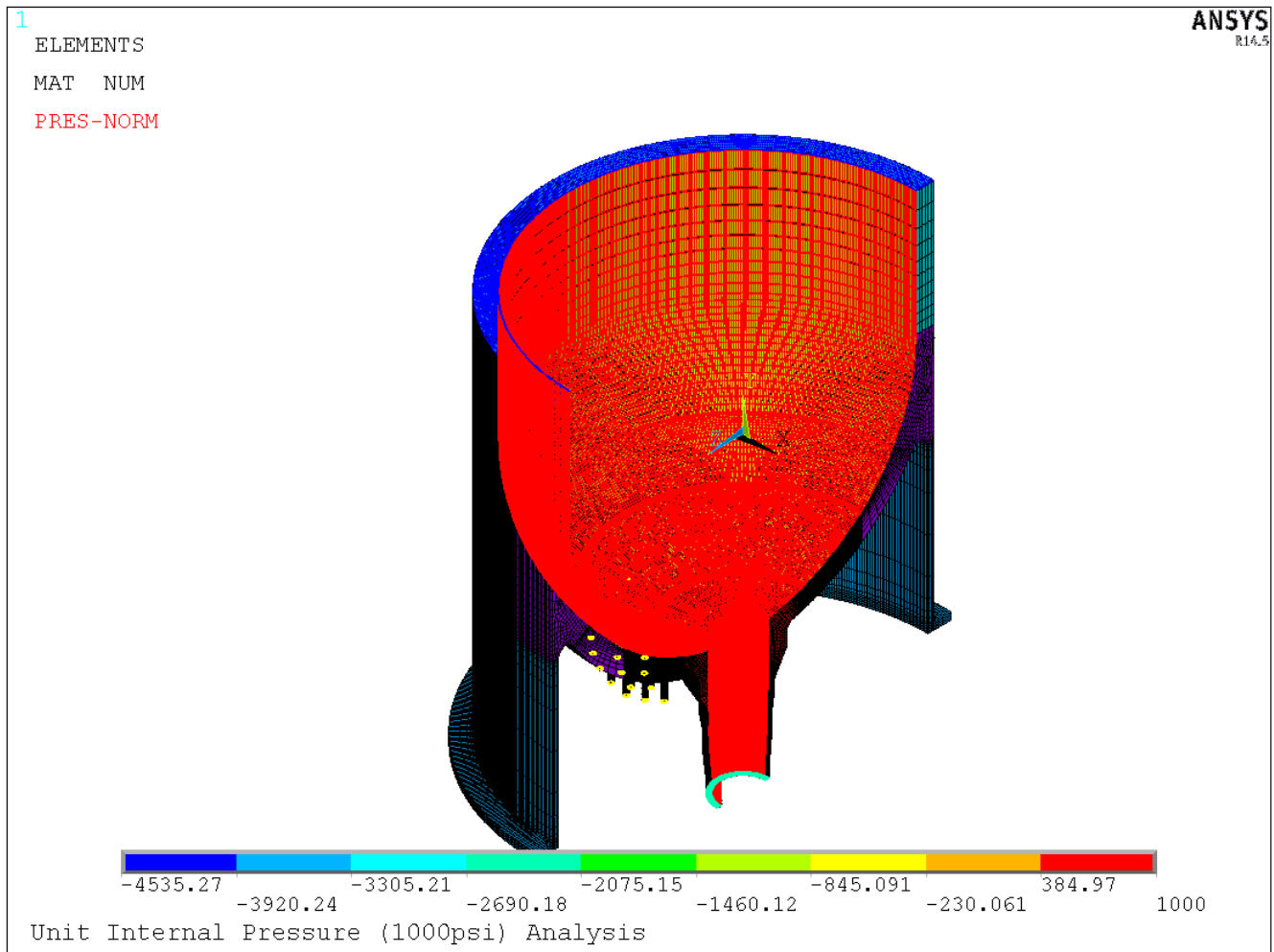


Figure 3: Pressure Boundary Conditions, Unit Pressure Run

4.0 CALCULATIONS

All temperature and stress component calculations are performed using ANSYS. Appendix A contains a list of the input and output files used in the analyses.

5.0 RESULTS OF ANALYSIS

The bounding location for EAF is at the toe of the cover fillet weld on the downhill side of the outer heater well, based on a previous 3D analysis of a similar Westinghouse lower head [4, Table 3 and Figure 7]. In the current analysis, this corresponds to a path from node 35521 (inside) to node 35698 (outside, wetted surface), as shown in Figure 4.

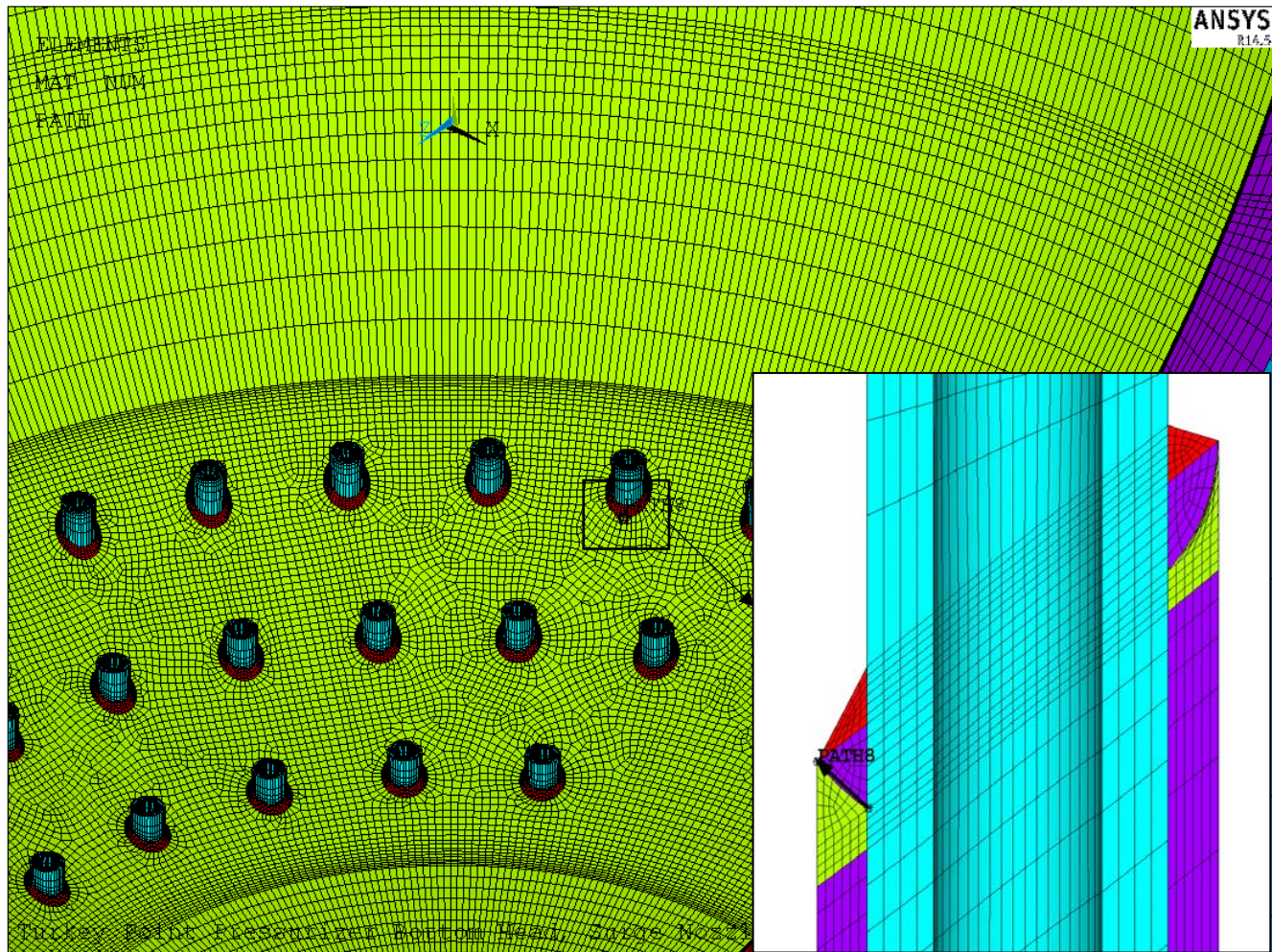


Figure 4: Bounding Path for EAF

The Green's function files are produced with a Structural Integrity Associates macro *GenGreen.mac*. This is an ANSYS post-processing macro that produces a text file ready to be used in the subsequent environmentally assisted fatigue calculations using **SI:FatiguePro 4 (FP4)** methodology. All relevant input and output files are included in the project supporting files, and filenames are listed in Appendix A.

6.0 CONCLUSIONS AND DISCUSSION

Green's functions for each of the four thermal zones are written to files with extension GRN, and unit pressure stress results are written to file *InternalPress.lin*, as shown in Appendix A. These files may be used as input to an EAF analysis of the bounding location for the PTN pressurizer lower head.

7.0 REFERENCES

1. SI Calculation Package No. 1700804.316P, Revision 0, *3-D Finite Element Model of Pressurizer Bottom Head, Skirt Assembly and Heater Wells*, CONTAINS VENDOR PROPRIETARY INFORMATION.
2. ANSYS Mechanical APDL, Release 14.5 (w/ Service Pack 1 UP20120918), September 2012, ANSYS, Inc.
3. SI Calculation Package No. FPL-09Q-302, Revision 0, *Pressurizer Surge Nozzle and Lower Head Finite Element Thermal Analysis*.
4. Paper No. PVP2013-98060, *Environmentally-Assisted Fatigue Management of PWR Pressurizer using Nonlinear Strain-Based Analysis*, Proceedings of the ASME 2013 Pressure Vessels and Piping Conference, PVP2013, July 14-18, 2013, Paris, France.
5. ASME Boiler and Pressure Vessel Code, 2010 Edition.

Appendix A

COMPUTER FILES

<i>1700804.317.xlsx</i>	Excel workbook to calculate thermal resistance and specific heat
<i>BottomHead.inp</i>	Original FEM input [1]
<i>BottomHeadGF.inp</i>	FEM input modified for Green's function and unit pressure analyses
<i>Batch.inp</i>	Overall input file used to launch other runs
<i>PZR_BottomHead_T*.inp</i>	Input file for Green's function thermal pass, where * = 1, 2, 3, or 4 and is the thermal zone
<i>CMNTR.MAC</i>	Macro to generate <i>PZR_BottomHead_T*_mntr.inp</i> files
<i>BottomHead_HTBC.INP</i>	Input file that applies heat transfer boundary conditions
<i>PZR_BottomHead_S*.inp</i>	Input file for Green's function stress pass, where * = 1, 2, 3, or 4 and is the thermal zone
<i>PZR_BottomHead_T*_mntr.inp</i>	Input file to apply thermal results to Green's function stress pass (automatically generated during thermal pass), where * = 1, 2, 3, or 4 and is the thermal zone
<i>GenGreen.mac</i>	Macro to generate Green's functions
<i>GETPATH.TXT</i>	File used by <i>GenGreen.mac</i> to define paths
<i>GRN-STR.INP</i>	Input file that calls <i>GenGreen.mac</i> for each of the four Green's function analyses
<i>InternalPress.inp</i>	Input file for unit pressure analysis
<i>linear.inp</i>	Input file that performs linearization for all stress pass runs
<i>InternalPress.lin</i>	Linearization output for unit pressure analysis
<i>PZR_BottomHead_S*.lin</i>	Linearization output for Green's function stress pass, where * = 1, 2, 3, or 4 and is the thermal zone
<i>PZR_BottomHead_S*_PATH8.GRN</i>	Green's function output for Green's function stress pass, where * = 1, 2, 3, or 4 and is the thermal zone



CALCULATION PACKAGE

File No.: 1700804.318

Project No.: 1700804

Quality Program Type: ☒ Nuclear ☐ Commercial

PROJECT NAME:

Turkey Point TLAA's for SLR – Component EAF Analyses

CONTRACT NO.:

2000243484, Rev. 1

CLIENT:

Florida Power & Light (FPL)

PLANT:

Turkey Point 3 and 4

CALCULATION TITLE:

Pressurizer Lower Head Loads, Fatigue and EAF Analysis



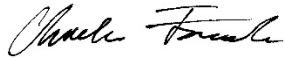
Document Revision	Affected Pages	Revision Description	Project Manager Approval Signature & Date	Preparer(s) & Checker(s) Signatures & Date
0	1 - 22 A-1 - A-3	Initial issue	 D.A. Gerber 11/7/2017	 T.D. Gilman 11/2/2017  C.J. Fourcade 11/7/2017

Table of Contents

1.0	OBJECTIVE AND INTRODUCTION	4
2.0	METHODOLOGY	4
2.1	Overall Methodology	4
2.2	FP4 “LGeneric” SBF Location	4
2.3	Location Analyzed	6
2.4	Loading	6
2.4.1	<i>Types of Loads</i>	7
2.4.2	<i>Loading for Heatups and Cooldowns</i>	7
2.4.3	<i>Loading for Other Transients</i>	8
2.5	Fatigue Analysis Methodology	8
2.6	Environmental Effects on Fatigue	8
3.0	ASSUMPTIONS AND DESIGN INPUTS	9
3.1	Assumptions	9
3.1.1	<i>Methodological Assumptions</i>	9
3.1.2	<i>Input Assumptions</i>	9
3.2	Inputs	10
3.3	Transient Inputs	10
3.3.1	<i>Heatups and Cooldown</i>	10
3.3.2	<i>Upset Transients</i>	10
3.4	Numbers of Cycles	10
3.5	FP4 Analysis Inputs	11
3.5.1	<i>Fatigue Strength Reduction Factor</i>	11
3.5.2	<i>Green’s Functions and Unit Stresses</i>	11
3.5.3	<i>Material Properties</i>	12
4.0	CALCULATIONS	13
4.1	Heatup and Cooldown Transients	13
4.2	Upset Transients	14
4.2.1	<i>Reactor Trip</i>	14
4.2.2	<i>Reactor Trip with Cooldown and SI</i>	16

4.2.3	<i>Large Step Load Decrease</i>	18
4.2.4	<i>Observations from Upset Transient Results</i>	20
5.0	RESULTS OF ANALYSIS	21
6.0	CONCLUSIONS	21
7.0	REFERENCES	22
	Appendix A COMPUTER FILES	A-1

List of Tables

Table 1:	Key Values for LGeneric SBF Location	5
Table 2:	Projected Cycles for Unit 3 Heatup and Cooldown for an 80-Year Plant Life	11
Table 3:	Projected Cycles for Unit 4 Heatup and Cooldown for an 80-Year Plant Life	11
Table 4:	Material Properties as Input to FP4	12
Table 5:	NUREG/CR-6909 Rev. 1 Fatigue Curve for Stainless-Steel	13
Table 6:	EAF Calculations for Heatups and Cooldowns	14
Table 7:	Overall Fatigue Usage Factor Results	21

List of Figures

Figure 1:	Bounding Path for EAF	6
Figure 2:	Thermal Zones	7
Figure 3:	Reactor Trip Simulation	15
Figure 4:	Stress Results for Reactor Trip	16
Figure 5:	Reactor Trip with CD and SI Simulation	17
Figure 6:	Stress Results for Reactor Trip with CD and SI	18
Figure 7:	Large Step Load Decrease Simulation	19
Figure 8:	Stress Results for Large Step Load Decrease	20

1.0 OBJECTIVE AND INTRODUCTION

The objective of this calculation package is to define the loading and compute the stresses and associated environmentally-assisted fatigue (EAF) of the pressurizer lower head heater penetrations due to insurge/outsurge stratification loading during plant heatups and cooldowns. The analysis will be used to support the 80-year Subsequent License Renewal (SLR) of Turkey Point (PTN) Units 3 and 4.

2.0 METHODOLOGY

2.1 Overall Methodology

The fatigue analysis will be performed in accordance with the methods in Subarticle NB-3200 of Section III of the ASME Code [1]. The calculations will be performed to address the concerns expressed in both NRC RIS 2008-30 [2] (use of all six stress components in the fatigue calculations) and RIS 2011-14 [3] (repeatability of the process of selecting stress peaks and valleys).

In accordance with Section X.M1 of the generic aging lessons learned report for subsequent license renewal (GALL-SLR) [4], F_{en} methodology and fatigue curves from DRAFT revision 1 of NUREG/CR-6909 [5, Appendix A] are used to account for environmental effects on fatigue.

SI's SI:FatiguePro 4.0 (FP4) stress-based fatigue (SBF) software [6] is used to perform the EAF analysis. FP4 is verified under SI's nuclear QA program and computes fatigue and EAF in accordance with ASME Subarticle NB-3200 methodology. It was specifically designed to address the NRC concerns expressed in NRC RIS 2008-30 [2] and RIS 2011-14 [3]. The technical basis for the SBF module was sponsored by EPRI and documented in the Reference [7] technical report.

Loading is applied, based on actual plant data, and applied using the Green's Function methodology described in the technical basis report [7] and accounts for the effects of insurge/outsurge and thermal stratification in the pressurizer lower head.

2.2 FP4 "LGeneric" SBF Location

The FP4 software contains a built-in location called "LGeneric". LGeneric allows for generic SBF calculations using an arbitrary number of Green's Functions and other unit loads such as pressure and piping interface loads. The location has a unique functionality, as described below.

LGeneric utilizes a generic transfer function with a number of "key values" that are configurable in the location parameters. These key values are shown in Table 1. Although LGeneric can handle an arbitrary number of thermal zones, this particular analysis uses four, and therefore the key values relevant to the four thermal zones are included in Table 1. In addition, piping interface loads due to thermal expansion are also not relevant to this analysis, so they are not shown in the table.

Table 1: Key Values for LGeneric SBF Location

Key	Value	Description
Grn1	L1_Grn1	Green's function for Thermal Zone #1
Grn2	L1_Grn2	Green's function for Thermal Zone #2
Grn3	L1_Grn3	Green's function for Thermal Zone #3
Grn4	L1_Grn4	Green's function for Thermal Zone #4
Tloc1	L1_Tloc1	Local temperature for Thermal Zone #1
Tloc2	L1_Tloc2	Local temperature for Thermal Zone #2
Tloc3	L1_Tloc3	Local temperature for Thermal Zone #3
Tloc4	L1_Tloc4	Local temperature for Thermal Zone #4
P_instr	L1_Press	Pressure instrument name
TE1_instr	L1_TE1_sf	Local temperature #1 instrument name
TE2_instr	L1_TE2_sf	Local temperature #2 instrument name
TE3_instr	L1_TE3_sf	Local temperature #3 instrument name
TE4_instr	L1_TE4_sf	Local temperature #4 instrument name
P_strs	SX,SY,SZ,SXY,SYZ,SXZ	Unit pressure total stress vector (from FEA)
P_strPQ	SX,SY,SZ,SXY,SYZ,SXZ	Unit pressure M+B stress vector (from FEA)
K1		Stress index (FSRF) applied to pressure stress
K3		Stress index (FSRF) applied to transient thermal stress
Tfree		Stress-free temperature for thermal stress calculations

Tloc1 through Tloc4 represent local temperatures for four separate thermal zones in a configurable location. The values for Tloc1 through Tloc4 (i.e., L1_Tloc1 through L1_Tloc4) are names of configured temperature instruments and are integrated with the four configurable Green's functions L1_Grn1 through L1_Grn4, respectively. The Tloc instruments are then simulated to generate transient thermal stresses using the Green's function methodology specified in Reference [7].

The value for P_instr (L1_Press) represents the pressure instrument name. The pressure instrument is a scale factor that is applied to the static unit pressure stresses P_strs (total) and P_strsPQ (M+B). The pressure instrument is simulated in FP4 to create time-varying pressure stresses.

K1 and K3 are stress indices or fatigue strength reduction factors (FSRFs) that are applied to the pressure and transient thermal stresses, respectively. K1 is the FSRF applicable to "static" pressure loads as specified in the Reference [7, Section 2.5.2] specification, and K3 is the FSRF applicable to the transient thermal stresses [7, Section 2.6.8].

Tfree represents the stress-free temperature for the thermal stress calculations. For example, if Tfree is set to 70.0, then when the component is at a uniform temperature of 70.0, the thermal stresses will all be zero. This value corresponds to T_{ref} described in Section 2.6.1 of [7].

2.3 Location Analyzed

The Reference [8] calculation package selected a limiting, wetted location for analysis. SI has performed several analyses of similarly-designed pressurizers, and documented one such analysis in the Reference [10] PVP paper. It was concluded that the limiting location for EAF was the toe of the stainless-steel J-groove cover fillet. The location is shown on Figure 1.

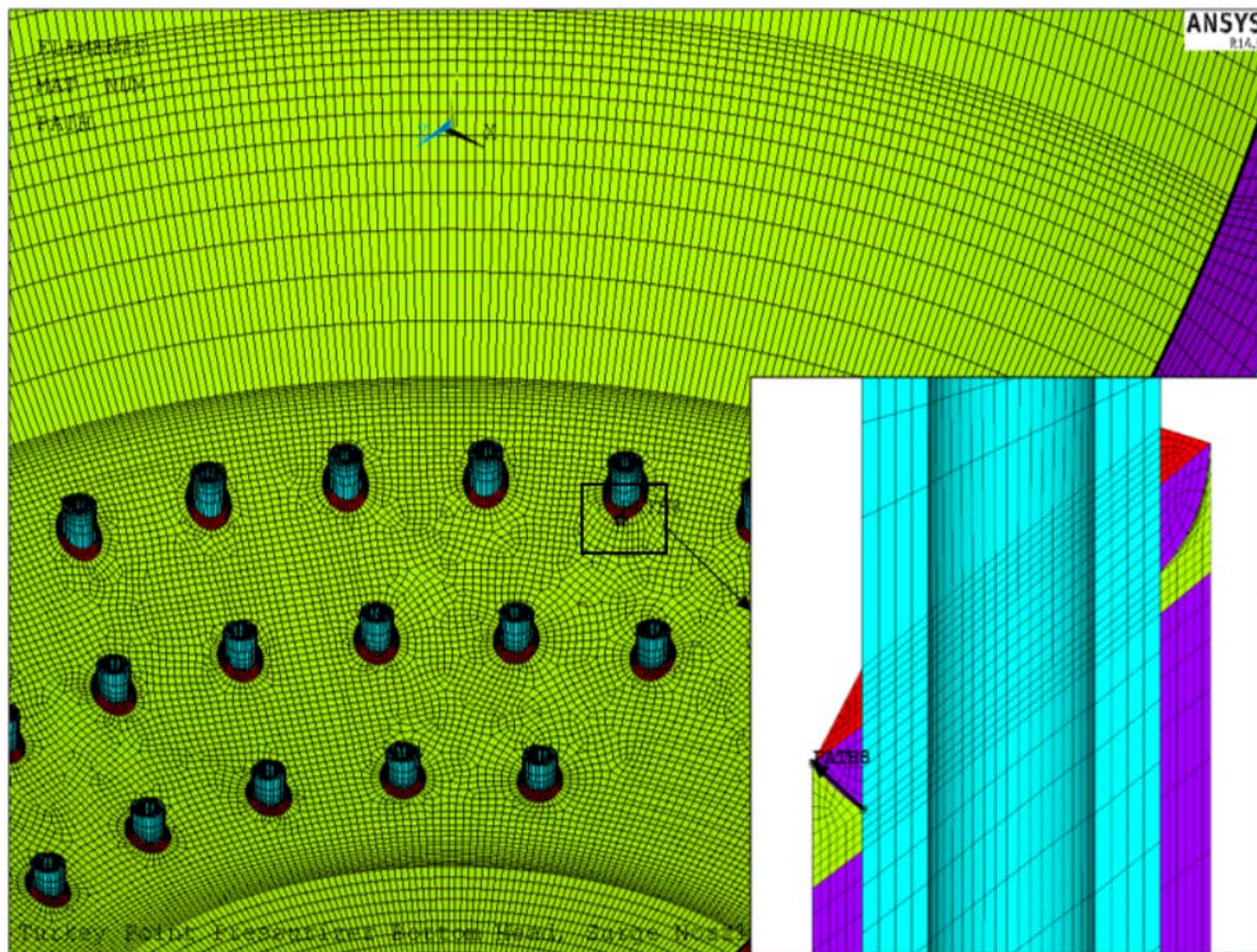


Figure 1: Bounding Path for EAF

2.4 Loading

The loading used in this analysis consists of previously developed loading, based on actual plant data during heatups and cooldowns at PTN-3/4. For other transients, plant data was selected from similarly designed plants, based on SI's extensive experience with fatigue monitoring. The approach is described in more detail below.

2.4.1 *Types of Loads*

Since actual plant data is used to characterize the loading, the Green's Function methodology was used. The Green's Function methodology is ideal for efficiently and accurately analyzing longer and more complex transients, especially for large, complex finite element models, as the one used here. The applied thermal loading consists of four different temperatures, representing the four separate thermal zones defined in the Reference [8] Green's Function calculation package and shown on Figure 2.

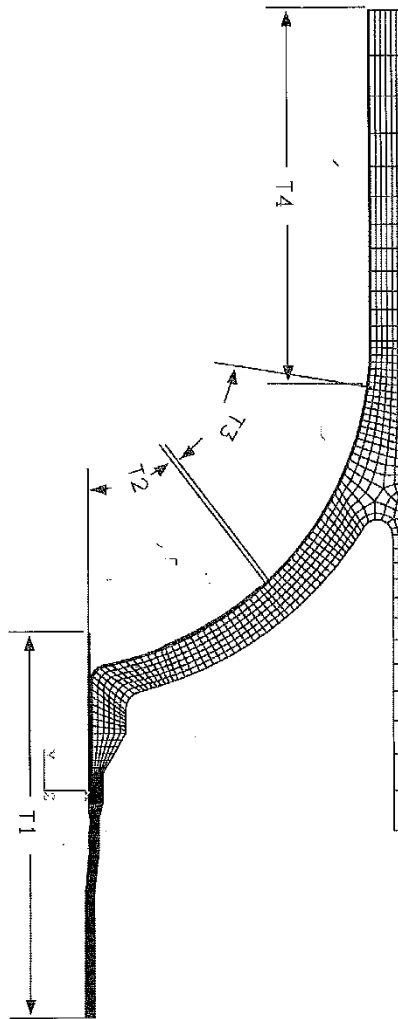


Figure 2: Thermal Zones

Internal pressure loads were also analyzed in Reference [8]. The resulting stresses are scaled to the indicated pressure.

2.4.2 *Loading for Heatups and Cooledowns*

Insurge/outsurge and thermal stratification in the pressurizer can occur during heatup and cooldown operations and are the chief contributors to fatigue at the location of interest in the pressurizer lower

head. These types of loads are caused by changes in reactor coolant inventory combined with a large temperature differential between the pressurizer and reactor coolant system hot leg. Therefore, it is essential that these loading effects are considered in the fatigue analysis and adequately characterized for various operational methods throughout plant history.

In a previous calculation package [9] for PTN's 60-year license renewal, a fatigue analysis was performed for the lower head heater penetrations, also using the Green's Function methodology but with a conservative, simplified 2-dimensional model. The analysis utilized a collection of plant data from PTN-3/4 for heatups and cooldowns during various modes of operation. This included time histories of pressurizer liquid temperature, reactor coolant system hot leg temperature, pressurizer pressure, and surge line flow rate. A thermal hydraulic model that accounts for insurge/outsurge and thermal stratification was used to calculate the resulting local temperature time histories for four thermal zones defined consistently with the analysis herein. The pressurizer pressure time history is used to directly scale the unit pressure stresses to the indicated pressure. These loads are used directly in this refined fatigue analysis, because they adequately represent PTN's operating practices.

2.4.3 Loading for Other Transients

For other (non-heatup and cooldown) events, a sample of actual plant data from similarly designed and operated Westinghouse plants is selected to investigate and quantify the effects on fatigue. Upset transients such as reactor trips, where significant pressure and/or temperature swing could occur, are evaluated to adequately account for any potential contributions from these transients to the overall usage.

2.5 Fatigue Analysis Methodology

The fatigue analysis is performed in accordance with ASME Section III, Subarticle NB-3200 methods. This consists of computing all six stress components for both the Primary Plus Secondary and the Total stress, plus the metal temperature, as described in detail in the Reference [7] report.

2.6 Environmental Effects on Fatigue

In accordance with Section X.M1 of the DRAFT generic aging lessons learned report for subsequent license renewal (GALL-SLR) [4], F_{en} methodology from DRAFT revision 1 of NUREG/CR-6909 [5, Appendix A] is used as appropriate for the material for each location. FP4 includes analysis options for this version of NUREG/CR-6909 and uses the Modified Rate integration method for computing F_{en} factors, as described in detail in Reference [7]. The F_{en} expression for the relevant stainless-steel analysis location is:

$$\text{For wrought and cast austenitic stainless steel (SS):} \quad F_{en} = \exp(-T' \dot{\epsilon}' O) \quad (2)$$

$$\begin{aligned} \text{where: } T' &= 0 && \text{for service temperature, } T < 100^{\circ}\text{C} \\ &= (T - 100)/250 && \text{for } 100^{\circ}\text{C} \leq T < 325^{\circ}\text{C} \\ \dot{\epsilon}' &= 0 && \text{for strain rate, } \dot{\epsilon} > 10\%/ \text{sec} \\ &= \ln(\dot{\epsilon}/10) && \text{for } 0.0004 \leq \dot{\epsilon} \leq 10\%/ \text{sec} \end{aligned}$$

$$\begin{aligned} &= \ln(0.0004/10) && \text{for } \dot{\epsilon} < 0.0004\%/ \text{sec} \\ O' &= 0.29 && \text{for dissolved oxygen (DO)} < 0.1 \text{ ppm} \\ &= 0.29 && \text{for sensitized high-carbon wrought and cast SS, any DO} \\ &= 0.14 && \text{for DO} \geq 0.1 \text{ ppm, all wrought SS except sensitized high-carbon SS} \end{aligned}$$

3.0 ASSUMPTIONS AND DESIGN INPUTS

3.1 Assumptions

Methodological and input assumptions, along with their respective justifications, are described as follows.

3.1.1 *Methodological Assumptions*

1. The maximum K_e factor is assumed to be 1.0. SI has performed multiple nonlinear elastic-plastic evaluations of similarly-designed pressurizer lower heads, as described in the Reference [10] PVP paper. In each case, results demonstrated that the location with highest strain range shakes down to elastic limits. Therefore, it is appropriate to limit the simplified elastic-plastic penalty factor K_e to 1.0.
2. The Modified Operating Procedure (MOP) heatups and cooldowns are conservatively assumed to be represented by the Modified Steam Bubble (MSB) results. Because a limited amount of Modified Operating Procedure (MOP) data is available, this period of operation is conservatively assumed to be represented by the pre-MOP behavior. The MOP is intended to mitigate stratification cycling and thereby minimize fatigue usage. Since the MSB operation is in reality a more severe operation than MOP with respect to fatigue, it is conservative to assume the MOP operation has a similar level of cycling. This conservative assumption also counts for contingency cycles that may occur in the future, despite the MOP. (Based on the results shown in Section 5.0, there remains adequate margin at 80 years of operation to make this assumption.)

3.1.2 *Input Assumptions*

Data for a sample of upset transients from other similarly-designed Westinghouse plants is assumed to be applicable to Turkey Point. Pressurizer temperature and pressure excursions resulting from events such as Reactor Trip and Large Step Load Decrease are similar for the various Westinghouse designed plants and judged to be adequately realistic to evaluate the fatigue contribution from these events.

3.2 Inputs

3.3 Transient Inputs

3.3.1 *Heatups and Cooldown*

Calculated local temperatures for each thermal zone in the pressurizer are taken from the electronic project files in Reference [9]. These include date/time histories of the local temperature values in comma separated format in files named *T1.csv*, *T2.csv*, *T3.csv*, and *T4.csv*. Time histories of pressurizer pressure values are taken from *Ppzzr.csv*.

As described in Reference [9] plant data was available for Turkey Point Units 3 and 4 for heatups and cooldowns during the following modes of operation.

Operation	Period (Unit 3)	Period (Unit 4)
1. Water Solid	8/72 – 7/86	5/73 – 7/86
2. Modified Steam Bubble	7/86 – 9/94 (both units)	
3. Modified Operating Procedure	9/94 – Present (both units)	

3.3.2 *Upset Transients*

SI reviewed previous FatiguePro baseline analyses from other similar Westinghouse-designed plants and selected relevant data from examples of upset transients from the FatiguePro data. The actual data selected is shown in Section 4.2.

3.4 Numbers of Cycles

80-year projected cycles are taken from Reference [13]. For the various modes of operation Heatup and Cooldown projected cycles are taken from Reference [14] and summarized in Table 2 and Table 3. Projected MOP cycle counts are taken as total 80 year projections (Station Heatup or Station Cooldown) minus the numbers of cycles from the respective Water Solid and Modified Steam Bubble operations.

Table 2: Projected Cycles for Unit 3 Heatup and Cooldown for an 80-Year Plant Life

Pressurizer Operating Mode	Cycle Counts (up to 2/2000)			Projected Cycle Counts 80-Year Plant Life (8/1972 – 8/2052)	
	Operating Period	Heatup Cycles	Cooldown Cycles	Total Heatup Cycles	Total Cooldown Cycles
Water Solid	8/1972 – 7/1986	64	63	64	63
Modified Steam Bubble	7/1986 – 9/1994	24	24	24	24
MOP	9/1994 – 2/2000	4	5	76	77
Total – All Modes	8/1972 – 2/2000	92	92	164	164

Table 3: Projected Cycles for Unit 4 Heatup and Cooldown for an 80-Year Plant Life

Pressurizer Operating Mode	Cycle Counts (up to 4/1999)			Projected Cycle Counts 80-Year Plant Life (5/1973 – 5/2053)	
	Operating Period	Heatup Cycles	Cooldown Cycles	Total Heatup Cycles	Total Cooldown Cycles
Water Solid	5/1973 – 7/1986	67	67	67	67
Modified Steam Bubble	7/1986 – 9/1994	30	29	30	29
MOP	9/1994 – 4/1999	5	5	84	85
Total – All Modes	5/1973 – 4/1999	102	101	181	181

3.5 FP4 Analysis Inputs

3.5.1 *Fatigue Strength Reduction Factor*

At the toe of the partial penetration J-groove weld cover fillet a fatigue strength reduction factor (FSRF) of 1.5 is applied, based on Welding Research Council (WRC) Bulletin 432 [11, Tables 1 and 2]. This is appropriate for shop welds with machined surfaces and relatively thorough inspections. The FSRF of 1.5 is applied for both K parameters (K_1 and K_3) described in Section 2.2.

3.5.2 *Green's Functions and Unit Stresses*

Green's Function files and unit pressure stresses were taken from the Reference [8] calculation package and loaded into the FP4 configuration. Since the pressure analysis used a 1000 psi loading, the input stresses were divided by 1000 to represent the stress due to 1 psi. In addition, the “outside” surface stresses for the selected path represents the wetted location. Therefore, the outside surface is specified in the FP4 location configuration for use.

3.5.3 *Material Properties*

Various material properties are required for the FP4 analysis. These properties and their input sources are as follows.

The elastic modulus versus temperature of the stainless-steel weld material is from ASME Section II Part D [1]. These values are the same as those defined for the stainless steel weld material in the finite element model calculation package [12]. Values are shown in Table 4.

Table 4: Material Properties as Input to FP4

Material	T, °F	E_{analysis}, psi
Stainless-Steel ER308	70	28,300,000
	200	27,500,000
	300	27,000,000
	400	26,400,000
	500	25,900,000
	600	25,300,000
	700	24,800,000

ASME Code parameters m , n , and S_m are used for K_e calculations, but are irrelevant here, because K_e is limited to 1.0.

The stainless-steel fatigue curve from NUREG/CR-6909 Revision 1 [5, Table A.2] is used, along with the respective elastic modulus of the curve ($E_c = 28,300,000$ psi).

Table 5: NUREG/CR-6909 Rev. 1 Fatigue Curve for Stainless-Steel

Number of Cycles	S_a, ksi Austenitic
10	870
20	624
50	399
100	287
200	209
500	141
1000	108
2000	85.6
5000	65.3
10000	53.4
20000	43.5
50000	34.1
100000	28.4
200000	24.4
500000	20.6
1000000	18.3
2.E+06	16.4
5.E+06	14.8
1.E+07	14.4
1.E+08	14.1
1.E+09	13.9
1.E+10	13.7
1.E+11	13.6

4.0 CALCULATIONS

For each transient, FP4 is used to calculate incremental fatigue usage factors. Transient loads are input by assigning the time histories of the four local temperatures and internal pressure using the FP4 simulation mode. Separate FP4 projects are created for each transient analyzed.

4.1 Heatup and Cooldown Transients

Table 6 provides a summary of the calculations. Average, incremental usage factors are calculated for each of the Water Solid (WS), Modified Steam Bubble (MSB), and Modified Operating Procedure (MOP) periods of operation. Computer files associated with each of these runs are listed in Appendix A. As was noted previously, the MOP period of operation is conservatively assumed to be represented by the Modified Steam Bubble Calculation results.

Table 6: EAF Calculations for Heatups and Cooldowns

Unit	Transient	Cycle #	Start	End	Oper.	Project	U _{inc}	U _{inc} (avg)	F _{en}	U _{en, inc}	U _{en, inc} (avg)
4	Heatup	46	12/08/81	12/09/81	WS	HU46.WS	0.000026		1.00	0.000026	
4	Cooldown	50	10/10/82	10/10/82	WS	CD50.WS	0.00009		4.19	0.000377	
4	Cooldown	52	08/08/83	08/08/83	WS	CD52.WS	0.000076		4.53	0.000343	
4	Cooldown	53	08/16/83	08/16/83	WS	CD53.WS	0.000125	0.000079	3.63	0.000455	0.000300
3	Heatup	80	05/29/90	06/03/90	MSB	HU80	0.000019		2.72	0.000053	
3	Cooldown	81	12/13/90	12/14/90	MSB	CD81	0.000162		3.68	0.000595	
3	Heatup	81	09/16/91	09/22/91	MSB	HU81	0.000063		1.00	0.000063	
3	Cooldown	83	08/23/92	08/24/92	MSB	CD83	0.000026		4.78	0.000124	
4	Cooldown	93	04/10/93	04/11/93	MSB	CD93	0.000059		4.65	0.000276	
4	Heatup	94	05/20/93	05/22/93	MSB	HU94	0.000101		1.70	0.000172	
4	Cooldown	96	03/10/94	03/11/94	MSB	CD96	0.000141		3.02	0.000425	
4	Heatup	97	03/15/94	03/17/94	MSB	HU97	0.000066	7.96E-05	2.05	0.000136	0.0002305
3/4	HU/CD				MOP*			7.96E-05			0.0002305

* MOP conservatively assumed to be the same as MSB

4.2 Upset Transients

The effect of transients other than Heatup and Cooldown were investigated to determine the impact on fatigue usage factors. Three sample upset events were selected, which have a non-trivial impact on the temperature and pressure in the pressurizer. These were Reactor Trip, Reactor Trip with Cooldown and Safety Injection, and Large Step Load Decrease. Computer files associated with each run are listed in Appendix A.

4.2.1 Reactor Trip

For the Reactor Trip event, the pressurizer bulk temperature and internal pressure was simulated, as shown on Figure 3. An FP4 analysis was performed, resulting in zero usage, because the maximum alternating stress intensity is below the endurance limit (13.6 ksi) of the fatigue curve. The stress results are shown on Figure 4, demonstrating a relatively minor perturbation in stresses.

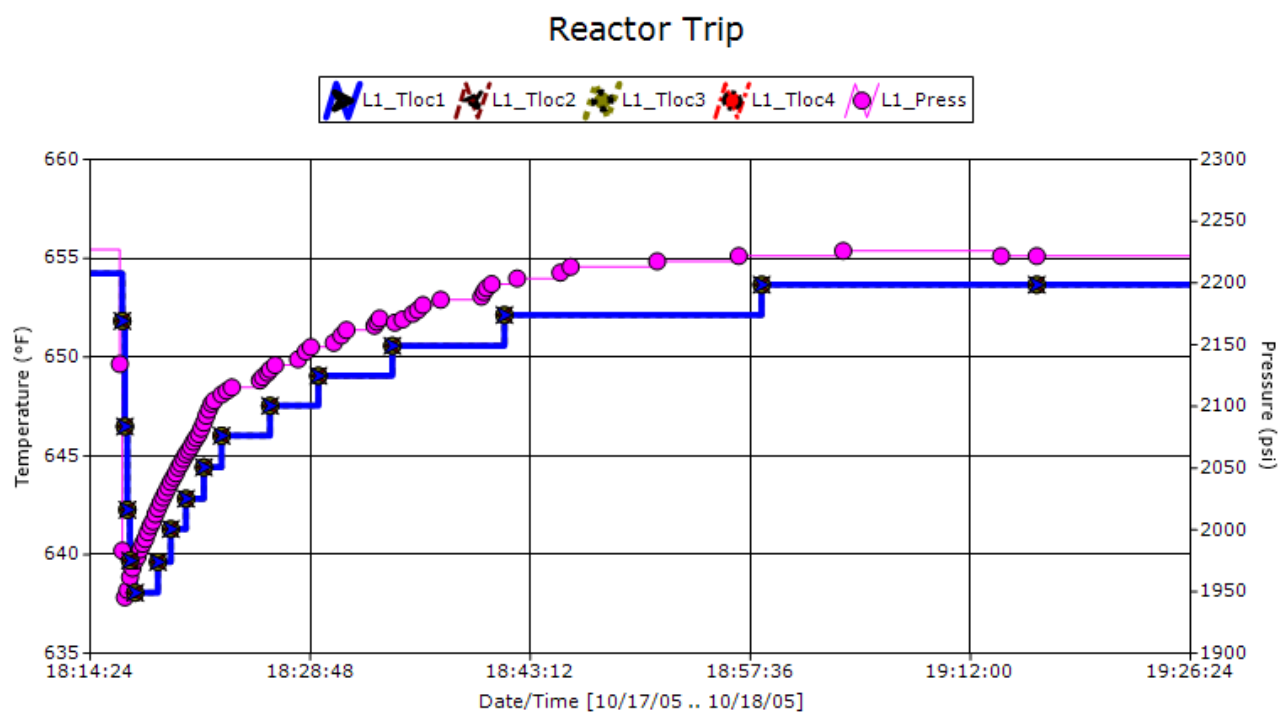


Figure 3: Reactor Trip Simulation

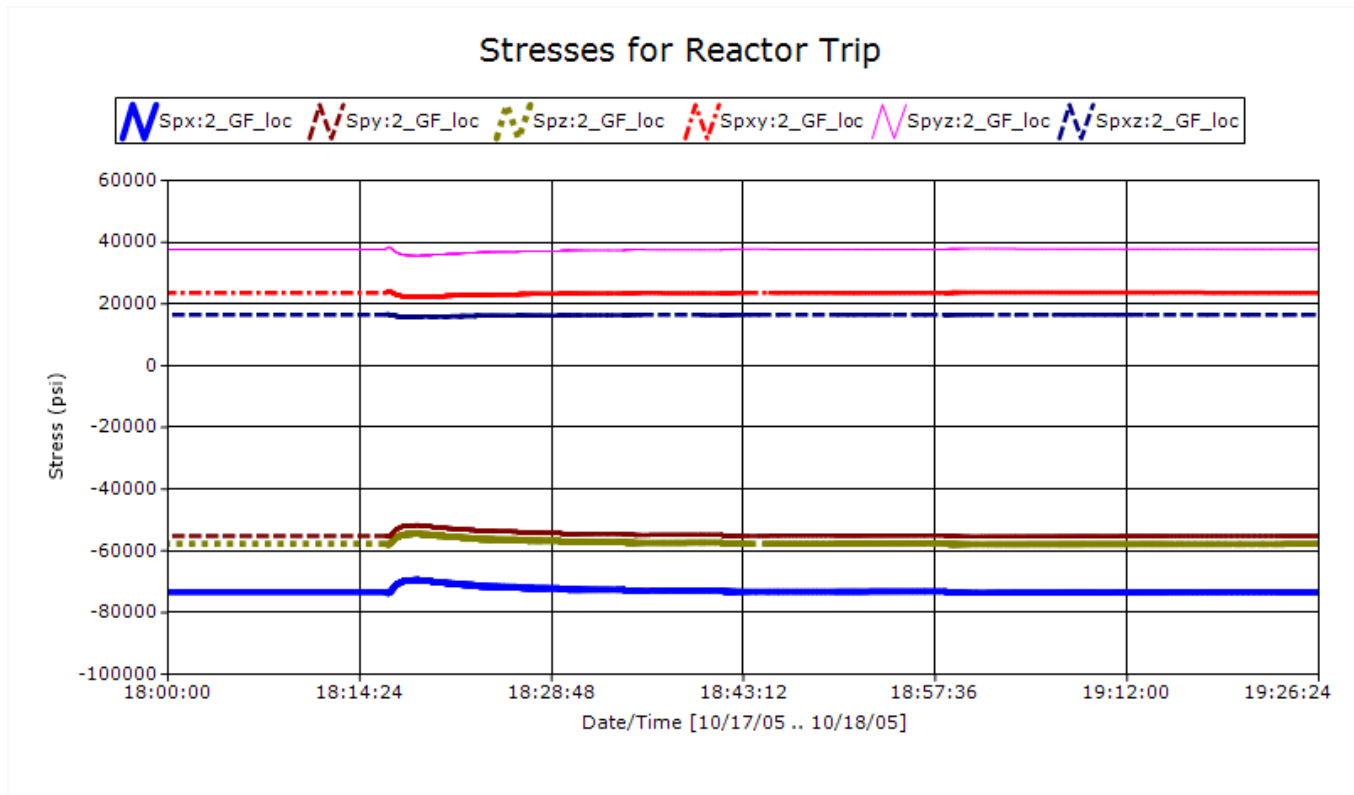


Figure 4: Stress Results for Reactor Trip

4.2.2 Reactor Trip with Cooldown and SI

For the Reactor Trip with Cooldown and SI event, the pressurizer bulk temperature and internal pressure was simulated, as shown on Figure 5. An FP4 analysis was performed, resulting in zero usage, because the maximum alternating stress intensity is below the endurance limit of the fatigue curve. The stress results are shown on Figure 6.

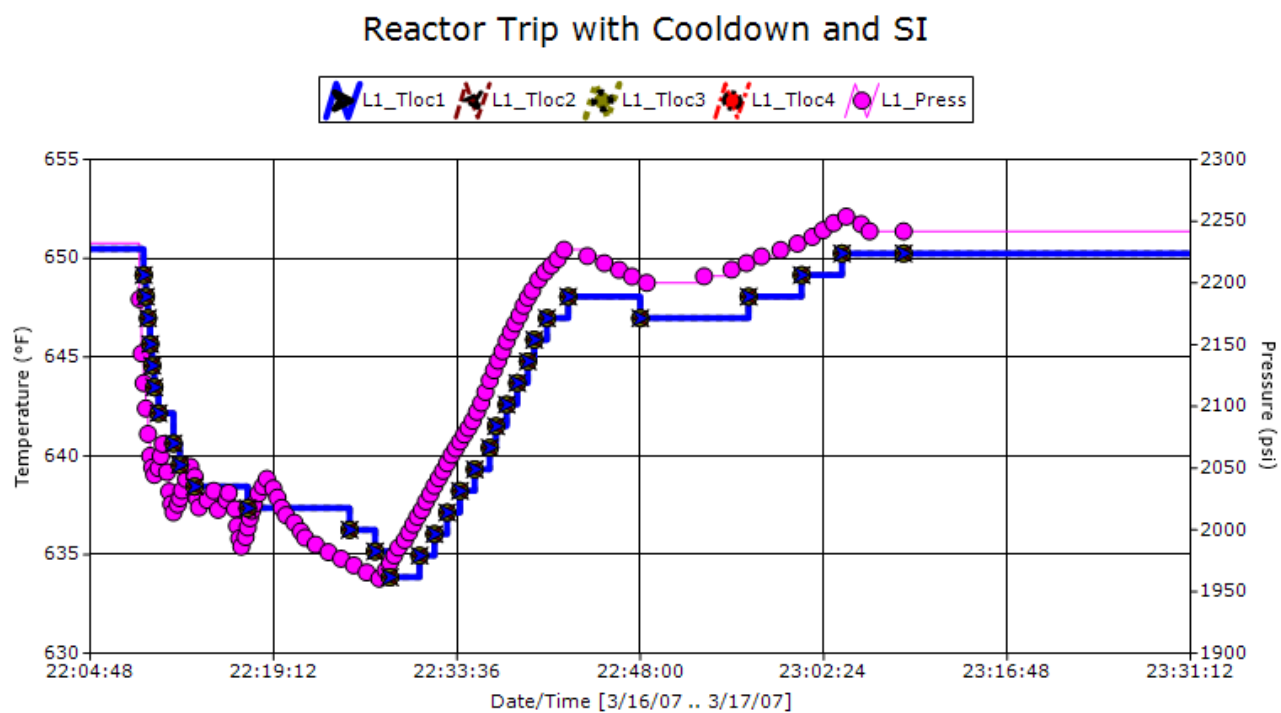


Figure 5: Reactor Trip with CD and SI Simulation

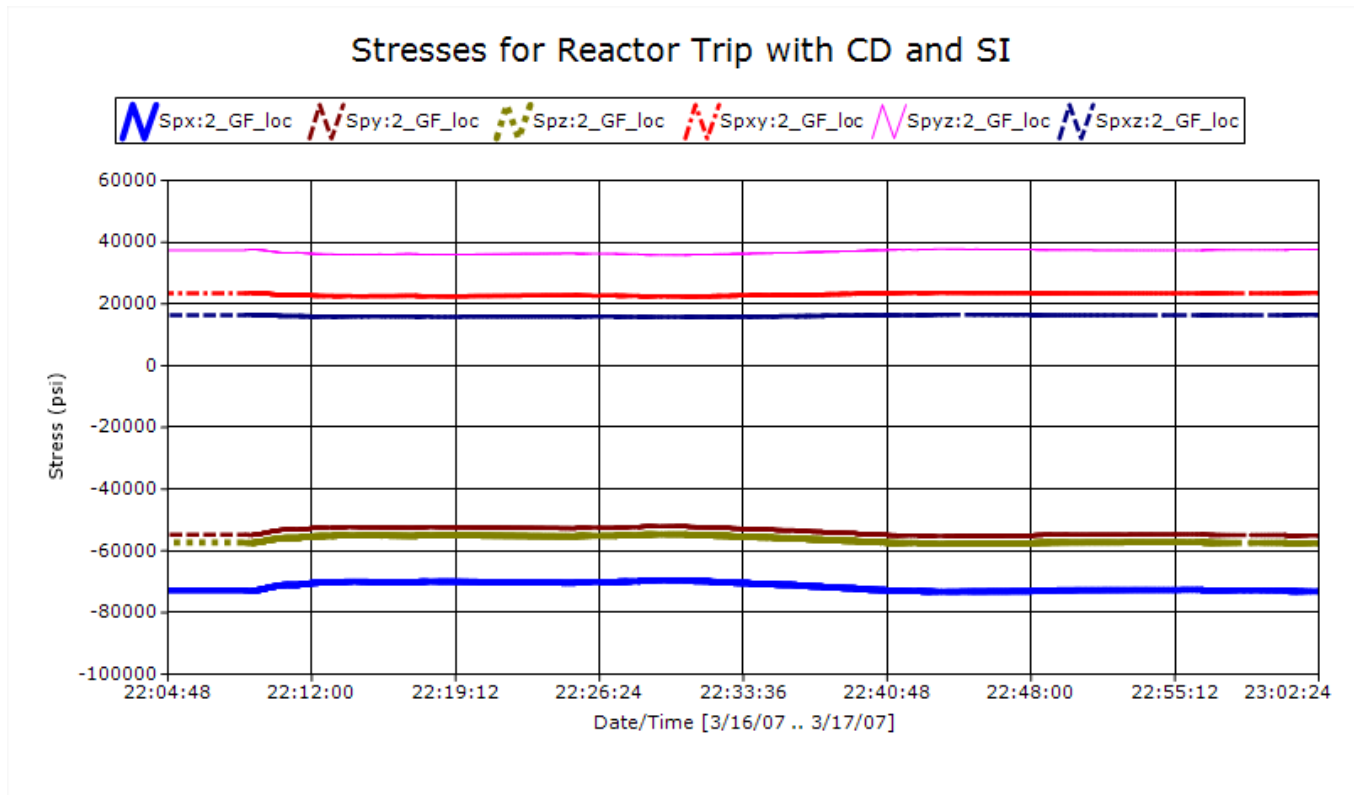


Figure 6: Stress Results for Reactor Trip with CD and SI

4.2.3 Large Step Load Decrease

For the Large Step Load Decrease event, the pressurizer bulk temperature and internal pressure was simulated, as shown on Figure 7. An FP4 analysis was performed, resulting in zero usage, because the maximum alternating stress intensity is below the endurance limit of the fatigue curve. The stress results are shown on Figure 8.

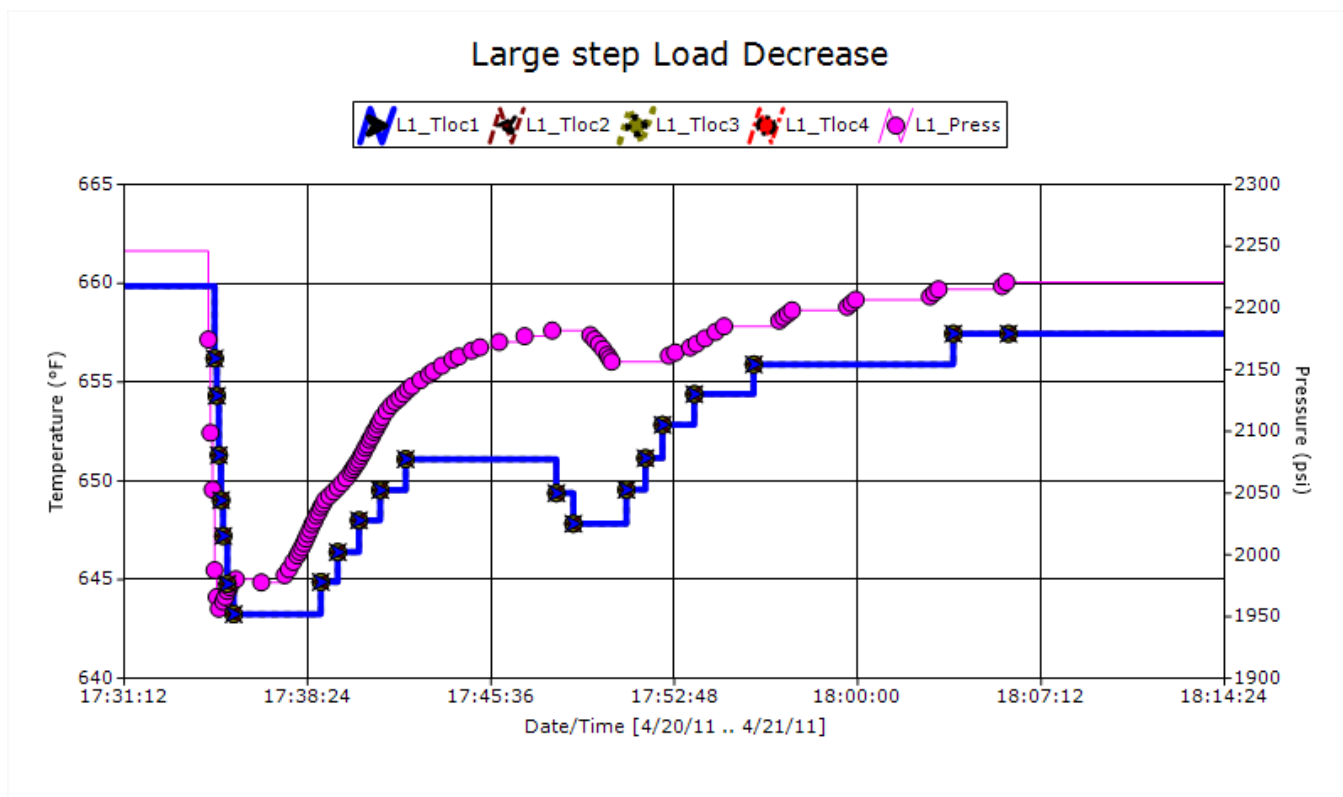


Figure 7: Large Step Load Decrease Simulation

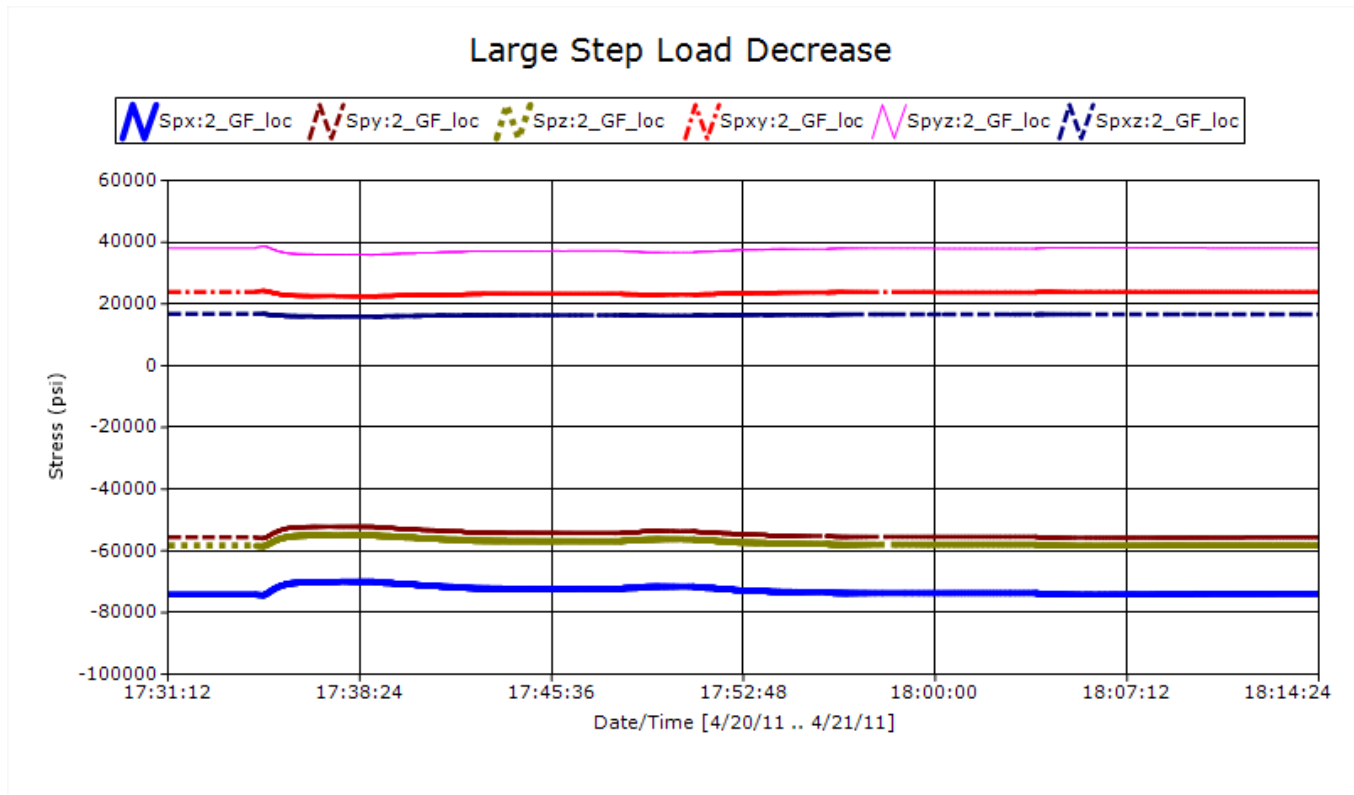


Figure 8: Stress Results for Large Step Load Decrease

4.2.4 Observations from Upset Transient Results

The fatigue calculation results for the upset transients shown above demonstrate even with non-trivial changes in temperature and pressure, the effect on usage considering realistic events is negligible or zero. Therefore, for low cycle fatigue, events not associated with heatup and cooldown and the insurge/outsurge stratification events which occur concurrently with them, will have a negligible contribution toward the overall usage factor.

5.0 RESULTS OF ANALYSIS

Based on the average incremental fatigue usage factors calculated previously, and the 80-year projected numbers of cycles, the usage factors, including environmental effects, are shown in Table 7. The results show that the usage, including environmental effects, is less than 0.1 at 80-years of operation.

Table 7: Overall Fatigue Usage Factor Results

Unit 3	Cycles	U_{inc}	U_{en inc}	F_{en}
# WS Operations =	127	0.010065	0.038132	3.79
# MSB Operations =	48	0.003822	0.011064	2.89
# MOP Operations ⁽¹⁾ =	153	0.012183	0.035267	2.89
	Total =	0.0261	0.0845	3.24
Unit 4	Cycles	U_{inc}	U_{en inc}	F_{en}
# WS Operations =	134	0.01062	0.040234	3.79
# MSB Operations =	59	0.004698	0.0136	2.89
# MOP Operations ⁽¹⁾ =	169	0.013457	0.038955	2.89
	Total =	0.0288	0.0928	3.22

Table notes:

(1) MOP operations were conservatively analyzed as MSB.

6.0 CONCLUSIONS

EAF for the pressurizer heater penetration was calculated for PTN-3/4 for 80-years of operation. The calculation was performed in accordance with ASME Section III, Subarticle NB-3200 methods, and with environmental effects as given in NUREG/CR-6909 Revision 1. Usage factors with environmental effects are acceptable for 80 years of operation, if cycle counts remain within the limits in Reference [13].

7.0 REFERENCES

1. ASME Boiler and Pressure Vessel Code, 2010 Edition.
2. NRC RIS-2008-30, *Fatigue Analysis of Nuclear Power Plant Components*, December 2008.
3. NRC RIS 2011-14, *Metal Fatigue Analysis Performed by Computer Software*, December 2011.
4. NUREG-2191, *Generic Aging Lessons Learned for Subsequent License Renewal (GALL-SLR) Report*, U. S. Nuclear Regulatory Commission, July 2017.
5. NUREG/CR-6909 (ANL-12/60), DRAFT Revision 1, *Effect of LWR Coolant Environments on the Fatigue Life of Reactor Materials*, March 2014.
6. Structural Integrity Associates Software, SI:FatiguePro 4.0 Generic Version Number 4.00.6079.23323, SI File No. FP-FP4-5044.
7. Structural Integrity Associates Report No. FP-FP4-403, Revision 1, *Stress-Based Fatigue Monitoring: Methodology for Fatigue Monitoring of Class 1 Nuclear Components in a Reactor Water Environment*. EPRI, Palo Alto, CA: 1022876.
8. SI Calculation Package, 1700804.317, Revision 0, October 2017, *Pressurizer Lower Head Green's Functions and Unit Pressure*,
9. SI Calculation Package, FPL-09Q-307P, Revision 0, August 2000, *Pressurizer Insurge/Outsurge Fatigue Analysis*, CONTAINS VENDOR PROPRIETARY INFORMATION.
10. Paper No. PVP2013-98060, *Environmentally-Assisted Fatigue Management of PWR Pressurizer using Nonlinear Strain-Based Analysis*, Proceedings of the ASME 2013 Pressure Vessels and Piping Conference, PVP2013, July 14-18, 2013, Paris, France.
11. Welding Research Council Bulletin 432, *Fatigue Strength Reduction and Stress Concentration Factors for Welds in Pressure Vessels and Piping*, June 1998.
12. SI Calculation Package No. 1700804.316P, Revision 0, *3-D Finite Element Model of Pressurizer Bottom Head, Skirt Assembly and Heater Wells*, CONTAINS VENDOR PROPRIETARY INFORMATION.
13. Project Correspondence Letter, DAG-17-003, Revision 3, "Formal Transmittal of Inputs for Westinghouse Evaluation of Turkey Point 3/4 Component Fatigue Usage for Environmentally Assisted Fatigue," October 12, 2017, SI File No. 1700109.102.
14. SI Calculation Package, FPL-09Q-301, Revision 0, *Development of Analysis Cases*.

Appendix A

COMPUTER FILES

1700804.318.xlsx Spreadsheet containing summary results

Files associated with the FP4 analyses are listed below. *.fpp are the FP4 project files. *.sqlite are the databases, which contain both configurations and results.

Directory FP4\CD50.WS
CD50.WS.fpp
CD50.WS.sqlite

Directory FP4\CD52.WS
CD52.WS.fpp
CD52.WS.sqlite

Directory FP4\CD53.WS
CD53.WS.fpp
CD53.WS.sqlite

Directory FP4\CD81
CD81.fpp
CD81.sqlite

Directory FP4\CD83
cd83.fpp
CD83.sqlite

Directory FP4\CD93
CD93.fpp
CD93.sqlite

Directory FP4\CD96
CD96.fpp
CD96.sqlite

Directory FP4\HU46.WS
HU46.WS.fpp
HU46.WS.sqlite

Directory FP4\HU80
HU80.fpp
HU80.sqlite

Directory FP4\HU81
HU81.fpp
HU81.sqlite

Directory FP4\HU94

HU94.fpp
HU94.sqlite

Directory FP4\HU97
HU97.fpp
HU97.sqlite

Directory FP4\LARGESTEP
LARGESTEP.fpp
LARGESTEP.sqlite

Directory FP4\RXTRIP
RXTRIP.fpp
RXTRIP.sqlite

Directory FP4\RXTRIP_CDSI
RXTRIP_CDSI.fpp
RXTRIP_CDSI.sqlite



CALCULATION PACKAGE

File No.: 1700804.313P - REDACTED

Project No.: 1700804

Quality Program Type: ☒ Nuclear ☐ Commercial

PROJECT NAME:

Turkey Point TLAA's for SLR – Component EAF Analyses

CONTRACT NO.:

2000243484, Revision 0

CLIENT:

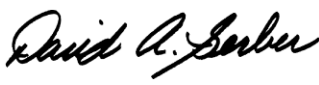


Florida Power and Light

PLANT:

Turkey Point Units 3 and 4

CALCULATION TITLE:

Pressurizer Spray Nozzle Loads

Document Revision	Affected Pages	Revision Description	Project Manager Approval Signature & Date	Preparer(s) & Checker(s) Signatures & Date
0	All	Initial Issue	David A. Gerber [DAG] 11/10/17	Kevin Wong [KLW] 11/10/17 Timothy D. Gilman [TDG] 11/10/17
1	All	Revised references, added heat transfer coefficient methodology, revised thermal transients.	 David A. Gerber [DAG] 12/7/17	 Kevin Wong [KLW] 12/7/17  Timothy D. Gilman [TDG] 12/7/17

THIS DOCUMENT CONTAINS CLIENT; DESIGN OR SUPPLIER PROPRIETARY INFORMATION. THIS DOCUMENT MAY NOT BE DISCLOSED, WHOLLY OR IN PART, TO ANY THIRD PARTIES WITHOUT THE PRIOR WRITTEN CONSENT OF STRUCTURAL INTEGRITY ASSOCIATES, INC.

PROPRIETARY INFORMATION NOTICE

THIS DOCUMENT CONTAINS PROPRIETARY INFORMATION. THE CLIENT MAY USE THE INFORMATION CONTAINED IN THIS DOCUMENT SOLELY FOR THEIR PURPOSES. IF THE DOCUMENT IS SUBMITTED TO THE NUCLEAR REGULATORY COMMISSION (NRC), STRUCTURAL INTEGRITY ASSOCIATES, INC. WILL PROVIDE PROPRIETARY AND NON-PROPRIETARY VERSIONS OF THE DOCUMENT FOR NRC USE ALONG WITH THE REQUIRED LETTER STATING THE PERMITTED USE BY THE NRC. THIS DOCUMENT MAY NOT BE DISCLOSED, WHOLLY OR IN PART, TO ANY THIRD PARTIES WITHOUT THE PRIOR WRITTEN CONSENT OF STRUCTURAL INTEGRITY ASSOCIATES, INC.

Note: Proprietary References are identified with a "P" in the SI File Number.

This entire document is considered Proprietary or Proprietary information used in the document is "Bracketed" ({ }).

Table of Contents

1.0	OBJECTIVE	4
2.0	METHODOLOGY	4
2.1	Internal Heat Transfer Coefficients, Forced Convection.....	4
2.2	Internal Heat Transfer Coefficients, Natural Convection.....	5
2.3	Internal Heat Transfer Coefficients, Condensation	6
2.4	Other Heat Transfer Coefficients.....	7
3.0	ASSUMPTIONS.....	7
4.0	PIPING INTERFACE LOADS	8
5.0	THERMAL TRANSIENTS.....	8
5.1	Inadvertent Auxiliary Spray Transient	8
5.2	Heatup and Cooldown Transients.....	9
6.0	REFERENCES	16

List of Tables

Table 1:	Piping Interface Loads.....	8
Table 2:	Projected Cycles for Unit 3 Heatup and Cooldown for an 80-Year Plant Life	11
Table 3:	Projected Cycles for Unit 4 Heatup and Cooldown for an 80-Year Plant Life	11
Table 4:	Heatup and Cooldown Transients for Unit 3.....	12
Table 5:	Heatup and Cooldown Transients for Unit 4.....	14

1.0 OBJECTIVE

The purpose of this calculation is to determine the loading conditions for the pressurizer spray nozzle at Turkey Point Nuclear Plant, Units 3 and 4. This includes piping interface loads, temperature and pressure histories for thermal transients, and projected cycle counts for thermal transients based on actual cycle counts.

2.0 METHODOLOGY

The loading developed herein will be used to perform stress analyses in accordance with the ASME Code [1].

This calculation will augment the design specifications to account for projected cycle counts for 80 years of plant operation and the three different pressurizer operating modes for heatup and cooldown - water solid (beginning of plant life to mid-1986), modified steam bubble (mid-1986 – mid-1994), and modified operating procedure (MOP) [3] (mid-1994 – present) [4].

Heat transfer coefficients are calculated in the supporting spreadsheet and are described in the subsequent sections.

2.1 Internal Heat Transfer Coefficients, Forced Convection

Holman [2, Eq. 6-4, pp. 226-227] gives the following equation for turbulent flow heating in tubes:

$$Nu = 0.023 Re^{0.8} Pr^{0.4}, \text{ where}$$

Nu = Nusselt number = hD/k

Re = Reynolds number = VD/ν

Pr = Prandtl number, non-dimensional

h = heat transfer coefficient, Btu/hr-ft²-°F

D = inside diameter, feet

k = thermal conductivity, Btu/hr-ft-°F

V = velocity, ft/sec = $Q/(\pi D^2/4)$

Q = volumetric flow rate, ft³/sec

ν = kinematic viscosity, ft²/sec

Solving for heat transfer coefficient and substituting $V = Q/(\pi D^2/4)$ yields:

$$h = 0.023 (k/D) (VD/\nu)^{0.8} Pr^{0.4}$$

$$h = 0.023 (k/D) [4QD/(\nu\pi D^2)]^{0.8} Pr^{0.4}$$

$$h = 0.023 (k/D) [4Q/(\nu\pi D)]^{0.8} Pr^{0.4}$$

$$h = 0.023 k [4Q/(\nu\pi)]^{0.8} 1/D^{1.8} Pr^{0.4}$$

It is convenient to express D in inches and Q in gallons per minute (gpm). In the equation, $Q/(vD)$ is dimensionless, and k/D must yield h units. Therefore, conversion factors from gpm to ft^3/sec for Q and inches to feet for D must be included:

$$h = 0.023 \left(\frac{4}{\pi} \times \frac{0.002228 \text{ ft}^3}{\text{sec} - \text{gpm}} \right)^{0.8} \left(\frac{\text{Pr}^{0.4} k}{v^{0.8}} \right) \left(\frac{12 \text{ in}}{\text{ft}} \right)^{1.8} (Q, \text{gpm})^{0.8} / (D, \text{in})^{1.8}$$

$$= 0.018472 \left(\frac{\text{Pr}^{0.4} k}{v^{0.8}} \right) \frac{Q^{0.8}}{D^{1.8}}$$

The temperature dependent factor, ϕ_1 , is defined as:

$$\phi_1 = 0.018472 \left(\frac{\text{Pr}^{0.4} k}{v^{0.8}} \right)$$

Thus:

$$h = \frac{\phi_1 Q^{0.8}}{D^{1.8}}$$

The above equation is valid for Reynolds number, Re, greater than 2300 [2, p. 172]; Re is given by:

$$\text{Re} = \frac{VD}{\nu} = \frac{4}{\pi} \left(\frac{0.002228 \text{ ft}^3}{\text{sec} - \text{gpm}} \right) \left(\frac{12 \text{ in}}{\text{ft}} \right) \frac{Q}{vD}$$

$$= \frac{\phi_2 Q}{D}, \text{ where}$$

$$\phi_2 = 0.034041/\nu$$

2.2 Internal Heat Transfer Coefficients, Natural Convection

For transients where flow rate is zero and the component is at steady-state conditions, heat transfer coefficients are determined based on natural circulation. Radiative heat transfer is deemed insignificant. For natural circulation in enclosed vertical or horizontal cylinders, Holman [2, Eq. 7-56, p. 289] gives the following formula:

$$\text{Nu}_f = 0.55 (\text{Gr}_f \text{Pr}_f)^{1/4}, \text{ where}$$

$$\begin{aligned} \text{Gr}_f &= \text{Grashof number, dimensionless} = g \beta \Delta T D^3 / \nu^2 \\ \beta &= \text{temperature coefficient of volume expansion (fluid), } 1/^\circ\text{F} \\ g &= \text{acceleration due to gravity} = 32.174 \text{ ft/sec}^2 \\ \Delta T &= \text{temperature difference between the fluid and wall, } ^\circ\text{F} \end{aligned}$$

ν = kinematic viscosity, ft²/sec

Other symbols are the same as previously defined. The subscript f indicates that the properties are evaluated at the film temperature, which is the average of the free-stream fluid temperature and the wall temperature [2, p. 273]. Separating constants and physical properties as before, the equation becomes:

$$\begin{aligned} h &= 0.55 (k/D) (g \beta \Delta T D^3 \text{Pr}_f/\nu^2)^{1/4} \\ h &= 0.55 k [g \beta \Delta T D^3 \text{Pr}_f/(D^4 \nu^2)]^{1/4} \\ h &= 0.55 k [g \beta \Delta T \text{Pr}_f/(D \nu^2)]^{1/4} \\ h &= \{0.55 k (g \beta \text{Pr}_f/\nu^2)^{1/4}\} (\Delta T/D)^{1/4} \end{aligned}$$

The portion inside the curly brackets is defined as ϕ_B , and is temperature dependent.

2.3 Internal Heat Transfer Coefficients, Condensation

When steam floods a relatively cold component (pipe wall or inner surface of thermal sleeve), the steam condenses on the component surface. Holman [2, p. 413] gives the following equation for average heat transfer coefficient for when turbulence is encountered in the film (the turbulent equation listed below applies when film Reynold's Number $\text{Re}_f > 1800$):

$$\bar{h} = C_0 / \{\mu^2 / [k^3 \rho (\rho - \rho_v) g]\}^{1/3}, \text{ where}$$

ρ = mass density of liquid

ρ_v = mass density of vapor

g = acceleration of gravity

k = conductivity of liquid at average temperature

μ = viscosity of liquid at average temperature

$$C_0 = 0.0077 \text{Re}_f^{0.4}$$

$$\text{Re}_f = 4 \bar{h} L (T_g - T_w) / [h'_{fg} \mu]$$

$$h'_{fg} = h_{fg} + 0.68c(T_g - T_w)$$

h_{fg} = heat of condensation at vapor temperature

c = specific heat of liquid at average temperature

T_g = saturated vapor temperature = T_{final}

T_w = pipe inner wall temperature = T_{initial}

L = Height of pipe

Steam properties are interpolated at T_g , and water properties are interpolated at the film temperature, $T_f = [(T_g + T_w)/2]$. Then, h'_{fg} and heat transfer coefficient \bar{h} are calculated for each set of steam properties at T_g , and water properties at T_w .

2.4 Other Heat Transfer Coefficients

All outside surfaces are assumed to be fully insulated and the insulation itself will be treated as perfect, allowing no heat transfer to or from the containment building environment. At the inside surface of the pressurizer shell the initial heat transfer coefficient calculated for the nozzle/safe end/pipe for each transient is applied to the pressurizer shell for the entirety of the transient. In addition, for those transients that consist of short term thermal shock events, the pressurizer shell is held at the initial temperature, which is consistent with a steam space environment condition.

3.0 ASSUMPTIONS

The following assumptions are used in this calculation:

1. It is assumed that there is only one occurrence of the Inadvertent Auxiliary Spray transient over the 80-year plant lifetime [8].
2. Inadvertent Auxiliary Spray is conservatively modeled as two instantaneous thermal shocks of $\Delta T = 553$ °F and $\Delta P = 1000$ psi.
3. In Section 6.0, several assumptions are made regarding pressurizer spray operation. Pressurizer spray is assumed not to operate when the heatup or cooldown ΔT exceeds the pressurizer spray operating limit.
4. It is assumed that there are 50 OBE cycles over 80 years of operation.
5. Piping interface loads for Unit 3 are assumed to be representative of the piping interface loads for Unit 4.
6. All outside surfaces are assumed to be fully insulated and the insulation itself will be treated as perfect, allowing no heat transfer to or from the containment building environment. The assumption is typical for most design activities and creates a conservative thermal stress field by maximizing through wall temperature gradients.
7. Piping interface loads for Unit 3 are assumed to be representative of the piping interface loads for Unit 4 due to both plants being of the same design and configuration

4.0 PIPING INTERFACE LOADS

Table 1 lists the piping interface loads for Unit 3 at the top of the nozzle (node 100) due to thermal expansion and operating basis earthquake (OBE) [5]. Consistent with original plant design, there are 50 OBE cycles over the life of the plant, which is now projected to be 80 years of operation. The y-direction is vertical; x and z are horizontal.

Table 1: Piping Interface Loads

Load Case	Forces, lb			Moments, lb-in		
	F _x	F _y	F _z	M _x	M _y	M _z
Thermal	172	-621	121	12,528	2424	-9084
OBE	842	145	775	19,476	44544	21,084

The thermal loads are applicable for a pressurizer temperature of 653°F, and are scaled to other temperatures using factors calculated as:

$$T_{\text{FACTOR}} = (T_{\text{fluid}} - 70)/(650 - 70)$$

T_{fluid} is equal to the fluid temperature during the given transient in °F.

5.0 THERMAL TRANSIENTS

Actual cycle counts through 10/24/16 [6, 7] have been used to calculate the projected cycles for an 80-year plant life. The beginning of plant life for Unit 3 and Unit 4 are August 1972 and May 1973 [3], respectively, and the actual cycle counts through 10/24/16 correspond to 44.2 years and 43.4 years of plant life for Unit 3 and Unit 4, respectively. Reference [3] provides a more detailed history of cycle counts subdivided by pressurizer operating modes for heatup and cooldown (See Section 5.2).

5.1 Inadvertent Auxiliary Spray Transient

Inadvertent Auxiliary Spray is modeled as two instantaneous thermal shocks with a ΔT of 553 °F when the pressurizer spray of 200 gpm is turned on and off. Between two thermal shocks, the pressure drops from a normal operating pressure of 2250 psia to approximately 1050 psia over a much longer period of time. Heat transfer coefficients are calculated in the supporting spreadsheet.

There have been no occurrences of Inadvertent Auxiliary Spray thus far [6, 7]. As such, it is assumed that there will only be one occurrence of the Inadvertent Auxiliary Spray transient over the 80-year plant lifetime [8].

5.2 Heatup and Cooldown Transients

Table 2 and Table 3 tabulate the actual and projected cycle counts [8] for different pressurizer operating modes during heatup and cooldown [obtained from 3, Tables 3-2 and 3-3]. Water solid and modified steam bubble are operating modes that were used during earlier plant life and have been replaced by the Modified Operating Procedure (MOP). Projected MOP cycle counts are taken as total 80-year projections (Station Heatup or Station Cooldown) minus the numbers of cycles from the respective Water Solid and Modified Steam Bubble operations.

Table 4 and Table 5 tabulate the heatup and cooldown transients for Units 3 and 4, respectively [9, Table 3]. Each design transient is representative of a thermal shock with the maximum ΔT . The three pressurizer operating modes for heatup and cooldown - water solid (beginning of plant life to mid-1986), modified steam bubble (mid-1986 – mid-1994), and modified operating procedure (MOP) (mid-1994 – present) [3] – are characterized using the heatup and cooldown design transients.

Water Solid $\Delta T \leq 200^{\circ}\text{F}$

Heatup for this operating mode with an operating limit of $\Delta T \leq 200^{\circ}\text{F}$ [3, Section 2.1] is characterized by Heatup Transients H4 ($\Delta T = 203^{\circ}\text{F}$) through H6 ($\Delta T = 125^{\circ}\text{F}$). As such, the 60 and 64 projected 80-year heatup cycles for Unit 3 and Unit 4, respectively, are added to the cycle counts for Heatup Transients H4 through H6. This assumes that pressurizer spray does not operate during the H1, H2 and H3 transients.

Cooldown for this operating mode with an operating limit of $\Delta T \leq 200^{\circ}\text{F}$ [3, Section 2.1] is characterized by Cooldown Transients C1 ($\Delta T = 125^{\circ}\text{F}$) through C3 ($\Delta T = 203^{\circ}\text{F}$). As such, the 60 and 63 projected 80-year cooldown cycles for Unit 3 and Unit 4, respectively, are added to the cycle counts for Cooldown Transients C1 through C3. This assumes that pressurizer spray does not operate during the C4 through C8 transients.

Water Solid $\Delta T \leq 320^{\circ}\text{F}$

Heatup for this operating mode with an operating limit of $\Delta T \leq 320^{\circ}\text{F}$ [3, Section 2.1] is characterized by Heatup Transients H1 ($\Delta T = 320^{\circ}\text{F}$) through H6 ($\Delta T = 125^{\circ}\text{F}$) and Cooldown Transients C1 ($\Delta T = 125^{\circ}\text{F}$) through C6 ($\Delta T = 320^{\circ}\text{F}$) and Cooldown Transient C8 ($\Delta T = 320^{\circ}\text{F}$). As such, the 4 and 3 projected 80-year heatup cycles for Unit 3 and Unit 4, respectively, are added to the cycle counts for Heatup Transients H1 through H6.

Cooldown for this operating mode with an operating limit of $\Delta T \leq 320^{\circ}\text{F}$ [3, Section 2.1] is characterized by Cooldown Transients C1 ($\Delta T = 125^{\circ}\text{F}$) through C6 ($\Delta T = 320^{\circ}\text{F}$) and Cooldown Transient C8 ($\Delta T = 320^{\circ}\text{F}$). As such, the 3 and 4 projected 80-year cooldown cycles for Unit 3 and Unit 4, respectively, are added to the cycle counts for Cooldown Transients C1 through C6 and Cooldown Transient C8. This assumes that the pressurizer spray does not operate during the C7 transient.

Modified Steam Bubble (OP-201.1 and 3-GOP-503/4-GOP-503)

Heatup for this operating mode with an operating limit of $\Delta T \leq 320^{\circ}\text{F}$ [3, Section 2.2] is characterized by Heatup Transients H1 ($\Delta T = 320^{\circ}\text{F}$) through H6 ($\Delta T = 125^{\circ}\text{F}$). As such, the 2 + 22 and 4 + 26 projected 80-year heatup cycles for Unit 3 and Unit 4, respectively, are added to the cycle counts for Heatup Transients H1 through H6.

Cooldown for this operating mode with an operating limit of $\Delta T \leq 320^{\circ}\text{F}$ [3, Section 2.2] is characterized by Cooldown Transients C1 ($\Delta T = 125^{\circ}\text{F}$) through C6 ($\Delta T = 320^{\circ}\text{F}$) and Cooldown Transient C8 ($\Delta T = 320^{\circ}\text{F}$). As such, the 2 + 22 and 4 + 25 projected 80-year cooldown cycles for Unit 3 and Unit 4, respectively, are added to the cycle counts for Cooldown Transients C1 through C6 and Cooldown Transient C8. This assumes that pressurizer spray does not operate during the C7 transient.

Modified Operating Procedure (MOP)

Heatup for this operating mode with an operating limit of $\Delta T \leq 320^{\circ}\text{F}$ [3, Section 2.3] is characterized as a single temperature shock increase with a gradual temperature change afterwards. As such, the MOP Heatup Transient ($\Delta T = 320^{\circ}\text{F}$) is modeled using the temperature shock increase of Heatup Transient H1 ($\Delta T = 320^{\circ}\text{F}$). The 76 and 84 projected 80-year MOP heatup cycles for Unit 3 and Unit 4, respectively, are applied to the MOP Heatup Transient ($\Delta T = 320^{\circ}\text{F}$).

Cooldown for this operating mode with an operating limit of $\Delta T \leq 320^{\circ}\text{F}$ is characterized as a single temperature shock decrease with a gradual temperature change afterwards [3, Section 2.3]. As such, the MOP Cooldown Transient ($\Delta T = 320^{\circ}\text{F}$) is modeled using the temperature shock increase of Cooldown Transient C6 ($\Delta T = 320^{\circ}\text{F}$). The 77 and 85 projected 80-year MOP cooldown cycles for Unit 3 and Unit 4, respectively, are applied to the MOP Cooldown Transient ($\Delta T = 320^{\circ}\text{F}$).

Table 2: Projected Cycles for Unit 3 Heatup and Cooldown for an 80-Year Plant Life

Pressurizer Operating Mode	Cycle Counts (up to 2/2000)			Projected Cycle Counts 80-Year Plant Life (8/1972 – 8/2052)	
	Operating Period	Heatup Cycles	Cooldown Cycles	Total Heatup Cycles	Total Cooldown Cycles
Water Solid $\Delta T \leq 200^{\circ}\text{F}$	8/1972 – 1/1986	60	60	60	60
Water Solid $\Delta T \leq 320^{\circ}\text{F}$	1/1986 – 5/1986	4	3	4	3
Modified Steam Bubble (OP-202.1)	7/1986 – 8/1986	2	2	2	2
Modified Steam Bubble (3-FOP-503)	12/1986 – 5/1994	22	22	22	22
MOP	9/1995 – 2/2000	4	5	76	77
Total – All Modes	8/1972 – 2/2000	92	92	164	164

Table 3: Projected Cycles for Unit 4 Heatup and Cooldown for an 80-Year Plant Life

Pressurizer Operating Mode	Cycle Counts (up to 4/1999)			Projected Cycle Counts 80-Year Plant Life (5/1973 – 5/2053)	
	Operating Period	Heatup Cycles	Cooldown Cycles	Total Heatup Cycles	Total Cooldown Cycles
Water Solid $\Delta T \leq 200^{\circ}\text{F}$	5/1973 – 12/1984	64	63	64	63
Water Solid $\Delta T \leq 320^{\circ}\text{F}$	1/1985 – 5/1986	3	4	3	4
Modified Steam Bubble (OP-202.1)	8/1986 – 10-1986	4	4	4	4
Modified Steam Bubble (4-FOP-503)	10/1986 – 3/1994	26	25	26	25
MOP	10/1994 – 4/1999	5	5	84	85
Total – All Modes	5/1973 – 4/1999	102	101	181	181



Table 4: Heatup and Cooldown Transients for Unit 3

[illegible]



Structural Integrity Associates, Inc.®

Table 4: Heatup and Cooldown Transients for Unit 3 (Continued)

[illegible]



Structural Integrity Associates, Inc.®

Table 5: Heatup and Cooldown Transients for Unit 4

Description	Time, sec	T, °F	Q, gpm	P, psia	Water Solid Cycles 80-year	Modified Steam Bubble Cycles 80-year	MOP Cycles 80-year	Total Cycles 80-year	h,
{									
}									



Structural Integrity Associates, Inc.®

Table 5: Heatup and Cooldown Transients for Unit 4 (Continued)

[illegible]

6.0 REFERENCES

1. ASME Boiler and Pressure Vessel Code, Section III, Rules for Construction of Nuclear Facility Components, 2007 Edition with Addenda through 2008a.
2. Holman, J.P., *Heat Transfer*, Fifth Edition, McGraw-Hill, 1981.
3. Structural Integrity Associates Calculation No. FPL-09Q-301, Revision 0, "Development of Analysis Cases."
4. Florida Power & Light Company Procedure No. 3-OP-041.2, "Pressurizer Operation," Approval Date 12/13/94, SI File No. FPL-09Q-206.
5. Teledyne Report TR-5322-35, Revision 1 (Unit 3), *USNRC I&E BULLETIN 79-14 ANALYSIS, TURKEY POINT 3 NUCLEAR POWER PLANT, REACTOR COOLANT SYSTEM (INSIDE CONTAINMENT) AND CHEMICAL AND VOLUME CONTROL SYSTEM, STRESS PROBLEM PS-1/023*, SI File No. 1100756.203.
6. NextEra Energy Work Order Package No. 4043903901, "U3 Maintaining Records for Design Cycles," SI File No. 1700109.203.
7. NextEra Energy Work Order Package No. 4045719701, "Maintaining Records for Design Cycles Unit 4," SI File No. 1700109.203.
8. Project Correspondence Letter, DAG-17-003, "Formal Transmittal of Inputs for Westinghouse Evaluation of Turkey Point 3/4 Component Fatigue Usage for Environmentally Assisted Fatigue," Revision 3, October 12, 2017, SI File No. 1700109.102.
9. LTR-SGMP-11-66, Revision 2, "Turkey Point Units 3 and 4 Data Package for Pressurizer Spray and Surge Nozzle Analysis," October 2011, Attachment 2 of FPL-11- 276, PROPRIETARY, SI File No. 1700804.203P.



CALCULATION PACKAGE

File No.: 1700804.314P - REDACTED

Project No.: 1700804

Quality Program Type: ☒ Nuclear ☐ Commercial

PROJECT NAME:

Turkey Point TLAA's for SLR – Component EAF Analyses

CONTRACT NO.:

2000243484, Revision 1

CLIENT:

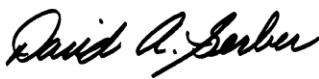


Florida Power and Light

PLANT:

Turkey Point

CALCULATION TITLE:

Pressurizer Spray Nozzle Finite Element Model and Stress Analyses

Document Revision	Affected Pages	Revision Description	Project Manager Approval Signature & Date	Preparer(s) & Checker(s) Signatures & Date
0	1 - 26 A1-A2	Initial Issue	David A. Gerber [DAG] 11/10/17	Aparna Alleshwaram [AA] 11/10/17 Wilson Wong [WW] 11/10/17
1	All	Deleted reference, revised methodology and assumptions, edited supporting files.	 David A. Gerber [DAG] 12/07/17	 Kevin Wong [KLW] 12/07/17  Wilson Wong [WW] 12/07/17
THIS DOCUMENT CONTAINS; CLIENT; DESIGN OR SUPPLIER PROPRIETARY INFORMATION. THIS DOCUMENT MAY NOT BE DISCLOSED, WHOLLY OR IN PART, TO ANY THIRD PARTIES WITHOUT THE PRIOR WRITTEN CONSENT OF STRUCTURAL INTEGRITY ASSOCIATES, INC.				

PROPRIETARY INFORMATION NOTICE

THIS DOCUMENT CONTAINS PROPRIETARY INFORMATION. IN ACCORDANCE WITH THE TERMS OF THE CLIENT CONTRACT. THE CLIENT MAY USE THE INFORMATION CONTAINED IN THIS DOCUMENT SOLELY FOR THEIR PURPOSES. IF THE DOCUMENT IS SUBMITTED TO THE NUCLEAR REGULATORY COMMISSION (NRC), STRUCTURAL INTEGRITY ASSOCIATES, INC. WILL PROVIDE PROPRIETARY AND NON-PROPRIETARY VERSIONS OF THE DOCUMENT FOR NRC USE ALONG WITH THE REQUIRED LETTER STATING THE PERMITTED USE BY THE NRC. THIS DOCUMENT MAY NOT BE DISCLOSED, WHOLLY OR IN PART, TO ANY THIRD PARTIES WITHOUT THE PRIOR WRITTEN CONSENT OF STRUCTURAL INTEGRITY ASSOCIATES, INC.

Note: Proprietary References are identified with a "P" in the SI File Number.

This entire document is considered Proprietary or Proprietary information used in the document is "Bracketed" ({ }).

Table of Contents

1.0	OBJECTIVE	5
2.0	METHODOLOGY	5
2.1	Overview	5
2.2	Software Used	6
3.0	DESIGN INPUT	6
3.1	Finite Element Model	6
3.2	Material Properties	6
3.3	Thermal Transient Definitions	6
4.0	ASSUMPTIONS	6
5.0	ANALYSIS	7
5.1	Mechanical Boundary Conditions	7
5.2	Thermal Analyses	7
5.3	Unit Internal Pressure Analysis	7
5.4	Unit Axial Piping Load Analysis	8
5.5	Unit Moment Load Analysis	8
6.0	RESULTS AND DISCUSSION	9
7.0	REFERENCES	10
	Appendix A COMPUTER FILES	A-1

List of Tables

Table 1: Inadvertent Auxiliary Spray Transient	11
Table 2: Heatup and Cooldown Transients for Unit 3	12
Table 3: Heatup and Cooldown Transients for Unit 4.....	14

List of Figures

Figure 1: Finite Element Model of the Pressurizer Spray Nozzle	16
Figure 2: Pressurizer Spray Nozzle Component Definitions.....	17
Figure 3: Applied Structural Boundary Conditions for Stress Analyses ⁷	18
Figure 4: Representative Heat Transfer Coefficients for Thermal Transients (H1 Shown)...	19
Figure 5: Representative Stress Intensity Contour for Transient H1 at Time = 8 Seconds....	20
Figure 6: Applied 1,000 psi Unit Internal Pressure and Induced End Cap Pressure	21
Figure 7: Stress Intensity Contour for Unit Internal Pressure	22
Figure 8: Applied 1,000 lb _f Unit Axial Piping Load	23
Figure 9: Stress Intensity Contour for Unit Axial Piping Load.....	24
Figure 10: Stress Intensity Contour for Unit Moment Piping Load	25
Figure 11: Path Definitions for Results Extraction.....	26

1.0 OBJECTIVE

The purpose of this calculation is to document the development of a finite element model and perform finite element stress analyses due to applicable thermal transients and unit mechanical loads on a representative pressurizer spray nozzle at Turkey Point Nuclear Plant (PTN), Units 3 and 4.

Linearized stresses, as well as mapped through-wall temperature time histories, are extracted through locations of geometric and material discontinuities or stress concentration regions. The stress and temperature outputs are stored in computer files and will be used in a separate fatigue evaluation in accordance with sub-article NB-3200 of Section III of the ASME Code [2].

2.0 METHODOLOGY

The finite element model and thermal analyses performed herein will be used in a separate fatigue evaluation in accordance with the ASME Code [2].

Previously, the finite element model and loading conditions were developed for stress and fatigue usage analyses of the pressurizer spray nozzle at Turkey Point Nuclear Plant, Units 3 and 4 [1 and 7]. Loads developed therein tabulated piping loads, design cycle counts, and design transients and calculated heat transfer coefficients for design transients.

This calculation will cite the previous finite element model calculation package [1] (including the Westinghouse source documents) and include additional information from the latest loads calculation package [4] to account for actual cycle counts and the three different pressurizer operating modes for heatup and cooldown - water solid (beginning of plant life to mid-1986), modified steam bubble (mid-1986 – mid-1994), and modified operating procedure (MOP) (mid-1994 – present).

2.1 Overview

The following is the order in which the analyses were conducted:

- Perform thermal analyses by applying the appropriate heat transfer coefficients and temperatures specified for each of the thermal transients in Tables 1 through 3 to inside surfaces of the finite element model.
- Perform thermal stress analyses using temperature results from thermal loading.
- Perform stress analysis for the unit pressure load case.
- Perform stress analysis for the unit axial and moment load cases.
- Review stress results and define paths at locations of discontinuities and stress concentrations.
- Extract mapped temperature history from the thermal analyses for the defined paths.
- Extract linearized stress history from the stress analyses for the defined paths.

2.2 Software Used

The ANSYS finite element software [6] was used to perform thermal and stress analyses for the loading conditions.

3.0 DESIGN INPUT

3.1 Finite Element Model

The finite element model was developed in a previous calculation package [1] using the ANSYS finite element software package [3]. The same input file is used to re-create the finite element model in the latest version of ANSYS [6]. Details of the two-dimensional (2-D) finite element model of the pressurizer spray nozzle are given in Reference 1. A 3-D model is not needed for this evaluation because the model has a perfectly axisymmetric geometry. All relevant stress components are calculated and used in the subsequent fatigue evaluation. The finite element model is shown in Figure 1, with the component definitions illustrated in Figure 2.

3.2 Material Properties

The material properties are included in Reference 1, and are used for the analyses performed herein.

3.3 Thermal Transient Definitions

The Inadvertent Auxiliary Spray transient is defined in Section 5.2 of Reference [4] and tabulated in Table 2. Heatup and Cooldown transients are documented in Tables 4 and 5 of Reference [4] and reproduced here in Tables 2 and 3.

4.0 ASSUMPTIONS

- All thermal transient and pressure analyses are performed with a stress-free reference temperature of 70°F. This is consistent with typical thermal transient stress evaluation methodology.
- { .}

For those transients that consist of short term thermal shock events, the pressurizer shell remains at the initial conditions, which is consistent with a steam space environment condition. For short term thermal shock events, there is enough thermal capacitance in the fluid in the pressurizer that it won't have any local effect on the shell. Hence the pressurizer shell remains at the initial conditions, which is consistent with a steam space environment condition.

5.0 ANALYSIS

5.1 Mechanical Boundary Conditions

In the stress analyses, symmetric boundary conditions are applied to the free end of the modeled local portion of the pressurizer head, while axial displacement (UY) couplings are applied to the modeled spray piping free end to simulate un-modeled connecting pipe. In addition, the entire model is constrained in the out-of-plane direction (UZ) to ensure axisymmetric behavior. The structural boundary conditions are the same for all thermal and unit load stress analyses, as shown in Figure 3.

5.2 Thermal Analyses

The PLANE75 element type was used to perform the thermal pass of the analyses. Table 1 through 3, are tabulated from Section 5.1 and Tables 4 and 5 of Reference [4] respectively, show the summary of transients that were analyzed for the pressurizer spray nozzle. For each of the thermal transient events, the bulk fluid temperatures and heat transfer coefficients listed in the tables are applied to the inside surface nodes of the local portion of the pressurizer head with cladding, nozzle support inner cylinder, thermal sleeve, safe-end and the local portion of the attached spray piping. An example heat transfer coefficient application is shown in Figure 4.

An additional time of 3600 seconds, followed by a steady state load step at the end, are appended to each transient to ensure that the model reaches equilibrium. For the annulus region between the nozzle and the thermal sleeve, water elements are included so that heat transfer across the annulus is properly considered in the analyses.

The PLANE25 element type was used to perform the stress pass of the analyses. Note that the water elements, as well as the thermal sleeve, the nozzle support cylinder, and nozzle liner, are deleted because they do not contribute structural stiffness to the nozzle assembly. A representative resulting stress intensity contour for thermal transient H1 (see Table 1) is shown in Figure 5.

5.3 Unit Internal Pressure Analysis

Non-structural components including the thermal sleeve, nozzle support cylinder, nozzle liner, and water elements are removed and a unit internal pressure of 1,000 psi is applied to the inside surfaces of the model. An induced end-cap load is applied to the free end of the spray piping in the form of tensile axial pressure and is calculated below. The boundary conditions applied to the model are the same as the boundary conditions applied for the thermal stress analyses (See Section 4.3). The applied loading for the unit pressure analysis are shown in Figure 6. Figure 7 shows the stress intensity results due to the unit pressure load.

where, $\{ \quad \}$

$P_{\text{end-cap-spray}}$ = End cap pressure on spray piping free end (psi)

P	= Unit Internal pressure (psi)
r _{inside}	= Inside radius of 4" Schedule 120 spray piping (in) [5]
r _{outside}	= Outside radius of 4" Schedule 120 spray piping (in) [5]

The unit pressure stresses will be scaled to the appropriate pressure loads in the subsequent fatigue evaluation, which is performed separately from this calculation package.

5.4 Unit Axial Piping Load Analysis

Non-structural components including the thermal sleeve, nozzle support cylinder, nozzle liner, and water elements are removed and a unit axial load of 1,000 lbf is applied to the free end of the attached spray piping. The applied loading for the unit axial piping load is shown in Figure 8. Figure 9 shows the stress intensity results due to the unit axial load.

The unit axial piping load stresses will be scaled to the appropriate piping force loads in the subsequent fatigue evaluation, which is performed separately from this calculation package.

5.5 Unit Moment Load Analysis

Similar to the unit axial piping load analysis, non-structural components including the thermal sleeve, nozzle support cylinder, nozzle liner, and water elements are removed and a unit moment load of 1,000 in-lb is applied as a force to the free end of the attached spray piping. Using the PLANE 25 elements for performing this analysis, an applied non-axisymmetric moment (M) load due to an axial input force (FY) for this case can be computed as follows:

$$M = \int_0^{2\pi} (\text{force per unit length}) * (\text{lever arm}) * (\text{increment length})$$

$$M = \int_0^{2\pi} (FY(\cos \theta)/2\pi R) * (R \cos \theta) * (R d\theta) = (FY)R/2$$

$$\begin{aligned} \text{Where } M &= 1000 \text{ in-lbs} \\ R &= (R_i + R_o)/2 \\ R_i &= 1.813'' \\ R_o &= 2.25'' \end{aligned}$$

$$\text{Hence axial force } FY = (1000 * 2) / ((1.813 + 2.25) / 2) = 984.49 \text{ lbs}$$

Figure 10 shows the stress intensity results due to the unit moment load. The unit moment piping load stresses will be scaled to the appropriate piping moment loads in the subsequent fatigue evaluation, which is performed separately from this calculation package.

6.0 RESULTS AND DISCUSSION

The stress results for all loading conditions are reviewed and linearized stress and mapped temperature time histories are extracted at the locations (Paths 1 through 5) shown in Figure 11. Note that Paths 3 through 5 start from the base metal interface because the nozzle liner and cladding materials are excluded from structural considerations.

linearized stresses and mapped temperature time histories are extracted using the global Cartesian coordinate system with the global Y axis parallel to the axial direction of the spray piping, and Z axis corresponds to the hoop direction of the model.

For the unit load analyses (pressure, axial and moment force), the stresses due to the appropriate loads will be included in the subsequent fatigue evaluation. In addition, the combined stresses due to the thermal transients and applicable pressure and piping loads will be combined in the subsequent fatigue evaluation, which is performed separately from this calculation package.

All output files are included with the project computer files.

7.0 REFERENCES

1. SI Calculation Package 1100768.302P, Rev. 0, “Finite Element Model of the Pressurizer Spray Nozzles.”
2. ASME Boiler and Pressure Vessel Code, Section III, Rules for Construction of Nuclear Facility Components, 2007 Edition with Addenda through 2008a.
3. ANSYS Mechanical APDL and PrepPost, Release 12.1 x64, ANSYS, Inc., November 2009.
4. SI Calculation Package 1700804.313P, Rev. 1, “Pressurizer Spray Nozzle Loads.”
5. Teledyne Engineering Services Drawing No. 5613-P-661-S, Sheet 1 of 5, Rev. 6, “Turkey Point Nuclear Power Plant Unit 3, Reactor Coolant System and CVCS, SYS. Nos. 41 & 47 Inside Containment, Stress Problem PS-1/023,” SI File No. 1100768.204.
6. ANSYS Mechanical APDL, Release 14.5 (w/ Service Pack 1 UP20120918), ANSYS, Inc., September 2012.



Structural Integrity Associates, Inc.[®]

Table 1: Inadvertent Auxiliary Spray Transient

Thermal Transient	Time, sec	T, °F	Q, gpm	P, psia	Projected Cycles 80-Year Plant Life		h, Btu/hr-ft ² -°F
					Unit 3	Unit 4	
{							}



Structural Integrity Associates, Inc.®

Table 2: Heatup and Cooldown Transients for Unit 3[illegible]



Structural Integrity Associates, Inc.®

Table 2: Heatup and Cooldown Transients for Unit 3 (Continued)

[illegible]

Notes: Table reproduced from Reference [4, Table 4].



Structural Integrity Associates, Inc.®

Table 3: Heatup and Cooldown Transients for Unit 4[illegible]



Structural Integrity Associates, Inc.®

Table 3: Heatup and Cooldown Transients for Unit 4 (Continued)

[illegible]

Notes: Table reproduced from Reference [4, Table 5].

{

}

Figure 1: Finite Element Model of the Pressurizer Spray Nozzle

{

}

Figure 2: Pressurizer Spray Nozzle Component Definitions

{

}

Figure 3: Applied Structural Boundary Conditions for Stress Analyses⁷

Note: The out-of-plane displacements on the entire model are also constrained (i.e., $U_Z = 0$)

{

}

Figure 4: Representative Heat Transfer Coefficients for Thermal Transients (H1 Shown)

Note: To be consistent with the units used in the analysis, the units for the applied heat transfer coefficients are in terms of Btu/sec-in²-°F

{

}

Figure 5: Representative Stress Intensity Contour for Transient H1 at Time = 8 Seconds

Note: Contour units are in terms of psi

{

}

Figure 6: Applied 1,000 psi Unit Internal Pressure and Induced End Cap Pressure

Note: Contour units are in terms of psi

{

}

Figure 7: Stress Intensity Contour for Unit Internal Pressure

Note: Contour units are in terms of psi

{

}

Figure 8: Applied 1,000 lbf Unit Axial Piping Load

Note: Force value is in terms of lbf

{

}

Figure 9: Stress Intensity Contour for Unit Axial Piping Load

Note: Contour units are in terms of psi

{

}

Figure 10: Stress Intensity Contour for Unit Moment Piping Load

Note: Contour units are in terms of psi

{

}

Figure 11: Path Definitions for Results Extraction

Appendix A

COMPUTER FILES

File Name	Description
spray.mac	ANSYS file to construct the 2-D axisymmetric model of spray nozzle.
matprop.mac	ANSYS file of temperature dependent linear elastic material properties, called by spray.mac.
SPRAY_\$.INP	ANSYS input file for thermal transients, where \$\$ denotes the thermal transient: H1=Heatup H1; H2=Heatup H2; H3=Heatup H3; H4=Heatup H4; H5=Heatup H5; H6=Heatup H6; C1=Cooldown C1; C2=Cooldown C2; C3=Cooldown C3; C4=Cooldown C4; C5=Cooldown C5; C6=Cooldown C6; C7=Cooldown C7; C8=Cooldown C8; IAS=Inadvertent Auxiliary Spray
SPRAY_\$_MNTR.INP	ANSYS input file for stress pass of thermal transients, where \$\$ denotes the thermal transient as denoted above.
SPRAY_PRESS.INP	ANSYS input file for unit internal pressure loading
SPRAY_FY.INP	ANSYS input file for unit axial spray pipe loading
SPRAY_Moment.INP	ANSYS input file for unit moment pipe loading
POST1_LIN.INP	ANSYS input file for linearized stress extraction
POST1_MAP.INP	ANSYS input file for mapped temperature history extraction
STR_\$_&&_LIN.OUT	ANSYS linearized stress output file for thermal transients, where \$\$ denotes the thermal transient (H1=Heatup H1; H2=Heatup H2; H3=Heatup H3; H4=Heatup H4; H5=Heatup H5; H6=Heatup H6; C1=Cooldown C1; C2=Cooldown C2; C3=Cooldown C3; C4=Cooldown C4; C5=Cooldown C5; C6=Cooldown C6; C7=Cooldown C7; C8=Cooldown C8; IAS=Inadvertent Auxiliary Spray and && denotes the 5 chosen paths (P1=Path 1; P2=Path 2; P3=Path 3; P4=Path 4; P5=Path 5)

File Name	Description
STR_PRESS_&&_LIN.OUT	ANSYS linearized stress output file for unit internal pressure loading, where && denotes the 5 chosen paths (P1=Path 1; P2=Path 2; P3=Path 3; P4=Path 4; P5=Path 5)
STR_FY_&&_LIN.OUT	ANSYS linearized stress output file for unit axial spray pipe loading, where && denotes the 5 chosen paths (P1=Path 1; P2=Path 2; P3=Path 3; P4=Path 4; P5=Path 5)
THM_\$\$_&&_TEMP.OUT	ANSYS mapped temperature history output file for thermal transients, where \$\$ denotes the thermal transient (H1=Heatup H1; H2=Heatup H2; H3=Heatup H3; H4=Heatup H4; H5=Heatup H5; H6=Heatup H6; C1=Cooldown C1; C2=Cooldown C2; C3=Cooldown C3; C4=Cooldown C4; C5=Cooldown C5; C6=Cooldown C6; C7=Cooldown C7; C8=Cooldown C8; IAS=Inadvertent Auxiliary Spray and && denotes the 5 chosen paths (P1=Path 1; P2=Path 2; P3=Path 3; P4=Path 4; P5=Path 5)



CALCULATION PACKAGE

File No.: 1700804.315P - REDACTED

Project No.: 1700804

Quality Program Type: ☒ Nuclear ☐ Commercial

PROJECT NAME:

Turkey Point TLAA's for SLR – Component EAF Analyses

CONTRACT NO.:

2000243484, Revision 1

CLIENT:




Florida Power & Light Company

PLANT:

Turkey Point Nuclear Station, Units 3 & 4

CALCULATION TITLE:

Pressurizer Spray Nozzle Fatigue Analysis

Document Revision	Affected Pages	Revision Description	Project Manager Approval Signature & Date	Preparer(s) & Checker(s) Signatures & Date
0	1 - 23	Initial issue	Terry J. Herrmann [TJH] 11/13/2017	Keith R. Evon [KRE] 11/10/2017 Kevin L. Wong [KLW] 11/10/2017
1	1 - 22	Revised to incorporate changes to references.	 Terry J. Herrmann [TJH] 12/7/2017	 Keith R. Evon [KRE] 12/7/2017  Kevin L. Wong [KLW] 12/7/2017
THIS DOCUMENT CONTAINS CLIENT; DESIGN OR SUPPLIER PROPRIETARY INFORMATION. THIS DOCUMENT MAY NOT BE DISCLOSED, WHOLLY OR IN PART, TO ANY THIRD PARTIES WITHOUT THE PRIOR WRITTEN CONSENT OF STRUCTURAL INTEGRITY ASSOCIATES, INC.				

PROPRIETARY INFORMATION NOTICE

THIS DOCUMENT CONTAINS PROPRIETARY INFORMATION. THE CLIENT MAY USE THE INFORMATION CONTAINED IN THIS DOCUMENT SOLELY FOR THEIR PURPOSES. IF THE DOCUMENT IS SUBMITTED TO THE NUCLEAR REGULATORY COMMISSION (NRC), STRUCTURAL INTEGRITY ASSOCIATES, INC. WILL PROVIDE PROPRIETARY AND NON-PROPRIETARY VERSIONS OF THE DOCUMENT FOR NRC USE ALONG WITH THE REQUIRED LETTER STATING THE PERMITTED USE BY THE NRC. THIS DOCUMENT MAY NOT BE DISCLOSED, WHOLLY OR IN PART, TO ANY THIRD PARTIES WITHOUT THE PRIOR WRITTEN CONSENT OF STRUCTURAL INTEGRITY ASSOCIATES, INC.

Note: Proprietary References are identified with a "P" in the SI File Number.

This entire document is considered Proprietary or Proprietary information used in the document is "Bracketed" ({ }).

Table of Contents

1.0	OBJECTIVE	4
2.0	METHODOLOGY	4
2.1	Air Curve Fatigue Usage	4
2.2	Environmentally-Assisted Fatigue Usage.....	6
3.0	DESIGN INPUTS AND ASSUMPTIONS	9
3.1	Stress Calculation	9
3.2	Load Sets	11
3.3	Material Properties.....	12
3.4	Assumptions	14
4.0	FATIGUE CALCULATIONS.....	14
5.0	ENVIRONMENTAL FATIGUE CALCULATIONS.....	16
6.0	RESULTS OF ANALYSIS	16
7.0	CONCLUSIONS AND DISCUSSION	16
8.0	REFERENCES	22

List of Tables

Table 1:	Load Sets as Input to VESLFAT	12
Table 2:	Material Properties as Input to VESLFAT	13
Table 3:	Fatigue Curves.....	14
Table 4:	Detailed Fatigue Usage Results, Path 1, Piping Properties (Run P1i)	17
Table 5:	Detailed Fatigue Usage Results, Path 2, Safe End Properties (Run P2i)	18
Table 6:	Detailed Fatigue Usage Results, Path 5, Nozzle Body Properties (Run P5i).....	19
Table 7:	Detailed U_{en} Results, Path 1, Piping Properties (Run P1i)	20
Table 8:	Detailed U_{en} Results, Path 2, Safe End Properties (Run P2i).....	21

List of Figures

Figure 1.	Summary of Stress Paths.....	10
-----------	------------------------------	----

1.0 OBJECTIVE

The purpose of this calculation package is to perform an ASME Code, Section III fatigue usage calculation for the pressurizer spray nozzle at Turkey Point (PTN) Units 3 and 4.

The calculations will be performed to address the concerns expressed in both NRC RIS 2008-30 [11] (use of all six stress components in the fatigue calculations) and RIS 2011-14 [12] (repeatability of the process of selecting stress peaks and valleys).

2.0 METHODOLOGY

2.1 Air Curve Fatigue Usage

A previous calculation package performed finite element analysis of the thermal and pressure transients and unit piping loads, and provided linearized stresses at multiple locations of interest [1]. Fatigue usage calculations are performed at the inside surface, which is in contact with reactor water and is therefore susceptible to environmentally-assisted fatigue (EAF) effects. Thermal transient stresses are added to stresses due to piping loads, which are linearly scaled based on the magnitude of the loads. Fatigue strength reduction factors (FSRFs) are applied as appropriate.

For the pipe region, excess conservatism is removed by taking guidance from Section 4.3 of NUREG/CR-6260 [4], which states, in part:

7. **Code analysis changes.** Did fatigue requirements change from the ASME Code edition of record for the design basis calculations to the current Code edition? For example, the ΔT_1 term was eliminated from the NB-3600 primary plus secondary stress equation (Equation 10) for piping in the 1977 edition, Summer 1979 addenda of the Code. A corresponding change was made to Table NB-3217-2.

The change in Table NB-3217-2 means that, for piping, stress due to linear radial temperature gradient was reclassified as peak stress. Therefore, the bending stress due to radial temperature gradient is subtracted from the primary plus secondary membrane stress plus bending stress for the applicable transients.

The fatigue calculation uses the methodology of Subarticle NB-3200 of Section III of the ASME Code [2] using the SI-developed VESLFAT program [3]. VESLFAT performs the analysis required by NB-3222.4(e) [2] for Service Levels A and B conditions defined by the user. The VESLFAT program computes the primary plus secondary and total (primary plus secondary plus peak [2, NB-3213.14]) stress ranges for all events and performs a correction for elastic-plastic analysis, if appropriate.

The program computes the stress intensity range based on the stress component ranges for all event pairs [2, NB-3216.2]. The program evaluates the stress ranges for primary plus secondary and primary plus secondary plus peak stress based upon six components of stress (3 direct and 3 shear stresses). Primary plus secondary stress intensity range (S_n) is calculated as [2, Figure NB-3222-1]:

$$S_n = P_L + P_b + P_e + Q, \text{ where}$$

P_L = primary local membrane stress intensity range
 P_b = primary bending stress intensity range
 P_e = secondary expansion stress intensity range
 Q = secondary membrane plus bending stress intensity range

If S_n is greater than $3S_m$, then the total stress range is increased by the factor K_e , as described in NB-3228.5 [2]. S_m is specified as a function of temperature. The input maximum temperature for either state of a load set pair is used to determine S_m from the user-defined values.

When more than one load set is defined for either of the event pair loadings, the stress differences are determined for all of the potential loadings, saving the maximum for the event pair, based on the pair producing the largest alternating total stress intensity (S_{alt}), including the effects of K_e . S_{alt} is calculated as [2, NB-3222.4(e) and NB-3228.5(b)]:

$$S_{alt} = (K_e S_p / 2) (E_c / E_a), \text{ where}$$

K_e = strain concentration factor
 S_p = primary plus secondary plus peak (total) stress intensity range
 E_c = modulus of elasticity shown on applicable fatigue curve
 E_a = modulus of elasticity used in the analysis, conservatively taken at the maximum input temperature for both sets of a load set pair

The principal stresses for the stress ranges are determined by solving for the roots of the cubic equation:

$$S^3 - (\sigma_x + \sigma_y + \sigma_z)S^2 + (\sigma_x \sigma_y + \sigma_y \sigma_z + \sigma_z \sigma_x - \tau_{xy}^2 - \tau_{xz}^2 - \tau_{yz}^2)S - (\sigma_x \sigma_y \sigma_z + 2 \tau_{xy} \tau_{xz} \tau_{yz} - \sigma_z \tau_{xy}^2 - \sigma_y \tau_{xz}^2 - \sigma_x \tau_{yz}^2) = 0$$

The stress intensity ranges for the event pairs are reordered in decreasing order of S_{alt} , including a correction for the ratio of modulus of elasticity (E) from the fatigue curve divided by E from the analysis. This allows a fatigue table to be created to eliminate the number of cycles available for each of the events of an event pair, allowing determination of fatigue usage per NB-3222.4(e) [2]. For each load set pair in the fatigue table, the allowable number of cycles is determined based on S_{alt} .

Unless justified otherwise, transients that consist of multiple extreme stress conditions (local maximum, or peak, and local minimum, or valley) are split so that each significant, extreme condition is treated as a separate event. The total stresses (primary plus secondary plus peak) are calculated and plotted versus time. Potential peaks and valleys are identified based on the change in sign of the slope of any of the three principal stresses. Intermediate peaks or valleys that produce obvious alternating stress intensities below the fatigue curve endurance limit are negligible and may therefore be filtered out (not split separately). If multiple peaks result from different principal stresses peaking at slightly different times due to the thermal response behavior of the location, then the peaks are determined to be simultaneous and are therefore grouped into a single event. Peaks and valleys in pressure vessels and piping are typically associated with upward and downward temperature or pressure ramps or abrupt changes in temperature slopes.

2.2 Environmentally-Assisted Fatigue Usage

In accordance with Section X.M1 of the DRAFT generic aging lessons learned report for subsequent license renewal (GALL-SLR) [13], F_{en} methodology from DRAFT revision 1 of NUREG/CR-6909 [14, Appendix A] is used as appropriate for the material for each location. The expressions are:

For carbon and low alloy steel:
$$F_{en} = \exp((0.003 - 0.031 \dot{\epsilon}^*) S^* T^* O^*) \quad (1)$$

where:

$S^* = 2.0 + 98 S$	for sulfur content, $S, \leq 0.015$ wt. %
$= 3.47$	for $S > 0.015$ wt. %
$T^* = 0.395$	for service temperature, $T < 150^\circ\text{C}$
$= (T - 75)/190$	for $150 \leq T \leq 325^\circ\text{C}$
$O^* = 1.49$	for dissolved oxygen, $DO < 0.04$ parts per million (ppm)
$= \ln(DO/0.009)$	for $0.04 \text{ ppm} \leq DO \leq 0.5 \text{ ppm}$
$= 4.02$	for $DO > 0.5 \text{ ppm}$
$\dot{\epsilon}^* = 0$	for strain rate, $\dot{\epsilon} > 2.2\%/ \text{sec}$
$= \ln(\dot{\epsilon}/2.2)$	for $0.0004 \leq \dot{\epsilon} \leq 2.2\%/ \text{sec}$
$= \ln(0.0004/2.2)$	for $\dot{\epsilon} < 0.0004\%/ \text{sec}$

For wrought and cast austenitic stainless steel (SS):
$$F_{en} = \exp(-T' \dot{\epsilon}' O') \quad (2)$$

where:

$T' = 0$	for service temperature, $T < 100^\circ\text{C}$
$= (T - 100)/250$	for $100^\circ\text{C} \leq T < 325^\circ\text{C}$
$\dot{\epsilon}' = 0$	for strain rate, $\dot{\epsilon} > 10\%/ \text{sec}$
$= \ln(\dot{\epsilon}/10)$	for $0.0004 \leq \dot{\epsilon} \leq 10\%/ \text{sec}$
$= \ln(0.0004/10)$	for $\dot{\epsilon} < 0.0004\%/ \text{sec}$
$O' = 0.29$	for dissolved oxygen (DO) $< 0.1 \text{ ppm}$
$= 0.29$	for sensitized high-carbon wrought and cast SS, any DO
$= 0.14$	for $DO \geq 0.1 \text{ ppm}$, all wrought SS except sensitized high-carbon SS

For Ni-Cr-Fe alloys:
$$F_{en} = \exp(-T' \dot{\epsilon}' O') \quad (3)$$

where:

$T' = 0$	for service temperature, $T < 50^\circ\text{C}$
$= (T - 50)/275$	for $50 \leq T \leq 325^\circ\text{C}$
$\dot{\epsilon}' = 0$	for strain rate, $\dot{\epsilon} > 5.0\%/ \text{sec}$
$= \ln(\dot{\epsilon}/5.0)$	for $0.0004 \leq \dot{\epsilon} \leq 5.0\%/ \text{sec}$
$= \ln(0.0004/5.0)$	for $\dot{\epsilon} < 0.0004\%/ \text{sec}$
$O' = 0.14$	for dissolved oxygen (DO) $< 0.1 \text{ ppm}$
$= 0.06$	for $DO \geq 0.1 \text{ ppm}$

For each material type, there is a strain amplitude threshold below which $F_{en} = 1.0$: 0.07% strain amplitude or 21.0 ksi stress amplitude for carbon steel and low alloy steel, and 0.10% strain amplitude or 28.3 ksi stress amplitude for SS and Ni-Cr-Fe [14, pp. A-1 to A-3].

Average temperature may be used for simple transients with a linear temperature response [14, p. A-6]. To avoid calculating an F_{en} that is too low, the applicable F_{en} formula threshold temperature (for example, 100°C for SS materials) is applied before averaging.

For load set pairs that contain dynamic loading, such as operating basis earthquake (OBE), the fatigue usage caused by the dynamic portion of the strain for that load pair has an F_{en} value of 1.0 [15, Section 4.2.6]. The effective F_{en} is then calculated as a weighted average of the value without dynamic loads and the value that is applicable for dynamic loads only (that is, 1.0).

The EAF usage factor, U_{en} , is determined as $U_{en} = (U) (F_{en})$, where U is the fatigue usage. F_{en} is typically calculated separately for each load set pair in a fatigue usage analysis, although a bounding F_{en} value may be used. For locations where EAF does not apply, $F_{en} = 1.0$ and $U_{en} = U$.

Section 4.6.4 of EPRI report [7] shows a modified rate approach to calculate F_{en} . The modified rate is described in NUREG/CR-6909 [14, Section 4.4]. NUREG/CR-6909 indicates that the modified rate approach, without the consideration of a strain threshold, gives the best estimates of life [14, Section 4.4, p. 4-75].

The F_{en} for a stress cycle is computed as:

$$F_{en} = \frac{\sum_{i=2}^n F_{en,i} \Delta \varepsilon_i}{\sum_{i=2}^n \Delta \varepsilon_i}$$

where:

- $F_{en,i}$ = F_{en} computed at Point $i = \text{fn}(\dot{\varepsilon}_i, T'_i \text{ or } T^*_i, O'_i \text{ or } O^*_i, S'_i \text{ or } S^*_i)$. This function is specific to the applicable regulatory document and the material of interest.
- n = Number of time points in the stress cycle.
- i = The collection of points (n) for the stress cycle, where the time increases with increasing i .
- $T'_i \text{ or } T^*_i$ = $\text{fn}(T)$, where T = maximum metal temperature of the current (i) and previous ($i-1$) time steps. This function is specific to the applicable regulatory document and the material of interest.
- $O'_i \text{ or } O^*_i$ = $\text{fn}(\text{DO})$, where DO is the dissolved oxygen level. This function and the DO value to use are specific to the applicable regulatory document material of interest.
- $S'_i \text{ or } S^*_i$ = $\text{fn}(S)$, where S is the sulfur content of the material. This function and the S value to use are specific to the applicable regulatory document and the material of interest.
- $\dot{\varepsilon}_i$ = Strain rate at Point i , %/sec

$$\begin{aligned} &= \Delta \varepsilon_i / \Delta t \cdot 100\% \\ \Delta t &= \text{Change in time at Point i, sec} \\ &= t_i - t_{i-1} \\ \Delta \varepsilon_i &= \text{Change in strain at Point i, in/in.} \end{aligned}$$

$\Delta \varepsilon_i$, based on all six components of the stress tensor, is computed by performing the following procedure.

First, the principal stress ranges and stress intensity range from Point i-1 to Point i are computed per NB-3216.2 [2], which uses all six stress components and considers the possibility of varying principal stress directions. Total P+Q+F stresses are used in the calculation of strain rate.

$$\begin{aligned} &= \frac{\begin{matrix} \sigma_{x,i} & \sigma_{y,i} & \sigma_{z,i} & \sigma_{xy,i} & \sigma_{yz,i} & \sigma_{xz,i} \\ \sigma_{x,i-1} & \sigma_{y,i-1} & \sigma_{z,i-1} & \sigma_{xy,i-1} & \sigma_{yz,i-1} & \sigma_{xz,i-1} \end{matrix}}{\begin{matrix} \sigma'_x & \sigma'_y & \sigma'_z & \sigma'_{xy} & \sigma'_{yz} & \sigma'_{xz} \end{matrix}} \end{aligned}$$

From σ'_x , σ'_y , etc. the principal stress ranges (σ'_1 , σ'_2 , σ'_3) and stress intensity range σ'_I are computed. Per convention, σ'_1 , σ'_2 , and σ'_3 are reordered so that $\sigma'_1 \geq \sigma'_2 \geq \sigma'_3$.

The sign of the principal total stress range from Point i-1 to i with the largest absolute value determines whether the strain increment is primarily increasingly tensile or increasingly compressive in nature.

The increasingly tensile change in strain, or the strain increment, $\Delta \varepsilon_i$, is computed as follows.

$$\Delta \varepsilon_i = \begin{cases} \frac{\sigma'_I}{E(T_{\min})} K_e & \text{if } Sgn = 1 \text{ and } range(S_i, S_v) > max_range \\ 0 & \text{Otherwise} \end{cases}$$

where:

$$Sgn = \begin{cases} \text{sgn}(\sigma'_1) & \text{if } |\sigma'_1| \geq |\sigma'_3| \\ \text{sgn}(\sigma'_3) & \text{Otherwise} \end{cases}$$

$\text{sgn}(\sigma) =$ The sign (-1 or +1) of σ .

$K_e =$ Plastic penalty factor for the load pair, based on previously performed NB-3228.5 [2] Simplified Elastic-Plastic Analysis. It is conservative to assume that $K_e = 1.0$. K_e used in the strain rate calculation shall not be greater than K_e used in the fatigue analysis for the stress cycle under consideration.

$E(T_{\min})$ = Elastic modulus at the minimum temperature, T_{\min} , of the current (i) and previous (i-1) time points. As a conservative alternative, the elastic modulus of the fatigue curve may be used.

S_i = Stress at (time) Point i.

S_v = Stress at the closest valley preceding Point i.

$range(S_i, S_v)$ = range function from Section 3.3.1 of Reference [7].

max_range = the largest range $range(S_j, S_v)$ for any stress value S_j between S_v and S_{i-1} .

The check against max_range is used because stresses computed using real data can have a large number of small reversals that are not peaks and valleys. This condition prevents the method from integrating over many small increments that do not increase the overall tensile strain range of the stress cycle.

Note that if the stress cycle under consideration is composed of two extreme stress states that are not chronologically continuous (e.g. the peak of one transient pairs with the valley of a different one), then the strain increment and strain rate within the discontinuity should not be considered in the F_{en} formulation (i.e., $\Delta\epsilon_i=0$).

3.0 DESIGN INPUTS AND ASSUMPTIONS

3.1 Stress Calculation

Linearized stress components at the inside surface of the linearization paths are used for the fatigue usage analysis. Stress linearization output file names have the extension “.OUT” [1]. The stress components from the thermal stress analyses are combined with stress components due to pressure and piping moments [1, 8]. Paths are defined as follows, as shown in Figure 1, which is obtained from [1, Figure 11]:

1. Centerline of safe end to piping butt weld: 1 to 3985
2. Geometric discontinuity in safe end: 138 to 117
3. Nozzle to safe end weld: 379 to 357
4. Geometric transition in nozzle: 518 to 1116
5. Nozzle corner: 844 to 1715

}

Figure 1. Summary of Stress Paths

FSRFs are applied to the primary plus secondary membrane plus bending stress components (P+Q) to yield total (primary plus secondary plus peak) stress components (P+Q+F). These FSRFs are conservatively applied to all six components (three normal, three shear) of the stress tensor.

For Path 1, the girth butt weld is assumed to be flush. For Unit 3, this assumption is justified because it has been inspected previously [6]. For Unit 4, no inspection has been performed [6]. An FSRF of 1.1 is chosen by taking guidance from the local stress indices (K indices) from NB-3600, for a flush girth butt weld [2, Table NB-3681(a)-1].

For the discontinuity at Path 2, the finite element model accounts for at least some portion of the peak stress caused by the notch. A stress concentration factor (K_t) was calculated based on a formulation in Reference

[9, p. 313]. The equation for K_t is shown below and is applicable for calculating stress concentration factors at a variable thickness transition section in a cylindrical vessel.

$$K_t = \frac{2 \tan \alpha}{\left(\alpha + \frac{1}{2} \sin 2\alpha\right)}$$

Where α is the angle of the taper. Using $\tan(\alpha) = \{ \quad \}$, based on the Reference [10] drawing, K_t is calculated to be $\{ \quad \}$.

To estimate the extent to which the finite element model accounts for at least some portion of the peak stress caused by the notch, the ratio of the total axial (SY) stress to the membrane axial stress was determined from the results in the ANSYS output file (unit moment) *STR_FY_P2_LIN.OUT*. This ratio is $176.3 / 92.78 = 1.9$. Therefore, based on the formulation above, the finite element model contains sufficient conservatism to account for peak stresses caused by the notch. An additional FSRF of 1.23 is applied for conservatism.

Paths 4 and 5 are through carbon steel material and therefore subject to different environmentally assisted fatigue formulas than the other locations. Path 5 has slightly higher stresses than path 4 and will therefore be evaluated. There is no weld or discontinuity at Path 5 so no FSRF need be applied.

Paths 3 and 4 were not explicitly analyzed. A review of the thermal stresses demonstrated that they were significantly lower than the stresses for Paths 1 and 2. Thermal stresses for Paths 3, 4 and 5 are each mitigated due to the presence of a thermal sleeve. Path 5 is included in the evaluation as it is carbon steel material and subject to different environmentally assisted fatigue formulas than Paths 1 or 2.

For thermal stresses, the peak stress components are added back into the total stress to capture the peak stress due to nonlinear radial temperature gradient, as follows:

$$P+Q+F = (\text{ANSYS membrane plus bending})\text{FSRF} + \text{ANSYS peak}$$

For the cylindrical Path 1 piping location, the distinction between radial and axial thermal gradient is easily made, because the axial thermal gradients are negligible. To remove excess conservatism for this location, thermal bending due to linear radial temperature gradient is removed in accordance with the piping rules for stress classification in Table NB-3217-2 [2]. However, for the other paths, the stresses result from a combination of both axial and radial thermal gradients. In addition, for the paths in the nozzle classified as vessel locations (as opposed to piping), the linear radial thermal gradient stresses must be secondary, per Table NB-3217-1. Therefore, for Path 2, the linear portions of thermal stresses were conservatively considered to be secondary stresses.

3.2 Load Sets

Table 1 shows the number of cycles for each event analyzed for 80 years of plant operation. The numbers of cycles in Table 1 are from the Reference [8] loads calculation, except as noted, and are entered in VESLFAT input files with extension CYC. Heatup – H1 includes 60 cycles of MOP heatup. Cooldown – C6 includes 60 cycles of MOP cooldown.

Table 1: Load Sets as Input to VESLFAT

Load Set	Transient	Description	Abbreviation	U3 Cycles	U4 Cycles
{					
}					

Table Notes:

1. Includes 76 cycles of MOP Heatup for Unit 3 and 84 cycles for Unit 4.
2. Includes 77 cycles of MOP Cooldown for Unit 3 and 85 cycles for Unit 4.

3.3 Material Properties

Material properties are entered in VESLFAT input files with extension FDT. Table 2 lists the temperature-dependent material properties for use in the fatigue usage analysis [2, Section II Part D], and Table 3 lists the fatigue curves for the materials [14, Table A.2]. VESLFAT automatically scales the stresses by the ratio of E_{curve} to E_{analysis} (See Section 2.0), for purposes of determining allowable numbers of cycles, as required by the ASME Code.

Other material properties are input as follows:

Stainless Steel Safe End and Weld:

$m = 1.7$, $n = 0.3$, parameters used to calculate K_e [2, Table NB-3228.5(b)-1]

$E_{\text{curve}} = 28,300$ ksi [2, Appendix I, Figure I-9.2.1] [14, Appendix A, Figure A-1]

Carbon Steel Nozzle Body:

$m = 3.0$, $n = 0.2$, parameters used to calculate K_e [2, Table NB-3228.5(b)-1]

$E_{\text{curve}} = 30,000$ ksi [2, Appendix I, Figure I-9.1] [14, Appendix A, Figure A-1]

(Note: VESLFAT Inputs labeled “Max membrane stress per psi applied pressure”, “NB-3222.5(b) limit on S_y if large number of cycles”, and S_y values are not used in this analysis.)

Table 2: Material Properties as Input to VESLFAT

Material	T, °F	$E_{analysis}$, ksi	S_m, ksi
SA216 WCC (Carbon Steel) Nozzle Body	40	29,400	23.3
	70	29,400	23.3
	200	28,800	23.2
	300	28,300	22.4
	400	27,900	21.6
	500	27,300	20.6
	600	26,500	19.4
	700	25,500	18.1
SA376 Tp. 316 (16Cr-12Ni-2Mo) Spray Piping	40	28,300	20.0
	70	28,300	20.0
	200	27,500	20.0
	300	27,000	20.0
	400	26,400	19.3
	500	25,900	18.0
	600	25,300	17.0
	700	24,800	16.3
SA182 Tp. 316 (16Cr-12Ni-2Mo) Safe End	40	28,300	20.0
	70	28,300	20.0
	200	27,500	20.0
	300	27,000	20.0
	400	26,400	19.3
	500	25,900	18.0
	600	25,300	17.0
	700	24,800	16.3

Table 3: Fatigue Curves

Number of Cycles	S _a , ksi Austenitic	S _a , ksi Carbon Steel
10	870	777
20	624	556
50	399	364
100	287	264
200	209	197
500	141	136
1000	108	106
2000	85.6	84.7
5000	65.3	65.4
10000	53.4	54.1
20000	43.5	44.2
50000	34.1	34.5
100000	28.4	29.2
200000	24.4	25.5
500000	20.6	22.3
1000000	18.3	20.6
2.E+06	16.4	18.9
5.E+06	14.8	17.4
1.E+07	14.4	16.7
2.E+07		16.0
5.E+07		15.2
1.E+08	14.1	14.7
1.E+09	13.9	13.1
1.E+10	13.7	11.7
1.E+11	13.6	10.4

3.4 Assumptions

For Path 1, the girth butt weld is assumed to be flush. For Unit 3, this assumption is justified because it has been inspected previously [6]. For Unit 4, because no inspection has been performed [6], the flush weld assumption requires FPL confirmation.

4.0 FATIGUE CALCULATIONS

VESLFAT stress input is calculated in Excel workbooks *StressComboPath?i.xls*, where "?" represents the path number. These files contain one sheet per transient, plus a sheet at the end containing the stress input to VESLFAT.

- Input: Columns A through O of each transient sheet contain input as follows:
 - Folder containing ANSYS output files
 - Transient name
 - Minimum temperature, °F
 - Inside node number (for specifying the path)
 - Surface (inside or outside)
 - Magnitude of unit pressure, psi

- Flag for whether this is a piping location with no through-wall bending stress due to axial temperature gradient; if set to 1, then P+Q stress will not include thermal transient bending stress
 - File names for thermal, pressure, and other stresses
 - Overall scaling factors
 - FSRFs; if FSRFs are not used, this is set to 1
 - Time-dependent scaling factors for pressure and other stresses
- **ANSYS Output:** When the Stress Combo macro is run, columns P through AI of the active transient sheet are populated with membrane plus bending and total (membrane plus bending plus peak) stress components (six components each) for unit pressure (one set), other unit loads (one set each), and thermal (several sets since thermal transient stresses are functions of time). The macro reads the stress components from the ANSYS linearization output files, and rearranges them to conform to VESLFAT input format (including switching the shear stress components S_{xz} and S_{yz} as required by VESLFAT).
 - **Combined Results:** When the Stress Combo macro is run, columns AT through BH of the active transient sheet are populated with the following:
 - Name, taken as the first eight characters of the input name plus the time in seconds
 - Combined primary plus secondary and total stress components, calculated using the factors in the Input section and the stress components from the ANSYS output
 - Time-varying metal temperature, from the ANSYS output, used by VESLFAT to determine temperature-dependent properties from the values in Table 2
 - Time-varying pressure, based on the value of unit pressure times the time-varying pressure scaling factor (not used for this analysis)
 - **STR file sheet:** The Make STR macro populates this sheet with the stress components, temperatures, and pressures from the Combined Results portions of the transient sheets. Load set numbers are entered by hand based on review of the stresses and transient definitions (see Table 1) to ensure that multiple peaks in each transient are captured. The sheet is saved as a formatted text file with extension STR, the VESLFAT stress input file.

All VESLFAT input and output files are saved in the project computer files.

Tables 4, 5 and 6 provide detailed results of the VESLFAT runs from VESLFAT output files with extension FAT and rounded appropriately; these runs have file names of the form *P1i.** (for Path 1), *P2i.** (for Path 2), and *P5i.** (for Path 5) where "*" is the extension. There are two cycle files named U3.cyc and U4.cyc as the cycles are the same between paths. Only the cycles for Unit 4 were run as they bound Unit 3. All results presented are based on bounding Unit 4. The fatigue results files are named *P1iU#.fat* (for Path 1), *P2iU#.fat* (for Path 2), and *P5iU#.fat* (for Path 5) where "#" is the unit number.

These calculation results are based on design inputs furnished by FPL/Westinghouse.

5.0 ENVIRONMENTAL FATIGUE CALCULATIONS

The methodology in Section 2.2 is used to calculate F_{en} factors for the three locations based on the material type for those locations.

As shown in Table 4, the usage result for stainless steel Path 1 is less than 0.1. A bounding approach for this location is to calculate F_{en} values on a load pair basis using maximum temperature for that load pair. The U_{en} for this location is 0.410768 as shown in Table 7.

As shown in Table 5, the usage result for stainless steel Path 2 is 0.072149. The resulting U_{en} for this location is 0.528909 as shown in Table 8.

As shown in Table 6, the usage for the carbon steel location, Path 5, is very low. A bounding approach is therefore used in the calculation of F_{en} for this location. In a PWR environment, DO is less than 0.04 ppm so an O^* value of 1.49 is appropriate. Based on a maximum temperature of 653°F, T^* is 1.42. The maximum S^* value is 3.47. The most conservative value of strain rate is -8.613. A bounding F_{en} value for carbon steel is therefore 7.27. The resulting conservative U_{en} for this carbon steel location is $0.0000002 \times 7.27 = 0.00000145$. Note that an F_{en} value of 1.0 could be used as the alternating stress is below the threshold value of 28.3 ksi for all load pairs.

6.0 RESULTS OF ANALYSIS

Usage including the effects of environment is calculated for stainless steel paths 1 and 2 and carbon steel path 5. Tables 4, 5 and 6 provide detailed usage results of the VESLFAT runs from VESLFAT output files with extension FAT and rounded appropriately; these runs have file names of the form $Pl.i.^*$ (for Path 1), $P2i.^*$ (for Path 2), and $P5i.^*$ (for Path 5) where "*" is the extension. Section 5.0 contains the U_{en} results for all three locations. Unit 4 results bound Unit 3, bounding results for both units are as follows:

Location	U	U_{en}
Path 1	0.060962	0.410768
Path 2	0.072149	0.528909
Path 5	0.0000002	0.00000145

Note: The U_{en} for Path 2 considering four IAS events is $0.5289 + 3 \times 0.1249 = 0.9036$.

7.0 CONCLUSIONS AND DISCUSSION

The cumulative fatigue usage, including the effects of EAF, is less than 1.0 for all locations. Stainless steel Path 2 is the bounding location with a cumulative fatigue usage of 0.528909. Since this value is less than the allowable value of 1.0, the ASME Code requirement is met, if actual cycle counts remain within the limits shown in Table 1. As shown in Table 1, only one inadvertent auxiliary spray (IAS) event is projected to occur. The bounding stainless steel Path 2 location can sustain up to four IAS events and remain below an allowable value of 1.0. The U_{en} for Path 2 considering four IAS events is $0.5289 + 3 \times 0.1249 = 0.9036$. U_{en} results are based on NUREG/CR-6909 DRAFT Revision 1 [14].



Table 4: Detailed Fatigue Usage Results, Path 1, Piping Properties (Run P1i)

[illegible]

Table 5: Detailed Fatigue Usage Results, Path 2, Safe End Properties (Run P2i)

I	Load Set A	Load Set B	Cycles	S_n	K_e	S_{alt}	N_{allowed}	Usage
(

								}
								$\Sigma = 0.072149$



Structural Integrity Associates, Inc.[®]

Table 6: Detailed Fatigue Usage Results, Path 5, Nozzle Body Properties (Run P5i)

[illegible]

Table 7: Detailed U_{en} Results, Path 1, Piping Properties (Run P1i)

Max						
I	Load Set A	Load Set B	Usage	Temp (°F)	F _{en}	U _{en}
{						

}						
				$\square =$	0.410768	

Note: 1. From this pair down alternating stress is below the threshold value of 28.3 ksi. See Table 4 and Section 2.2.

Table 8: Detailed U_{en} Results, Path 2, Safe End Properties (Run P2i)

I	Load Set A	Load Set B	Usage	Max Temp (°F)	F_{en}	U_{en}
{						

						}
					<input type="checkbox"/> = 0.528909	

- Notes:
1. The modified rate approach was used to determine F_{en}.
 2. For this pair alternating stress is below the threshold value of 28.3 ksi. See Table 5 and Section 2.2.

8.0 REFERENCES

1. SI Calculation Package, *Pressurizer Spray Nozzle Finite Element Model and Stress Analyses*, Revision 1, SI File No. 1700804.314P, PROPRIETARY.
2. ASME Boiler and Pressure Vessel Code, Section 2007 Edition with Addenda through 2008a.
3. VESLFAT, Version 1.42, 02/06/07, Structural Integrity Associates.
4. NUREG/CR-6260 (INEL-95/0045), *Application of NUREG/CR-5999 Interim Fatigue Curves to Selected Nuclear Power Plant Components*, March 1995.
5. SI Report SIR-00-089, Revision 0, *Position Document to Address GSI-190 Issues Related to Fatigue Evaluation for Turkey Point Units 3 and 4*, July 2000, SI File No. FPL-10Q-401.
6. E-mail from Satyan-Sharma, Tirumani (FPL) to Gilman, Tim (SI), Subject: FW: Pressurizer spray nozzle safe end to piping butt weld, Sent: Tuesday, December 06, 2011 10:46 AM, SI File 1100768.103.
7. *Stress-Based Fatigue Monitoring: Methodology for Fatigue Monitoring of Class 1 Nuclear Components in a Reactor Water Environment*. EPRI, Palo Alto, CA: 1022876.
8. SI Calculation Package, *Pressurizer Spray Nozzle Loads*, Revision 1, SI File No. 1700804.313P, PROPRIETARY.
9. Harvey, J.F., *Theory and Design of Modern Pressure Vessels*, Second Edition, 1974, Van Nostrand Reinhold Company, New York, NY.
10. Westinghouse Design Inputs, LTR-SGMP-11-66, Revision 2, "Turkey Point Units 3 and 4 Data Package for Pressurizer Spray and Surge Nozzle Analysis," October 2011, Attachment 2 of FPL-11-276, PROPRIETARY, SI File No. 1700804.203P.
11. NRC RIS-2008-30, *Fatigue Analysis of Nuclear Power Plant Components*, December 2008.
12. NRC RIS 2011-14, *Metal Fatigue Analysis Performed by Computer Software*, December 2011.
13. NUREG-2191, *Generic Aging Lessons Learned for Subsequent License Renewal (GALL-SLR) Report*, U. S. Nuclear Regulatory Commission, July 2017.
14. NUREG/CR-6909 (ANL-12/60), DRAFT Revision 1, *Effect of LWR Coolant Environments on the Fatigue Life of Reactor Materials*, March 2014.
15. *Materials Reliability Program: Guidelines for Addressing Fatigue Environmental Effects in a License Renewal Application (MRP-47 Revision 1)*. EPRI, Palo Alto, CA: 2005. 1012017.

Enclosure 4
Non-proprietary Reference Documents
and
Redacted Versions of Proprietary
Reference Documents
(Public Version)
Attachment 7

Westinghouse Environmentally Assisted Fatigue Calculations

LTR-SDA-II-17-13-NP, Rev. 2

Environmentally Assisted Fatigue Evaluation of the Turkey Point Unit 3 and Unit 4 Pressurizer Upper Head and Shell and Reactor Vessel Core Support Blocks, November 30, 2017

LTR-CECO-17-025-NP, Rev. 1

Environmentally Assisted Fatigue Evaluation of the Turkey Point Unit 3 and Unit 4 Replacement Steam Generators, November 30, 2017

(8 Total Pages, including cover sheets)



1000 Westinghouse Drive
Cranberry Twp., PA 16066

To: John Ahearn

Date: November 30, 2017

From: Structural Design & Analysis II

Ext: 412-374-4196

Our ref: LTR-SDA-II-17-13-NP, Rev. 2

Fax: 724-940-8565

Subject: Environmentally Assisted Fatigue Evaluation of the Turkey Point Unit 3 and Unit 4 Pressurizer Upper Head and Shell and Reactor Vessel Core Support Blocks

References:

1. Westinghouse Letter, LTR-AMER-MKG-17-1375, Rev. 0, "Westinghouse Offer for Evaluation of Environmentally Assisted Fatigue at Turkey Point Units 3 & 4."
2. Westinghouse Calculation, CN-SDA-II-17-003, Rev. 0, "Turkey Point Units 3 and 4 Subsequent License Renewal Environmentally Assisted Fatigue Evaluation of Pressurizer Upper Head." (Westinghouse Proprietary Class 2)
3. Westinghouse Calculation, CN-SDA-17-5, Rev. 0, "Environmentally Assisted Fatigue Analysis of the Turkey Point Units 3 and 4 Reactor Vessel Core Support Blocks for Subsequent License Renewal." (Westinghouse Proprietary Class 2)
4. US Nuclear Regulatory Commission (NRC) Regulatory Guide, NUREG/CR-6909, Rev. 1 (Draft Report for Comment), "Effect of the LWR Coolant Environments on the Fatigue Life of Reactor Materials."
5. Florida Power & Light Letter, NNPWEC-17-0219, Rev. 0, "Formal Transmittal of Inputs for Westinghouse Evaluation of Environmentally Assisted Fatigue at Turkey Point Units 3 & 4."
6. Electric Power Research Institute (EPRI) Document, "Pressurized Water Reactor Primary Water Chemistry Guidelines," Volume 1, Revision 7, EPRI, Palo Alto, CA: 2014.3002000505.
7. Florida Power & Light Letter, NNPWEC-17-0227, Rev. 0, "Formal Transmittal of Inputs for Westinghouse Evaluation of Environmentally Assisted Fatigue at Turkey Point Units 3 & 4."

The purpose of this letter is to provide the results from the environmentally assisted fatigue (EAF) analysis performed for the Turkey Point Units 3 and 4 pressurizer (PZR) upper head and shell and the reactor vessel (RV) core support blocks in support of Subsequent License Renewal (SLR). This Westinghouse Proprietary Class 2 letter supplements the non-proprietary letter report deliverable outlined in Reference 1. Revision 1 of this letter updated Note 1 under Table 1 for clarity. **Revision 2 of this letter is generated to identify data considered to be proprietary to Westinghouse consistent with the requirements of Westinghouse procedure BMS-LGL-84 for information to be transmitted to the NRC. A "Proprietary Class 2" and "Non-Proprietary Class 3" version of this document is generated as this Revision 2 letter with the designator of "-P" and "-NP" added to the letter number to designate proprietary and non-proprietary, respectively. There is no change to the Revision 1 data as presented.** Revision 2 changes are marked with a vertical bar in the left margin.

Table 1 summarizes the cumulative usage factors (CUF) considering environmental effects (CUF_{en}) from References 2 and 3 applicable for 80 years of operation. CUF_{en} was determined conservatively by applying the appropriate environmental fatigue correction factor (F_{en}) for the material calculated

using the methods from Reference 4 considering the pressurized water reactor (PWR) environment. It is noted that, although Reference 4 is only issued as a draft report for comment, Reference 5 communicates acceptance of this method from Florida Power and Light. Dissolved oxygen content was considered in the F_{en} calculation consistent with the guidelines for PWR primary water chemistry given in Reference 6.

Projected transient cycles for 80 years of operation were also transmitted in Reference 5. It was demonstrated that the current licensing basis transient cycles were bounding for the 80 year projected cycles for all transients. Therefore, current licensing basis transient cycles were used for all fatigue pairings, except where noted in Table 1. Projected cycles were selectively applied to a limited extent to achieve CUF_{en} within the allowable, to maintain conservatism in the evaluation. It is noted that Reference 7 transmits updated projected cycle data for some transients. A review of the updated projected cycle data from Reference 7 demonstrates that the changes do not affect the transients where projected cycles were used in the Reference 2 and 3 evaluations. Therefore, the results presented in Table 1 using projected cycle data from Reference 5 remain valid.

Table 1: PZR Upper Head and Shell and RV Core Support Block EAF Results for SLR

Equipment	Component	Material	CUF	F_{en}	CUF_{en}
PZR	Upper Head and Shell	Low Alloy Steel	[] ^{a,c}	[] ^{a,c}	0.974 ⁽¹⁾
RV	Core Support Blocks	Low Alloy Steel	[] ^{a,c}	[] ^{a,c}	0.910 ⁽²⁾

⁽¹⁾ CUF_{en} was calculated by crediting 80 year projected cycles for station loading at 5% of full power/min and station unloading at 5% of full power/min.

⁽²⁾ CUF_{en} was calculated by crediting 80 year projected cycles for the hydrostatic test at 2485 psig pressure and 400°F temperature.

As shown in Table 1, the CUF_{en} values for the PZR upper head and shell and RV core support blocks are below the allowable value of 1.0 for 80 years of operation and are therefore acceptable for SLR.

If you have any questions, please contact the undersigned.

Author: Elliott L. Burdwood*
Structural Design & Analysis II

Verifier: Gregory M. Imbrogno*
Structural Design & Analysis II

Manager: Benjamin A. Leber*
Structural Design & Analysis II

**Electronically approved records are authenticated in the electronic document management system.*

This page was added to the quality record by the PRIME system upon its validation and shall not be considered in the page numbering of this document.

Approval Information

Author Approval Burdwood Elliott L Dec-01-2017 15:11:17

Verifier Approval Imbrogno Greg M Dec-01-2017 15:16:25

Manager Approval Leber Benjamin A Dec-01-2017 15:45:06

Files approved on Dec-01-2017

*** This record was final approved on 12/1/2017 3:45:06 PM. (This statement was added by the PRIME system upon its validation)



To: John T. Ahearn

Date: November 30, 2017

cc: David P. Lytle
Nicole D. Vitale

From: Kim J. Romanko

Your ref:

Ext: 724-722-5104

Our ref: LTR-CECO-17-025-NP, Rev. 1

Fax: (724) 722-5889

Subject: **Environmentally Assisted Fatigue Evaluation of the Turkey Point Unit 3 and Unit 4 Replacement Steam Generators**

- References:
1. FPL Purchase Order: 2000249045, September 29, 2017. (Attached in EDMS)
 2. Calculation Note: CN-CECO-17-002, Revision 0, "Evaluation of the Turkey Point Units 3 and 4 Divider Plate and Tube Fatigue for an 80-year Plant Life," October 2017. (Westinghouse Proprietary)
 3. FPL Letter: NNPWEC-17-0227, Revision 0, "Formal Transmittal of Inputs for Westinghouse Evaluation of Environmentally Assisted Fatigue at Turkey Point Units 3 & 4," October 17, 2017.
 4. US NRC Regulatory Guide: NUREG/CR-6909, Rev. 1 DRAFT, "Effect of LWR Coolant Environments on the Fatigue Life of Reactor Materials – Draft Report for Comment."
 5. Design Specification: 953362, Revision 3, "Florida Power & Light Turkey Point Units 3 & 4 Replacement Steam Generators – Reactor Coolant System," April 2009.

Revision 1 of this letter is generated to identify data considered to be proprietary to Westinghouse consistent with the requirements of Westinghouse procedure BMS-LGL-84 for information to be transmitted to the NRC. A "Proprietary Class 2" and "Non-Proprietary Class 3" version of this document is generated as this Revision 1 letter with the designator of "-P" and "-NP" added to the letter number to designate proprietary and non-proprietary, respectively. There is no change to the Revision 0 data as presented.

The purpose of this letter is to provide results from the environmentally assisted fatigue (EAF) analysis performed for the Turkey Point Unit 3 and Unit 4 replacement steam generators (RSGs) primary side subcomponents in support of Subsequent License Renewal (SLR). This letter provides the letter report deliverable, outlined in Purchase Order 2000249045, Reference 1.

Described in Reference 1, the screening EAF evaluation is performed for two (2) sentinel RSG locations, divider plate and tubes, for which Westinghouse has the analyses of record (AOR). The EAF analysis, Reference 2, is an internal calculation, from which the results reported below were extracted. The calculation, Reference 2, is based on design transient information provided in Reference 3. Table 1 summarizes the results of the RSG EAF evaluations, including the baseline fatigue cumulative usage factors (CUF), the environmental fatigue correction factors (F_{en}), and the final EAF cumulative usage factors (CUF_{en}) for the critical RSG sub-

components, Reference 1. The analyses documented in Reference 2 were performed considering the F_{en} formulas and fatigue curves from Reference 4. The basis for the CUF_{en} utilizes both design and projected transient cycles, References 5 and 3, respectively. The transient cycles used for the two (2) RSG subcomponents, divider plate and tubes, is provided in Table 2. The transient cycles defined in Table 2 now constitute the RSG design basis for the EAF analysis.

Table 1: EAF Evaluation Results

Equipment	Component	Material	$CUF^{(1)}$	F_{en}	CUF_{en}
RSG	Divider Plate	Ni-Cr-Fe Alloy (SB-168)	[] ^{a,c}	[] ^{a,c}	0.881
RSG	Tubes	Ni-Cr-Fe Alloy (SB-163)	[] ^{a,c}	[] ^{a,c}	0.903

Notes:

1. The CUF is derived by using design and projected design transient cycles defined in Table 2 below.

Table 2: Design and Projected Cycles Used in the EAF Evaluation

Transient	Number of Cycles D-Spec.	Projected Cycles Envelope
Heatup	---	181
Cooldown	---	181
Plant Loading	---	533
Plant Unloading	---	533 ⁽¹⁾
10% Step Load Increase	---	164 ⁽²⁾
10% Step Load Decrease	---	164
Reactor Trip	400	---
50% Step Load Decrease	200	---
Hot Standby	25000	---
Steady-State Fluctuations	Infinite	---
Loss of Flow	80	---
Loss of Load	80	---
Initial Primary Hydro Test	1	---
Subsequent Primary Hydro Test	50	---
Initial Secondary Hydro Test	10	---
Secondary Pressure Test	50	---
Primary/Secondary Leak Test	15	---
Secondary/Primary Leak Test	15	---

Notes:

1. Projected cycle envelope for Turkey Point Unit 3 and 4 is 451 cycles. Conservatively made the number of cycles to be the same as the "Plant Unloading" projected cycles.
2. Projected cycle envelope for Turkey Point Unit 3 and 4 is 82 cycles. Conservatively made the number of cycles to be the same as the "10% Step Load Decrease" projected cycles.

If you have any questions, please contact the undersigned.

Thank you,

Author: Electronically Approved *

Kim J. Romanko
Component Engineering & Chemistry Operations

Verifier: Electronically Approved *

John S. Rees
Component Engineering & Chemistry Operations

Approved: Electronically Approved *

Nicole D. Vitale, Manager
Component Engineering & Chemistry Operations

© 2017 Westinghouse Electric Company LLC
All Rights Reserved

** Electronically Approved Records Are Authenticated in the Electronic Document Management System*

This page was added to the quality record by the PRIME system upon its validation and shall not be considered in the page numbering of this document.

Approval Information

Author Approval Romanko Kim Nov-30-2017 08:56:42

Verifier Approval Rees John Nov-30-2017 10:22:50

Manager Approval Vitale Nicole Nov-30-2017 11:44:53

Files approved on Nov-30-2017

*** This record was final approved on 11/30/2017 11:44:53 AM. (This statement was added by the PRIME system upon its validation)

Enclosure 4
Non-proprietary Reference Documents
and
Redacted Versions of Proprietary
Reference Documents
(Public Version)
Attachment 8

Areva Environmentally Assisted Fatigue Calculations:

Areva Letter No. AREVA-17-02742, dated December 6, 2017

Final CUF_{EN} Results – Turkey Point 3 & 4 – SLR EAF Analyses

1. 32-9280707, Rev. 0, Turkey Point 3 & 4 CRDM Nozzle to Adapter Weld Connection EAF Evaluation, December 15, 2017
2. 32-9280708, Rev. 0, Turkey Point 3 & 4 Replacement RVCH J Groove, December 12, 2017
3. 32-9280709, Rev. 0, 12/15/17, TP CRDM Latch Housing Environmentally Assisted Fatigue, December 15, 2017
4. 32-9280710, Rev. 0, TP Vent Nozzle Environmentally Assisted Fatigue, December 14, 2017
5. 32-9280711, Rev. 0, Turkey Point SLR EAF Analysis for Reactor Vessel Flange, December 14, 2017
6. 32-9280712, Rev. 0, TP CRDM Lower Joint Environmentally Assisted Fatigue, December 15, 2017

(146 Total Pages, including cover sheets)



December 6, 2017
AREVA-17-02742

Mr. William Maher
Sr. Licensing Director
Juno Beach Office
Juno Beach
700 Universe Boulevard
Juno Beach, FL 33408-2657

Subject: Final CUF_{EN} Results – Turkey Point 3 & 4 - SLR EAF Analyses

References: 1. Florida Power & Light Company Purchase Order 2000252727, Revision 1
2. AREVA-17-02624, November 22, 2017, “CUF_{EN} Results – Turkey Point 3 & 4 - SLR EAF Analyses”

Dear Mr. Maher:

Per the reference 1 contract pertaining to the Turkey Point 3 and 4 Subsequent License Renewal (SLR) Environmentally Assisted Fatigue (EAF) Evaluation, AREVA provided FP&L with the reference 2 “partially reviewed” Cumulative Usage Factor Environmental Assisted (CUF_{EN}) results. Listed below is a complete listing of the final CUF_{EN} values. All documents have been reviewed and approved by FP&L.

LOCATION	CUF _{EN} (MAXIMUM) =	AREVA DOCUMENT SOURCE
CRDM Nozzle / J-Groove	0.274	32-9279212-000
CRDM Latch Housing	0.269	32-9279367-000
CRDM Nozzle to Adapter Weld	0.695	32-9279174-000
CRDM Lower Connection	0.420 [Unit 3] 0.749 [Unit 4]	32-9280202-000
RV Flange	0.373	32-9279161-000
RV Vent Nozzle	0.230	32-9279362-000

Note: Maximum Allowable CUF_{EN} = 1.0.

AREVA INC.

3315 Old Forest Road, P.O. Box 10935, Lynchburg, VA 24506-0935
Tel.: (434) 832-3000 - Fax: (434) 832-3840 www.areva.com

The above CUF_{EN} results may be used in FP&L's SLR application without an affidavit as the results alone are considered non-proprietary, even though they were derived from an AREVA proprietary calculation.

Should you have any questions or require additional information, please contact me at 434-832-2341 or by E-mail at Alan.Stalker@areva.com.

Sincerely,



Alan Stalker PE, PMP
Project Manager
IBPE - NSSS Engineering

cc: Mr. Paul Jacobs
Mr. Raul Febre
Records Center T1.2 / F.504146

AREVA INC.

3315 Old Forest Road, P.O. Box 10935, Lynchburg, VA 24506-0935
Tel.: (434) 832-3000 - Fax: (434) 832-3840 www.areva.com



CALCULATION SUMMARY SHEET (CSS)

Document No. 32 - 9280707 - 000

Safety Related: ☒ Yes ☐ No

Title Turkey Point -3 & 4 CRDM Nozzle to Adapter Weld Connection EAF Evaluation – Non-Proprietary

PURPOSE AND SUMMARY OF RESULTS:

Purpose:

The purpose of this document is to calculate the Cumulative Usage Factor for the CRDM Nozzle to Adapter Weld Connection and adjust for Environmentally Assisted Fatigue per NUREG/CR-6909 Rev 1(Reference [1]).

The proprietary version of this document is 32-9279174-001.

Results:

For 80 years plant operation, the CUF criterion is met with $0.695 < 1$ []

If the computer software used herein is not the latest version per the EASI list, AP 0402-01 requires that justification be provided.

THE FOLLOWING COMPUTER CODES HAVE BEEN USED IN THIS DOCUMENT:

CODE/VERSION/REV	CODE/VERSION/REV
_____	_____
_____	_____
_____	_____

THE DOCUMENT CONTAINS ASSUMPTIONS THAT SHALL BE VERIFIED PRIOR TO USE

☐ Yes

☒ No

Turkey Point -3 & 4 CRDM Nozzle to Adapter Weld Connection EAF Evaluation – Non-Proprietary

Review Method: ☒ Design Review (Detailed Check)

☐ Alternate Calculation

Does this document establish design or technical requirements? ☐ YES ☒ NO

Does this document contain Customer Required Format? ☐ YES ☒ NO

Signature Block

Name and Title (printed or typed)	Signature	P/R/A/M and LP/LR	Date	Pages/Sections Prepared/Reviewed/Approved
Caleb Tomlin Engineer II CAFM	David Cofflin for Caleb Tomlin per e-mail David R. Cofflin	P	12/15/17	All
Kaihong Wang Principal Engineer CAFM	[Signature]	R	12/15/17	All
David Cofflin Manager CAFM	David R. Cofflin	A	12/15/17	All

Notes: P/R/A designates Preparer (P), Reviewer (R), Approver (A);
LP/LR designates Lead Preparer (LP), Lead Reviewer (LR);
M designates Mentor (M)

In preparing, reviewing and approving revisions, the lead preparer/reviewer/approver shall use 'All' or 'All except ___' in the pages/sections reviewed/approved. 'All' or 'All except ___' means that the changes and the effect of the changes on the entire document have been prepared/reviewed/approved. It does not mean that the lead preparer/reviewer/approver has prepared/reviewed/approved all the pages of the document.

Project Manager Approval of Customer References and/or Customer Formatting (N/A if not applicable)

Name (printed or typed)	Title (printed or typed)	Signature	Date
N/A	N/A	N/A	N/A

Turkey Point -3 & 4 CRDM Nozzle to Adapter Weld Connection EAF Evaluation – Non-Proprietary

Record of Revision

Revision No.	Pages/Sections/Paragraphs Changed	Brief Description / Change Authorization
000	All	Original Issue. The proprietary version of this document is 32-9279174-001.

Table of Contents

Page

SIGNATURE BLOCK.....	2
RECORD OF REVISION	3
LIST OF TABLES	5
1.0 PURPOSE.....	6
1.1 Background	6
2.0 METHODOLOGY	6
2.1 General Approach to Calculating the F_{en} and Usage Factor.....	6
3.0 ASSUMPTIONS	7
3.1 Unverified Assumptions.....	7
3.2 Justified Assumptions.....	7
4.0 COMPUTER USAGE	7
5.0 INPUTS	7
6.0 ANALYSIS	7
6.1 Evaluation using Existing CUF	7
6.2 Refinement of CUF	8
6.2.1 F_{en} Calculation	8
6.2.2 CUF Considering EAF	11
7.0 CONCLUSION	12
8.0 REFERENCES	12

List of Tables

Page

Table 6-1: Input Data and Stress Difference Calculation.....	9
Table 6-2: Calculation of Various Intermediate Parameters Needed to Determine F_{en}	10
Table 6-3: [.....]	11
Table 6-4: [.....]	12

1.0 PURPOSE

The purpose of this document is to address the concerns of Environmentally Assisted Fatigue for the CRDM Nozzle and Adapter Weld Connection utilizing NUREG/CR-6909 Rev 1 (Reference [1]). The analysis is subsequent to the analysis that was originally performed for the replacement components in Reference [2].

1.1 Background

The ASME Code provides rules for the design of Class 1 components. The Code also provides fatigue design curves for applicable structural materials. However, the curves were developed using in-air testing and did not account for light water reactor coolant environments. Subsequent testing has shown that the LWR environment can substantially reduce fatigue lives for components, [

]

[

]

2.0 METHODOLOGY

- 1.) Evaluate the existing in air cumulative usage factors (CUF) for the reported wetted surface to determine if applying the maximum F_{en} can produce a CUF_{en} less than 1.0.

- 2.) [

]. A

detailed F_{en} will be calculated and applied to the recalculated in-air CUF. The in-air CUF will be recalculated using the updated fatigue curves from NUREG/CR-6909 Rev 1 (Reference [1]).

2.1 General Approach to Calculating the F_{en} and Usage Factor

- (1) Calculate the stress range between time point n-1 and n on the component stresses according to NB-3216.2. The stress ranges are $\sigma'_{ij} = \sigma^{(n)}_{ij} - \sigma^{(n-1)}_{ij}$. The principal stresses ($\sigma_1, \sigma_2, \sigma_3$) are then calculated based on the stress ranges σ'_{ij} , and arranged such that $\sigma_1 \geq \sigma_2 \geq \sigma_3$. The stress intensity (SI) range is then $\sigma_{int} = \sigma_1 - \sigma_3$.
- (2) Calculate the strain range by $\Delta\epsilon_n = \sigma_{int} / E$, where E is the Young's modulus of the material at the average metal temperature between the two time points.
- (3) Calculate the strain rate by $\epsilon'_n = \Delta\epsilon_n / \Delta t_n$, where Δt_n in seconds is the time increment between point n-1 and n.
- (4) Determine whether or not the F_{en} for step n shall be calculated. Since only the strain increment of increasingly tensile is considered (i.e., no negative ϵ' is permitted), the methodology presented in Reference [3] is adopted to determine if the strain range shall be kept:

If $|\sigma_3| \leq |\sigma_1|$, the F_{en} for step n shall be calculated based on the strain rate (Step 3) and other applicable parameters (S^* , T^* and O^*) according to corresponding equations listed in Sub-Section 6.1;

If $|\sigma_3| > |\sigma_1|$, the strain range is excluded in the next step, and no F_{en} is calculated.

- (5) Calculate the F_{en} factor between the two extreme time points of pair number k using the Multi-Linear Strain Based F_{en} approach presented in Reference [1] (Section 6 Equation (68)):

Turkey Point -3 & 4 CRDM Nozzle to Adapter Weld Connection EAF Evaluation – Non-Proprietary

$$F_{en} = \frac{\sum F_{en,i} \Delta \varepsilon_i}{\sum \Delta \varepsilon_i}$$

(6) Calculate the overall CUF with EAF for the location: $U_{en} = F_{en,1}U_1 + F_{en,2}U_2 + F_{en,3}U_3 + \dots$.

3.0 ASSUMPTIONS

3.1 Unverified Assumptions

There are no unverified assumptions within this calculation.

3.2 Justified Assumptions

- 1.) []
- 2.) Transient and External loads as analyzed in Reference [2] are unchanged.
- 3.) []

]

4.0 COMPUTER USAGE

No engineering software is used in this calculation.

5.0 INPUTS

The inputs for this calculation are taken from Reference [2] []

6.0 ANALYSIS

6.1 Evaluation using Existing CUF

Turkey Point -3 & 4 CRDM Nozzle to Adapter Weld Connection EAF Evaluation – Non-Proprietary

Applying the resulting F_{en} to the existing CUF results in a CUF_{en} greater than of 1:

$$F_{en} * CUF = [\quad]$$

This is an unacceptable result and therefore additional analysis is required.

6.2 Refinement of CUF

[] The transients and their combinations which were analyzed in Reference [2] are utilized within this analysis.

[] As stated in NB-3213.17 of the ASME Code “Fatigue strength reduction factor is a stress intensification factor which accounts for the effects of a local structural discontinuity (stress concentration) on the fatigue strength.” []

[]

The existing K_e factor, from Reference [2] Section 5.4.2, of [] is then applied to the maximum Total SI Range of []

[]

6.2.1 F_{en} Calculation

Table 6-1 provides the output from [] in Reference [2] which is used as input for the detailed F_{en} and Table 6-2 calculates the Detailed F_{en} . []

[]

Table 6-1: Input Data and Stress Difference Calculation

Table 6-2: Calculation of Various Intermediate Parameters Needed to Determine Fen

Based on the above calculations for $\Delta\epsilon_n$ and $F_{en} * \Delta\epsilon_n$, the usage factor can be recalculated to account for the EAF.

$$F_{en} = \frac{\sum F_{en,i} \Delta\epsilon_i}{\sum \Delta\epsilon_i} = [\quad]$$

6.2.2 CUF Considering EAF

Table 6-3: []

Table 6-4: []

7.0 CONCLUSION

For 80 years plant operation, the CUF criterion is met with $0.695 < 1$ []

8.0 REFERENCES

1. NUREG/CR-6909, Rev 1, “Effect of LWR Coolant Environments on the Fatigue Life of Reactor Materials,” March 2014 (Draft Report for Comments).
2. AREVA Document, 32-5029862-009, “Turkey Point -3 & 4 CRDM Nozzle to Adapter Weld Connection.”
3. Mark A. Gray, et al., “Strain Rate Calculation Approach in Environmental Fatigue Evaluations,” *Transaction of the ASME Journal of Pressure Vessel Technology*, Vol. 136, August 2014.
4. AREVA Document 38-9279661-000, Formal Transmittal of inputs for Areva Evaluation of Environmentally Assisted Fatigue at Turkey Point Units 3 and 4.



CALCULATION SUMMARY SHEET (CSS)

Document No. 32 - 9280708 - 000

Safety Related: ☒ Yes ☐ No

Title Turkey Point 3 & 4 Replacement RVCH CRDM Nozzle EAF Analysis- Non-Proprietary

PURPOSE AND SUMMARY OF RESULTS:

Purpose: The purpose of this document is to evaluate the Environmentally Adjusted Cumulative Usage Factor (CUF_{en}) at the wetted surface of CRDM nozzle and J-Groove weld for the replacement RVCH at Turkey Point Units 3 and 4.

The proprietary version of this document is 32-9279212-001.

Summary of Results: The $CUF_{en} = 0.274$ [], which meets the criterion of $CUF_{en} < 1.0$.

If the computer software used herein is not the latest version per the EASI list, AP 0402-01 requires that justification be provided.

THE FOLLOWING COMPUTER CODES HAVE BEEN USED IN THIS DOCUMENT:

CODE/VERSION/REV	CODE/VERSION/REV
ANSYS 15.0.7	
StressRange20.exe	

THE DOCUMENT CONTAINS ASSUMPTIONS THAT SHALL BE VERIFIED PRIOR TO USE

☐ Yes

☒ No

Turkey Point 3 & 4 Replacement RVCH CRDM Nozzle EAF Analysis- Non-Proprietary

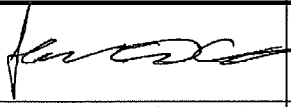
Review Method: ☒ Design Review (Detailed Check)

☐ Alternate Calculation

Does this document establish design or technical requirements? ☐ YES ☒ NO

Does this document contain Customer Required Format? ☐ YES ☒ NO

Signature Block

Name and Title (printed or typed)	Signature	P/R/A/M and LP/LR	Date	Pages/Sections Prepared/Reviewed/Approved
Jasmine Cao Principal Engineer		P	12/12/2017	All
Don Kim Supervisory Engineer	David Cofflin for Don Kim Per e-mail David R. Cofflin	R	12/12/17	All
David Cofflin Manager	David R. Cofflin	A	12/12/17	All

Notes: P/R/A designates Preparer (P), Reviewer (R), Approver (A);
LP/LR designates Lead Preparer (LP), Lead Reviewer (LR);
M designates Mentor (M)

In preparing, reviewing and approving revisions, the lead preparer/reviewer/approver shall use 'All' or 'All except ___' in the pages/sections reviewed/approved. 'All' or 'All except ___' means that the changes and the effect of the changes on the entire document have been prepared/reviewed/approved. It does not mean that the lead preparer/reviewer/approver has prepared/reviewed/approved all the pages of the document.

Project Manager Approval of Customer References and/or Customer Formatting (N/A if not applicable)

Name (printed or typed)	Title (printed or typed)	Signature	Date
N/A	N/A	N/A	N/A

Turkey Point 3 & 4 Replacement RVCH CRDM Nozzle EAF Analysis- Non-Proprietary

Record of Revision

Revision No.	Pages/Sections/Paragraphs Changed	Brief Description / Change Authorization
000	All	Initial Release. The proprietary version of this document is 32-9279212-001.

Table of Contents

	Page
SIGNATURE BLOCK.....	2
RECORD OF REVISION	3
LIST OF TABLES	5
LIST OF FIGURES	6
1.0 INTRODUCTION.....	7
2.0 METHODOLOGY	7
3.0 ASSUMPTIONS	7
3.1 Unverified Assumptions.....	7
3.2 Justified Assumptions.....	7
4.0 DESIGN INPUT	8
4.1 Geometry.....	8
4.2 Finite Element Model.....	9
4.3 Materials.....	9
4.4 Boundary Conditions	10
4.5 Loads.....	10
5.0 COMPUTER USAGE	12
5.1 Software and Hardware.....	12
5.2 Computer files	12
6.0 RESULTS.....	14
6.1 Design Condition	14
6.2 Thermal Analysis Results.....	15
6.3 Structural Analysis Results	17
6.4 Stress from External Load due to OBE	19
6.5 In-Air Fatigue Usage Calculation	19
6.6 CUF _{en} Calculation.....	21
7.0 CONCLUSIONS	22
8.0 REFERENCES	22
APPENDIX A : COMPARISON BETWEEN RESULTS FROM THE ORIGINAL AND NEW MODELS.....	A-1
APPENDIX B : MESH-SENSITIVITY STUDY AND SCF DETERMINATION	B-1

List of Tables

	Page
Table 4-1: [].....	11
Table 4-2: [].....	11
Table 5-1: Computer Files	12
Table 6-1: Nodes of interest for evaluation of temperature gradients.....	16
Table 6-2: Temperature Gradients of Interest.....	16
Table 6-3: Time Points of Interest for the Transients.....	16
Table 6-4: Path Lines – Node Number and Coordinates	17
Table 6-5: [].....	19
Table 6-6: [].....	20
Table 6-7: [].....	20

List of Figures

	Page
Figure 4-1: Finite Element Model.....	9
Figure 6-1: Deformation and Stress Intensity Contours – Design Condition	15
Figure 6-2: Path Lines for Stress Linearization.....	18
Figure A-1: Displacement Contours of the Original (Left) and Refined (Right) FEMs	A-2
Figure A-2: Stress Intensity Contours of the Original (Left) and Refined (Right) FEMs.....	A-2
Figure A-3: Original (Left) vs. Refined (Right) – dT Time History – []	A-3
Figure A-4: Original (Left) vs. Refined (Right) – Temperature Contour – []	A-3
Figure A-5: Original (Left) vs. Refined (Right) – dT Time History – []	A-4
Figure A-6: Original (Left) vs. Refined (Right) – Temperature Contour – []	A-4
Figure B-1: FEM1 vs. FEM2	B-1
Figure B-2: Displacement Contours – FEM1 (Left) vs. FEM2 (Right).....	B-2
Figure B-3: Stress Intensity Contours (Overall) – FEM1 (Left) vs. FEM2 (Right)	B-3
Figure B-4: Stress Intensity Contours (Local) – FEM1 (Left) vs. FEM2 (Right)	B-3
Figure B-5: Stress Comparison of Key Locations – FEM1 (Left) vs. FEM2 (Right)	B-4

1.0 INTRODUCTION

Florida Power & Light Co. (FPL) is planning to submit their License Amendment Request (LAR) for Subsequent License Renewal (SLR = life to 80 years) to the NRC, for the replacement Reactor Vessel Closure Head (RVCH) and Control Rod Drive Mechanisms (CRDM) assembly at Turkey Point 3 and 4. In order to be approved for 80 year life, the NRC requires utilities to address Environmentally-Assisted Fatigue (EAF) at susceptible locations in the RCS.

Six susceptible locations are identified within the replacement RVCH and CRDM assembly as described in the scope document [4].

The purpose of this document is to evaluate the EAF within the replacement CRDM assembly. The scope of the document herein is limited to the wetted surface of the locations evaluated in Reference [3], i.e., the path lines defined on the wetted surface of the nozzle and the J-Groove weld.

2.0 METHODOLOGY

The methodology is outlined below:

- (1) Resurrect the geometry from the existing ANSYS model used in the existing analyses. Redefine the node and element by re-meshing the geometry to meet discretization requirements of the analysis documented herein. Modify the ANSYS input files accordingly and create new ANSYS input files as needed.
- (2) Removal of obvious conservatisms, such as in transient groupings, FSRF, etc., as needed.
- (3) Execute the modified input files with the new database (model) and compare key results to those documented in the previous analyses in order to validate that the modified input file is correct.
- (4) Perform the thermal and structural analyses considered in the previous analysis performed by AREVA.
- (5) Define stress classification path lines and determine the maximum fatigue cumulative usage factor at the wetted surface using the in-air fatigue curve given in NUREG/CR-6909 (Reference [1]). The attempt will be made to calculate the in-air CUF according to the design number of cycles of transients. If the in-air CUF is lower enough that the expected CUF_{en} would meet the criteria of less than 1.0, no further analysis will be performed. []
- (6) Calculate F_{en} , per RG 1.207 Rev. 1 (Reference [2]) and NUREG 6909 Rev. 1 (Reference [1]) for the wetted location having the highest in-air cumulative usage factor (CUF) to arrive at the CUF_{en} for the locations of interest being examined.
- (7) Complete documentation and perform final review.

3.0 ASSUMPTIONS

3.1 Unverified Assumptions

There are no unverified assumptions used for the calculation herein.

3.2 Justified Assumptions

Justified assumptions are listed in the body of the calculation where applicable.

- (1) The CRDM nozzle joint consists of a piece of RV head, a CRDM nozzle, J-Groove weld and a piece of cladding. The cladding is exposed to the fluid. However, since cladding is not a structural component and is assumed to be failed in the analysis herein, it is not evaluated for the EAF requirement.

Turkey Point 3 & 4 Replacement RVCH CRDM Nozzle EAF Analysis- Non-Proprietary

(2) The RV head is not exposed to fluid since it is covered by the cladding on its inside surface. However, since the cladding is assumed to be failed, the head is evaluated against the EAF requirement. This is conservative and acceptable.

(3) [

]

(4) [

]

4.0 DESIGN INPUT

4.1 Geometry

As indicated in Step (1) of Section 2.0, the geometry is from the existing analysis as documented in Reference [3].

[The key dimensions are taken from Reference [3] and listed below for convenience:

RV Head inside radius to base metal = []

RV Head thickness = []

RV Head cladding thickness = []

Penetration diameter = []

CRDM nozzle OD = []

CRDM nozzle ID = []

J-groove outer radius = []

Buttering Weld layer thickness = []

Angle between weld and nozzle = []

4.2 Finite Element Model

The finite element model is shown in Figure 4-1. [

]

The finite element model is documented in database file “TP_CRDM_Model_new.cdb”, in the form of ANSYS commands.

[

]

A mesh sensitivity study is performed and documented in Appendix B. The results show that the discretization of the model, as shown in Figure 4-1, for the regions of interest is able to properly capture the stresses needed for the purpose of the analysis.



Figure 4-1: Finite Element Model

4.3 Materials

Material properties of analyzed components are taken from Reference [3]:

RV Head = []

CRDM nozzle = []

Cladding = []

J-Groove buttering = []

J-Groove filler = []

4.4 Boundary Conditions

The same boundary conditions, as described in Reference [3], are applied to the new finite element model, with the exception of the simulation of the interface between the outside diameter of the nozzle and inside diameter of the head penetration in the thermal analysis:

[

] This is confirmed from the

comparison documented in Appendix A;

[

]

• [

] This is conservative and acceptable;

• [

]

4.5 Loads

The same loads, as documented in Section 3.5 of Reference [3], are used in the analyses performed herein.

External load:

The external loads due to OBE will be used in the fatigue analysis. The OBE loads are taken from Reference [3] and listed below for convenience:

[]

Operating Transient Load:

The heat transfer coefficients used in the thermal analysis are taken from subsection 3.5.3 of Reference [3] and listed below for convenience:

• [

]

• [

]

[

] The same practice is adopted in the analysis

documented herein. The transient loads are taken from Tables 10 through 15 of Reference [3].

[
]

Table 4-1: []

--

Table 4-2: []

--

Note:

--

5.0 COMPUTER USAGE

5.1 Software and Hardware

The finite element analysis documented in this report is performed using ANSYS 15.0.7, Reference [6]. The error notices of this version of ANSYS have been reviewed and concluded that ANSYS 15.0.7 is acceptable to use.

All computer runs are performed on the following computer:

- (1) AUSLYNCHPCI06; Intel® Xeon® CPU E5-2640 v3 @ 2.60GHz; 396 GB RAM; Operating System: Red Hat Enterprise Server v6.4 (Linux); Kernel: 2.6.32-358.el6.x86_64
- (2) Person running the tests: Jasmine Cao
- (3) ANSYS Verification Files Test Date: 11/09/2017 and 11/17/2017.

Table 5-1 lists the ANSYS verification run results. Evaluation of the verification results shows all tests were successful.

5.2 Computer files

The computer files have been uploaded to ColdStor and listed in Table 5-1 below.

Table 5-1: Computer Files

/[cold]/[General-Access]/[32]/[32-9000000]/[32-9279212-000]/[official]/[database]/						
Name	Size	Date/Time Modified	CRC	Perm	Owner	
TP_CRDM_Model_new.cdb	26864121	Oct 31 2017 08:03:55	30205	trw-dc	mocao	
ft_alloy690 ASME 2009.mac	3102	Nov 09 2017 13:16:31	52691	trw-dc	mocao	
ft_sa508Gr3Cl2_psi.mac	2894	Nov 23 2017 20:08:19	14862	-rw-dc	mocao	
/[cold]/[General-Access]/[32]/[32-9000000]/[32-9279212-000]/[official]/[DesignCondition]/						
Name	Size	Date/Time Modified	CRC	Perm	Owner	
TP_CRDM_DesignCond.out	51008	Nov 08 2017 11:01:17	63780	-rw-dc	mocao	
run_DesignCon.inp	8301	Nov 09 2017 13:17:18	16258	-rw-dc	mocao	
/[cold]/[General-Access]/[32]/[32-9000000]/[32-9279212-000]/[official]/[obe]/						
Name	Size	Date/Time Modified	CRC	Perm	Owner	
TP_CRDM_OBE_afterEUP_rough.out	30670	Nov 23 2017 18:18:03	18693	-rw-dc	mocao	
TP_CRDM_OBE_afterEUP_rough_post.Class_Line_Summary(M+B).dat	27089	Nov 24 2017 14:57:33	26783	-rw-dc	mocao	
TP_CRDM_OBE_afterEUP_rough_post.Class_Line_Summary(Total).dat	27132	Nov 24 2017 14:57:07	65014	-rw-dc	mocao	
TP_CRDM_OBE_afterEUP_rough_post.out	168565	Nov 23 2017 18:20:58	41006	-rw-dc	mocao	
post_OBECon.inp	5234	Nov 23 2017 18:18:22	47675	-rw-dc	mocao	
run_OBECon_afterEUP_rough.inp	14307	Nov 23 2017 18:18:23	40666	-rw-dc	mocao	

Turkey Point 3 & 4 Replacement RVCH CRDM Nozzle EAF Analysis- Non-Proprietary

[\[/\[cold\]/\[General-Access\]/\[32\]/\[32-9000000\]/\[32-9279212-000\]/\[official\]/\[ThermalRuns\]/](#)

Name	Size	Date/Time Modified	CRC	Perm	Owner
TP_CD_tr.mac	4807	Nov 09 2017 13:16:13	37189	-rw-dc	mocao
TP_CRDM_CD_th.out	100111	Oct 28 2017 17:41:03	37874	-rw-dc	mocao
TP_CRDM_CD_th_post.out	30523	Oct 29 2017 15:39:50	29678	-rw-dc	mocao
TP_CRDM_HU_th.out	99823	Oct 28 2017 17:41:08	11213	-rw-dc	mocao
TP_CRDM_HU_th_post.out	30351	Oct 29 2017 15:39:47	25226	-rw-dc	mocao
TP_CRDM_PL_th.out	69671	Oct 28 2017 17:41:13	58224	-rw-dc	mocao
TP_CRDM_PL_th_post.out	22439	Oct 29 2017 15:39:42	60093	-rw-dc	mocao
TP_CRDM_PU_th.out	82707	Oct 28 2017 17:41:19	22647	-rw-dc	mocao
TP_CRDM_PU_th_post.out	25363	Oct 29 2017 15:39:38	34787	-rw-dc	mocao
TP_CRDM_RD_th.out	90184	Oct 28 2017 17:41:29	58931	-rw-dc	mocao
TP_CRDM_RD_th_post.out	26395	Oct 29 2017 15:39:25	14819	-rw-dc	mocao
TP_CRDM_RI_th.out	74808	Oct 28 2017 17:41:35	08232	-rw-dc	mocao
TP_CRDM_RI_th_post.out	24331	Oct 29 2017 15:39:19	41424	-rw-dc	mocao
TP_HU_tr.mac	4891	Nov 09 2017 13:16:13	05388	-rw-dc	mocao
TP_PL_tr.mac	5068	Nov 09 2017 13:16:13	52845	-rw-dc	mocao
TP_PU_tr.mac	5119	Nov 09 2017 13:16:13	61354	-rw-dc	mocao
TP_RD_tr.mac	5505	Nov 09 2017 13:16:13	08828	-rw-dc	mocao
TP_RI_tr.mac	4454	Nov 09 2017 13:16:13	00989	-rw-dc	mocao
run_TP_CRDM_th.inp	9721	Nov 09 2017 13:17:08	22899	-rw-dc	mocao
tp_post_th_dt.inp	3348	Nov 09 2017 13:16:41	26948	-rw-dc	mocao

[\[/\[cold\]/\[General-Access\]/\[32\]/\[32-9000000\]/\[32-9279212-000\]/\[official\]/\[StructuralRuns\]/](#)

Name	Size	Date/Time Modified	CRC	Perm	Owner
TP_CD_Pr_tr.mac	4906	Nov 09 2017 13:16:21	36403	-rw-dc	mocao
TP_HU_Pr_tr.mac	4844	Nov 09 2017 13:16:21	63035	-rw-dc	mocao
TP_PL_Pr_tr.mac	5071	Nov 09 2017 13:16:21	28146	-rw-dc	mocao
TP_PU_Pr_tr.mac	5218	Nov 09 2017 13:16:21	22109	-rw-dc	mocao
TP_RD_Pr_tr.mac	5606	Nov 09 2017 13:16:21	48339	-rw-dc	mocao
TP_RI_Pr_tr.mac	4642	Nov 09 2017 13:16:21	11537	-rw-dc	mocao
run_TP_CRDM_st.inp	7206	Nov 09 2017 13:17:05	29923	-rw-dc	mocao
tp_st_CD_post.out	1988277	Nov 09 2017 11:43:54	60709	-rw-dc	mocao
tp_st_HU_post.out	1943753	Nov 09 2017 13:08:09	35270	-rw-dc	mocao
tp_st_PL_post.out	377085	Nov 09 2017 13:08:12	49108	-rw-dc	mocao
tp_st_PU_post.out	511245	Nov 09 2017 13:08:15	10859	-rw-dc	mocao
tp_st_RD_post.out	690469	Nov 09 2017 13:08:17	64995	-rw-dc	mocao
tp_st_RI_post.out	19530	Nov 09 2017 13:08:23	26608	-rw-dc	mocao

Turkey Point 3 & 4 Replacement RVCH CRDM Nozzle EAF Analysis- Non-Proprietary

[/[cold]/[General-Access]/[32]/[32-9000000]/[32-9279212-000]/[official]/[FatigueAnalysis]/						
Name	Size	Date/Time Modified	CRC	Perm	Owner	
ft_80proj_new_2_HEAD_1.dat	4343	Nov 24 2017 14:52:25	28129	-rw-dc	mocao	
ft_80proj_new_2_HEAD_2.dat	4344	Nov 24 2017 14:52:23	32986	-rw-dc	mocao	
ft_80proj_new_8_NPath1.dat	4272	Nov 23 2017 23:17:57	23763	-rw-dc	mocao	
ft_80proj_new_8_NPath2.dat	4269	Nov 23 2017 23:17:48	45901	-rw-dc	mocao	
ft_80proj_new_8_NPath3.dat	4273	Nov 23 2017 23:17:56	31365	-rw-dc	mocao	
ft_80proj_new_8_NPath4.dat	4270	Nov 23 2017 23:17:59	54993	-rw-dc	mocao	
ft_80proj_new_8_NPath5.dat	4273	Nov 23 2017 23:17:47	19896	-rw-dc	mocao	
ft_80proj_new_8_NPath6.dat	4273	Nov 23 2017 23:17:56	13400	-rw-dc	mocao	
ft_80proj_new_8_WPath1.dat	4334	Nov 23 2017 23:17:59	25428	-rw-dc	mocao	
ft_80proj_new_8_WPath2.dat	4330	Nov 23 2017 23:17:55	01699	-rw-dc	mocao	
ft_DesignCycles_2_HEAD_1.dat	4343	Nov 24 2017 19:54:58	19873	-rw-dc	mocao	
ft_DesignCycles_2_HEAD_2.dat	4344	Nov 24 2017 19:54:59	50656	-rw-dc	mocao	
ft_DesignCycles_8_NPath1.dat	4272	Nov 23 2017 23:17:42	53305	-rw-dc	mocao	
ft_DesignCycles_8_NPath2.dat	4269	Nov 23 2017 23:17:45	28411	-rw-dc	mocao	
ft_DesignCycles_8_NPath3.dat	4273	Nov 23 2017 23:17:45	19859	-rw-dc	mocao	
ft_DesignCycles_8_NPath4.dat	4270	Nov 23 2017 23:17:41	32756	-rw-dc	mocao	
ft_DesignCycles_8_NPath5.dat	4273	Nov 23 2017 23:17:42	24348	-rw-dc	mocao	
ft_DesignCycles_8_NPath6.dat	4273	Nov 23 2017 23:17:41	46397	-rw-dc	mocao	
ft_DesignCycles_8_WPath1.dat	4334	Nov 23 2017 23:17:41	34478	-rw-dc	mocao	
ft_DesignCycles_8_WPath2.dat	4330	Nov 23 2017 23:17:41	26886	-rw-dc	mocao	
post_tp_st_CUFair_80proj_new_2.inp	8116	Nov 24 2017 14:40:11	26588	-rw-dc	mocao	
post_tp_st_CUFair_80proj_new_8.inp	13140	Nov 24 2017 13:53:47	20432	-rw-dc	mocao	
post_tp_st_CUFair_DesignCycles_2.inp	8116	Nov 24 2017 14:41:31	36912	-rw-dc	mocao	
post_tp_st_CUFair_DesignCycles_8.inp	13116	Nov 23 2017 23:17:46	32944	-rw-dc	mocao	
tp_st_CUFair_80proj_new_2_3rd_set.fatq	154353	Nov 24 2017 14:52:23	37596	-rw-dc	mocao	
tp_st_CUFair_80proj_new_2_post.out	903611	Nov 24 2017 14:52:26	01502	-rw-dc	mocao	
tp_st_CUFair_80proj_new_8_1st_set.fatq	460537	Nov 23 2017 23:17:59	29255	-rw-dc	mocao	
tp_st_CUFair_80proj_new_8_2nd_set.fatq	154353	Nov 23 2017 23:17:57	27445	-rw-dc	mocao	
tp_st_CUFair_80proj_new_8_post.out	3488557	Nov 23 2017 23:17:59	51319	-rw-dc	mocao	
tp_st_CUFair_DesignCycles_2_3rd_set.fatq	154353	Nov 24 2017 19:55:00	42107	-rw-dc	mocao	
tp_st_CUFair_DesignCycles_2_post.out	903627	Nov 24 2017 19:54:59	00074	-rw-dc	mocao	
tp_st_CUFair_DesignCycles_8_1st_set.fatq	460537	Nov 23 2017 23:17:43	16371	-rw-dc	mocao	
tp_st_CUFair_DesignCycles_8_2nd_set.fatq	154353	Nov 23 2017 23:17:43	15682	-rw-dc	mocao	
tp_st_CUFair_DesignCycles_8_post.out	3488537	Nov 23 2017 23:17:54	38780	-rw-dc	mocao	
[/[cold]/[General-Access]/[32]/[32-9000000]/[32-9279212-000]/[official]/[AppendixA]/						
Name	Size	Date/Time Modified	CRC	Perm	Owner	
TP_CRDM_Model.cdb	8570036	Oct 25 2017 13:12:05	57829	-rw-dc	mocao	
[/[cold]/[General-Access]/[32]/[32-9000000]/[32-9279212-000]/[official]/[AppendixB]/						
Name	Size	Date/Time Modified	CRC	Perm	Owner	
TP_CRDM_Model_scf.cdb	38226580	Nov 03 2017 14:47:16	49463	-rw-dc	mocao	
TP_CRDM_scf.out	50968	Nov 09 2017 13:10:03	22384	-rw-dc	mocao	
[/[cold]/[General-Access]/[32]/[32-9000000]/[32-9279212-000]/[official]/[InstallationVerification]/						
Name	Size	Date/Time Modified	CRC	Perm	Owner	
vm162.out	13894	Nov 09 2017 11:43:41	56665	trw-dc	mocao	
vm246.out	19340	Nov 09 2017 11:43:39	22438	trw-dc	mocao	
vm_vm162_2.out	13904	Nov 29 2017 14:28:27	35677	-rw-dc	mocao	
vm_vm246_2.out	19350	Nov 29 2017 14:28:29	17137	-rw-dc	mocao	

6.0 RESULTS

6.1 Design Condition

Stress analysis under the design pressure is performed to verify the behavior of the new model is as expected. The design condition stress analysis is documented in ANSYS output file “TP_CRDM_DesignCond.out”.

Turkey Point 3 & 4 Replacement RVCH CRDM Nozzle EAF Analysis- Non-Proprietary

Figure 6-1 shows the model deformation and stress intensity contours of the model under the design pressure. It is seen that the deformation and the stress intensity distribution of the model are as expected.

Figure 6-1: Deformation and Stress Intensity Contours – Design Condition

6.2 Thermal Analysis Results

Thermal analysis is performed using the enveloped or grouped transients as documented in Reference [3].

The transient loads are documented in the ANSYS input files “TP_*_tr.mac”, where * represents the name of the transients, i.e., []

The thermal analysis is documented in ANSYS output files “TP_CRDM_*_th.out”, where * represents the name of the transients, i.e. []

The results of the thermal analysis are evaluated to identify the peaks and valleys of the temperature gradients time history between key locations of interest. The temperature distributions at the time points of these peaks and valleys are used as temperature loads in the structural analysis to calculate thermal stresses.

The same key locations as those documented in Reference [3] are selected for temperature gradient evaluation. Due to re-discretization of the finite element model, node numbers are different from the original document. Table 6-1 summarizes the nodes of interest for evaluation of temperature gradients. The temperature gradients of the same pairs of the locations, as documented in Table 17 of Reference [3], are used in the evaluation. The temperature gradient of interest is summarized in Table 6-2 for convenience.

The temperature gradient evaluation is documented in the ANSYS output files “TP_CRDM_*_th_post.out”, where * represents the name of the transients, i.e. []

Besides the time points when the extrema occur in the temperature gradient time history, the time points when the pressure time history start, change, or end are also selected in the structural analysis. The time points to be used for structural analysis are summarized in Table 6-3.

[]

Table 6-1: Nodes of interest for evaluation of temperature gradients

Table 6-2: Temperature Gradients of Interest

Table 6-3: Time Points of Interest for the Transients

In addition, the results from the thermal analysis are compared to the results from the original analysis. The comparison shows that the results from the new model are in agreement with the original results. The comparison is documented in Appendix A.

6.3 Structural Analysis Results

Structural analysis is performed to calculate the stresses due to thermal and pressure transient loads.

The transient loads and the time points are documented in ANSYS files “TP_*_Pr_tr.mac”, where * represents the name of the transients, i.e. [] Note that the transient data stored in these files are exactly the same as those for thermal transient analysis, except the time points at which analysis is to be performed are different.

The analysis is documented in ANSYS output files “tp_st_*.out

The path lines for stress linearization are shown in Figure 6-2 and listed in Table 6-4.

Table 6-4: Path Lines – Node Number and Coordinates

Note: * These nodes are not located on the wetted surface (refer to Figure 6-2) and the cumulative usage factors of these nodes are not calculated and reported in the document herein.

The figure area is a large, empty rectangular frame with a black border, intended for the visualization of path lines for stress linearization.

Figure 6-2: Path Lines for Stress Linearization

6.4 Stress from External Load due to OBE

Stresses due to OBE external loads are calculated and documented in ANSYS output file “TP_CRDM_OBE_afterEUP_rough.out”. The stresses for each path line is extracted and documented in “TP_CRDM_OBE_afterEUP_rough_post.out”. The stress intensity range is calculated using EASI list engineering tool StressRange20.exe (Reference [7]) and documented in following files:

- “TP_CRDM_OBE_afterEUP_rough_post.Class_Line_Summary(M+B).dat”
- “TP_CRDM_OBE_afterEUP_rough_post.Class_Line_Summary(Total).dat”

The stress range calculated based on total stress is used in the fatigue calculation. The stress due to OBE load is combined with the stress due to transient loads in the fatigue calculation. [

] This is conservative and acceptable.

6.5 In-Air Fatigue Usage Calculation

ANSYS Fatigue module is utilized to calculate the in-air cumulative usage factor. Total stresses are used in the fatigue calculation for all locations investigated.

Per Appendix B, the discretization of the model is refined enough to properly capture the peak stress of the locations of interest. [

]

The calculation of the maximum in-air CUF is detailed in Table 6-5.

Table 6-5: [

]

Turkey Point 3 & 4 Replacement RVCH CRDM Nozzle EAF Analysis- Non-Proprietary

CUF based on [] :

[

] The maximum in-air CUF occurs at the uphill side of the weld fillet. The calculation is detailed in Table 6-7.

Table 6-6: []

Note: Stress due to OBE load is included in the CUF calculation.

Table 6-7: []

Note:

- (1) This value reflects the number of used cycles for event pair []
- (2) The value is based on the alternating stress including OBE loads;

6.6 CUF_{en} Calculation

As mentioned in Assumption (1) in Subsection 3.2, cladding (stainless steel) is not evaluated for the EAF requirement. The EAF evaluations for J-groove weld and CRDM [] and RV head [] are as follows:

Locations in J-Groove Weld and CRDM Nozzle [] :

The wetted location with the highest in-air CUF is WPATH2, [] The CUF reported in Section 6.5 for this location is [] and the maximum stress intensity range is []

This is an acceptable result and therefore no additional analysis is required.

Locations in Head [] :

The base metal of head does not expose to the fluid. However, it is conservatively assumed that the cladding has crack therefore the inside surface of the head need to be qualified to the EAF criterion.

Turkey Point 3 & 4 Replacement RVCH CRDM Nozzle EAF Analysis- Non-Proprietary

This is an acceptable result and therefore no additional analysis is required.

7.0 CONCLUSIONS

The environmental aided fatigue cumulative usage factor [] is 0.274, which is well below the requirement of 1.0, therefore meet the fatigue criterion.

8.0 REFERENCES

- [1] NUREG/CR-6909, Rev. 1, Effect of LWR Coolant Environments on the Fatigue Life of Reactor Materials, Draft Report for Comment, U.S. NRC
- [2] REGULATORY GUIDE 1.207, Guidelines for Evaluating Fatigue Analyses Incorporating the Life Reduction of Metal Components due to the Effects of the Light-Water Reactor Environment for New Reactors
- [3] AREVA Document, 32-5037379-008, Turkey Point -3 & 4 Replacement RVCH CRDM Nozzle Connection
- [4] AREVA Document 51-9277194-000, Turkey Point Units 3 and 4 Environmentally Assisted Fatigue Evaluation
- [5] AREVA Document 38-9279661-000, Formal Transmittal of inputs for AREVA Evaluation of Environmentally Assisted Fatigue at Turkey Point Units 3 and 4
- [6] ANSYS Release 15.0.7, UP20140420, LINUX x64, ANSYS Inc., Canonsburg, P.A.
- [7] AREVA EASI Software, StressRange2.0.

APPENDIX A: COMPARISON BETWEEN RESULTS FROM THE ORIGINAL AND NEW MODELS

A.1 Background

The original FEM documented Reference [3] is created in ANSYS 7.0. The FEM is able to be loaded in ANSYS 15.0.7. The model has been converted into a database file in the form of ANSYS commands file and uploaded into ColdStor.

The original FEM was meshed in [

] were conservatively used in the fatigue calculation to cover any uncaptured peak stresses due to discretization of the original mesh. In order to remove this conservatism, a refined model is built based on the same geometry as in the original document.

A refined model is created and benchmarked to the original results.

The following comparisons are made between the results from the refined and original FEMs.

- For Design Condition:
 - Total displacement contour;
 - Stress intensity contour;
- For thermal analysis:
 - Differential temperature (dT) time history;
 - Temperature contour comparison for a randomly selected time point.

A.2 Design Condition Comparison

The total displacement and stress intensity contours from the original and the refined FEMs are shown Figure A-1 and Figure A-2.

It is seen from Figure A-1 that the patterns of the displacement contours of the two FEMs are very similar. [

]

It is seen from Figure A-2 that the patterns of the stress intensity contours of the two FEMs are similar. The maximum stress intensities from both models occur at the weld fillet regions. The magnitude of the maximum stress intensity from the refined model is higher than that of the original model, as expected.

Figure A-1: Displacement Contours of the Original (Left) and Refined (Right) FEMs

Figure A-2: Stress Intensity Contours of the Original (Left) and Refined (Right) FEMs

A.3 Thermal Analysis Comparison

The dT time histories and temperature distribution contours at a randomly selected time point for [] transients are shown in Figure A-3, Figure A-4, Figure A-5 and Figure A-6.

It is seen the dT time histories and the temperature distribution from both models are very close, though the transition of temperature contour is smoother for the refined model than that of the original coarse model.

It is concluded that the refined FEM produces comparable (very close) results as the original FEM for the thermal analysis, as expected.

Turkey Point 3 & 4 Replacement RVCH CRDM Nozzle EAF Analysis- Non-Proprietary



Figure A-3: Original (Left) vs. Refined (Right) – dT Time History – []



Figure A-4: Original (Left) vs. Refined (Right) – Temperature Contour – []

Turkey Point 3 & 4 Replacement RVCH CRDM Nozzle EAF Analysis- Non-Proprietary

Figure A-5: Original (Left) vs. Refined (Right) – dT Time History – []

Figure A-6: Original (Left) vs. Refined (Right) – Temperature Contour – []

APPENDIX B: MESH-SENSITIVITY STUDY AND SCF DETERMINATION

B.1 Background

The FEM from the original document has been refined to form the FEM used in the analysis documented herein, in order to properly capture peak stress. This FEM is labeled as FEM1.

Mesh sensitivity study is performed for the regions of interest, i.e., the weld fillet and the CRDM nozzle wall. Two cases are compared:

- Case 1: [] This model is used in the analysis;
- Case 2: [] This model is considered to be able to produce more accurate stresses in the region of interest.

The comparison of the results from the two cases is taken as the base for FSRF determination.

Design pressure produces tensile and bending stresses in the region of interest, therefore is good for use of mesh sensitivity study and FSRF determination.

B.2 The Two Finite Element Models

A comparison of the two FEMs is shown in Figure B-1.



Figure B-1: FEM1 vs. FEM2

B.3 Results and Conclusion

The overall deformations of the two models are shown in

Figure B-2. It is seen that the overall deformation of the two models are comparable, as expected.

The over stress intensity of the two models are shown in Figure B-3. The overall maximum SINT from both FEMs occur at the crevice between the CRDM nozzle and the bore of the head. [

]

Figure B-4 shows the detailed stress intensity distribution at the weld fillet region from the two models. [

]

Figure B-5 shows a comparison of the stress intensities at the key locations of the two models.

It is seen that the differences of the results from the two models are negligible indicating that model FEM1 is good enough for the purposed analysis. [

]

Figure B-2: Displacement Contours – FEM1 (Left) vs. FEM2 (Right)

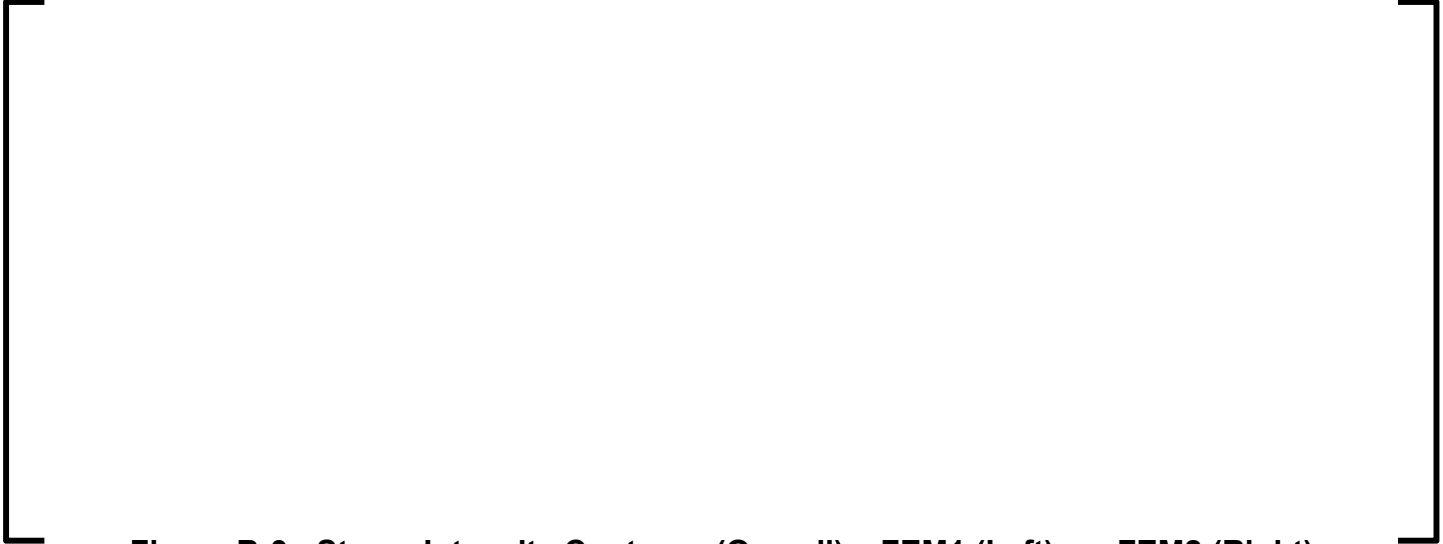
The figure area for Figure B-3 is currently blank, enclosed by a large black L-shaped bracket on the left and top.

Figure B-3: Stress Intensity Contours (Overall) – FEM1 (Left) vs. FEM2 (Right)

The figure area for Figure B-4 is currently blank, enclosed by a large black L-shaped bracket on the left and top.

Figure B-4: Stress Intensity Contours (Local) – FEM1 (Left) vs. FEM2 (Right)



Figure B-5: Stress Comparison of Key Locations – FEM1 (Left) vs. FEM2 (Right)



CALCULATION SUMMARY SHEET (CSS)

Document No. 32 - 9280709 - 000

Safety Related: ☒ Yes ☐ No

Title TP CRDM Latch Housing Environmentally Assisted Fatigue - Non-Proprietary

PURPOSE AND SUMMARY OF RESULTS:

Purpose

The purpose of this calculation is to determine the effects of environmental assisted fatigue on the Latch Housing. The basis used for the determination is DRAFT Regulatory Guide 1.207 and DRAFT NUREG/CR-6909 Revision 1.

The proprietary version of this document is 32-9279367-001.

Results

The results indicate that the Latch Housing fatigue remains acceptable when the Environmental Assisted Fatigue (EAF) is considered. The EAF usage factor is calculated [] and is acceptable. The maximum calculated EAF usage factor including the environmental assisted fatigue is, $U_{en} = 0.269$ []

If the computer software used herein is not the latest version per the EASI list, AP 0402-01 requires that justification be provided.

THE FOLLOWING COMPUTER CODES HAVE BEEN USED IN THIS DOCUMENT:

CODE/VERSION/REV	CODE/VERSION/REV
_____	_____
_____	_____
_____	_____

THE DOCUMENT CONTAINS ASSUMPTIONS THAT SHALL BE VERIFIED PRIOR TO USE

☐ Yes

☒ No

TP CRDM Latch Housing Environmentally Assisted Fatigue - Non-Proprietary




Review Method: ☒ Design Review (Detailed Check)

☐ Alternate Calculation

Does this document establish design or technical requirements? ☐ YES ☒ NO

Does this document contain Customer Required Format? ☐ YES ☒ NO

Signature Block

Name and Title (printed or typed)	Signature	P/R/A/M and LP/LR	Date	Pages/Sections Prepared/Reviewed/Approved
Thomas M. Washko Engineer		P	12-15-2017	All
HT Harrison Advisory Engineer		R	12/15/17	All
David Cofflin Engineering Manager		MA DRC	12/15/17	All

Notes: P/R/A designates Preparer (P), Reviewer (R), Approver (A);
LP/LR designates Lead Preparer (LP), Lead Reviewer (LR);
M designates Mentor (M)

In preparing, reviewing and approving revisions, the lead preparer/reviewer/approver shall use 'All' or 'All except ___' in the pages/sections reviewed/approved. 'All' or 'All except ___' means that the changes and the effect of the changes on the entire document have been prepared/reviewed/approved. It does not mean that the lead preparer/reviewer/approver has prepared/reviewed/approved all the pages of the document.

Project Manager Approval of Customer References and/or Customer Formatting (N/A if not applicable)

Name (printed or typed)	Title (printed or typed)	Signature	Date
N/A			

TP CRDM Latch Housing Environmentally Assisted Fatigue - Non-Proprietary

Record of Revision

Revision No.	Pages/Sections/Paragraphs Changed	Brief Description / Change Authorization
000	All	Original Issue. The proprietary version of this document is 32-9279367-001.

Table of Contents

Page

SIGNATURE BLOCK.....	2
RECORD OF REVISION	3
LIST OF TABLES	5
LIST OF FIGURES	6
1.0 OBJECTIVE	7
2.0 METHODOLOGY	7
2.1 General Approach to Calculating the Fen and EAF Usage Factor	7
2.2 Detailed Method of Calculation of the Fen for Latch Housing.....	7
3.0 ASSUMPTIONS	8
4.0 DESIGN INPUTS	8
5.0 COMPUTER USAGE	8
6.0 CALCULATIONS.....	8
6.1 Transients To Be Evaluated	8
6.2 EXCEL Spreadsheet Calculations	12
7.0 RESULTS.....	20
8.0 REFERENCES.....	21
APPENDIX A : BASIS FOR PRINCIPAL STRESS CALCUATIONS.....	A-1

List of Tables

	Page
Table 6-1: Input Data and Stress Difference Calculation for Transients 3 and 16.....	14
Table 6-2: Calculation of Various Intermediate Parameters Needed to Determine Fen.....	15
Table 6-3 Input Data and Stress Difference Calculation for Transient 1.....	16
Table 6-4 Calculation of Various Intermediate Parameters Needed to Determine Fen for Transient 1	17
Table 6-5: [.....].....	18
Table 6-6: [.....]	19

List of Figures

	Page
Figure 6-1: Time History Stresses for Transients 16 and 3	9
Figure 6-2: Transients 16 and 3 Stress Versus Time	10
Figure 6-3: Strain Versus Time for Two Transients	10
Figure 6-4: Fen Versus Strain for Two Transients	11
Figure 6-5 Time History Stresses for Transients 16 and 1	11
Figure 6-6: S-N Curve Showing Significance of NUREG/CR-6909 to ASME III	20

1.0 OBJECTIVE

The component to be qualified for EAF in this calculation is the CRDM latch housing. Only the inside wetted location is to be considered. A fatigue usage factor is to be calculated considering the EAF and the objective is to obtain a value that is less than 1.0.

2.0 METHODOLOGY

Calculations are performed based on the criteria below, which is based on DRAFT NUREG/CR-6909, Reference [1]. The applicable code is ASME III, 1989 edition with no Addenda Reference [2].

2.1 General Approach to Calculating the Fen and EAF Usage Factor

Time-history stresses are provided for various transients in Reference [3]. From this information, the following procedure is used to calculate the Fen and resulting EAF usage factor.

- (1) Calculate the stress range between time point n-1 and n on the component stresses according to NB-3216.2. The stress ranges are $\sigma'_{ij} = \sigma^{(n)}_{ij} - \sigma^{(n-1)}_{ij}$. The principal stresses ($\sigma_1, \sigma_2, \sigma_3$) are then calculated based on the stress ranges σ'_{ij} , and arranged such that $\sigma_1 \geq \sigma_2 \geq \sigma_3$. The stress intensity (SI) range is then $\sigma_{int} = \sigma_1 - \sigma_3$.
- (2) Calculate the strain range by $\Delta \epsilon_n = \sigma_{int} / E$, where E is the Young's modulus of the material at the average metal temperature between the two time points.
- (3) Calculate the strain rate by $\epsilon'_n = \Delta \epsilon_n / \Delta t_n$, where Δt_n in second is the time increment between point n-1 and n.
- (4) Determine whether or not an F_{en} for step n shall be calculated. Since only the strain increment of increasingly tensile strain is considered (i.e., no negative ϵ' is permitted), the following methodology is adopted to determine if the strain range shall be kept:

If $|\sigma_3| \leq |\sigma_1|$, the F_{en} for step n shall be calculated based on the strain rate (Step 3) and other applicable parameters (S^* , T^* and O^*) according to Eqs. (2), (3) or (4);

If $|\sigma_3| > |\sigma_1|$, the strain range is excluded in the next step, and no F_{en} is calculated.

- (5) Calculate the F_{en} factor between the two extreme time points of pair number k using the "Multi-Linear Strain Based Method" F_{en} approach presented in Reference [1].

$$F_{en,k} = \frac{\sum F_{en,i} \Delta \epsilon_i}{\sum \Delta \epsilon_i} \quad \text{Equation (68) of Reference [1].}$$

- (6) Calculate the overall EAF_{en} usage factor for the location: $U_{en} = F_{en,1}U_1 + F_{en,2}U_2 + F_{en,3}U_3 + \dots$.

2.2 Detailed Method of Calculation of the Fen for Latch Housing

Detailed description of the F_{en} calculation applicable to the latch housing:

3.0 ASSUMPTIONS

No assumptions or Modeling Simplifications were used.

4.0 DESIGN INPUTS

The plant design, past and projected operating information was provided in Reference [3], Reference [5], and Reference [6].

5.0 COMPUTER USAGE

EXCEL spreadsheet only.

6.0 CALCULATIONS

Calculations are performed based on the methodology of Reference [1].

Based on the information provided in Reference [3], the total “in-air” usage factor was calculated to be []
This total usage is mostly from a range between transients 16 and 1, 16 and 3. The stress time-histories are also provided in a table in this same calculation and an example is displayed in the following plot, Figure 6-1. []

6.1 Transients To Be Evaluated

The following transients will be shown to be the contributors to the EAF usage factor:

Figure 6-1: Time History Stresses for Transients 16 and 3

The plots in Figure 6-2 are shown to establish the basis for the strain rate calculations. [

]

Figure 6-2: Transients 16 and 3 Stress Versus Time



An example of two transients to be integrated are shown below in Figure 6-3. The hand-drawn figures below are for demonstration of methodology and do not represent the exact data.

Figure 6-3: Strain Versus Time for Two Transients

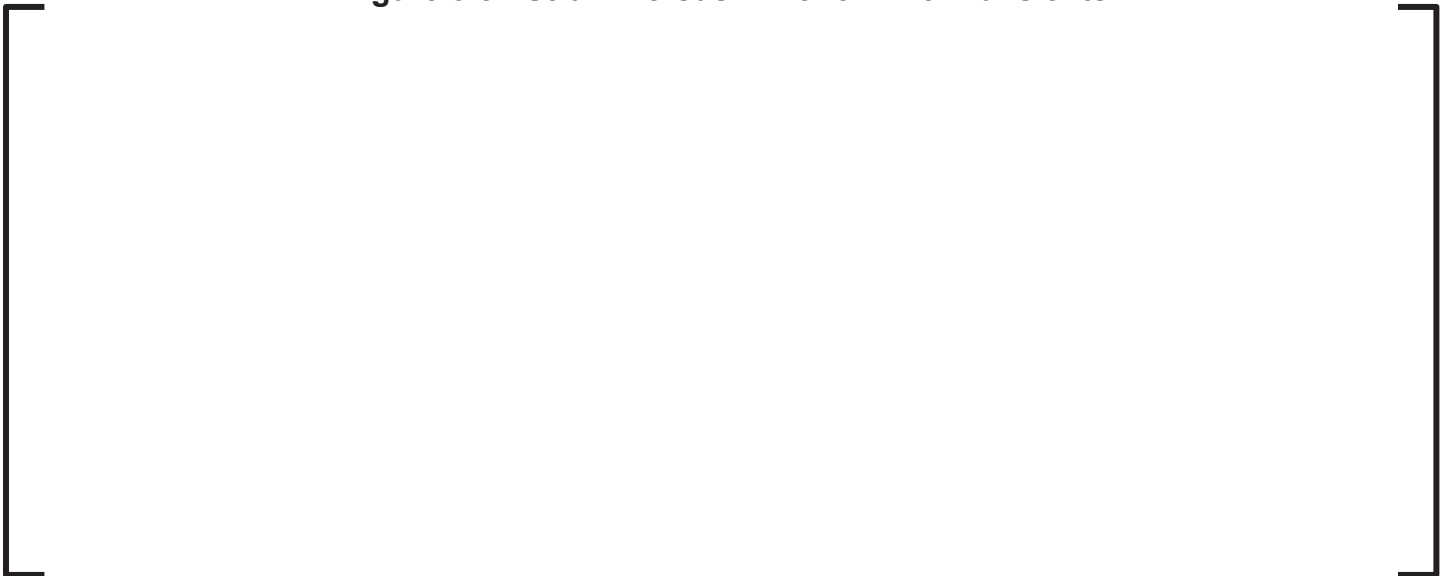


Figure 6-4: Fen Versus Strain for Two Transients



Figure 6-5 Time History Stresses for Transients 16 and 1

Transients 1 and 16 are plotted below. Due to the differences in the time durations of transients 1 and 16, refer to the preceding figures for a better view of the time history of transient 16. [

]



6.2 EXCEL Spreadsheet Calculations

The calculations necessary to perform this evaluation were done with EXCEL. The following is an explanation of the equations used in the spreadsheet.

For Sheet: "Latch Housing"

TP CRDM Latch Housing Environmentally Assisted Fatigue - Non-Proprietary

]

Table 6-1: Input Data and Stress Difference Calculation for Transients 3 and 16

Table 6-2: Calculation of Various Intermediate Parameters Needed to Determine Fen

--

Table 6-3 Input Data and Stress Difference Calculation for Transient 1

--	--

Table 6-4 Calculation of Various Intermediate Parameters Needed to Determine Fen for Transient 1

--	--

TP CRDM Latch Housing Environmentally Assisted Fatigue - Non-Proprietary

For Transients 3 and 16:

Based on the above calculations for $\Delta\epsilon_n$ and $F_{en} * \Delta\epsilon_n$, the usage factor can be recalculated to account for the EAF.

$$F_{en} = \frac{\sum F_{en,i} \Delta\epsilon_i}{\sum \Delta\epsilon_i} = [\quad]$$

For Transients 1 and 16:

Based on the above calculations for $\Delta\epsilon_n$ and $F_{en} * \Delta\epsilon_n$, the usage factor can be recalculated to account for the EAF.

$$F_{en} = \frac{\sum F_{en,i} \Delta\epsilon_i}{\sum \Delta\epsilon_i} = [\quad]$$

[

]

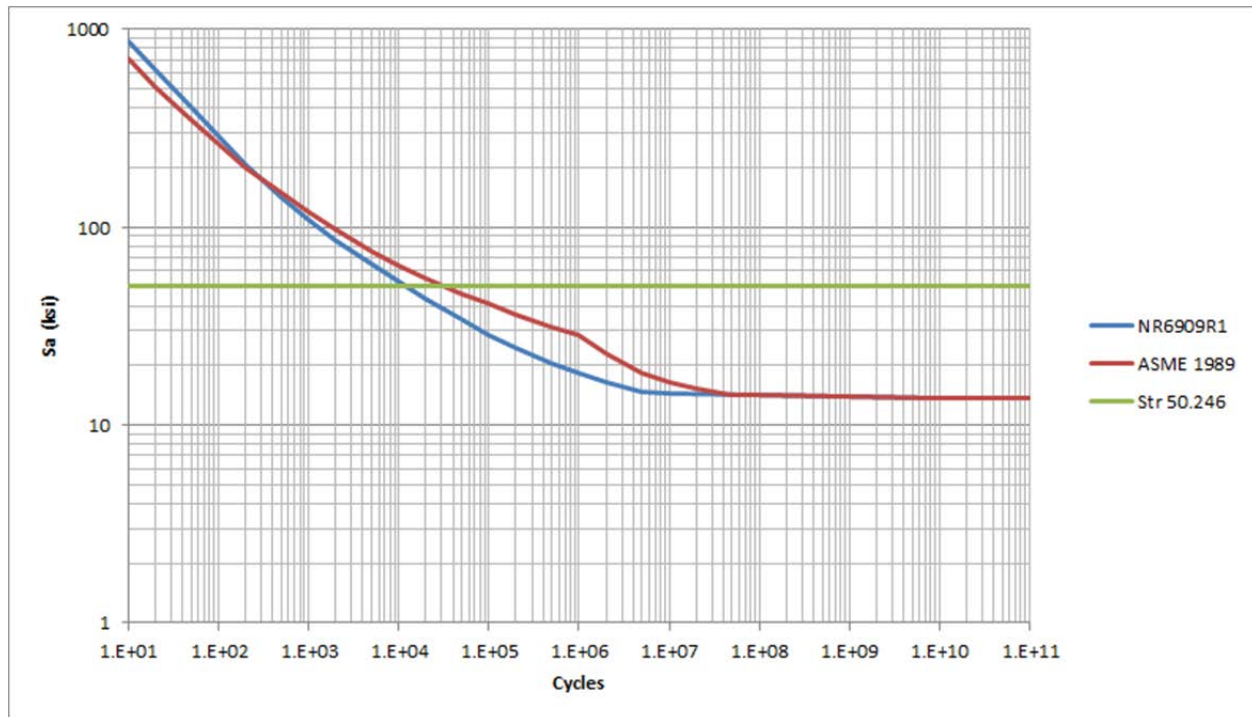
Table 6-5: [

]

TP CRDM Latch Housing Environmentally Assisted Fatigue - Non-Proprietary

The following S-N curve is based on NUREG/CR-6909, Reference [1] and ASME III 1989, Reference [2] and shows the significance of including the NUREG/CR-6909 curve which reduces the number of allowable cycles significantly for an alternating stress of 50.246 ksi.

Figure 6-6: S-N Curve Showing Significance of NUREG/CR-6909 to ASME III



7.0 RESULTS

Per Table 6-4, the EAF usage factor has been recalculated and shown to be less than 1.0 []

8.0 REFERENCES

References identified with an (*) are maintained within Turkey Point Nuclear Power Plant Records System and are not retrievable from AREVA Records Management. These are acceptable references per AREVA Administrative Procedure 0402-01, Attachment 8. See page 2 for Project Manager Approval of customer references.

1. NUREG/CR-6909, Revision 1, “Effect of LWR Coolant Environments on the Fatigue Life of Reactor Materials”, DRAFT, March 2014.
2. ASME B&PV Code Sec. III, SubSection 1989 edition with no Addenda.
3. AREVA Document 38-9279681-000, JSPM Document 17NI0548, Rev. B, “Turkey Point Power Plant – Data for the fatigue analysis of the critical points of latch housing and canopy joint”.
4. Textbook, “Advanced Strength and Applied Elasticity The SI Version”, A.C. Ugural, S.K. Fenster, 1982, Elsevier Science Publishing Co.
5. AREVA Document 33-9127371-001, “Turkey Point Plant Extended Power Uprate Control Rod Drive Mechanism Pressure Housing Assembly Appurtenances ASME Class 1”.
6. AREVA Document 08-5036747-003, JSPM Document 6GA4571 Rev. H, “Turkey Point Nuclear Power Plant Units 3 & 4 Control Rod Drive Mechanism Pressure Housing Assembly Appurtenances ASME III Class 1 Design Specification”.
7. Areva Document 38-9279661-000, [NNPARV-17-0241, NNPARV-17-0243], “Formal Transmittal of inputs for Areva Evaluation of Environmentally Assisted Fatigue at Turkey Point Units 3 and 4”.

APPENDIX A: BASIS FOR PRINCIPAL STRESS CALCUATIONS

A.1 Equations for Principal Stress Calculations

The source equations from the text, “Advanced Strength and Applied Elasticity The SI Version”, [4] are shown here for documentation purposes.

Advanced Strength and Applied Elasticity The SI Version

A.C. Ugural
Fairleigh Dickinson University

S. K. Fenster
New Jersey Institute of Technology

Elsevier Science Publishing Co., Inc.
52 Vanderbilt Avenue, New York, New York

Distributors outside the United States and Canada:
Elsevier Science Publishers B.V.
P.O. 211, 1000 AE Amsterdam, The Netherlands

©1981 by Elsevier Science Publishing Co., Inc.
Second Printing, 1982

Library of Congress Cataloging in Publication Data

Ugural, A.C.
Advanced strength and applied elasticity: The SI version.
Includes bibliographical references and index.
1. Strength materials. 2. Elasticity. I. Fenster,
Saul K., 1933– joint author. II. Title.
TA405.U42 1981 620.1'12 80-26638
ISBN 0-444-00428-9

Desk Editor Louise Calabro Schreiber
Design Edmée Froment
Art Editor Glen Burris
Cover Design Paul Agule Design
Production Manager Joanne Jay
Compositor Science Typographers, Inc.
Printer Haddon Craftsmen

Manufactured in the United States of America

Appendix B

A Practical Approach to the Stress Cubic Equation and Direction Cosines

B.1 Principal Stresses

There are many methods in common usage for solving a cubic equation. A simple approach for dealing with Eq. (1.20) is to find one root, say σ_1 , by plotting it (σ as abscissa) or by trial and error. The cubic equation is then factored by dividing by $(\sigma_p - \sigma_1)$ to arrive at a quadratic equation. The remaining roots can be obtained by applying the familiar general solution of a quadratic equation. This process requires considerable time and algebraic work, however.

What follows is a practical approach for determining the roots of stress cubic equation (1.20):

$$\sigma_p^3 - I_1\sigma_p^2 + I_2\sigma_p - I_3 = 0 \quad (a)$$

where

$$\begin{aligned} I_1 &= \sigma_x + \sigma_y + \sigma_z \\ I_2 &= \sigma_x\sigma_y + \sigma_x\sigma_z + \sigma_y\sigma_z - \tau_{xy}^2 - \tau_{yz}^2 - \tau_{xz}^2 \\ I_3 &= \sigma_x\sigma_y\sigma_z + 2\tau_{xy}\tau_{yz}\tau_{xz} - \sigma_x\tau_{yz}^2 - \sigma_y\tau_{xz}^2 - \sigma_z\tau_{xy}^2 \end{aligned} \quad (B.1)$$

According to the method, expressions that provide direct means for solving both two-dimensional and three-dimensional stress problems are*

$$\begin{aligned} \sigma_a &= 2S[\cos(\alpha/3)] + \frac{1}{3}I_1 \\ \sigma_b &= 2S\{\cos[(\alpha/3) + 120^\circ]\} + \frac{1}{3}I_1 \\ \sigma_c &= 2S\{\cos[(\alpha/3) + 240^\circ]\} + \frac{1}{3}I_1 \end{aligned} \quad (B.2)$$

*See E. E. Messal, Finding true maximum shear stress, *Machine Design* pp. 166–169 (December 7, 1978).

408 A Practical Approach to the Stress Cubic Equation and Direction Cosines

Here the constants are given by

$$\begin{aligned}
 S &= \left(\frac{1}{3}R\right)^{1/2} \\
 \alpha &= \cos^{-1}\left(-\frac{Q}{2T}\right) \\
 R &= \frac{1}{3}I_1^2 - I_2 \\
 Q &= \frac{1}{3}I_1I_2 - I_3 - \frac{2}{27}I_1^3 \\
 T &= \left(\frac{1}{27}R^3\right)^{1/2}
 \end{aligned} \tag{B.3}$$

and invariants I_1 , I_2 , and I_3 are represented in terms of the given stress components by Eqs. (B.1).

The principal stresses found from Eqs. (B.2) are *redesignated* using numerical subscripts so that $\sigma_1 > \sigma_2 > \sigma_3$. The above procedure is well adapted to a pocket calculator or digital computer.



CALCULATION SUMMARY SHEET (CSS)

Document No. 32 - 9280710 - 000

Safety Related: ☒ Yes ☐ No

Title TP Vent Nozzle Environmentally Assisted Fatigue – Non-Proprietary

PURPOSE AND SUMMARY OF RESULTS:

PURPOSE:

The purpose of the analysis is to evaluate the Environmentally Assisted Fatigue (EAF) of the Reactor Vessel Closure Head Vent Nozzle for Turkey Point Units 3 and 4, according to the F_{en} methodology provided in NUREG/CR-6909 Rev. 1 (Reference [1]).

The proprietary version of this document is 32-9279362-001.

RESULTS:

The maximum cumulative fatigue usage factor considering EAF is 0.23 [

]

If the computer software used herein is not the latest version per the EASI list, AP 0402-01 requires that justification be provided.

THE FOLLOWING COMPUTER CODES HAVE BEEN USED IN THIS DOCUMENT:

CODE/VERSION/REV	CODE/VERSION/REV
<u>ANSYS 16.0</u>	<u></u>
<u></u>	<u></u>

THE DOCUMENT CONTAINS
ASSUMPTIONS THAT SHALL BE
VERIFIED PRIOR TO USE

☐ Yes

☒ No

TP Vent Nozzle Environmentally Assisted Fatigue – Non-Proprietary



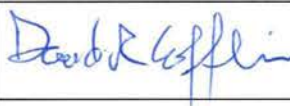
Review Method: ☒ Design Review (Detailed Check)

☐ Alternate Calculation

Does this document establish design or technical requirements? ☐ YES ☒ NO

Does this document contain Customer Required Format? ☐ YES ☒ NO

Signature Block

Name and Title (printed or typed)	Signature	P/R/A/M and LP/LR	Date	Pages/Sections Prepared/Reviewed/Approved
Kaihong Wang, Principal Engineer		P	12/13/17	All.
Thomas Washko, Engineer		R	12-14-2017	All, detailed review.
David Cofflin, Manager		A	12/14/17	All.

Notes: P/R/A designates Preparer (P), Reviewer (R), Approver (A);
LP/LR designates Lead Preparer (LP), Lead Reviewer (LR);
M designates Mentor (M)

In preparing, reviewing and approving revisions, the lead preparer/reviewer/approver shall use 'All' or 'All except ___' in the pages/sections reviewed/approved. 'All' or 'All except ___' means that the changes and the effect of the changes on the entire document have been prepared/reviewed/approved. It does not mean that the lead preparer/reviewer/approver has prepared/reviewed/approved all the pages of the document.

Project Manager Approval of Customer References and/or Customer Formatting (N/A if not applicable)

Name (printed or typed)	Title (printed or typed)	Signature	Date
N/A	N/A	N/A	N/A

TP Vent Nozzle Environmentally Assisted Fatigue – Non-Proprietary

Record of Revision

Revision No.	Pages/Sections/Paragraphs Changed	Brief Description / Change Authorization
000	Initial release	The proprietary version of this document is 32-9279362-001.

Table of Contents

	Page
SIGNATURE BLOCK.....	2
RECORD OF REVISION	3
LIST OF TABLES	5
LIST OF FIGURES	6
1.0 INTRODUCTION.....	7
2.0 PURPOSE AND SCOPE.....	7
3.0 ANALYTICAL METHODOLOGY	7
3.1 ASME Section III In-Air Fatigue Usage.....	7
3.2 F_{en} Methodology	8
4.0 ASSUMPTIONS	9
4.1 Unverified Assumptions.....	9
4.2 Justified Assumptions.....	9
4.3 Modeling Simplifications.....	10
5.0 DESIGN INPUTS	10
5.1 Geometry.....	10
5.2 Material.....	11
5.3 Finite Element Model.....	11
5.4 Loads.....	14
6.0 COMPUTER USAGE	16
6.1 Software	16
6.2 Computer Files	16
7.0 CALCULATIONS	18
7.1 Design Conditions	18
7.2 Thermal Analysis.....	19
7.3 Stress Analysis.....	24
7.4 Cumulative Fatigue Usage Factor.....	25
8.0 RESULTS SUMMARY AND CONCLUSION	28
9.0 REFERENCES	29

List of Tables

	Page
Table 5-1: Enveloped Affecting Transients for Fatigue Evaluation	15
Table 5-2: Enveloped Transients	15
Table 7-1: Locations for Temperature Gradients	20
Table 7-2: Time Points in Structural Analysis	24
Table 7-3: Nozzle EAF Usage Factor	26
Table 7-4: J-Groove Weld EAF Usage Factor	27
Table 7-5: RV Head EAF Usage Factor.....	27

List of Figures

	Page
Figure 5-1: 2-D Solid Model.....	12
Figure 5-2: Meshed Finite Element Model	13
Figure 5-3: Thermal Boundary Conditions	13
Figure 5-4: Structural Boundary Conditions	14
Figure 7-1: Displacement in Design Conditions (inch).....	18
Figure 7-2: Stress Intensity in Design Conditions (psi).....	19
Figure 7-3: Locations for Evaluation of Temperature Gradients.....	20
Figure 7-4: []	21
Figure 7-5: []	21
Figure 7-6: []	22
Figure 7-7: []	22
Figure 7-8: []	23
Figure 7-9: []	23
Figure 7-10: Locations for EAF Evaluation	25

1.0 INTRODUCTION

Florida Power & Light Co. (FPL) is planning to submit a License Amendment Request (LAR) for Subsequent License Renewal (SLR = life to 80 years) to the NRC for the replacement Reactor Vessel Closure Head (RVCH) and CRDM assembly at Turkey Point Units 3 and 4. As required by the NRC, the Environmentally-Assisted Fatigue (EAF) at susceptible locations in the RCS needs to be evaluated.

2.0 PURPOSE AND SCOPE

The purpose of this document is to calculate the EAF usage factors for the RVCH Vent Nozzle. The EAF evaluation is based on the F_{en} methodology provided in NUREG/CR-6909 Rev. 1 (Reference [1]). The original ASME Section III analysis of the Vent Nozzle is documented in Reference [2], in which the plant EPU transients are considered.

Since the original analysis does not include the fatigue usage calculation for the inside surfaces of the J-Groove weld and the nozzle that are exposed to the RCS coolant, a finite element analysis is re-performed to calculate the stresses and fatigue usage factors at the inside surfaces, followed by the evaluation of EAF usage based on the F_{en} methodology.

The scope is to calculate the cumulative usage factor (CUF) considering EAF on the inside surfaces of:

- Vent Nozzle near the J-Groove weld []
- J-Groove weld including the buttering []
- RV closure head near the J-Groove weld []

The list above covers all material types in the component.

ASME Section III stress and fatigue analyses are contained in the original analysis (Reference [2]), which remains valid. Note that the original stress and fatigue analysis qualifies the Vent Nozzle to the ASME Code 1989 Edition with no addenda. The current analysis calculate the in-air fatigue usage factor based on the fatigue design curves developed in NUREG/CR-6909 Rev. 1 (Reference [1]), as part of the LAR commitment.

3.0 ANALYTICAL METHODOLOGY

3.1 ASME Section III In-Air Fatigue Usage

A finite element analysis is performed, with the same steps as described in Reference [2] to calculate stresses due to design transients and nozzle external loads:

1. [] There are two finite element models consisting of thermal and structural elements respectively so as to enable the thermal and structural analysis.
2. Applying the design conditions of pressure and temperature to the structural finite element model and obtaining the deformation and stresses in the model. The deformation field is used to verify the correct behavior of the model and correct modeling of boundary and load conditions.

TP Vent Nozzle Environmentally Assisted Fatigue – Non-Proprietary

3. Applying the thermal loads pertaining to the power transients (in the form of transient temperatures and corresponding heat transfer coefficients versus time). Each of the major power transients requires a separate run on the thermal finite element model.
4. Evaluating the results of the thermal analysis by examination of the magnitude of temperature differences between key locations of the model at corresponding times (for example between nozzle and wall). The time points of maximum temperature gradient are the time points at which the maximum thermal stresses develop or the biggest pressure exists.
5. Applying the corresponding mechanical (pressure) and thermal loads (temperature gradients) at each time point identified in step 4 on the structural finite element model.
6. Applying the stress intensity due to the OBE loads calculated in Reference [2] to applicable locations on the nozzle.
7. Calculating the in-air CUF on the inside surfaces of the nozzle, J-Groove weld and RV head based on the fatigue design curves as summarized in Appendix A of Reference [1].

This analysis does not use the simplified methodology described in NRC RIS 2008-30 where the influence function and only one value of stress is used in the fatigue evaluation. This is a detailed finite element analysis, meeting the requirements of ASME III, NB-3216.2, where all six stress components are used in calculating fatigue usage factors.

3.2 F_{en} Methodology

The F_{en} method is developed in NUREG/CR-6909 Rev. 1 (Reference [1]). This sub-section summarizes the formulas provided in Appendix A of Reference [1].

The F_{en} method is an acceptable approach in the EAF evaluation, in which the F_{en} factor is a nominal correction value defined as the ratio of fatigue life in air at room temperature ($N_{air,RT}$) to that in LWR coolant environments at service temperature (N_{water}):

$$F_{en} = \frac{N_{air,RT}}{N_{water}}$$

TP Vent Nozzle Environmentally Assisted Fatigue – Non-Proprietary

The final fatigue usage considering EAF is then: $CUF_{en} = F_{en,1}U_1 + F_{en,2}U_2 + F_{en,3}U_3 + \dots$ where U_i is the in-air fatigue usage factor.

4.0 ASSUMPTIONS

4.1 Unverified Assumptions

There are no unverified assumptions within this calculation.

4.2 Justified Assumptions

1. The loading conditions (design transients, nozzle external loads) are the same as those used in the original analysis.

TP Vent Nozzle Environmentally Assisted Fatigue – Non-Proprietary

2. []
3. The RV head inside surfaces are covered with cladding. For EAF evaluation, the head inside surface near the J-Groove weld is considered being exposed to the RCS coolant although it is covered with cladding.
4. []
5. []
6. In NUREG/CR-6909 Rev. 1 (Reference [1]), when calculating T^* or T' in Appendix A, the upper bound limit of equation for T is 325°C (617°F). []

4.3 Modeling Simplifications

Simplifications in modeling and simulation in the analysis are the same as in the original analysis.

5.0 DESIGN INPUTS

5.1 Geometry

The geometry of the model is based on the drawings provided in References [3], [4] and [5], same as in the original analysis.

RV Head inside radius to base metal	= []
RV Head thickness	= []
RV Head cladding thickness, min.	= []

TP Vent Nozzle Environmentally Assisted Fatigue – Non-Proprietary

Vent nozzle OD, min. = []

Vent nozzle ID, max. = []

J-Groove weld height = []

Buttering weld layer height = []

Angle between weld and nozzle = []

[]

5.2 Material

The materials designation is provided in Reference [3] and [7]. Same as in the original analysis, the material designations of various sub-components as listed as follows:

RV Head = [] Reference [3]

Vent nozzle = [] Reference [7]

Cladding⁽¹⁾ = [] Reference [7]

J-Groove buttering⁽²⁾ = [] Reference [4]

J-Groove filler⁽²⁾ = [] Reference [4]

Notes:

(1) Thermal properties in ASME code are grouped by their chemical composition. []

]

(2) Section 4.4 of Reference [7] identifies the weld material in accordance with ASME Code Cases 2142-1 and 2143-1. These code cases provided specification of weld filler metal and welding electrode, respectively. []

]

The analysis herein uses the thermal properties – mean coefficient of thermal expansion (α), specific heat (C), thermal conductivity (k) and the mechanical properties – modulus of elasticity (E), Poisson's ratio (μ), density (ρ). The detailed values (thermal & structural) for these materials are listed in Tables 3-1 to 3-3 of Reference [2].

5.3 Finite Element Model

The finite element model is developed with ANSYS (Reference [8]). The solid model is shown in Figure 5-1. The model is meshed with []

[] The meshed model is shown in Figure 5-2.

The ANSYS finite element model is documented in the file “TPVent_Geo.dat” and “TPVent_Geo.out.”

TP Vent Nozzle Environmentally Assisted Fatigue – Non-Proprietary

The same boundary conditions as used in the original analysis are applied in both thermal and structural analyses.

[

]

In structural analysis, symmetric boundary conditions are applied to the head cut-off cross-section. End-cap pressure load is applied to the nozzle cut-off cross-section. [

]



Figure 5-1: 2-D Solid Model

TP Vent Nozzle Environmentally Assisted Fatigue – Non-Proprietary

Figure 5-2: Meshed Finite Element Model

Figure 5-3: Thermal Boundary Conditions



Figure 5-4: Structural Boundary Conditions

5.4 Loads

The external nozzle loads are provided in Reference [9]. The forces and moments along with the corresponding locations are summarized in the tables in Sub-Section 3.5.1 of the original analysis (Reference [2]). As with the fatigue usage, a conservative value of [] due to nozzle external loads is determined from the original analysis (Sub-Section 5.4.2.2 in Reference [9]), which will be added to the stress intensity ranges for nodes on the nozzle. [

]

The reactor vessel head is designed to satisfy the ASME code criteria when operating at a pressure of [] and a temperature of [] (Reference [7]). The design conditions are simulated on the model by applying a uniform and reference temperature of [] throughout the model and a uniform pressure of [] on all those surfaces in contact with the primary reactor coolant. These surfaces include the inside surfaces of the reactor vessel head, inside surfaces of the vent nozzle, and the surface of the weld joining the nozzle to the reactor head.

The Normal and Upset transients are listed in Table 3-8 of Reference [2]. The enveloped affecting transients for fatigue evaluation are listed in Table 3-9 of Reference [2], as repeated in Table 5-1. Per Reference [6], the number of cycles for the analyzed transients is applicable for 80 years plant operation.

Table 5-1: Enveloped Affecting Transients for Fatigue Evaluation

In Table 5-1 the enveloped transients as well as the total number of cycles are the same as listed in Table 3-9 of Reference [2].

The corresponding transient data as listed in Tables 3-10 to 3-15 of Reference [2] are listed as follows. [

]

Table 5-2: Enveloped Transients

6.0 COMPUTER USAGE

6.1 Software

ANSYS Release 16.0 is used in this calculation. Verification tests are listed as follows:

Computer programs tested: ANSYS Release 16.0.

Verification Tests: [

Verification output files are identified in the computer listing, using the naming convention of pre/post_ * where “*” represents the Test Name.

Computer hardware used:

- 1) Computer Name: SC-MJEHGTA. Hardware: Intel (R) Xeon™ CPU E5645@2.40GHz, 24GB RAM. Operating System: Windows 7 Enterprise, Service Pack 1, 64-Bit.
- 2) Name of person running the tests: Kaihong Wang.
- 3) Date of tests: 11/7/2017 and 11/12/2017.

Acceptability: Output files of all verification tests have been reviewed and found to be successful. Verification output files are also uploaded to AREVA ColdStor.

6.2 Computer Files

Computer files generated for this analysis and the verification tests have been uploaded to AREVA ColdStor in the directory “\cold\General-Access\32\32-9000000\32-9279362-000\official\.”

A complete directory listing of all filenames, sizes, dates and sub-directories has been provided in the following under the abovementioned directory. All times in the listing file and below are the U.S. Central Standard Time (CST).

[last modified date/time]-----		[file size]--	[filename]
11/12/2017	06:36 PM	1,274,273	InAirCUF_Head.out
11/12/2017	06:36 PM	4,325	InAirCUF_HEAD.txt
11/12/2017	06:38 PM	3,024,099	InAirCUF_JWeld.out
11/12/2017	06:38 PM	10,523	InAirCUF_JWeld.txt
11/12/2017	06:39 PM	2,447,746	InAirCUF_Noz.out
11/12/2017	06:39 PM	8,457	InAirCUF_NOZ.txt
11/07/2017	09:49 AM	1,821	TH_dt.mac
11/12/2017	06:27 PM	31,373	TPVent_Des.out
11/04/2017	12:08 PM	1,621,522	TPVent_Geo.dat
11/07/2017	09:50 AM	85,943	TPVent_Geo.out
11/05/2017	12:16 PM	946	TR01.mac
11/07/2017	09:58 AM	93,854	TR01_st.out
11/07/2017	09:56 AM	673,036	TR01_th.out
11/05/2017	12:16 PM	978	TR02.mac
11/07/2017	11:43 AM	93,101	TR02_st.out
11/07/2017	11:41 AM	673,036	TR02_th.out
11/05/2017	11:25 PM	1,512	TR03.mac
11/07/2017	10:17 AM	85,817	TR03_st.out
11/07/2017	10:15 AM	593,619	TR03_th.out
11/05/2017	11:26 PM	1,682	TR04.mac
11/07/2017	10:24 AM	85,825	TR04_st.out
11/07/2017	10:22 AM	723,844	TR04_th.out
11/12/2017	06:23 PM	1,420	TR05.mac

TP Vent Nozzle Environmentally Assisted Fatigue – Non-Proprietary

11/12/2017	06:35	PM	81,253	TR05_st.out
11/12/2017	06:33	PM	871,187	TR05_th.out
11/05/2017	11:30	PM	1,848	TR06.mac
11/07/2017	10:41	AM	87,506	TR06_st.out
11/07/2017	10:39	AM	902,396	TR06_th.out
11/12/2017	06:40	PM	31,422	VM112_post.out
11/07/2017	09:39	AM	31,608	VM112_pre.out
11/12/2017	06:45	PM	79,248	VM211_post.out
11/07/2017	09:46	AM	79,434	VM211_pre.out

7.0 CALCULATIONS

7.1 Design Conditions

Design conditions are simulated in the model by applying a uniform and reference temperature of [] throughout the model and uniform pressure of [] (Reference [7]). The purpose is to provide a basis for verification of the correct behavior of the model, the structural boundary conditions, and to verify stress attenuation at regions away from the nozzle. The ASME Section III primary stress analysis of Design Conditions is included in Reference [2]. The general deformation and the stress intensity (SI) plots are shown in Figure 7-1 and Figure 7-2, respectively.

Design Conditions analysis is documented in the ANSYS file “TPVent_Des.out.”



Figure 7-1: Displacement in Design Conditions (inch)

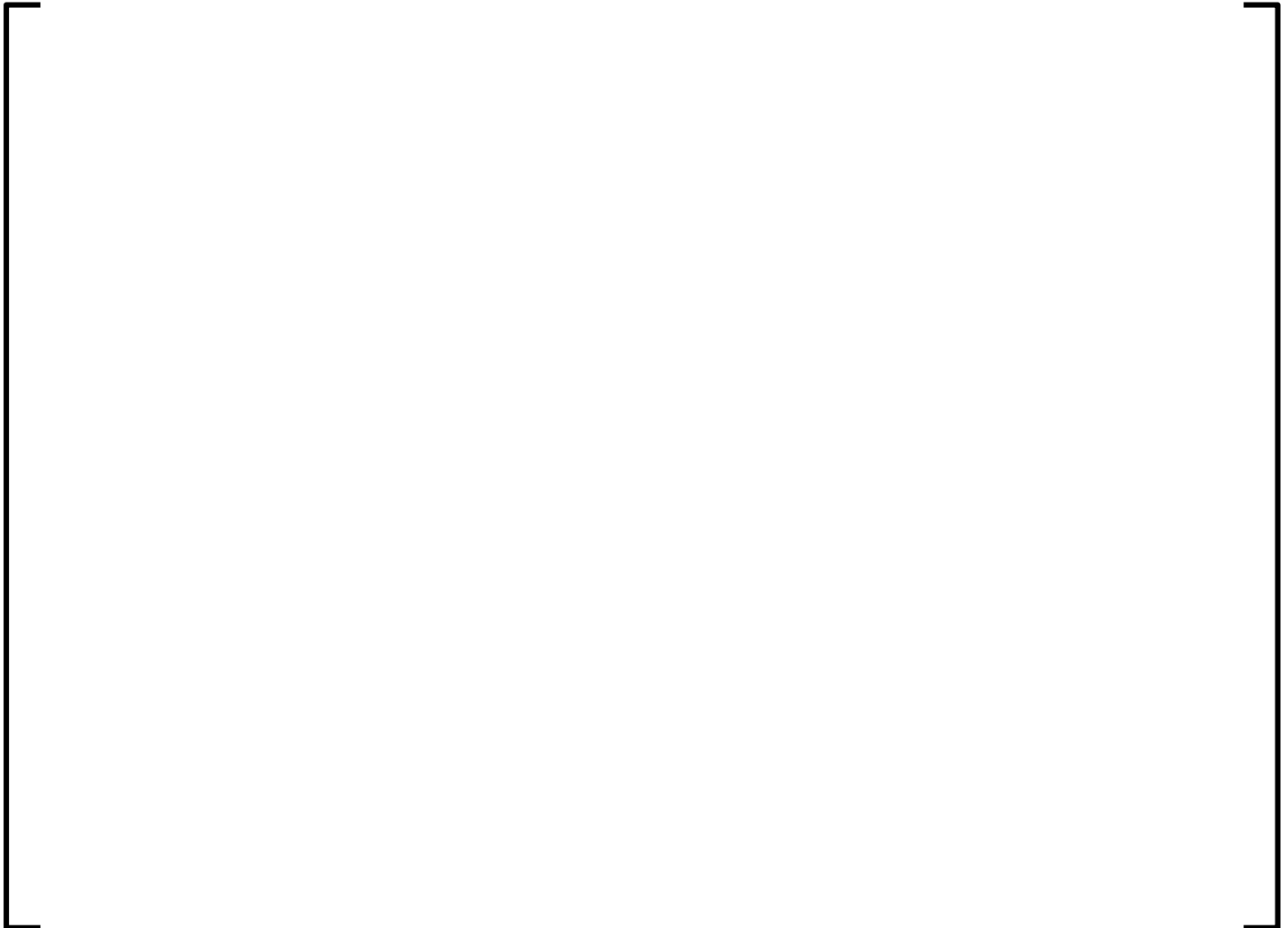


Figure 7-2: Stress Intensity in Design Conditions (psi)

7.2 Thermal Analysis

The results of the thermal analyses are evaluated to identify the maximum and minimum temperature gradients between critical locations in the model and the corresponding time points. These temperature gradients generate maximum and minimum thermal stresses, which in turn contribute to the maximum range of stress intensities in the model.

Similar locations as in the original stress analysis (Reference [2]) are selected. The node numbers corresponding to the two locations for evaluation of temperature gradient are listed in Table 7-1 for the model, as shown in Figure 7-3.

The corresponding ANSYS output files are listed in Section 6.2 with the file name convention as “TR*_th.out” for thermal output file. Here the asterisk “*” is to be substituted by the transient number as 01, 02, ..., 06 as listed in Table 5-2. Transient input files are named as “TR*.mac” that include the temperature and internal pressure all as a function of time and are called by each of the “TR*_th.inp” file. The input file for location definition is “TH_dt.mac.”

Table 7-1: Locations for Temperature Gradients

The temperature gradients between the two nodes as a function of time are shown in Figure 7-4 to Figure 7-9. These figures are provided to show the trend and for visual aid only. Specific values are taken from the ANSYS output files

Figure 7-3: Locations for Evaluation of Temperature Gradients

TP Vent Nozzle Environmentally Assisted Fatigue – Non-Proprietary

Figure 7-4: []

Figure 7-5: []

TP Vent Nozzle Environmentally Assisted Fatigue – Non-Proprietary

Figure 7-6: []

Figure 7-7: []

TP Vent Nozzle Environmentally Assisted Fatigue – Non-Proprietary

Figure 7-8: []

Figure 7-9: []

7.3 Stress Analysis

Nodal solution of the thermal analysis is loaded into the structural analysis with ANSYS. Time points selected from the thermal analysis include those with max/min temperature gradients as well as those where the internal pressure changes in linear interpolations. These time points are tabulated in tables below. Internal pressure at each time point is added as the mechanical load.

The ANSYS output files are listed in Section 6.2 with the file name convention as “*_st.out” where “*” is to be substituted by the transient index as listed in Table 5-2. Pressure input tables are defined in “TR*.mac.”

Table 7-2: Time Points in Structural Analysis

7.4 Cumulative Fatigue Usage Factor

For consideration of fatigue usage, the total stress intensity ranges are calculated. [

] Based on the stress contours, fatigue locations are selected as shown in Figure 7-10 where the FEM node numbers are indicated.

The bounding transients (and the corresponding cycles) that have a potential impact on fatigue usage factor are listed in Section 5.4. [

] The in-air cumulative fatigue usage factor is calculated using the ranges obtained from the stress results and the design cycles listed in Table 5-1. The in-air CUF is calculated based on the design fatigue curves in NUREG/CR-6909 Rev. 1 (Reference [1]). The corresponding maximum F_{en} value for the subject material (see Sub-Section 3.2) is then multiplied with the in-air CUF to obtain the final EAF CUF_{en} .



Figure 7-10: Locations for EAF Evaluation

TP Vent Nozzle Environmentally Assisted Fatigue – Non-Proprietary

In the following tables (Table 7-10 to Table 7-12), only the locations having the highest cumulative usage factors and only SI ranges having nonzero partial usage factors for each component are documented. The detailed calculation includes:

- (1) Req'd Cycles – the number of cycles.
- (2) Peak SI range – the extreme Total stress intensity range between two load steps, including SI range due to external loads if applicable.
- (3) $S_a = (\text{Peak SI range} \cdot E_{\text{ratio}})/2$, where $E_{\text{ratio}} = E_{\text{curve}}/E_{\text{material}}$

Table 7-3: Nozzle EAF Usage Factor

Note:

- (1) $E_{\text{ratio}} = E_{\text{curve}}/E_{\text{material}}$, where E_{material} is the nozzle material Young's module at [] and E_{curve} is the Young's module of the testing material in the design fatigue curve.
- (2) []

Table 7-4: J-Groove Weld EAF Usage Factor

Note:

- (1) $E_{ratio} = E_{curve} / E_{material}$, where $E_{material}$ is the nozzle material Young's module at [] and E_{curve} is the Young's module of the testing material in the design fatigue curve.

Table 7-5: RV Head EAF Usage Factor

Note:

- (1) $E_{ratio} = E_{curve} / E_{material}$, where $E_{material}$ is the nozzle material Young's module at [] and E_{curve} is the Young's module of the testing material in the design fatigue curve.

8.0 RESULTS SUMMARY AND CONCLUSION

Finite element analysis of the Turkey Point Units 3 and 4 RVCH Vent Nozzle is performed, similar to the original stress analysis (Reference [2]), in order to obtain the in-air CUF at the wetted surfaces near the J-Groove weld. An EAF analysis using the F_{en} method documented in Reference [1] is then performed. [] the highest CUF_{en} considering EAF is found to be 0.23 []

9.0 REFERENCES

1. NUREG/CR-6909, “Effect of LWR Coolant Environments on the Fatigue Life of Reactor Materials,” Rev. 1, March 2014 (draft for comments).
2. AREVA Document 32-5037640-006, “Turkey Point Units 3 and 4 Reactor Vessel Head Vent Nozzle Qualification.”
3. AREVA Drawing 02-5023321E-10, “Specification Drawing For Replacement Reactor Vessel Closure Head Turkey Point, Units 3 and 4.”
4. AREVA Drawing 02-5027458E-04, “Turkey Point Units 3 and 4, J-Groove Weld Details.”
5. AREVA Drawing 02-5028736D-01, “Vent Pipe Assembly for FPL, Turkey Point, Units 3 and 4.”
6. AREVA Document 38-9279661-000, “Formal Transmittal of inputs for Areva Evaluation of Environmentally Assisted Fatigue at Turkey Point Units 3 and 4.”
7. AREVA Document 08-5023846-04, “Certified Design Specification – Reactor Vessel Closure Head Replacement, Florida Power and Light Company, Turkey Point, Units 3 and 4,” as amended by SA-PTN 3/4-02.
8. “ANSYS” Finite Element Computer Code, Version 16.0, ANSYS, Inc., Canonsburg, Pa.
9. AREVA Document 18-5027466-05, “Loading Specification and Design Transients for Reactor Vessel Closure Head, Control Rod Drive and Integrated Head Assembly Replacements Turkey Point - Units 3 and 4.”



CALCULATION SUMMARY SHEET (CSS)

Document No. 32 - 9280711 - 000

Safety Related: ☒ Yes ☐ No

Title Turkey Point SLR EAF Analysis for Reactor Vessel Flange – Non-Proprietary

PURPOSE AND SUMMARY OF RESULTS:

PURPOSE:

The purpose of the analysis is to evaluate the Environmentally Assisted Fatigue (EAF) of the Reactor Vessel Flange for Turkey Point Units 3 and 4, according to the F_{en} methodology provided in NUREG/CR-6909 Rev 1 [1].

The proprietary version of this document is 32-9279161-001.

RESULTS:

[] the cumulative fatigue usage factor
considering EAF is 0.373. []

If the computer software used herein is not the latest version per the EASI list, AP 0402-01 requires that justification be provided.

THE FOLLOWING COMPUTER CODES HAVE BEEN USED IN THIS DOCUMENT:

CODE/VERSION/REV	CODE/VERSION/REV
<u>None</u>	<u></u>
<u></u>	<u></u>
<u></u>	<u></u>

THE DOCUMENT CONTAINS
ASSUMPTIONS THAT SHALL BE
VERIFIED PRIOR TO USE

☐ Yes

☒ No

Turkey Point SLR EAF Analysis for Reactor Vessel Flange – Non-Proprietary

Review Method: ☒ Design Review (Detailed Check)

☐ Alternate Calculation

Does this document establish design or technical requirements? ☐ YES ☒ NO

Does this document contain Customer Required Format? ☐ YES ☒ NO

Signature Block

Name and Title (printed or typed)	Signature	P/R/A/M and LP/LR	Date	Pages/Sections Prepared/Reviewed/Approved
Milan KOPINEC Engineer	David Cofflin for Milan Kopinec personal David R Cofflin	P	12/14/17	All.
Kaihong Wang Principal Engineer	[Signature]	R	12/14/17	All, detailed review.
David Cofflin Manager	David R Cofflin	A	12/14/17	All.

Notes: P/R/A designates Preparer (P), Reviewer (R), Approver (A);
LP/LR designates Lead Preparer (LP), Lead Reviewer (LR);
M designates Mentor (M)

In preparing, reviewing and approving revisions, the lead preparer/reviewer/approver shall use 'All' or 'All except ___' in the pages/sections reviewed/approved. 'All' or 'All except ___' means that the changes and the effect of the changes on the entire document have been prepared/reviewed/approved. It does not mean that the lead preparer/reviewer/approver has prepared/reviewed/approved all the pages of the document.

Project Manager Approval of Customer References and/or Customer Formatting (N/A if not applicable)

Name (printed or typed)	Title (printed or typed)	Signature	Date
N/A	N/A	N/A	N/A

Turkey Point SLR EAF Analysis for Reactor Vessel Flange – Non-Proprietary

Record of Revision

Revision No.	Pages/Sections/Paragraphs Changed	Brief Description / Change Authorization
000	All	Initial Revision. The proprietary version of this document is 32-9279161-001.

Table of Contents

Page

SIGNATURE BLOCK.....	2
RECORD OF REVISION	3
LIST OF TABLES	5
LIST OF FIGURES	6
1.0 INTRODUCTION.....	7
2.0 PURPOSE AND SCOPE.....	7
3.0 ANALYTICAL METHODOLOGY	7
4.0 ASSUMPTIONS	8
4.1 Unverified Assumptions.....	8
4.2 Justified Assumptions.....	8
5.0 DESIGN INPUTS	8
6.0 COMPUTER USAGE	9
7.0 CALCULATIONS.....	10
7.1 In-Air Fatigue Usage Factor	10
7.2 Stresses (prior to EPU)	15
7.3 F_{en} Calculation (prior to EPU).....	18
7.4 Environmentally Assisted Fatigue Usage.....	20
8.0 CONCLUSION	21
9.0 REFERENCES.....	22

List of Tables

	Page
Table 7-1: Fatigue Usage Factor from [2] prior to EPU	11
Table 7-2: Fatigue Usage Factor from [2] with EPU	11
Table 7-3: In-Air Fatigue Usage Factor using ANL Fatigue Design Curve, prior to EPU.....	12
Table 7-4: In-Air Fatigue Usage Factor using ANL Fatigue Design Curve, with EPU	13
Table 7-5: Total Stresses prior to EPU	15
Table 7-6: [.....]	17
Table 7-7: Calculation Summary of Strain Increments	19
Table 7-8: Calculation Summary of F_{en}	19
Table 7-9: [.....]	21

List of Figures

	Page
Figure 7-1: Critical Fatigue Location	10
Figure 7-2: Temperature Gradients in Thermal Analysis	10
Figure 7-3: Transients Contributing to the Fatigue Usage	14
Figure 7-4: Temperature Difference Plots and Time Points Chosen for Structural Analysis	16

1.0 INTRODUCTION

Florida Power & Light Co. is planning to submit a License Amendment Request for Subsequent License Renewal (SLR = life to 80 years) to the NRC for the replacement Reactor Vessel Closure Head (RVCH) and CRDM assembly at Turkey Point Units 3 and 4. In order to be approved for 80 year life, the NRC requires utilities to address Environmentally-Assisted Fatigue (EAF) at susceptible locations in the RCS.

2.0 PURPOSE AND SCOPE

Six susceptible locations are identified within the replacement RVCH and CRDM assembly as described in the scope document [1]. This report is focused on the EAF analysis of the Reactor Vessel Flange which is one of the identified locations. The analysis takes advantage of the calculation results documented in [2], which is a detailed stress and fatigue calculation of Turkey Point 3 and 4 replacement RVCH following rules specified in ASME Code Section III 1998 edition no addenda.

The EAF analysis herein is based on the guidelines given in NUREG/CR-6909 Rev 1 [3] so that the environmental effects are incorporated into ASME Code Section III fatigue evaluation performed in [2] with environmental correction factor ' F_{en} '.

3.0 ANALYTICAL METHODOLOGY

The EAF analysis of the Reactor Vessel Flange (RV Flange) is performed with the stress and fatigue results documented in [2] along with environmental correction factor ' F_{en} ' determined in accordance with [3].

The following steps outline the analytical methodology used:

- 1) The critical location for the fatigue damage determined in [2] is identified.
- 2) Recalculation of in-air fatigue usage factor with the ANL fatigue design curve from [3] and number of cycles specified in [4]. As reported in the original stress analysis [2] for the usage factor with transients prior to EPU and with EPU, the in-air usage factor is re-calculated also with both sets of transients. The results are reviewed to determine which set of transients is bounding in the subsequent EAF usage calculation.
- 3) The component stresses from [2] are retrieved at the critical location at each time point of the transients contributing to the total fatigue usage factor.
- 4) Review of the calculated stress states in the course of the transients and their applicability for EAF analysis.
- 5) Calculation of F_{en} in accordance with NUREG/CR-6909 Rev 1 [3].
- 6) Multiplication by the F_{en} factor for each contributing transient pair identified in step no. 2) to obtain final EAF usage factor.

4.0 ASSUMPTIONS

4.1 Unverified Assumptions

There are no unverified assumptions within this calculation.

4.2 Justified Assumptions

1. The loading conditions (design transients, nozzle external loads) are the same as those used in the original analysis.
 2. The RV head and vessel inside surfaces are covered with cladding. []
 3. []
-] .

5.0 DESIGN INPUTS

The analysis of EAF of RV Flange is based on:

- calculation results from [2] (see also Section 6.0)
- calculation guidelines [3]
- []
- []
- []

6.0 COMPUTER USAGE

All calculations are made within MS Excel 2010. No further software was used. Computer files retrieved from AREVA ColdStor which were generated in [2] are listed as follows:

Total Stress Intensity Ranges:

Ranges(total).out	11/25/2008
-------------------	------------

Ranges(Total)_EPU.out	11/16/2009
-----------------------	------------

Temperature differences through the vessel wall:

HUCD_DeltaTs.out	11/25/2008
------------------	------------

PLUL_DeltaTs.out	11/25/2008
------------------	------------

RIRD_DeltaTs.out	11/25/2008
------------------	------------

Stress components:

TP_ST_HUCD_Path.out	11/25/2008
---------------------	------------

TP_ST_PLUL_Path.out	11/25/2008
---------------------	------------

TP_ST_PLPU_EPU_Path.out	11/15/2009
-------------------------	------------

TP_ST_RIRD_Path.out	11/25/2008
---------------------	------------

TP_ST_RIRD_EPU_Path.out	11/12/2009
-------------------------	------------

7.0 CALCULATIONS

7.1 In-Air Fatigue Usage Factor

The in-air ASME Code Section III maximum usage factor of the RV Flange calculated in [2] is [] The location is shown in Figure 7-1 (inside node of Path 6, also the location labeled with G in thermal analysis shown in Figure 7-2). The usage is based on the transients and design number of cycles defined in [5]. The fatigue calculation summary from [2] at the inside node of Path 6 is provided in Table 7-1.

Figure 7-1: Critical Fatigue Location

Figure 7-2: Temperature Gradients in Thermal Analysis

Turkey Point SLR EAF Analysis for Reactor Vessel Flange – Non-Proprietary

In the following fatigue usage calculation, [] that can be combined with any other transient stress conditions to calculate the stress intensity range.

Table 7-1: Fatigue Usage Factor from [2] prior to EPU

The Revision 004 of [2] has also analyzed the impact of the Extended Power Uprate (EPU). []

[] However, this assumption is not necessarily conservative in terms of EAF evaluation, since ‘F_{en}’ factor might be actually larger for the contributing transient pair having smaller stress amplitude with a smaller strain rate in comparison to the one with larger stress amplitude and larger strain rate. The fatigue calculation summary from [2] at the inside node of Path 6 with EPU transients is provided in Table 7-2.

Table 7-2: Fatigue Usage Factor from [2] with EPU

In order to calculate the EAF usage factor using the F_{en} method, [] needs to be applied to calculate the in-air fatigue usage factor. Since the ANL fatigue design curve is located above the ASME fatigue curve used in the original analysis, the usage factor decreases along with

Turkey Point SLR EAF Analysis for Reactor Vessel Flange – Non-Proprietary

reduction of conservatisms described in [3]. [

] This simplification increases the E_{ratio} factor and so the adjusted alternating stress.

With the ANL fatigue design curve [] the in-air fatigue usage calculation is re-performed with aforementioned changes.

The stresses and metal temperatures at the node no. 202260 (inside node of Path 6) for the load combinations contributing to usage factor are retrieved from these computer outputs:

TP_ST_HUCD_Path.out,

TP_ST_PLUL_Path.out,

TP_ST_PLPU_EPU_Path.out

TP_ST_RIRD_Path.out,

TP_ST_RIRD_EPU_Path.out

Ranges(total).out,

Ranges(Total)_EPU.out

The fatigue usage recalculation is documented in Table 7-3 for the inside node of Path 6 prior to EPU, and in Table 7-4 for the same node with EPU. In Table 7-3 and Table 7-4, [

] In the table:

LC 1 and 2 – ANSYS Load Cases comprising the load combination

Time 1 and 2 – time points associated with the load cases and transient pair under consideration

Range – total stress intensity range

$E_{mat,min}$ – Young's modulus at metal temperature. [

]

E_{curve} – Young's modulus [

]

S_{alt} – calculated alternating stress intensity range from ANSYS

Table 7-3: In-Air Fatigue Usage Factor using ANL Fatigue Design Curve, prior to EPU

Table 7-4: In-Air Fatigue Usage Factor using ANL Fatigue Design Curve, with EPU

The fatigue recalculation shows a significant decrease of in-air usage factor from [] for transients prior to EPU and from [] for transients with EPU.

[

]

For the total usage factor with EPU transients, the second combination is between []

The [] transients are plotted in Figure 7-3.

Turkey Point SLR EAF Analysis for Reactor Vessel Flange – Non-Proprietary



Figure 7-3: Transients Contributing to the Fatigue Usage

7.2 Stresses (prior to EPU)

The component stresses for [] transients for all calculated time points prior to EPU are retrieved from the “Ranges(total).out” computer file and are summarized in Table 7-5.

Table 7-5: Total Stresses prior to EPU

Turkey Point SLR EAF Analysis for Reactor Vessel Flange – Non-Proprietary

Temperature difference plots between inside and outside vessel walls at the location of Path 6 for both transients are shown in Figure 7-4. The plots also depict the time points at which the stresses were calculated (black dots).

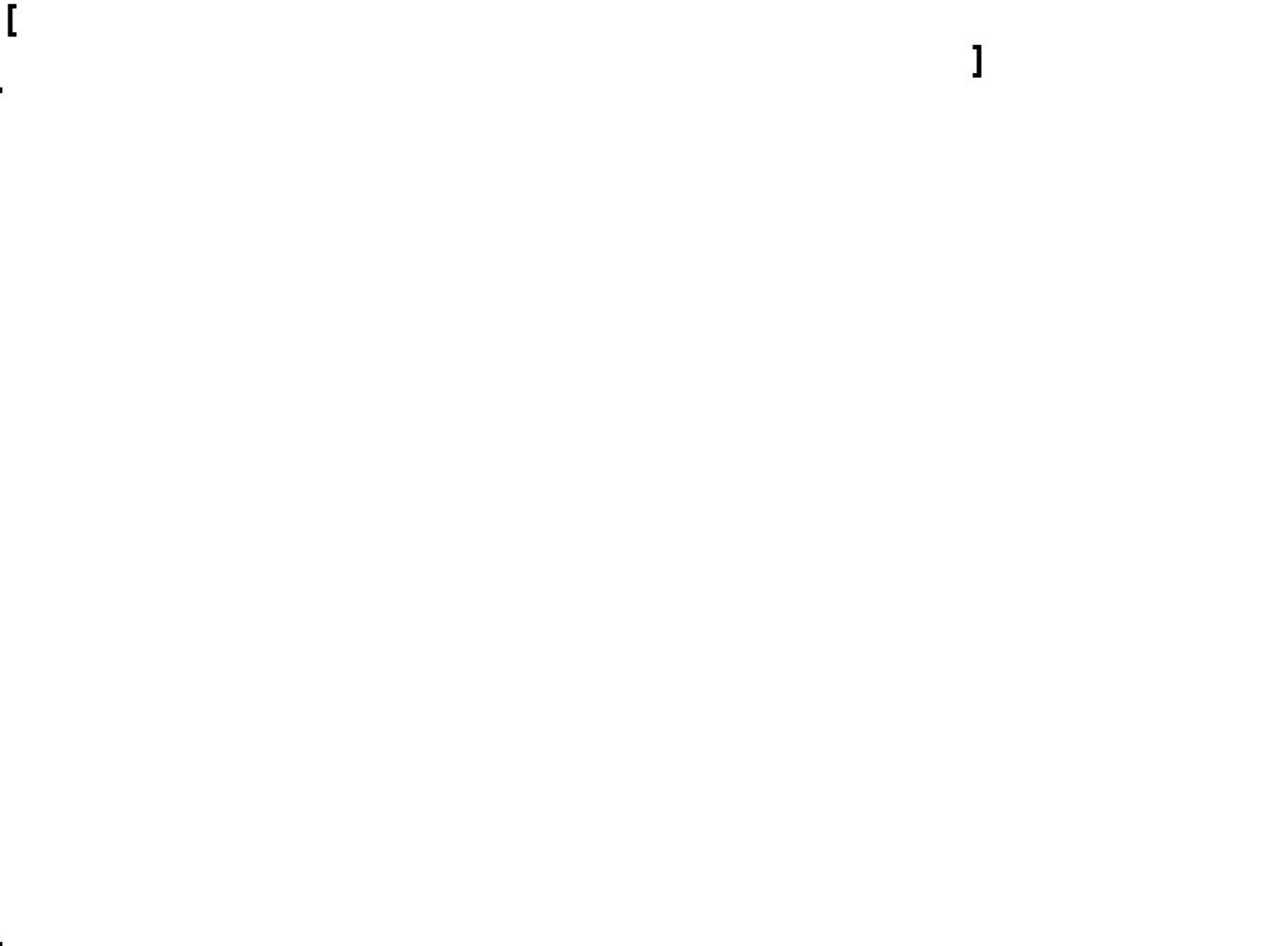


Figure 7-4: Temperature Difference Plots and Time Points Chosen for Structural Analysis

Turkey Point SLR EAF Analysis for Reactor Vessel Flange – Non-Proprietary

Table 7-6: []

[] **Transient**

The logic used for [] transient is also used for the [] transient. []

7.3 F_{en} Calculation (prior to EPU)

[

] This approach is described in detail in Section 6 of [3]. The calculation steps are repeated herein:

- 1) Calculate the stress range between time points $n - 1$ and n on the component stresses according to NB-3216.2. The stress ranges are $\sigma'_{ij} = \sigma_{ij}^{(n)} - \sigma_{ij}^{(n-1)}$. The principal stresses ($\sigma_1, \sigma_2, \sigma_3$) are then calculated based on the stress ranges σ'_{ij} , and arranged such that $\sigma_1 \geq \sigma_2 \geq \sigma_3$. The stress intensity (SI) range is then $\sigma_{int} = \sigma_1 - \sigma_3$.
- 2) Calculate the strain range by $\Delta\epsilon_n = \sigma_{int}/E$, where E is the Young's module of the material at the average temperature of the metal between the two time points.
- 3) Calculate the stain rate by $\epsilon_n = \Delta\epsilon_n/\Delta t_n$, where Δt_n in second is the time increment between time points $n - 1$ and n .
- 4) Determine whether or not a F_{en} for step n shall be calculated. Since only the strain increment of increasingly tensile is considered (i.e., no negative ϵ is permitted), the following criterion from [6] is adopted to determine if the strain range shall be kept:

If $|\sigma_3| \leq |\sigma_1|$, the F_{en} for step n shall be calculated based on the strain rate (Step 3) and other applicable parameters (S^* , T^* and O^*) according to equations shown below in text;

If $|\sigma_3| > |\sigma_1|$, the strain range is excluded in the next step, and no F_{en} is calculated.

- 5) Calculate the F_{en} factor between the two extreme time points of pair number k using the Multi-Linear Strain Based approach provided in [3] (see Section 6 Equation (68) in [3]): $F_{en,k} = \frac{\sum F_{en,n} \Delta\epsilon_n}{\sum \Delta\epsilon_n}$.
- 6) Calculate the overall EAF usage factor for the location: $U_{en} = F_{en,1}U_1 + F_{en,2}U_2 + F_{en,3}U_3 + \dots$.

The value for dissolved oxygen (DO) is obtained from [4]:

[

]

Finally, the F_{en} can be calculated using [document the calculation of strain increments and calculation of 'F_{en}', respectively.

] Table 7-7 and Table 7-8

Table 7-7: Calculation Summary of Strain Increments

Note¹⁾: Negative sign signifies a compressive strain increment.

Table 7-8: Calculation Summary of F_{en}

7.4 Environmentally Assisted Fatigue Usage

The combination of in-air cumulative usage factors (U_i) from Table 7-3 with corresponding $F_{en,i}$ factors from Table 7-8 gives the final environmentally assisted fatigue usage:

$$CUF_{en} = F_{en1} \cdot U_1 + F_{en2} \cdot U_2 = [\quad]$$

$$[\quad]$$

$$[\quad]$$

$$[\quad]$$

$$[\quad]$$

The environmentally assisted fatigue usage for [] is:

$$CUF_{en} = F_{en1} \cdot U_1 + F_{en2} \cdot U_2 = [\quad]$$

In Section 7.1 it was stated that in-air fatigue usage assuming EPU could potentially result in a larger fatigue usage provided that F_{en} factors determined for the combinations including EPU transient are sufficiently larger than the ones calculated in Table 7-8 because of their smaller strain rates. [] fulfilled

]

$$\Delta \epsilon^* = [\quad]$$

Moreover, the values O^* and S^* are unchanged and so these two variables also cannot increase the F_{en} factors. []

[] For these reasons, the calculated CUF_{en} which is based on the transients prior to EPU is bounding.

Table 7-9: []

8.0 CONCLUSION

The former in-air ASME Code Section III fatigue usage analysis made in [2] calculates the usage of []
[]

The above calculated usage factors are based on []
[] the usage is significantly reduced to 0.373.

9.0 REFERENCES

1. AREVA Document 51-9277194-000, “Turkey Point Units 3 and 4 Environmentally Assisted Fatigue Evaluation.”
2. AREVA Document 32-5040304-006, “Turkey Point Units - 3 & 4 Closure Analysis w/ Replacement Head.”
3. NUREG/CR-6909, “Effect of LWR Coolant Environments on the Fatigue Life of Reactor Materials,” Rev. 1, March 2014 (Draft Report for comment).
4. AREVA Document 38-9279661-000, “Formal Transmittal of inputs for Areva Evaluation of Environmentally Assisted Fatigue at Turkey Point Units 3 and 4.”
5. AREVA Document 18-5027466-05, “Loading Specification and Design Transients for Reactor Vessel Closure Head, Control Rod Drive and Integrated Head Assembly Replacements Turkey Point - Units 3 and 4.”
6. Mark A. Gray, et al., “Strain Rate Calculation Approach in Environmental Fatigue Evaluations,” *Transaction of the ASME Journal of Pressure Vessel Technology*, Vol. 136, August 2014.



CALCULATION SUMMARY SHEET (CSS)

Document No. 32 - 9280712 - 000

Safety Related: ☒ Yes ☐ No

Title TP CRDM Lower Joint Environmentally Assisted Fatigue – Non-Proprietary

PURPOSE AND SUMMARY OF RESULTS:

Purpose

The purpose of this calculation is to determine the effects of EAF (environmental assisted fatigue) on the Lower Joint. The basis used for the determination is DRAFT NUREG/CR-6909 Revision 1.

The proprietary version of this document is 32-9280202-001.

Results

The results indicate that the Lower Joint fatigue remains acceptable when the Environmental Assisted Fatigue is considered. The calculated EAF usage factor including the environmental assisted fatigue is 0.420 for Unit 3 and 0.749 for Unit 4, []

If the computer software used herein is not the latest version per the EASI list, AP 0402-01 requires that justification be provided.

THE FOLLOWING COMPUTER CODES HAVE BEEN USED IN THIS DOCUMENT:

CODE/VERSION/REV	CODE/VERSION/REV
_____	_____
_____	_____
_____	_____

THE DOCUMENT CONTAINS
ASSUMPTIONS THAT SHALL BE
VERIFIED PRIOR TO USE

☐ Yes

☒ No

TP CRDM Lower Joint Environmentally Assisted Fatigue – Non-Proprietary




Review Method: ☒ Design Review (Detailed Check)

☐ Alternate Calculation

Does this document establish design or technical requirements? ☐ YES ☒ NO

Does this document contain Customer Required Format? ☐ YES ☒ NO

Signature Block

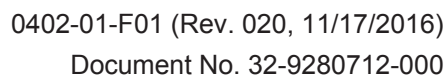
Name and Title (printed or typed)	Signature	P/R/A/M and LP/LR	Date	Pages/Sections Prepared/Reviewed/Approved
Thomas M. Washko Engineer		P	12-15-2017	All
HT Harrison Advisory Engineer		R	12/15/17	All
David Cofflin Engineering Manager		M A DRC	12/15/17	All

Notes: P/R/A designates Preparer (P), Reviewer (R), Approver (A);
LP/LR designates Lead Preparer (LP), Lead Reviewer (LR);
M designates Mentor (M)

In preparing, reviewing and approving revisions, the lead preparer/reviewer/approver shall use 'All' or 'All except ___' in the pages/sections reviewed/approved. 'All' or 'All except ___' means that the changes and the effect of the changes on the entire document have been prepared/reviewed/approved. It does not mean that the lead preparer/reviewer/approver has prepared/reviewed/approved all the pages of the document.

Project Manager Approval of Customer References and/or Customer Formatting (N/A if not applicable)

Name (printed or typed)	Title (printed or typed)	Signature	Date
N/A	N/A	N/A	N/A



Record of Revision

[illegible]

Table of Contents

Page

SIGNATURE BLOCK.....	2
RECORD OF REVISION	3
LIST OF TABLES	5
LIST OF FIGURES	6
1.0 OBJECTIVE	7
2.0 METHODOLOGY	7
2.1 General Approach to Calculating the Fen and Usage Factor	7
2.2 Detailed Method of Calculation of the Fen for Lower Joint	7
3.0 ASSUMPTIONS	8
4.0 DESIGN INPUTS	8
5.0 COMPUTER USAGE	8
6.0 CALCULATIONS	8
6.1 Transients To Be Evaluated	8
6.2 EXCEL Spreadsheet Calculations	11
7.0 RESULTS	22
8.0 REFERENCES	23
APPENDIX A : BASIS FOR PRINCIPAL STRESS CALCULATIONS.....	A-1

List of Tables

	Page
Table 6-1: Input Data and Stress Difference Calculation for Transients 1 and 7	14
Table 6-2: Calculation of Various Intermediate Parameters Needed to Determine Fen for Transients 1 and 7	15
Table 6-3: Input Data and Stress Difference Calculation for Transients 10 and 11	16
Table 6-4: Calculation of Various Intermediate Parameters Needed to Determine Fen for Transients 10 and 11	17
Table 6-5 [.....].....	19
Table 6-6 [.....].....	19
Table 6-7 [.....].....	20
Table 6-8 [.....].....	21

List of Figures

	Page
Figure 6-1 Time History Stresses for Transient 1	9
Figure 6-2 Time History Stresses for Transient 7	10
Figure 6-3 Time History Stresses for Transient 10	10
Figure 6-4 Time History Stresses for Transient 11	11
Figure 6-5 [.....]	19

1.0 OBJECTIVE

The component to be qualified for EAF (environmental assisted fatigue) in this calculation is the CRDM Lower Joint. Only the inside wetted location is to be considered. A fatigue usage factor is to be calculated considering the EAF and the objective is to obtain a value that is less than 1.0.

2.0 METHODOLOGY

Calculations are performed based on the criteria below, which is based on DRAFT NUREG/CR-6909, Reference [1]. The applicable code is ASME III, 1989 edition with no Addenda Reference [2].

2.1 General Approach to Calculating the Fen and Usage Factor

Time-history stresses are provided for various transients in Reference [4]. From this information, the following procedure is used to calculate the Fen and resulting EAF usage factor.

- (1) Calculate the stress range between time point n-1 and n on the component stresses according to NB-3216.2. The stress ranges are $\sigma'_{ij} = \sigma^{(n)}_{ij} - \sigma^{(n-1)}_{ij}$. The principal stresses ($\sigma_1, \sigma_2, \sigma_3$) are then calculated based on the stress ranges σ'_{ij} , and arranged such that $\sigma_1 \geq \sigma_2 \geq \sigma_3$. The stress intensity (SI) range is then $\sigma_{int} = \sigma_1 - \sigma_3$.
- (2) Calculate the strain range by $\Delta \epsilon_n = \sigma_{int} / E$, where E is the Young's modulus of the material at the average metal temperature between the two time points.
- (3) Calculate the strain rate by $\epsilon'_n = \Delta \epsilon_n / \Delta t_n$, where Δt_n in second is the time increment between point n-1 and n.
- (4) Determine whether or not an F_{en} for step n shall be calculated. Since only the strain increment of increasingly tensile strain is considered (i.e., no negative ϵ' is permitted), the following methodology is adopted to determine if the strain range shall be kept:

If $|\sigma_3| \leq |\sigma_1|$, the F_{en} for step n shall be calculated based on the strain rate (Step 3) and other applicable parameters (S^* , T^* and O^*) according to Eqs. (2), (3) or (4);

If $|\sigma_3| > |\sigma_1|$, the strain range is excluded in the next step, and no F_{en} is calculated.

- (5) Calculate the F_{en} factor between the two extreme time points of pair number k using the "Multi-Linear Strain Based Method" F_{en} approach presented in Reference [1].

$$F_{en,k} = \frac{\sum F_{en,i} \Delta \epsilon_i}{\sum \Delta \epsilon_i} \quad \text{Equation (68) of Reference [1].}$$

- (6) Calculate the overall EAF_{en} usage factor for the location: $U_{en} = F_{en,1}U_1 + F_{en,2}U_2 + F_{en,3}U_3 + \dots$.

2.2 Detailed Method of Calculation of the Fen for Lower Joint

Detailed description of the F_{en} calculation applicable to the Lower Joint:

TP CRDM Lower Joint Environmentally Assisted Fatigue – Non-Proprietary

3.0 ASSUMPTIONS

[

]

4.0 DESIGN INPUTS

The plant design, past and projected operating information was provided in Reference [3], Reference [4] and Reference [7].

5.0 COMPUTER USAGE

EXCEL spreadsheet only.

6.0 CALCULATIONS

Calculations are performed based on the methodology of Reference [1].

Based on the information provided in Reference [4], the total usage factor associated with various transients including consideration of dynamic seismic events was calculated to be [] The stress time-histories are also provided in a table in this same calculation and are displayed in the following plot. []

6.1 Transients To Be Evaluated

The following transients were considered to be included in the calculation of the EAF usage factor for this component.

[]

The following plots show the time history loading of the transients involved. The decreases in stresses in these plots will generally correspond to the times of negative strain shown later in Tables 6-2 and 6-4.

Figure 6-1 Time History Stresses for Transient 1



Figure 6-2 Time History Stresses for Transient 7**Figure 6-3 Time History Stresses for Transient 10**

Figure 6-4 Time History Stresses for Transient 11

6.2 EXCEL Spreadsheet Calculations

The calculations necessary to perform this evaluation were done with EXCEL. The following is an explanation of the equations used in the spreadsheet.

For Sheet: “Lower Joint”

TP CRDM Lower Joint Environmentally Assisted Fatigue – Non-Proprietary

TP CRDM Lower Joint Environmentally Assisted Fatigue – Non-Proprietary

Table 6-1: Input Data and Stress Difference Calculation for Transients 1 and 7

--	--

Table 6-2: Calculation of Various Intermediate Parameters Needed to Determine Fen for Transients 1 and 7

--	--

Table 6-3: Input Data and Stress Difference Calculation for Transients 10 and 11

--	--

Table 6-4: Calculation of Various Intermediate Parameters Needed to Determine Fen for Transients 10 and 11

--

TP CRDM Lower Joint Environmentally Assisted Fatigue – Non-Proprietary

Based on the above calculations for $\Delta \epsilon_n$ and $F_{en} * \Delta \epsilon_n$, the usage factor can be recalculated to account for the EAF.

For Transients 1 and 7,

$$F_{en} = \frac{\sum F_{en,i} \Delta \epsilon_i}{\sum \Delta \epsilon_i} = [\quad]$$

For Transients 1 and 10,

$$F_{en} = \frac{\sum F_{en,i} \Delta \epsilon_i}{\sum \Delta \epsilon_i} = [\quad]$$

For Transients 1 and 11,

$$F_{en} = \frac{\sum F_{en,i} \Delta \epsilon_i}{\sum \Delta \epsilon_i} = [\quad]$$

[This will be used for the Transient 1 and 5 combination.

Transient 16 []

The temperature loading is shown to be a maximum of [] on page 39 of Reference [6].
Conservatively using this temperature for the lower joint:

[]

[]

[]

[This will be used for the Transient 1 and 16 combination.

The following Tables 6-5 and 6-6 show the calculation of cycles of transients available []

Figure 6-5 []

Table 6-5 []

(1) Reference [3], (2) Reference [7] .

Table 6-6 []

(1) Reference [3], (2) Reference[7].

Table 6-7 [

]

		EAF Usage Factor Total U_{en}⁽²⁾ =	0.420
--	--	--	--------------

Notes:

- (1) The EAF Usage Factors above were calculated with the Fatigue Design Curve from Reference [1], Table A.2.
- (2) Per Section 2.1, the overall EAF_{en} usage factor for the location is: $U_{en} = F_{en,1}U_1 + F_{en,2}U_2 + F_{en,3}U_3 + \dots$.

(3) [

]

(4) [

]

Table 6-8 [

]

--	--	--	--	--	--	--	--	--	--	--	--	--	--	--	--	--	--	--	--	--	--	--	--	--	--	--	--	--	--	--	--	--	--	--	--	--	--	--	--	--	--	--	--	--	--	--	--	--	--	--	--	--	--	--	--	--	--	--	--	--	--	--	--	--	--	--	--	--	--	--	--	--	--	--	--	--	--	--	--	--	--	--	--	--	--	--	--	--	--	--	--	--	--	--	--	--	--	--	--	--	--	--	--	--	--	--	--	--	--	--	--	--	--	--	--	--	--	--	--	--	--	--	--	--	--	--	--	--	--	--	--	--	--	--	--	--	--	--	--	--	--	--	--	--	--	--	--	--	--	--	--	--	--	--	--	--	--	--	--	--	--	--	--	--	--	--	--	--	--	--	--	--	--	--	--	--	--	--	--	--	--	--	--	--	--	--	--	--	--	--	--	--	--	--	--	--	--	--	--	--	--	--	--	--	--	--	--	--	--	--	--	--	--	--	--	--	--	--	--	--	--	--	--	--	--	--	--	--	--	--	--	--	--	--	--	--	--	--	--	--	--	--	--	--	--	--	--	--	--	--	--	--	--	--	--	--	--	--	--	--	--	--	--	--	--	--	--	--	--	--	--	--	--	--	--	--	--	--	--	--	--	--	--	--	--	--	--	--	--	--	--	--	--	--	--	--	--	--	--	--	--	--	--	--	--	--	--	--	--	--	--	--	--	--	--	--	--	--	--	--	--	--	--	--	--	--	--	--	--	--	--	--	--	--	--	--	--	--	--	--	--	--	--	--	--	--	--	--	--	--	--	--	--	--	--	--	--	--	--	--	--	--	--	--	--	--	--	--	--	--	--	--	--	--	--	--	--	--	--	--	--	--	--	--	--	--	--	--	--	--	--	--	--	--	--	--	--	--	--	--	--	--	--	--	--	--	--	--	--	--	--	--	--	--	--	--	--	--	--	--	--	--	--	--	--	--	--	--	--	--	--	--	--	--	--	--	--	--	--	--	--	--	--	--	--	--	--	--	--	--	--	--	--	--	--	--	--	--	--	--	--	--	--	--	--	--	--	--	--	--	--	--	--	--	--	--	--	--	--	--	--	--	--	--	--	--	--	--	--	--	--	--	--	--	--	--	--	--	--	--	--	--	--	--	--	--	--	--	--	--	--	--	--	--	--	--	--	--	--	--	--	--	--	--	--	--	--	--	--	--	--	--	--	--	--	--	--	--	--	--	--	--	--	--	--	--	--	--	--	--	--	--	--	--	--	--	--	--	--	--	--	--	--	--	--	--	--	--	--	--	--	--	--	--	--	--	--	--	--	--	--	--	--	--	--	--	--	--	--	--	--	--	--	--	--	--	--	--	--	--	--	--	--	--	--	--	--	--	--	--	--	--	--	--	--	--	--	--	--	--	--	--	--	--	--	--	--	--	--	--	--	--	--	--	--	--	--	--	--	--	--	--	--	--	--	--	--	--	--	--	--	--	--	--	--	--	--	--	--	--	--	--	--	--	--	--	--	--	--	--	--	--	--	--	--	--	--	--	--	--	--	--	--	--	--	--	--	--	--	--	--	--	--	--	--	--	--	--	--	--	--	--	--	--	--	--	--	--	--	--	--	--	--	--	--	--	--	--	--	--	--	--	--	--	--	--	--	--	--	--	--	--	--	--	--	--	--	--	--	--	--	--	--	--	--	--	--	--	--	--	--	--	--	--	--	--	--	--	--	--	--	--	--	--	--	--	--	--	--	--	--	--	--	--	--	--	--	--	--	--	--	--	--	--	--	--	--	--	--	--	--	--	--	--	--	--	--	--	--	--	--	--	--	--	--	--	--	--	--	--	--	--	--	--	--	--	--	--	--	--	--	--	--	--	--	--	--	--	--	--	--	--	--	--	--	--	--	--	--	--	--	--	--	--	--	--	--	--	--	--	--	--	--	--	--	--	--	--	--	--	--	--	--	--	--	--	--	--	--	--	--	--	--	--	--	--	--	--	--	--	--	--	--	--	--	--	--	--	--	--	--	--	--	--	--	--	--	--	--	--	--	--	--	--	--	--	--	--	--	--	--	--	--	--	--	--	--	--	--	--	--	--	--	--	--	--	--	--	--	--	--	--	--	--	--	--	--	--	--	--	--	--	--	--	--	--	--	--	--	--	--	--	--	--	--	--	--	--	--	--	--	--	--	--	--	--	--	--	--	--	--	--	--	--	--	--	--	--	--	--	--	--	--	--	--	--	--	--	--	--	--	--	--	--	--	--	--	--	--	--	--	--	--	--	--	--	--	--	--	--	--	--	--	--	--	--	--	--	--	--	--	--	--	--	--	--	--	--	--	--	--	--	--	--	--	--	--	--	--	--	--	--	--	--	--	--	--	--	--	--	--	--	--	--	--	--	--	--	--	--	--	--	--	--	--	--	--	--	--	--	--	--	--	--	--	--	--	--	--	--	--	--	--	--	--	--	--	--	--	--	--	--	--	--	--	--	--	--	--	--	--	--	--	--	--	--	--	--	--	--	--	--	--	--	--	--	--	--	--	--	--	--	--	--	--	--	--	--	--	--	--	--	--	--	--	--	--	--	--	--	--	--	--	--	--	--	--	--	--	--	--	--	--	--	--	--	--	--	--	--	--	--	--	--	--	--	--	--	--	--	--	--	--	--	--	--	--	--	--	--	--	--	--	--	--	--	--	--	--	--	--	--	--	--	--	--	--	--	--	--	--	--	--	--	--	--	--	--	--	--	--	--	--	--	--	--	--	--	--	--	--	--	--	--	--	--	--	--	--	--	--	--	--	--	--	--	--	--	--	--	--	--	--	--	--	--	--	--	--	--	--	--	--	--	--	--	--	--	--	--	--	--	--	--	--	--	--	--	--	--	--	--	--	--	--	--	--	--	--	--	--	--	--	--	--	--	--	--	--	--	--	--	--	--	--	--	--	--	--	--	--	--	--	--	--	--	--	--	--	--	--	--	--	--	--	--	--	--	--	--	--	--	--	--	--	--	--	--	--	--	--	--	--	--	--	--	--	--	--	--	--	--	--	--	--	--	--	--	--	--	--	--	--	--	--	--	--	--	--	--	--	--	--	--	--	--	--	--	--	--	--	--	--	--	--	--	--	--	--	--	--	--	--	--	--	--	--	--	--	--	--	--	--	--	--	--	--	--	--	--	--	--	--	--	--	--	--	--	--	--	--	--	--	--	--	--	--	--	--	--	--	--	--	--	--	--	--	--	--	--	--	--	--	--	--	--	--	--	--	--	--	--	--	--	--	--	--	--	--	--	--	--	--	--	--	--	--	--	--	--	--	--	--	--	--	--	--	--	--	--

Notes:

(1) The EAF Usage Factors above were calculated with the Fatigue Design Curve from Reference [1], Table A.2.

(2) Per Section 2.1, the overall EAF_{en} usage factor for the location is: $U_{en} = F_{en,1}U_1 + F_{en,2}U_2 + F_{en,3}U_3 + \dots$.

(3) [

(4) [

]

]

7.0 RESULTS

Per Tables 6-7 and 6-8, the EAF usage factors have been recalculated and shown to be less than 1.0 [

However removing this conservatism provides a more accurate and realistic usage factor as presented in these calculations.]

8.0 REFERENCES

References identified with an (*) are maintained within Turkey Point Nuclear Power Plant Records System and are not retrievable from AREVA Records Management. These are acceptable references per AREVA Administrative Procedure 0402-01, Attachment 8. See page 2 for Project Manager Approval of customer references.

1. NUREG/CR-6909, Revision 1, “Effect of LWR Coolant Environments on the Fatigue Life of Reactor Materials”, DRAFT, March 2014.
2. ASME B&PV Code Sec. III, SubSection 1989 edition with no Addenda.
3. Areva Document 38-9279661-000, [NNPARV-17-0241, NNPARV-17-0243], “Formal Transmittal of inputs for Areva Evaluation of Environmentally Assisted Fatigue at Turkey Point Units 3 and 4”.
4. AREVA Document 38-9279681-000, JSPM Document 17NI0548, Rev. B, “Turkey Point Power Plant – Data for the fatigue analysis of the criticals points of latch housing and canopy joint”.
5. Textbook, “Advanced Strength and Applied Elasticity The SI Version”, A.C. Ugural, S.K. Fenster, 1982, Elsevier Science Publishing Co.
6. AREVA Document 33-9127371-001, “Turkey Point Plant Extended Power Uprate Control Rod Drive Mechanism Pressure Housing Assembly Appurtenances ASME Class 1”.
7. AREVA Document 38-9280092-000, [NNPARV-17-0268], “Formal Transmittal of input for Areva Evaluation of Environmentally Assisted Fatigue at Turkey Point Units 3 and 4”.

APPENDIX A: BASIS FOR PRINCIPAL STRESS CALCULATIONS

A.1 Equations for Principal Stress Calculations

The source equations from the text, “Advanced Strength and Applied Elasticity The SI Version”, [5] are shown here for documentation purposes.

Advanced Strength and Applied Elasticity The SI Version

A.C. Ugural
Fairleigh Dickinson University

S. K. Fenster
New Jersey Institute of Technology

Elsevier Science Publishing Co., Inc.
52 Vanderbilt Avenue, New York, New York

Distributors outside the United States and Canada:
Elsevier Science Publishers B.V.
P.O. 211, 1000 AE Amsterdam, The Netherlands

©1981 by Elsevier Science Publishing Co., Inc.
Second Printing, 1982

Library of Congress Cataloging in Publication Data

Ugural, A.C.
Advanced strength and applied elasticity: The SI version.
Includes bibliographical references and index.
1. Strength materials. 2. Elasticity. I. Fenster,
Saul K., 1933– joint author. II. Title.
TA405.U42 1981 620.1'12 80-26638
ISBN 0-444-00428-9

Desk Editor Louise Calabro Schreiber
Design Edmée Froment
Art Editor Glen Burris
Cover Design Paul Agule Design
Production Manager Joanne Jay
Compositor Science Typographers, Inc.
Printer Haddon Craftsmen

Manufactured in the United States of America

Appendix B

A Practical Approach to the Stress Cubic Equation and Direction Cosines

B.1 Principal Stresses

There are many methods in common usage for solving a cubic equation. A simple approach for dealing with Eq. (1.20) is to find one root, say σ_1 , by plotting it (σ as abscissa) or by trial and error. The cubic equation is then factored by dividing by $(\sigma_p - \sigma_1)$ to arrive at a quadratic equation. The remaining roots can be obtained by applying the familiar general solution of a quadratic equation. This process requires considerable time and algebraic work, however.

What follows is a practical approach for determining the roots of stress cubic equation (1.20):

$$\sigma_p^3 - I_1\sigma_p^2 + I_2\sigma_p - I_3 = 0 \quad (a)$$

where

$$\begin{aligned} I_1 &= \sigma_x + \sigma_y + \sigma_z \\ I_2 &= \sigma_x\sigma_y + \sigma_x\sigma_z + \sigma_y\sigma_z - \tau_{xy}^2 - \tau_{yz}^2 - \tau_{xz}^2 \\ I_3 &= \sigma_x\sigma_y\sigma_z + 2\tau_{xy}\tau_{yz}\tau_{xz} - \sigma_x\tau_{yz}^2 - \sigma_y\tau_{xz}^2 - \sigma_z\tau_{xy}^2 \end{aligned} \quad (B.1)$$

According to the method, expressions that provide direct means for solving both two-dimensional and three-dimensional stress problems are*

$$\begin{aligned} \sigma_a &= 2S[\cos(\alpha/3)] + \frac{1}{3}I_1 \\ \sigma_b &= 2S\{\cos[(\alpha/3) + 120^\circ]\} + \frac{1}{3}I_1 \\ \sigma_c &= 2S\{\cos[(\alpha/3) + 240^\circ]\} + \frac{1}{3}I_1 \end{aligned} \quad (B.2)$$

*See E. E. Messal, Finding true maximum shear stress, *Machine Design* pp. 166–169 (December 7, 1978).

408 A Practical Approach to the Stress Cubic Equation and Direction Cosines

Here the constants are given by

$$\begin{aligned}
 S &= \left(\frac{1}{3}R\right)^{1/2} \\
 \alpha &= \cos^{-1}\left(-\frac{Q}{2T}\right) \\
 R &= \frac{1}{3}I_1^2 - I_2 \\
 Q &= \frac{1}{3}I_1I_2 - I_3 - \frac{2}{27}I_1^3 \\
 T &= \left(\frac{1}{27}R^3\right)^{1/2}
 \end{aligned} \tag{B.3}$$

and invariants I_1 , I_2 , and I_3 are represented in terms of the given stress components by Eqs. (B.1).

The principal stresses found from Eqs. (B.2) are *redesignated* using numerical subscripts so that $\sigma_1 > \sigma_2 > \sigma_3$. The above procedure is well adapted to a pocket calculator or digital computer.

Enclosure 4
Non-proprietary Reference Documents
and
Redacted Versions of Proprietary
Reference Documents
(Public Version)
Attachment 9

PWROG-17031-NP, Rev. 0

Update for Subsequent License Renewal: WCAP-15338-A

**A Review of Cracking Associated with Weld Deposited
Cladding in Operating PWR Plants, August 2017**

(34 Total Pages, including cover sheets)



PWROG-17031-NP
Revision 0

WESTINGHOUSE NON-PROPRIETARY CLASS 3

Update for Subsequent License Renewal: WCAP-15338-A, “A Review of Cracking Associated with Weld Deposited Cladding in Operating PWR Plants”

Materials Committee

PA-MS-C-1497

August 2017

PWROG-17031-NP
Revision 0

Update for Subsequent License Renewal: WCAP-15338-A, “A Review of Cracking Associated with Weld Deposited Cladding in Operating PWR Plants”

PA-MS-C-1497

Gordon Z. Hall*
Major Reactor Component Design and Analysis I
August 2017

Reviewer: Thomas E. Demers *
Major Reactor Component Design and Analysis I

Approved: Carl J. Gimbrone* for Stephen P. Rigby, Manager
Major Reactor Component Design and Analysis - I

Approved: James P. Molkenhuth*, Program Director
PWR Owners Group PMO

*Electronically approved records are authenticated in the electronic document management system.

Westinghouse Electric Company LLC
1000 Westinghouse Drive
Cranberry Township, PA 16066, USA

© 2017 Westinghouse Electric Company LLC
All Rights Reserved

ACKNOWLEDGEMENTS

This report was developed and funded by the PWR Owners Group under the leadership of the participating utility representatives of the Materials Committee.

WESTINGHOUSE ELECTRIC COMPANY LLC PROPRIETARY**LEGAL NOTICE:**

This report was prepared as an account of work performed by Westinghouse Electric Company LLC. Neither Westinghouse Electric Company LLC, nor any person acting on its behalf:

1. Makes any warranty or representation, express or implied including the warranties of fitness for a particular purpose or merchantability, with respect to the accuracy, completeness, or usefulness of the information contained in this report, or that the use of any information, apparatus, method, or process disclosed in this report may not infringe privately owned rights; or
2. Assumes any liabilities with respect to the use of, or for damages resulting from the use of, any information, apparatus, method, or process disclosed in this report.

COPYRIGHT NOTICE:

This report has been prepared by Westinghouse Electric Company LLC and bears a Westinghouse Electric Company copyright notice. Information in this report is the property of, and contains copyright material owned by, Westinghouse Electric Company LLC and /or its subcontractors and suppliers. It is transmitted to you in confidence and trust, and you agree to treat this document and the material contained therein in strict accordance with the terms and conditions of the agreement under which it was provided to you.

DISTRIBUTION NOTICE

This report was prepared for the PWR Owners Group. This Distribution Notice is intended to establish guidance for access to this information. This report (including proprietary and non-proprietary versions) is not to be provided to any individual or organization outside of the PWR Owners Group program participants without prior written approval of the PWR Owners Group Program Management Office. However, prior written approval is not required for program participants to provide copies of Class 3 Non-Proprietary reports to third parties that are supporting implementation at their plant, or for submittals to the USNRC.

PWR Owners Group
United States Member Participation* for PA-MSC-1497

Utility Member	Plant Site(s)	Participant	
		Yes	No
Ameren Missouri	Callaway (W)		X
American Electric Power	D.C. Cook 1 & 2 (W)	X	
Arizona Public Service	Palo Verde Unit 1, 2, & 3 (CE)		X
Dominion Connecticut	Millstone 2 (CE)		X
	Millstone 3 (W)	X	
Dominion VA	North Anna 1 & 2 (W)	X	
	Surry 1 & 2 (W)	X	
Duke Energy Carolinas	Catawba 1 & 2 (W)	X	
	McGuire 1 & 2 (W)	X	
	Oconee 1 (B&W)	X	
	Oconee 2, & 3 (B&W)		X
Duke Energy Progress	Robinson 2 (W)	X	
	Shearon Harris (W)	X	
Entergy Palisades	Palisades (CE)		X
Entergy Nuclear Northeast	Indian Point 2 & 3 (W)		X
Entergy Operations South	Arkansas 1 (B&W)		X
	Arkansas 2 (CE)		X
	Waterford 3 (CE)		X
Exelon Generation Co. LLC	Braidwood 1 & 2 (W)	X	
	Byron 1 & 2 (W)	X	
	TMI 1 (B&W)		X
	Calvert Cliffs 1 & 2 (CE)		X
	Ginna (W)		X
FirstEnergy Nuclear Operating Co.	Beaver Valley 1 & 2 (W)		X
	Davis-Besse (B&W)		X
Florida Power & Light \ NextEra	St. Lucie 1 & 2 (CE)		X
	Turkey Point 3 & 4 (W)	X	
	Seabrook (W)		X
	Pt. Beach 1 & 2 (W)	X	

**PWR Owners Group
United States Member Participation* for PA-MSC-1497**

Utility Member	Plant Site(s)	Participant	
		Yes	No
Luminant Power	Comanche Peak 1 & 2 (W)		X
Omaha Public Power District	Fort Calhoun (CE)		X
Pacific Gas & Electric	Diablo Canyon 1 & 2 (W)		X
PSEG – Nuclear	Salem 1 & 2 (W)		X
South Carolina Electric & Gas	V.C. Summer (W)	X	
So. Texas Project Nuclear Operating Co.	South Texas Project 1 & 2 (W)		X
Southern Nuclear Operating Co.	Farley 1 & 2 (W)		X
	Vogtle 1 & 2 (W)		X
Tennessee Valley Authority	Sequoyah 1 & 2 (W)		X
	Watts Bar 1 & 2 (W)		X
Wolf Creek Nuclear Operating Co.	Wolf Creek (W)		X
Xcel Energy	Prairie Island 1 & 2 (W)	X	

* Project participants as of the date the final deliverable was completed. On occasion, additional members will join a project. Please contact the PWR Owners Group Program Management Office to verify participation before sending this document to participants not listed above.

**PWR Owners Group
International Member Participation* for PA-MS-1497**

Utility Member	Plant Site(s)	Participant	
		Yes	No
Asociación Nuclear Ascó-Vandellòs	Asco 1 & 2 (W)		X
	Vandellos 2 (W)		X
Axpo AG	Beznau 1 & 2 (W)		X
Centrales Nucleares Almaraz-Trillo	Almaraz 1 & 2 (W)		X
EDF Energy	Sizewell B (W)		X
Electrabel	Doel 1, 2 & 4 (W)		X
	Tihange 1 & 3 (W)		X
Electricite de France	58 Units		X
Eletronuclear-Eletronuclear	Angra 1 (W)		X
Emirates Nuclear Energy Corporation	Barakah 1 & 2		X
EPZ	Borssele		X
Eskom	Koeberg 1 & 2 (W)		X
Hokkaido	Tomari 1, 2 & 3 (MHI)		X
Japan Atomic Power Company	Tsuruga 2 (MHI)		X
Kansai Electric Co., LTD	Mihama 3 (W)		X
	Ohi 1, 2, 3 & 4 (W & MHI)		X
	Takahama 1, 2, 3 & 4 (W & MHI)		X
Korea Hydro & Nuclear Power Corp.	Kori 1, 2, 3 & 4 (W)		X
	Hanbit 1 & 2 (W)		X
	Hanbit 3, 4, 5 & 6 (CE)		X
	Hanul 3, 4, 5 & 6 (CE)		X
Kyushu	Genkai 2, 3 & 4 (MHI)		X
	Sendai 1 & 2 (MHI)		X
Nuklearna Elektrarna KRSKO	Krsko (W)		X
Ringhals AB	Ringhals 2, 3 & 4 (W)		X
Shikoku	Ikata 1, 2 & 3 (MHI)		X
Taiwan Power Co.	Maanshan 1 & 2 (W)		X

* Project participants as of the date the final deliverable was completed. On occasion, additional members will join a project. Please contact the PWR Owners Group Program Management Office to verify participation before sending this document to participants not listed above.

TABLE OF CONTENTS

1	Background and Introduction	1-1
2	Mechanisms of Cracking Associated with Weld Deposited Cladding.....	2-1
3	Plant Experience with Defects in and under the Weld-deposited Cladding	3-1
3.1	PWR Plants	3-1
3.1.1	Reactor Vessel Experience: Underclad Cracks.....	3-1
3.1.2	Reactor Vessel Experience: Exposed Base Metal	3-3
3.1.3	Other Primary System Component Experience.....	3-4
3.2	BWR Plants	3-4
3.3	PWR Service Experience Since 1999	3-5
4	Effects of Cladding on Fracture Analysis.....	4-1
5	Vessel Integrity Assessment	5-1
5.1	Potential for Inservice Exposure of the Vessel Base Metal To Reactor Coolant Water..	5-1
5.2	Fatigue Usage	5-1
5.3	Acceptance Criteria	5-2
5.3.1	ASME Section XI – IWB-3500	5-2
5.3.2	ASME Section XI – IWB-3600	5-2
5.4	Fatigue crack growth	5-3
5.5	Allowable Flaw Size – Normal, Upset & Test Conditions	5-8
5.6	Sensitivity of Inservice Inspections	5-11
5.7	Allowable Flaw Size – Emergency & Faulted Conditions.....	5-11
6	Summary and Conclusions	6-1
7	References	7-1

1 Background and Introduction

Underclad cracking was initially detected at the Rotterdam Dockyard Manufacturing (RDM) Company during magnetic particle inspections of a reactor vessel in January 1971. These inspections were performed as part of an investigation initiated by RDM as a result of industry observations reported in December 1970. Subsequent evaluations by Westinghouse [1, 2 and 3] concluded that these underclad cracks would not have an impact on the integrity of reactor vessels for a full 40 years of operation. The evaluation was submitted to the Atomic Energy Commission in 1972, and the AEC review concurred [4]. This type of underclad cracking is now commonly referred to as reheat cracking.

In late 1979, a new form of underclad cracking ("cold" cracking) was observed. Westinghouse isolated it to a select group of vessels (only 6 are operating in the U.S.) which were considered suspect. Supplemental inspections of these vessels confirmed the presence of flaw indications indicative of 'cold' cracking. Such flaw indications were determined to be acceptable to the standards in the ASME Boiler and Pressure Vessel Code, Section XI, Paragraph IWB-3500. Furthermore, fracture evaluations of the reported flaw indications concluded that there would be no impact on the integrity of the reactor vessels for 40 years of operation.

A number of reactor vessels with confirmed flaw indications indicative of underclad cracks remain in service, and the potential for such cracks cannot be conclusively ruled out in any vessel with weld-deposited cladding. The cracks are in base metal immediately beneath the clad, and are created as a result of the weld deposited cladding process.

The purpose of this report is to update the 60 year fatigue crack growth analysis in [26] and confirm the analysis remains appropriate for application to subsequent license renewal (SLR), up to 80 years of operation. More specifically:

- Revise the fatigue crack growth analysis for 80 years of operation.
- Confirm fracture toughness values used in Appendix A of [26] are bounding for 80 years of operation.
- Update operating experience as discussed in Sections 2 and 3 of [26].
- Include discussion of state of the art inspection techniques and capabilities for detecting and characterizing cracks associated with manufacturing processes as well as those due to potentially service-induced mechanisms.

This report is applicable to all Westinghouse plants.

2 Mechanisms of Cracking Associated with Weld Deposited Cladding

Underclad cracking was initially detected in 1970, and has been extensively investigated by Westinghouse and others over the past 30 years. This cracking has been relatively widespread, having occurred in France and Japan, as well as the USA.

The cracking has occurred in the low alloy steel base metal heat-affected zone (HAZ) beneath the austenitic stainless steel weld overlay that is deposited to protect the ferritic material from corrosion. Two types of underclad cracking have been identified.

Reheat cracking has occurred as a result of post weld heat treatment of single-layer austenitic stainless steel cladding applied using high-heat-input welding processes on ASME SA-508, Class 2 forgings. The high-heat-input welding processes effecting reheat cracking, based upon tests of both laboratory samples and clad nozzle cutouts, include strip clad, six-wire clad and manual inert gas (MIG) cladding processes. Testing also revealed that reheat cracking did not occur with one-wire and two-wire submerged arc cladding processes [1 and 3]. The cracks are often numerous and are located in the base metal region directly beneath the cladding. They are confined to a region approximately 0.125 inch deep and 0.4 inch long [5].

Cold cracking has occurred in ASME SA-508, Class 3 forgings after deposition of the second and third layers of cladding, where no pre-heating or post-heating was applied during the cladding procedure. The cold cracking was determined to be attributable to residual stresses near the yield strength in the weld metal and base metal interface after cladding deposition, combined with a crack-sensitive microstructure in the HAZ and high levels of diffusible hydrogen in the austenitic stainless steel or Inconel weld metals. The hydrogen diffused into the HAZ and caused cold (hydrogen-induced) cracking as the HAZ cooled [14]. Destructive analyses have demonstrated that these cracks vary in depth from 0.007 inch to 0.295 inch and in length from 0.078 inch to 2.0 inches. Typical cold crack dimensions were 0.078 inch to 0.157 inch in depth, and 0.196 inch to 0.59 inch in length. As with the reheat cracks, these cracks initiate at or near the clad/base metal fusion line and penetrate into the base metal [15].

3 Plant Experience with Defects in and under the Weld-deposited Cladding

This section updates the historic operating experience data in [26].

3.1 PWR Plants

The U.S. nuclear industry has had many years of service experience with fabrication related defects and/or flaw indications in the cladding, through the cladding into the base metal, and in the base metal just below the cladding. None of these anomalies have challenged the integrity of the reactor vessels in over 2000 reactor years of service experience.

3.1.1 Reactor Vessel Experience: Underclad Cracks

An industry task group was established by the Pressure Vessel Research Council (PVRC) as a result of the underclad reheating cracking issue, and this group did a survey of the industry in 1973-74 to identify the number of underclad cracking events which had been observed. A total of 96 survey forms were returned, covering manufactured vessels by 11 different firms on three continents. Of these, five were European, five were American, and one was Japanese.

Of the 96 surveys return, 26 cases of underclad cracking were reported. The cracking cases were confined to forging materials, SA-508 Class 2 (25 cases of 47 surveys) and SA-508 Class 3 (1 of 9 surveys). There were no reported cases in SA-533B, SA-302B, SA-302B nickel modified, or A387D plate materials. The report of the task group [5] contains a statistical study performed to identify the influence of chemistry, tensile strength, and post weld heat treatment on cracking sensitivity. This work was used by the fabricators to refine their process to minimize cracking in the vessels fabricated thereafter.

Westinghouse participated in the PVRC task group, and also performed a large number of preservice inspections of reactor vessels during the 1970s and 1980s to baseline the condition of reactor vessels for future inservice inspections. A number of occurrences of underclad reheating cracking were identified during these examinations. Subsequent inservice inspections of these same vessels with ASME Section XI/Regulatory Guide 1.150 inspection techniques have revealed no measurable growth in these flaw indications.

In late 1979, underclad cold cracking was reported by a European Nuclear Steam Supply System (NSSS) provider. This type of cracking was observed in SA-508, Class 3 nozzles clad with multiple-layer, strip-electrode, and submerged-arc welding processes where preheating and post-heating were applied to the first layer but not to subsequent layers [14]. A review of cladding practices used on vessel nozzle bores in Westinghouse domestic and Japanese plants indicated that a number of vessels were considered suspect in terms of underclad 'cold' cracking [16].

The nozzle bores in all six of the domestic plants considered suspect were examined ultrasonically in 1980 and 1981 using a special underclad cracking technique to determine the extent of the underclad “cold” cracking issue [17 - 21]. This ultrasonic technique was demonstrated to be 5 times more sensitive than the ASME Section XI mandated sensitivities [15]. Five of the six vessels contained flaw indications indicative of underclad “cold” cracking; all the reported flaw indications met the acceptance standards of the ASME Code Section XI [17 - 21]. Four of the reported flaw indications were destructively analyzed and found to be within the depth/length bounds of 0.295 inch in depth and 2 inches in length for underclad cold cracking [22].

Subsequently, these vessels have since undergone inservice inspections (ISI, 40-month and/or 10-year) in accordance with the ASME Code Section XI with no reported issues. These follow-up examinations make comparisons difficult because of the changing ISI methods through time as well as the different sensitivities applied. One detailed comparison by Rishel and Bamford [6] was reported for inspections of the Sequoyah Unit 1 reactor vessel nozzle bores, in 1993. A special preservice examination of the Sequoyah Unit 1 reactor vessel nozzle bores was done in 1980, by Westinghouse which revealed the extent of any potential underclad cold cracks, including their location and lengths [20]. During the first 10-year inservice inspection for the Sequoyah Unit 1 reactor vessel, performed by Southwest Research (SwRI), flaw indications indicative of underclad cold cracks were detected again using ASME Section XI/USNRC Regulatory Guide 1.150 inspection procedures. It is noted that a specific goal of this inservice inspection was to determine if any of the previously recorded flaw indications had grown during service. The comparison report concluded that there was no observable increase in the size of the assumed underclad cold cracks during the 13 year duration (including at least 10 years of service), but the conclusion was somewhat uncertain because of the different inspection methods employed for the two examinations. A fatigue crack growth analysis showed that little or no growth would be expected, and all the flaws were acceptable to the standards of the ASME Code Section XI, so no further evaluation was required [6].

In the 1983 10-Year ISI of the Palisades reactor vessel welds, two small clusters of reheat cracks situated on either side of an intermediate shell longitudinal seam were detected using 60-degree longitudinal wave UT techniques. These indications were individually assigned a conservative flaw size and were determined to be within the allowable limits of Section XI, IWB-3500. In the 1995 10-year Inservice Inspection, similar clusters were detected in the same area using 70-degree longitudinal wave UT techniques. The indication depths (0.3 inch), the echodynamic signature of the indication responses, and the rate of occurrence were consistent with the previous interpretation of reheat cracking. There was no evidence that these bands of indications had expanded in number or size.

Additionally, underclad cracks are being monitored in various French plants every 10 years to determine whether there is any measurable growth. No integrity issues have been reported to date.

3.1.2 Reactor Vessel Experience: Exposed Base Metal

Various reactor vessels have been operating with exposed base metal surfaces as a result of the removal of the cladding. The reactor vessel experiences listed below showed exposed base metal does not affect the reactor vessel's integrity. Therefore, it has been shown to be acceptable even if underclad cracks become a surface crack exposing the base metal to RCS fluid.

1. Yankee Rowe Reactor Vessel

Two clad areas (approximately 1" x 1" and 2" x 4") in the Yankee Rowe reactor vessel were removed due to wear caused by a loose surveillance capsule. These areas had been observed during shutdown. Subsequent measurements of these areas using underwater replication techniques and after approximately 16 years of service have revealed no measurable penetration into the base metal. This result is consistent with the analyses performed for acceptance of these areas [23].

The stainless steel cladding was stitch clad (resistance welded) using 4 ft. x 8 ft. plates. An analysis considering corrosion of these 4 ft. by 8 ft. areas of the bare base metal was performed. It was assumed that with the worn clad areas and cracking in the cladding, the complete cladding/base metal interface would be exposed to the reactor water environment. This analysis showed that this condition was acceptable.

2. Connecticut Yankee Reactor Vessel

The Connecticut Yankee reactor vessel also had the weld-deposited stainless cladding on the reactor vessel worn through because of a surveillance capsule which had come loose. No detrimental effects were observed in over 25 years of service, although the plant is now closed, for other reasons. The reason for this excellent performance has been attributed to primary system chemistry controls.

3. Watts Bar Unit 1 Reactor Vessel Inlet Nozzles

As a result of ultrasonic examination of the Watts Bar Unit 1 nozzles for the assessment of underclad cold cracks, three areas in two inlet nozzles were destructively examined by grinding to determine the depth of four indications [22]. The three clad-removed areas remain in the nozzle. The total size of the three areas is approximately 3 square inches. As of 2002, the plant has operated for at least 7 years with no problems, again because of tight primary system chemistry control.

4. McGuire Unit 2 Bottom Head Dutchman

The McGuire Unit 2 reactor vessel has an area in the bottom head transition piece between the lower head and vessel shell where stainless steel cladding has been removed. The low alloy steel base metal is exposed to reactor water. The area is 4 to 5 inches long circumferentially, ½ to 1 inches wide vertically and 0.25 inch deep. It is located in the lower head transition cone at 270° approximately 1 1/2 inch above the bottom head to transition cone weld. As of 2002, the plant has continued operation with no repair of the exposed area for over ten years with no reported problems.

3.1.3 Other Primary System Component Experience

Crack-like indications have been found in the cladding of a number of pressurizers and steam generators. Most of these indications have been found in the narrow zone between adjacent strips of cladding. In a number of cases, Westinghouse has been involved in the inspection and disposition of these indications, and in every case, the owners and vendors determined that no repair was needed, and the USNRC concurred.

There are at least seven plants where these indications have been found in the steam generator channel head region including:

- Indian Point 3 (replaced in 1989)
- Salem 1 and 2
- Turkey Point 3 and 4
- Beznau 1 and 2 (Switzerland) [replaced in 1996]

In each of these plants a surveillance program was established to monitor the growth of these indications. Two follow-up inspections were conducted after the initial findings. In most cases, the monitoring inspections were conducted every 40 months, in conjunction with regular ISI. In the five U. S. Plants above, these surveillances detected no significant changes in the indications. This led to the USNRC allowing for the termination of these programs. For the Beznau plants, the surveillances continued until the steam generators were replaced in the early 1990s, with no issues.

In 1990, a number of indications were discovered in the pressurizer cladding at the Connecticut Yankee Plant, as a result of a camera inspection of the bottom head and surge nozzle region. Ultrasonic inspection confirmed that the indications did not penetrate into the ferritic base metal, and so they were acceptable without further action, according to the rules of the ASME Code Section XI. As before, a surveillance program was put in place. After two follow-up inspections showed no change, the USNRC allowed the surveillance program to stop [24].

While these observations are reassuring, it should be pointed out that in several of the cases cited above, the regulators required fracture mechanics analyses to be completed to identify the acceptable flaw size in the region where the indications were found. These analyses have demonstrated that the cladding indications which have been identified will not compromise the integrity of the pressurizers or steam generators.

The Connecticut Yankee pressurizer also contains some small areas of the base metal exposed to RCS fluid as a result of grinding. This repair was performed in 1965 and was intended to remove underclad cracks. At the time of decommissioning, the pressurizer had operated for over 30 years with no detrimental effects. Westinghouse performed an engineering evaluation of this condition, considering the effects of both operating and shutdown plant environments, the effect of flow rates, and the effects of galvanic corrosion. The results showed the predicted maximum corrosion penetration for the remaining life of the plant was 0.173 inch [24]. The actual wall loss was not measured.

3.2 BWR Plants

Further evidence of acceptable plant operation with cladding removed and base metal exposed can be found in BWR plants.

A decision was made in 1980 to grind off the weld-deposited cladding around the entire circumference of the Feedwater nozzles in most U. S. BWR plants. Since that time, both surface and ultrasonic examinations have been required each fuel cycle, and no cracking or corrosion effects have been observed. Therefore, it has been shown to be acceptable even if underclad cracks become a surface crack exposing the base metal to RCS fluid.

3.3 PWR Service Experience Since 1999

A review was made of recent service experience resulting from degraded cladding, and very few new examples were found. The three cases below are the only known new cases [29] and [30]. Plants cited in Sections 3.1 and 3.2 which are still in operation continue to experience no detrimental effects of the missing cladding. Therefore, it has been shown to be acceptable even if underclad cracks become a surface crack exposing the base metal to RCS fluid.

1. Callaway Reactor Vessel Bottom Head Region

An indication in the cladding region at the bottom of the reactor vessel was found visually, due to a rust stain that was indicative of exposed low alloy steel. The indication was determined to encompass an area of 1.5 inch x 0.75 inch. The location was characterized as 302.94 degrees from the vessel "0" location, and 384.89 degrees from the flange surface. The plant has operated since 2004 with no issues, as verified by three separate inspections, each of which involved removing the core barrel.

2. Diablo Canyon Unit Reactor Vessel Inlet Nozzle

During the 2005 inspection for Diablo Canyon Unit 1 inlet nozzle inner radius, visual examination found an area of approximately 1.025 inch x 0.53 inch of clad scraping (spall) at 10 degrees from the bottom dead center of the nozzle. This particular region was re-examined visually in 2014, and it was determined that there was no noticeable change in the past 9 years. No degradation was identified and nor is it expected because the PWR environment is de-oxygenated, since the oxygen is scavenged by the hydrogen overpressure which is present during operation.

3. Qinshan Reactor Vessel Bottom Head Region

Indications were discovered in the bottom head region of Qinshan Phase 1 reactor vessel when it was examined in 1999. As discussed in [30], it was unclear whether the base metal was exposed. Due to the irregularity of the surface in the vicinity of the indication, a replication was made of the area and the shape of the degradation scar was determined by a laser scan. Since the original examination, the region has been examined three times, and no change has been observed.

The evaluation in [30] concluded that Qinshan is safe to operate until 2041 as requested, a total of 50 years (end of design life).

4 Effects of Cladding on Fracture Analysis

The effects of cladding on the fracture analysis were discussed in detail in Section 4 of [26]. Experiments were performed and measurements were taken. Fracture analyses of reactor pressure vessels subjected to thermal shock have employed various assumptions regarding the behavior of the cladding and its influence on the fracture resistance of the vessel. The effect of cladding is also important because of its relevance to underclad cracks. For the most part, it was assumed that the welded clad layer, being lower in strength and higher in ductility than the low-alloy pressure vessel steel, would produce no observable effect on the strength or apparent fracture toughness of the pressure vessel. In a positive sense, the clad layer was presumed to have a sufficient strength to reduce the stress intensity factor, or crack driving force.

Bend bar tests were conducted in [7 and 8] to study the effect of cladding on the structure behavior in the operating reactor vessels. Residual stress measurements performed in [9, 10, and 11] were discussed in [26] in detail. The residual stress measurement confirmed the bend bar test results. It was concluded in [26] that the effects of cladding will be more important at lower temperatures, where the stresses are higher. At temperatures over 180°F (82°C) the cladding has virtually no impact on fracture behavior, and this is the very lower end of the temperature range of the plant operation. The effects of the cladding is considered for flaws that penetrate the cladding into the base metal. For this report, the actual impact of the cladding residual stress on the fracture evaluation is negligible, even for irradiated materials, as also concluded by McCabe [13].

5 Vessel Integrity Assessment

This section discusses the reactor vessel integrity evaluation and assessment.

5.1 Potential for Inservice Exposure of the Vessel Base Metal To Reactor Coolant Water

The occurrence of wastage or wall thinning of the carbon steel vessel base metal requires the breaching of the complete thickness of the cladding so that the base metal is exposed to the reactor coolant system (RCS) environment. Thus the total process consists of two sequential steps:

1. Cracking and separation of a portion of the clad weld metal resulting in the exposure of the base metal to the primary water, and
2. Corrosive attack and wastage of the carbon steel base metal due to its exposure to the primary water

Delamination and separation of the complete clad thickness can occur either by mechanical distress or by micro-cracking induced by metallurgical degradation mechanisms. Examples of mechanical distress are denting and overload (overloads can result in metal plasticity and cracking) cracking caused by mechanical impact loads such as those due to a loose part. Metallurgical mechanisms include intergranular stress corrosion cracking (IGSCC) and transgranular stress corrosion cracking (TGSCC) mechanisms.

IGSCC of the clad metal can occur if the weld is sensitized (chromium depleted grain boundaries) and is exposed to oxygenated water. TGSCC can occur in the cladding only in the presence of a chloride environment. The typical PWR service and shut down RCS chemistry contains oxygen and chloride levels that are significantly below the threshold levels required to initiate either IGSCC or TGSCC.

Thus there is no degradation mechanism that can contribute to additional breaching of the clad thickness and result in any exposure of the vessel base metal. Even if the base metal were exposed, the degree of corrosive attack and wastage due to operation is insignificant as evidenced by operational histories and analyses based on corrosion tests.

5.2 Fatigue Usage

Review of the reactor vessel shell fatigue analysis in representative Westinghouse reactor vessels reveals that maximum cumulative fatigue usage factor is 0.04 or less for 60 years of operation. Assuming transient cycles linearly scale from 60 to 80 years, the maximum usage factor would be 0.053. This shows that the likelihood of fatigue cracks initiating during service is very low, even for the 80-year SLR application.

5.3 Acceptance Criteria

5.3.1 ASME Section XI – IWB-3500

The underclad cracks which have been identified over the years are very shallow, with a maximum depth of 0.295 inch (7.5mm). The flaw indications indicative of underclad cracks that have been found during pre-service and inservice inspections are all within the flaw acceptance standard of the ASME Code Section XI, Paragraph IWB-3500. Nonetheless, the USNRC RAI [26, Section 8] stated that the ASME Section XI IWB-3600 criteria should be used as evaluation criteria. Appendix A of [26] responded to the USNRC RAI questions, and was subsequently accepted by USNRC.

5.3.2 ASME Section XI – IWB-3600

There are two alternative sets of flaw acceptance criteria for ferritic components, for continued service without repair in paragraph IWB-3600 of ASME Code Section XI. Either of the criteria below may be used, at the convenience of the user.

(1) Acceptance criteria based on flaw size (IWB-3611)

(2) Acceptance criteria based on stress intensity factor, K_I (IWB-3612)

Both criteria are comparable for thick sections, and the acceptance criteria based on stress intensity factor have been determined by past experience to be less restrictive for thin sections, and for outside surface flaws in many cases. In all cases, the most beneficial criteria have been used in the evaluation to be presented here.

5.3.2.1 Criteria Based on Flaw Size

The code acceptance criteria stated in IWB-3611 of Section XI for ferritic steel components 4 inches and greater in wall thickness are:

$$\begin{aligned} a_f &< 0.1 a_c && \text{for normal conditions (including upset and test conditions) and,} \\ a_f &< 0.5 a_i && \text{for faulted conditions (including emergency conditions)} \end{aligned}$$

where

a_f = The maximum size to which the detected flaw is calculated to grow until the next inspection. An 80 year period is considered in the calculation herein.

a_c = The minimum critical flaw size under normal operating conditions.

a_i = The minimum critical flaw size for initiation of non-arresting growth under postulated faulted conditions.

5.3.2.2 Criteria Based on Applied Stress Intensity Factors

Alternatively, the code acceptance criteria stated in IWB-3612 of Section XI for ferritic steel components criteria based on applied stress intensity factors may be used:

$$\begin{aligned} K_I &< \frac{K_{Ia}}{\sqrt{10}} && \text{for normal conditions (including upset and test conditions)} \\ K_I &< \frac{K_{Ic}}{\sqrt{2}} && \text{for faulted conditions (including emergency conditions)} \end{aligned}$$

where

K_I = the maximum applied stress intensity factor for the final flaw size after crack growth.

K_{Ia} = Fracture toughness based on crack arrest for the corresponding crack tip temperature.

K_{Ic} = Fracture toughness based on fracture initiation for the corresponding crack tip temperature.

5.4 Fatigue crack growth

A series of fatigue crack growth (FCG) calculations were carried out to provide a prediction of future growth of underclad cracks for service periods up through 60 years in [26]. The FCG calculation is revised and updated herein for the 80-year SLR application.

To complete the fatigue crack growth analysis, the methodology of Section XI of the ASME Code was used, with the entire set of design transients applied over a 80 year period. The cycles applicable to 40 years of operation were conservatively multiplied by a factor of 2 to account for 80 years of operation. The analysis assumes a flaw of a specified size and shape, and considers each design transient in turn, calculating the crack growth, adding the crack growth increment to the original flaw size, and then repeating the process until all transient cycles have been accounted for.

The crack growth was conservatively calculated using the ASME Section XI, Appendix A, A-4300, crack growth rate for water environments [27]. This is the most current crack growth rate and is comparable to the rate in the original analysis in [26], which dates back to the ASME Code in 1979. This crack growth law is shown in Figure 5-1. Even though the underclad cracks are not exposed to the PWR water environment, the water crack growth rate was used in response to USNRC RAI in [26]. This is a conservative assumption.

A series of flaw types were postulated to include the various possible shapes for the underclad cracks. Specifically, the postulated flaw depths ranged from 0.05 inch (1.3mm) to 0.30 inch (7.6mm), which is beyond the 0.295 inch (7.5mm) maximum depth of an underclad cold crack. The shape of the flaws analyzed (flaw depth/flaw length) ranged from 0.01 through 0.5. The results are shown in Table 5-1 through Table 5-3. The maximum flaw size of 0.4267 inch at the end of 80 years is less than the minimum allowable flaw size of 0.67 inch, presented in Section 5.5.

Therefore, it may be concluded that the crack growth is insignificant for any type of flaw which might exist at the clad/base metal interface and into the base metal for both nozzle bore and vessel shell regions.

Table 5-1: Fatigue Crack Growth Result for Beltline Region, Axial Flaw (Water Environment)

Initial Flaw Depth	Depth after 20 years	Depth after 40 years	Depth after 60 years	Depth after 80 years
Flaw Shape AR = l/a = 2				
0.050	0.0504	0.0504	0.0504	0.0504
0.125	0.1256	0.1263	0.1263	0.1271
0.200	0.2023	0.2038	0.2054	0.2077
0.250	0.2534	0.2573	0.2612	0.2651
0.300	0.3046	0.3092	0.3147	0.3193
Flaw Shape AR = l/a = 6				
0.050	0.0504	0.0512	0.0512	0.0519
0.125	0.1302	0.1349	0.1403	0.1465
0.200	0.2108	0.2224	0.2341	0.2472
0.250	0.2643	0.2790	0.2945	0.3116
0.300	0.3178	0.3364	0.3557	0.3767
Continuous Flaw (l/a = 100)				
0.050	0.0507	0.0513	0.0520	0.0527
0.125	0.1323	0.1399	0.1481	0.1578
0.200	0.2156	0.2318	0.2495	0.2693
0.250	0.2713	0.2937	0.3187	0.3469
0.300	0.3277	0.3569	0.3895	0.4267

Note: Aspect Ratio l/a = flaw length / flaw depth. Depths are in inches.

Table 5-2: FCG Results for Beltline Region, Circumferential Flaw in Water

Initial Flaw Depth	Depth after 20 years	Depth after 40 years	Depth after 60 years	Depth after 80 years
Flaw Shape AR = l/a = 2				
0.050	0.0504	0.0504	0.0504	0.0504
0.125	0.1250	0.1256	0.1256	0.1256
0.200	0.2000	0.2007	0.2007	0.2015
0.250	0.2503	0.2511	0.2519	0.2519
0.300	0.3007	0.3015	0.3023	0.3030
Flaw Shape AR = l/a = 6				
0.050	0.0504	0.0504	0.0504	0.0504
0.125	0.1263	0.1271	0.1279	0.1287
0.200	0.2031	0.2062	0.2093	0.2124
0.250	0.2550	0.2604	0.2658	0.2720
0.300	0.3077	0.3147	0.3216	0.3294
Continuous Flaw (l/a = 100)				
0.050	0.0501	0.0502	0.0503	0.0504
0.125	0.1265	0.1278	0.1291	0.1305
0.200	0.2043	0.2083	0.2124	0.2167
0.250	0.2573	0.2646	0.2721	0.2801
0.300	0.3106	0.3208	0.3315	0.3429

Note: Aspect Ratio l/a = flaw length / flaw depth. Depths are in inches.

Table 5-3: FCG Results for Inlet Nozzle to Shell Weld, Axial Flaw in Water

Initial Flaw Depth	Depth after 20 years	Depth after 40 years	Depth after 60 years	Depth after 80 years
Flaw Shape AR = l/a = 2				
0.050	0.0500	0.0500	0.0500	0.0505
0.125	0.1253	0.1253	0.1253	0.1253
0.200	0.2001	0.2011	0.2011	0.2011
0.250	0.2506	0.2506	0.2517	0.2517
0.300	0.3012	0.3022	0.3022	0.3033
Flaw Shape AR = l/a = 6				
0.050	0.0505	0.0505	0.0505	0.0505
0.125	0.1264	0.1274	0.1274	0.1285
0.200	0.2032	0.2064	0.2095	0.2127
0.250	0.2559	0.2611	0.2664	0.2717
0.300	0.3085	0.3159	0.3243	0.3327
Continuous Flaw (l/a = 100)				
0.0500	0.0502	0.0503	0.0505	0.0506
0.1250	0.1271	0.1287	0.1303	0.1321
0.2000	0.2059	0.2111	0.2164	0.2222
0.2500	0.2597	0.2693	0.2796	0.2908
0.3000	0.3141	0.3276	0.3419	0.3576

Note: Aspect Ratio l/a = flaw length / flaw depth. Depths are in inches.

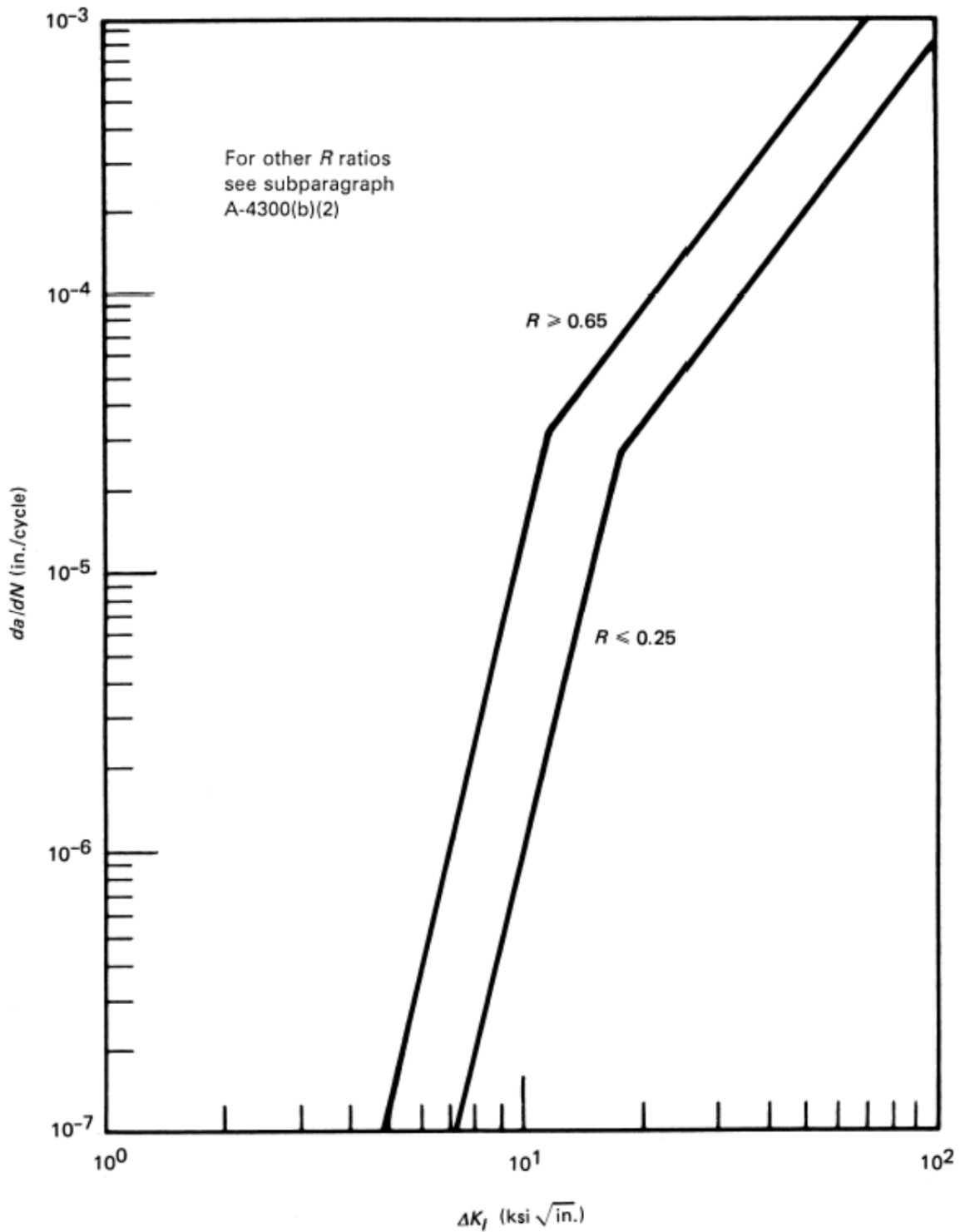


Figure 5-1: Reference Fatigue Crack Growth Curves for Carbon and Low Alloy Ferritic Steels Exposed to Water Environment [27, Fig. A-4300-2]

5.5 Allowable Flaw Size – Normal, Upset & Test Conditions

The allowable flaw size for normal, upset and test conditions was calculated and documented in [26], using the criteria in Section 5.3.2.2. The fracture toughness for ferritic steels has been taken directly from the reference curves of Appendix A, ASME Section XI. In the transition temperature region, these curves can be represented by the following equations:

$$K_{Ic} = 33.2 + 20.734 \exp [0.02 (T - RT_{NDT})]$$

$$K_{Ia} = 26.8 + 12.445 \exp. [0.0145 (T - RT_{NDT})]$$

where K_{Ic} and K_{Ia} are in $\text{ksi}\sqrt{\text{in}}$.

While these equations are the simplified form in the current ASME Section XI, they are mathematically identical to those presented in [26], there is no impact on the results.

The upper shelf temperature regime requires utilization of a shelf toughness, which is not specified in the ASME Code. A value of $200 \text{ ksi}\sqrt{\text{in}}$ has been used here. This conservative value is consistent with general practice in such evaluations. As shown in Table 5-4, the governing transients are in the upper temperature range. Fracture toughness, K_{Ic} per ASME Section XI, A-4200 would yield values higher than $200 \text{ ksi}\sqrt{\text{in}}$. Lower temperature transients are protected by the pressure-temperature (P-T) limits per ASME Section XI, Appendix G, assuming a 1/4T flaw, which is much larger than those flaws evaluated herein.

The evaluation detailed herein for normal operating, upset and test conditions is for a typical plant, and is expected to apply to any Westinghouse operating plant for an operating period of at least 80 years. Use of the upper shelf toughness to evaluate the normal operating, upset, and test condition transients is expected to remain appropriate for an 80 year life. Portions of the heatup and cooldown transients that drop to temperatures below the upper shelf region are governed by plant-specific P-T curves. Therefore, the allowable flaw size determined in Appendix A of [26] remains applicable for the 80-year SLR application.

As documented in [26], the minimum allowable flaw size was calculated using the most governing transients under normal operating conditions for the location of interest. To select the most governing transients for the beltline region, the stress intensity factors (K_I) for several normal, upset and test conditions were calculated for axial flaws in the beltline region. The axial flaws were chosen since the hoop stresses are higher than the axial stresses in the beltline region, as can be evident from the crack growth results in Table 5-1 and Table 5-2. The stress intensity factors are plotted in Figure 5-2 through Figure 5-4 for three different flaw shapes. Note that several transients were considered for each flaw shape, to ensure that the most governing transient would be chosen. The allowable flaw depth was chosen as the intersection of the stress intensity factor curve with the allowable fracture toughness, which is $200/\sqrt{10} = 63.2 \text{ ksi}\sqrt{\text{in}}$. The allowable flaw size results for normal, upset and test conditions are provided in Table 5-4. The minimum allowable flaw size is 0.67 inch.

Note that the analysis was performed using $200 \text{ ksi}\sqrt{\text{in}}$. The temperatures of the transients considered correspond to the upper shelf for the material. The selection of

this criterion remains conservative for the 80 year lifetime of the plant. Applicability of the peak thermal shock event governed by USNRC 10CFR50.61 is independent of the operation of the plant (whether 60 or 80 years).

Table 5-4: Allowable Flaw Size Summary for Beltline Region – Normal, Upset & Test Conditions

Flaw Shape	Governing Transient	Allowable Flaw Size	
		inches	(a/t)
Aspect Ratio 2:1	Inadvertent Safety Injection	4.07	(0.525)
Aspect Ratio 6:1	Reactor Trip with Cooldown and S.I.	1.34	(0.173)
Continuous Flaw	Excessive Feedwater Flow	0.67	(0.086)

Note: Wall Thickness = 7.75" is used here.

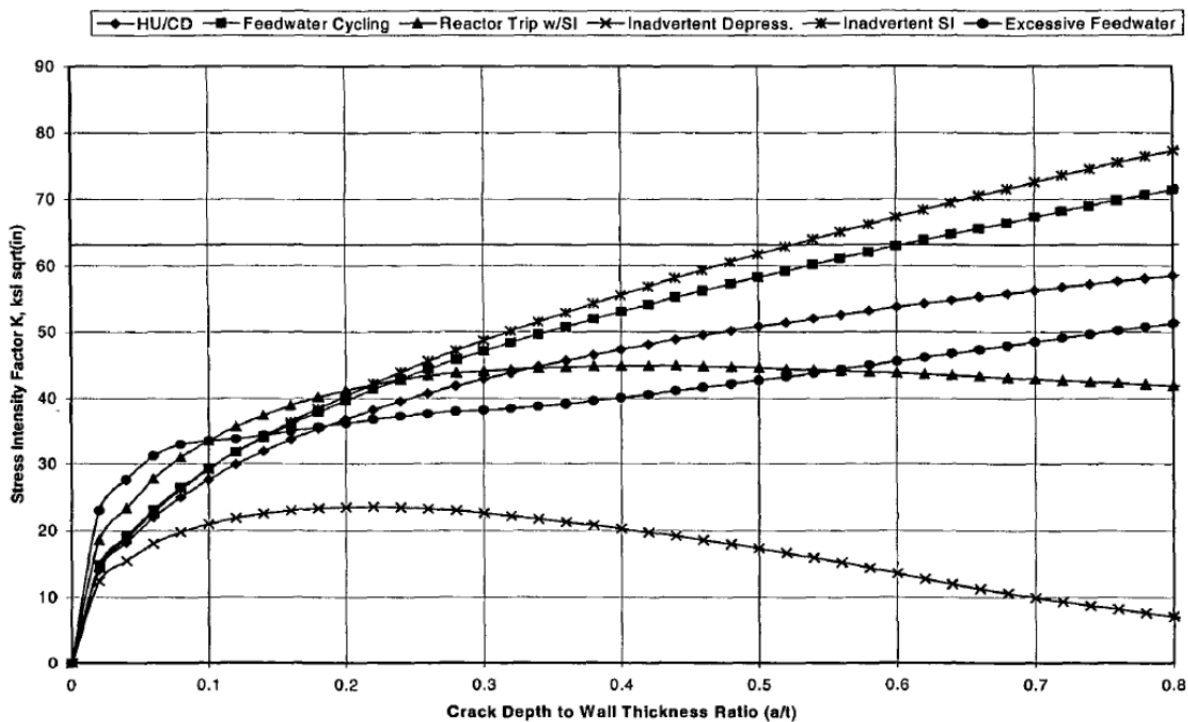


Figure 5-2: Allowable Flaw Size Determination – Beltline Region, Axial Flaw, AR 2:1

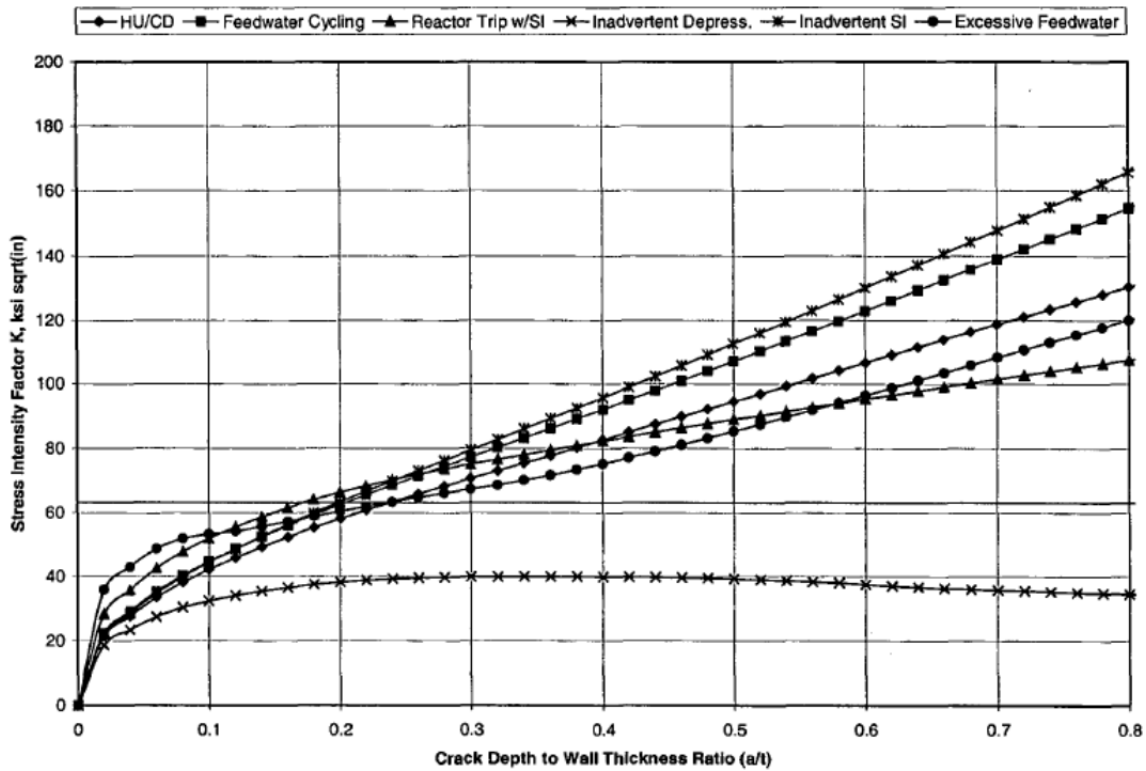


Figure 5-3: Allowable Flaw Size Determination – Beltline Region, Axial Flaw, AR 6:1

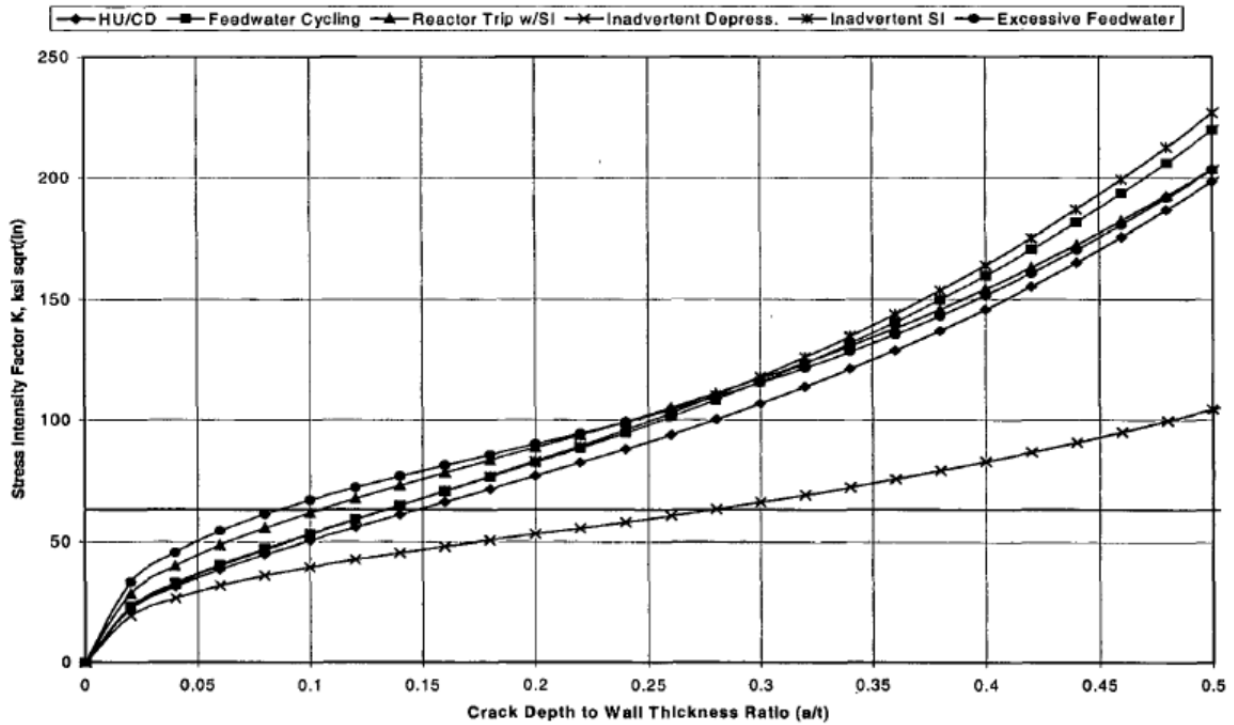


Figure 5-4: Allowable Flaw Size Determination – Beltline Region, Axial Flaw, Continuous

5.6 Sensitivity of Inservice Inspections

Regular inservice inspections of the vessel will continue to provide a monitor for assessing the integrity of the vessel. The capability to detect and size near-surface indications such as these was significantly improved with the advent of Regulatory Guide 1.150, in the early 1980s. This process was replaced by the performance demonstration requirements of ASME Section XI, Appendix VIII, Supplement 4 [27], and the Performance Demonstration Initiative (PDI) as mandated and amended by USNRC regulations (10CFR50.55(a)). This process requires that no surface connected flaw greater than 0.25-inch through-wall be missed and that the through-wall size of such flaws be measured within a 0.150-inch RMS (root mean square) tolerance. This process is currently used and will continue in the future to provide the capability for detection of flawed conditions and better characterization of any detected flaw indications.

5.7 Allowable Flaw Size – Emergency & Faulted Conditions

The allowable flaw sizes for emergency and faulted conditions were also documented in [26]. The selection of the governing transient for emergency and faulted conditions was not as straightforward as the selection for normal, upset and test conditions, primarily due to the pressurized thermal shock (PTS) issue. This issue had previously resulted in an extensive probabilistic risk assessment study by Westinghouse Owners' Group (WOG) to identify the overall risk from PTS on a typical Westinghouse plant. The study included all transients that could potentially result in a pressurized thermal shock of the reactor vessel. The summary of the WOG risk assessment for PTS showed that the key contributors to the total risk occur from small LOCA and steam generator tube rupture (SGTR), because of the combination of severe transient characteristics with relatively high frequencies of transient occurrence.

The ASME Code in its present form, however, does not take transient frequencies into consideration and requires an evaluation of flaw indications using the most limiting emergency/faulted condition transient. Therefore, the WOG PTS risk analysis results could not be used directly, but they were used to guide the determination of the key transients to be considered here.

To determine the governing emergency and faulted conditions for a generic Westinghouse 3-loop reactor vessel, a series of transients were studied. These transients included the large LOCA and large steamline break (LSB) and the dominating transients from the WOG pressurized thermal shock studies. This work led to the conclusion that the following transients should be considered in the deterministic assessments for the beltline region:

- Steam Generator Tube Rupture (SGTR)
- Small LOCA
- Large LOCA
- Large Steamline Break (LSB)

Thermal stress and fracture analyses were performed for the beltline region, utilizing the characteristics of the above four transients. The limiting circumferential and axial flaws were used in performing the fracture analyses. ASME Section XI, IWB-3611 was used for the acceptance criteria. The resulting critical flaw depths for a range of shapes are shown in Table 5-5. The longitudinal/axial flaws are bounding for all transients considered. Table 5-6 shows the allowable axial flaw sizes which is 1/2 of the limiting values in Table 5-5.

Table 5-5: Critical Flaw Size Summary for Beltline Region – Emergency & Faulted Conditions

Emergency/Faulted Condition	Flaw	Continuous Flaw		Aspect Ratio 6:1		Aspect Ratio 2:1	
	Orientation	(inches)	(a/t)	(inches)	(a/t)	(inches)	(a/t)
Steam Generator Tube Rupture	Longitudinal	$a_i = 2.50$	0.323	$a_i = 5.51$	0.711	$a_i = 7.75$	1.000
	Circumferential	$a_i = 7.75$	1.000	$a_i = 7.75$	1.000	$a_i = 7.75$	1.000
Large Steamline Break	Longitudinal	$a_i = 2.50$	0.323	$a_i = 3.39$	0.437	$a_i = 7.75$	1.000
	Circumferential	$a_i = 2.21$	0.285	$a_i = 7.75$	1.000	$a_i = 7.75$	1.000
Small LOCA	Longitudinal	$a_i = 2.56$	0.330	$a_i = 5.74$	0.741	$a_i = 7.75$	1.000
	Circumferential	$a_i = 7.75$	1.000	$a_i = 7.75$	1.000	$a_i = 7.75$	1.000
Large LOCA	Longitudinal	$a_i = 7.75$	1.000	$a_i = 7.75$	1.000	$a_i = 7.75$	1.000
	Circumferential	$a_i = 7.75$	1.000	$a_i = 7.75$	1.000	$a_i = 7.75$	1.000

Note: Wall Thickness = 7.75" is used here.

Table 5-6: Allowable Axial Flaw Sizes for Beltline Region – Emergency and Faulted Conditions

Flaw Shape	Allowable Flaw Size	
	Depth (inches)	Through-wall Ratio (a/t)
Aspect Ratio 2:1	3.88	0.501
Aspect Ratio 6:1	1.70	0.219
Continuous Flaw	1.25	0.162

Note: Wall Thickness = 7.75" is used here.

The emergency and faulted conditions were evaluated for a typical plant. As discussed in [26, Appendix A], the emergency and faulted conditions are ultimately governed by plant specific treatment of pressurized thermal shock (PTS). The RT_{NDT} is not expected to change significantly for 80 years, and it would not impact any of the evaluations summarized herein. Additionally, the normal operating, upset, and test condition transients result in the most limiting allowable flaw size. There are also several conservatisms built into the analysis. Underclad cracks are assumed to be surface cracks which results in a conservative K_I . Conservatively assuming the flaw is exposed to water, the crack growth rate for water environment is used. This results in a higher

growth rate than assuming an air environment. The full flaw depth is assumed to be in the base material, and linear elastic fracture mechanics is used to determine the allowable flaw sizes. Therefore, the calculation of allowable flaw size for 60 years in [26] remains applicable for 80 years. Note that the largest flaw size of 0.4267 inch at the end of 80 years shown in Table 5-1 is below the minimum allowable flaw size of 0.67 inch Table 5-4.

As discussed in Section 5.5, the analysis assumed an upper shelf value of 200 ksi√in. The temperatures of the transients considered correspond to the upper shelf for the material. The selection of this criterion remains conservative for the 80 year lifetime of the plant. Applicability of the peak thermal shock event governed by USNRC 10CFR50.61 is independent of the operation of the plant (whether 60 or 80 years).

As discussed in Section 2, destructive analyses have demonstrated that cracks vary in depth from 0.007 inch to 0.295 inch, and in length from 0.078 inch to 2.0 inches. The continuous flaw was considered in order to bound all possible flaw geometries, including potential flaws with large aspect ratios (length/depth). The fatigue crack growth analysis for continuous flaw used an aspect ratio of 100. While the results in Table 5-5 indicate critical flaws with $a/t = 1.0$ for some conditions, this does not literally indicate a 100% through-thickness is allowed. It indicates that the load is very low ($K_I < K_{IC}$) even as the flaw depth approaches 100% of the wall thickness (i.e., critical flaw size $a/t = 1.0$). The original analysis summarized in WCAP-15338-A [26] determined that these were sufficiently close to a through-wall flaw to be summarized as $a/t = 1.0$. The actual allowable flaw depth is $\frac{1}{2}$ of the critical flaw, which means an a/t of 0.5 is allowed for these cases. In any case, the analysis for normal, upset and test conditions generated the limiting allowable flaw size, calculated using K_{IC} reduced by the appropriate factor.

6 Summary and Conclusions

The purpose of this report is to update the 60 year fatigue crack growth analysis in [26] and confirm the analysis remains appropriate for application to SLR, up to 80 years of operation. More specifically:

- Revise the fatigue crack growth analysis for 80 years of operation.
- Confirm fracture toughness values used in Appendix A of [26] is bounding for 80 years of operation.
- Update operating experience as discussed in Sections 2 and 3 of [26].
- Include discussion of state of the art inspection techniques and capabilities for detecting and characterizing cracks associated with manufacturing processes as well as those due to potentially service-induced mechanisms.

As summarized in [26], there are many levels of defense in depth relative to the underclad cracks. There is no known mechanism for the creation of additional flaws in this region, so the only concern is the potential propagation of the existing flaws.

In 1971, Westinghouse submitted an assessment of the underclad reheat cracking issue [2] to the regulatory authorities, then the Atomic Energy Commission evaluating underclad cracks for an operating period of 40 years. The Commission reviewed the assessment, and issued the following conclusion:

SUMMARY OF REGULATORY POSITON:

“We concur with Westinghouse’s finding that the integrity of a vessel having flaws such as described in the subject report would not be compromised during the life of the plant. This report is acceptable and may be referenced in future applications where similar underclad grain boundary separations have been detected. However, such flaws should be avoided, and we recommend that future applicants state in their PSARs what steps they plan to take in this regard.”

Flaw indications indicative of underclad cracks have been evaluated in accordance with the acceptance criteria of the ASME Code Section XI. Such indications have been found during pre-service and inservice inspections of plants considered to have cladding conditions which are suspect with respect to underclad cracking. These flaw indications have been dispositioned as being acceptable for further service without repair or detailed evaluation, because they meet the conservative requirements of the ASME Code Section XI, Paragraph IWB-3500.

Fracture evaluations have also been performed to evaluate underclad cracks, and the results have always been that the flaws are acceptable.

A number of field examples were summarized which have involved cladding cracks, as well as exposure of the base metal due to cladding removal. In several cases the cladding cracks have been suspected to extend into the base metal, and have been analyzed as such. In these cases the cracks were suspected to be exposed to the water environment, and successive monitoring inspections were conducted on the area of concern. No changes were found due to propagation or further deterioration of any type.

Based on these observations, the USNRC then allowed the surveillance to be discontinued.

Finally, underclad cracks found during pre-service and inservice inspections have been evaluated in accordance with the acceptance criteria of the ASME Code Section XI. The observed underclad cracks are very shallow, confined in depth to less than 0.295 inch and have lengths up to 2.0 inches. The fatigue crack growth assessment for these small cracks shows very little extension over 80 years, even if they were exposed to the reactor water and with crack tip pressure of 2,500 psi. For the worst case scenario, a 0.30 inch deep continuous axial flaw in the beltline region would grow to 0.43 inch after 80 years. The minimum allowable axial flaw size for normal, upset and test conditions is 0.67 inch and for emergency and faulted conditions is 1.25 inches. Since the maximum flaw depth of 0.4267 inch after 80 years of fatigue crack growth is below the minimum allowable flaw size of 0.67 inch, underclad cracks of any shape are acceptable for service for 80 years, regardless of the size or orientation of the flaws. Therefore, it may be concluded that underclad cracks are of no concern relative to structural integrity of the reactor vessel for a period of 80 years.

7 References

1. Westinghouse Report, WCAP-7673-L, Rev. 0, "Reactor Vessels Weld Cladding- Base Metal Interaction," April 1971.
2. Westinghouse Report, WCAP-7733, Rev. 0, "Reactor Vessels Weld Cladding- Base Metal Interaction," July 1971.
3. Westinghouse Report, WCAP-7673-L-AD1, Rev. 0, Addendum 1, Reactor Vessels Weld Cladding – Base Metal Interaction," August 1971.
4. U.S. Atomic Energy Commission Letter, "Topical Report Evaluation on Reactor Vessels, Weld Cladding - Base Metal Interaction," September 22, 1972.
5. Vinckier, A. G. and Pense, A. W., "A Review of Underclad Cracking in Pressure Vessel Components," Welding Research Bulletin 197, Welding Research Council, New York, NY, August 1974.
6. Rishel, R. D. and Bamford, W. H., "Evaluation of the Ultrasonic Test Results from the 1993151 on the Underclad Flaw Indications in the Sequoyah Unit 1 Reactor Vessel Nozzles," Westinghouse Report MEM-MNA-296 (83) Rev. 2, July 13, 1993.
7. McCabe, D. E., "Fracture Evaluation of Surface Cracks Embedded in Reactor Vessel Cladding," Report NUREG/CR-4841, May 1987.
8. McCabe, D. E., "Fracture Resistance of Irradiated Steel Clad Vessels," in Effects of Radiation on Materials: 14th International Symposium. ASTM STP 1046, Philadelphia, PA 1990, pp. 348-360.
9. A. J. Bush and F. J. Kromer, "Simplification of the Hole-Drilling Method of Residual Stress Measurement," ISA Transactions, Volume 12, No. 3, 1973, pp. 249-259.
10. "Standard Method for Determining Residual Stresses by the Hole-Drilling Strain-Gage Method," ASTM E837, 1982.
11. J. E. Brynum, "Modifications to the Hole-Drilling Technique of Measuring Residual Stresses for Improved Accuracy and Reproducibility," Experimental Mechanics, January 1981, pp. 21-33.
12. Not used.
13. McCabe, D. E., "Assessment of Metallurgical Effects that Impact Pressure Vessel Safe Margin Issues," ORNL/NRC/LTR-94/26, October 1994.
14. Westinghouse Report, WCAP-9704, Rev. 0, "Metallurgical Investigation of the Offshore Power Company Reactor Vessel Outlet Nozzle Cracks," April, 1980.
15. Westinghouse Report, WCAP-9980, Rev. 0, "Detection of Underclad Cold Cracking by Immersion Ultrasonic Techniques," September 1981.
16. Westinghouse Letter, PE-RVP-2806, Rev. 0, "Summary of RV Vendor Nozzle Clad Practice Survey," November 19, 1979.
17. Westinghouse Letter, MT-MNA-2642, Rev. 0, "Preservice Inspection Results – Watts Bar Unit 2 Reactor Vessel Nozzle Bores," March 3, 1981. (Attachment, MT-MNA-2609,

“Assessment of Ultrasonic Reflectors in the Watts Bar Unit II Reactor Vessel Nozzle Bores.”).

18. Adamortis, D. C., and Rishel, R. D., “Ultrasonic Examination of Prairie Island Unit II Outlet Nozzle Bores for Detection of Underclad Cracking,” Westinghouse Report, MT-MNA-2822-81, June 4, 1981.
19. Mager, T. R., “Pre-Service Inspection Results - McGuire Unit II Reactor Vessel Nozzles Bores,” Westinghouse Report, MT-MNA-2398, October 30, 1980.
20. Adamortis, D. C., and Rishel, R. D., “Ultrasonic Examination of the Sequoyah Unit I Reactor Vessel Nozzles for Detection of Cracks Beneath the Stainless Steel Cladding,” Westinghouse Report, MT-MNA-947, February 18 & March 11, 1980.
21. Mager, T. R., “Pre-Service Inspection Results - Catawba Unit 1 Reactor Vessel Nozzle Bores,” Westinghouse Report, MT-MNA-2396, November 5, 1980.
22. Rishel, R. D., “Destructive Analysis of Four Indications Found in an Earlier Ultrasonic Examination of Reactor Vessel Nozzle Bores in Watts Bar Unit 1,” Westinghouse Report, MT-MNA-2577-81, February 3, 1981.
23. Westinghouse Report, WCAP-2855, Rev. 0, “Evaluation of Yankee Vessel Cladding Penetrations,” October 15, 1965.
24. Westinghouse Report, WCAP-12653, Rev. 0 Handbook on Flaw Evaluation for Hadam Neck Pressurizer Lower Head Region,” July 1990.
25. Westinghouse Calculation Note, CN-SMT-01-59, Rev. 0, “Flaw Evaluation of Underclad Cracking in Reactor Vessels,” June 11, 2001.
26. Westinghouse Report, WCAP-15338-A, Rev. 0, “A Review of Cracking Associated with Weld Deposited Cladding in Operating PWR Plants,” October 2002.
27. ASME Boiler & Pressure Vessel Code Section XI, 2001 Edition through 2003 Addenda.
28. PWROG Project Authorization, PA-MS-1497, Rev. 0, “Update for Subsequent License Renewal: WCAP-15338-A, “A Review of Cracking Associated with Weld Deposited Cladding in Operating PWR Plants,” September 2016.
29. Westinghouse Letter, LTR-PSDR-TAM-14-003, Rev. 0, “Reactor Vessel Inlet Nozzle Cladding Damage Assessment for Diablo Canyon Unit 1,” February 2014.
30. Westinghouse Report, WCAP-18158-P, Rev. 0, “Qinshan Phase I Reactor Vessel Cladding Wear Evaluation for Operating Life Extension up to 50 years,” October 2016.

Enclosure 4
Non-proprietary Reference Documents
and
Redacted Versions of Proprietary
Reference Documents
(Public Version)
Attachment 10

PWR Owners Group, PWROG-17011-NP, Rev. 0
Update for Subsequent License Renewal
WCAP-14535A, Topical Report on Reactor Coolant Pump
Flywheel Inspection Elimination
And
WCAP-15666-A, Extension of Reactor Coolant Pump Motor
Flywheel Examination, November 2017

(64 Total Pages, including cover sheets)



PWROG-17011-NP
Revision 0

WESTINGHOUSE NON-PROPRIETARY CLASS 3

Update for Subsequent License Renewal: WCAP-14535A, “Topical Report on Reactor Coolant Pump Flywheel Inspection Elimination” and WCAP-15666-A, “Extension of Reactor Coolant Pump Motor Flywheel Examination”

Materials Committee

PA-MS-C-1500

November 2017



PWROG-17011-NP
Revision 0

Update for Subsequent License Renewal: WCAP-14535A, “Topical Report on Reactor Coolant Pump Flywheel Inspection Elimination” and WCAP-15666-A, “Extension of Reactor Coolant Pump Motor Flywheel Examination”

PA-MSC-1500

Gordon Z. Hall*
Structural Design and Analysis - I

Raymond E. Schneider*
Risk Applications and Methods - II

November 2017

Reviewer: Thomas E. Demers*
Structural Design and Analysis - I

Reviewer: John White*
Risk Applications and Methods - II

Approved: John McFadden*, Manager
Aging Management & License Renewal

Approved: James P. Molkenthin*, Program Director
PWR Owners Group PMO

*Electronically approved records are authenticated in the electronic document management system.

Westinghouse Electric Company LLC
1000 Westinghouse Drive
Cranberry Township, PA 16066, USA

© 2017 Westinghouse Electric Company LLC
All Rights Reserved

ACKNOWLEDGEMENTS

This report was developed and funded by the PWR Owners Group under the leadership of the participating utility representatives of the Materials Committee.

WESTINGHOUSE ELECTRIC COMPANY LLC PROPRIETARY**LEGAL NOTICE**

This report was prepared as an account of work performed by Westinghouse Electric Company LLC. Neither Westinghouse Electric Company LLC, nor any person acting on its behalf:

1. Makes any warranty or representation, express or implied including the warranties of fitness for a particular purpose or merchantability, with respect to the accuracy, completeness, or usefulness of the information contained in this report, or that the use of any information, apparatus, method, or process disclosed in this report may not infringe privately owned rights; or
2. Assumes any liabilities with respect to the use of, or for damages resulting from the use of, any information, apparatus, method, or process disclosed in this report.

COPYRIGHT NOTICE

This report has been prepared by Westinghouse Electric Company LLC and bears a Westinghouse Electric Company copyright notice. Information in this report is the property of, and contains copyright material owned by, Westinghouse Electric Company LLC and /or its subcontractors and suppliers. It is transmitted to you in confidence and trust, and you agree to treat this document and the material contained therein in strict accordance with the terms and conditions of the agreement under which it was provided to you.

DISTRIBUTION NOTICE

This report was prepared for the PWR Owners Group. This Distribution Notice is intended to establish guidance for access to this information. This report (including proprietary and non-proprietary versions) is not to be provided to any individual or organization outside of the PWR Owners Group program participants without prior written approval of the PWR Owners Group Program Management Office. However, prior written approval is not required for program participants to provide copies of Class 3 Non-Proprietary reports to third parties that are supporting implementation at their plant, or for submittals to the USNRC.

**PWR Owners Group
United States Member Participation* for PA-MSC-1500**

Utility Member	Plant Site(s)	Participant	
		Yes	No
Ameren Missouri	Callaway (W)	X	
American Electric Power	D.C. Cook 1 & 2 (W)	X	
Arizona Public Service	Palo Verde Unit 1, 2, & 3 (CE)		X
Dominion Connecticut	Millstone 2 (CE)		X
	Millstone 3 (W)	X	
Dominion VA	North Anna 1 & 2 (W)	X	
	Surry 1 & 2 (W)	X	
Duke Energy Carolinas	Catawba 1 & 2 (W)	X	
	McGuire 1 & 2 (W)	X	
	Oconee 1, 2, & 3 (B&W)	X	
Duke Energy Progress	Robinson 2 (W)	X	
	Shearon Harris (W)	X	
Entergy Palisades	Palisades (CE)		X
Entergy Nuclear Northeast	Indian Point 2 & 3 (W)		X
Entergy Operations South	Arkansas 1 (B&W)		X
	Arkansas 2 (CE)		X
	Waterford 3 (CE)		X
Exelon Generation Co. LLC	Braidwood 1 & 2 (W)	X	
	Byron 1 & 2 (W)	X	
	TMI 1 (B&W)		X
	Calvert Cliffs 1 & 2 (CE)	X	
	Ginna (W)		X
FirstEnergy Nuclear Operating Co.	Beaver Valley 1 & 2 (W)		X
	Davis-Besse (B&W)		X
Florida Power & Light \ NextEra	St. Lucie 1 & 2 (CE)		X
	Turkey Point 3 & 4 (W)	X	
	Seabrook (W)	X	
	Pt. Beach 1 & 2 (W)	X	
Luminant Power	Comanche Peak 1 & 2 (W)		X
Omaha Public Power District	Fort Calhoun (CE)		X
Pacific Gas & Electric	Diablo Canyon 1 & 2 (W)		X
PSEG – Nuclear	Salem 1 & 2 (W)		X
South Carolina Electric & Gas	V.C. Summer (W)	X	
So. Texas Project Nuclear Operating Co.	South Texas Project 1 & 2 (W)		X
Southern Nuclear Operating Co.	Farley 1 & 2 (W)		X
	Vogtle 1 & 2 (W)		X
Tennessee Valley Authority	Sequoyah 1 & 2 (W)		X
	Watts Bar 1 & 2 (W)		X
Wolf Creek Nuclear Operating Co.	Wolf Creek (W)		X
Xcel Energy	Prairie Island 1 & 2 (W)	X	

* **Project participants as of the date the final deliverable was completed. On occasion, additional members will join a project. Please contact the PWR Owners Group Program Management Office to verify participation before sending this document to participants not listed above.**

PWR Owners Group
International Member Participation* for PA-MSC-1500

Utility Member	Plant Site(s)	Participant	
		Yes	No
Asociación Nuclear Ascó-Vandellòs	Asco 1 & 2 (W)		X
	Vandellos 2 (W)		X
Axpo AG	Beznau 1 & 2 (W)		X
Centrales Nucleares Almaraz-Trillo	Almaraz 1 & 2 (W)		X
EDF Energy	Sizewell B (W)		X
Electrabel	Doel 1, 2 & 4 (W)		X
	Tihange 1 & 3 (W)		X
Electricite de France	58 Units		X
Eletronuclear-Elektrobras	Angra 1 (W)		X
Emirates Nuclear Energy Corporation	Barakah 1 & 2		X
EPZ	Borssele		X
Eskom	Koeberg 1 & 2 (W)		X
Hokkaido	Tomari 1, 2 & 3 (MHI)		X
Japan Atomic Power Company	Tsuruga 2 (MHI)		X
Kansai Electric Co., LTD	Mihama 3 (W)		X
	Ohi 1, 2, 3 & 4 (W & MHI)		X
	Takahama 1, 2, 3 & 4 (W & MHI)		X
Korea Hydro & Nuclear Power Corp.	Kori 1, 2, 3 & 4 (W)		X
	Hanbit 1 & 2 (W)		X
	Hanbit 3, 4, 5 & 6 (CE)		X
	Hanul 3, 4, 5 & 6 (CE)		X
Kyushu	Genkai 2, 3 & 4 (MHI)		X
	Sendai 1 & 2 (MHI)		X
Nuklearna Elektrarna KRSKO	Krsko (W)		X
Ringhals AB	Ringhals 2, 3 & 4 (W)		X
Shikoku	Ikata 1, 2 & 3 (MHI)		X
Taiwan Power Co.	Maanshan 1 & 2 (W)		X

* **Project participants as of the date the final deliverable was completed. On occasion, additional members will join a project. Please contact the PWR Owners Group Program Management Office to verify participation before sending this document to participants not listed above.**

TABLE OF CONTENTS

1	INTRODUCTION.....	1-1
2	BACKGROUND	2-1
2.1	DESIGN AND FABRICATION.....	2-2
2.2	INSPECTION	2-5
2.3	STRESS AND FRACTURE EVALUATION.....	2-10
2.3.1	Selection of Flywheel Groups for Evaluation	2-10
2.3.2	Ductile Failure Analysis.....	2-11
2.3.3	Nonductile Failure Analysis.....	2-12
2.3.4	Fatigue Crack Growth	2-12
2.3.5	Excessive Deformation Analysis	2-13
2.4	SUMMARY OF STRESS AND FRACTURE RESULTS	2-14
3	RISK ASSESSMENT	3-1
3.1	RISK-INFORMED REGULATORY GUIDE 1.174 METHODOLOGY	3-1
3.2	FAILURE MODES AND EFFECTS ANALYSIS	3-7
3.3	FLYWHEEL FAILURE PROBABILITY	3-10
3.3.1	Method of Calculation Failure Probabilities.....	3-10
3.3.2	Sensitivity Study	3-15
3.3.3	Failure Probability Assessment Conclusions	3-17
3.4	CORE DAMAGE EVALUATION	3-22
3.4.1	What is the Likelihood of the Event.....	3-23
3.4.2	What are the Consequences?.....	3-24
3.4.3	Risk Calculation.....	3-24
3.5	CONSIDERATION OF UNCERTAINTY	3-30
3.5.1	Initiating Event Frequency.....	3-31
3.5.2	Conditional Flywheel Failure Probability	3-31
3.5.3	Conditional Core Damage/Large Early Release Probability Given Flywheel Failure Event	3-31
3.5.4	Conclusion Regarding Treatment of Uncertainty	3-32
3.6	RISK RESULTS AND CONCLUSIONS	3-32
4	CONCLUSIONS.....	4-1
5	REFERENCES.....	5-1
APPENDIX A : CALVERT CLIFFS UNIT 1 & 2 RCP MOTOR FLYWHEEL EVALUATIONS FOR EXTENSION OF ISI INTERVAL		A-1

List of Tables

Table 2-1: Westinghouse Domestic Plant Alpha Designation Listing	2-1
Table 2-2: Summary of Westinghouse Domestic Plant RCP Motor Flywheel Information [3]	2-3
Table 2-3: Flywheel Inspection Result from MUHP-5042 Study [2, 3]	2-5
Table 2-4: Summary of Recordable Indications from MUHP-5042 Study [2, 3]	2-7
Table 2-5: Flywheel Inspection Data per [8]	2-8
Table 2-6: Flywheel Inspection Data per [8]	2-9
Table 2-7: Flywheel Groups Evaluated for Program MUHP-5043 [3].....	2-10
Table 2-8: Ductile Failure Limiting Speed.....	2-11
Table 2-9: Critical Crack Lengths for Flywheel Overspeed of 1500 rpm (Considering LBB)....	2-12
Table 2-10: Fatigue Crack Growth Assuming 6000 RCP Starts and Stops	2-13
Table 2-11: Flywheel Deformation at 1500 rpm.....	2-13
Table 2-12: Shrink Fit Lost at 1500 rpm [2]	2-14
Table 3-1: Variables for RCP Motor Flywheel Failure Probability Model	3-11
Table 3-2: Input Values for RCP Motor Flywheel Failure Probability Model	3-13
Table 3-3: Cumulative Probability of Failure over 40, 60 and 80 Years with and without Inservice Inspection ⁽¹⁾	3-15
Table 3-4: Effect of Flywheel Risk Parameter on Failure Probability	3-16
Table 3-5: Summary of Flywheel Analysis Parameters	3-22
Table 3-6: Estimated RCP Motor Flywheel Failure Probabilities	3-23
Table 3-7: Westinghouse RCP Motor Flywheel Evaluation Group 1	3-27
Table 3-8: RCP Motor Flywheel Evaluation Group 2.....	3-28
Table 3-9: Calvert Cliffs Units 1 and 2 RCP Motor Flywheel Evaluation	3-29
Table 3-10: CDF Sensitivity to Variations in PRA evaluation assumptions for RCP Flywheel Failure Risk Assessment for Extending 10 year inspection intervals to 20 years for Flywheel operation to 80 years –(Flywheel Group 1).....	3-32
Table 3-11: Evaluation with Respect to Regulatory Guide 1.174 (Key Principles)	3-33
Table A-1: Critical Crack Length in Inches and % Through Flywheel.....	A-2

List of Figures

Figure 2-1: Example of a Typical Westinghouse RCP Motor Flywheel	2-4
Figure 2-2: Result of Typical Westinghouse RCP Motor Flywheel Overspeed Evaluation	2-10
Figure 3-1: NRC Regulatory Guide 1.174 Basic Steps	3-2
Figure 3-2: Principles of Risk-Informed Regulation [9]	3-4
Figure 3-3: Westinghouse PROF Program Flow Chart for Calculating Failure Probability	3-18
Figure 3-4: Probability of Failure for Flywheel Evaluation Group 1	3-19
Figure 3-5: Probability of Failure for Flywheel Evaluation Group 2	3-20
Figure 3-6: Probability of Failure for Calvert Cliffs Units 1 and 2	3-21

List of Acronyms

B&W	Babcock and Wilcox
CCDP	conditional core damage probability
CCL	critical crack length
CCNPP	Calvert Cliffs Nuclear Power Plant
CDF	core damage frequency
CE	Combustion Engineering
DEGB	double ended guillotine break
DLE	design limiting events
FCG	fatigue crack growth
FSAR	final safety analysis report
FSAR	final safety analysis report
GQA	graded quality assurance
ISI	inservice inspection
IST	inservice testing
LBB	leak-before-break
LERF	large early release frequency
LOCA	loss of coolant accident
LOOP	loss offsite power
MT	magnetic particle testing
NDE	non-destructive examination
NRC	Nuclear Regulatory Commission
OD	outer diameter
PMSC	Pump & Motor Services
PRA	probabilistic risk assessment
PROF	probability of failure
PT	penetrant testing
PWROG	Pressurized Water Reactor Owners Group
RCP	reactor coolant pump
RCPM	reactor coolant pump motor
RCS	reactor coolant system
RG	regulatory guide
rpm	revolutions per minute
RT _{NDT}	reference nil-ductility transition temperature
SER	safety evaluation report
SLR	subsequent license renewal
SRP	standard review plan
SRRA	structural reliability and risk assessment
SSCs	systems, structures and components
USAR	updated safety analysis report
UT	ultrasonic examination/ultrasonic test
W	Westinghouse
WOG	Westinghouse Owners Group
W-PROF	Westinghouse PROF Software Library

1 INTRODUCTION

WCAP-14535A [2] is a Westinghouse report published in November of 1996 to provide the technical basis for the elimination of inspection requirements for the reactor coolant pump (RCP) motor flywheels for all operating domestic Westinghouse and several B&W plants. The NRC issued a Safety Evaluation Report (SER) in September 1996, wherein they accepted the technical arguments but did not allow for total elimination of examinations. The SER provided partial relief from examination requirements of NRC RG 1.14 [4], by allowing for an extension of examination frequency from 40 months to 10 years. It further relaxed the examination guidance by recommending an in-place ultrasonic examination (UT) over the volume from the inner bore of the flywheel to the circle of one-half the outer radius or an alternative surface examination, i.e., magnetic particle testing (MT) and/or liquid penetrant testing (PT), of exposed surfaces defined by the volume of disassembled flywheel. NRC's decision was only based on the deterministic methodology in [2].

WCAP-15666-A [3] is a follow-up report published in October of 2003 for the Westinghouse Owners Group in an effort to extend the 10 year inspection interval from [2] to 20 years. The report shows that the results from [2] remain valid and performed a failure probability analysis to show that the change in risks for a 20 year inspection interval satisfies the RG 1.174 acceptable guidelines. The NRC SER deemed both the deterministic and probabilistic calculations in [3] acceptable, and granted the 20-year inspection interval. It was stated the potential for failure of the RCP flywheel is, and will continue to be negligible during normal and accident conditions.

WCAP-14535A explicitly states that it is applicable to operating domestic Westinghouse plants and several Babcock and Wilcox (B&W) plants (including Crystal River 3, Oconee 1, 2, and 3, Davis Besse, and Three Mile Island Unit 1). While WCAP-15666-A [3] did include some data for B&W plants, the topical report and related NRC SER did not specifically address the applicability of the risk assessments and other evaluations to B&W plants. The NRC acknowledged that some of the supporting material may help support plant-specific applications for B&W units included in portions of WCAP-15666-A [3]. This same applicability is carried over for the SLR update report presented herein.

Per PA-MSC-1500 [1], this report is not applicable to Combustion Engineering (CE) plants, as they fall outside of the scope of [1].

Calvert Cliffs had Westinghouse perform a site-specific evaluation to apply the methodology of these WCAPs for 60 years of operation. This was unique among CE plants. Calvert Cliffs was included within the scope of PA-MSC-1500.

The purpose of this report, as described in Tasks 2 and 3 of [1] is update the WCAPs [2 and 3], or confirm that the analysis remains appropriate for application to SLR of up to 80 years of operation.

2 BACKGROUND

In previous Westinghouse owners group (WOG) programs MUHP-5042 and MUH-5043, summarized in [2 and 3], respectively, the engineering basis was established that led to NRC approval of extending the surveillance interval for the RCP motor flywheel from 40 months to 10 years, and then to 20 years.

The various aspects of these previous programs are discussed in the following subsections. Applicable plants for the earlier program MUHP-5042 included all operating domestic WOG plants and several B&W plants including Crystal River 3, Oconee 1, 2 and 3, Davis Besse and Three Mile Island 1, as reported in [2]. While some data for B&W plants was included in [3], the MUH-5043 program and NRC SER applies only to operating domestic WOG plants. Plant alpha designations used in the report are identified in Table 2-1.

Table 2-1: Westinghouse Domestic Plant Alpha Designation Listing

Plant Alpha Designation(s)	Plant(s)
AEP/AMP	D.C. Cook Units 1 and 2
ALA/APR	J.M. Farley Units 1 and 2
CAE/CBE	Byron Units 1 and 2
CCE/CDE	Braidwood Units 1 and 2
CGE	V.C. Summer
CPL	H.B. Robinson Unit 2
CQL	Shearon Harris
DAP/DBP	McGuire Units 1 and 2
DCP/DDP	Catawba Units 1 and 2
DLW/DMW	Beaver Valley Units 1 and 2
FPL/FLA	Turkey Point Units 3 and 4
GAE/GBE	Vogtle Units 1 and 2
IPP/INT	Indian Point Units 2 and 3
NAH	Seabrook
NEU	Millstone Unit 3
NSP/NRP	Prairie Island Units 1 and 2
PGE/PEG	Diablo Canyon Units 1 and 2
PSE/PNJ	Salem Units 1 and 2
RGE	Ginna
SAP	Wolf Creek
SCP	Callaway
TBX/TCX	Comanche Peak Units 1 and 2
TVA/TEN	Sequoyah Units 1 and 2
TGX/THX	South Texas Units 1 and 2
VGB/VRA	North Anna Units 1 and 2
VPA/VIR	Surry Units 1 and 2
WAT	Watts Bar Unit 1
WEP/WIS	Point Beach Units 1 and 2
WPS	Kewaunee

2.1 DESIGN AND FABRICATION

Westinghouse RCP motor flywheels consist of two large steel discs that are shrunk fit directly to the RCP motor shaft. The individual flywheel discs are bolted together to form an integral flywheel assembly, which is located above the RCP rotor core. Typically, each flywheel disc is keyed to the motor shaft by means of three vertical keyways, positioned at 120° intervals. The bottom disc usually has a circumferential notch along the outside diameter bottom surface for placement of anti-rotation pawls. See Figure 2-1 for the configuration of a typical Westinghouse flywheel.

Westinghouse manufactured the RCP motors for all of the Westinghouse plants. All of the RCP motor flywheels for operating Westinghouse plants are made of SA-533 Grade B Class 1 steel. As discussed in [3], it was not possible to locate each of the certified material test reports for all of the flywheels. A sample is provided in Appendix D of [2]. The ordering specifications for the Westinghouse flywheel materials (the first specification is dated December 1969) required that the RT_{NDT} from both longitudinal and transverse Charpy specimens be less than 10°F. The Westinghouse equipment specification was changed in January 1973 to require both Charpy and drop weight tests to ensure that RT_{NDT} is no greater than 10°F. Even though it is likely that most, if not all, of the flywheels in operation have an RT_{NDT} of 10°F or less, a range of RT_{NDT} values from 0°F to 60°F was assumed in the integrity evaluations of [2], which are discussed later in this report.

A summary of pertinent flywheel parameters is provided in Table 2-2. Note that for the evaluations performed in [2], and summarized in this report, the larger flywheel outside diameter for a particular flywheel assembly was used, since this was judged to be conservative with respect to stress and fracture. This larger dimension is provided in Table 2-2.

Table 2-2: Summary of Westinghouse Domestic Plant RCP Motor Flywheel Information [3]

Group	Outer Diam. (inch)	Bore (inch)	Keyway Radial Length (inch)	Pump & Motor Inertia (lbm-ft ²)	Material Type	Applicable Plants (Plant Alpha Designation)
1	76.50	9.375	0.937	110,000	SA-533B	TGX/THX/Spare
2	75.75	8.375	0.906	82,000	SA-533B	PSE ⁽³⁾ /PNJ/Spare
3	75.00	9.375	0.937	95,000	SA-533B	CQL; CAE/CBE/CCE/CDE ⁽¹⁾ ; DAP/DBP/DCP/DDP; GAE/GBE ⁽¹⁾ ; SAP/SPARE; NEU; NAH; CGE/Spare; WAT/Spare; TBX/TCX/Spare; SCP; VRA/VGB/Spare
4	75.00	9.375	0.937	83,000	SA-533B	TVAT/TEN/Spare
5	75.00	9.375	0.937	82,000	SA-533B	ALA/APR/Spare; AEP/AMP/Spare; DLW/DMW, PGE Spare ^{(1), (6)}
6	75.00	9.375	0.937	80,000	SA-533B	NSP/NRP ⁽²⁾ ; WPS ⁽²⁾
7	75.00	9.375	0.911	82,000	SA-533B	INT Spare, PGE Spare ^{(5), (6)}
8	75.00	8.375	0.906	82,000	SA-533B	IPP/INT; PGE/PEG
9	75.00	8.375	0.906	80,000	SA-533B	WEP ⁽⁴⁾ /WIS
12	72.00	8.375	0.906	80,000	SA-533B	RGE ⁽³⁾
13	72.00	8.375	0.906	70,000	SA-533B	CPL/Spare; FPL/FLA/Spare; VPA/VIR ⁽⁴⁾

Notes:

- (1) Spare has a keyway radial length of 0.855”.
- (2) Spare has a keyway radial length of 0.853”.
- (3) Spare has a keyway radial length of 0.911”.
- (4) Spare has a keyway radial length of 0.937”.
- (5) Spare has a keyway radial length of 0.863”.
- (6) The spares for PGE/PEG are bounded by [2].
- (7) Groups 10, 11, 15 and 16 included non-WOG plants in [2]. Group 14 includes Haddam Neck, which is no longer in service. These groups are not included in the WOG program MUHP-5043 (WCAP-15666-A [3]), and are therefore not summarized in this report.

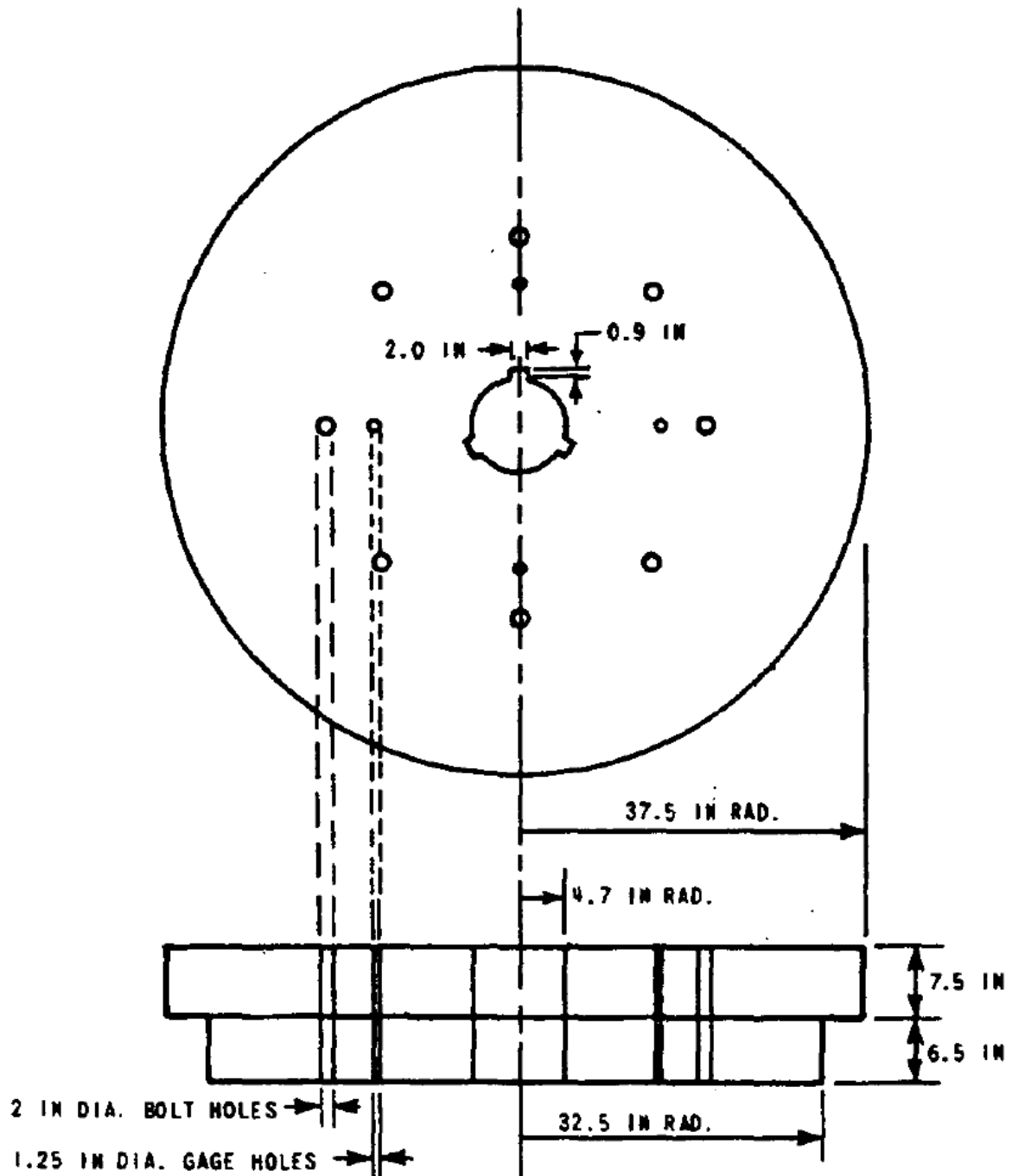


Figure 2-1: Example of a Typical Westinghouse RCP Motor Flywheel

2.2 INSPECTION

Flywheels are inspected at the plant or during motor refurbishment. Inspections are conducted under the ASME Boiler and Pressure Vessel Code, Section XI [6] standard practice for control of instrumentation and personnel qualification. Ultrasonic test (UT) level II and III examiners conduct the inspections.

WCAP-15666-A [3] discussed the examination volume, approach, access and exposure in detail. This discussion remains applicable for the application to SLR up to 80 years of operation.

Inspection History

WCAP-15666-A [3] discussed a survey conducted for the historical plant ISI results in the previous MUHP-5042 project with contributions from all member utilities including B&W plants. The flywheel population surveyed was a total of 214. A total of 729 examination results were reported, and no indications that would affect the integrity of the flywheels were found. These results are summarized on a plant by plant basis in Table 2-3.

A summary of recordable indications from the previous MUHP-5042 program is provided in Table 2-4. It was noted in [2, 3] that a number of indications in the form of nicks and gashes were found in the keyway area, having been created by the act of removing or reassembling the flywheel. Table 2-4 listed recordable indications at the keyway area from surface examination for a number of plants, namely CAE/CBE, CWE, FPL/FLA, VGB/VRA and WAT. These were dispositioned as not affecting flywheel integrity, but are clear evidence that the act of disassembly and reassembly for refurbishment and inspection can produce damage.

Indications were found at the Haddam Neck plant, in the weld used to join the two flywheel plates together. The indications identified were associated with this seal weld and resulted in no radially oriented cracking, and no impact on the integrity of the flywheels. A detailed summary of this finding is given in Appendix B of [2]. Sample flywheel inspection procedures are provided in Appendix C of [2].

Per [3], no flaws were discovered among the flywheel inspections performed between the times of publication for WCAP-14535A [2] and WCAP-15666-A [3].

Table 2-3: Flywheel Inspection Result from MUHP-5042 Study [2, 3]

Plant Alpha Designation	Plant	Number of Flywheels	Total Number of Flywheel Inspections	Total Number of Inspection with No Indications or Non-recordable Indications	Total Number of Inspection With Recordable Indications	Number of Indications Affecting Flywheel Integrity
AEP	Cook 1	4	14	13	1	0
AMP	Cook 2	4	12	12	0	0
ALA	Farley 1	3	17	17	0	0
APR	Farley 2	3	19	19	0	0
CAE/CBE	Byron 1 & 2	8	20	19	1	0
CCE	Braidwood 1	4	13	11	2	0
CDE	Braidwood 2	4	9	8	1	0

Table 2-3: Flywheel Inspection Result from MUHP-5042 Study [2, 3], continued

Plant Alpha Designation	Plant	Number of Flywheels	Total Number of Flywheel Inspections	Total Number of Inspection with No Indications or Non-recordable Indications	Total Number of Inspection With Recordable Indications	Number of Indications Affecting Flywheel Integrity
CGE	Summer	4	10	10	0	0
CWE	Zion 1	4	10	9	1	0
COM	Zion 2	4	16	16	0	0
CPL	Robinson 2	4	22	20	2	0
CQL	Harris	3	17	17	0	0
CYW	Haddam Neck	4	32	28	4	0
DAP	McGuire 1	4	13	13	0	0
DBP	McGuire 2	4	8	8	0	0
DCP	Catawba 1	4	6	6	0	0
DDP	Catawba 2	4	6	6	0	0
DLW	Beaver Valley 1	3	15	11	4	0
DMW	Beaver Valley 2	3	5	5	0	0
FPL/FLA	Turkey Point 3 & 4	7	36	34	2	0
GAE/GBE	Vogtle 1 and 2	9	19	19	0	0
IPP	Indian Point 2	5	21	21	0	0
INT	Indian Point 3	5	17	17	0	0
NAH	Seabrook	4	8	8	0	0
NEU	Millstone 3	5	12	12	0	0
NSP	Prairie Island 1	2	13	12	1	0
NRP	Prairie Island 2	2	11	10	1	0
PGE	Diablo Canyon 1	4	12	11	1	0
PEG	Diablo Canyon 2	4	11	11	0	0
PSE/PNJ	Salem 1 and 2	9	24	13	11	0
RGE	Ginna	3	21	21	0	0
SAP	Wolf Creek	4	13	12	1	0
SCP	Callaway	4	11	11	0	0
TBX	Comanche Peak 1	4	8	8	0	0
TCX	Comanche Peak 2	4	4	4	0	0
TVA/TEN	Sequoyah 1 and 2	9	37	36	1	0
TGX	South Texas 1	4	12	12	0	0
THX	South Texas 2	4	12	12	0	0
VGB/VRA	North Anna 1 & 2	7	37	33	4	0
VPA/VIR	Surry 1 and 2	7	17	17	0	0
WAT	Watts Bar 1	4	4	2	2	0
WEP	Point Beach 1	2	12	12	0	0
WIS	Point Beach 2	2	13	13	0	0
WPS	Kewaunee	3	6	5	1	0
BCRY3	Crystal River 3	4	30	30	0	0
BDAV1	Davis Besse	5	24	22	2	0
BOCO1	Oconee 1	4	6	6	0	0
BOCO2	Oconee 2	4	2	2	0	0
BOCO3	Oconee 3	4	3	3	0	0
B3MI1	Three Mile Island 1	4	9	9	0	0
TOTALS	57	217	729	686	43	0

Table 2-4: Summary of Recordable Indications from MUHP-5042 Study [2, 3]

Plant Alpha Designation	Year	Description of Recordable Indications
AEP	1987	Surface examination of RCP flywheel no. 13 showed two 3/8" long recordable indications. Surface Chatter removed by minor surface reconditioning.
CAE/CBE	1993	0.45" Rounded indications in RCP flywheel 1B keyway area (surface exam) characterized as minor tool mark.
CCE	1991	PT indications on RCP "A" flywheel were acceptable.
	1994	Indications noted on RCP "B" flywheel with PT and VT-1 were resurfaced and found to be acceptable.
CDE	1994	Four 1/16" rounded indications noted in various areas located approximately 0.8" below top surface of RCP "C" flywheel. One linear indication noted (circ. oriented). Indications were acceptable.
CWE	1986	PT recordable indication in loop 1 RCP flywheel, bleed out from gouges and metal folds in keyways.
CPL	1984	PT recordable indication on RCP "C" flywheel bore was filed out and reexamined.
	1992	Gouge on spare flywheel blended out to 3 to 1 taper.
DLW	1980	PT indication, unsatisfactory mechanical damage from removal of RCP "B" flywheel. Grinding repaired condition.
	1987	PT recordable indication dispositioned as satisfactory for RCP "A" flywheel. Damage from handling.
	1993	UT recordable indication in RCP "B" flywheel due to geometry, dispositioned as satisfactory. PT recordable indication due to handling, dispositioned as satisfactory.
	1994	UT recordable indication in RCP "C" flywheel due to geometry, dispositioned as satisfactory.
FPL/FLA	1974	Laminations mid-wall (UT) in motor 1S-76P499 flywheel accepted as-is.
	1993	Torn metal in keyway (PT) on motor 2S-76P499 flywheel removed by buffing.
NSP	1994	MT of flywheel no. 11 periphery (0.4 inch) to be re-examined in January 1996 outage.
NRP	1995	MT indications in periphery of flywheel no. 21 (which were buffed in 1993) were found to be unchanged.
PGE	1995	Multiple MT linear indications (laminations) on lower periphery RCP 1-4 flywheel, accept as-is, monitor.
PSE/PNJ	1983-1995	Eleven recorded indications from surface examinations on seven flywheels were identified as minor chatter marks in keyway from original rough machine cuts due to the arbor tool used during manufacture. Accept as is.
SAP	1995	Wear marks on bottom surface of RCP 1 flywheel within seal ring (circular like spacers wear) – removed.
TVA/TEN	1993	Recorded indications (10 year MT) in flywheel 3S-81P352. Laminations in edge, dispositioned as acceptable.
VGB/VRA	1983	Tool marks noted in keyway of flywheel 2S-81P355.
	1986	Four PT indications in the keyway of flywheel 3S-81P355 caused by incorrect installation.
	1988	Six reportable indications from keyway scratches in flywheel 3S-81P777.
	1993	Three acceptable rounded indications in the keyway of flywheel 2S-81P777.

Table 2-4: Summary of Recordable Indications from MUHP-5042 Study [2, 3], continued

Plant Alpha Designation	Year	Description of Recordable Indications
WAT	1986	PT recorded indication in keyway area of RCP 1 flywheel resulted from tool chatter that occurred during manufacture of the flywheel. The indications were formed by the tearing and smearing of the raised metal (introduced by the tool chatter) at disassembly and reassembly of the keys.
	1986	VT recorded indication in keyway area of RCP 4 flywheel.
WPS	1976	Visual recorded indication in RCP "A" flywheel. Machine chips in five small holes in center of shaft.
BDAV1	1975	Volumetric preservice indication in RCP flywheel found to be acceptable. Surface tears in keyway removed by surface conditioning.
	1988	Surface gouges in bore of RCP 4 flywheel from flywheel removal found to be acceptable.
CYW	1971	See Appendix B of [2]

Inspection History Update

In 2017, AREVA PMSC was contracted by the PWROG to perform a study of all refurbished Westinghouse RCPMs at PMSC and document the results of flywheel NDE testing.

The method used for verifying findings was review of historical data packages, NDE data sheets, and/or Incoming/Final Refurbishment Reports. Ultimately, there were four flywheels with recordable indications discovered, all of which were deemed to be non-relevant; no repairs were required on any flywheels with recordable indications.

A summary of all Westinghouse RCPM flywheels inspected by AREVA can be found in Table 2-5. A description of all recordable indications can be found in Table 2-6.

Table 2-5: Flywheel Inspection Data per [8]

Plant	Number of Flywheels	Total Number of Flywheel Inspections	Total Number of Inspection with No Indications or Non-recordable Indications	Total Number of Inspection With Recordable Indications	Number of Indications Affecting Flywheel Integrity
Calvert Cliffs	9	9	8	1	0
Catawba	9	9	8	1	0
Davis Besse	2	2	2	0	0
DC Cook	9	14	14	0	0
Ginna	2	2	2	0	0
HB Robinson	3	3	3	0	0
McGuire	7	7	7	0	0
Oconee	13	13	13	0	0
Prairie Island	1	1	1	0	0
Salem	9	9	8	1	0
Sequoyah	1	1	1	0	0
South Texas Project	8	9	8	1	0
Surry	1	1	1	0	0
Turkey Point	1	1	1	0	0
Total	75	81	77	4	0

Table 2-6: Flywheel Inspection Data per [8]

Plant	Year	Description of Recordable Indications
Calvert Cliffs	2015	Recordable UT indication – Accepted. Lamination with 50% back wall loss 1" x 4". Testing performed by Exelon personnel.
Catawba	2006	Procedurally recordable UT indications found in the bottom flywheel plate during the 45 degree shear wave examination. – Accepted per NB-2530.
Salem	2005	Indications in two of three keyways in the lower thickness. The recordable indications were recorded in the flywheel examination evaluation report SRCP-001. PSEG was informed of the recorded indications. These same indications were previously recorded and dispositioned as acceptable by PSEG. "Indications accepted as-in in accordance with PIRS 00950906482 dated 10/24/95 supplied by PSEG. Indications are considered non-relevant due to machining process."
South Texas Project	2012	Non-relevant indications. Several low amplitude (<20% DAC) responses were noted during the radial examinations. These responses were indicative of small machine grooves or marks that extend 360°.

2.3 STRESS AND FRACTURE EVALUATION

WCAP-15666-A [3] summarized the detailed stress and fracture evaluation. The ductile and brittle failure mechanisms were considered in flywheel evaluation. Figure 2-2 shows the results of a typical flywheel overspeed evaluation, where the flywheel failure speed was calculated for a range of postulated crack depths. Note that the brittle failure limit governs for large flaws. The limiting speed increases for small flaws. Using brittle fracture considerations alone, the limiting speed would approach infinity for vanishingly small flaws. The ductile failure limit governs for these situations. This was proven by scale model tests as reported in [5]. The evaluation requirements are per RG 1.14 [4].

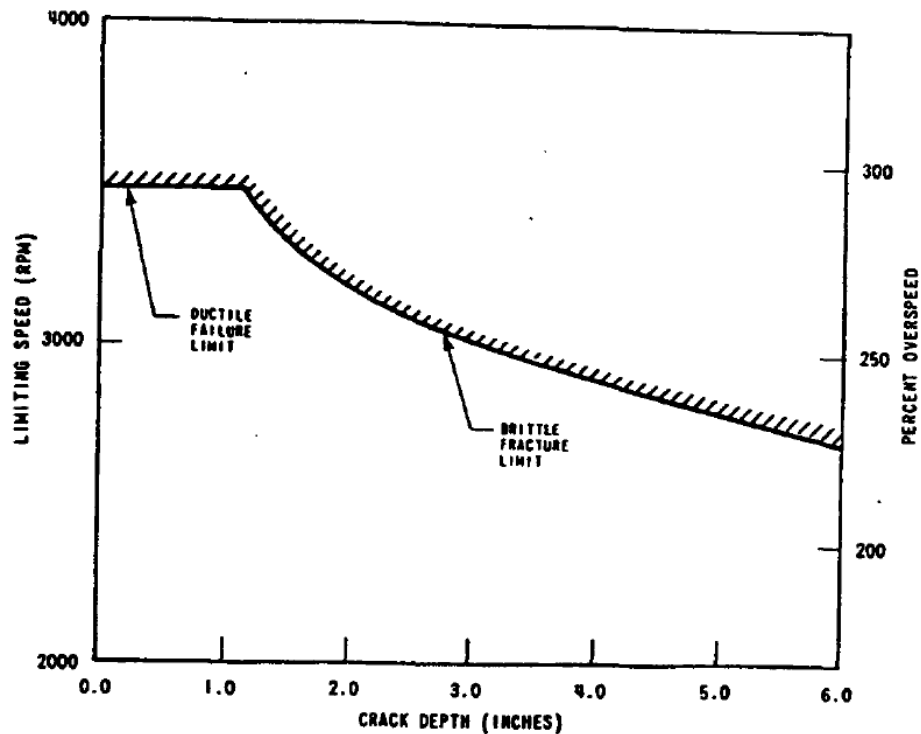


Figure 2-2: Result of Typical Westinghouse RCP Motor Flywheel Overspeed Evaluation Asymptotically

2.3.1 Selection of Flywheel Groups for Evaluation

As discussed in [3], stresses in the flywheel are a strong function of the outer diameter (approximately proportional to the OD^2). Therefore, the two groups shown in Table 2-7 with the largest flywheel outer diameter (Groups 1 and 2) bound all other groups in Table 2-2, and were selected for the deterministic and probabilistic evaluations.

Table 2-7: Flywheel Groups Evaluated for Program MUHP-5043 [3]

Flywheel Evaluation Group	Outer Diameter (inch)	Bore (inch)	Keyway Radial Length (inch)	Comments
1	76.50	9.375	0.937	Maximum OD.
2	75.75	8.375	0.906	Large OD, minimum bore.

2.3.2 Ductile Failure Analysis

The flywheel stresses are dependent on dimensions and rotation speed. Extending the operating period to 80 years does not affect the stress calculation. Therefore, the ductile failure analysis in [3] remains valid for 80 years of operation.

As discussed in [3], ASME Section III faulted condition stress limits are used as criteria. The faulted limit for elastic analysis (P_m and P_m+P_b) are $0.7 S_u$ and $1.05 S_u$, where S_u of 80 ksi was the minimum specified ultimate tensile stress for SA-533 Grade B, Class 1. The closed form equations for calculating P_m and P_m+P_b are shown in equations 1 through 6 of [3]. The ductile failure limiting speeds were determined in [3] for each selected flywheel group, assuming that cracks are not present and neglecting the local stress effects from holes and keyways. The limiting speeds were also calculated considering the reduced cross sectional area resulting from the keyway, and that cracks may be present, emanating radially from the maximum radial location of the keyway, through the full thickness of the flywheel. The limiting speeds are calculated by iterating the rotation speed until the stress limit is reached. These results from [3] are summarized in Table 2-8.

Table 2-8: Ductile Failure Limiting Speed

Flywheel Evaluation Group	Assuming No Cracks		Crack Length (as measured from the maximum radial location of the keyway)			
	Neglecting Keyway Radial Length	Considering Keyway Radial Length	1" Crack	2" Crack	5" Crack	10" Crack
1	3487	3430	3378	3333	3240	3012
2	3553	3493	3435	3386	3281	3060

Per RG 1.14, Rev. 1, Section C, item 2f [4], the normal speed should be less than one-half of the lowest of the critical speeds as calculated for ductile failure, nonductile failure, and excessive deformation. Assuming no cracks, the normal operating flywheel speed of 1200 rpm is less than 1715 rpm, half of the minimum calculated limiting speed of 3430 rpm. Item 2f of RG 1.14 is satisfied for ductile failure with no cracks present. Assuming a rather large crack of 10" in depth, item 2f is still satisfied for ductile failure since one-half of the lowest calculated critical speed (3012 rpm) is 1506 rpm, which is higher than the normal operating flywheel speed of 1200 rpm.

Per item 2g of Section C of RG 1.14, the predicted LOCA overspeed should be less than the lowest of the critical speeds calculated for ductile failure, nonductile failure, and excessive deformation. Since the predicted LOCA overspeed is in all cases less than 1500 rpm considering LBB, and all calculated limiting speed for ductile failure shown in Table 2-8 are higher than 1500 rpm, item 2g of RG 1.14 is satisfied for ductile failure, even if a large, 10" crack is present.

Therefore, RG 1.14 acceptance criteria for ductile failure of the flywheels are satisfied.

2.3.3 Nonductile Failure Analysis

The flywheel stress intensity factor, K_I , is dependent on geometry, postulated flaw dimensions and stress condition (due to rotation speed). Extending the operating period to 80 years does not affect the K_I calculations. Furthermore, the flywheel is remote from the reactor core and the effect of irradiated embrittlement is negligible. The fracture toughness, K_{Ic} would not change due to the 80 year extension, unlike the reactor vessel. Therefore, the nonductile failure analysis in [3] remains valid for 80 years of operation.

The results from [3] are shown in Table 2-9. The ambient temperature of 70°F was conservatively used as the operating temperature, while the typical containment ambient temperature is 100°F to 120°F. At the maximum flywheel overspeed condition of 1500 rpm (considering LBB), the critical crack lengths were calculated for cracks emanating radially from the keyway. The crack length is defined as radially from the keyway. The percentage through the flywheel is defined as the crack length divided by the radial length from the maximum radial keyway location to the flywheel outer radius, i.e., percentage through-wall. Note that an intermediate RT_{NDT} of 30°F ($K_{Ic} = 79.3 \text{ ksi}\sqrt{\text{in}}$) is included in the table. The critical crack lengths are quite large, even when considering higher values of RT_{NDT} and a lower than expected operating temperature.

Table 2-9: Critical Crack Lengths for Flywheel Overspeed of 1500 rpm (Considering LBB)

Flywheel Evaluation Group	Critical Crack Length in Inches and % through Flywheel		
	$RT_{NDT} = 0^\circ\text{F}$	$RT_{NDT} = 30^\circ\text{F}$	$RT_{NDT} = 60^\circ\text{F}$
1	16.6" (50%)	7.7" (24%)	3.1" (9%)
2	17.5" (53%)	8.5" (26%)	3.6" (11%)

2.3.4 Fatigue Crack Growth

FCG is dependent on flywheel K_I at operating and rest states (ΔK_I), and the number of start and stop cycles. As discussed previously, the 80 year extension has no impact on the K_I calculations. Additionally, it was confirmed by several participants that the 6000 cycles used in the FCG calculation of [3] remains bounding and applicable for 80 years of operation. Individual plants should confirm the applicability of the 6000 cycles for the 80-year operation period when referencing this report.

The FCG calculations assumed the 6000 cycles of RCP start and stop for the 80-year plant life. The FCG results from [3] are applicable and are shown in Table 2-10. The crack growth is negligible over an 80-year life of the flywheel, even when assuming a large initial crack length.

Table 2-10: Fatigue Crack Growth Assuming 6000 RCP Starts and Stops

Flywheel Evaluation Group	Flywheel OD (inch)	Flywheel Bore (inch)	Keyway Radial Length (inch)	Length From Keyway to OD (inch)	Assumed Initial Crack Length (inch)	ΔK_I (ksi $\sqrt{\text{in}}$)	Crack Growth after 6000 cycles (inch)
1	76.50	9.375	0.937	32.63	3.26	38	0.08
2	75.75	8.375	0.906	32.78	3.28	37	0.08

2.3.5 Excessive Deformation Analysis

The deformation of the flywheel is only dependent on the rotation speed and physical attributes of the flywheel. The 80-year extension has no impact on the excessive deformation analysis of the flywheel. The results in [3] remain applicable to 80 years of operation.

At the flywheel over speed condition of 1500 rpm (157.08 radians/second), the change in the bore radius and outer radius is shown in Table 2-11. A maximum deformation of 0.006 inch is anticipated for the flywheel over speed condition. As deformation is proportional to the square of angular speed, ω^2 , this represents an increase of 56% over the normal operating deformation of 0.004 inch. This increase would not result in any adverse conditions such as excessive vibrational stress leading to crack propagation, since the flywheel assemblies are typically shrunk fit to the flywheel shaft, and the deformations as calculated are negligible.

Table 2-11: Flywheel Deformation at 1500 rpm

Flywheel Evaluation Group	Change in Bore Radius (inch)	Change in Outer Radius (inch)
1	0.003	0.006
2	0.003	0.006

Additionally, Appendix E of [2], "Response to Item 5" of NRC request for additional information (RAI), addressed the potential of loss of shrink fit. The evaluation assumed 0.0052 inch for shrink fit, which is representative for Group 1, Beaver Valley Units 1 and 2 flywheels. As summarized in Table 2-12, there is more than 50% shrink fit at 1500 rpm. Furthermore, [4] defines excessive deformation as "any deformation such as an enlargement of the bore that could cause separation directly or could cause an unbalance of flywheel leading to structural failure or separation of the flywheel from the shaft." Therefore, the concern about excessive deformation is not related to loss of shrink fit, but relates to the amount of deformation which could cause unbalance or failure. The speed at which excessive deformations could occur is greater than or equal to the limiting flywheel speed for ductile failure. As shown in Table 2-8, the ductile failure of the flywheel would occur at 3012 rpm, with a 10-inch crack. This is more than the maximum overspeed of 1500 rpm, satisfying item C.2.g [4].

Table 2-12: Shrink Fit Lost at 1500 rpm [2]

Flywheel Group	Flywheel Outer Radius (inch)	Flywheel Bore Radius (inch)	Assumed Shrink Fit (inch)	Shaft Radial Expansion (inch)	Flywheel Bore Radial Expansion (inch)	Shrink Fit at 1500 rpm (inch)	Shrink Fit Lost at 1500 rpm (%)
1	38.250	4.6875	0.0052	0.0000	0.0034	0.0018	65
2	37.875	4.1875	0.0052	0.0000	0.0030	0.0022	58

Notes:

- (1) Shrink Fit at 1500 rpm = Assumed Shrink Fit + Shaft Radial Expansion – Flywheel Bore Radial Expansion.
 (2) Shrink Fit Lost at 1500 rpm = (Assume Shrink Fit – Shrink Fit at 1500 rpm)/Assume Shrink Fit.

2.4 SUMMARY OF STRESS AND FRACTURE RESULTS

The deterministic integrity evaluations in [3] remains applicable for 80 years of operation. It has shown that the RCP motor flywheels have a very high tolerance for the presence of flaws, especially with the 1500 rpm overspeed due to the application of LBB [3]. As noted in [3], the probabilistic assessment evaluates all credible flywheel speeds. This report uses the same probabilistic assessment methodology as [3], which will be discussed in Section 3.

There are no significant mechanisms for inservice degradation of the flywheels, since they are isolated from the primary coolant environment. The evaluations presented in this section have shown there is no significant deformation of the flywheels, even at maximum overspeed conditions. FCG calculations have shown that even with a large assumed flaw, the crack growth for 80 years of operation is negligible. Therefore, based on these deterministic evaluations, the flywheel inspections completed prior to service are sufficient to ensure their integrity during service. As discussed in Section 2.2 and [2 and 3], the most likely source of inservice degradation is damage to the keyway region that could occur during disassembly or reassembly for refurbishment and inspection.

3 RISK ASSESSMENT

The quantitative risk assessment discussed below provides justification for applying the WCAP-15666-A [3] 20-year flywheel inspection interval for 60 years and beyond (up to 80 years of operation). Specifically, the risk analyses confirms that applying the inspection extension to flywheels in operation in excess of 60 years up to 80 years has negligible impact on risk (CDF and LERF), i.e., it is within the bounds of RG 1.174 [9]. This section provides a discussion on the requirements of [9], and extends the previous flywheel failure probability assessment of [3].

Risk assessments included in this section apply to all Westinghouse RCP/flywheel combinations, as well as the Calvert Cliffs Units 1 and 2 RCP/flywheels which employ a Byron Jackson [18] RCP with a Westinghouse flywheel.

3.1 RISK-INFORMED REGULATORY GUIDE 1.174 METHODOLOGY

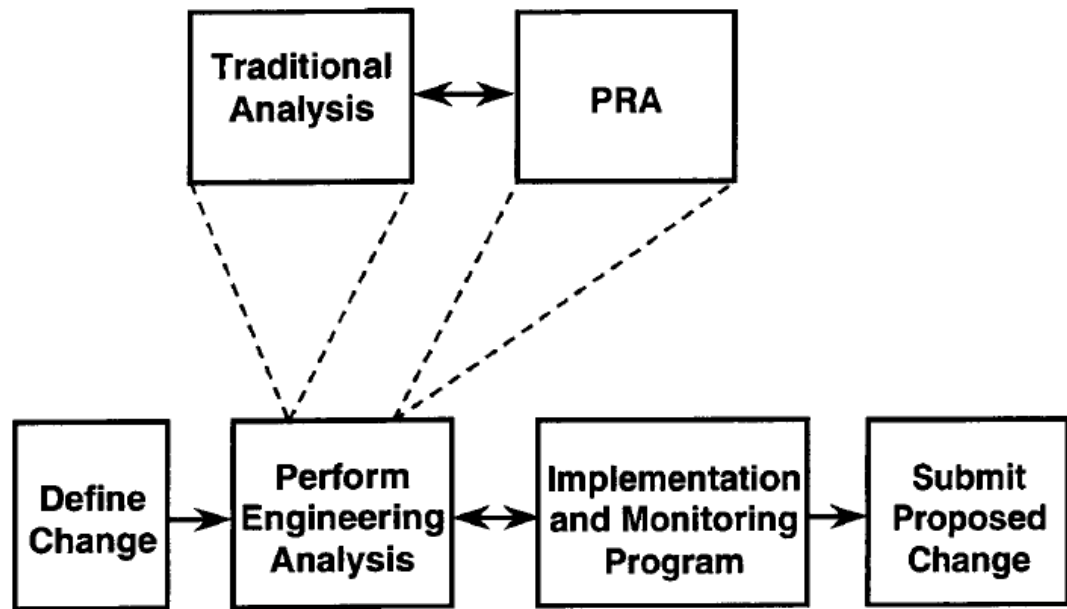
The NRC risk-informed regulatory framework for modifying a plant's licensing basis is contained in the NRC issued RG 1.174, Revision 2, "An Approach for Using Probabilistic Risk Assessment in Risk-Informed Decisions on Plant-Specific Changes to the Licensing Basis" [9]. The intent of this risk-informed process is to allow insights derived from probabilistic risk assessments to be used in combination with traditional engineering analysis to focus licensee and regulatory attention on issues commensurate with their importance to safety. Additional regulatory guidance to the NRC is contained in [10].

In addition, the NRC issued application-specific RGs and SRPs:

- RG-1.175 and SRP Chapter 3.9.7, related to inservice testing (IST) programs,
- RG-1.176, related to graded quality assurance (GQA) programs,
- RG-1.177 and SRP Chapter 16.1, related to technical specifications, and
- RG-1.178 and SRP-3.9.8, related to inservice inspection of piping programs.

These RGs and SRPs chapters provide guidance in their respective application-specific subject areas to reactor licensees and the NRC staff regarding the submittal and review of risk-informed proposals that would change the licensing basis for a power reactor facility.

The approach described in RG-1.174 is used in each of the application-specific RGs/SRPs, and has four basic steps as shown in Figure 3-1. The four (4) basic steps are discussed below.



**Principal Elements of Risk-Informed, Plant-Specific
Decisionmaking (from NRC Regulatory Guide RG-1.174)**

Figure 3-1: NRC Regulatory Guide 1.174 Basic Steps

Step 1: Define the proposed change

This element includes identifying:

1. Those aspects of the plant's licensing bases that may be affected by the change
2. All systems, structures, and components (SSCs), procedures, and activities that are covered by the change and consider the original reasons for inclusion of each program requirement
3. Any engineering studies, methods, codes, applicable plant-specific and industry data and operational experience, PRA findings, and research and analysis results relevant to the proposed change.

Step 2: Perform engineering analysis

This element includes performing the evaluation to show that the fundamental safety principles on which the plant design was based are not compromised (defense-in-depth attributes are maintained) and that sufficient safety margins are maintained. The engineering analysis includes both traditional deterministic analysis and probabilistic risk assessment. The evaluation of risk impact should also assess the expected change in CDF and LERF, including a treatment of uncertainties. The results from the traditional

analysis and the probabilistic risk assessment must be considered in an integrated manner when making a decision.

Step 3: Define implementation and monitoring program

This element's goal is to assess SSC performance under the proposed change by establishing performance monitoring strategies to confirm assumptions and analyses that were conducted to justify the change.

This is to ensure that no unexpected adverse safety degradation occurs because of the changes. Decisions concerning implementation of changes should be made in light of the uncertainty associated with the results of the evaluation. A monitoring program should have measurable parameters, objective criteria, and parameters that provide an early indication of problems before becoming a safety concern. In addition, the monitoring program should include a cause determination and corrective action plan.

Step 4: Submit proposed change

This element includes:

1. Carefully reviewing the proposed change in order to determine the appropriate form of the change request
2. Assuring that information required by the relevant regulation(s) in support of the request is developed
3. Preparing and submitting the request in accordance with relevant procedural requirements.

Five (5) fundamental safety principles are described which should be met for each application for a modification. These are shown in Figure 3-2 and are discussed below.

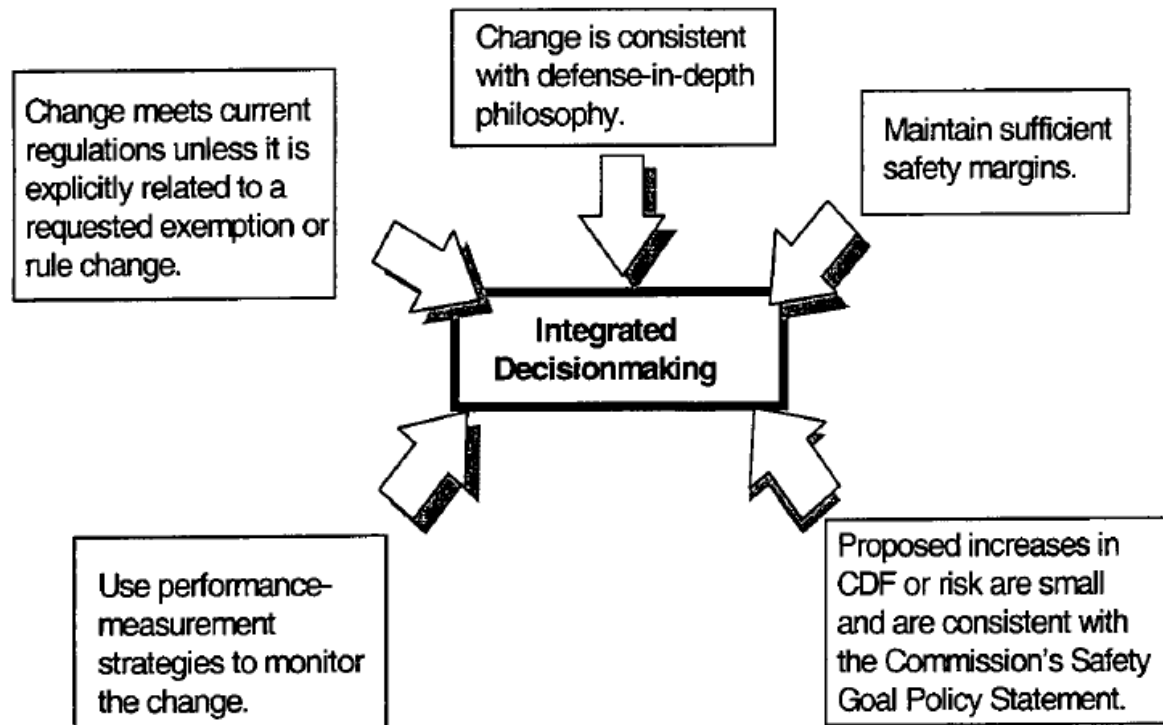


Figure 3-2: Principles of Risk-Informed Regulation [9]

Principle 1: Change meets current regulations unless it is explicitly related to a requested exemption or rule change

The proposed change is evaluated against the current regulations (including the general design criteria) to either identify where changes are proposed to the current regulations (e.g., technical specification, license conditions, and FSAR), or where additional information may be required to meet the current regulations.

Principle 2: Change is consistent with defense-in-depth philosophy

Defense-in-depth has traditionally been applied in reactor design and operation to provide a multiple means to accomplish safety functions and prevent the release of radioactive material. As defined in RG-1.174, defense-in-depth is maintained by assuring that:

- A reasonable balance among prevention of core damage, prevention of containment failure, and consequence mitigation is preserved
- Over-reliance on programmatic activities to compensate for weaknesses in plant design is avoided

- System redundancy, independence, and diversity are preserved commensurate with the expected frequency and consequences to the system (e.g., no risk outliers)
- Defenses against potential common cause failures are preserved and the potential for introduction of new common cause failure mechanisms is assessed.
- Independence of barriers is not degraded (the barriers are identified as the fuel cladding, reactor coolant pressure boundary, and containment structure)
- Defenses against human errors are preserved

Defense-in-depth philosophy is not expected to change unless:

- A significant increase in the existing challenges to the integrity of the barriers occurs
- The probability of failure of each barrier changes significantly,
- New or additional failure dependencies are introduced that increase the likelihood of failure compared to the existing conditions, or
- The overall redundancy and diversity in the barriers changes.

Principle 3: Maintain sufficient safety margins

Safety margins must also be maintained. As described in RG-1.174, sufficient safety margins are maintained by assuring that:

- Codes and standards, or alternatives proposed for use by the NRC, are met, and
- Safety analysis acceptance criteria in the licensing basis (e.g., FSARs, supporting analyses) are met, or proposed revisions provide sufficient margin to account for analysis and data uncertainty.

Principle 4: Proposed increases in CDF or risk are small and are consistent with the Commissions Safety Goal Policy Statement

To evaluate the proposed change with regard to a possible increase in risk, the risk assessment should be of sufficient quality to evaluate the change. The expected change in CDF and LERF are evaluated to address this principle. An assessment of the uncertainties associated with the evaluation is conducted. Additional qualitative assessments are also performed.

There are two acceptance guidelines, one for CDF and one for LERF, both of which should be used.

The guidelines for CDF are:

- If the application can be clearly shown to result in a decrease in CDF, the change will be considered to have satisfied the relevant principle of risk-informed regulation with respect to CDF.
- When the calculated increase in CDF is very small, which is taken as less than 10^{-6} per reactor year, the change will be considered regardless of whether there is a calculation of the total CDF.

- When the calculated increase in CDF is in the range of 10^{-6} per reactor year to 10^{-5} per reactor year, applications will be considered only if it can be reasonably shown that the total CDF is less than 10^{-4} per reactor year.
- Applications which result in increases to CDF above 10^{-5} per reactor year would not normally be considered.

AND

The guidelines for LERF are:

- If the application can be clearly shown to result in a decrease in LERF, the change will be considered to have satisfied the relevant principle of risk-informed regulation with respect to LERF
- When the calculated increase in LERF is very small, which is taken as being less than 10^{-7} per reactor year, the change will be considered regardless of whether there is a calculation of the total LERF.
- When the calculated increase in LERF is in the range of 10^{-7} per reactor year to 10^{-6} per reactor year, applications will be considered only if it can be reasonably shown that the total LERF is less than 10^{-5} per reactor year.
- Applications which result in increases to LERF above 10^{-6} per reactor year would not normally be considered.

These guidelines are intended to provide assurance that proposed increases in CDF and LERF are small and are consistent with the intent of the Commission's Safety Goal Policy Statement.

Principle 5: The impact of the proposed change should be monitored using performance-measurement strategies to monitor the change

Performance-based implementation and monitoring strategies are also addressed as part of the key elements of the evaluation as described previously.

The following sections address the principle elements of the RG-1.174 process and the principles of risk-informed regulation to RCP motor flywheel examination frequency reduction.

3.2 FAILURE MODES AND EFFECTS ANALYSIS

A failure modes and effects analysis is used to identify the potential failure modes of a RCP motor flywheel and the effect that each failure mode would have on the plant SSCs in relation to overall plant safety.

Failure Modes

The primary failure mode of the RCP motor flywheel is growth of an undetected fabrication induced flaw in the keyway of the flywheel that emanates radially from that location to a point such that it reaches a critical flaw size during normal or accident conditions. Once the critical flaw size is reached during plant operation, the flywheel has the potential to catastrophically fail, resulting in flywheel fragments, which are essentially high energy missiles that could impact other SSCs important to plant safety. The growth of a flaw is primarily related to stresses generated from changes in the flywheel speed. The flywheel inspection process, which itself has the potential to introduce flywheel damage as discussed in [2], is not considered in the assessment. This is because the purpose of the assessment is to support interval extension, which will reduce unnecessary occurrences for introducing potential damage.

As discussed in [5], the normal operating speed of the RCP motor flywheel for Westinghouse RCPs is 1189 revolutions per minute (rpm), with a synchronous speed of 1200 rpm. It is designed for an overspeed of 1500 rpm, which is 125% of the synchronous speed. The flywheel speed can be altered, however, as a result of plant events, including accidents such as a DEGB in the main reactor coolant loop piping.

Westinghouse designed flywheels are also used for Calvert Cliffs Units 1 and 2. These plants include Byron-Jackson designed pumps and motors and therefore have different normal flywheel operating speeds and different flywheel accident responses. The normal operating speed of the RCP motor flywheel for these RCPs is 900 revolutions per minute (rpm), with a design limiting speed of 1125 rpm. Maximum overspeed following a design basis LOCA is limited by 1368 rpm.

When operating as a motor, the rotor of a polyphase induction machine rotates in the direction of, but slightly lower than, the rotating magnetic flux provided by the stator. This slight speed difference is usually expressed in percent and designated slip. If the shaft of the machine is driven above synchronous speed by a prime mover (with line voltage maintained on the stator) the rotor conductors rotate faster than the magnetic flux and the slip becomes negative. The rotor current and consequently the stator current reverse under the condition of negative slip and the machine operates as an induction, or asynchronous, generator. The RCP motor functions as an efficient torque producer under normal conditions. In the unlikely event that a hydraulic torque is applied to the motor shaft in the direction of increasing shaft speed (thus acting as a prime mover), the slip would become negative and, with the stator connected to the grid, the motor would function as a dynamic brake.

If the power supply to the motor is interrupted (zero voltage), the motor torque would be reduced to a negligible value, since torque is proportional to the supplied voltage. However, a design feature of Westinghouse PWR plants assures that the electrical

power supply to the RCP will be maintained for at least 30 seconds after the turbine trip following a LOCA. This situation is true for the assumption of loss of offsite power (LOOP); for the expected case of available off-site power, power to the RCP would continue through the LOCA transient. As a result, reverse torque is provided.

WCAP-8163 also performed several sensitivity studies to evaluate the effect of break opening area on RCP flywheel speed for typical Westinghouse PWRs. Specifically, break sizes equal to DEGB, 60% of DEGB, and 3 ft² have been analyzed. (Note that a 3 ft² break size corresponds to a pipe approximately 23 inches in inside diameter; the only RCS pipes greater than this size are those associated with the main coolant loop piping.) The first two breaks have blowdown times equal to or less than the RCP trip time; the applied voltage prevents overspeed. The latter break has an extended blowdown time, but the RCP flow at the time of RCP trip is reduced such that the speed decreases. Hence, smaller breaks are not limiting even though the voltage is maintained for only 30 seconds. Results of these studies were discussed in [5].

To investigate consequences of RCP overspeed, [3] analyzed a spectrum of LOCA events leading to a range of flywheel transients. Results of that analysis indicated that the limiting event was the DEGB with an instantaneous loss of power, this led to a peak flywheel speed of 3321 rpm. It was also noted that the 3 ft² break area case showed a decrease in speed such that normal operating speed is not exceeded.

Based on the WCAP-15666-A assessments, the following scenarios are associated with the primary mode of potential failure in the Westinghouse RCP motor flywheel that are related to operating speed and potential overspeed during various conditions:

- Failure during normal plant operation resulting in a plant trip (1200 rpm peak speed)
- Failure of the RCP motor flywheel given a plant transient or LOCA event with no loss of electrical power to the RCP (1200 rpm peak speed)
- Failure of the RCP motor flywheel given a plant transient or LOCA event (up to 3 ft² with an instantaneous loss of electrical power to the RCP (1200 rpm peak speed)
- Failure of the RCP motor flywheel given a DEGB coincident with an instantaneous loss of electrical power, such as LOOP (3321 rpm peak speed). This case bounds and is conservatively assumed to apply to all flywheel transients for LOCA break areas.

WCAP-15666-A [3] was limited in scope to RCPs with Westinghouse supplied pumps and flywheels. It is also the intent of this topical report to extend the applicability of the flywheel inspection extension to Calvert Cliffs Units 1 and 2 which employ Byron Jackson RCPs but use Westinghouse supplied flywheels. It is important to note that as a result of significant design differences between the Westinghouse and Calvert Cliffs units, the Calvert Cliffs RCP operational and transient conditions are different. Specifically, Calvert Cliffs pumps normally operate at 900 rpm with a design speed of 1125 rpm. Furthermore, the peak RCP post LOCA speed is limited to 1368 rpm.

Therefore, the Calvert Cliffs Units 1 and 2 Pump/Flywheel Combinations analyses were based on the following:

- Failure during normal plant operation resulting in a plant trip (1125 rpm peak speed)
- Failure of the RCP motor flywheel given a plant transient or LOCA event with no loss of electrical power to the RCP (1125 rpm peak speed)
- Failure of the RCP motor flywheel given a plant transient or LOCA event (up to 3 ft²) with an instantaneous loss of electrical power to the RCP (1125 rpm peak speed)
- Failure of the RCP motor flywheel given a DEGB coincident with an instantaneous loss of electrical power, such as, loss of offsite power (LOOP) (1368 rpm peak speed). As for the Westinghouse flywheel analysis, this case is conservatively assumed to bound all flywheel transients for LOCA break areas resulting from equivalent reactor coolant pipe breaks greater than a 3.0 ft² break and less than a double ended break.

Failure Effects

The failure of the RCP motor flywheel during normal plant operation would directly result in a reactor trip. However, the potential indirect or spatial effects associated with a postulated flywheel failure present a greater challenge in terms of failure effects or consequences. As mentioned previously, the flywheel has the potential to catastrophically fail, resulting in flywheel fragments, which are essentially high energy missiles, which could impact other SSCs important to plant safety. Failure of these other SSCs could present a threat to overall plant safety in terms of core damage (e.g., as a result of the loss of safety injection) or large, early release (as a result of potential impacts on containment structures or systems).

Initial investigations have been performed to determine if any SSCs important to plant safety may pass through the RCP compartments in Westinghouse PWR plants. These investigations indicate that there is not much uniformity with respect to the layout of critical targets that potential flywheel fragments could impact given its failure. In order to address this situation on a generic basis, it is conservatively assumed that failure of the RCP motor flywheel results in core damage and large early release, i.e., the flywheel failure frequency is equal to CDF and LERF.

Section 3.3 describes the process for estimating the likelihood of the primary failure mode of the RCP motor flywheel. Section 3.4 then combines this failure probability estimation with the likelihood of various plant events and consequences to estimate the change in risk for extending the flywheel examination interval from 10 years to 20 years, for RCP/Flywheels in service up to 80 years.

3.3 FLYWHEEL FAILURE PROBABILITY

To investigate the effect of flywheel inspections on the risk of failure, a structural reliability and risk assessment is performed; a 40-year plant life including the potential for an extended plant life of 80 years. Twelve (12) month operating cycles are conservatively assumed for the evaluation. This section describes the methodology used and summarizes the results from this assessment.

As described in Section 3.2, the Westinghouse RCP has a normal operating speed of 1189 rpm, a synchronous speed of 1200 rpm, and a design speed of 1500 rpm, per [3]. Therefore, a peak speed of 1500 rpm is conservatively used in the evaluation of RCP motor flywheel integrity to represent all conditions except a DEGB coincident with an instantaneous loss of electrical power. For this more limiting event, a peak speed of 3321 rpm is used.

The structural reliability evaluation for the Westinghouse RCP makes use of work previously performed and summarized in [2], where the 1500 rpm design speed had been assumed based on arguments that were appropriate for the evaluation that was performed at that time. In addition, this evaluation builds upon the initial analysis presented in [3].

The structural reliability evaluation for the Calvert Cliffs RCP is based on plant specific analyses presented in the Calvert Cliffs USAR. For this assessment flywheel failure probabilities are based on nominal and transient flywheel operation at 1125 rpm and a post design basis LOCA flywheel transient overspeed of 1368 rpm.

3.3.1 Method of Calculation Failure Probabilities

The method for calculating flywheel failure probabilities is based on WCAP-15666-A.

The probability of failure of the RCP motor flywheel as a function of operating time t , $Pr(t < t_1)$, is calculated directly for each set of input values using Monte-Carlo simulation with importance sampling. The Monte-Carlo simulation does not force the calculated distribution of time to failure to be of a fixed type (e.g., Weibull, Log-normal or Extreme Value). The actual failure distribution is estimated based upon the distributions of the uncertainties in the key structural reliability model parameters and plant specific input parameters. Importance sampling, as described by Witt [11], is a variance reduction technique to greatly reduce the number of trials required for calculating small failure probabilities. In this very effective technique, random values are selected from the more severe high or low regions of their distributions so as to promote failure. However, when failure is calculated, the count is corrected to account for the lower probability of simultaneously obtaining all of the more severe random values.

To apply this simulation method to RCP motor flywheel failure, the existing Westinghouse PROF Software System (object library) is combined with the problem-specific structural analysis models described previously in [3]. The PROF library provides standard input and output, and probabilistic analysis capabilities (e.g., random number generation, importance sampling). The result is the executable program RPFWPROF.EXE for calculation of RCP motor flywheel failure probability with time. The failure mode being simulated by the program is an initial flaw, undetected during pre-

service inspection, growing by fatigue crack growth due to RCP startup and shutdown until a critical length is obtained. The critical length is that which causes the stress intensity factor of the flaw due to RCP overspeed during the design-limiting event to exceed the fracture toughness of the flywheel material.

The Westinghouse PROF Software Library (W-PROF), which was used to generate the RPFWPROF program [7], has been verified and benchmarked in a number of ways. A discussion of that verification and results of associated sensitivity studies are contained in [3]. Verification results demonstrated that W-PROF calculated values agree very well (less than 4% error) with results of hand calculations for various sample cases.

The calculation of failure probability using the W-PROF methods and importance sampling was also compared to that calculated by an alternative method using more complex models. The more complex model also included the uncertainties in growth rate, which were also a function of the crack depth. The alternative method was the @RISK add-in for Lotus 1-2-3 spreadsheets [12]. Results of the comparison were reported in [3]. These results demonstrated that the W-PROF calculated probabilities are excellent at the low probability values, where importance sampling is normally used.

The input to the RPFWPROF program, which is described in Table 3-1, includes the key parameters needed for failure probability calculation. Its usage in the program is specified as shown in the last column of Table 3-2 and schematically in the flow chart of Figure 3-3. "Initial" conditions do not change with time, "Steady-State" is not needed for RPFWPROF, "Transient" calculates fatigue crack growth and "Failure" checks to see if the accumulated crack length exceeds the critical length. In addition, parameter RPM-DLE is included in the model to address the impact of design limiting events (DLE) such as external events (e.g., seismic or failure of other RCP components). Thus, inclusion of this parameter is used to support the proposed RCP motor flywheel ISI interval.

Table 3-1: Variables for RCP Motor Flywheel Failure Probability Model			
No.	Name	Description of Input Variable	Usage Type
1	ORADIUS	Outer Flywheel Radius (inch)	Initial
2	IRADIUS	Inner Flywheel Radius (inch)	Initial
3	PFE-PSI	Probability of Flaw Existing (PFE) after Preservice ISI	Initial
4	ILENGTH	Initial Radial Flaw Length (inch)	Initial
5	CY1-ISI	Operating Cycle for First Inservice Inspection	Inspection
6	DCY-ISI	Operating Cycle between Inservice Inspections	Inspection
7	POD-ISI	Flaw Detection Probability per Inservice Inspection	Inspection
8	DFP-ISI	Fraction PFE Increases per Inservice Inspection	Inspection
9	NOTR/CY	Number of Transients per Operating Cycle	Transient
10	DRPM-TR	Speed Change per Transient (RPM)	Transient
11	RATE-FCG	Fatigue Crack Growth Rate (Inch/Transient)	Transient
12	KEXP-FCG	Fatigue Crack Growth Rate SIF Exponent	Transient
13	RPM-DLE	Speed for Design Limiting Event (RPM)	Failure
14	TEMP-F	Temperature for Design Limiting Event (F)	Failure
15	RT-NDT	Reference Nil Ductility Transition Temperature (F)	Failure
16	F-KIC	Crack Initiation Toughness Factor	Failure
17	DLENGTH	Flywheel Keyway Radial Length (Inch)	Failure

Variables 5 to 8 are available to calculate the effects of an ISI in the RPFWPROF program. The effect of ISI calculated using these equations, which are used in the SRRA model for the effect of ISI, are consistent with those described in the pc-PRAISE Code User's Manual [14]. The results are somewhat optimistic since there is no correlation between successive inspections of the same material, which may systematically occur in actual practice. The parameters needed to describe the selected ISI program are the time of the first inspection, the frequency of subsequent inspections (expressed as the number of fuel or operating cycles between inspections) and the probability of non-detection as a function of crack length. For the RCP motor flywheel, the non-detection probability, which is independent of crack length, is simply one minus a constant value of detection probability, variable 7 (POD-ISI) in Table 3-1. An increase in failure probability due to RCP inspection (chance of incorrect disassembly and reassembly) is included in the ISI model but conservatively not used (variable 8 set to zero) in this evaluation.

The median input values and their uncertainties for each of the parameters of Table 3-1 are shown in Table 3-2. The median is the value at 50% probability (half above and half below this value); it is also the mean (average) value for symmetric distributions, like the normal (bell-shaped curve) distribution.

Uncertainties are based upon expert engineering judgement and previous structural reliability modeling experience. For example, the fracture toughness for initiation as a function of the RT_{NDT} and the uncertainties on these parameters are based upon prior probabilistic fracture mechanics analyses of the pressure vessel [15]. Also note that the stress intensity factor calculation for crack growth and failure used the flywheel keyway radial length (variable 17, DLENGTH) in addition to the calculated flaw length.

Table 3-2: Input Values for RCP Motor Flywheel Failure Probability Model				
No.	Name	Median	Distribution	Uncertainty*
1	ORADIUS	Per Flywheel Group	Constant	-----
2	IRADIUS	Per Flywheel Group	Constant	-----
3	PFE-PSI	1.000E-01	Constant	-----
4	ILENGTH	1.000E-01	Log-Normal	2.153E+00
5	CY1-ISI	3.000E+00	Constant	-----
6	DCY-ISI	4.000E+00	Constant	-----
7	POD-ISI	5.000E-01	Constant	-----
8	DFP-ISI	0.000E+00	Constant	-----
9	NOTR-CY	1.000E+02	Normal	1.000E+01
10	DRPM-TR****	9.00E+02 (CCNPP) 1.200E+03 (W)	Normal	9.00E+01 (CCNPP) 1.200E+02 (W)
11	RATE-FCG	9.950E-11	Log-Normal	1.414E+00
12	KEXP-FCG	3.070E+00	Constant	-----
13	RPM-DLE	1.500E+03**	Normal	1.500E+02**
14	TEMP-F***	7.0E+01 (CCNPP) 9.500E+01 (W)	Normal	1.250E+01
15	RT-NDT	3.000E+01	Normal	1.700E+01
16	F-KIC	1.000E+00	Normal	1.000E-01
17	DLENGTH	Per Flywheel Group	Constant	-----

Notes:

- * Uncertainty is normal standard deviation, the range (median to maximum) for uniform distributions or the corresponding factor for logarithmic distributions.
- ** RPM-DLE is modified in each case to allow for Design Level Events for both Westinghouse Plants and Calvert Cliffs Units 1 and 2.
- *** TEMP-F is set to 95°F for Westinghouse Plants (W) and 70°F for Calvert Cliffs Units 1 and 2 (CCNPP).
- **** DRPM-TR is set to 1200 RPM for Westinghouse Plants (W) and 900 RPM for Calvert Cliffs Units 1 and 2 (CCNPP).

Group specific input variables used in the probability of failure calculations are summarized below:

Flywheel Group	ORadius (inch)	IRadius (inch)	DLength (inch)
Group1	38.25	4.6875	0.937
Group 2	38.875	4.1875	0.906
Calvert Cliffs	41.00	4.719	0.937

Evaluations were performed to determine the effect on the probability of flywheel failure for continuing the current inservice inspections over the life of the plant and for discontinuing the inspections. Since most plants have been in operation for at least ten years, the evaluation also calculated the effects of the inspections being discontinued after ten years. This calculation would bound the effects of any subsequent inservice inspections at 10 to 20 year intervals.

It is important to keep in mind that the probability of failure determined by these evaluations is considered to be a conservatively calculated parameter. The reason for this is that the evaluation conservatively assumes that the probability of a flaw existing after preservice inspection is 10%, and that the ISI flaw detection probability is only 50%. In reality, most preservice and ISI flaws would be detected, especially for the larger flaw depths which may lead to failure. Therefore, the calculated values are very conservative. (The effects of some important parameters on the calculated probability of failure are discussed later in this section). The most important result of the evaluation is the change in calculated probability of failure from continuing versus discontinuing the ISI after ten years (cycles) of plant life.

As shown in Figure 3-4, Figure 3-5 and Figure 3-6 and Table 3-3, the ISI provides little benefit on minimizing the potential for failure of the flywheel. The results of this assessment are summarized as follows for a plant life of 40, 60 and 80 years.

Table 3-3: Cumulative Probability of Failure over 40, 60 and 80 Years with and without Inservice Inspection ⁽¹⁾

Flywheel Group	Design Limiting Speed (rpm)	Cumulative Probability of Flywheel Failure with ISI at 4-Year Intervals	Cumulative Probability of Flywheel Failure with ISI at 4-Year Intervals Prior to 10 Years and without ISI after 10 Years			% Increase in Cumulative Failure Probability for Eliminating Inspections		
		Over 40, 60 & 80 Years	Over 40 Years	Over 60 Years	Over 80 Years	Over 40 Years	Over 60 Years	Over 80 Years
1	1500	2.39E-7	2.44E-7	2.49E-7	2.52E-7	2.2%	4.5%	5.4%
2	1500	1.29E-7	1.32E-7	1.34E-7	1.35E-7	2.4%	3.5%	4.5%
1	3321	9.87E-3	9.89E-3	9.89E-3	9.99E-3	0.1%	0.2%	1.2%
2	3321	9.01E-3	9.09E-3	9.09E-3	9.09E-3	0.1%	0.1%	0.1%
Calvert Cliffs	1125	1.50E-8	1.51E-8	1.51E-8	1.52E-8	0.5%	0.6%	0.8%
Calvert Cliffs	1368	5.56E-6	5.56E-6	5.62E-6	5.63E-6	0.3%	1.4%	1.5%

Note: (1) Results are slightly different from Table 3-8 in [3]. Differences are on the order of 2%. These differences are likely due to changes in the operating platform and do not impact any conclusions drawn in this analysis or in [3].

As can be seen in Table 3-3, continuing inspection after 10 years has a very minimal impact on the failure probabilities.

Note that for the limiting speed of 3321 rpm, the flywheel failure probability is $\sim 1.0\text{E-}2$ from the first through the 80th year of operation for Flywheel Group 1. It is approximately constant at $9.09\text{E-}3$ from the first through the 80th year of operation for Flywheel Group 2. The post LOCA limiting speed of Calvert Cliffs Units 1 and 2 of 1368 RPM yielded much reduced failure probabilities, with the equivalent post-LOCA failure probability for a Westinghouse RCP (with a peak speed of 3321 rpm). The Calvert Cliffs cumulative flywheel failure probability given a limiting LOCA event was only $\sim 5.6\text{E-}6$.

3.3.2 Sensitivity Study

A sensitivity study was performed to determine the effect of some important flywheel risk assessment parameters on the probability of failure. Sensitivity studies were performed on a Westinghouse Group 10 flywheel. The parameters evaluated included the probability of detection and the initial flaw length. The results of this study are summarized in the Table 3-4. Note that consistent with [3] this study was performed for only 40 years of flywheel operation, utilizing Flywheel Group 10 as a generic base case.

**Table 3-4: Effect of Flywheel Risk Parameter on Failure Probability
(Flywheel Group 10)**

Description of Flywheel Risk Parameter Varied	Probability of Flywheel Failure after 40 years with ISI prior to and after 10 years	Probability of Flywheel Failure after 40 years with ISI prior to 10 years and without ISI after 10 years
Base Case (Group 10 of [2])	1.00E-07	1.04E-07
Probability of Detection of 10%	1.02E-07	1.04E-07
Probability of Detection of 80%	1.00E-07	1.04E-07
Initial flaw length of 0.05 inches	4.57E-08	4.71E-08
Initial flaw length of 0.20 inches	2.97E-07	3.00E-07

The values for the base case were for:

- 10% probability of a flaw existing after preservice inspection
- Initial flaw length of 0.10 inch (1.006 inch with keyway)
- Initial ISI at 3 years of plant life, and subsequent inspections at 4-year intervals
- Probability of detection of 50% per ISI (see [2], Table 5-5, flywheel Group 10)

A discussion of the results of the sensitivity studies are summarized below.

3.3.2.1 Sensitivity to Change in Flaw Detection Probability

The flaw detection probability was varied from the base case 50% to 10% and 80%. The failure probability increased approximately 3% for a decrease in flaw detection probability from 50% to 10%. The failure probability did not change for an increase in flaw detection probability from 50% to 80%. Therefore, the flaw detection probability, which is a measure of how well the inspections are performed, has essentially no effect on flywheel failure probability.

3.3.2.2 Sensitivity to Initial Flaw Length

The initial flaw length was varied from the base case value of 0.10 inch to 0.05 inch and 0.20 inches. The failure probability decreased by 54% for a decrease in initial flaw length from 0.10 inch to 0.05 inch, and the failure probability tripled for an increase in initial flaw length from 0.10 inch to 0.20 inches. Therefore, the initial flaw length does affect flywheel failure probability, but the failure probability is small, even for larger initial flaw lengths. Moreover, the probability of the larger flaw being missed during preservice inspection would be even smaller than the assumed 10%.

3.3.3 Failure Probability Assessment Conclusions

An evaluation of flywheel structural reliability was performed for each of the flywheel groups selected for evaluation, using methods that have been sufficiently verified and benchmarked.

Using conservative input values for preservice flaw existence, initial flaw length, inservice flaw detection capability and RCP start/stop transients, it was shown that flywheel inspections beyond ten years of plant life have no significant benefit relative to the probability of flywheel failure. The reasons for this are that most flaws that could lead to failure would be detected during preservice inspection or at worst early in the plant life, and crack growth is negligible over the plant life. It should be noted that the effect on potential flywheel failure from damage through disassembly and reassembly for inspection has not been evaluated. This is because the purpose of the assessment is to support interval extension, which will reduce unnecessary occurrences for introducing potential damage.

Sensitivity studies showed that improved flaw detection capability and more inspections result in a small relative change in calculated failure probability. Failure probability is most affected by the initial flaw length and its uncertainty. These parameters are determined by the accuracy of the preservice inspection. The uncertainty could be reduced using the results from the first inservice inspection, but would probably not change much during subsequent inspections.

The failure probability estimates identified in [3] show that inspections after 10 years have a very minimal impact on the failure probabilities. These results would bound the effects of any subsequent ISI at 10 to 20 year intervals. No credit has been taken for other indications of potential degradation such as pump vibration monitoring and pump maintenance.

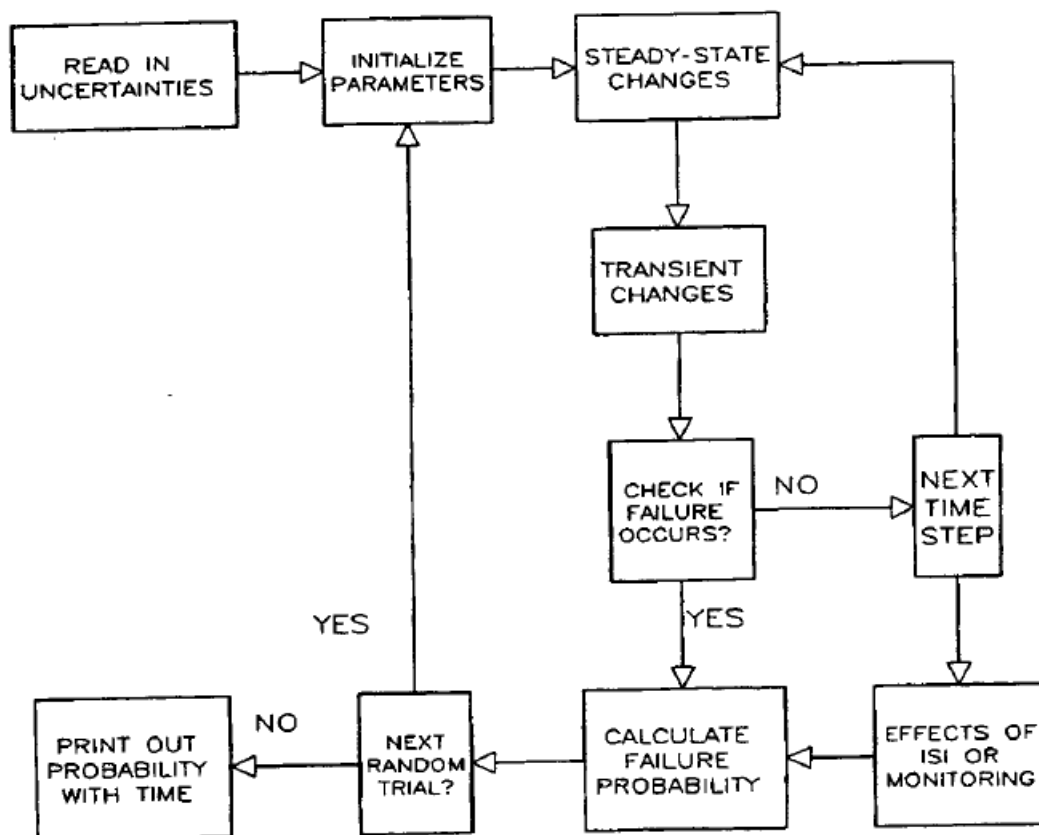


Figure 3-3: Westinghouse PROF Program Flow Chart for Calculating Failure Probability

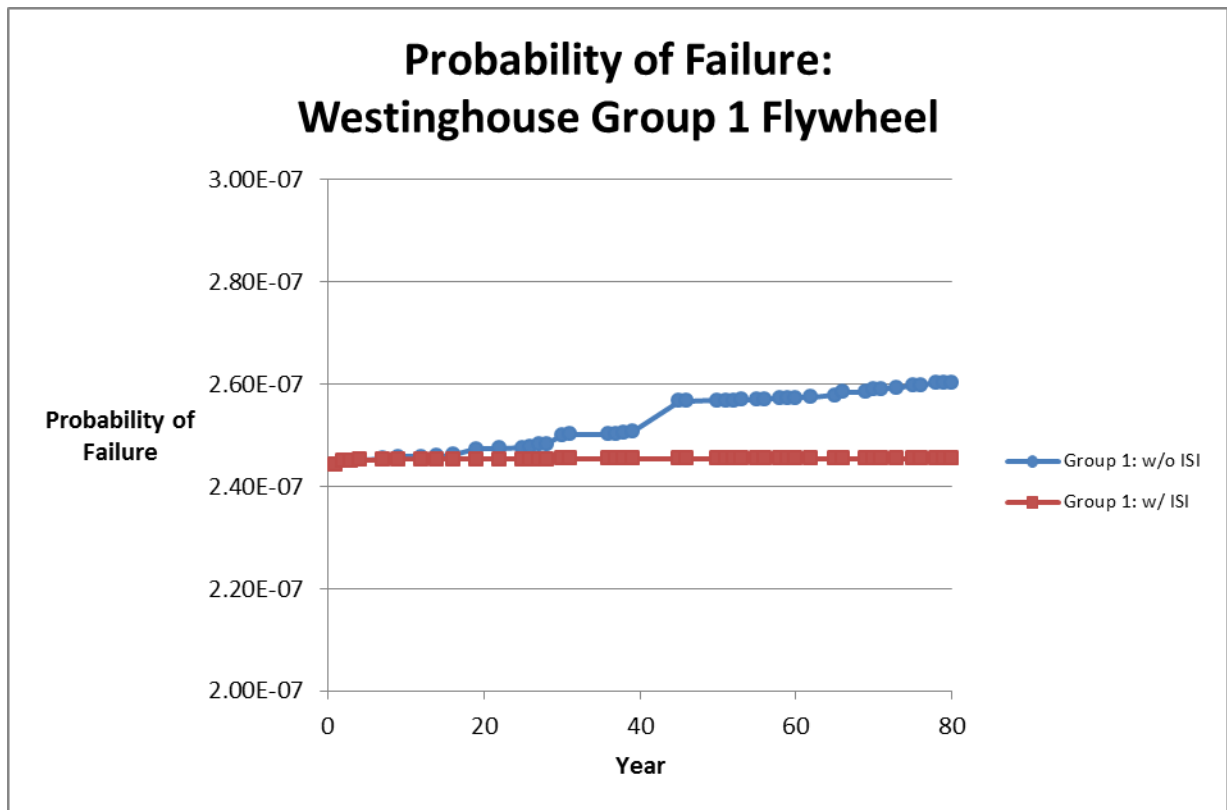


Figure 3-4: Probability of Failure for Flywheel Evaluation Group 1

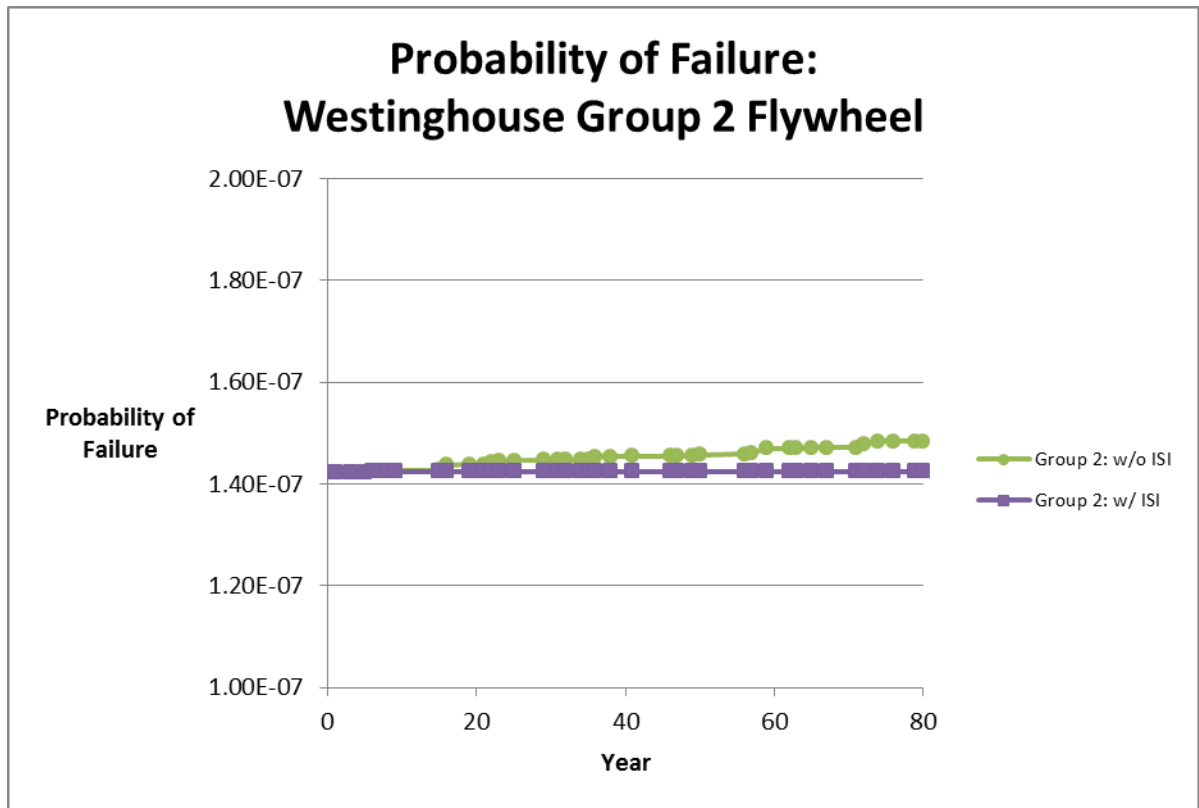


Figure 3-5: Probability of Failure for Flywheel Evaluation Group 2

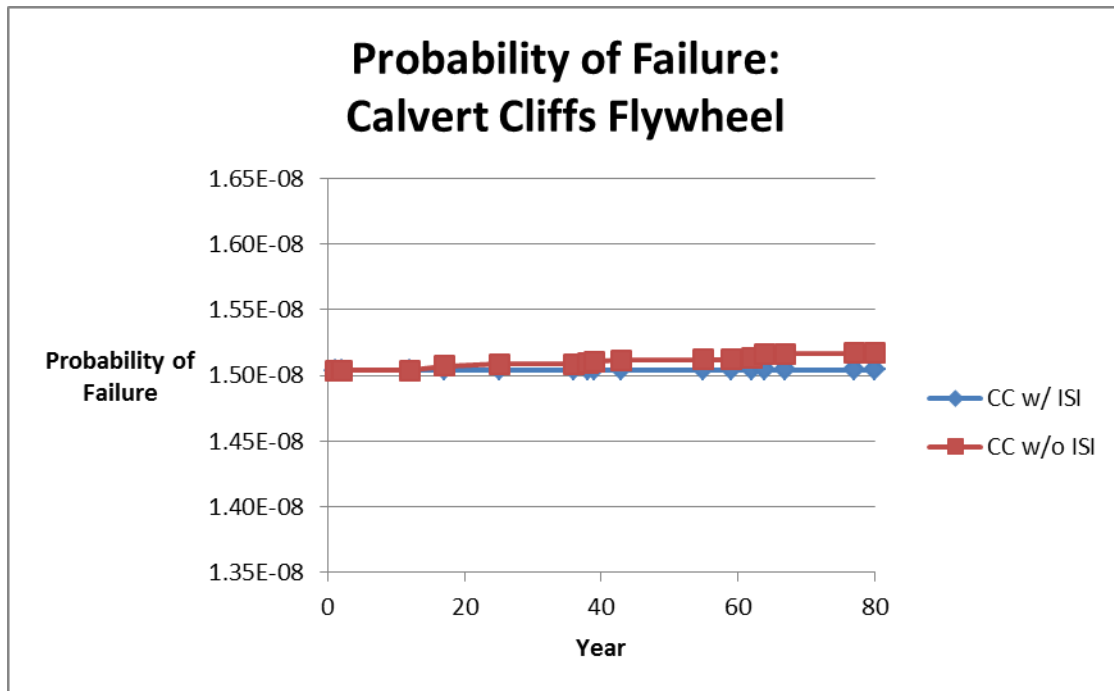


Figure 3-6: Probability of Failure for Calvert Cliffs Units 1 and 2

3.4 CORE DAMAGE EVALUATION

The objective of the risk assessment is to evaluate the core damage risk from the extension of the examination of the RCP motor flywheel, over an extended 80 year in-service duration, relative to other plant risk contributors through a qualitative and quantitative evaluation.

RG 1.174, Revision 2 [9] provides the basis for this evaluation and also provides the acceptance guidelines to make a change to the current licensing basis.

Risk is defined as the combination of likelihood of an event and severity of consequences of an event. Therefore, the following two questions are addressed:

- What is the likelihood of the event?
- What are the consequences?

The following sections describe the likelihood and postulated consequences. The likelihood and consequences are then combined in the risk calculation and the results of the evaluation are presented.

Several different scenarios have been identified for potential RCP motor flywheel failures that are related to its operating speed and potential overspeed under certain conditions. These scenarios are summarized in Table 3-5.

Table 3-5: Summary of Flywheel Analysis Parameters

	Westinghouse RCP/Flywheel (rpm)	Calvert Cliffs RCP/Flywheel (rpm)
Failure during normal plant operation resulting in a plant trip	1500*	1125*
Failure of the RCP motor flywheel given a plant transient or LOCA event with NO loss of electrical power to the RCP	1500*	1125*
Failure of the RCP motor flywheel given a plant transient or LOCA event (up to a three square foot break in the main loop) with loss of electrical power to the RCP	1500*	1125*
Failure of the RCP motor flywheel given a large LOCA (from a greater than 3 ft ² break up to the DEGB of the RC loop piping) coincident with an instantaneous electrical power loss (e.g., loss of offsite power (LOOP) or loss of electrical power to the RCP) and therefore no electrical braking to the RCP	3321	1368

Notes: * RPM are based on maximum design speed

3.4.1 What is the Likelihood of the Event

The likelihood is addressed by identifying a plant transient or LOCA event combined with the postulated failure of the flywheel and estimating the probability/frequency of these events. The likelihood of the flywheel failure is discussed in Section 3.3 and the results are provided in Table 3-3 for the two flywheel evaluation groups that bound the other flywheel groups and for Calvert Cliffs Units 1 and 2 flywheels. The estimated failure probabilities for the different conditions for the various flywheel types and event combinations are shown in Table 3-6.

Table 3-6: Estimated RCP Motor Flywheel Failure Probabilities

Flywheel Group and Conditions*	Cumulative Probabilities of Flywheel Failure over 60 Years*		Cumulative Probabilities of Flywheel Failure over 80 Years*	
	With ISI at 4-Year Intervals	With ISI at 4-Year Intervals Prior to 10 Years and without ISI after 10 Years	With ISI at 4-Year Intervals	With ISI at 4-Year Intervals Prior to 10 Years, and without ISI after 10 Years
Group 1 – Normal/Accident*	2.39E-07	2.49E-07	2.39E-07	2.52E-07
Group 1 – LOCA/LOOP*	9.87E-03	9.89E-03	9.87E-03	9.99E-03***
Group 2 – Normal/Accident*	1.29E-07	1.34E-07	1.29E-07	1.35E-07
Group 2 – LOCA/LOOP*	9.09E-03	9.09E-03	9.09E-03	9.09E-03
Calvert Cliffs Units 1&2 – Normal/Accident**	1.50E-08	1.51E-08	1.50E-08	1.52E-08
Calvert Cliffs Units 1&2-LOCA/LOOP**	5.54E-06	5.62E-06	5.54E-06	5.63E-06

Notes:

* For the failure probability calculations the mean flywheel speed for normal/accident conditions is 1500 rpm; for LOCA/LOOP is it 3321 rpm.

** For the failure probability calculations the mean flywheel speed for normal/accident conditions is 1125 rpm; for LOCA/LOOP is it 1368 rpm.

*** Selected as bounding value

3.4.2 What are the Consequences?

The consequence evaluation is performed to identify the potential consequences from the failure of the RCP motor flywheel from an integrity standpoint. The consequences are briefly discussed in Section 3.2.

The consequence evaluation includes both direct effects and indirect effects of flywheel failure. Direct effects are those effects associated directly with the component being evaluated, such as loss of process fluid flow. Indirect effects are those effects on surrounding equipment that may be impacted by mechanisms such as jet impingement, pipe whip, missiles, and flooding.

The direct consequences are defined as failure of the RCP motor flywheel resulting in a failure of the RCP. With failure of the RCP, a reactor trip would be required.

The potential indirect or spatial effects associated with the postulated flywheel failure are associated with the potential missiles generated from the fragmented portions of the flywheel given a significant flywheel crack.

For this evaluation, the conditional core damage probability given the failure of the flywheel will be assumed to be 1.0 (no credit for safety system actuation to mitigate the consequences of the failure).

3.4.3 Risk Calculation

This methodology is described in detail in the Westinghouse Owners Group Risk-Informed Inservice Inspection Methodology for Piping, WCAP-14572, Revision 1-NP-A [13]. For failures that cause only an initiating event, the portion of the PRA model that is impacted is the initiating event and its frequency. The core damage frequency from the failure is calculated by:

$$CDF = IE * CCDP_{IE}$$

Where:

CDF = Core Damage Frequency from a failure (events per year)

$CCDP_{IE}$ = Conditional Core Damage Probability for the Initiator

IE = Initiating Event Frequency (in events per year)

The initiating event frequency (in events per year) is obtained differently given the different conditions. For the normal operating mode, the initiating event frequency is determined from the RCP motor flywheel failure probability model as described in Section 3.3. Because the model generates a probability, the probability must be transformed into a failure rate. The cumulative probability at a given time is divided by the number of years to end of license. In other words,

$$IE = FP/EOL$$

where:

FP = Failure probability from failure probability model (dimensionless)

EOL = Number of years used in failure probability model (80 years used to cover an extended plant life). Between 40 and 80 years, the failure probability is relatively constant.

For a RCP motor flywheel failure following a plant event, the core damage frequency of associated with that event (initiating event with flywheel failure) is defined as:

$$CDF = (IE * CFP) * CCDP$$

where:

CDF = Core Damage Frequency from a failure (events per year)

CCDP = Conditional Core Damage Probability for the initiator and flywheel failure

IE = Initiating Event frequency (in events per year)

CFP = Conditional Failure Probability of the flywheel by initiating event

The frequencies of the initiating events for the different conditions were identified as follows:

The initiating event frequency for a plant trip or non-LOCA transient is estimated as 1 event/year (plants on average experience 1 plant trip per year).

The probability of a loss of offsite power or loss of power to the RCP following a plant trip was conservatively established from NUREG/CR-6890 [19] as 0.01. This value was based on the observation that the conditional LOOP probability had increased from 0.003 in the 1986-1996 time frame to 0.0053 based on 1997 to 2004 data. Furthermore, the authors noted that the conditional probability in the summer months increase to 0.0091. The LOOP conditional on a LOCA event was estimated from Table 4.2 of NUREG/CR-6538 [17] as 1.4E-02 for PWR plants. As LOCAs < 3 ft² and other plant transient events were conservatively combined, the probability of a plant transient concurrent with a LOOP was set as 0.014.

The frequency of a large break LOCA events with break areas in excess of 3 ft² (~23 inches in diameter) was estimated from NUREG-1829 [16]. Mean failure rates of piping are presented in Table 7.19 of that reference. Using 25 and 40 year failure rates, failure rates provided in that table were linearly extrapolated to 60 years and 80 years and then interpolated to obtain a mean frequency of exceeding 3.0 ft². Using this process the LOCA exceedance frequency for break areas > 3 ft² was estimated to be about 3.8E-07 per year. For purposes of the analysis the LOCA IE was assigned a bounding value of 1E-06 per year.

Table 3-7, Table 3-8 and Table 3-9 show the calculations to estimate the frequency of the initiating event combined with the probability of the RCP motor flywheel failure. These calculations are also estimates of the core damage frequency given that the assumption of the CCDP is set to 1.0 (no credit taken for safety systems).

The resulting calculations show that the change in CDF for flywheel Evaluation Group 1 is 1.33E-08/year/RCP, the change in the CDF for flywheel Evaluation Group 2 is 6.00E-09/year/RCP and the change in the CDF for the Calvert Cliffs flywheel is 1.30E-10/year/RCP. The RG-1.174 criteria for an acceptable change in risk for CDF are

1E-06/year and for LERF is 1E-07/year. These calculations show the change in risk from extending the inspection interval for the RCP motor flywheel continues to remain below the acceptance criteria.

Table 3-7: Westinghouse RCP Motor Flywheel Evaluation Group 1

Condition	Initiating Event Frequency	Likelihood of RCP Motor Flywheel Failure (@80 years)		Event with RCP Motor Flywheel Failure (and Core Damage Frequency given CDP = 1.0) (per year)	
		With ISI after 10 Years	Without ISI after 10 Years	With ISI After 10 Years	Without ISI after 10 Years
1. Normal Operating Condition	N/A	2.39E-07	2.52E-07	2.98E-09	3.15E-09
2. Failure of the RCP motor flywheel given a plant with NO loss of electrical power to the RCP (1200 rpm peak speed)**	1	2.39E-07	2.52E-07	2.39E-07	2.52E-07
3. Failure of the RCP motor flywheel given a plant transient (including LOCA event (up to a 3 ft ² break in the RCS loop piping)) with loss of electrical power to the RCP (1200 rpm peak speed)** 1.0 x (1.4E-02)	1.40E-02	2.39E-07	2.52E-07	3.34E-09	3.52E-09
4. Failure of the RCP motor flywheel given large LOCA (from a greater than 3 ft' break up to a DEGB of the RCS loop piping) coincident with an instantaneous power loss (e.g., loss of offsite power (LOOP) or loss of electrical power to the RCP) and therefore no electrical braking effects (3321 rpm peak speed)	1.40E-08	9.87E-03	9.99E-03	1.38E-10	1.4E-10
Totals				2.45E-07	2.588E-07
Change in CDF for one Flywheel (per RCP risk)					1.33E-08
Change in CDF for 4 RCPs (4 Flywheels)					5.32E-08

Notes:

** The peak speed is 1200 rpm, however, 1500 rpm is used for the failure probability calculations

Table 3-8: RCP Motor Flywheel Evaluation Group 2

Condition	Initiating Event Frequency (per year)	Likelihood of RCP Motor Flywheel Failure (@80 years)		Event with RCP Motor Flywheel Failure (and Core Damage Frequency given CDP = 1.0) (per year)	
		With ISI after 10 Years	Without ISI after 10 Years	With ISI After 10 Years	Without ISI after 10 Years
1. Normal Operating Condition	N/A	1.29E-07	1.35E-07	1.61E-09	1.69E-09
2. Failure of the RCP motor flywheel given a plant with NO loss of electrical power to the RCP (1200 rpm peak speed)**	1	1.29E-07	1.35E-07	1.29E-07	1.35E-07
3. Failure of the RCP motor flywheel given a plant transient (including LOCA event (up to a 3 ft ² break in the RCS loop piping)) with loss of electrical power to the RCP (1200 rpm peak speed)** 1.0 x (1.4E-02)	1.40E-02	1.29E-07	1.35E-07	1.81E-09	1.89E-09
4. Failure of the RCP motor flywheel given large LOCA (from a greater than 3 ft' break up to a DEGB of the RCS loop piping) coincident with an instantaneous power loss (e.g., loss of offsite power (LOOP) or loss of electrical power to the RCP) and therefore no electrical braking effects (3321 rpm peak speed)	1.40E-08	9.09E-03	9.09E-03	1.27E-10	1.273E-10
Totals				1.33E-07	1.39E-07
Change in CDF for one Flywheel (per RCP risk)					6.00E-09
Change in CDF for 4 RCPs (4 Flywheels)					2.40E-08

Notes:

** The peak speed is 1200 rpm, however, 1500 rpm is used for the failure probability calculations

Table 3-9: Calvert Cliffs Units 1 and 2 RCP Motor Flywheel Evaluation

Condition	Initiating Event Frequency	Likelihood of RCP Motor Flywheel Failure (@80 years)		Event with RCP Motor Flywheel Failure (and Core Damage Frequency given CDP = 1.0) (per year)	
		With ISI after 10 Years	Without ISI after 10 Years	With ISI After 10 Years	Without ISI after 10 Years
1. Normal Operating Condition	N/A	1.50E-08	1.52E-08	1.88E-10	1.90E-10
2. Failure of the RCP motor flywheel given a plant with NO loss of electrical power to the RCP (900 rpm peak speed)**	1	1.50E-08	1.52E-08	1.50E-08	1.52E-08
3. Failure of the RCP motor flywheel given a plant transient (including LOCA event (up to a 3 ft ² break in the RCS loop piping)) with loss of electrical power to the RCP (900 rpm peak speed)** 1.0 x (1.4E-02)	1.40E-02	1.50E-08	1.52E-08	2.11E-10	2.12E-10
4. Failure of the RCP motor flywheel given large LOCA (from a greater than 3 ft' break up to a DEGB of the RCS loop piping) coincident with an instantaneous power loss (e.g., loss of offsite power (LOOP) or loss of electrical power to the RCP) and therefore no electrical braking effects (3321 rpm peak speed)	1.40E-08	5.54E-06	5.63E-06	7.76E-14	7.87E-14
Totals				1.54E-08	1.557E-08
Change in CDF for one Flywheel (per RCP risk)					1.30E-10
Change in CDF for 4 RCPs (4 Flywheels)					5.20E-10

Notes:

** The peak speed is 900 rpm, however, 1125 rpm is used for the failure probability calculations

3.5 CONSIDERATION OF UNCERTAINTY

This section provides a discussion of uncertainties associated with the core damage risk assessment. The discussion follows the general guidance of NUREG-1855 [20] in that the potential key model assumptions and uncertainties are identified and their impact is evaluated with respect to the current application.

The baseline risk assessment presented in Section 3.4 includes several significant conservatisms which are intended to bias the results of the analysis in a conservative direction. Specifically, these assumptions include:

1. All flywheel failure events result in both core damage and a large early release. This tacitly assumes that the missiles generated by the flywheel will result in both an unrecoverable LOCA and a loss in containment integrity sufficient to support a large release of radionuclides. This is a highly unlikely sequence as events resulting from reactor trip would have rods inserted prior to failure and the potential for flywheel fragments to render all safety injection paths unavailable is unlikely. Furthermore, there is virtually no likelihood that flywheel fragments could significantly impact the ability of the containment to perform its function or prevent containment isolation.
2. Flywheel failure probability is based on bounding selection of rotational flywheel speeds. This assumption is intended to simplify the event grouping while upwardly biasing flywheel failure probabilities. The flywheel failure probability model used to assess failure probability has been developed as a realistic model. Details of that model are provided in [3] and a sensitivity study to typical input assumptions is provided in Section 3.2.
3. Non-LOCA plant events that could result in a LOOP were assigned a LOOP probability of 0.014. This value is representative of the conditional LOCA/LOOP failure probability and as previously discussed overstates the LOOP potential for the more likely events.
4. Failure probabilities of flywheels are based on the cumulative failure probability over the lifetime of the flywheel. This provides some conservatism, however, failure rates are observed to stabilize during the later years of operation

While these assumptions are intended to provide a bounding estimate of risk, uncertainty associated with other parameters may be of interest in understanding the potential risks of the requested extension. As discussed in Section 3.4 the risk of the proposed change has three elements: the frequency of the initiating event, probability of flywheel failure given an event and the conditional probability of core damage given the failure. Sensitivity studies were performed to investigate the potential impact in changes to risk assessment modeling assumptions. Results of these studies are included in Table 3-10. The uncertainty associated with each of these factors is discussed below.

3.5.1 Initiating Event Frequency

As discussed in Table 3-7 through Table 3-9 the flywheel failure risks are assigned to four bins: normal operation, plant transient events without loss of off-site power, plant transient events (non-large LOCA) with loss of off-site power and large LOCA events with loss of offsite power. Nominal operational events are based on flywheel operating life and a bounding number of start-up and shutdown cycles. This is a low contributor to flywheel failure risks. Transient events are assumed to result in acceleration of the flywheel to design speeds. The risk assessment assumed that the plant will experience one transient event per year. A review of plant operation in the United States in the recent past suggests that overall plant operation has improved and more typical plant failure probabilities are less than 0.80 per year¹. The impact of the reduction in the plant trip frequency results in a 2.6E-09 per year per RCP reduction in CDF from the baseline value. The conditional LOOP probability contributes to the event frequencies for transient and LOCA events. Increasing the conditional LOOP probability from 0.014 to 0.05 only increases the incremental CDF by 5E-10 per year per RCP. Finally, the frequency of a large LOCA has a significant uncertainty attached to its mean value. In this study the large LOCA frequency (for breaks greater than 3 ft²) was increased an order of magnitude from 1E-06 per year to 1E-05 per year with no observable impact on plant risk.

3.5.2 Conditional Flywheel Failure Probability

To simplify analyses flywheel failure probabilities were based on 80 year end of life failure assumption and, with the exception of the large LOCA event, the assumption that the flywheel failure condition occurs at the plant design flywheel speed. For Westinghouse plants this was 1500 rpm. However, many plant transients are expected to result in events with lower flywheel speeds closer to that of nominal operation. Assuming flywheel failure probabilities associated with 1200 rpm operation, per RCP core damage frequency would reduce to 1E-11 per year.

3.5.3 Conditional Core Damage/Large Early Release Probability Given Flywheel Failure Event

The baseline analysis assumes a conditional core damage probability and a conditional large early release probability of 1.0. As discussed above this is a limiting assumption and expected values would be much lower, and in particular it is judged that conditional LERP probabilities would be negligible.

¹ IN/EXT-16-39534, Initiating Event Rates at U.S. Nuclear Power Plants: 1988-2015, INL, May 2016.

Table 3-10: CDF Sensitivity to Variations in PRA evaluation assumptions for RCP Flywheel Failure Risk Assessment for Extending 10 year inspection intervals to 20 years for Flywheel operation to 80 years –(Flywheel Group 1)

	Incremental Change in CDF (per Year)	
	Risk Impact of Single Flywheel Failure	Risk impact of Flywheel Failure (4 RCP Plant)
Baseline Change in CDF	1.33E-08	5.32E-08
PWR general and other transient reduction to 0.8 per year	1.07E-08	4.28E-08
Increase Conditional LOOP probability to 0.05	1.38E-08	5.51E-08
Increase LOCA frequency for breaks >3 ft ² to 1 E-05/year	1.33E-08	5.33E-08
Flywheel Failure probability reduced for normal operation and non-large LOCA transient based on 1200 rpm	1.00E-11	4.01E-11

3.5.4 Conclusion Regarding Treatment of Uncertainty

The above sensitivity studies confirm that even for a relatively large increase in modeling parameters, the incremental CDF would continue to remain below the 1.0E-06 per year core damage and 1.0E-07 per year LERF criteria in [9] supporting a conclusion of a very small risk increase. The present treatment assumes the incremental LERF and incremental CDF are equal. This is an extremely conservative assumption.

3.6 RISK RESULTS AND CONCLUSIONS

Given the extremely low failure probabilities for the RCP motor flywheel during normal/accident conditions and the extremely low probability of LOCA/LOOP, and even assuming a CDDP of 1.0 (complete failure of safety systems), the CDF and change in risk would still not exceed the NRC's acceptable guidelines in [9] ($\Delta\text{CDF} < 1.0\text{E-}6$ per year and $\Delta\text{LERF} < 1.0\text{E-}07$ per year).

Even considering the uncertainties involved in this evaluation, the risk associated with the postulated failure of an RCP motor flywheel is significantly low. Even when all four RCP motor flywheels are considered in the bounding plant configuration case, the risk is still acceptably low.

Because of the evaluation results for core damage frequency and the conservative assumption that failure of the RCP motor flywheel results in core damage and large early release, the calculations were not performed for the LERF. If detailed LERF analyses were performed, it is expected that the relative LERF contribution arising from these events would be significantly less than 20%. Regardless, this assessment assumes the calculated CDF is equal to LERF and that results are below the NRC's LERF acceptance guidelines (taken as 1E-07/reactor year).

As part of this evaluation, the key principles identified in RG-1.174 are reviewed and the responses based on the evaluation are provided in Table 3-11.

This evaluation, in conjunction with the previous deterministic calculations described throughout the report, concludes that extension of the RCP motor flywheel examination from 10 to 20 years, for flywheels in service up to 80 years would not be expected to result in a significant increase in risk and therefore the proposed change is acceptable.

Table 3-11: Evaluation with Respect to Regulatory Guide 1.174 (Key Principles)

Key Principles	Evaluation Response
Change meets current regulations unless it is explicitly related to a requested exemption or rule change	Change to current Regulatory Guide 1.14 Requirements [4]. No exemption or rule change is requested.
Change is consistent with defense-in-depth philosophy	Potential for failure of the RCP motor flywheel is negligible during normal accident conditions, and does not threaten plant barriers
Maintain sufficient safety margins	No safety analysis margins are changed
Proposed increases in CDF or risk are small and are consistent with the Commission's Safety Goal Policy Statement	Proposed increase in risk is estimated to be negligible. Leakage expected before a piping LOCA occurs (no core damage consequences associated with leakage), No credit taken for leak detection
Use performance-measurement to monitor the change	NDE examinations still conducted, but on a less frequent basis not to exceed 20 years for equipment having in-service durations exceeding 60 years up to 80 years. Other indications of potential degradation of RCP motor flywheel available (e.g., pump vibration monitoring, pump maintenance)

4 CONCLUSIONS

Results from the previous WOG program MUHP-5042, as summarized in WCAP-14535A [2], remain valid and are reiterated below:

1. Flywheels are carefully designed and manufactured from excellent quality steel, which has high fracture toughness.
2. Flywheel overspeed is the critical loading, but LBB has limited the maximum speed to 1500 rpm. *(Note however that the LBB exclusion for LBLOCA does not pertain to the risk assessment contained in the WCAP-15666-A [3] report, which does consider the overspeed due to LBLOCA.)*
3. Flywheel inspections have been performed for over 20 years, with no service-induced flaws.
4. Flywheel integrity evaluations show a very high flaw tolerance for the flywheels.
5. Crack extension during service is negligible.
6. Structural reliability studies show that eliminating inspections will not change the probability of failure.
7. Inspections result in man-rem exposure and the potential for flywheel damage during assembly and reassembly.

The deterministic results from the previous WOG program MUHP-5043, as summarized in WCAP-15666-A [3] remain applicable for 80 years of operation. The risk assessments are updated and presented in Section 3 of in this report.

1. The failure probabilities for the RCP motor flywheels are small.
2. The change in risk is below the Regulatory Guide 1.174 CDF and LERF acceptable guidelines.
3. The 20-year ISI frequency for the RCP motor flywheel, granted by NRC in [3] remains applicable for the 80-year SLR application.

5 REFERENCES

1. PWROG Project Authorization, PA-MS-1500, Rev. 0, "Update for Subsequent License Renewal: WCAP-14535A, "Topical Report on Reactor Coolant Pump Flywheel Inspection Elimination" and WCAP-15666-A, "Extension of Reactor Coolant Pump Motor Flywheel Examination", December 2016.
2. Westinghouse Report, WCAP-14535A, Rev. 0, "Topical Report on Reactor Coolant Pump Flywheel Inspection Elimination," November 1996.
3. Westinghouse Report, WCAP-15666-A, Rev. 1, "Extension of Reactor Coolant Pump Motor Flywheel Examination," October 2003.
4. United States Nuclear Regulatory Commission, Office of Standards Development, Regulatory Guide 1.14, "Reactor Coolant Pump Flywheel Integrity," Revision 1, August 1975.
5. Westinghouse Report, WCAP-8163, Rev. 0, "Reactor Coolant Pump Integrity in LOCA," September 1973.
6. ASME Boiler and Pressure Vessel Code, Section XI, 2007 Edition with 2008 Addenda.
7. Westinghouse Letter, SRPLO 95-031, "Program RPFWPROF for Reactor Pump Flywheel Probability of Failure," December 29, 1995.
8. AREVA Engineering Information Record, 51-9271850-000, "Pressurized Water Reactor Owners Group Westinghouse Flywheel ISI Study," May 17, 2017.
9. United States Nuclear Regulatory Commission, Regulatory Guide 1.174, Revision 2, "An Approach for Using Probabilistic Risk Assessment in Risk-Informed Decisions on Plant-Specific Changes to the Licensing Basis," May 2011.
10. Standard Review Plan 19.0, "Use of Probabilistic Risk Assessment in Plant Specific Risk- Informed Decision Making: General Guidance," NUREG-800.
11. "Development and Applications of Probabilistic Fracture Mechanics for Critical Nuclear Reactor Components," pages 55-70, Advances in Probabilistic Fracture Mechanics, ASME PVP-Vol. 92, F. J. Witt, 1984.
12. @RISK, Risk Analysis and Simulation add-In for Lotus 1-2-3, Version 2.01 Users Guide, Palisade Corporation, Newfield, NY, February 6, 1992.
13. Westinghouse report WCAP-14572, Supplement 1, "Westinghouse Structural Reliability and Risk Assessment (SRRA) Model for Piping Risk-Informed Inservice Inspection," Revision 1-NP-A, February 1999.
14. NUREG/CR-5864, Theoretical and User's Manual for pc-PRAISE, A Probabilistic Fracture Mechanics Computer Code for Piping Reliability Analysis, Harris and Dedhia, July 1992.
15. EPRI TR-105001, Documentation of Probabilistic Fracture Mechanics Codes Used for Reactor Pressure Vessels Subjected to Pressurized Thermal Shock Loading, K. R. Balkey and F. J. Witt (Part 1) and B. A. Bishop (Part 2), June 1995.

16. NUREG-1829, "Estimating Loss-of-Coolant Accident (LOCA) Frequencies through the Elicitation Process," April 2008.
17. "Evaluation of LOCA With Delayed Loop and Loop With Delayed LOCA Accident Scenarios," NUREG/CR-6538, July 1997.
18. Westinghouse Shop Order 79P528, "Byron Jackson, induction motor, Stock Order No. 79P528, test reports and drawing lists for Baltimore #2," 1/20/72.
19. NUREG/CR-6890, "Reevaluation of Station Blackout Risk at Nuclear Power Plants: Analysis of Loss of Offsite Power Events," 1986-2004," S.A. Eide, et. al., Idaho National Laboratory, USNRC, December 2005.
20. NUREG-1855, Revision 1, "Guidance on the Treatment of Uncertainties Associated with PRAs in Risk-Informed Decisionmaking: Final report", USNRC, July, 2016.

APPENDIX A: CALVERT CLIFFS UNIT 1 & 2 RCP MOTOR FLYWHEEL EVALUATIONS FOR EXTENSION OF ISI INTERVAL

Background and Purpose

WCAP-15666-A [3] extended the ISI intervals for Westinghouse RCP motors from 10 to 20 years. Although Calvert Cliffs plants are Combustion Engineering design, they have Westinghouse RCP Motors and flywheels, the motor operating speeds are different than those evaluated in WCAP-15666-A [3]. A Calvert Cliffs plant specific deterministic calculation and a probabilistic evaluation were performed using the methodology [3] to justify 20-year ISI interval for 60 years of plant operation.

The probabilistic evaluations for Calvert Cliffs were updated in Section 3 of this report for 80-year plant operation. The purpose of this Appendix is to evaluate and extend the applicability of [3] to 80-year plant operation for Calvert Cliffs Units 1 and 2.

Ductile Failure Analysis

As discussed in Section 2.3.2 of this report, the flywheel stresses are dependent on dimensions and rotation speed. Extending the operating period to 80 years does not affect the stress calculation. Therefore, the current ductile failure analysis for 60 years remains valid for 80 years of operation.

Ductile failure limiting speed was determined for the flywheel for two cases. Case 1 considered that no cracks were present but accounted for the reduced cross sectional area resulting from the keyway. Case 2 considered that a 10-inch radial crack existed emanating from the center of the keyway through the full thickness of the flywheel.

The calculated limiting speeds are:

Case 1: 3219 rpm (considering keyway only, no crack)

Case 2: 2856 rpm (considering keyway and 10" crack)

Given the nominal operating speed of 900 rpm for Calvert Cliffs plants, criterion item f [4] is satisfied since this is lower than one half of the lowest calculated critical speed of $2856/2 = 1428$ rpm, considering both no cracks present and a large crack present.

Given the LOCA over speed of 1368 rpm for Calvert Cliffs plants, criterion item f [4] is satisfied since this is lower than any calculated critical speeds considering both no cracks present and a large crack present.

Nonductile Failure Analysis

As discussed in Section 2.3.3 of this report, extending the operating period to 80 years does not affect the K_I calculations, and the flywheel fracture toughness, K_{Ic} would not change due to the 80 year extension. Therefore, the current nonductile failure analysis for 60 years remains valid for 80 years of operation. As in discussed in Section 2.3.3, Table 2-9, RT_{NDT} values of 0°F, 30°F and 60°F were used to calculate critical flaw sizes shown in Table A-1.

Table A-1: Critical Crack Length in Inches and % Through Flywheel

RT_{NDT}	0°F	30°F	60°F
Critical Crack Length	18.5"	8.8"	3.7"
% Through Flywheel	52%	25%	10%

Note: % through flywheel is calculated as CCL in the table divided by the radial length from the maximum radial keyway location to the flywheel outer radius $[CCL / (41.0" - 4.7188" - 0.937")]$.

Fatigue Crack Growth

As discussed in Section 2.3.4 of this report, extending the operating period to 80 years does not affect the K_I and ΔK_I calculations. As confirmed by a number of participating plants, the 6000 design cycles of start and stop remain applicable for 80 years of operation. Actual start and stop cycles are likely to be much lower than 6000. Therefore, the current FCG evaluation and results for 60 years remain applicable for 80-year plant operation. The FCG of 0.025 inch after 80 years or 6000 cycles is negligible even when assuming a large initial crack length of 3.7 inches.

Excessive Deformation Analysis

As discussed in Section 2.3.5 of this report, the 80-year extension has no impact on the excessive deformation analysis of the flywheel. The current deformation results for 60 years remain applicable to 80 years of operation.

The change in flywheel bore radius and outer diameter at overspeed condition of 1368 rpm are:

$$\Delta a = \text{the change in the flywheel bore radius at overspeed} = 0.003 \text{ inch}$$

$$\Delta b = \text{the change in the flywheel outside radius at overspeed} = 0.006 \text{ inch}$$

Since Δ is proportional to ω^2 , this represents a 231% increase $[(\omega_{os}/\omega_n)^2 = (1368 / 900)^2 = 2.31 = 231\%]$ over the deformation at normal operating speed.

This increase would not result in any adverse conditions, such as excessive flywheel vibrational stresses leading to crack propagation since the flywheel assemblies are interference fit to the flywheel shaft and the calculated deformations are small and considered insignificant. It is noted that the deformation for Calvert Cliffs flywheels is less than the that of Westinghouse flywheels reported in Section 2.3.5 of this report.

Conclusion

The current Calvert Cliffs evaluation and results for 60 years are applicable for the 80-year plant operation. The Calvert Cliffs flywheels exhibit stresses and operational limits consistent with the flywheels evaluated in [3]. The probabilistic risk evaluation, in conjunction with the deterministic calculations described above, concludes that extension of the RCP motor flywheel ISI from 10 to 20 years, for flywheels in service up to 80 years is acceptable.

Enclosure 4
Non-proprietary Reference Documents
and
Redacted Versions of Proprietary
Reference Documents
(Public Version)
Attachment 11

WCAP-15354-NP, Revision 1

**Technical Justification for Eliminating Primary Loop Pipe
Rupture as a Structural Design Basis for Turkey Point
Units 3 and 4 Nuclear Power Plants for the Subsequent
License Renewal Time-Limited Aging Analysis Program
(80 Years) Leak-Before-Break Evaluation, August 2017**

(59 Total Pages, including cover sheets)

Technical Justification for Eliminating Large Primary Loop Pipe Rupture as the Structural Design Basis for Turkey Point Units 3 and 4 Nuclear Power Plants for the Subsequent License Renewal Time-Limited Aging Analysis Program (80 Years) Leak-Before-Break Evaluation

WCAP-15354-NP
Revision 1

**Technical Justification for Eliminating Large Primary
Loop Pipe Rupture as the Structural Design Basis for
Turkey Point Units 3 and 4 Nuclear Power Plants for
the Subsequent License Renewal Time-Limited Aging
Analysis Program (80 Years) Leak-Before-Break
Evaluation**

August 2017

Author: Momo Wiratmo*
Piping Analysis and Fracture Mechanics

Reviewer: Eric D. Johnson*
Piping Analysis and Fracture Mechanics

Anees Udyawar*
Piping Analysis and Fracture Mechanics

Approved: Ben A. Leber*, Manager
Piping Analysis and Fracture Mechanics

*Electronically approved records are authenticated in the electronic document management system.

Westinghouse Electric Company LLC
1000 Westinghouse Drive
Cranberry Township, PA 16066, USA

© 2017 Westinghouse Electric Company LLC
All Rights Reserved

Record of Revisions

Rev	Date	Revision Description
0	January 2000	Original Issue. Primary Object Name: WCAP-15354, Rev. 0 A Westinghouse Proprietary Class 2 Report
1	August 2017	<p>This WCAP report is revised to include Leak-Before-Break (LBB) evaluations for the Subsequent License Renewal Time-Limited Aging Analyses (SLR TLAA) Program, i.e., plant operation extension to 80 years of service, for Turkey Point Units 3 and 4.</p> <p>The WCAP report also incorporates the LBB results of the Extended Power Uprate (EPU) evaluation performed in 2009.</p>

FOREWORD

This document contains Westinghouse Electric Company LLC proprietary information and data which has been identified by brackets. Coding^(a,c,e) associated with the brackets sets forth the basis on which the information is considered proprietary. These code letters are listed with their meanings in BMS-LGL-84 (April 2017), "Protection of Proprietary Information Regarding Submittals to the USNRC including Safety Analysis Reports for Commercial Nuclear Power Plants." The code letters are defined as follows:

- a. The information reveals the distinguishing aspects of a process (or component, structure, tool, method, etc.), where the prevention of its use by any of Westinghouse's competitors without license from Westinghouse constitutes a competitive economic advantage over other companies.
- c. The information, if used by a competitor, would reduce the competitor's expenditure of resources or improve the competitor's advantage in the design, manufacture, shipment, installation, assurance of quality, or licensing of a similar product.
- e. The information reveals aspects of past, present, or future Westinghouse or customer funded development plans and programs of potential commercial value to Westinghouse.

The proprietary information and data contained within the brackets in this report were obtained at considerable Westinghouse expense and its release could seriously affect our competitive position. This information is to be withheld from public disclosure in accordance with the Rules of Practice 10CFR2.790 and the information presented herein be safeguarded in accordance with 10CFR2.903. Withholding of this information does not adversely affect the public interest.

This information has been provided for your internal use only and should not be released to persons or organizations outside the Directorate of Regulation and the ACRS without the express written approval of Westinghouse Electric Company LLC. Should it become necessary to release this information to such persons as part of the review procedure, please contact Westinghouse Electric Company LLC, which will make the necessary arrangements required to protect the Company's proprietary interests.

TABLE OF CONTENTS

1.0	Introduction	1-1
1.1	Purpose	1-1
1.2	Background Information	1-1
1.3	Scope and Objectives	1-2
1.4	References	1-3
2.0	Operation and Stability of the Reactor Coolant System	2-1
2.1	Stress Corrosion Cracking	2-1
2.2	Water Hammer	2-2
2.3	Low Cycle and High Cycle Fatigue	2-3
2.4	Wall Thinning, Creep, and Cleavage	2-3
2.5	References	2-3
3.0	Pipe Geometry and Loading	3-1
3.1	Introduction to Methodology	3-1
3.2	Calculation of Loads and Stresses	3-1
3.3	Loads for Leak Rate Evaluation	3-2
3.4	Load Combination for Crack Stability Analyses	3-3
3.5	References	3-3
4.0	Material Characterization	4-1
4.1	Primary Loop Pipe and Fittings Materials	4-1
4.2	Tensile Properties	4-1
4.3	Fracture Toughness Properties	4-1
4.4	References	4-4
5.0	Critical Location and Evaluation Criteria	5-1
5.1	Critical Locations	5-1
5.2	Fracture Criteria	5-1
6.0	Leak Rate Predictions	6-1
6.1	Introduction	6-1
6.2	General Considerations	6-1
6.3	Calculation Method	6-1
6.4	Leak Rate Calculations	6-2
6.5	References	6-2
7.0	Fracture Mechanics Evaluation	7-1
7.1	Local Failure Mechanism	7-1
7.2	Global Failure Mechanism	7-2
7.3	Crack Stability Evaluations	7-3
7.4	References	7-3
8.0	Fatigue Crack Growth Analysis	8-1
8.1	References	8-2
9.0	Assessment of Margins	9-1
10.0	Conclusions	10-1
	Appendix A: Limit Moment	A-1

LIST OF TABLES

Table 3-1	Dimensions, Normal Loads and Stresses for Turkey Point Units 3 and 4	3-4
Table 3-2	Faulted Loads and Stresses for Turkey Point Units 3 and 4	3-5
Table 4-1	Measured Tensile Properties for Turkey Point Units 3 and 4 Primary Loop Piping	4-5
Table 4-2	Measured Room Temperature Tensile Properties for Turkey Point Units 3 and 4 Primary Loop Elbow Fittings.....	4-8
Table 4-3	Mechanical Properties for Turkey Point Units 3 and 4 Materials at Operating Temperatures.....	4-10
Table 4-4	Chemistry and Fracture Toughness Properties of the Material Heats of Turkey Point Units 3 and 4	4-11
Table 4-5	Fracture Toughness Properties for Turkey Point Units 3 and 4 Primary Loops for Leak-Before-Break Evaluation at Critical Locations.....	4-13
Table 6-1	Flaw Sizes Yielding a Leak Rate of 10 gpm at the Governing Locations.....	6-3
Table 7-1	Stability Results for Turkey Point Units 3 and 4 Based on Elastic-Plastic J-Integral Evaluations	7-4
Table 7-2	Stability Results for Turkey Point Units 3 and 4 Based on Limit Load.....	7-4
Table 8-1	Summary of Reactor Vessel Transients for Turkey Point Units 3 and 4.....	8-3
Table 8-2	Typical Fatigue Crack Growth at [.....] ^{a,c,e}	8-4
Table 9-1	Leakage Flaw Sizes, Critical Flaw Sizes and Margins for Turkey Point Units 3 and 4	9-2

LIST OF FIGURES

Figure 3-1	Hot Leg Coolant Pipe.....	3-6
Figure 3-2	Schematic Diagram of Turkey Point Units 3 and 4 Primary Loop Showing Weld Locations.....	3-7
Figure 4-1	Pre-Service J vs. Δa for SA351 CF8M Cast Stainless Steel at 600°F	4-14
Figure 6-1	Analytical Predictions of Critical Flow Rates of Steam-Water Mixtures.....	6-4
Figure 6-2	[] ^{a,c,e} Pressure Ratio as a Function of L/D	6-5
Figure 6-3	Idealized Pressure Drop Profile Through a Postulated Crack.....	6-6
Figure 7-1	[] ^{a,c,e} Stress Distribution	7-5
Figure 8-1	Typical Cross-Section of [] ^{a,c,e}	8-5
Figure 8-2	Reference Fatigue Crack Growth Curves for [] ^{a,c,e}	8-6
Figure A-1	Pipe with a Through-Wall Crack in Bending	A-2

EXECUTIVE SUMMARY

Westinghouse had originally performed a plant specific primary loop piping leak-before-break (LBB) analysis for the Turkey Point Units 3 and 4 in 1994. The results of the analysis were documented in WCAP-14237 (Reference 1-2). The NRC reviewed WCAP-14237 and approved it for Turkey Point Units 3 and 4 in a letter dated June 23, 1995 (Reference 1-3). Subsequently, in 2000 the LBB analysis was updated for Turkey Point Units 3 and 4 nuclear power plants for the 60 year plant service (license renewal program) and documented in WCAP-15354 (Reference 1-1). In the current report herein, WCAP-15354 is revised to include LBB evaluations performed for the Subsequent License Renewal Time-Limited Aging Analysis (SLR TLAA) for 80 years of operation for Turkey Point Units 3 and 4. This report also includes the LBB results of the EPU (Extended Power Uprate) Program evaluation that was performed in 2009.

Specifically, this report demonstrates compliance with LBB technology for the Turkey Point reactor coolant system piping for the 80 year plant service. The report documents the plant specific geometry, loading, and material properties used in the fracture mechanics evaluation. The report also examines potential material degradation due to thermal aging. While the Turkey Point Units 3 and 4 primary loop forged stainless steel piping (A376-TP316) does not degrade due to thermal aging, the primary loop cast austenitic stainless steel elbow fittings (A351-CF8M) are susceptible to thermal aging at the reactor operating temperature, that is, about 290°C (550°F). Thermal aging of cast austenitic stainless steel elbow fittings results in embrittlement, that is, a decrease in the ductility, impact strength, and fracture toughness of the material.

The report documents the fully aged fracture toughness properties for 80 years of plant service using revised correlations per NUREG/CR-4513 Revision 2 (Reference 1-12) in predicting the fracture toughness properties for the primary loop elbow fittings based on primary coolant loop operating temperatures applicable for the SLR TLAA Program. The fully aged condition is applicable for plants operating at beyond 15 EFPY (Effective Full Power Years) for the CF8M materials (elbows for Turkey Point Units 3 and 4). As of June 1, 2017, Turkey Point Units 3 and 4 are operating at 33.16 and 33.23 EFPY, respectively. Therefore, the use of the fracture toughness correlations described herein are applicable for the fully aged or saturated condition of the Turkey Point Units 3 and 4 elbow materials made of CF8M to demonstrate stability of the reactor coolant system due to any postulated cracks for 80 years of plant service.

Specific factors that may potentially generate stress corrosion cracking have been verified including the existence of Alloy 82/182. Since there is no Alloy 82/182 in the Turkey Point Units 3 and 4 primary loop piping, potential of primary water stress corrosion cracking can be precluded in Turkey Point Units 3 and 4 for 80 years of plant service.

In conclusion, the current report had demonstrated compliance with LBB technology for the Turkey Point reactor coolant system piping for the 80 year plant service based on a plant specific analysis. The LBB evaluation had also demonstrated that dynamic effects of reactor coolant system primary loop pipe breaks need not be considered in the structural design basis of the Turkey Point Units 3 and 4 Nuclear Power Plants for the 80 year plant service.

1.0 INTRODUCTION

1.1 PURPOSE

This report applies to the Turkey Point Units 3 and 4 Reactor Coolant System (RCS) primary loop piping. It is intended to demonstrate that for the specific parameters of the Turkey Point Units 3 and 4 Nuclear Power Plants, RCS primary loop pipe breaks need not be considered in the structural design basis for 80 years of service life (Subsequent License Renewal Time-Limited Aging Analyses or SLR TLAA Program). The approach taken has been accepted by the Nuclear Regulatory Commission (NRC) per USNRC Generic Letter 84-04 (Reference 1-4).

1.2 BACKGROUND INFORMATION

Westinghouse has performed considerable testing and analysis to demonstrate that RCS primary loop pipe breaks can be eliminated from the structural design basis of all Westinghouse plants. The concept of eliminating pipe breaks in the RCS primary loop was first presented to the NRC in 1978 in WCAP-9283 (Reference 1-5). That topical report employed a deterministic fracture mechanics evaluation and a probabilistic analysis to support the elimination of RCS primary loop pipe breaks. That approach was then used as a means of addressing Generic Issue A-2 and Asymmetric LOCA Loads.

Westinghouse performed additional testing and analysis to justify the elimination of RCS primary loop pipe breaks. This material was provided to the NRC along with Letter Report NS-EPR-2519 (Reference 1-6).

The NRC funded research through Lawrence Livermore National Laboratory (LLNL) to address this same issue using a probabilistic approach. As part of the LLNL research effort, Westinghouse performed extensive evaluations of specific plant loads, material properties, transients, and system geometries to demonstrate that the analysis and testing previously performed by Westinghouse and the research performed by LLNL applied to all Westinghouse plants (References 1-7 and 1-8). The results from the LLNL study were released at a March 28, 1983, ACRS Subcommittee meeting. These studies, which are applicable to all Westinghouse plants east of the Rocky Mountains, determined the mean probability of a direct LOCA (RCS primary loop pipe break) to be 4.4×10^{-12} per reactor year and the mean probability of an indirect LOCA to be 10^{-7} per reactor year. Thus, the results previously obtained by Westinghouse (Reference 1-5) were confirmed by an independent NRC research study.

Based on the studies by Westinghouse, LLNL, the ACRS, and the AIF, the NRC completed a safety review of the Westinghouse reports submitted to address asymmetric blowdown loads that result from a number of discrete break locations on the PWR primary systems. The NRC Staff evaluation (Reference 1-4) concludes that an acceptable technical basis has been provided so that asymmetric blowdown loads need not be considered for those plants that can demonstrate the applicability of the modeling and conclusions contained in the Westinghouse response or can provide an equivalent fracture mechanics demonstration of the primary coolant loop integrity. In a more formal recognition of leak-before-break (LBB) methodology applicability for PWRs, the NRC appropriately modified 10 CFR 50, General Design Criterion 4,

"Requirements for Protection Against Dynamic Effects of Postulated Pipe Ruptures" (Reference 1-9).

1.3 SCOPE AND OBJECTIVES

The general purpose of this investigation is to demonstrate leak-before-break for the primary loops in Turkey Point Units 3 and 4 on a plant specific basis for 80 years of plant service. The recommendations and criteria proposed in References 1-10 and 1-11 are used in this evaluation. These criteria and resulting steps of the evaluation procedure can be briefly summarized as follows:

1. Calculate the applied loads. Identify the locations at which the highest stress occurs.
2. Identify the materials and the associated material properties.
3. Postulate a surface flaw at the governing locations. Determine fatigue crack growth. Show that a through-wall crack will not result.
4. Postulate a through-wall flaw at the governing locations. The size of the flaw should be large enough so that the leakage is assured of detection with margin using the installed leak detection equipment when the pipe is subjected to normal operating loads. A margin of 10 is demonstrated between the calculated leak rate and the leak detection capability.
5. Using faulted loads, demonstrate that there is a margin of 2 between the leakage flow size and the critical flaw size.
6. Review the operating history to ascertain that operating experience has indicated no particular susceptibility to failure from the effects of corrosion, water hammer or low and high cycle fatigue.
7. For the materials actually used in the plant, provide the properties including toughness and tensile test data. Evaluate long term effects such as thermal aging.
8. Demonstrate margin on applied load.

This report provides a fracture mechanics demonstration of primary loop integrity for the Turkey Point Units 3 and 4 plants consistent with the NRC position for exemption from consideration of dynamic effects, and reflects the LBB evaluation results based on the Extended Power Uprate (EPU) program and for the SLR TLAA Program.

It should be noted that the terms "flaw" and "crack" have the same meaning and are used interchangeably. "Governing location" and "critical location" are also used interchangeably throughout the report.

The computer codes used in this evaluation for leak rate and fracture mechanics calculations have been validated and used for all the LBB applications by Westinghouse.

1.4 REFERENCES

- 1-1 WCAP-15354, "Technical Justification for Eliminating Large Primary Loop Pipe Rupture as the Structural Design Basis for the Turkey Point Units 3 and 4 Nuclear Power Plant For the 60 Year Plant Life (License Renewal Program)," January 2000.
- 1-2 WCAP-14237, "Technical Justification for Eliminating Large Primary Loop Pipe Rupture as the Structural Design Basis for the Turkey Point Units 3 and 4 Nuclear Power Plant," December 1994.
- 1-3 Nuclear Regulatory Commission Docket #'s 50-250 and 50-251 Letter from Richard P. Croteau, Project Manager, Project Directorate II-I, Division of Reactor Projects- I/II, NRC, to Mr. J. H. Goldberg, President, Florida Power and Light Company, Subject: "Turkey Point Units 3 and 4, Approval to Utilize Leak-Before-Break Methodology for Reactor Coolant System Piping (TAC Nos. M91494 and M91495)," dated 6/23/95.
- 1-4 USNRC Generic Letter 84-04, Subject: "Safety Evaluation of Westinghouse Topical Reports Dealing with Elimination of Postulated Pipe Breaks in PWR Primary Main Loops," February 1, 1984.
- 1-5 WCAP-9283, "The Integrity of Primary Piping Systems of Westinghouse Nuclear Power Plants During Postulated Seismic Events," March, 1978.
- 1-6 Letter Report NS-EPR-2519, Westinghouse (E. P. Rahe) to NRC (D. G. Eisenhut), Westinghouse Proprietary Class 2, November 10, 1981.
- 1-7 Letter from Westinghouse (E. P. Rahe) to NRC (W. V. Johnston) dated April 25, 1983.
- 1-8 Letter from Westinghouse (E. P. Rahe) to NRC (W. V. Johnston) dated July 25, 1983.
- 1-9 Nuclear Regulatory Commission, 10 CFR 50, Modification of General Design Criteria 4 Requirements for Protection Against Dynamic Effects of Postulated Pipe Ruptures, Final Rule, Federal Register/Vol. 52, No. 207/Tuesday, October 27, 1987/Rules and Regulations, pp. 41288-41295.
- 1-10 Standard Review Plan: Public Comments Solicited; 3.6.3 Leak-Before-Break Evaluation Procedures; Federal Register/Vol. 52, No. 167/Friday August 28, 1987/Notices, pp. 32626-32633.
- 1-11 NUREG-0800 Revision 1, March 2007, Standard Review Plan: 3.6.3 Leak-Before-Break Evaluation Procedures.
- 1-12 O. K. Chopra, "Estimation of Fracture Toughness of Cast Stainless Steels During Thermal Aging in LWR Systems," NUREG/CR-4513, Revision 2, U.S. Nuclear Regulatory Commission, Washington, DC, May 2016.

2.0 OPERATION AND STABILITY OF THE REACTOR COOLANT SYSTEM

2.1 STRESS CORROSION CRACKING

The Westinghouse reactor coolant system primary loops have an operating history that demonstrates the inherent operating stability characteristics of the design. This includes a low susceptibility to cracking failure from the effects of corrosion (e.g., intergranular stress corrosion cracking (IGSCC)). This operating history totals over 1400 reactor-years, including 16 plants each having over 30 years of operation, 10 other plants each with over 25 years of operation, 11 plants each with over 20 years of operation, and 12 plants each with over 15 years of operation.

In 1978, the United States Nuclear Regulatory Commission (USNRC) formed the second Pipe Crack Study Group. (The first Pipe Crack Study Group (PCSG) established in 1975, addressed cracking in boiling water reactors only). One of the objectives of the second PCSG was to include a review of the potential for stress corrosion cracking in Pressurized Water Reactors (PWR's). The results of the study performed by the PCSG were presented in NUREG-0531 (Reference 2-1) entitled "Investigation and Evaluation of Stress Corrosion Cracking in Piping of Light Water Reactor Plants." In that report the PCSG stated:

"The PCSG has determined that the potential for stress corrosion cracking in PWR primary system piping is extremely low because the ingredients that produce IGSCC are not all present. The use of hydrazine additives and a hydrogen overpressure limit the oxygen in the coolant to very low levels. Other impurities that might cause stress corrosion cracking, such as halides or caustic, are also rigidly controlled. Only for brief periods during reactor shutdown when the coolant is exposed to the air and during the subsequent startup are conditions even marginally capable of producing stress corrosion cracking in the primary systems of PWRs. Operating experience in PWRs supports this determination. To date, no stress corrosion cracking has been reported in the primary piping or safe ends of any PWR."

During 1979, several instances of cracking in PWR feedwater piping led to the establishment of the third PCSG. The investigations of the PCSG reported in NUREG-0691 (Reference 2-2) further confirmed that no occurrences of IGSCC have been reported for PWR primary coolant systems.

As stated above, for the Westinghouse plants there is no history of cracking failure in the reactor coolant system loop. The discussion below further qualifies the PCSG's findings.

For stress corrosion cracking (SCC) to occur in piping, the following three conditions must exist simultaneously: high tensile stresses, susceptible material, and a corrosive environment. Since some residual stresses and some degree of material susceptibility exist in any stainless steel piping, the potential for stress corrosion is minimized by properly selecting a material immune to SCC as well as preventing the occurrence of a

corrosive environment. The material specifications consider compatibility with the system's operating environment (both internal and external) as well as other material in the system, applicable ASME Code rules, fracture toughness, welding, fabrication, and processing.

The elements of a water environment known to increase the susceptibility of austenitic stainless steel to stress corrosion are: oxygen, fluorides, chlorides, hydroxides, hydrogen peroxide, and reduced forms of sulfur (e.g., sulfides, sulfites, and thionates). Strict pipe cleaning standards prior to operation and careful control of water chemistry during plant operation are used to prevent the occurrence of a corrosive environment. Prior to being put into service, the piping is cleaned internally and externally. During flushes and preoperational testing, water chemistry is controlled in accordance with written specifications. Requirements on chlorides, fluorides, conductivity, and pH are included in the acceptance criteria for the piping.

During plant operation, the reactor coolant water chemistry is monitored and maintained within very specific limits. Contaminant concentrations are kept below the thresholds known to be conducive to stress corrosion cracking with the major water chemistry control standards being included in the plant operating procedures as a condition for plant operation. For example, during normal power operation, oxygen concentration in the RCS is expected to be in the ppb range by controlling charging flow chemistry and maintaining hydrogen in the reactor coolant at specified concentrations. Halogen concentrations are also stringently controlled by maintaining concentrations of chlorides and fluorides within the specified limits. Thus during plant operation, the likelihood of stress corrosion cracking is minimized.

It should be noted that there are no primary water stress corrosion cracking material such as Alloy 82/182 in the dissimilar metal welds in the Turkey Point Units 3 and 4 Reactor Coolant System (RCS) primary loop piping.

2.2 WATER HAMMER

Overall, there is a low potential for water hammer in the RCS since it is designed and operated to preclude the voiding condition in normally filled lines. The reactor coolant system, including piping and primary components, is designed for normal, upset, emergency, and faulted condition transients. The design requirements are conservative relative to both the number of transients and their severity. Relief valve actuation and the associated hydraulic transients following valve opening are considered in the system design. Other valve and pump actuations are relatively slow transients with no significant effect on the system dynamic loads. To ensure dynamic system stability, reactor coolant parameters are stringently controlled. Temperature during normal operation is maintained within a narrow range; pressure is controlled by pressurizer heaters and pressurizer spray also within a narrow range for steady-state conditions. The flow characteristics of the system remain constant during a fuel cycle because the only governing parameters, namely system resistance and the reactor coolant pump characteristics, are controlled in the design process. Additionally, Westinghouse has instrumented typical reactor coolant systems to verify the flow and vibration characteristics of the system. Preoperational

testing and operating experience have verified the Westinghouse approach. The operating transients of the RCS primary piping are such that no significant water hammer can occur.

2.3 LOW CYCLE AND HIGH CYCLE FATIGUE

An assessment of the low cycle fatigue loadings was carried out as part of this study in the form of a fatigue crack growth analysis, as discussed in Section 8.0.

High cycle fatigue loads in the system would result primarily from pump vibrations. These are minimized by restrictions placed on shaft vibrations during hot functional testing and operation. During operation, an alarm signals the exceedance of the vibration limits. Field measurements have been made on a number of plants during hot functional testing, including plants similar to Turkey Point Units 3 and 4. Stresses in the elbow below the reactor coolant pump resulting from system vibration have been found to be very small, between 2 and 3 ksi at the highest. These stresses are well below the fatigue endurance limit for the material and would also result in an applied stress intensity factor below the threshold for fatigue crack growth.

2.4 WALL THINNING, CREEP, AND CLEAVAGE

Wall thinning by erosion and erosion corrosion effects should not occur in the primary loop piping due to the low velocity, typically less than 1.0 ft/sec and the stainless steel material, which is highly resistant to these degradation mechanisms. The cause of wall thinning is related to the high water velocity and is therefore clearly not a mechanism that would affect the primary loop piping.

Creep is typical experienced for temperatures over 700°F for stainless steel material, and the maximum operating temperature of the primary loop piping is well below this temperature; therefore, there would be no significant mechanical creep damage in stainless steel piping.

Cleavage type failures are not a concern for the operating temperatures and the stainless steel material used in the primary loop piping.

2.5 REFERENCES

- 2-1 Investigation and Evaluation of Stress-Corrosion Cracking in Piping of Light Water Reactor Plants, NUREG-0531, U.S. Nuclear Regulatory Commission, February 1979.
- 2-2 Investigation and Evaluation of Cracking Incidents in Piping in Pressurized Water Reactors, NUREG-0691, U.S. Nuclear Regulatory Commission, September 1980.

3.0 PIPE GEOMETRY AND LOADING

3.1 INTRODUCTION TO METHODOLOGY

The general approach is discussed first. As an example a segment of the primary coolant hot leg pipe is shown in Figure 3-1. The as-built outside diameter and minimum wall thickness of the pipe are 34.00 in. and 2.395 in., respectively, as shown in the figure. The normal stresses at the weld locations are from the load combination procedure discussed in Section 3.3 whereas the faulted loads are as described in Section 3.4. The components for normal loads are pressure, dead weight and thermal expansion. An additional component, Safe Shutdown Earthquake (SSE), is considered for faulted loads. As seen from Table 3-2, the highest stressed location in the entire loop is at Location 1 at the reactor vessel outlet nozzle to pipe weld. This is one of the locations at which, as an enveloping location, leak-before-break is to be established. Essentially a circumferential flaw is postulated to exist at this location which is subjected to both the normal loads and faulted loads to assess leakage and stability, respectively. The loads (developed below) at this location are also given in Figure 3-1.

Since the elbows are made of different materials than the pipe, locations other than the highest stressed pipe location were examined taking into consideration both fracture toughness and stress. The three most critical locations among the entire primary loop are identified after the full analysis is completed. Once loads (this section) and fracture toughnesses (Section 4.0) are obtained, the critical locations are determined (Section 5.0). At these locations, leak rate evaluations (Section 6.0) and fracture mechanics evaluations (Section 7.0) are performed per the guidance of References 3-1 and 3-2. Fatigue crack growth (Section 8.0) assessment and stability margins are also evaluated (Section 9.0). All the weld locations considered for the LBB evaluation are those shown in Figure 3-2.

Note that the piping loads and stresses based on the EPU Program were considered in the LBB evaluation as part of Revision 1 of this WCAP report.

3.2 CALCULATION OF LOADS AND STRESSES

The stresses due to axial loads and bending moments are calculated by the following equation:

$$\sigma = \frac{F}{A} + \frac{M}{Z} \quad (3-1)$$

where,

σ	=	stress, ksi
F	=	axial load, kips
M	=	bending moment, in-kips
A	=	pipe cross-sectional area, in ²
Z	=	section modulus, in ³

The bending moments for the desired loading combinations are calculated by the following equation:

$$M = \sqrt{M_Y^2 + M_Z^2} \quad (3-2)$$

where,

M = total moment for required loading

M_Y = Y component of bending moment

M_Z = Z component of bending moment

The axial load and bending moments for leak rate predictions and crack stability analyses are computed by the methods to be explained in Sections 3.3 and 3.4.

3.3 LOADS FOR LEAK RATE EVALUATION

The normal operating loads for leak rate predictions are calculated by the following equations:

$$F = F_{DW} + F_{TH} + F_P \quad (3-3)$$

$$M_Y = (M_Y)_{DW} + (M_Y)_{TH} \quad (3-4)$$

$$M_Z = (M_Z)_{DW} + (M_Z)_{TH} \quad (3-5)$$

The subscripts of the above equations represent the following loading cases:

DW = deadweight

TH = normal thermal expansion

P = load due to internal pressure

This method of combining loads is often referred to as the algebraic sum method (References 3-1 and 3-2).

The loads based on this method of combination are provided in Table 3-1 at all the weld locations identified in Figure 3-2. The as-built dimensions are also given in Table 3-1.

3.4 LOAD COMBINATION FOR CRACK STABILITY ANALYSES

In accordance with Standard Review Plan 3.6.3 (References 3-1 and 3-2), the margin in terms of applied loads needs to be demonstrated by crack stability analysis. Margin on loads of 1.4 ($\sqrt{2}$) can be demonstrated if normal plus Safe Shutdown Earthquake (SSE) are applied. The 1.4 ($\sqrt{2}$) margin should be reduced to 1.0 if the deadweight, thermal expansion, internal pressure, SSEINERTIA and seismic anchor motion (SAM) loads are combined based on individual absolute values as shown below.

The absolute sum of loading components is used for the LBB analysis which results in higher magnitude of combined loads and thus satisfies a margin on loads of 1.0. The absolute summation of loads is shown in the following equations:

$$F = |F_{DW}| + |F_{TH}| + |F_P| + |F_{SSEINERTIA}| + |F_{SSEAM}| \quad (3-6)$$

$$M_Y = |(M_Y)_{DW}| + |(M_Y)_{TH}| + |(M_Y)_{SSEINERTIA}| + |(M_Y)_{SSEAM}| \quad (3-7)$$

$$M_Z = |(M_Z)_{DW}| + |(M_Z)_{TH}| + |(M_Z)_{SSEINERTIA}| + |(M_Z)_{SSEAM}| \quad (3-8)$$

where subscript SSEINERTIA refers to safe shutdown earthquake inertia, SSEAM is safe shutdown earthquake anchor motion, respectively.

The loads so determined are used in the fracture mechanics evaluations (Section 7.0) to demonstrate the LBB margins at the locations established to be the governing locations. These loads at all the weld locations (see Figure 3-2) are given in Table 3-2.

3.5 REFERENCES

- 3-1 Standard Review Plan: Public Comments Solicited; 3.6.3 Leak-Before-Break Evaluation Procedures; Federal Register/Vol. 52, No. 167/Friday, August 28, 1987/Notices, pp. 32626-32633.
- 3-2 NUREG-0800 Revision 1, March 2007, Standard Review Plan: 3.6.3 Leak-Before-Break Evaluation Procedures.

Table 3-1 Dimensions, Normal Loads and Stresses for Turkey Point Units 3 and 4					
Location^a	Outside Diameter (in)	Minimum Thickness (in)	Axial Load^b (kips)	Moment (in-kips)	Total Stress (ksi)
1	34.00	2.395	1336	24063	19.32
2	34.00	2.395	1336	11563	12.20
3	37.75	3.270	1574	18263	10.93
4	37.62	3.205	1715	3800	6.33
5	36.25	2.520	1657	4354	8.27
6	36.25	2.520	1653	4448	8.30
7	36.25	2.520	1719	785	6.81
8	36.25	2.520	1716	3735	8.20
9	37.63	3.208	1819	8843	8.46
10	32.25	2.270	1363	6903	10.98
11	32.25	2.270	1363	6918	10.99
12	33.56	2.930	1363	7803	8.77

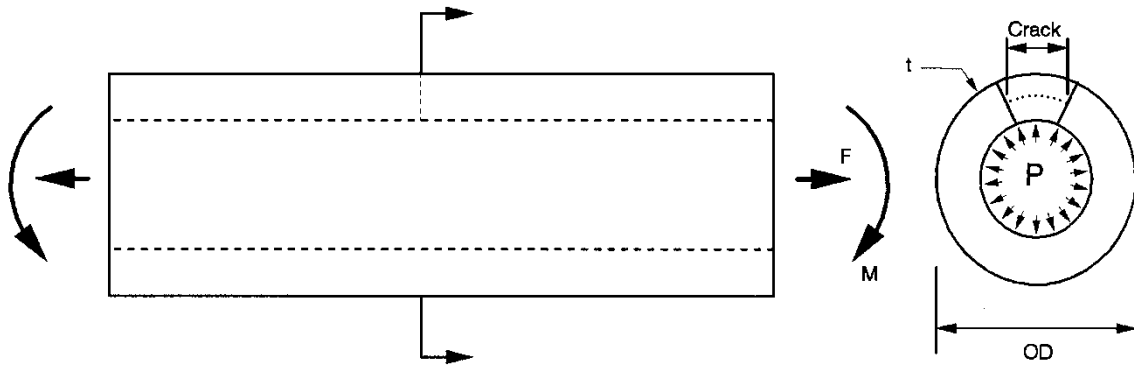
Notes:

- a. See Figure 3-2
- b. Included Pressure

Table 3-2 Faulted Loads and Stresses for Turkey Point Units 3 and 4			
Location^{a,b}	Axial Load^c (kips)	Moment (in-kips)	Total Stress (ksi)
1	1881	24638	21.94
2	1881	12209	14.86
3	2011	21361	13.27
4	1745	5065	6.88
5	1825	5260	9.33
6	1821	4859	9.13
7	1743	1172	7.08
8	1745	4408	8.63
9	1832	10754	9.19
10	1434	9642	13.15
11	1435	8137	12.14
12	1430	9375	9.80

Notes:

- a. See Figure 3-2
- b. See Table 3-1 for dimensions
- c. Included Pressure



Location 1

$OD^a = 34.00$ in
 $t^a = 2.395$ in

Normal Loads^a

Faulted Loads^b

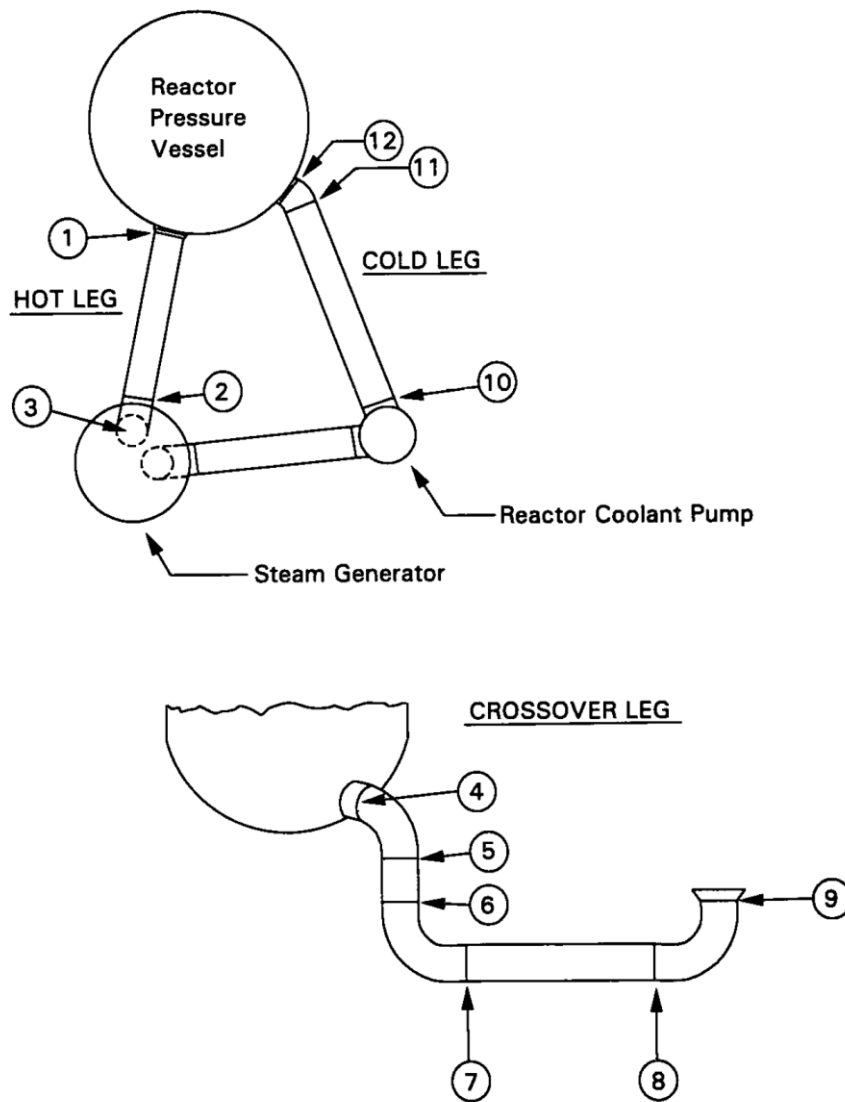
Force ^c :	1336 kips	Force ^c :	1881 kips
Bending Moment:	24063 in-kips	Bending Moment:	24638 in-kips

^a See Table 3-1

^b See Table 3-2

^c Includes the force due to a pressure of 2250 psia

Figure 3-1 Hot Leg Coolant Pipe



HOT LEG

Temperature 616.8°F Pressure: 2250 psia

CROSS-OVER LEG

Temperature 548.9°F Pressure: 2250 psia

COLD LEG

Temperature 549.2°F Pressure: 2250 psia

**Figure 3-2 Schematic Diagram of Turkey Point Units 3 and 4
Primary Loop Showing Weld Locations**

4.0 MATERIAL CHARACTERIZATION

4.1 PRIMARY LOOP PIPE AND FITTINGS MATERIALS

The Turkey Point Units 3 and 4 primary loop pipe materials are A376-TP316 and the elbow fitting materials are A351-CF8M.

4.2 TENSILE PROPERTIES

The pipe and elbow fitting Certified Materials Test Reports (CMTRs) for Turkey Point Units 3 and 4 were used to establish the tensile properties for the leak-before-break analyses. The pipe CMTRs include tensile properties at room temperature and at 650°F for each of the heats of material, while the elbow fitting CMTRs include tensile properties at room temperature. The tensile properties (yield and ultimate strengths) are given in Table 4-1 for piping and in Table 4-2 for elbow fittings.

For the A376-TP316 material, the representative properties at 616.8°F (hot leg temperature) were established from the tensile properties at 650°F given in Table 4-1 by utilizing Section III of the 1989 ASME Boiler and Pressure Vessel Code (Reference 4-1). Code tensile properties at 616.8°F were obtained by interpolating between the 600°F and 650°F tensile properties. Ratios of the code tensile properties at 616.8°F to the corresponding tensile properties at 650°F were then applied to the 650°F tensile properties given in Table 4-1 to obtain the plant specific properties for A376-TP316 at 616.8°F. It should be noted that there is no significant impact on the LBB analysis by using the 1989 ASME Code Section III edition for material properties, as compared to the Turkey Point ASME code of record.

For the A351-CF8M material, the representative properties at 616.8°F and 549.2°F (cold leg temperature conservatively bounds crossover leg temperature) were established from the tensile properties at room temperature given in Table 4-2 by utilizing Section III of the 1989 ASME Boiler and Pressure Vessel Code (Reference 4-1). Code tensile properties at 616.8°F and 549.2°F were established by interpolating between the 500°F, 600°F and the 650°F tensile properties. Ratios of the code tensile properties at 616.8°F and 549.2°F to the corresponding properties at room temperature were then applied to the room temperature properties given in Table 4-2 to obtain the plant specific representative properties for A351-CF8M at 616.8°F and 549.2°F.

The average and lower bound yield strengths and ultimate strengths are given in Table 4-3. The ASME Code moduli of elasticity are also given, and Poisson's ratio was taken as 0.3.

4.3 FRACTURE TOUGHNESS PROPERTIES

To support the Subsequent License Renewal Time-Limited Aging Analyses (SLR TLAA) Program, the fracture toughness properties of the Turkey Point Units 3 and 4 primary loop piping structural integrity need to be demonstrated to meet the stability criteria for 80 years of service life. The stability criteria are provided in Section 5.2.

The Turkey Point Units 3 and 4 primary loop forged stainless steel piping (A376-TP316) does not degrade due to thermal aging; however, the primary loop cast stainless steel elbow fittings (A351-CF8M) in a high temperature environment are potentially susceptible to degradation due to thermal aging. Therefore, this section of the report provides the aged end of life fracture toughness properties for Turkey Point Units 3 and 4 cast CF8M elbows due to thermal aging embrittlement.

The pre-service fracture toughness (J) of cast stainless steels that are of interest are in terms of J_{ic} (J at Crack Initiation) and have been found to be very high at 600°F. [

^{a,c,e} However, cast stainless steel is susceptible to thermal aging at the reactor operating temperature, that is, about 290°C (550°F). Thermal aging of cast stainless steel results in embrittlement, that is, a decrease in the ductility, impact strength, and fracture toughness of the material. Depending on the material composition, the Charpy impact energy of a cast stainless steel component could decrease to a small fraction of its original value after exposure to reactor temperatures during service.

The susceptibility of the material to thermal aging increases with increasing ferrite contents. The molybdenum bearing CF8M shows increased susceptibility to thermal aging.

In 1994, the Argonne National Laboratory (ANL) completed an extensive research program in assessing the extent of thermal aging of cast stainless steel materials (Reference 4-2). The ANL research program measured mechanical properties of cast stainless steel materials after they had been heated in controlled ovens for long periods of time. ANL compiled a data base, both from data within ANL and from international sources, of about 85 compositions of cast stainless steel exposed to a temperature range of 290-400°C (550-750°F) for up to 58,000 hours (6.5 years). In 2015 the work done by ANL was augmented, and the fracture toughness database for the Cast Austenitic Stainless Steel (CASS) materials was aged to 100,000 hours at 290-350°C (554-633°F). The methodology for estimating fracture properties has been extended to cover CASS materials with a ferrite content of up to 40%. From this database (NUREG/CR-4513, Revision 2), ANL developed correlations for estimating the extent of thermal aging of cast stainless steel (Reference 4-3).

ANL developed the fracture toughness estimation procedures by correlating data in the database conservatively. After developing the correlations, ANL validated the estimation procedures by comparing the estimated fracture toughness with the measured value for several cast stainless steel plant components removed from actual plant service. The procedure developed by ANL in Reference 4-3 was used to calculate the end of life fracture toughness values for this analysis. The ANL research program was sponsored and the procedure was accepted by the NRC.

Based on NUREG/CR-4513, Revision 2, the fracture toughness correlations used for the full aged condition is applicable for plants operating at and beyond 15 EFPY (Effective Full Power Years) for the CF8M materials (elbows for Turkey Point Units 3 and 4). As of June 1, 2017, Turkey Point Units 3 and 4 are operating at 33.16 and 33.23 EFPY respectively. Therefore, the

use of the fracture toughness correlations described below is applicable for the fully aged or saturated condition of the Turkey Point Units 3 and 4 elbow materials made of CF8M.

The method described below was used to calculate the end of life toughness properties for the cast material of the Turkey Point Units 3 and 4 primary coolant loop elbows.

The chemical compositions of the Turkey Point Units 3 and 4 primary loop elbow fitting material are available from CMTRs and are provided in Table 4-4. The following equations are taken from Reference 4-3 and applicable for CF8M type material:

$$Cr_{eq} = Cr + 1.21(Mo) + 0.48(Si) - 4.99 = (\text{Chromium equivalent}) \quad (4-1)$$

$$Ni_{eq} = (Ni) + 0.11(Mn) - 0.0086(Mn)^2 + 18.4(N) + 24.5(C) + 2.77 = (\text{Nickel equivalent}) \quad (4-2)$$

$$\delta_c = 100.3(Cr_{eq} / Ni_{eq})^2 - 170.72(Cr_{eq} / Ni_{eq}) + 74.22 = (\text{Ferrite Content}) \quad (4-3)$$

where the elements are in percent weight and δ_c is ferrite in percent volume.

The saturation room temperature (RT at 77°F) impact energies of the cast stainless steel materials were determined from the chemical compositions available from CMTRs and provided in Table 4-4.

For CF8M steel with < 10% Ni, the saturation value of RT impact energy Cv_{sat} (J/cm²) is the lower value determined from

$$\log_{10} Cv_{sat} = 0.27 + 2.81 \exp(-0.022\phi) \quad (4-4)$$

where the material parameter ϕ is expressed as

$$\phi = \delta_c (Ni + Si + Mn)^2 (C + 0.4N) / 5.0 \quad (4-5)$$

and from

$$\log_{10} Cv_{sat} = 7.28 - 0.011\delta_c - 0.185Cr - 0.369Mo - 0.451Si - 0.007Ni - 4.71(C + 0.4N) \quad (4-6)$$

For CF8M steel with $\geq 10\%$ Ni, the saturation value of RT impact energy Cv_{sat} (J/cm²) is the lower value determined from

$$\log_{10} Cv_{sat} = 0.84 + 2.54 \exp(-0.047\phi) \quad (4-7)$$

where the material parameter ϕ is expressed as

$$\phi = \delta_c (Ni + Si + Mn)^2 (C + 0.4N) / 5.0 \quad (4-8)$$

and from

$$\log_{10} Cv_{sat} = 7.28 - 0.011\delta_c - 0.185Cr - 0.369Mo - 0.451Si - 0.007Ni - 4.71(C + 0.4N) \quad (4-9)$$

The saturation J-R curve at RT, for static-cast CF8M steel is given by

$$J_d = 1.44 (Cv_{sat})^{1.35} (\Delta a)^n \quad \text{for } Cv_{sat} < 35 \text{ J/cm}^2 \quad (4-10)$$

$$J_d = 16 (Cv_{sat})^{0.67} (\Delta a)^n \quad \text{for } Cv_{sat} \geq 35 \text{ J/cm}^2 \quad (4-11)$$

$$n = 0.20 + 0.08 \log_{10} (Cv_{sat}) \quad (4-12)$$

where J_d is the “deformation J” in kJ/m^2 and Δa is the crack extension in mm.

The saturation J-R curve at 290-320°C (554-608°F), for static-cast CF8M steel is given by

$$J_d = 5.5 (Cv_{\text{sat}})^{0.98} (\Delta a)^n \quad \text{for } Cv_{\text{sat}} < 46 \text{ J/cm}^2 \quad (4-13)$$

$$J_d = 49 (Cv_{\text{sat}})^{0.41} (\Delta a)^n \quad \text{for } Cv_{\text{sat}} \geq 46 \text{ J/cm}^2 \quad (4-14)$$

$$n = 0.19 + 0.07 \log_{10} (Cv_{\text{sat}}) \quad (4-15)$$

where J_d is the “deformation J” in kJ/m^2 and Δa is the crack extension in mm.

[

$J^{a,c,e}$

[

$J^{a,c,e}$

The results from the ANL Research Program indicate that the lower-bound fracture toughness of thermally aged cast stainless steel is similar to that of submerged arc welds (SAWs). The applied value of the J-integral for a flaw in the weld regions will be lower than that in the base metal because the yield stress for the weld materials is much higher at the temperature.¹

Therefore, weld regions are less limiting than the cast material.

In the fracture mechanics analyses that follow, the fracture toughness properties given in Table 4-5 will be used as the criteria against which the applied fracture toughness values will be compared.

4.4 REFERENCES

- 4-1 ASME Boiler and Pressure Vessel Code 1989, Section III.
- 4-2 O. K. Chopra and W. J. Shack, "Assessment of Thermal Embrittlement of Cast Stainless Steels," NUREG/CR-6177, U.S. Nuclear Regulatory Commission, Washington, DC, May 1994.
- 4-3 O. K. Chopra, "Estimation of Fracture Toughness of Cast Stainless Steels During Thermal Aging in LWR Systems," NUREG/CR-4513, Revision 2, U.S. Nuclear Regulatory Commission, Washington, DC, May 2016.

¹ In the report all the applied J values were conservatively determined by using base metal strength properties.

Table 4-1
Measured Tensile Properties for Turkey Point Units 3 and 4 Primary Loop Piping

Component	Heat Num.	Yield Room Temp (psi)	Ultimate Room Temp (psi)	Yield Temp 650°F (psi)	Ultimate Temp 650°F (psi)	Material Type
Hot Leg	F0070 #2646	38200	79000	21000	60800	A376-TP316
Hot Leg	F0070 #2646	34100	78200	21000	60800	A376-TP316
Hot Leg	F0214 #2850	42000	83300	22400	62300	A376-TP316
Hot Leg	F0214 #2850	43000	82800	22400	62300	A376-TP316
Hot Leg	F0188 #2844	39200	83400	26100	67000	A376-TP316
Hot Leg	F0188 #2844	38900	84000	26100	67000	A376-TP316
Hot Leg	D8549 #1170	30100	75000	22100	63400	A376-TP316
Hot Leg	D8549 #1170	36900	79000	22100	63400	A376-TP316
Hot Leg	F0215 #2892X	43000	83000	21700	66800	A376-TP316
Hot Leg	F0215 #2892X	42000	84600	21700	66800	A376-TP316
Hot Leg	F0225 #2895X	42000	85900	22100	68200	A376-TP316
Hot Leg	F0225 #2895X	46000	88800	22100	68200	A376-TP316
Hot Leg	E-1493 #3356	42000	83100	25500	69200	A376-TP316
Hot Leg	E-1493 #3356	42600	84500	25500	69200	A376-TP316
Hot Leg	E-1485 #3352X	42300	85400	27500	72200	A376-TP316
Hot Leg	E-1485 #3352X	45400	87400	27500	72200	A376-TP316
Hot Leg	E-1482 #3355	40900	82700	24500	66200	A376-TP316
Hot Leg	E-1482 #3355	48600	88800	24500	66200	A376-TP316
Hot Leg	E-1483 #3357	42100	85000	23700	52100	A376-TP316
Hot Leg	E-1483 #3357	43000	85200	23700	52100	A376-TP316
Hot Leg	E-1490 #3348Y	46000	85700	23700	68600	A376-TP316
Hot Leg	E-1490 #3348Y	40900	83300	23700	68600	A376-TP316
Hot Leg	E-1490 #3347X	43100	86000	23700	68600	A376-TP316
Hot Leg	E-1490 #3347X	43000	82700	23700	68600	A376-TP316

Table 4-1 (Continued)
Measured Tensile Properties for Turkey Point Units 3 and 4 Primary Loop Piping

Component	Heat Num.	Yield Room Temp (psi)	Ultimate Room Temp (psi)	Yield Temp 650°F (psi)	Ultimate Temp 650°F (psi)	Material Type
Cold Leg	D8777 #2874X	35300	79200	24100	65600	A376-TP316
Cold Leg	D8777 #2874X	34900	78200	24100	65600	A376-TP316
Cold Leg	D8913 #2877	35100	79200	23100	64200	A376-TP316
Cold Leg	D8913 #2877	38100	79600	23100	64200	A376-TP316
Cold Leg	D8915 #2876	34100	78400	22500	63600	A376-TP316
Cold Leg	D8915 #2876	32800	78600	22500	63600	A376-TP316
Cold Leg	F0230 #2993	48000	88100	21700	70200	A376-TP316
Cold Leg	F0230 #2993	47000	90900	21700	70200	A376-TP316
Cold Leg	F0162 #2858	43700	83100	27600	69400	A376-TP316
Cold Leg	F0162 #2858	46200	84900	27600	69400	A376-TP316
Cold Leg	F0371 #3130	47000	88700	25600	72300	A376-TP316
Cold Leg	F0371 #3130	44000	88800	25600	72300	A376-TP316
Cold Leg	F0228 #2949	42200	86100	24700	69800	A376-TP316
Cold Leg	F0228 #2949	45000	89900	24700	69800	A376-TP316
Cold Leg	F0373 #3166	40100	86900	25600	71900	A376-TP316
Cold Leg	F0373 #3166	45500	91900	25600	71900	A376-TP316
Cold Leg	F0244 #2997	42900	85400	25400	69900	A376-TP316
Cold Leg	F0244 #2997	47500	88100	25400	69900	A376-TP316
Cold Leg	F0229 #2950	41000	85700	24500	68200	A376-TP316
Cold Leg	F0229 #2950	44400	86400	24500	68200	A376-TP316
Cold Leg	F0371 #3128	46800	78700	25600	72300	A376-TP316
Cold Leg	F0371 #3128	36900	84700	25600	72300	A376-TP316

Table 4-1 (Continued) Measured Tensile Properties for Turkey Point Units 3 and 4 Primary Loop Piping						
Component	Heat Num.	Yield Room Temp (psi)	Ultimate Room Temp (psi)	Yield Temp 650°F (psi)	Ultimate Temp 650°F (psi)	Material Type
Xover Leg	F0189 #2868Z	37700	80600	25200	70000	A376-TP316
Xover Leg	F0189 #2868Z	44100	91000	25200	70000	A376-TP316
Xover Leg	F0189 #2870X	41300	82200	25200	70000	A376-TP316
Xover Leg	F0189 #2870X	42900	84200	25200	70000	A376-TP316
Xover Leg	F0189 #2870Y	41300	82200	25200	70000	A376-TP316
Xover Leg	F0189 #2870Y	42900	84200	25200	70000	A376-TP316
Xover Leg	D8775 #2880	34100	75800	24000	60400	A376-TP316
Xover Leg	D8775 #2880	41100	77800	24000	60400	A376-TP316
Xover Leg	D8777 #2879	38100	78200	20200	60000	A376-TP316
Xover Leg	D8777 #2879	38500	78200	20200	60000	A376-TP316
Xover Leg	D8785 #2881	32900	78200	20400	57200	A376-TP316
Xover Leg	D8785 #2881	34100	79000	20400	57200	A376-TP316
Xover Leg	E-1485 #3361Y	38300	83900	23600	70700	A376-TP316
Xover Leg	E-1485 #3361Y	45900	91400	23600	70700	A376-TP316
Xover Leg	F-0215 #2892	40000	84800	21700	82300	A376-TP316
Xover Leg	F-0215 #2892	41900	87700	21700	82300	A376-TP316
Xover Leg	F-0221 #2866	41000	83900	21600	65200	A376-TP316
Xover Leg	F-0221 #2866	41500	83000	21600	65200	A376-TP316
Xover Leg	E-1484 #3360X	39600	83300	23600	63600	A376-TP316
Xover Leg	E-1484 #3360X	44500	88800	23600	63600	A376-TP316
Xover Leg	F-0212 #2887	43500	85100	23400	67400	A376-TP316
Xover Leg	F-0212 #2887	43200	88000	23400	67400	A376-TP316
Xover Leg	E-1484 #3360Y	39600	83300	23600	63600	A376-TP316
Xover Leg	E-1484 #3360Y	44500	88800	23600	63600	A376-TP316

Note: Xover Leg = Cross-over Leg

Table 4-2
Measured Room Temperature Tensile Properties for Turkey Point Units 3 and 4
Primary Loop Elbow Fittings

Component	Heat Num.	Yield Room Temp (psi)	Ultimate Room Temp (psi)	Material Type
Hot Leg	11897-2	39000	76000	A351-CF8M
Hot Leg	12121-2	43500	85000	A351-CF8M
Hot Leg	12012-2	39000	77000	A351-CF8M
Hot Leg	08368-1	43500	87500	A351-CF8M
Hot Leg	08247-1	46500	88000	A351-CF8M
Hot Leg	08586-1	40000	84000	A351-CF8M
Cold Leg	16037-1	37500	75000	A351-CF8M
Cold Leg	10865-2	42000	81500	A351-CF8M
Cold Leg	12393-4	42000	83000	A351-CF8M
Cold Leg	05872-2	49500	89000	A351-CF8M
Cold Leg	05769-5	52500	93500	A351-CF8M
Cold Leg	05715-2	51000	90000	A351-CF8M
Xover Leg	10048-1	45000	87000	A351-CF8M
Xover Leg	10763-1	44250	81000	A351-CF8M
Xover Leg	10008-1	46500	88000	A351-CF8M
Xover Leg	10804-1	43500	81000	A351-CF8M
Xover Leg	10091-1	42000	86500	A351-CF8M
Xover Leg	10128-1	46500	89000	A351-CF8M
Xover Leg	10320-1	48000	91500	A351-CF8M
Xover Leg	10563-1	43500	88000	A351-CF8M
Xover Leg	10283-1	48000	91500	A351-CF8M
Xover Leg	10243-1	46500	90000	A351-CF8M
Xover Leg	10400-1	48000	91500	A351-CF8M

Table 4-2 (Continued)
Measured Room Temperature Tensile Properties for Turkey Point Units 3 and 4
Primary Loop Elbow Fittings

Component	Heat Num.	Yield Room Temp (psi)	Ultimate Room Temp (psi)	Material Type
Xover Leg	10644-1	49500	91000	A351-CF8M
Xover Leg	09476-3	45000	88000	A351-CF8M
Xover Leg	09027-1	48000	90500	A351-CF8M
Xover Leg	06239-2	48000	88000	A351-CF8M
Xover Leg	12511-2	46500	89000	A351-CF8M
Xover Leg	12584-2	40500	83250	A351-CF8M
Xover Leg	12357-7	42000	82500	A351-CF8M
Xover Leg	12432-5	45000	86000	A351-CF8M
Xover Leg	11518-1	42000	83750	A351-CF8M
Xover Leg	12087-1	39000	79000	A351-CF8M
Xover Leg	13498-3	45750	87250	A351-CF8M
Xover Leg	14206-1	45000	86250	A351-CF8M
Xover Leg	13378-3	42000	84250	A351-CF8M
Xover Leg	15258-1	42000	83750	A351-CF8M
Xover Leg	12660-2	42000	85000	A351-CF8M
Xover Leg	12857-1	42000	83500	A351-CF8M
Xover Leg	14048-1	40500	78500	A351-CF8M
Xover Leg	14335-1	51000	88500	A351-CF8M
Xover Leg	13133-2	45000	87000	A351-CF8M

Note: Xover Leg = Cross-over Leg

Table 4-3
Mechanical Properties for Turkey Point Units 3 and 4 Materials
at Operating Temperatures

a,c,e

Modulus of Elasticity

$E = 25.22 \times 10^6$ psi at 616.8°F
$E = 25.55 \times 10^6$ psi at 549.2°F
Poisson's ratio: 0.3

Note: The material properties for the crossover leg temperature (548.9°F) is represented by the cold leg temperature (549.2°F), as the difference in material properties based on the two temperature will be insignificant.

Table 4-4 Chemistry and Fracture Toughness Properties of the Material Heats of Turkey Point Units 3 and 4

a,c,e

Table 4-4 Chemistry and Fracture Toughness Properties of the Material Heats of Turkey Point Units 3 and 4 (Continued)

a,c,e

Table 4-5
Fracture Toughness Properties for Turkey Point Units 3 and 4 Primary Loops
for Leak-Before-Break Evaluation at Critical Locations

a,c,e

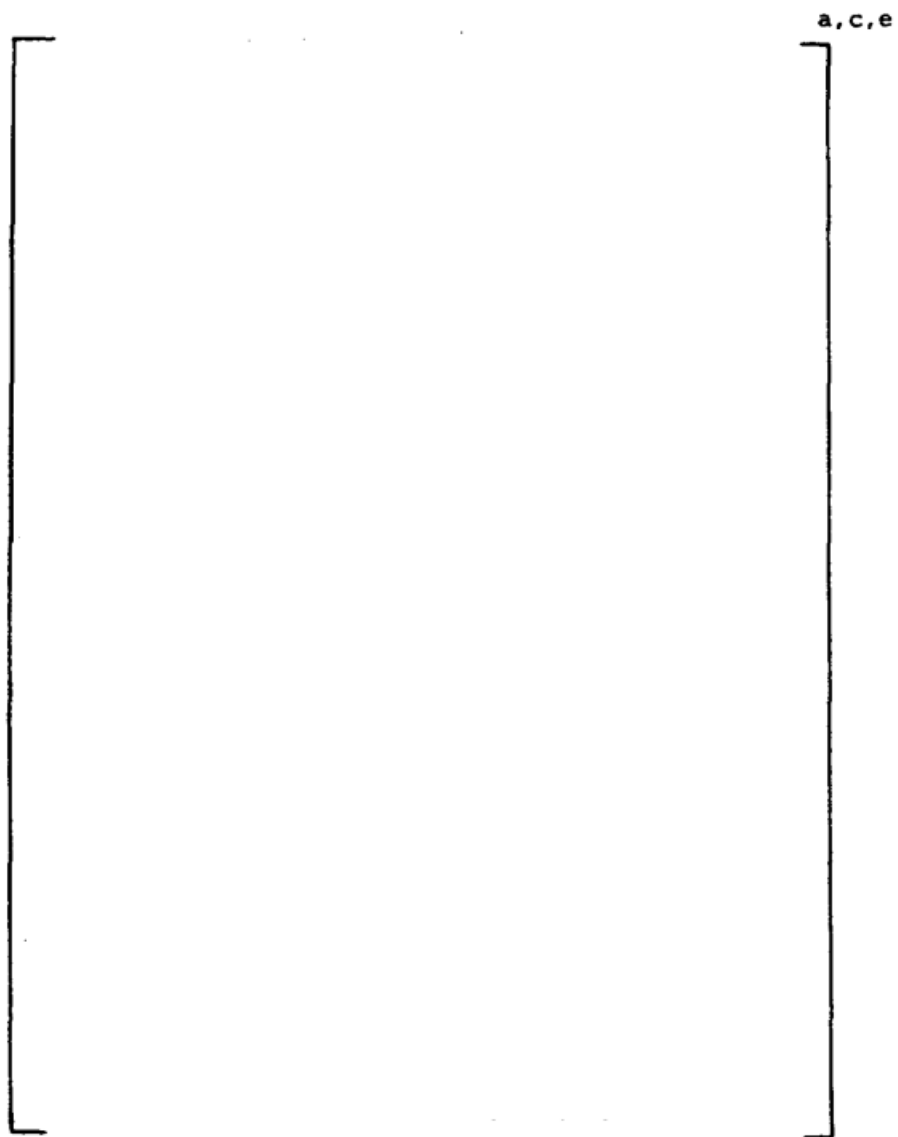


Figure 4-1 Pre-Service J vs. Δa for SA351-CF8M Cast Stainless Steel at 600°F

5.0 CRITICAL LOCATION AND EVALUATION CRITERIA

5.1 CRITICAL LOCATIONS

The leak-before-break (LBB) evaluation margins are to be demonstrated for the limiting locations (governing locations). Such locations are established based on the loads (Section 3.0) and the material properties established in Section 4.0. These locations are defined below for Turkey Point Units 3 and 4. Table 3-2 as well as Figure 3-2 are used for this evaluation.

Critical Locations

The highest stressed location for the entire primary loop is at location 1 (in the Hot Leg) (See Figure 3-2) at the reactor vessel outlet nozzle to pipe weld. Therefore, Location 1 is critical for all the weld locations of the pipe.

Since the elbows are made of cast materials and can be susceptible to thermal aging, the critical locations for the elbows are also analyzed. Per Section 4.3, the critical heat locations for the elbows are Heat number 08368-1 (Location 2) and Heat number 05769-5 (Location 11), due to low toughness. Note that the lowest toughness heat for the crossover leg is at Heat number 14048-1; however, based on both stresses and toughness, crossover leg locations are less critical than the two critical locations mentioned above; therefore, the crossover leg locations will be bounded by the critical locations at the Hot Leg and Cold Leg.

It is thus concluded that the enveloping locations in Turkey Point Units 3 and 4 for which LBB methodology is to be applied are locations 1, 2, and 11 (based on loads and stresses) and locations 2 and 11 (based on toughness). For the critical locations, the tensile properties are shown in Table 4-3 and the allowable toughness properties are shown in Table 4-5.

5.2 FRACTURE CRITERIA

As will be discussed later, fracture mechanics analyses are made based on loads and postulated flaw sizes related to leakage. The stability criteria against which the calculated J and tearing modulus are compared are:

- (1) If $J_{app} < J_{lc}$, then the crack will not initiate and the crack is stable;
- (2) If $J_{app} \geq J_{lc}$; and $T_{app} < T_{mat}$ and $J_{app} < J_{max}$, then the crack is stable.

Where:

J_{app}	=	Applied J
J_{lc}	=	J at Crack Initiation
T_{app}	=	Applied Tearing Modulus
T_{mat}	=	Material Tearing Modulus
J_{max}	=	Maximum J value of the material

For critical locations, the limit load method discussed in Section 7.0 was also used.

6.0 LEAK RATE PREDICTIONS

6.1 INTRODUCTION

The purpose of this section is to discuss the method which is used to predict the flow through postulated through-wall cracks and present the leak rate calculation results for through-wall circumferential cracks.

6.2 GENERAL CONSIDERATIONS

The flow of hot pressurized water through an opening to a lower back pressure causes flashing which can result in choking. For long channels where the ratio of the channel length, L , to hydraulic diameter, D_H , (L/D_H) is greater than [

$$j^{a,c,e}$$

6.3 CALCULATION METHOD

The basic method used in the leak rate calculations is the method developed by [

$$j^{a,c,e}$$

The flow rate through a crack was calculated in the following manner. Figure 6-1 from Reference 6-2 was used to estimate the critical pressure, P_c , for the primary loop enthalpy condition and an assumed flow. Once P_c was found for a given mass flow, the [

$j^{a,c,e}$ was found from Figure 6-2 (taken from Reference 6-2). For all cases considered, since [$j^{a,c,e}$

Therefore, this method will yield the two-phase pressure drop due to momentum effects as illustrated in Figure 6-3, where P_o is the operating pressure. Now using the assumed flow rate, G , the frictional pressure drop can be calculated using

$$\Delta P_f = [j^{a,c,e} \quad (6-1)$$

where the friction factor f is determined using the [$j^{a,c,e}$ The crack relative roughness, ε , was obtained from fatigue crack data on stainless steel samples. The relative roughness value used in these calculations was [$j^{a,c,e}$

The frictional pressure drop using equation 6-1 is then calculated for the assumed flow rate and added to the [$j^{a,c,e}$ to obtain the total pressure drop from the primary system to the atmosphere. That is, for the primary loop:

$$\text{Absolute Pressure} - 14.7 = [j^{a,c,e} \quad (6-2)$$

for a given assumed flow rate G . If the right-hand side of equation 6-2 does not agree with the pressure difference between the primary loop and the atmosphere, then the procedure is repeated until equation 6-2 is satisfied to within an acceptable tolerance which in turn leads to flow rate value for a given crack size.

6.4 LEAK RATE CALCULATIONS

Leak rate calculations were made as a function of crack length at the governing locations previously identified in Section 5.1. The normal operating loads of Table 3-1 were applied in these calculations. The crack opening areas were estimated using the method of Reference 6-3, and the leak rates were calculated using the two-phase flow formulation described above. The average material properties of Section 4.0 (see Table 4-3) were used for these calculations.

The flaw sizes to yield a leak rate of 10 gpm were calculated at the governing locations and are given in Table 6-1 for Turkey Point Units 3 and 4. The flaw sizes so determined are called leakage flaw sizes.

The Turkey Point Units 3 and 4 RCS pressure boundary leak detection system meets the intent of Regulatory Guide 1.45, and the plant leak detection capability is 1 gpm. Thus, to satisfy the margin of 10 on the leak rate, the flaw sizes (leakage flaw sizes) are determined which yield a leak rate of 10 gpm.

6.5 REFERENCES

- 6-1 [
- $]^{a,c,e}$
- 6-2 M. M, El-Wakil, "Nuclear Heat Transport, International Textbook Company," New York, N.Y, 1971.
- 6-3 Tada, H., "The Effects of Shell Corrections on Stress Intensity Factors and the Crack Opening Area of Circumferential and a Longitudinal Through-Crack in a Pipe," Section II-1, NUREG/CR-3464, September 1983.

Table 6-1
Flaw Sizes Yielding a Leak Rate of 10 gpm
at the Governing Locations

a,c,e

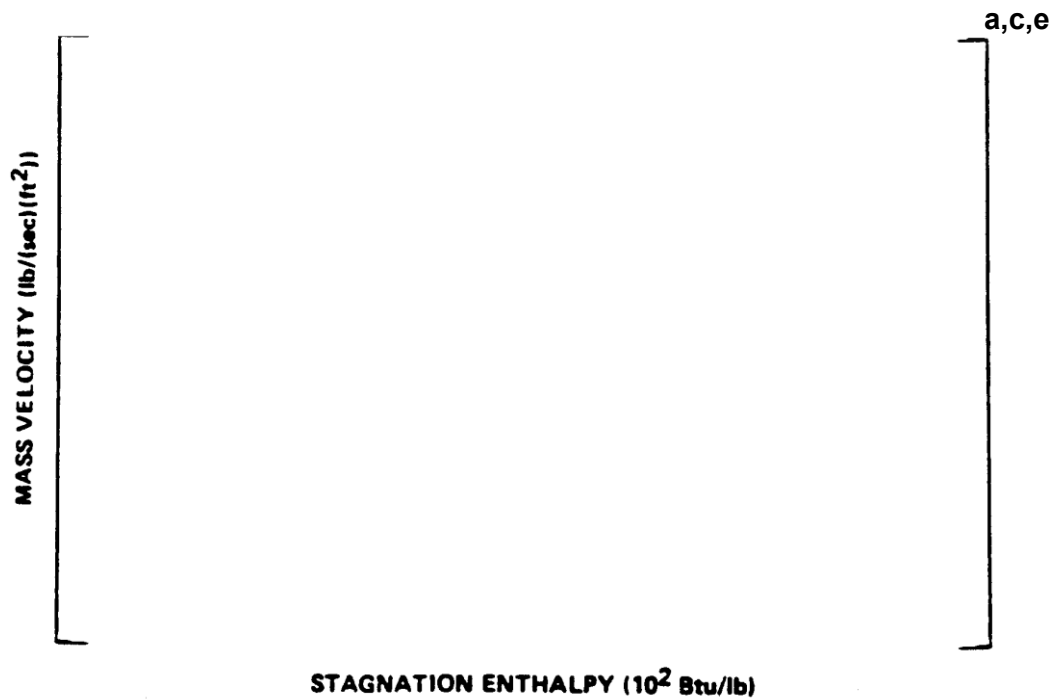


Figure 6-1 Analytical Predictions of Critical Flow Rates of Steam-Water Mixtures



Figure 6-2 []^{a,c,e} Pressure Ratio as a Function of L/D

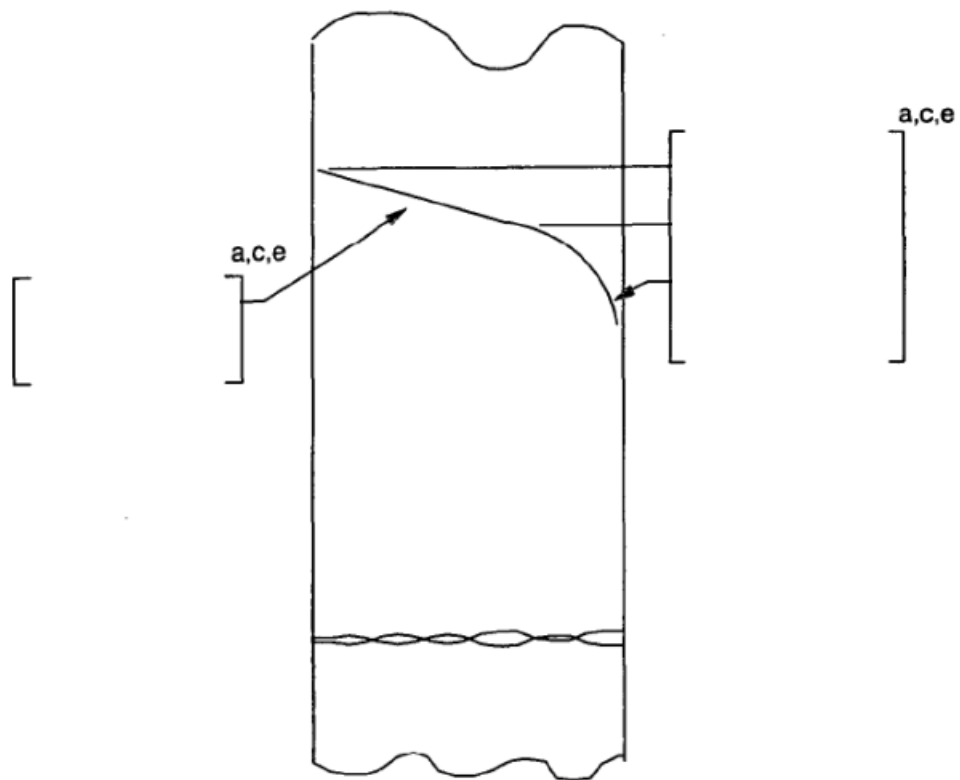


Figure 6-3 Idealized Pressure Drop Profile Through a Postulated Crack

7.0 FRACTURE MECHANICS EVALUATION

7.1 LOCAL FAILURE MECHANISM

The local mechanism of failure is primarily dominated by the crack tip behavior in terms of crack-tip blunting, initiation, extension and final crack instability. The local stability will be assumed if the crack does not initiate at all. It has been accepted that the initiation toughness measured in terms of J_{Ic} from a J-integral resistance curve is a material parameter defining the crack initiation. If, for a given load, the calculated J-integral value is shown to be less than the J_{Ic} of the material, then the crack will not initiate. If the initiation criterion is not met, one can calculate the tearing modulus as defined by the following relation:

$$T_{app} = \frac{dJ}{da} \times \frac{E}{\sigma_f^2}$$

where:

T_{app}	=	applied tearing modulus
E	=	modulus of elasticity
σ_f	=	$0.5 (\sigma_y + \sigma_u)$ = flow stress
a	=	crack length
σ_y, σ_u	=	yield and ultimate strength of the material, respectively

Stability is said to exist when ductile tearing does not occur if T_{app} is less than T_{mat} , the experimentally determined tearing modulus. Since a constant T_{mat} is assumed a further restriction is placed in J_{app} . J_{app} must be less than J_{max} where J_{max} is the maximum value of J for which the experimental T_{mat} is greater than or equal to the T_{app} used.

As discussed in Section 5.2 the local crack stability criteria is a two-step process:

- (1) If $J_{app} < J_{Ic}$, then the crack will not initiate and the crack is stable;
- (2) If $J_{app} \geq J_{Ic}$; and $T_{app} < T_{mat}$ and $J_{app} < J_{max}$, then the crack is stable.

7.2 GLOBAL FAILURE MECHANISM

Determination of the conditions which lead to failure in stainless steel should be done with plastic fracture methodology because of the large amount of deformation accompanying fracture. One method for predicting the failure of ductile material is the plastic instability method, based on traditional plastic limit load concepts, but accounting for strain hardening and taking into account the presence of a flaw. The flawed pipe is predicted to fail when the remaining net section reaches a stress level at which a plastic hinge is formed. The stress level at which this occurs is termed as the flow stress. The flow stress is generally taken as the average of the yield and ultimate tensile strength of the material at the temperature of interest. This methodology has been shown to be applicable to ductile piping through a large number of experiments and will be used here to predict the critical flaw size in the primary coolant piping. The failure criterion has been obtained by requiring equilibrium of the section containing the flaw (Figure 7-1) when loads are applied. The detailed development is provided in Appendix A for a through-wall circumferential flaw in a pipe with internal pressure, axial force, and imposed bending moments. The limit moment for such a pipe is given by:

$$\sigma_f = 0.5 (\sigma_y + \sigma_u) = \text{flow stress, psi}$$

The analytical model described above accurately accounts for the piping internal pressure as well as imposed axial force as they affect the limit moment. Good agreement was found between the analytical predictions and the experimental results (Reference 7-1). For application of the limit load methodology, the material, including consideration of the configuration, must have a sufficient ductility and ductile tearing resistance to sustain the limit load.

7.3 RESULTS OF CRACK STABILITY EVALUATION

Stability analyses were performed at the critical locations established in Section 5.1. The elastic-plastic fracture mechanics (EPFM) J-integral analyses for through-wall circumferential cracks in a cylinder were performed using the procedure in the EPRI fracture mechanics handbook (Reference 7-2).

The lower-bound material properties of Section 4.0 were applied (see Table 4-3). The fracture toughness properties established in Section 4.3 and the normal plus SSE loads given in Table 3-2 were used for the EPFM calculations. Evaluations were performed at the toughness critical locations identified in Section 5.1. The results of the elastic-plastic fracture mechanics J-integral evaluations are given in Table 7-1.

The critical locations were also identified in Section 5.1. A stability analysis based on limit load was performed for these locations as described in Section 7.2. The welds at these locations are assumed conservatively as SAW weld (SAW gives highest "Z" factor correction). The "Z" factor correction for SAW was applied (Reference 7-3) as follows:

$$Z = 1.30 [1.0 + 0.010 (OD-4)]$$

where OD is the outer diameter of the pipe in inches.

The Z-factors were calculated for the critical locations, using the dimensions given in Table 3-1. The Z factor was 1.69 for locations 1 and 2. The Z factor was 1.67 for location 11. Table 7-2 summarizes the results of the stability analyses based on limit load. The leakage size flaws are presented on the same table.

7.4 REFERENCES

- 7-1 Kanninen, M. F., et. al., "Mechanical Fracture Predictions for Sensitized Stainless Steel Piping with Circumferential Cracks," EPRI NP-192, September 1976.
- 7-2 Kumar, V., German, M. D. and Shih, C. P., "An Engineering Approach for Elastic-Plastic Fracture Analysis," EPRI Report NP-1931, Project 1237-1, Electric Power Research Institute, July 1981.
- 7-3 Standard Review Plan; Public Comment Solicited; 3.6.3 Leak-Before-Break Evaluation Procedures; Federal Register /Vol. 52, No. 167/Friday, August 28, 1987/Notices, pp. 32626-32633.

Table 7-1
Stability Results for Turkey Point Units 3 and 4
Based on Elastic-Plastic J-Integral Evaluations

a,c,e

Table 7-2
Stability Results for Turkey Point Units 3 and 4
Based on Limit Load

a,c,e

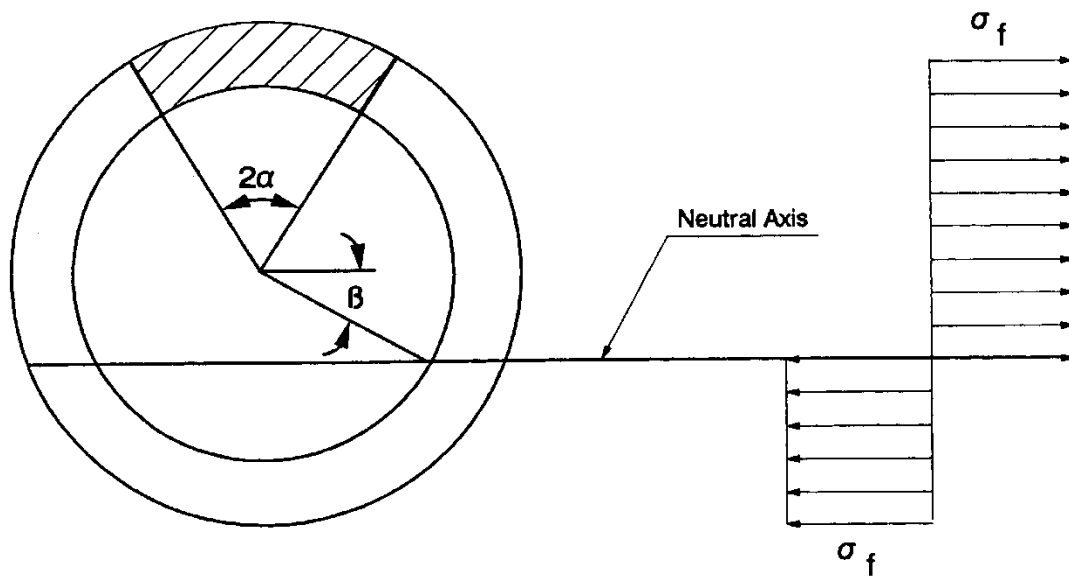


Figure 7-1 []^{a,c,e} Stress Distribution

8.0 FATIGUE CRACK GROWTH ANALYSIS

To determine the sensitivity of the primary coolant system to the presence of small cracks, a plant specific fatigue crack growth analysis for 60 year plant service was carried out in Revision 0 of WCAP-15354 report, for the []^{a,c,e} region (see Location []^{a,c,e} of Figure 3-2). This region was selected because crack growth calculated here will be typical (i.e. the design transient thermal and pressure stresses will be representative) of that in the entire primary loop. The crack growth at the []^{a,c,e} will demonstrate that small surface flaws would not develop to through-wall flaws during the plant design life. Crack growths calculated at other locations can be expected to show less than 10% variation.

Also, in Revision 0 of WCAP-15354 report, Westinghouse performed an investigation (Reference 8-1) to predict the transients and cycles for the 60 year plant service of Turkey Point Units 3 and 4. This was done by reviewing the actual plant operating transient severity and the frequency of occurrences. Reference 8-1 concluded that the design transients and cycles of the Turkey Point Units 3 and 4 for the 60 year plant service are bounded by the 40 year design plant service transient and cycles. The main conclusions derived from Reference 8-1 was that the number of cycles predicted for the 60 year plant service are still less than the design basis cycles. Reference 8-2 shows the uprating transients for Turkey Point Units 3 and 4. By reviewing References 8-1 and 8-2 all the significant normal, upset and test conditions were considered for the plant specific fatigue crack growth analysis. A summary of applied transients is provided in Table 8-1. The list of transient/cycles in Table 8-1 that was originally applicable for 60 years of plant service has been compared with the transients list for 80 years of plant service. The comparison shows that 60 year transient/cycles as shown in Table 8-1 remains applicable and bounding for 80 years of plant service transient/cycles. Therefore, the FCG evaluation provided herein for Turkey Point will remain applicable for 80 years of plant service transient/cycles as well.

A brief summary of the FCG evaluation is provided herein. It should be noted that circumferentially oriented surface flaws were postulated in the region of interest at the []^{a,c,e}. The postulated flaw was located in two different locations, as shown in Figure 8-1. Specifically, these were:

Cross Section A: []^{a,c,e}

Cross Section B: []^{a,c,e}

Fatigue crack growth rate laws were used []

[]^{a,c,e} For stainless steel, the fatigue crack growth formula is:

[]

] ^{a,c,e}

The calculated fatigue crack growth for semi-elliptic surface flaws of circumferential orientation and various depths is summarized in Table 8-2, and shows that the crack growth is very small, regardless of which material is assumed. It is therefore concluded that the generic fatigue crack growth analysis shown in Table 8-2 is representative of the Turkey Point plants for 80 years of operations.

It should be noted that the fatigue crack growth evaluation is a defense in depth review, and it is no longer a requirement for the leak-before-break (LBB) analysis, since the LBB analysis is based on the postulation of through-wall flaw, whereas the FCG analysis is performed based on the surface flaw. In addition Reference 8-4 has indicated that, "the Commission deleted the fatigue crack growth analysis in the proposed rule. This requirement was found to be unnecessary because it was bounded by the crack stability analysis." Nevertheless, the fatigue crack growth analysis is retained herein for information purposes to show that small surface flaws do not result in through-wall flaws over the life of the plant.

8.1 REFERENCES

- 8-1 WCAP-15370, "Turkey Point Units 3 and 4 Design Basis Transient Evaluation for License Renewal," January 2000.
- 8-2 WCAP-14291, "Turkey Point Units 3 and 4 Upgrading Engineering Report," December 1995.
- 8-3 Bamford, W. H., "Fatigue Crack Growth of Stainless Steel Piping in a Pressurized Water Reactor Environment," Trans. ASME Journal of Pressure Vessel Technology, Vol. 101, Feb. 1979.
- 8-4 Nuclear Regulatory Commission, 10 CFR 50, Modification of General Design Criteria 4 Requirements for Protection Against Dynamic Effects of Postulated Pipe Ruptures, Final Rule, Federal Register/Vol. 52, No. 207/Tuesday, October 27, 1987/Rules and Regulations, pp. 41288-41295.

Table 8-1 Summary of Reactor Vessel Transients for Turkey Point Units 3 and 4		
Number	Typical Transient Identification	Number of Cycles
	<u>Normal Conditions</u>	
1	Heatup and Cooldown at 100°F / hr	200
2	Plant Loading/Unloading at 5% of full power / min.	14500
3	10% Step Load Increase/Decrease	2000
4	Large Step Load Decrease	200
5	Steady State Fluctuation (Initial)	150000
6	Steady State Fluctuation (Random)	3000000
7	Feedwater Cycling/Hot Standby	2000
8	Boron Concentration Equalization	36000
9	Refueling	80
	<u>Upset Conditions</u>	
10	Loss of Load	80
11	Loss of Power	40
12	Reactor Trip	400
13	Loss of Flow	80
14	Inadvertent Auxiliary Spray	10
	<u>Test Conditions</u>	
15	Plant Hydrostatic Turbine Test (cold)	5
16	Plant Hydrostatic Test (hot)	5

Table 8-2
Typical Fatigue Crack Growth at [

]^{a,c,e}

FINAL FLAW (in.)

a,c,e



Figure 8-1 Typical Cross-Section of [**]**^{a,c,e}

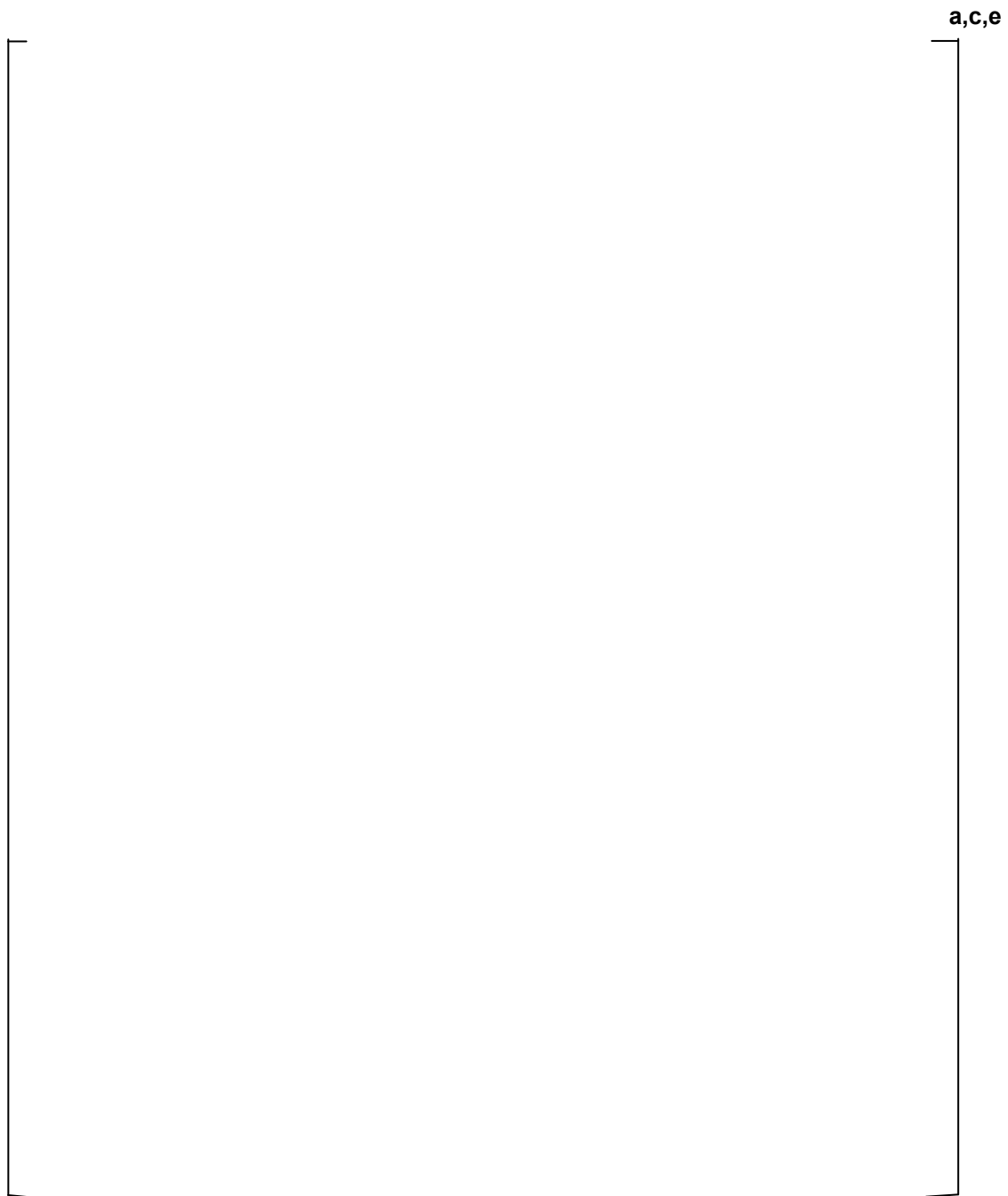


Figure 8-2 Reference Fatigue Crack Growth Curves for [
]^{a,c,e}

9.0 ASSESSMENT OF MARGINS

The results of the leak rates of Section 6.4 and the corresponding stability and fracture toughness evaluations of Sections 7.1, 7.2 and 7.3 are used in performing the assessment of margins. Margins are shown in Table 9-1. All of the LBB recommended margins are satisfied.

In summary, at all the critical locations relative to:

1. Flaw Size - Using faulted loads obtained by the absolute sum method, a margin of 2 or more exists between the critical flaw and the flaw having a leak rate of 10 gpm (the leakage flaw).
2. Leak Rate - A margin of 10 exists between the calculated leak rate from the leakage flaw and the plant leak detection capability of 1 gpm.
3. Loads - At the critical locations the leakage flaw was shown to be stable using the faulted loads obtained by the absolute sum method (i.e., a flaw twice the leakage flaw size is shown to be stable; hence the leakage flaw size is stable). A margin of 1 on loads using the absolute summation of faulted load combinations is satisfied.

Table 9-1
Leakage Flaw Sizes, Critical Flaw Sizes and Margins for Turkey Point Units 3 and 4

a,c,e

10.0 CONCLUSIONS

This report justifies the elimination of RCS primary loop pipe breaks from the structural design basis for the 80 year plant service of Turkey Point Units 3 and 4 as follows:

- a. Stress corrosion cracking is precluded by use of fracture resistant materials in the piping system and controls on reactor coolant chemistry, temperature, pressure, and flow during normal operation. There is no Alloy 82/182 material present in the welds for the Turkey Point Units 3 and 4 Reactor Coolant System (RCS) primary loop piping.
- b. Water hammer should not occur in the RCS piping because of system design, testing, and operational considerations.
- c. The effects of low and high cycle fatigue on the integrity of the primary piping are negligible.
- d. Ample margin exists between the leak rate of small stable flaws and the capability of the Turkey Point Units 3 and 4 reactor coolant system pressure boundary Leakage Detection System.
- e. Ample margin exists between the small stable flaw sizes of item (d) and larger stable flaws.
- f. Ample margin exists in the material properties used to demonstrate end-of-service life (fully aged) stability of the critical flaws.

For the critical locations, postulated flaws will be stable because of the ample margins described in d, e, and f above.

Based on the above, the leak-before-break conditions and margins are satisfied for the Turkey Point Units 3 and 4 primary loop piping. All the recommended margins are satisfied. It is therefore concluded that dynamic effects of RCS primary loop pipe breaks need not be considered in the structural design basis for Turkey Point Units 3 and 4 Nuclear Power Plants for 80 years of plant service (Subsequent License Renewal Time-Limited Aging Analysis Program).

APPENDIX A: LIMIT MOMENT

[

$J^{a,c,e}$



Figure A-1 Pipe with a Through-Wall Crack in Bending

Enclosure 4
Non-proprietary Reference Documents
and
Redacted Versions of Proprietary
Reference Documents
(Public Version)
Attachment 12

SIA Leak-Before-Break Evaluation for Auxiliary Lines

0901350.401, Revision 3

Leak-Before-Break Evaluation Accumulator, Pressurizer Surge and
Residual Heat Removal Lines Turkey Point Units 3 and 4, September
2017

0901350.304, Revision 3

Fatigue Crack Growth Evaluation, September 18, 2017

(149 Total Pages, including cover sheets)

Report No.: 0901350.401
Revision No.: 3
Project No.: 1700109
File No.: 0901350.401
Sept 2017

**Leak-Before-Break Evaluation
Accumulator, Pressurizer Surge and Residual Heat Removal Lines
Turkey Point Units 3 and 4**

Prepared for:

Florida Power & Light Company
Purchase Order No. 2000230248

Prepared by:

Structural Integrity Associates, Inc.
San Jose, California

Prepared by: Wilson Wong
Wilson Wong

Date: 09/18/17

Reviewed by: Do Jun Shim
Do Jun Shim

Date: 09/18/17

Reviewed &

Approved by: Gary L. Stevens
Gary L. Stevens, P.E.

Date: 09/18/17

REVISION CONTROL SHEET

Document Number: 0901350.401

Title: Leak-Before-Break Evaluation, Accumulator, Pressurizer Surge and Residual Heat
Removal Lines, Turkey Point Units 3 and 4

Client: Florida Power & Light Company

SI Project Number: 1700109

Section	Pages	Revision	Date	Comments
Summary 1.0 2.0 3.0 4.0 5.0 6.0 7.0 8.0	iii – x 1-1 – 1-7 2-1 – 2-2 3-1 – 3-3 4-1 – 4-15 5-1 – 5-18 6-1 – 6-13 7-1 – 7-2 8-1 – 8-5	0	4/15/2010	INITIAL ISSUE
3.0 4.0 5.0 6.0 8.0	3-2 4-1, 4-6 5-5, 5-6, 5-13 – 5-19 6-4 8-4	1	5/6/2010	Clients' Comments Addressed
Summary 1.0 6.0 7.0 8.0	v, viii-x 1-1 6-1 – 6-14 7-1 – 7-2 8-4 – 8-5	2	7/10/2017	Updated 60-year results in response to CAR 17-012. Extended evaluation to cover 80 years of operation and to use updated fatigue crack growth law.
Summary 1.0 2.0 3.0 4.0 5.0 6.0 7.0	v 1-1, 1-3 2-1 3-1, 3-2, 3-3 4-2 – 4-5, 4-9, 4-10 5-1 6-2, 6-5, 6-8 – 6-10, 6-13 7-1	3	9/18/2017	Addressed client editorial comments

SUMMARY

This report presents a leak-before-break (LBB) evaluation for the following lines at Turkey Point Nuclear Plant (PTN) Units 3 and 4 operated by Florida Power & Light Company (FPL). These lines are attached to the reactor coolant loop (RCL) and span from the connection to the RCL to the first isolation valve or the pressurizer as applicable:

1. 10" diameter Accumulator Lines – 3 lines (one per RCL connected to cold leg)
2. 12" pressurizer Surge Line – 1 line attached to "B" loop
3. 14" residual heat removal line – 1 line attached to "C" loop in Unit 3 and "A" loop in Unit 4 (connected to hot leg)

The evaluation was performed to eliminate consideration of the dynamic effects of the postulated large pipe rupture for these lines. The LBB evaluation was performed in accordance with the 10 CFR 50, Appendix A GDC-4 and NUREG-1061, Vol. 3 [6] as supplemented by NUREG-0800, Standard Review Plan 3.6.3 [7].

The methodology used in determining LBB capabilities of the above lines at PTN Units 3 and 4 consisted of several steps. First, the relationship between the critical through-wall flaw length and the applied stress (or moments) was determined on a generic basis for circumferential flaws. The critical flaw size as used herein refers to the through-wall flaw length that becomes unstable under a given set of applied loads. Critical flaw sizes were calculated using the net limit load (net section plastic collapse) approach with conservative material properties. NUREG-1061[6] requires that the load combination considered in determining the through-wall flaw length include the normal operating loads (NOP), which consists of internal pressure, dead weight, and thermal expansion loads, plus the safe shutdown earthquake (SSE). Once the NOP+SSE load for a given location is known, the critical flaw length can be determined from the generic relationship. The "leakage flaw size" was determined as the minimum of one half the critical flaw size with a factor of unity on normal operating plus SSE loads. Thus, the leakage flaw size as referred herein maintains a safety factor of 2 on the critical flaw size under normal plus SSE loads.

Leakage rates were determined as a function of stress (or moment) on a generic basis for a given through-wall flaw length. NUREG-1061, Vol. 3 [6] requires that the NOP loads be used to determine the leakage. On a generic basis, a family of curves was developed relating the leakage with the NOP loads to the through-wall flaw length.

Given the relationships between the leakage flow size versus NOP+SSE moments and leakage flow size versus NOP moments above (for a particular leak rate), a relationship was developed between the NOP+SSE moments and the NOP moments that would result in a particular leak rate. This results in the bounding analysis curve (BAC). The actual piping NOP+SSE and NOP loads were then used to determine if the combination of those loads would meet that leakage (fall below the BAC). This particular scheme is very convenient for determining whether or not a particular leakage will be met for a piping system with many nodal points and associated moments, such as the auxiliary RCL piping lines considered in this evaluation.

A fatigue crack growth analysis was also performed to determine the growth of postulated semi-elliptical, inside surface flaws with an initial size based on ASME Code, Section XI [26] acceptance standards. This showed that crack growth due to cyclic loadings was not significant such that it could be managed by the Section XI inspection program. In addition, a fatigue crack growth analysis was performed to show that a through-wall crack would not grow significantly, hereby, insuring that the leakage size flaw will not grow to the critical crack size.

The following summary of the LBB evaluation is formatted along the lines of the “Recommendations for Application of the LBB Approach” in the NUREG-1061 Vol. 3 [6] executive summary:

- (a) The three piping systems considered in this evaluation are constructed of A 376 Type 316 stainless steel piping. At the operating temperature of these piping lines of 550°F to 653°F, this material is very ductile and it is not susceptible to cleavage-type fracture. In addition, these systems have been shown not to be susceptible to the effects of corrosion, high cycle fatigue or water hammer.

- (b) Loadings have been determined from the original piping analysis, and are based upon pressure, dead weight, thermal expansion, and safe shutdown earthquake. All stress locations in these piping systems from the connection to the RCL to the first isolation valve or pressurizer, as applicable, were considered.
- (c) Minimum ASME Code material properties were used to establish conservative lower bound stress-strain properties to be used in the evaluations. For the fracture toughness properties, lower-bound generic industry material properties for the piping and welds have been conservatively used in the evaluations.
- (d) Crack growth analysis was conducted at the most critical locations on the evaluated piping, considering the cyclic stresses predicted to occur over the life of the plant. For a hypothetical flaw with aspect ratio of 10:1 and an initial flaw depth of 12.5% of pipe wall, the final flaw size after considering all plant transients for both 60 years and 80 years of operation is less than ASME Code Section XI allowable flaw size of 75%. Hence, fatigue crack growth is well within the allowable flaw size for the auxiliary RCL piping.
- (e) The LBB evaluation is performed for leakage rates of 2 GPM (gallons per minute), 5 GPM and 10 GPM. All piping locations considered in the evaluation exhibit a minimum leakage rate of 10 GPM based on the normal operating and normal plus dynamic loads. NUREG-1061 Vol. 3 recommends that the leakage detection system be capable of measuring leakage rates 1/10 of the minimum leakage rate. The plant leak detection capability for both Units 3 and 4 is 1 GPM [8], thereby satisfying the leakage rate requirement.
- (f) Each of the piping systems considered in this evaluation is less than 51.2 feet in length and is not geometrically complex.

- (g) Crack growth of a leakage size crack in the length direction due to a seismic event was small compared to the total circumference and insignificant compared to the margin between the leakage-size crack size and the critical crack size.
- (h) For all locations, the critical size circumferential crack was determined for the combination of absolute values of normal operating plus SSE loads. The leakage size flaw was chosen such that its length was no greater than the critical crack size reduced by a factor of two for conservatism. Axial cracks were not considered as they are known to exhibit much higher leakage and more margin than circumferentially oriented cracks.
- (i) Another LBB acceptance criterion is, for all locations, determine the critical crack size for the combination of 1.4 times the normal plus SSE loads and select the leakage crack no greater than this critical crack size. Based on previous experience, this criterion is always bounded by the criterion of (h) above. Hence, in this evaluation, only the evolution based on criterion of (h) is performed.
- (j-n) No special testing was conducted to determine material properties for fracture mechanics evaluation. Instead, ASME Code minimum properties were utilized in the evaluations. The material properties so determined have been shown to be applicable near the upper range of normal plant operation and exhibit ductile behavior at these temperatures.
- (o) Limit load analysis as outlined in NUREG-0800, SRP 3.6.3, was utilized in this evaluation in order to determine the critical flaw sizes since the materials involved in this evaluation are stainless steel piping.

Thus, the three piping systems evaluated in this report for PTN Units 3 and 4 qualify for the application of leak-before-break analysis to demonstrate that it is very unlikely that the piping could experience a large pipe break prior to leakage detection. Results of the evaluation show that for all applicable pipe stresses, leak-before-break can be justified for a plant leak detection system of 1 GPM.

Table of Contents

<u>Section</u>	<u>Page</u>
1.0 INTRODUCTION	1-1
1.1 Background	1-1
1.2 Leak-Before-Break Methodology	1-2
1.3 Leak Detection Requirement	1-4
2.0 CRITERIA FOR APPLICATION OF LEAK-BEFORE-BREAK	2-1
2.1 Criteria for Through-Wall Flaws	2-1
2.2 Criteria for Part-Through-Wall Flaws	2-2
2.3 Consideration of Other Mechanisms	2-2
3.0 CONSIDERATION OF WATER HAMMER, CORROSION AND FATIGUE	3-1
3.1 Water Hammer	3-1
3.2 Corrosion	3-2
3.3 Fatigue	3-3
4.0 PIPING MATERIALS AND STRESSES	4-1
4.1 Piping System Description, Operating Conditions and Geometry	4-1
4.1.1 Accumulator Lines	4-1
4.1.2 Pressurizer Surge Line	4-1
4.1.3 RHR Line	4-2
4.2 Material Properties	4-2
4.2.1 Calculation of Z Factors for Fracture Mechanics Analysis	4-3
4.2.2 Determination of Ramberg-Osgood Material Parameters	4-3
4.3 Applicable Stresses	4-4
5.0 LEAK-BEFORE-BREAK EVALUATION	5-1
5.1 Evaluation of Critical Flaw Sizes	5-1
5.2 Leak Rate Determination	5-3
5.3 Bounding Analysis Curves	5-4
5.4 LBB Evaluation Results and Discussions	5-6
6.0 EVALUATION OF FATIGUE CRACK GROWTH OF SURFACE FLAWS	6-1
6.1 Plant Transients	6-1
6.2 Stresses for Crack Growth Evaluation	6-1
6.3 Allowable Flaw Size	6-3
6.4 Fatigue Crack Growth Analysis	6-4
6.4.1 Fatigue Crack Growth Law Used for 60-Year Operation Calculations	6-4
6.4.2 Fatigue Crack Growth Law Used for 80-Year Operation Calculations	6-5
6.4.3 Part Through-Wall Crack Growth	6-6
6.4.4 Through-Wall Crack Growth	6-6
7.0 CONCLUSIONS	7-1
8.0 REFERENCES	8-1

List of Tables

<u>Table</u>	<u>Page</u>
Table 4-1. Normal Operating Conditions for Leakage Evaluation.....	4-6
Table 4-2: Operating Conditions for Critical Flaw Size Evaluation.....	4-6
Table 4-3: Pipe Geometry Inputs for Leakage Evaluation	4-6
Table 4-4: Pipe Geometry Inputs for Critical Flaw Size Evaluation	4-7
Table 4-5: ASME Code Strength at Normal Operating Temperatures for Leakage Calculation.....	4-7
Table 4-6: ASME Code Strength at Normal Operating Temperatures for Critical Flaw Size Calculation	4-8
Table 4-7: Ramberg-Osgood Parameters for Leakage Calculation	4-8
Table 4-8. Load Points for Accumulator Lines	4-9
Table 4-9. Load Points for RHR Lines	4-11
Table 4-10. Loads for Units 3 and 4 Pressurizer Surge Lines	4-11
Table 6-1. Accumulator Line Operating Condition Transients ¹	6-9
Table 6-2. RHR Line Operating Condition Transients [33]	6-9
Table 6-3 Surge Line Operating Condition Transients [57]	6-10
Table 6-4. Piping Loads for Accumulator and RHR Lines	6-11
Table 6-5. Accumulator Line Maximum and Minimum Transient Stresses	6-11
Table 6-6. RHR Line Maximum and Minimum Transient Stresses	6-11
Table 6-7. Stress Range for Accumulator Line	6-12
Table 6-8. Stress Range for RHR Line	6-12
Table 6-9. Stress Range for Surge Line	6-13
Table 6-10. Results of Fatigue Crack Growth Analysis	6-13

List of Figures

<u>Figure</u>	<u>Page</u>
Figure 1-1. Representation of Postulated Cracks in Pipes for Fracture Mechanics Leak-Before-Break Analysis.....	1-5
Figure 1-2. Conceptual Illustration of ISI (UT)/Leak Detection Approach to Protection Against Pipe Rupture	1-6
Figure 1-3. Leak-Before-Break Approach Based on Fracture Mechanics Analysis with In-service Inspection and Leak Detection	1-7
Figure 4-1. Schematic of Piping Model and Selected Node Points for Accumulator Lines (Loops A, B and C), PTN Unit 3 [34, 35, 36].....	4-12
Figure 4-2. Schematic of Piping Model and Selected Node Points for Accumulator Lines (Loops A, B and C), PTN Unit 4 [39, 40, 41].....	4-13
Figure 4-3. Schematic of Piping Model and Selected Node Points for Pressurizer Surge Line, PTN Unit 3 [38].....	4-14
Figure 4-4. Schematic of Piping Model and Selected Node Points for Pressurizer Surge Line, PTN Unit 4 [43].....	4-14
Figure 4-5. Schematic of Piping Model and Selected Node Points for RHR Line, PTN Unit 3 [37].....	4-15
Figure 4-6. Schematic of Piping Model and Selected Node Points for RHR Line, PTN Unit 4 [42].....	4-15
Figure 5-1. Leakage Flaw Size versus Normal Operating Stress of Accumulator Lines	5-7
Figure 5-2. Leakage Flaw Size versus Normal Operating Stress of Pressurizer Surge Lines (Pipe Side at Pressurizer End).....	5-8
Figure 5-3. Leakage Flaw Size versus Normal Operating Stress of Pressurizer Surge Lines (Nozzle Side at Pressurizer End)	5-9
Figure 5-4. Leakage Flaw Size versus Normal Operating Stress of Pressurizer Surge Line (Nozzle Side at Hot Leg End).....	5-10
Figure 5-5. Leakage Flaw Size versus Normal Operating Stress of Pressurizer Surge Line at Hot Leg End.....	5-11
Figure 5-6. Leakage Flaw Size versus Normal Operating Stress of RHR Line at Hot Leg End	5-12
Figure 5-7. BACs and Load Points for Accumulator Lines.....	5-13
Figure 5-8. BACs and Load Points for RHR Lines	5-14
Figure 5-9. BACs and Load Points for Pressurizer Surge Lines (Nozzle Side at Pressurizer End).....	5-15
Figure 5-10. BACs and Load Points for Pressurizer Surge Line (Nozzle Side at Hot Leg End).....	5-16
Figure 5-11. BACs and Load Points for Pressurizer Surge Lines (Pipe Side at Pressurizer End).....	5-17
Figure 5-12. BACs and Load Points for Pressurizer Surge Lines (Pipe Side at Hot Leg End).....	5-18
Figure 5-13. 10 GPM BAC Curve for Pipe/Elbow of Accumulator Lines.....	5-19

1.0 INTRODUCTION

1.1 Background

In 2009, Florida Power & Light Company (FPL) embarked on an Extended Power Uprate (EPU) project at Turkey Point Nuclear Plant (PTN) Units 3 and 4. Prior to EPU implementation, each of the PTN units was licensed to a core power rating of 2300 MWth. The EPU resulted in a new core power rating of 2644 MWth at PTN, which includes a 1.7% Measurement Uncertainty Recapture (MUR) [1]. Reactor coolant loop (RCL) pipe break design basis scenarios generally produce large hydrodynamic loads that must be considered in the design of plant safety systems. At PTN, the leak-before-break (LBB) methodology was applied to the primary RCL piping and approved by the US Nuclear Regulatory Commission (NRC). Branch lines connected to the RCL also benefit from the use of LBB methodology, which eliminates from the plant design basis the consideration of those auxiliary pipe break loads.

This report documents evaluations performed by Structural Integrity Associates (SIA) to determine LBB capabilities of the high energy, non-isolable, auxiliary piping attached to the RCL at PTN Units 3 and 4. In this revision of the report, the previous fatigue crack growth evaluation for 60 years is updated to use the current version of the **pc-CRACK** software (**pc-CRACK 4.1** [49a]) and to correct for the errors documented in Corrective Action Report (CAR) 17-012 [54]. The new fatigue crack growth results are shown in Table 6-10. Also, fatigue crack growth for 80 years of operation is added to address Subsequent License Renewal (SLR) operation utilizing the updated ASME Code Case N-809 [53] fatigue crack growth rate.

The following lines at PTN Units 3 and 4 are considered in this evaluation.

1. 10" diameter Accumulator Lines – 3 lines (one per RCL connected to cold leg)
2. 12" pressurizer Surge Line – 1 line attached to "B" loop
3. 14" residual heat removal line – 1 line attached to "C" loop in Unit 3 and "A" loop in Unit 4 (connected to hot leg)

The approach taken to address LBB for the lines at PTN delineated above is consistent with that used by SI in recent LBB submittals for other plants [2, 3, 4].

1.2 Leak-Before-Break Methodology

NRC SECY-87-213 [5] covers a rule to modify General Design Criterion 4 (GDC-4) of Appendix A, 10 CFR Part 50. This amendment to GDC-4 allows exclusion from the design basis of all dynamic effects associated with high energy pipe rupture by application of LBB technology.

Definition of the LBB approach and criteria for its use are provided in NUREG-1061 [6], supplemented by NUREG-0800, SRP 3.6.3 [7]. Volume 3 of NUREG-1061 defines LBB as "...the application of fracture mechanics technology to demonstrate that high energy fluid piping is very unlikely to experience double-ended ruptures or their equivalent as longitudinal or diagonal splits." The particular crack types of interest include circumferential through-wall cracks (TWC) and part-through-wall cracks (PTWC), as well as axial or longitudinal through-wall cracks (TWC), as shown in Figure 1-1.

LBB is based on a combination of in-service inspection (ISI) and leak detection to detect cracks, coupled with fracture mechanics analysis to show that pipe rupture will not occur for cracks smaller than those detectable by these methods. A discussion of the criteria for application of LBB is presented in Section 2 of this report, which summarizes NUREG-1061, Vol. 3 requirements.

The approach to LBB which has gained acceptance for demonstrating protection against high energy line break (HELB) in safety-related nuclear piping systems is schematically illustrated in Figure 1-2. Essential elements of this technique include critical flaw size evaluation, crack propagation analysis, volumetric nondestructive examination (NDE) for flaw detection/sizing, leak detection, and service experience. In Figure 1-2, a limiting circumferential crack is modeled as having both a short through-wall component, or an axisymmetric part-through-wall crack component. Leak detection establishes an upper bound for the through-wall crack component while volumetric ISI limits the size of undetected part-through-wall defects. These detection methods

complement each other, since volumetric NDE techniques are well suited to the detection of long cracks while leakage monitoring is effective in detecting short through-wall cracks. The level of NDE required to support LBB involves volumetric inspection at intervals determined by fracture mechanics crack growth analysis, which would preclude the growth of detectable part-through-wall cracks to a critical size during an inspection interval. A fatigue evaluation is performed to ensure that an undetected flaw acceptable per ASME Section III will not grow significantly during service. For through-wall defects, crack opening areas and resultant leak rates are compared with leak detection limits.

The net effect of complementary leak detection and ISI is illustrated by the shaded region of Figure 1-2 as the largest undetected defect that can exist in the piping at any given time. Critical flaw size evaluation, based on elastic-plastic fracture mechanics techniques, is used to determine the length and depth of defects that would be predicted to cause pipe rupture under specific design basis loading conditions, including abnormal conditions such as a seismic event and including appropriate safety margins for each loading condition. Crack propagation analysis is used to determine the time interval in which the largest undetected crack could grow to a size which would impact plant safety margins. A summary of the elements for a leak-before-break analysis is shown in Figure 1-3. Service experience, where available, is useful to confirm analytical predictions as well as to verify that such cracking tends to develop into "leak" as opposed to "break" geometries.

In accordance with NUREG-1061, Vol. 3 [6] and NUREG-0800, SRP 3.6.3 [7], the leak-before-break technique for the high energy piping systems evaluated in this report included the following considerations.

- Elastic-plastic fracture mechanics analysis of load carrying capacity of cracked pipes under worst case normal loading, with safe-shutdown earthquake (SSE) and other dynamic loads included. Such analysis includes elastic-plastic fracture data applicable to pipe weldments and weld heat affected zones where appropriate. In this evaluation, elastic-plastic fracture mechanics (EPFM) was not applied.

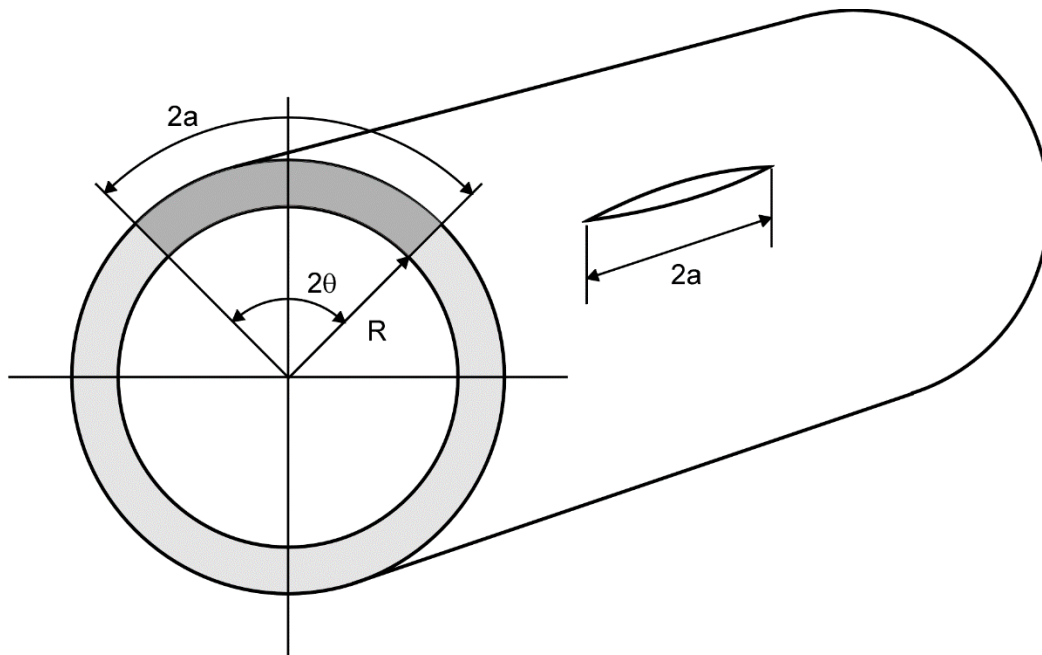
- Limit-load analysis in lieu of the elastic-plastic fracture mechanics analysis described above can be used to determine critical flaw sizes. Because the material for all the piping systems considered in this evaluation is stainless steel, limit load analysis was used.
- Linear elastic fracture mechanics analysis of subcritical crack propagation to determine ISI (in-service inspection) intervals for long, part-through-wall cracks.

Piping stresses have a dual role in LBB evaluations. On one hand, higher maximum (design basis) stresses tend to yield lower critical flaw sizes, which result in smaller flaw sizes for assessing leakage. On the other hand, higher operating stresses tend to open cracks more for a given crack size and create a higher leakage rate. Because of this duality, the use of a single maximum stress location for a piping system may result in a non-conservative LBB evaluation. Thus, the LBB evaluation reported herein has been performed for each nodal location addressed in the plant piping system analysis for the affected portions.

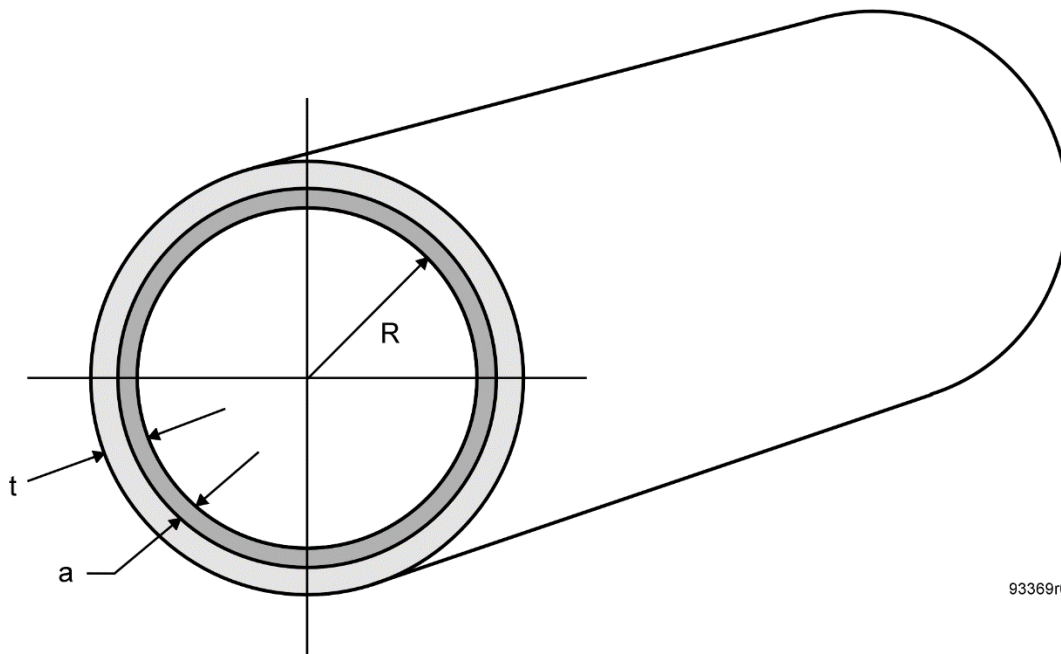
1.3 Leak Detection Requirement

Application of LBB evaluation methodology is predicated on having a very reliable leak detection system at the plant. This evaluation will determine the minimum leakage rate based on the normal operating and normal plus dynamic loads for the five auxiliary RCL piping lines in each Units 3 and 4. NUREG-1061 requires the demonstration of leak detection capability of leak rates of 1/10 of this amount. Per reference 8, the leak detection system at PTN is capable of detecting 1 GPM.

FPL is committed to US Nuclear Regulatory Commission (NRC) Generic Letter (GL) 84-04 [52] which considers a four hour response time for detecting 1 GPM leak rate.

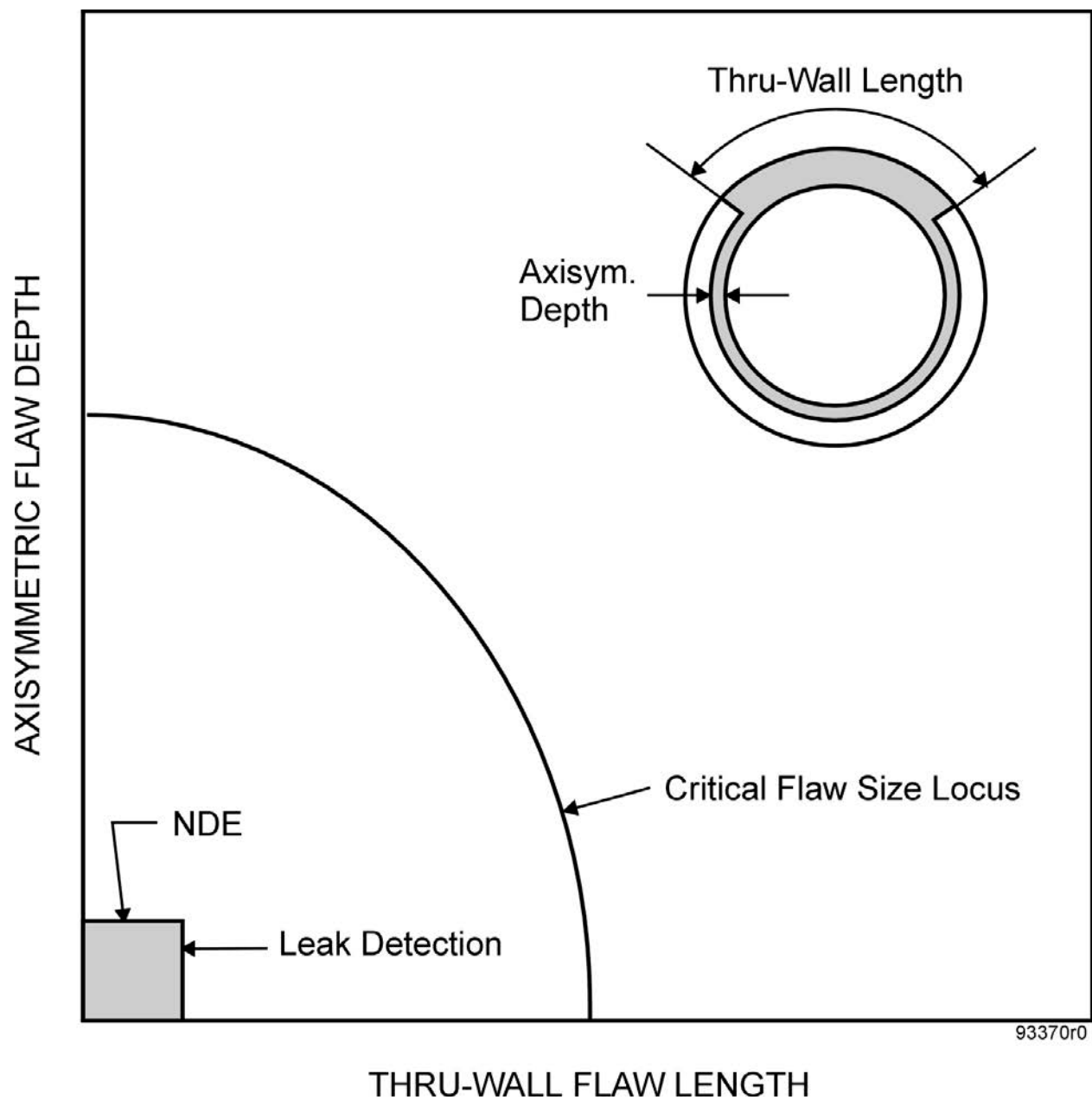


a. Circumferential and Longitudinal Through-Wall Cracks of Length $2a$.



b. Circumferential 360° Part-Through-Wall Crack of Depth a .

Figure 1-1. Representation of Postulated Cracks in Pipes for Fracture Mechanics Leak-Before-Break Analysis



93370r0

Figure 1-2. Conceptual Illustration of ISI (UT)/Leak Detection Approach to Protection Against Pipe Rupture

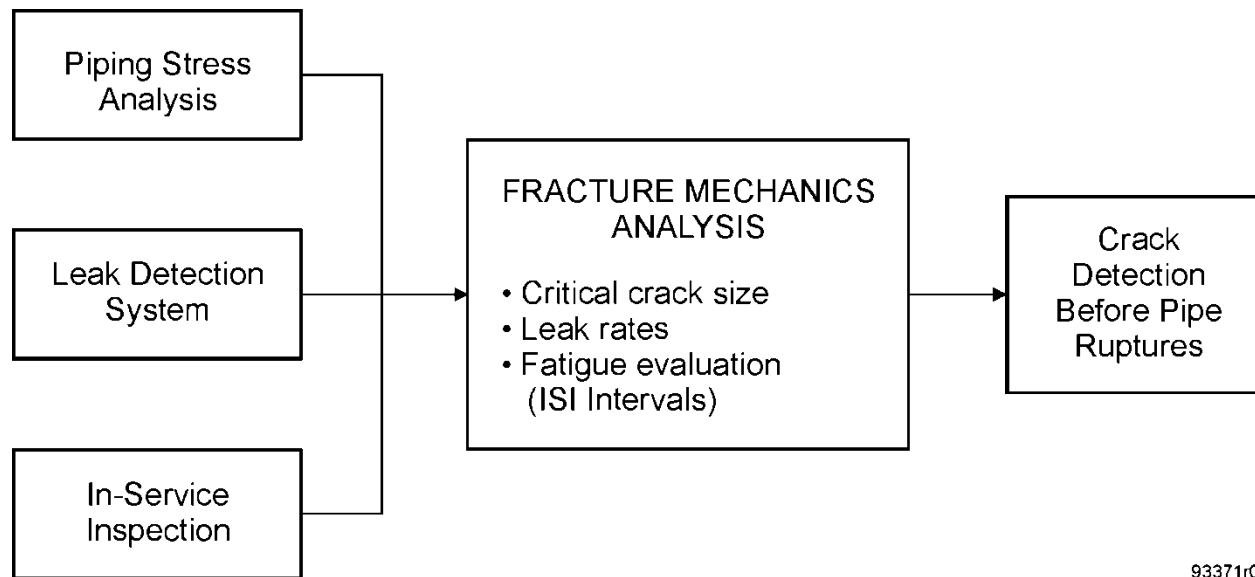


Figure 1-3. Leak-Before-Break Approach Based on Fracture Mechanics Analysis with In-service Inspection and Leak Detection

2.0 CRITERIA FOR APPLICATION OF LEAK-BEFORE-BREAK

NUREG-1061, Vol. 3 [6] identifies several criteria to be considered in determining applicability of the leak-before-break approach to piping systems. Section 5.2 of NUREG-1061, Vol. 3 provides extensive discussions of the criteria for performing leak-before-break analyses. These requirements are restated in NUREG-0800, SRP 3.6.3 [7]. The details of the discussions are not repeated here; the following summarizes the key elements:

2.1 Criteria for Through-Wall Flaws

Acceptance criteria for critical flaws may be stated as follows:

1. A critical flaw size shall be determined for normal operating conditions plus safe shutdown earthquake (SSE) loads. Leakage for normal operating conditions must be detectable for this flaw size reduced by a factor of two.
2. A critical flaw size shall be determined for normal operating conditions plus SSE loads multiplied by a factor of $\sqrt{2}$. Leakage for normal operating conditions must be detectable for this flaw size.

Previous evaluations conducted by Structural Integrity Associates (SIA) have found through experience from previous LBB analyses that the first criterion bounds the second. Hence, in this evaluation, only the first criterion was considered. Previous evaluations have found that the critical through-wall flaw length for an axial flaw is always greater than that of a circumferential flaw. Also, the higher hoop stress results in more leakage for an axial flaw compared to a circumferential flaw of the same length. Since axial flaws have both a larger critical through wall flaw length and more leakage for a given flaw size compared to circumferential flaws, only circumferential flaws are considered in this evaluation.

Either elastic-plastic fracture mechanics instability analysis or limit load analysis may be used in determining critical flaw sizes. Since the material of the piping systems considered at PTN is stainless steel, which is ductile at high temperatures, the limit load methodology is used in this evaluation to determine the critical flaw sizes.

2.2 Criteria for Part-Through-Wall Flaws

NUREG-1061, Vol. 3 [6] requires demonstration that a long part-through-wall flaw which is detectable by ultrasonic means will not grow due to fatigue to a depth which would produce instability over the life of the plant. This is demonstrated in Section 6.0 of this report, where the analysis of subcritical crack growth is discussed.

2.3 Consideration of Other Mechanisms

NUREG-1061, Vol. 3 [6] limits applicability of the leak-before-break approach to those locations where degradation or failure by mechanisms such as water hammer, erosion/corrosion, fatigue, and intergranular stress corrosion cracking (IGSCC) is not a significant possibility. These mechanisms were considered for the auxiliary RCL piping at PTN Units 3 and 4, as reported in Section 3 of this report.

3.0 CONSIDERATION OF WATER HAMMER, CORROSION AND FATIGUE

NUREG-1061, Vol. 3 [6] states that LBB should not be applied to high energy lines susceptible to failure from the effects of water hammer, corrosion or fatigue. These potential failure mechanisms are thus discussed below with regard to the affected RCL piping at PTN Units 3 and 4, and the above failure mechanisms are determined not to invalidate the use of LBB for this piping.

3.1 Water Hammer

A comprehensive study performed in NUREG-0927 [9] indicated that the probability of water hammer occurrence in the residual heat removal systems of a pressurized water reactor (PWR) is very low. In NUREG-0927, only a single event of water hammer was reported for PWR residual heat removal systems with the cause being incorrect valve alignment. There was no indication as to which portion of the system was affected but it would not be that portion adjacent to the reactor coolant system (RCS) attached piping evaluated for LBB.

NUREG-0927 also reported that the safety significance of water hammer events in the safety injection system is moderate. With four water hammer events reported in the safety injection systems, three of these events were associated with voided lines and the other event was associated with steam bubble collapse. Although there was no indication of the affected portions of the safety injection system, the portions susceptible to water hammer would not be that adjacent to the RCS-attached piping evaluated for LBB.

The portions of the piping evaluated for LBB are inboard of the first isolation valves for the safety injection (accumulator) and residual heat removal (RHR) piping. Thus, during normal operation, these lines experience reactor coolant pressure and temperature conditions such that there is no potential for steam/water mixtures that might lead to water hammer. The portions of these systems that are adjacent to the reactor coolant piping are not in use during normal operation. The RHR system is not used except during low-pressure low-temperature cooldown conditions. The safety injection system is used only during loss of coolant-accident (LOCA) conditions. During normal plant operation, the portions of the system beyond the first isolation valve are expected to run at low

temperature conditions. Thus, there should never be any voiding or potential for steam bubble collapse, which could result in water hammer loads on the piping attached directly to the RCS considered in this evaluation. To date, there has been no experience related to water hammer events in either the RHR or safety injection systems at PTN.

Per Reference 52, a search of FPL's condition report databases was performed to verify if water hammer events have occurred on the RHR Lines being analyzed for LBB evaluation. The search looked back as early as 1992 for past events of water hammer in RHR Lines and none were found in the Condition Reports Databases of PTN, Units 3 and 4. Therefore, water hammer is highly unlikely for the piping systems under consideration in this report. Hence, this phenomenon will have no impact on the LBB analysis for the affected portions of the safety injection and residual heat removal systems at PTN.

The surge line also experiences reactor coolant pressure and temperature conditions such that there is no potential for steam/water mixtures that might lead to water hammer.

3.2 Corrosion

Two corrosion damage mechanisms which can lead to rapid piping failure are intergranular stress corrosion cracking (IGSCC) in austenitic stainless steel pipes and flow-assisted corrosion (FAC) in carbon steel pipes. IGSCC has principally been an issue in austenitic stainless steel piping in boiling water reactors [10] resulting from a combination of tensile stresses, susceptible material and oxygenated environment. IGSCC is not typically a problem for the primary loop of a PWR fabricated from stainless steel such as the SI accumulator, Surge Line and RHR systems under consideration since the environment has relatively low concentrations of oxygen. There are no Alloy 600/82/182 materials in the 5 auxiliary lines evaluated in this report. Hence, PWSCC (IGSCC in primary water environment of PWRs) is not an active degradation mechanism.

FAC is a problem for carbon steel piping with two-phase flow [11]. FAC is not anticipated for the systems under consideration in this report since the piping is fabricated from stainless steel which is not susceptible to FAC.

3.3 High Cycle Fatigue

Metal fatigue in piping systems connected to the reactor coolant loops of Westinghouse-designed pressurized water reactor was identified in Bulletin 88-08 [12]. Evaluations performed by FPL and submitted to the Nuclear Regulatory Commission have concluded that the bulletin does not apply to PTN [52]. For the SI accumulator piping, there is no interconnection to the charging pumps that will lead to inleakage leading to cracking such as was identified at Farley and Tihange. For the RHR piping, any outleakage at the isolation valve leak off lines is monitored and can be corrected such that cracking similar to that identified at the Japanese Genkai plant will not occur. Thus, there is no potential for unidentified high cycle fatigue.

Known fatigue loadings and the resultant possible crack growth have been considered by the analyses reported in Section 6.0 of this report. Based on the results presented in Section 6.0, it is concluded that fatigue will not be a significant issue for the piping systems under consideration at PTN Units 3 and 4.

4.0 PIPING MATERIALS AND STRESSES

4.1 Piping System Description, Operating Conditions and Geometry

The piping systems considered in this evaluation have been described in Section 1.1. Schematics of these lines including selected nodal points are shown in Figures 4-1 through 4-6.

4.1.1 *Accumulator Lines*

The normal operating temperature and pressure for the 10" Accumulator Lines are 555 °F and 2485 psig for all the three RCLs (A, B, and C) in both units 3 and 4 [13, 14].

Per Reference 14 for Unit 4 Accumulator Lines, per Reference 44(a) for Unit 3 Accumulator Lines, and per the standard piping schedule [15] for Unit 3 Accumulator Lines, the pipe outer diameter (OD) is 10.75" and the pipe thickness is 1".

4.1.2 *Pressurizer Surge Line*

The normal operating temperature and pressure for the 12" pressurizer Surge Line are 653 °F and 2235 psig (RCL B only) in both units 3 and 4 for the pressurizer end [16]. For the hot leg end, the normal operating temperatures and pressure are 602.1/602.3/610.9 °F and 2235 psig (RCL B only) in both units 3 and 4 [17, 18]. The different temperatures at the hot leg end come from different specification documents as listed in References 17 and 18. For critical flaw size calculations a higher temperature gives lower material properties (less plastic moment) and hence is conservative. For leakage calculations a lower temperature gives higher material properties (less crack opening) and hence is conservative. Therefore, at the hot leg end of the pressurizer Surge Line, a temperature of 602.1 °F will be considered for leakage and a temperature of 610.9 °F will be considered for critical flaw size evaluation.

Per Reference 16, the nominal pipe OD of the pressurizer Surge Line is 12" and it is a schedule 140 pipe made of stainless steel material for both Units 3 and 4. Therefore, from the standard piping schedule [15] the pipe outer diameter (OD) is 12.75" and the pipe thickness is 1.125".

From References 38, 43 and 16, a 14" to 12" reducer is present at the pressurizer Surge Line nozzle. Per Reference 46, the Surge Line pipe OD is $14" + 4 * \tan(10^\circ) = 15.41"$ and the thickness is 1.765" at the centerline of the pressurizer nozzle. Since the thermal sleeve starts from the nozzle weld it will be conservatively considered for the leakage purpose as it increases the flow path length. Per Reference 46 the thermal sleeve thickness is 0.19". Since a similar 14" to 12" reducer is used at the hot leg end [38, 43] also, the same pipe geometry will be used.

4.1.3 RHR Line

The normal operating temperatures and pressure for the 14" RHR Line are 602.1/602.3/610.9 °F and 2235 psig (RCL C for Unit 3 and RCL A for Unit 4) in both units 3 and 4 for the hot leg end [17, 18].

Therefore, for leakage evaluation a hot leg temperature of 602.1 °F will be considered. For critical flaw size evaluation a hot leg temperature of 610.9 °F will be considered.

Per References 19 and 47 the pipe OD is 14" and the pipe thickness is 1.25".

A summary of the operating conditions for the five lines are presented in Tables 4-1 and 4-2 for leakage and critical flaw size calculations, respectively. A summary of the pipe geometry for these lines is provided in Tables 4-3 and 4-4 for leakage and critical flaw size calculations, respectively.

4.2 Material Properties

From the material specification documents [21], the base material used for all the piping systems with diameters between 10" and 16" is SA 376 Type 316 (corresponds to ASME designation of A 376). From Reference 22, the welding procedure is either gas tungsten arc weld (GTAW) or shielded metal arc weld (SMAW) except for the nozzle welds which are TIG (tungsten inert gas) welds [23]. Since SMAW weld has a lower toughness (i.e., higher Z factor per ASME Section XI, IWB-3640 rules) than GTAW/TIG welds, it is assumed conservatively to be the only weld

process used for all the cases. Per Reference 24, the weld material used is Type 316/317/317L. A Type 317L material is conservatively used for the flaw size calculation as it provides lower yield strength compared to that of the base material A 376 Type 316, which is conservatively used for the leakage evaluation. Similarly, A 376 Type 316 material gives lower Ramberg-Osgood parameters compared to Type 317L material and are therefore, is used for the leakage calculation.

The material properties per ASME Code Section II, Part D [25] are summarized in Tables 4-5 and 4-7 for the leakage evaluation and in Table 4-6 for the critical flaw size evaluation.

4.2.1 Calculation of Z Factors for Fracture Mechanics Analysis

The pressurizer surge, the accumulator, and the RHR Lines are made of austenitic stainless steel weld materials. Per ASME Code, Section XI, Appendix C [26], Section C-6330, the Z factor of austenitic stainless steel weld materials fabricated using the SMAW process is calculated as follows:

$$Z = 1.30[1 + 0.010(NPS - 4)] \quad \text{for submerged arc weld (SAW) (used conservatively since Z factor for SAW is higher than for SMAW)}$$

where:

NPS = nominal pipe size, in; NPS is taken as the outside diameter (OD) of the component.

Z factors for the weld material used in the flaw size calculation are shown in Table 4-6. Since wrought stainless steel (A 376 Type 316) is used for the pipe material (elbow and straight sections), a Z factor of 1.0 can be applied.

4.2.2 Determination of Ramberg-Osgood Material Parameters

For the leakage calculation, the Ramberg-Osgood material parameters are required. The Ramberg-Osgood stress-strain parameters used to describe the true stress-strain curve were obtained from the mechanical properties using the correlations developed in Reference 27. The true stress-true strain curve can be represented by the following relationship:

$$\frac{\varepsilon}{\varepsilon_0} = \frac{\sigma}{\sigma_0} + \alpha \left(\frac{\sigma}{\sigma_0} \right)^n \quad (4-1)$$

where: ε , σ are the true strain and true stress,

ε_0 , σ_0 are the yield strain and yield stress, and

α , n are the Ramberg-Osgood parameters.

The values of α and n are then obtained from the relationship provided in Reference 27 as:

$$n = \frac{1}{\ln(1 + e_u)} \quad (4-2)$$

$$\alpha = \left[\frac{\ln(1 + e_u)}{\ln\left(1 + \frac{S_y}{E}\right)} - \frac{S_u(1 + e_u)}{S_y\left(1 + \frac{S_y}{E}\right)} \right] \left[\frac{S_u(1 + e_u)}{S_y\left(1 + \frac{S_y}{E}\right)} \right]^{-n} \quad (4-3)$$

where, e_u is the ultimate elongation, S_y/S_u is yield/ultimate strength, and E is the elastic modulus.

All the stress-strain properties used in this evaluation are provided in Table 4-7.

4.3 Applicable Stresses

The piping moments and stresses considered in the LBB evaluation are due to pressure (P), dead weight (DW), thermal expansion (TE), thermal stratification (STRAT, if present), safe shutdown earthquake inertia (SSE) and seismic anchor movements (SAM) consistent with the guidance provided in NUREG-1061, Vol. 3. Per the guidance provided in NUREG-1061, other secondary stresses such as residual stresses and through-wall thermal stresses were not included in the evaluation.

For calculation of leakage, the normal operating (NOP) loads consisting of pressure, dead weight and thermal expansion loads are used. For calculation of critical flaw size, the maximum of

STRAT and SSE with SAM loads is added to the NOP loads (referred to as the NOP + SSE loading condition).

The applicable loads to be used in conjunction with the bounding analysis curves (BAC) developed based on plant operating conditions, pipe geometry, material properties are reported in Tables 4-8 through 4-13 [16, 44, 45, 46, 47, 48].

The axial stress due to normal operating pressure is calculated from the expression:

$$\sigma_p = \frac{pD_i^2}{D_o^2 - D_i^2}$$

where p is the internal pressure, D_o is the outside diameter of the pipe and D_i is the inside diameter.

The bending stress due to dead weight, thermal expansion and SSE is calculated from the bending moments using the expression:

$$\sigma_m = \frac{M_r}{Z}$$

where:

Z = the section modulus and,
M_r = the resultant moment.

Axial forces due to dead weight, thermal expansion, seismic, were not considered in the evaluation. The stresses due to axial forces are not significant compared to those from pressure loads, so their exclusion does not significantly affect the results of this evaluation. This has been shown in a previous LBB submittal [4].

Table 4-1. Normal Operating Conditions for Leakage Evaluation

Parameter	Accumulator Line	Surge Line		R H R Line
	Cold Leg End	Pressurizer End	Hot Leg End	Hot Leg End
Temperature, °F	555 ⁽¹⁾	653 ⁽²⁾	602.1 ⁽²⁾	602.1 ⁽³⁾
Pressure, psig	2485 ⁽¹⁾	2235 ⁽²⁾		2235 ⁽³⁾

Notes:

1. Normal operating temperature and pressure for all three RCLs A, B, and C in both Units 3 and 4.
2. Normal operating temperature and pressure for RCL B only in both Units 3 and 4.
3. Normal operating temperatures and pressure for RCL C and RCL A in Units 3 and 4, respectively, for the hot leg.

Table 4-2. Operating Conditions for Critical Flaw Size Evaluation

Parameter	Accumulator Line	Surge Line		R H R Line
	Cold Leg End	Pressurizer End	Hot Leg End	Hot Leg End
Temperature, °F	555 ⁽¹⁾	653 ⁽²⁾	610.9 ⁽²⁾	610.9 ⁽³⁾
Pressure, psig	2485 ⁽¹⁾	2235 ⁽²⁾		2235 ⁽³⁾

Notes:

1. Normal operating temperature and pressure for all three RCLs A, B, and C in both Units 3 and 4.
2. Normal operating temperature and pressure for RCL B only in both Units 3 and 4.
3. Normal operating temperatures and pressure for RCL C and RCL A in Units 3 and 4, respectively, for the hot leg.

Table 4-3. Pipe Geometry Inputs for Leakage Evaluation

	Accumulator Line	Surge Line		R H R Line
		Pipe Side	Nozzle Side	
Outside Diameter, in	10.75	12.75	15.41	14.00
Thickness, in	1.00	1.125	1.955 ^{(1), (2)}	1.25

Note:

- 1) For the leakage evaluation, as explained in Section 4.1.2, the thickness of the Surge Line at the nozzle side (1.955 in) includes the thickness of the thermal sleeve (0.19 in) and that of the nozzle side (1.955 in = 1.765 in + 0.19 in).
- 2) Used for nozzle sides at hot leg end and the pressurizer end.

Table 4-4. Pipe Geometry Inputs for Critical Flaw Size Evaluation

	Accumulator Line	Surge Line		R H R Line
		Pipe Side	Nozzle Side	
O. D. , in	10.75	12.75	15.41	14.00
Thickness, in	1.00	1.125	1.765	1.25

Table 4-5. ASME Code Strength at Normal Operating Temperatures for Leakage Calculation

Components	Material Designation	Leakage			
		S _y (ksi)	S _u (ksi)	σ _{flow} (ksi) ⁽¹⁾	E (ksi)
Surge Line at Hot Leg (602.1°F)	A-376 TP316	18.88	71.80	45.34	25289.5
Surge Line at Pressurizer (653°F)	A-376 TP316	18.48	71.80	45.14	25035.0
RHR Line at Hot Leg (602.1°F)	A-376 TP316	18.88	71.80	45.34	25289.5
Accumulator Line (546.2°F) ⁽²⁾	A-376 TP316	20.00	71.80	45.90	25569.0

Note:

- 1) Per Reference 7, the flow stress (σ_{flow}) is the average of the ultimate strength, S_u, and the yield strength, S_y at normal operating temperature [σ_{flow} = 0.5(S_u + S_y)].
- 2) Conservatively assumed cold leg normal operating temperature [17, 18] which is less than 555°F.

Table 4-6. ASME Code Strength at Normal Operating Temperatures for Critical Flaw Size Calculation

Components	Material Designation	S _y (ksi)	S _u (ksi)	σ _{flow} (ksi) ⁽¹⁾	Z factor
Surge Line at Hot Leg (610.9°F)	Type 317L (SA-240 ⁽²⁾)	18.61	66.10	42.36	1.466 ⁽³⁾ , 1.500 ⁽⁴⁾
Surge Line at Pressurizer (653°F)	Type 317L (SA-240 ⁽²⁾)	18.28	66.09	42.19	1.466 ⁽³⁾ , 1.500 ⁽⁴⁾
RHR Line at Hot Leg (610.9°F)	Type 317L (SA-240 ⁽²⁾)	18.61	66.10	42.36	1.482
Accumulator Line at Cold Leg (555°F)	Type 317L (SA-240 ⁽²⁾)	19.15	66.15	42.65	1.444

Note:

1. Per Reference 7, the flow stress (σ_{flow}) is the average of the ultimate strength, S_u, and the yield strength, S_y at normal operating temperature [σ_{flow} = 0.5(S_u + S_y)].

2. SA-240 assumed for conservatism.

3. Pipe side.

4. Nozzle side.

Table 4-7. Ramberg-Osgood Parameters for Leakage Calculation

	Ramberg Osgood Parameter α	Ramberg Osgood Exponent n
Surge Line at Hot Leg (602.1°F)	2.679	2.988
Surge Line at Pressurizer (653°F)	2.709	2.946
RHR Line at Hot Leg (602.1°F)	2.679	2.988
RHR Line at Cold Leg (546.2°F)	3.557	3.104
Accumulator Line (555°F)	2.567	3.093

Table 4-8. Load Points for Accumulator Lines

Unit 3		
NODE POINTS	NOP (ksi)	MAX (ksi)
460	6.3595407	13.13421
460	6.3595407	13.13421
470 B	5.0286469	8.0064046
470 B	5.0286469	12.026137
470 M	5.8448435	9.6070015
470 M	5.8448435	9.6070015
470 E	6.5103769	11.547761
470 E	6.510492	11.585303
475 B	6.5287801	11.628064
475 B	6.5288367	11.58679
475 M	7.7986352	14.739055
475 M	7.7986352	14.739055
475 E	8.641909	18.087145
475 E	8.6420909	18.540287
480	8.7326104	19.024855
610	4.9364849	7.148956
610	4.9364849	7.148956
615	5.2555545	8.4411515
615	5.2555545	8.4411515
625 B	5.2546522	8.3181221
625 B	5.2546522	8.3181997
625 M	5.271894	8.0773594
625 M	5.271894	8.0773594
625 E	5.3389725	7.8955707
625 E	5.3389725	7.8957902
630 B	5.4250361	8.015566
630 B	5.4250596	8.0155966
630 M	5.5590757	8.5960804
630 M	5.5590757	8.5960804
635 B	5.7404138	8.4769993
635 B	5.7405555	8.62194
635 M	5.9553124	9.2302237
635 M	5.9553124	9.2302237
636	6.1454537	10.271527
636	6.1456297	10.271453
637	6.1969734	10.603023

Unit 4		
NODE POINTS	NOP (ksi)	MAX (ksi)
110	5.8290139	11.465209
110	5.8290433	11.465263
120 B	6.8707021	12.531389
120 B	6.8705541	12.531548
120 M	7.4736314	14.131029
120 M	7.4736314	14.131029
120 E	7.5070712	14.804157
120 E	7.5076533	15.210674
122 B	7.5073396	15.210887
122 B	7.5073191	14.865775
122 M	7.656345	16.240519
122 M	7.656345	16.240519
124	8.5255197	18.173109
124	8.5255633	18.172721
200 B	5.4518614	9.3544977
200 E	5.4518091	9.3544479
204	5.4834917	7.9301628
204	5.3945135	7.9300164
206 B	5.4733183	7.7320302
206 B	5.396645	7.7320562
206 M	5.3413536	7.4375186
206 M	5.6637209	7.2925118
206 E	5.5640694	7.5952068
206 E	5.5640694	8.77403
208 B	6.0785518	8.8644482
208 B	6.0785518	11.00678
208 B	7.0049967	11.185453
208 B	7.0024718	12.956097
208 E	7.4932366	13.128829
208 E	7.4931974	13.072252
210 B	7.4864591	13.207919
210 B	7.494673	16.124818
210 M	8.06121	16.031819
210 M	8.06121	18.616902
210 E	8.6170688	18.752244
210 E	8.6169865	18.878764

Table 4-8 Load Points for Accumulator Lines (Continued)

637	6.1969936	10.64815
638	6.2180447	10.952796
638	6.2180447	10.95268
640	6.4547571	13.549134
800	5.7158749	9.3088684
800	5.7158749	9.3088684
805	5.1524623	8.3020868
805	5.1524623	8.3020529
810 B	5.1662935	8.320744
810 B	5.166334	8.3208273
810 M	5.3366771	8.9805324
810 M	5.3366771	8.9805324
815 B	5.2628912	10.434542
815 B	5.2628619	10.451851
815 M	5.3651255	12.006181
815 M	5.3651255	12.006315
815 E	5.8468804	13.118519
815 E	5.8468804	13.118519
820	6.0901454	13.432265
820	6.0900336	13.490592
822	6.2892547	13.537187
822	6.2892203	13.537289
825	6.8968736	10.650437

214	8.6497894	18.891922
322	7.0546833	11.900655
322	7.0546833	11.900655
326 B	7.3554734	9.6145431
326 B	7.2352558	9.6145431
326 M	7.3058349	9.1636999
326 M	7.605257	9.232953
326 E	7.7419177	9.8984831
326 E	7.7052035	9.9156199
328 B	7.8333652	9.9205456
328 B	7.912834	9.9949405
328 M	8.2738851	10.915342
328 M	7.9881243	10.915342
328 E	8.1464338	11.156846
328 E	8.0220912	11.156393
332	8.0339007	11.219414
332	7.2641944	11.505724
334	6.1235217	13.039712

Table 4-9. Load Points for RHR Lines

Unit 3			Unit 4		
NODE POINTS	NOP (ksi)	MAX (ksi)	NODE POINTS	NOP (ksi)	MAX (ksi)
5	9.771646	16.02175	90	9.359497	11.26326
10	8.81243	13.662224	90	9.359497	11.26326
10	8.812194	13.66267	90	9.359497	11.26326
15B	8.33433	12.433241	100	9.745627	12.21927
15B	8.334239	12.433202	110	10.32247	13.83366
15M	8.193514	12.21	110	10.32247	13.83366
15M	8.193514	12.21	110	10.32247	13.83366
15E	7.862934	11.812618	C7A	11.03248	15.74399
15E	7.445539	12.308857	C7A	11.03248	15.74399
20B	7.412785	11.517703	C7A	11.03248	15.74399
20B	7.412785	11.517657	C7B	11.33993	16.88578
20M	7.419432	11.548954	C7B	11.33993	16.88578
20M	7.419432	11.548954	C7B	11.33993	17.00477
20E	6.980055	11.030674	C8A	11.13434	16.7923
20E	6.980055	11.030674	C8A	11.13434	16.7923
25	4.87816	9.8406019	C8A	11.13434	16.53698
25	4.87816	9.8406019	C8B	10.94254	16.6974
30	7.179935	9.4883349	C8B	10.94254	16.6974
30	7.179935	9.4883349	C8B	10.94254	16.6974
35	7.653121	9.8729014	120	10.8842	17.37851
35	7.653121	9.8255048			
40	8.01412	10.127955			

Table 4-10. Loads for Units 3 and 4 Pressurizer Surge Lines

NODE POINTS ⁽¹⁾	NOP (ksi)	MAX (ksi)
Pipe	23.910	24.732
Nozzle ⁽²⁾	12.323	16.822

Notes:

- (1) Node points correspond to one bounding location each on the 12'' pipe and the 14'' pipe at the nozzle end.
 (2) To calculate bending stresses, thickness of thermal sleeve is neglected.

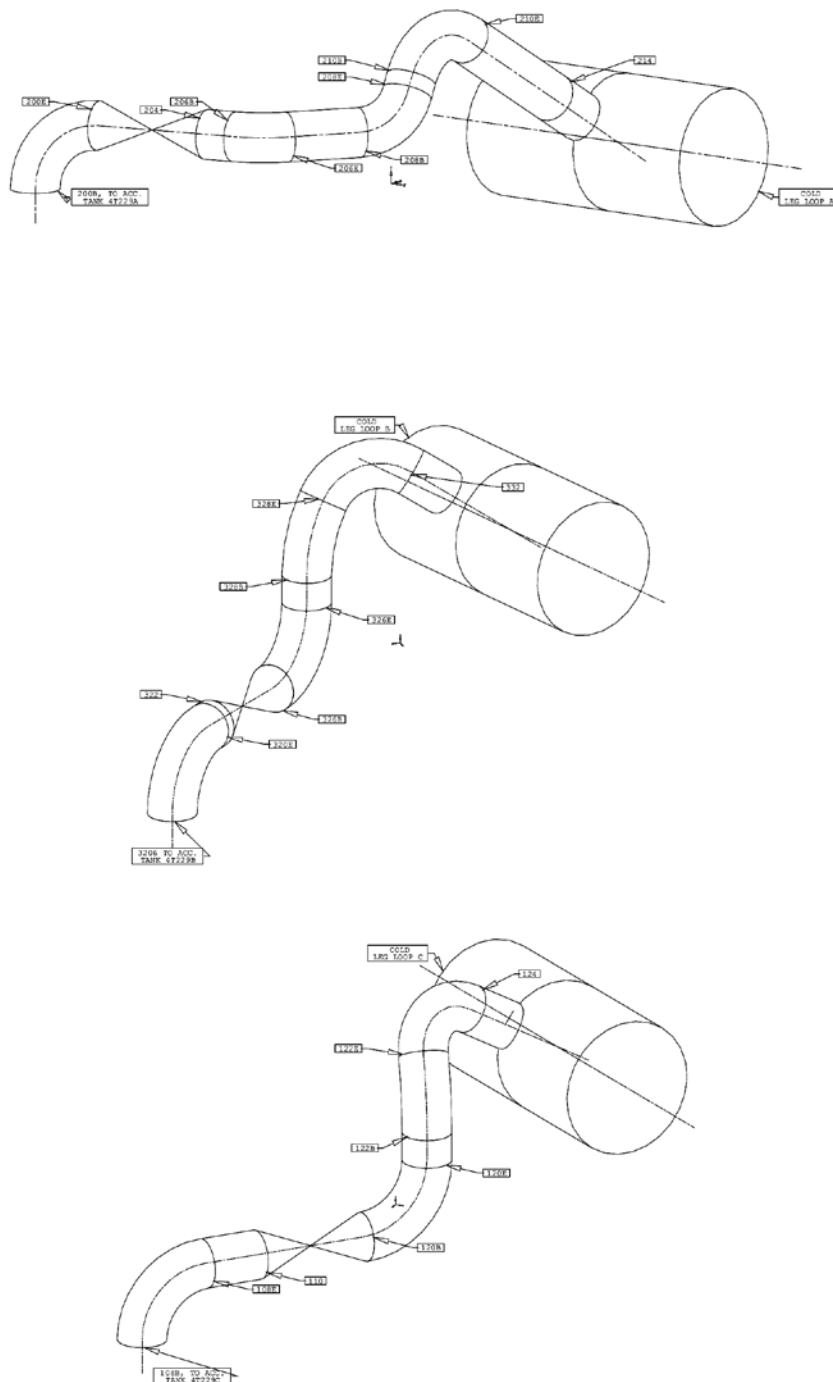


Figure 4-2. Schematic of Piping Model and Selected Node Points for Accumulator Lines (Loops A, B and C), PTN Unit 4 [39, 40, 41]

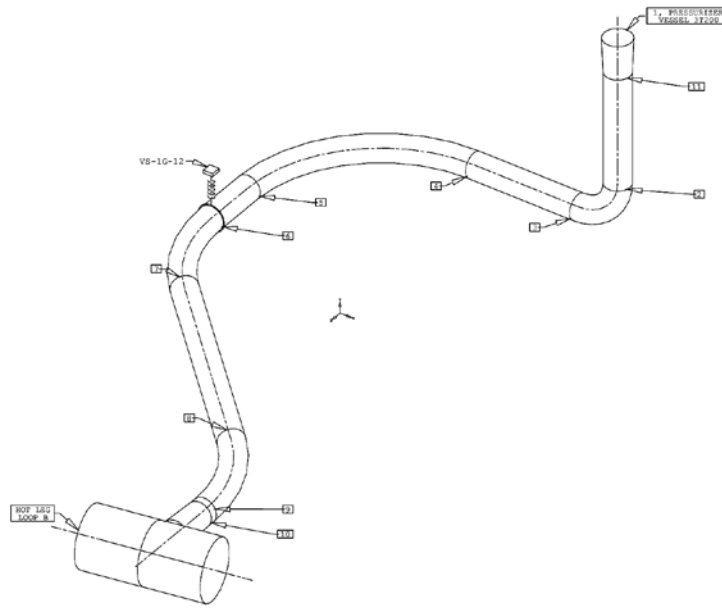


Figure 4-3. Schematic of Piping Model and Selected Node Points for Pressurizer Surge Line, PTN Unit 3 [38]

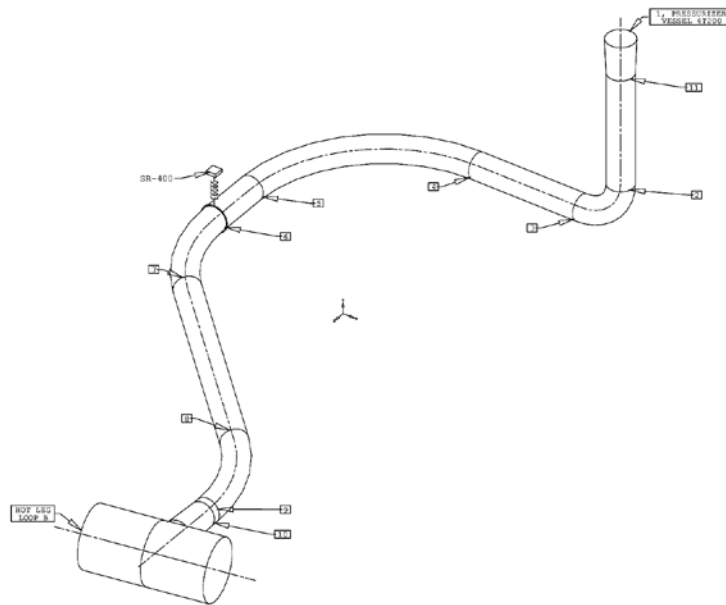


Figure 4-4. Schematic of Piping Model and Selected Node Points for Pressurizer Surge Line, PTN Unit 4 [43]

5.0 LEAK-BEFORE-BREAK EVALUATION

The LBB approach involves the determination of critical flaw sizes and leakage through flaws. The critical flaw length for a through-wall flaw is that length for which, under a given set of applied stresses, the flaw would become marginally unstable. Similarly, the critical stress is that stress at which a given flaw size becomes marginally unstable. NUREG-1061, Vol. 3 [6] defines required margins of safety on both flaw length and applied stress. Both of these criteria have been examined in this evaluation. Circumferential flaws are more restrictive than axial flaws since axial flaws are only affected by pressure stress and thus have larger critical flaw sizes with larger crack opening areas for leakage due to out of plane displacements. In this evaluation, only circumferential flaws are considered for all the piping systems.

5.1 Evaluation of Critical Flaw Sizes

Critical flaw sizes may be determined using either limit load/net section collapse criterion (NSCC) approach or J-Integral/Tearing Modulus (J/T) methodology. In this evaluation, as permitted by NUREG-0800, SRP 3.6.3, the limit load methodology was used to determine the critical flaw sizes since the piping material for all the piping systems under consideration is stainless steel which is ductile.

The methodology provided in NUREG-0800 [7] for calculation of critical flaw sizes by net section collapse (NSC-limit load) analysis was used to determine the critical flaw sizes. This methodology involves constructing a master curve where a stress index, SI, given by

$$SI = S + M P_m \quad (5-1)$$

is plotted as a function of postulated total circumferential through-wall flaw length, L, defined by

$$L = 2 \theta R \quad (5-2)$$

where

$$S = \frac{2\sigma_f}{\pi} [2 \sin \beta - \sin \theta] \quad (5-3)$$

$$\beta = 0.5 [(\pi - \theta) - \pi (P_m / \sigma_f)], \quad (5-4)$$

- θ = half angle in radians of the postulated through-wall circumferential flaw,
 R = pipe mean radius, that is, the average between the inner and outer radius,
 P_m = the combined membrane stress, including pressure, deadweight, and seismic components,
 M = the margin associated with the load combination method (that is, absolute or algebraic sum) selected for the analysis. Since the absolute sum of the moments was used here, a value of 1.0 recommended in Reference 7 was used.
 σ_f = flow stress for stainless steel pipe material categories.

If $\theta + \beta$ from Eqs. (5-1) and (5-5) is greater than π , then

$$S = \frac{2\sigma_f}{\pi} [\sin \beta], \quad (5-5)$$

where

$$\beta = -\pi (P_m / \sigma_f) \quad (5-6)$$

The critical flaw sizes correspond to the value of θ that result is S being greater than zero from Eqs. 5-3 and 5-5.

The value of SI used to enter the master curve for piping material is

$$SI = M (P_m + P_b) \quad (5-7)$$

where

P_b = the combined primary bending stress, including deadweight and seismic components

The value of SI used to enter the master curve for SMAW and SAW is

$$SI = M (P_m + P_b + P_e) Z \quad (5-8)$$

where

P_e = combined thermal expansion stress at normal operation,
 Z = $1.15 [1.0 + 0.013 (OD-4)]$ for SMAW, (5-9)

Z = $1.30 [1.0 + 0.010 (OD-4)]$ for SAW, (5-10)

OD = pipe outer diameter in inches.

Since SMAW weld has a lower toughness (i.e., higher Z factor) than GTAW/TIG welds, it is assumed to be the only weld process used for all the cases. The leakage size was determined as one half the flaw size based on the master curve.

5.2 Leak Rate Determination

The determination of leak rate is performed using the EPRI program, PICEP [28]. The flow rate equations in PICEP are based on a modification of Henry's homogeneous non-equilibrium critical flow model [29]. The program accounts for non-equilibrium mass transfer between liquid and vapor phases, fluid friction due to surface roughness and convergent flow paths. The model was validated for steam and water leakage conditions [28].

In the determination of leak rates using PICEP, the following assumptions are made:

- A plastic zone correction is included in calculating the crack opening displacement. This is consistent with fracture mechanics principles for ductile materials.
- The crack is assumed to be elliptical in shape. This is the most appropriate representation for a crack that has the maximum crack opening displacement at the center of the crack that is available in PICEP for calculations of leakage.
- Crack roughness is taken as 0.000197 inches [30].
- There are no turning losses included since there are no mechanisms to cause intergranular cracking in the piping.
- The cracks are assumed to have a constant through wall depth and include a sharp-edged entrance loss factor of 0.61 (PICEP default).
- The default friction factors of PICEP are utilized.
- The crack opening area at the inlet and outlet are the same.
- The stress combinations included those for NOP conditions.

The leakage flow sizes with respect to the leak rate of 2, 5 and 10 GPM were calculated for the operating pressures and temperatures shown in Tables 4-1 and 4-2 as appropriate using different moment stresses ranging from 0 to 45 ksi and material properties from Tables 4-5 and 4-7. The leakage flow size curves are plotted in Figure 5-1 through Figure 5-6.

5.3 Bounding Analysis Curves

The bounding analysis curves (BACs) represent the maximum allowable membrane (pressure) plus bending stress (as determined from piping analysis for the system) as a function of the applied membrane (pressure) plus bending stress during normal plant operation. The latter condition represents the conditions during which leakage would have to be detected.

To determine a BAC point, the following steps are taken:

- A normal operating stress (membrane plus bending) is assumed.
- Using the curve of leakage flow size versus normal condition applied stress, the crack length that will yield the required leakage rate (including the factor of 10 on top of the detectable leakage rate) is determined. This crack length is the total crack length (2a).

- The maximum allowable bending stress is determined from the curve of critical crack size (a) versus applied bending moment such that $a_{\text{critical}} = 2a_{\text{leakage}}$.
- This yields a point on the BAC curve for the maximum allowable.
- The BAC point so determined is corrected further, since it is based on shell theory stresses and the pipe bending stresses are determined in accordance with piping rules. The bending stress portion of the normal operating stress and the maximum stress must be corrected by the factor:

$$P_{b,BAC} = P_{b,analysis} \times (\pi R^2 t) / (2I/D)$$

where

$P_{b,analysis}$ = bending stress prior to correction

R = mean radius of pipe

t = pipe wall thickness

I = pipe section moment of inertia

D = pipe outside diameter

This process is completed for the complete range of bending stresses from zero to ~50 ksi. The BAC curve so developed contains no other limitation. Membrane stress due to pressure (P) is calculated using the following formula:

$$\sigma_m = \frac{P \pi (R_{in})^2}{2 \pi R_m t}$$

R_m = mean pipe radius

t = pipe wall thickness

R_{in} = inside radius of pipe.

The calculated BACs for Accumulator Line, RHR Line and Surge Lines are plotted in Figure 5-7 through Figure 5-12 respectively. Load points were calculated based on the loads listed in Table 4-8 through Table 4-17 for both Units 3 and 4. The corresponding load points for each of the pipe lines are plotted in Figure 5-7 through Figure 5-12 as well.

5.4 LBB Evaluation Results and Discussions

From the BACs and load points plotted in Figure 5-7 to Figure 5-12 all the stress points for both Units 3 and 4 are below 10 GPM BACs except for stress point 210M in the Unit 4 Accumulator Line as shown in Figure 5-7. Since the stress point 210M is in the middle of an elbow, removing the conservatism in using the weld material Z factor for pipe/elbow materials, the BAC is plotted using a Z factor of 1.0 as shown in Figure 5-13. Using a Z factor of 1.0, stress point 210M is under the 10 GPM BAC .

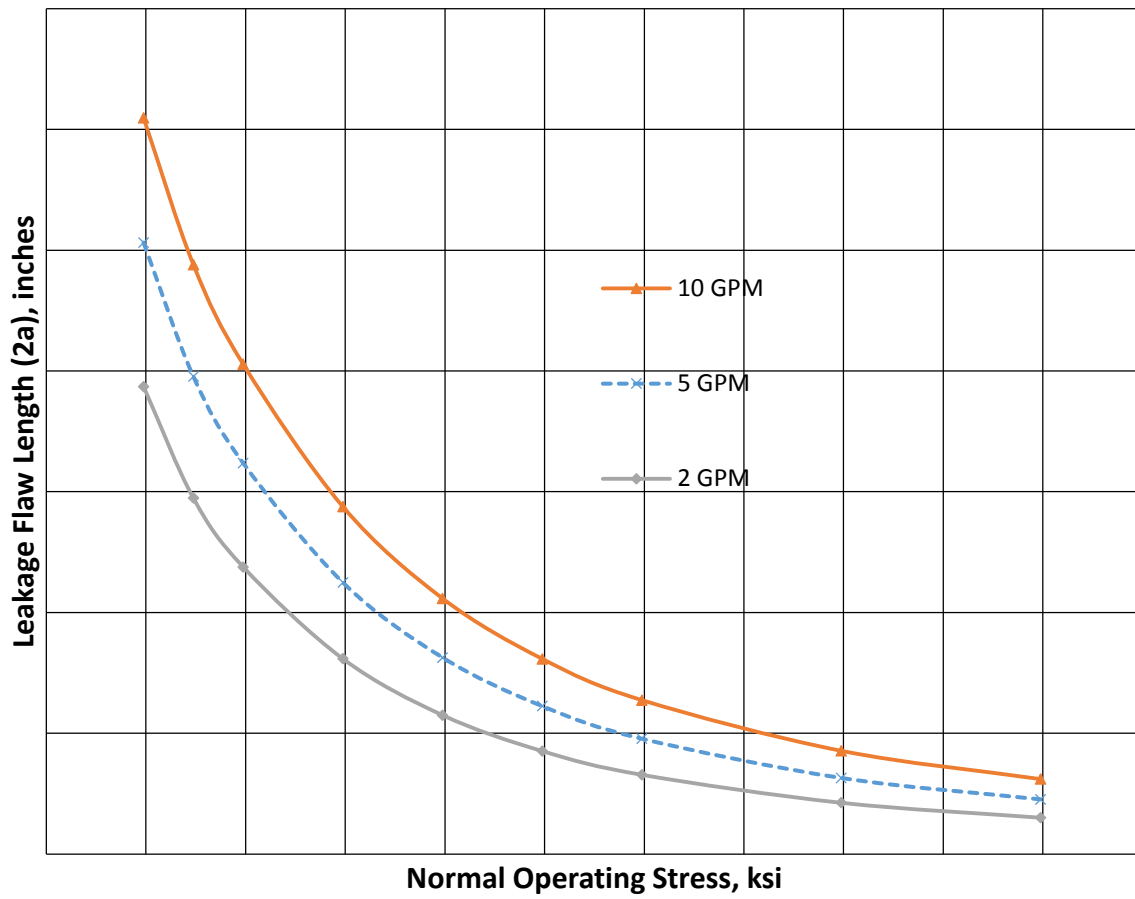


Figure 5-1. Leakage Flaw Size versus Normal Operating Stress of Accumulator Lines

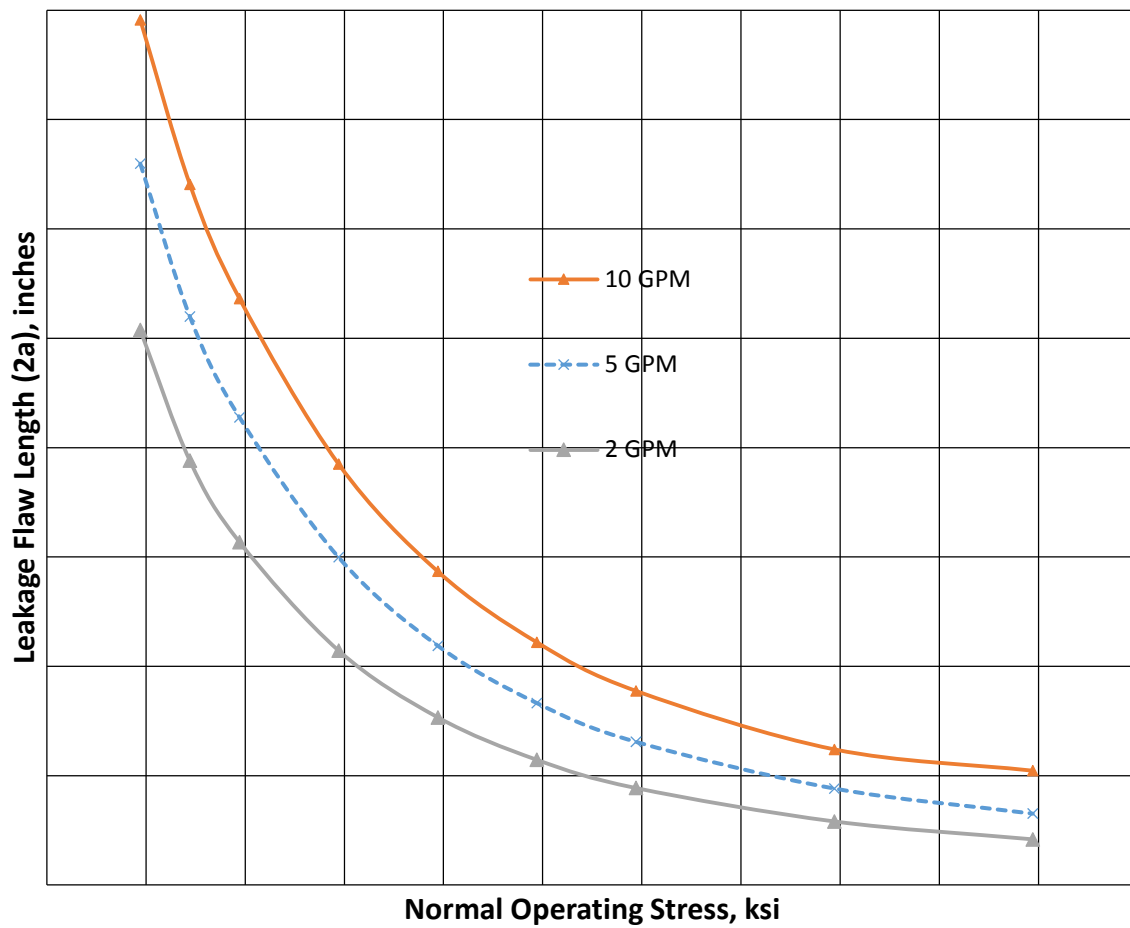


Figure 5-2. Leakage Flow Size versus Normal Operating Stress of Pressurizer Surge Lines
(Pipe Side at Pressurizer End)

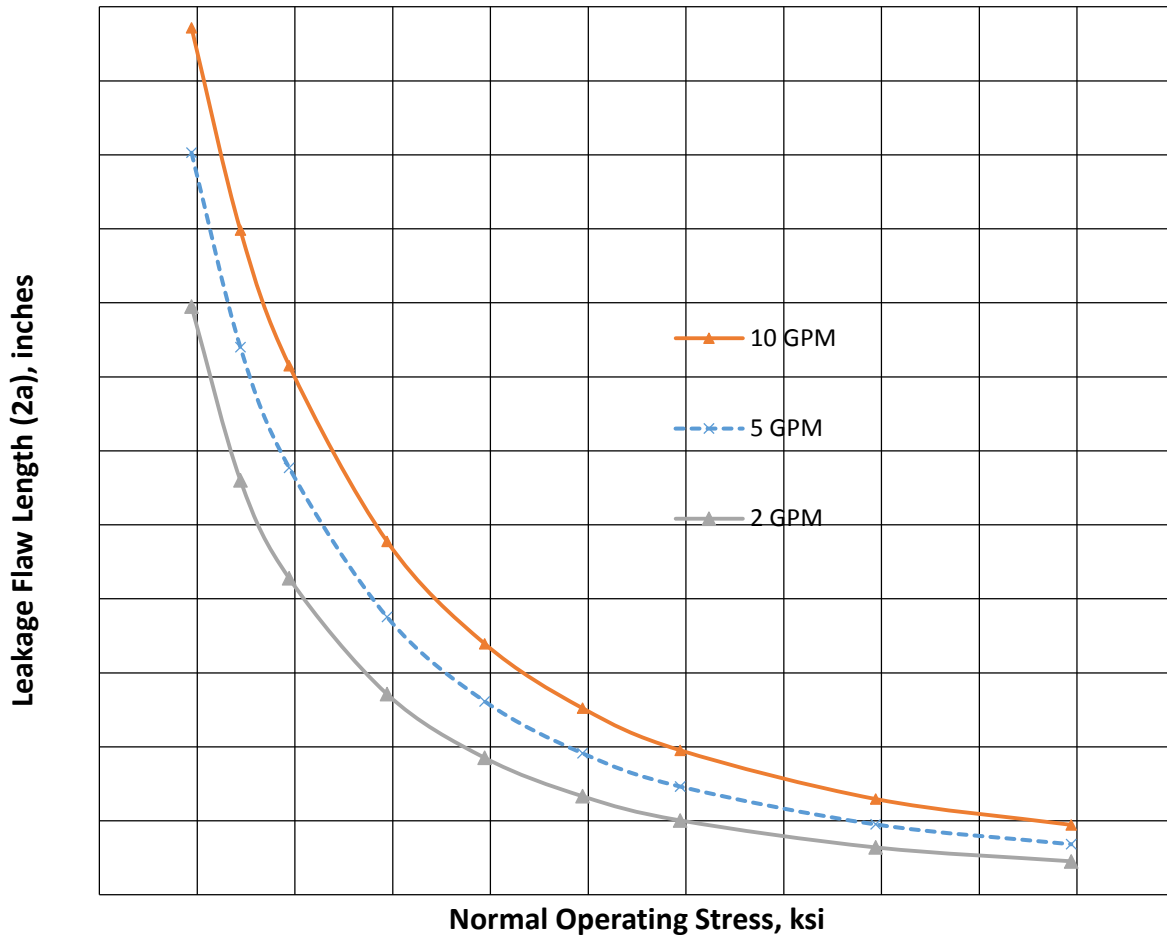


Figure 5-3. Leakage Flaw Size versus Normal Operating Stress of Pressurizer Surge Lines (Nozzle Side at Pressurizer End)

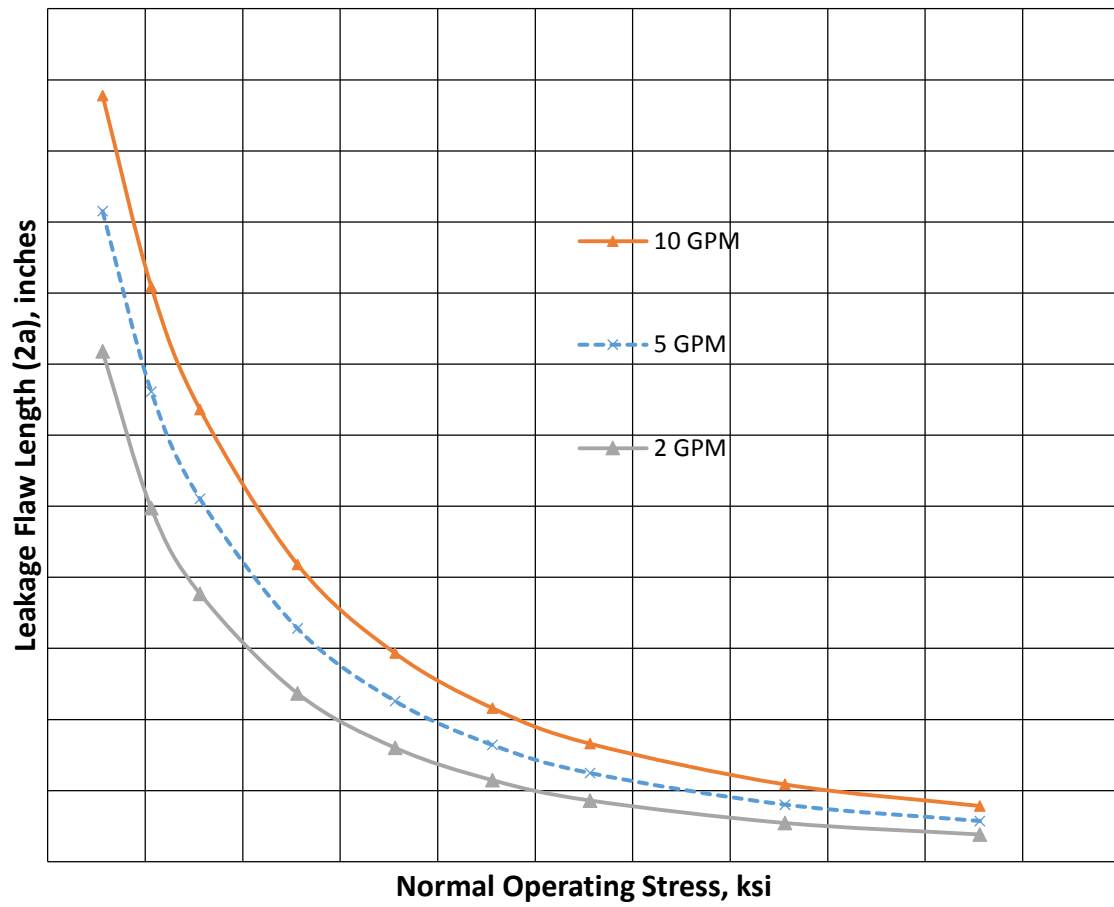


Figure 5-4. Leakage Flaw Size versus Normal Operating Stress of Pressurizer Surge Line (Nozzle Side at Hot Leg End)

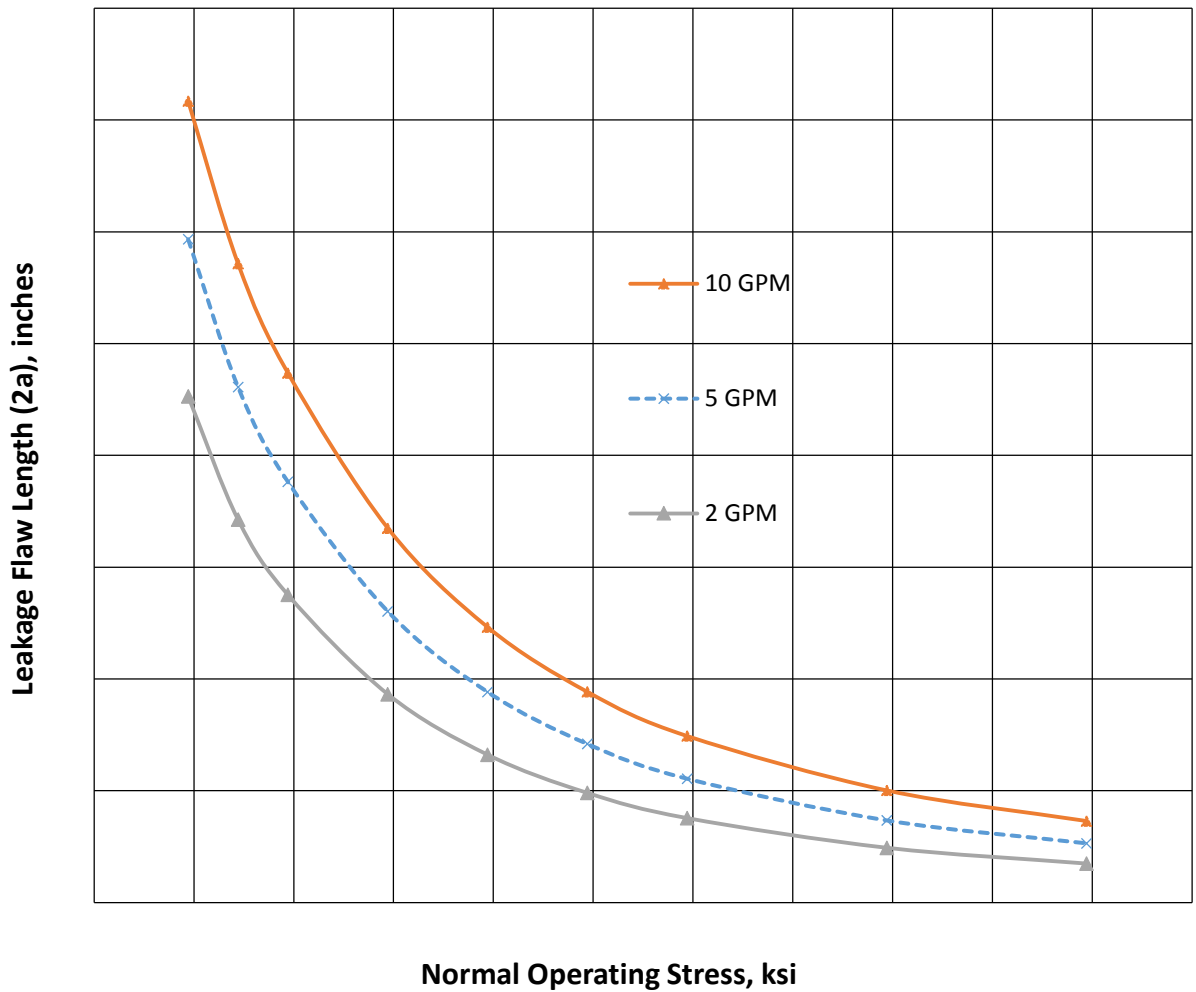


Figure 5-5. Leakage Flaw Size versus Normal Operating Stress of Pressurizer Surge Line at Hot Leg End

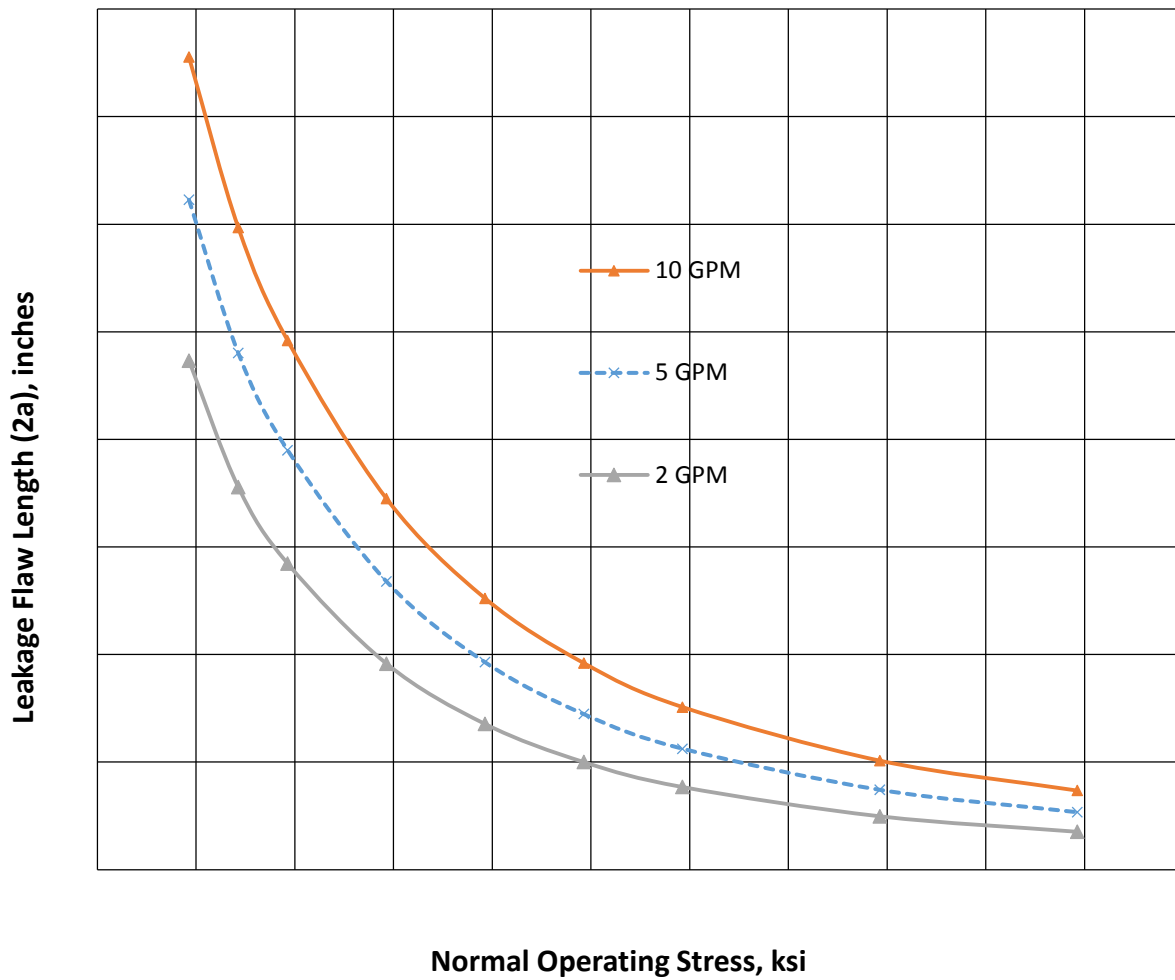


Figure 5-6. Leakage Flow Size versus Normal Operating Stress of RHR Line at Hot Leg End

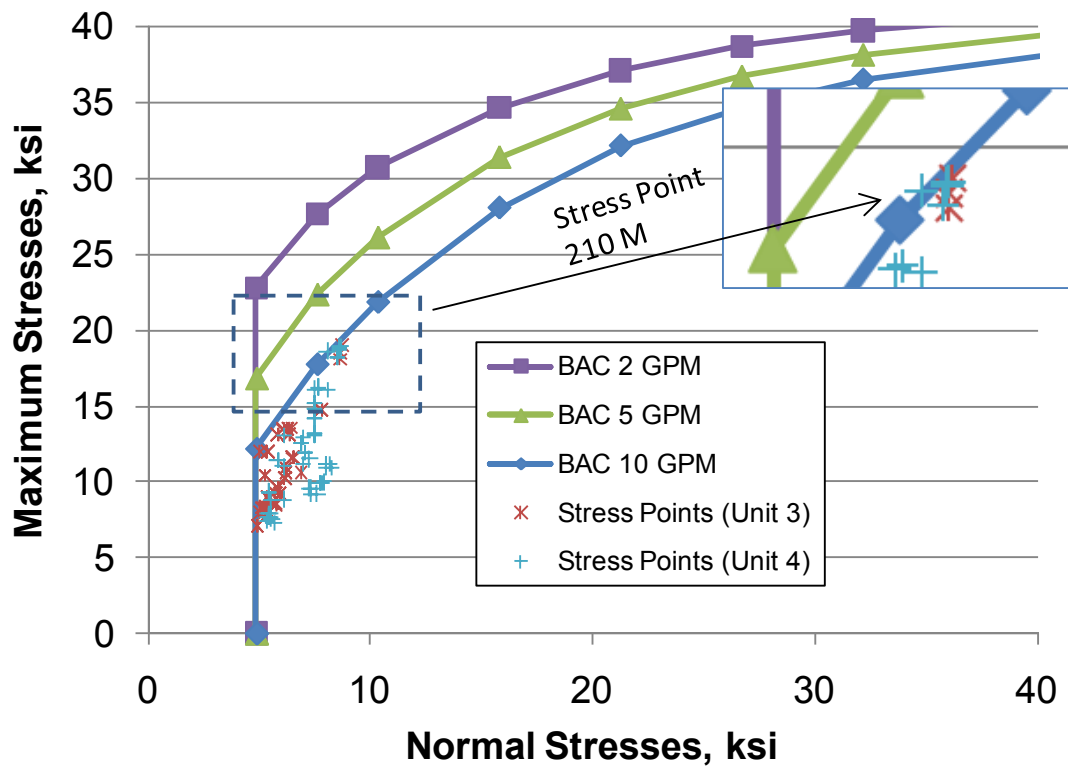


Figure 5-7. BACs and Load Points for Accumulator Lines

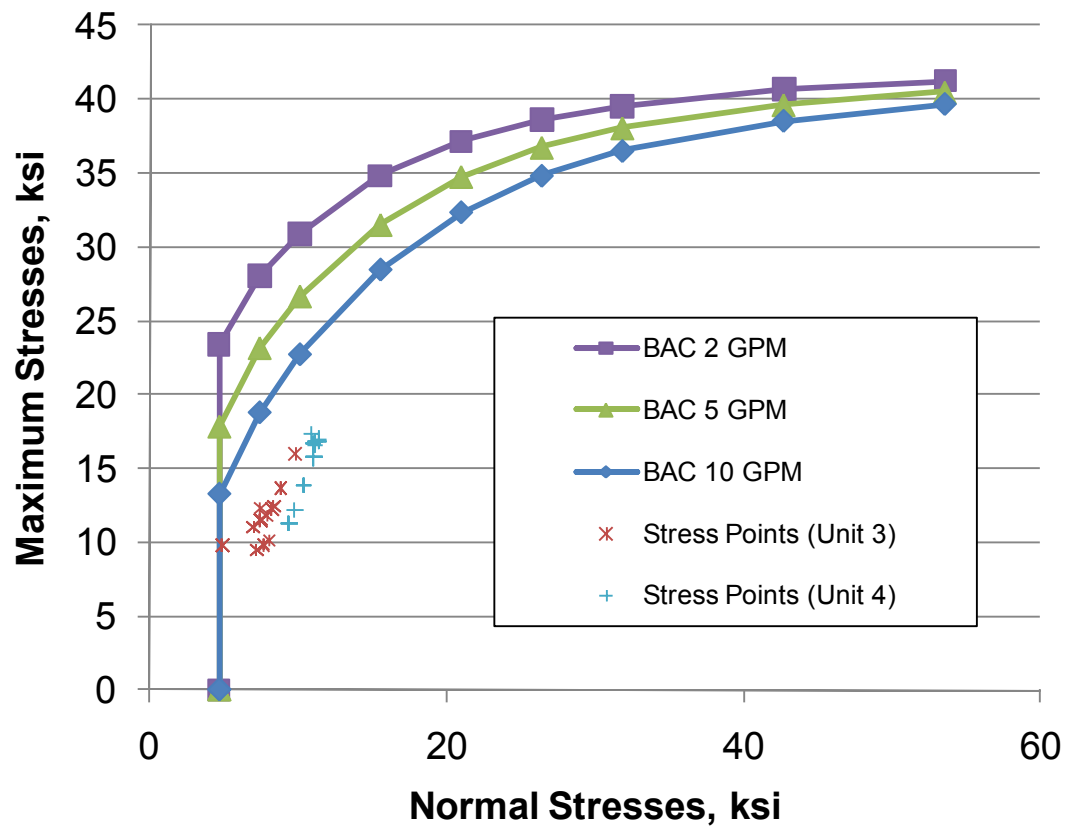


Figure 5-8. BACs and Load Points for RHR Lines

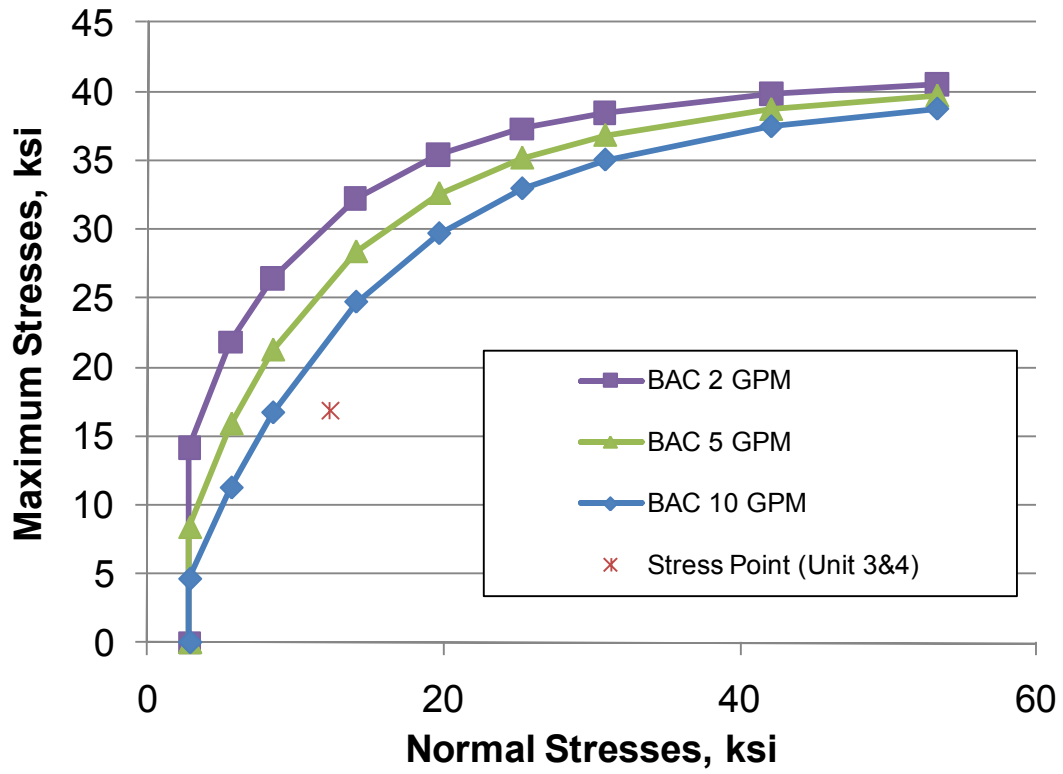


Figure 5-9. BACs and Load Points for Pressurizer Surge Lines (Nozzle Side at Pressurizer End)

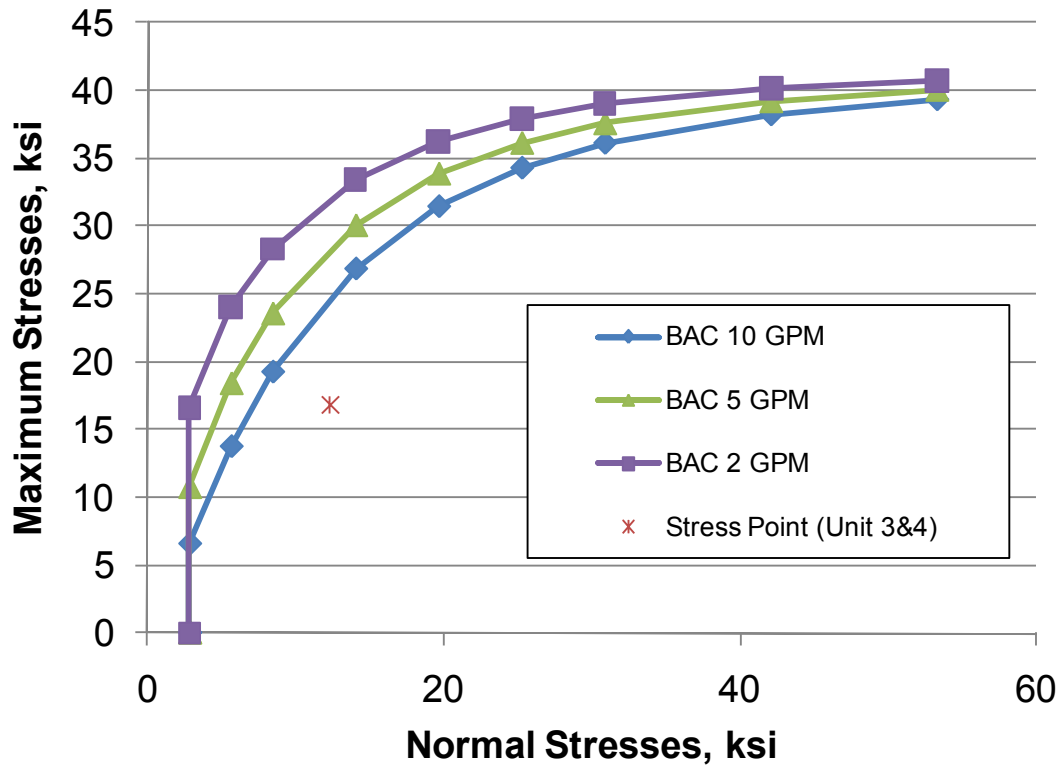


Figure 5-10. BACs and Load Points for Pressurizer Surge Line (Nozzle Side at Hot Leg End)

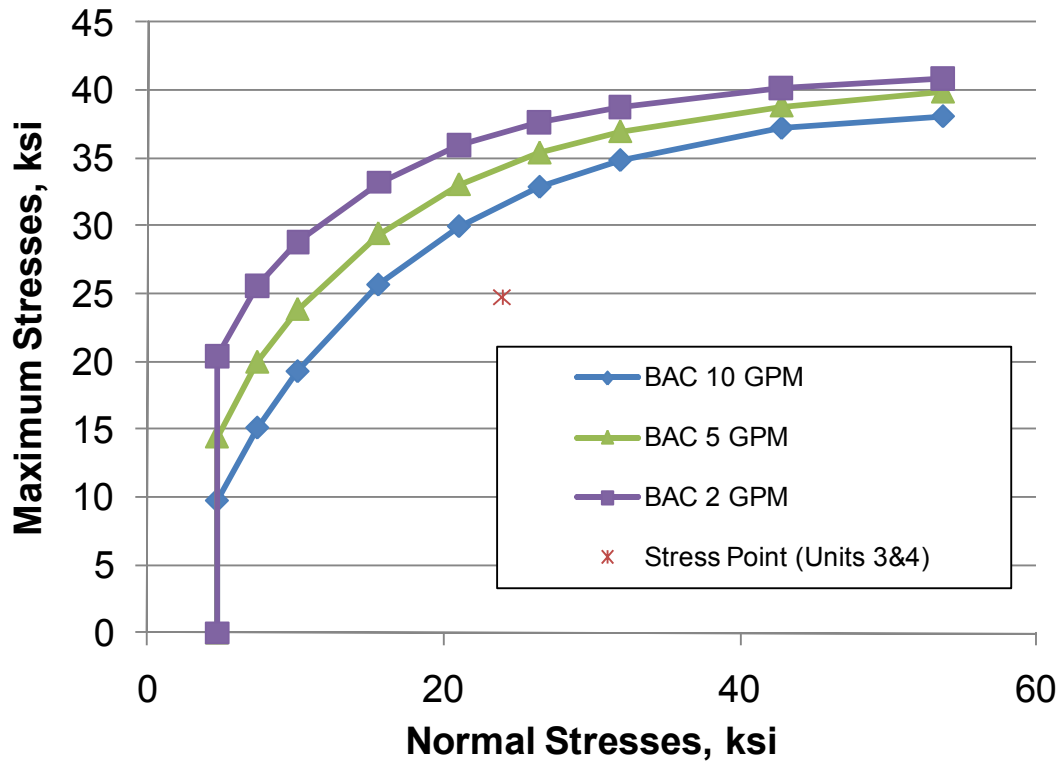


Figure 5-11. BACs and Load Points for Pressurizer Surge Lines (Pipe Side at Pressurizer End)

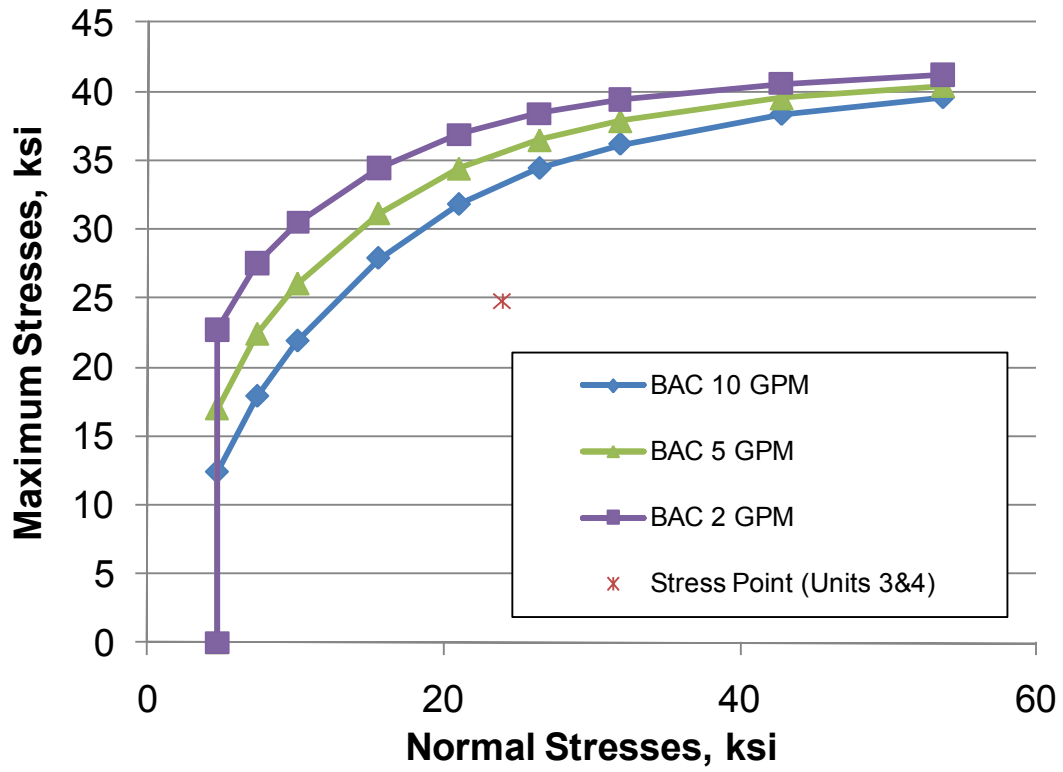


Figure 5-12. BACs and Load Points for Pressurizer Surge Lines (Pipe Side at Hot Leg End)

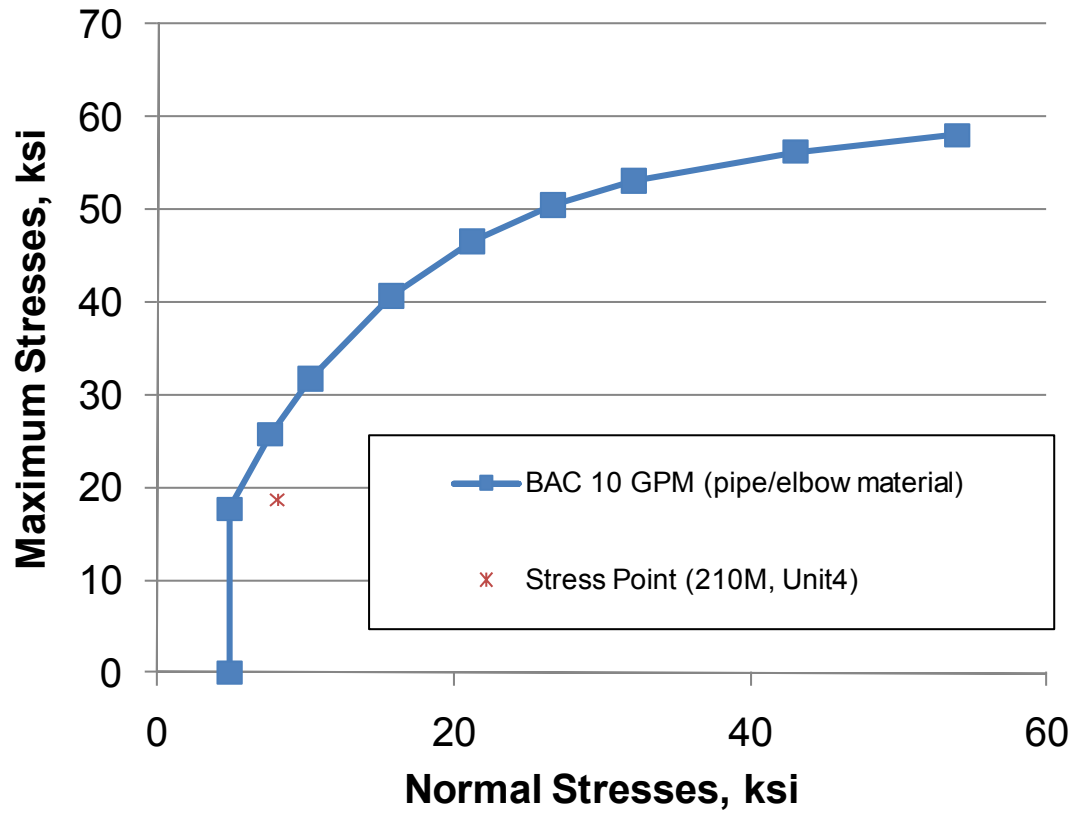


Figure 5-13. 10 GPM BAC Curve for Pipe/Elbow of Accumulator Lines

6.0 EVALUATION OF FATIGUE CRACK GROWTH OF SURFACE FLAWS

In accordance with the NRC criteria [6] set forth in Section 2 of this report, the growth of postulated surface cracks by fatigue is evaluated to demonstrate that such growth is insignificant for the plant life, when initial flaw sizes meeting ASME Code Section XI IWB-3514 acceptance standards [26] are postulated.

6.1 Plant Transients

Since PTN RCS attached piping lines were designed to the requirements of ANSI B31.1, no specific line unique transients exist in the design basis. Hence, transient information from generic Westinghouse nuclear steam supply system documents [31, 32] was obtained to perform the crack growth evaluation. The plant transients for crack growth affecting the auxiliary lines of PTN Units 3 and 4, provided in References 31 and 32, are presented in Table 6-1 for the Accumulator Line and in Table 6-2 for the Residual Heat Removal (RHR) Line.

In addition, the Surge Line experiences thermal stratification which results in larger stress ranges, thus more fatigue growth during transients. A Westinghouse fatigue calculation [50] was conducted considering thermal stratification during the transients. The definition of transients for crack growth, number of cycles, as well as the stress range for each transient are obtained from this calculation, and reproduced in Table 6-3.

6.2 Stresses for Crack Growth Evaluation

The axial stresses due to pressure and thermal loads are calculated as described below. For pressure loads, P, the axial stress is calculated as:

$$\sigma_p = P \frac{D_i^2}{D_o^2 - D_i^2}$$

where D_o is the outside diameter and D_i is the inside diameter of the pipe.

Bending stress is given by $\sigma_b = D_o(M)/2I$,

where

M = bending moment

I = moment of inertia

$$= (\pi/64) \times (D_o^4 - D_i^4)$$

For thermal expansion moments, the maximum operating thermal moments ($M_{\max \text{ oper}}$), from Section 4, are scaled by the ratio of the transient temperature range (ΔT) to the operating temperature range (ΔT_{oper}):

$$M_t = M_{\max \text{ oper}} (\Delta T / \Delta T_{\text{oper}}),$$

where ΔT_{oper} is based on the temperatures at which the thermal expansion moments were calculated. $\Delta T_{\text{oper}} = T_{\text{oper}} - 70$. The operating temperature for the Accumulator and RHR Lines are obtained from Section 4.0. The temperature range for the transients of the Accumulator and RHR Lines are obtained from References 32 and 50 and reproduced in Table 6-1 and Table 6-2, respectively.

For the Accumulator and RHR Lines, the moments from deadweight, thermal and operating basis earthquake (OBE) are obtained as the maximum moments from Tables 4-7 through Table 4-15 and shown in Table 6-4. The calculated maximum and minimum axial pressure, thermal, and dead weight stresses for each of the plant transients are presented in Table 6-5 for the Accumulator Line and Table 6-6 for the RHR Line. The computed stress ranges for transients using Table 6-5 and Table 6-6 are presented in Table 6-7 and Table 6-8 for the Accumulator and RHR Lines, respectively. For the Surge Line, the stress ranges are computed from maximum and minimum stresses in Table 6-3 and presented in Table 6-9.

For all the lines, the weld residual stress is conservatively represented by a pure through-wall bending stress equal to the yield stress of the pipe material at the operating temperature. Since Accumulator, RHR and Surge Lines are made of materials of similar type, the most conservative yield stress was chosen for all three types of lines. Thus, $S_y = 18.28$ ksi of Material Type 316 at 653°F is used in this analyses.

The number of OBE event occurrences are 50, obtained from Reference 32. This number is applicable to 80 years of operation per Reference 51. Note that OBE loads are conservatively assumed to be the same as SSE loads where OBE loads are not directly available.

6.3 Allowable Flaw Size

Since the stainless steel piping material behaves in a ductile manner, the net section plastic collapse methodology in Appendix C of ASME Code Section XI [26] can be used to determine the allowable flaw size. The load combination used for determining the allowable flaw size is pressure, deadweight, thermal expansion and seismic. The flow stress, σ_f for all three types of lines is conservatively assumed as 45.14 ksi (Type 316 at 653°F).

For the Accumulator Line, the total stress for this load combination is 19.02 ksi. The stress ratio $(\sigma_m + \sigma_b) / \sigma_f = 0.42$. With an aspect ratio a/l of 0.1 and a thickness of 1.0 inch, starting with the maximum allowable flaw depth-to-thickness ratio of 0.75, the maximum possible flaw length is 7.5 inches. The ratio of this flaw length to the pipe circumference is 0.22. Using Table C-5310-3 Table C-5310-4 for emergency and faulted conditions, the allowable end-of-evaluation period flaw depth-to- thickness ratio is determined to be 0.75.

For the RHR Line, the total stress for this load combination is 24.73 ksi. The stress ratio $(\sigma_m + \sigma_b) / \sigma_f = 0.55$. With an aspect ratio a/l of 0.1 and a thickness of 1.25 inch, starting with the maximum allowable flaw depth-to-thickness ratio of 0.75, the maximum possible flaw length is 9.34 inches. The ratio of this flaw length to the pipe circumference is 0.22. Using Table C-5310-

3 Table C-5310-4 for emergency and faulted conditions, the allowable end-of-evaluation period flaw depth-to- thickness ratio is determined to be 0.70.

For the Surge Line, the total stress for this load combination is 17.38 ksi. The stress ratio $(\sigma_m + \sigma_b) / \sigma_f = 0.39$. With an aspect ratio a/l of 0.1 and a thickness of 1.125 inch, starting with the maximum allowable flaw depth-to-thickness ratio of 0.75, the maximum possible flaw length is 8.44 inches. The ratio of this flaw length to the pipe circumference is 0.21. Using Table C-5310-3 Table C-5310-4 for emergency and faulted conditions, the allowable end-of-evaluation period flaw depth-to- thickness ratio is determined to be 0.75.

6.4 Fatigue Crack Growth Analysis

The fatigue crack growth analysis is performed for the number of cycles corresponding to the 40-year design plant life shown in Section 6.1. These cycles are applicable to both 60 years of operation per Reference [55], and 80 years of operation per Reference [51]. In the definition of the stress ranges, the stresses are cycled around the sum of deadweight and weld residual stresses, which are always in effect. For each enveloping transient category, the appropriate scaling factors (transient stress/reference stress) are input to obtain the actual K values for the fatigue crack growth.

6.4.1 Fatigue Crack Growth Law Used for 60-Year Operation Calculations

Crack growth in stainless steel for 60 years is calculated using the austenitic steel fatigue crack growth law in air from Article C-3210 of the ASME, Section XI [26]. Reference [33] indicates a factor of 2 may be applied to account for a PWR environment. This is accounted for in **pc-CRACK 4.1** [49a] by doubling the number of cycles.

$$(da/dN)_{\text{air}} = C_0(\Delta K)^n, \text{ units of inch/cycle}$$

where:

da/dN = crack growth per cycle, a is the crack depth, N is the number of cycles

C_0 = $C \cdot S$

C = $10^{[-10.009 + 8.12 \times 10^{-4}T - 1.13 \times 10^{-6}T^2 + 1.02 \times 10^{-9}T^3]}$

$$\begin{aligned}
S &= 1.0 && \text{when } R \leq 0 \\
&= 1.0 + 1.8R && \text{when } 0 < R \leq 0.79 \\
&= -43.35 + 57.97R && \text{when } 0.79 < R < 1.0 \\
T &= \text{metal temperature, } ^\circ\text{F (taken as the maximum during the transient)} \\
R &= \text{R-ratio} = (K_{\min}/K_{\max}) \\
\Delta K &= K_{\max} - K_{\min} = \text{range of stress intensity factor, ksi-in}^{0.5} \\
n &= 3.3 \text{ per Section XI, Appendix C [26]}
\end{aligned}$$

Note that for negative R-ratios ($K_{\min} < 0$ and $K_{\max} > 0$), the “S” value is 1.0, which could lead to over conservative crack growth for the stainless steel weld. The max C_0 and thus most conservative growth rate is used for each transient considered.

6.4.2 Fatigue Crack Growth Law Used for 80-Year Operation Calculations

Crack growth in stainless steel for 80 years uses the fatigue crack growth (FCG) law for stainless steels and associated weld metals from ASME Code Case N-809 [53]:

$$da/dN = C_0 \cdot \Delta K^n, \text{ units of inch/cycle}$$

where:

$$\begin{aligned}
C_0 &= \text{scaling parameter that accounts for the effect of loading rate and environment on fatigue crack growth rate} \\
&= C S_T S_R S_{ENV} \\
n &= \text{slope of the log (da/dN) versus log (ΔK) curve} = 2.25 \\
C &= \text{nominal fatigue crack growth rate constant} \\
&= 4.43 \times 10^{-7} \text{ for } \Delta K \geq \Delta K_{th} \\
&= 0 \text{ for } \Delta K < \Delta K_{th} \\
\Delta K &= \text{stress intensity factor range, ksi}\sqrt{\text{in}} \\
\Delta K_{th} &= 1.10 \text{ ksi}\sqrt{\text{in}} \\
S_T &= \text{parameter defining effect of temperature on FCG rate} \\
&= e^{-2516/T_K} \text{ for } 300^\circ\text{F} \leq T \leq 650^\circ\text{F} \\
&= 3.39 \times 10^5 e^{[(-2516/T_K) - 0.0301T_K]} \text{ for } 70^\circ\text{F} \leq T < 300^\circ\text{F} \\
T &= \text{metal temperature, } ^\circ\text{F} \\
S_R &= \text{parameter defining the effect of R-ratio on FCG rate} \\
&= 1.0 \text{ for } R < 0 \\
&= 1 + e^{8.02(R-0.748)} \text{ for } 0 \leq R < 1.0 \\
R &= K_{\min}/K_{\max} = \text{R ratio} \\
S_{ENV} &= \text{parameter defining the environmental effects on FCG rate} \\
&= T_R^{0.3} \\
T_R &= \text{loading rise time, sec} \\
T_K &= [(T-32)/1.8+273.15], K
\end{aligned}$$

The metal temperature of 653°F is applied to calculate the crack growth rate. A conservative loading rise time of 15,000 seconds is applied to calculate the crack growth rate.

The crack growth rate changes based on the R-ratio. The da/dN for selected ΔK is calculated for different R-ratios and entered into **pc-CRACK 4.1** [49a] to calculate crack growth using Code Case N-809 FCG equation.

6.4.3 Part Through-Wall Crack Growth

The crack growth analysis is performed using the fracture mechanics software program **pc-CRACK 4.1** [49a]. Based on the guidelines of ASME Code Section XI, IWB-3514, an initial flaw size equal to the allowable depth of up to 12.5% of wall thickness is postulated. For the crack growth analysis, an aspect ratio a/l of 0.1 is conservatively assumed for the initial flaw, where 'a' is the flaw depth and 'l' is the flaw length.

The results are shown in Table 6-10. Considering the larger growth of 80 years using the crack growth law from ASME Code Case N-809, the results show that the postulated partial through wall crack ($a/t = 0.125$, $a/l = 0.1$) does not grow during the design plant life for the Accumulator Line. For the RHR Line, the postulated crack ($a/t = 0.125$, $a/l = 0.1$) grows only 0.0014 inch during the design plant life to a final a/t ratio of 0.1262. This final a/t ratio is less than the allowable ratio of 0.70 documented in Section 6.3. For the Surge Line, the postulated crack ($a/t = 0.125$, $a/l = 0.1$) grows 0.0855 inch during the design plant life to a final a/t ratio of 0.2010. This final a/t ratio is less than the allowable ratio of 0.75 documented in Section 6.3.

Hence, the integrity of the auxiliary line piping is not jeopardized between in-service inspections.

6.4.4 Through-Wall Crack Growth

NUREG-1061, Section 5.2 (g) [6] requires that an evaluation be performed to show that the leakage flaw size is stable during an SSE event. A very simple approach is taken to determine the

crack growth of a through-wall leakage size flaw to demonstrate stability. The initial through-wall flaw is assumed to correspond to the leakage flow length for the most limiting location. A crack model in **pc-CRACK™** [49b] for a through-wall circumferential crack in a cylinder under tension and bending is used for the stress intensity K calculation. In this evaluation, the maximum $\sigma_m + \sigma_b$ is conservatively applied as tension stress in the **pc-CRACK™** input.

For the Accumulator Line, the maximum $\sigma_m + \sigma_b$ is 19.02 ksi (including internal pressure), and the bounding leakage flow size is 2.53 inches with bending stress = 0 for 5GPM (Figure 5-1). The resultant stress intensity factor K is $65.66 \text{ ksi}\sqrt{\text{in}}$. Using a conservative R ratio (0.99) in the ASME Code Section XI crack growth curve for stainless steels in a water environment (Figure C-8410-1) gives a crack growth per cycle of 5.9×10^{-3} inches, whereas the ASME Code Case N-809 crack growth curve gives 1.32×10^{-2} inches per cycle. For assumed 1 SSE and 50 OBE cycles, this translates into 0.301 inches for ASME Section XI crack growth law and 0.673 inches for Code Case N-809 crack growth law. This crack growth is insignificant compared to the total circumference of 33.77 inches.

For the RHR Line, the maximum $\sigma_m + \sigma_b$ is 17.38 ksi (including internal pressure), and the leakage flow size is 3.12 inches with bending stress = 0 for 5GPM (Figure 5-2). The stress intensity factor K, can be calculated as $54.41 \text{ ksi}\sqrt{\text{in}}$. Using a conservative R ratio (0.99) in the ASME Code Section XI crack growth curve for stainless steels in a water environment (Figure C-8410-1), the crack growth per cycle is 5.9×10^{-3} inches, whereas the ASME Code Case N-809 crack growth curve gives 1.33×10^{-2} inches per cycle. For assumed 1 SSE and 50 OBE cycles, this translates into 0.301 inches for ASME Section XI crack growth law and 0.678 inches for Code Case N-809 crack growth law. This crack growth is insignificant compared to the total circumference of 43.98 inches.

For the Surge Line, the maximum $\sigma_m + \sigma_b$ is 2.73 ksi (including internal pressure), and the bounding leakage flow size is 3.30 inches with bending stress = 0 for 5GPM (Figures 5-3 to 5-6). The stress intensity factor K, can be calculated as $101.77 \text{ ksi}\sqrt{\text{in}}$. Using a conservative R ratio

(0.99) in the ASME Code Section XI crack growth curve for stainless steels in a water environment (Figure C-8410-1), the crack growth per cycle is 2.49×10^{-2} inches, whereas the ASME Code Case N-809 crack growth curve gives 3.55×10^{-2} inches per cycle. For assumed 1 SSE and 50 OBE cycles, this translates into 1.27 inches for ASME Section XI crack growth law and 1.81 inches for Code Case N-809 crack growth law. This crack growth is insignificant compared to the total circumference of 40.06 inches.

As shown in Table 6-10, for a partial through-wall crack in the RHR Line, the crack growth in the depth direction is 0.0014 inch and the crack growth in the length direction is 0.0004 inch. This is about 0.0009% of the 43.96 inch circumference length, and compared to the crack growth of 0.12% (12.50% to 12.62% in Table 4-1) in the depth direction, it is relatively small. For the Surge Line, the crack growth in the depth direction is 0.0855 inch and the crack growth in the length direction is 0.0452 inch. This is 0.113% of the 40.03 inch circumference length, and compared to the 7.6% (12.50% to 20.10% in Table 4-1) in the depth direction, it is relatively small. Overall, for the RHR and surge lines, the partial through-wall cracks tend to grow in the depth direction and through-wall before extending significantly in the length (circumferentially) direction. There is no growth in the accumulator line.

Table 6-1. Accumulator Line Operating Condition Transients⁽¹⁾

Transient	Design Transients	Occurrences ⁽²⁾	$\Delta P^{(3)}$ (psi)	ΔT (°F)
1	Inadvertent RCS Depressurization	20	1,117	490
2	Inadvertent Accumulator Blowdown	4	232	330
3	Post LOCA Operation	1	1,117	490
4	OBE	50 ⁽⁴⁾		

- Notes:
1. Per Reference [31].
 2. The above event counts reflect the 40-year design life, which is applicable to both 60 years and 80 years of operation per References [51] and [55].
 3. Conservatively calculated as the pressure difference between the saturated steam pressure at high temperature and ambient pressure.
 4. Assumed the same as in Surge Line, obtained from Reference [32].

Table 6-2. RHR Line Operating Condition Transients [32]

Transient	Design Transients	Occurrences ⁽¹⁾	ΔP (psi)	ΔT (°F)
1	Heat Up /Cooldown	200 each	1925	437
2	Unit Load/Unload at 0-15% Full power	500 each	0	9.6
3	Unit Load /Unload at 5% Full power	13,200	68	55
4	Step Load Increase/Decrease of 10% Full power	2,000 each	109	8.7
5	Reactor Trip with Cooldown and Safety Injection	10	539	139
6	Primary Side Leakage Test	200	800	0 (Assumed)
7	OBE	50 ⁽²⁾		

- Notes
1. The above event counts reflect the 40-year design life, which is applicable to both 60 years and 80 years of operation per References [51] and [55].
 2. Assumed the same as in Surge Line, obtained from Reference [32].

Table 6-3 Surge Line Operating Condition Transients [50]

Transient #	Design Transients	Occurrences ⁽¹⁾	Max Stress ⁽³⁾ (ksi)	Min Stress ⁽³⁾ (ksi)
1	Heatup	200 ⁽²⁾	10.158	-8.179
2	Unit Loading	13,200 ⁽²⁾	14.583	11.150
3	Step Load Increase and Decrease	4000	15.465	9.599
4	Large Step Load Decrease with Steam Dump	200	14.470	9.430
5	SS Fluctuation	3,150,000	12.232	10.895
6	Loss of Load	80	18.677	9.340
7	Loss of Power	40	17.259	9.449
8	Loss of Flow	80	14.286	9.299
9	Reactor Trip	400	15.963	2.654
10	Inadvertent Auxiliary Spray	10	15.045	11.108
11	OBE	50	15.735	3.972
12	Unit Unloading	13,200 ⁽²⁾	14.583	11.150
13	Cool Down	200 ⁽²⁾	10.158	-8.179
14	Turbine Roll Test	10	2.292	0.000
15	Hydrotest @3107 psi	5	9.858	0.000
16	Leak Test @ 2485 psi	50	8.145	0.000

- Notes
1. The above event counts reflect the 40-year design life, which is applicable to both 60 years and 80 years of operation per References [51] and [55].
 2. Assumed the same as Accumulator Line [31].
 3. Values are assumed the same as unit loading transient.

Table 6-4. Piping Loads for Accumulator and RHR Lines

Components	Deadweight Moments (ft-lb)			Thermal Moments (ft-lb)			OBE Moments (ft-lb)		
	M _x	M _y	M _z	M _x	M _y	M _z	M _x	M _y	M _z
Accumulator Lines	2,847	5,545	25,236	38,919	33,733	26,644	40,607	38,813	17,688
RHR Lines	3,574	2,721	15,696	96,351	88,786	66,018	35,002	52,858	23,458

Table 6-5. Accumulator Line Maximum and Minimum Transient Stresses

Transient	Maximum Stresses (ksi)				Minimum Stresses (ksi)			
	Pressure	Thermal	DW	Total	Pressure	Thermal	DW	Total
1	2.193	10.169	0.000	0.000	22.838	2.193	33.007	0.000
2	2.648	17.017	1.737	3.320	22.838	2.648	39.856	1.737
3	4.386	20.338	0.000	0.000	22.838	4.386	43.176	0.000
4	4.878	0.000	4.558	19.764 ⁽¹⁾	4.878	0.000	4.558	-0.891 ⁽¹⁾

Note: (1) The OBE stress (10.32 ksi) is added to maximum stress and subtracted from minimum stress.

Table 6-6. RHR Line Maximum and Minimum Transient Stresses

Transient	Maximum Stresses (ksi)				Minimum Stresses (ksi)			
	Pressure	Thermal	DW	Total	Pressure	Thermal	DW	Total
1	3.993	10.810	1.335	16.139	0.000	0.000	1.335	1.335
2	3.993	11.048	1.335	16.376	3.993	10.573	1.335	15.901
3	4.134	12.171	1.335	17.640	3.852	9.450	1.335	14.637
4	4.220	11.025	1.335	16.580	3.767	10.595	1.335	15.697
5	5.112	14.249	1.335	20.695	2.875	7.372	1.335	11.582
6	5.653	10.810	1.335	17.798	2.334	10.810	1.335	14.479
7	4.637	0	1.335	11.499 ⁽¹⁾	4.637	0.000	1.335	0.444 ⁽¹⁾

Note: (1) The OBE stress (5.53 ksi) is added to maximum stress and subtracted from minimum stress.

Table 6-7. Stress Range for Accumulator Line

Group	Cyclic Stresses (ksi)				DW + Residual (ksi)	Total Stress Ranges (ksi)			
	Maximum		Minimum			Maximum		Minimum	
	Uniform	Linear	Uniform	Linear		Uniform	Linear	Uniform	Linear
1	2.193	10.169	0.000	0.000	22.838	2.193	33.007	0.00	22.838
2	2.648	17.017	1.737	3.320	22.838	2.648	39.856	1.737	26.159
3	4.386	20.338	0.000	0.000	22.838	4.386	43.176	0.000	22.838
4	4.878	10.328	4.878	-10.328	22.838	4.878	33.166	4.878	12.511

Table 6-8. Stress Range for RHR Line

	Cyclic Stresses (ksi)				DW +Residual(ksi)	Total Stress Ranges (ksi)			
	Maximum		Minimum			Maximum		Minimum	
Group	Uniform	Linear	Uniform	Linear		Uniform	Linear	Uniform	Linear
1	3.993	10.810	0	0	19.615	3.993	30.425	0	19.615
2	3.993	11.048	3.993	10.573	19.615	3.993	30.663	3.993	30.188
3	4.134	12.171	3.852	9.450	19.615	4.134	31.786	3.852	29.065
4	4.220	11.025	3.767	10.595	19.615	4.220	30.641	3.767	30.210
5	5.112	14.249	2.875	7.372	19.615	5.112	33.864	2.875	26.987
6	5.653	10.810	2.334	10.810	19.615	5.653	30.425	2.334	30.425
7	4.637	5.528	4.637	-5.528	19.615	4.6365	25.143	4.637	14.087

Table 6-9. Stress Range for Surge Line

Transient #	Total Stress Ranges (ksi)			
	Maximum ⁽¹⁾		Minimum	
	Uniform	Linear	Uniform	Linear
1	4.742	23.696	0.000	10.101
2	4.742	28.121	0.000	29.430
3	4.742	29.003	0.000	27.879
4	4.742	28.008	0.000	27.710
5	4.784 ⁽²⁾	25.728	4.700 ⁽²⁾	24.475
6	4.742	32.215	0.000	27.620
7	4.742	30.797	0.000	27.729
8	4.742	27.824	0.000	27.579
9	4.742	29.501	0.000	20.934
10	4.742	28.583	0.000	29.388
11	4.742	29.273	0.000	22.252
12	4.742	28.121	0.000	29.430
13	4.742	23.696	0.000	10.101
14	4.742	15.830	0.000	18.280
15	6.548 ⁽³⁾	21.590	0.000	18.280
16	5.237 ⁽⁴⁾	21.188	0.000	18.280

Note:

- (1) For all the transients with no pressure information, the operating pressure of 2250 psi is conservatively used to calculate the Maximum uniform stress.
- (2) For Transient 5 (steady state fluctuation as shown in Table 6-3), a typical pressure ± 20 psi was added to 2,250 to calculate the maximum and minimum uniform stress
- (3) The pressure of 3,107psi, as shown in Table 6-3, is used.
- (4) The pressure of 2,485 psi, as shown in Table 6-3, is used.

Table 6-10. Results of Fatigue Crack Growth Analysis

Auxiliary Lines	Postulated Initial Flaw			60 Years (ASME Section XI)			80 Years (ASME CC N-809)		
	a/t	Depth a _i (in)	Half Length c _i (in)	a/t	Depth a _r (in)	Half Length c _r (in)	a/t	Depth a _r (in)	Half Length c _r (in)
Accumulator Line	12.50%	0.1250	0.6250	12.50%	0.1250	0.6250	12.50%	0.1250	0.6250
RHR Line	12.50%	0.1563	0.7815	12.50%	0.1563	0.7815	12.62%	0.1577	0.7817
Surge Line	12.50%	0.1406	0.7030	12.57%	0.1414	0.7031	20.10%	0.2261	0.7256

7.0 CONCLUSIONS

Leak-before-break (LBB) evaluations are performed for RCS auxiliary piping at PTN Units 3 and 4 in accordance with the requirements of NUREG-1061. The evaluation included the following lines:

1. 10" diameter Accumulator Lines – 3 lines (one per RCL connected to cold leg)
2. 12" pressurizer Surge Line – 1 line attached to "B" loop
3. 14" residual heat removal line – 1 line attached to "C" loop in Unit 3 and "A" loop in Unit 4 (connected to hot leg)

The approach taken herein is consistent with SRP 3.6.3 and has been used in recent LBB submittals for other plants [2, 3, 4]. The analysis was performed using conservative lower bound material properties for the base metals and weldments and location specific stresses consisting of pressure, deadweight, thermal and SSE loads. The evaluations considered only circumferential flaws since previous evaluations have shown them to be more limiting than axial flaws. Critical flaw sizes and leakage flow sizes were calculated on a location specific basis using limit load analysis. The leakage flow size is defined as the minimum of one half the critical flaw size with a factor of one on the stresses. Leakage was then calculated through the leakage flow size. Bounding analysis curves (BAC) were then derived which provide loci of acceptable normal operating loads (for leakage calculation) and normal +SSE loads (for critical flaw size calculation) for a given leakage. Fatigue crack growth analysis was also performed to determine the extent of growth of any pre-existing flaws.

Based on these evaluations, the following conclusions can be made.

- For both PTN Units 3 and 4, all of the stress points of the 5 analyzed lines are under or very close to the BACs of 10 GPM leakage, which correspond to the 1 GPM detection capability.
- Fatigue crack growth of an assumed surface flaw is less than ASME Code Section XI allowable flaw size for the most limiting locations for all piping under consideration in this evaluation. In this revision of the report, the previous fatigue crack growth evaluation for 60 years is updated to use the current version of the pc-CRACK software

(**pc-CRACK 4.1** [49a]) and to correct for the errors documented in Corrective Action Report (CAR) 17-012 [54]. Also, fatigue crack growth for 80 years of operation is added to address Subsequent License Renewal (SLR) operation utilizing the updated ASME Code Case N-809 [53] fatigue crack growth rate.

- The effect of degradation mechanisms that could invalidate the LBB evaluations was considered in the evaluation. A determination was made that there is no potential for water hammer, intergranular stress corrosion cracking (IGSCC) and erosion-corrosion for the piping systems considered in the LBB evaluations.

In conclusion, the five auxiliary lines of the RCL piping systems of PTN Units 3 and 4 evaluated in this report qualify for the application of leak-before-break analysis to demonstrate that it is very unlikely that the piping could experience a large pipe break prior to leakage detection.

8.0 REFERENCES

1. EPU Bechtel/Engineering Services Project Scope Document, “Development of Technical Report to Apply Leak-Before-Break (LBB) Methodology to Auxiliary Lines Connected to Primary Reactor Coolant Loops at Turkey Point Units 3 and 4”.
2. Letter from G. S. Vissing (USNRC) to R. C. McCredy (RG&E) including Safety Evaluation Report, “Staff Review of the Submittal by Rochester Gas & Electric to Apply Leak Before Break Status to portions of R. E. Ginna Nuclear Power Plant Residual Heat Removal System Piping (TAC No. MA039)”, dated February 25, 1999, Docket No. 50-244.
3. Letter from R. B. Eaton (USNRC) to R. P. Necci (Northeast Nuclear Energy Company) including Safety Evaluation Report, “Staff Review of the Submittal by Northeast Nuclear Energy Company to Apply Leak Before Break Status to the Pressurizer Surge Line, Millstone Nuclear Power Station Unit 2 (TAC No. MA4146)”, dated May 4, 1999, Docket No. 50-336.
4. Letter from J. G. Lamb (USNRC) to T. Contu (Nuclear Management Company, LLC) including Safety Evaluation Report, “Kewaunee Nuclear Power Plant - Review of the Leak Before Break Evaluation for the Residual Heat Removal, Accumulator Injection Line, and Safety Injection System (TAC No. MB1301)”, dated September 5, 2002, Docket No. 50-305.
5. Stello, Jr., V., “Final Broad Scope Rule to Modify General Design Criterion 4 of Appendix A, 10 CFR Part 50,” NRC SECY-87-213, Rulemaking Issue (Affirmation), August 21, 1987.
6. NUREG-1061, Volumes 1-5, “Report of the U. S. Nuclear Regulatory Commission Piping Review Committee,” prepared by the Piping Review Committee, NRC, April 1985.
7. NUREG-0800, “U.S. Nuclear Regulatory Commission Standard Revision Plan, Office of Nuclear Reactor Regulation, Section 3.6.3, Leak-Before-Break Evaluation Procedure,” August 1987.
8. FPL Document, “ Leak Detection Capabilities 3/4.4.6,” SI File 0901350.206.
9. NUREG-0927, “Evaluation of Water Hammer Occurrence in Nuclear Power Plants,” Revision 1.
10. W. S. Hazelton and W. H. Koo, “Technical Report on Material Selection and Processing Guidelines for BWR Coolant Pressure Boundary Piping,” NUREG-0313, Rev. 2, USNRC, January 1988.

11. EPRI Report No. NP-3944, "Erosion/Corrosion in Nuclear Power Plant Steam Piping: Causes and Inspection Program Guidelines," April 1985
12. NRC Bulletin No. 88-08, "Thermal Stresses in Piping Connected to Reactor Coolant Systems," June 22, 1988.
13. FPL Stress Report SP-13, 14, 15 (TR 5322-43) "Unit 3 Book 1 of 16-Technical Report".
14. FPL Stress Report SP-13, 14, 15 SP-044 (TR-5322-126), "Unit 4 book 1 of 7-Technical Report".
15. Crane Co., Technical Paper No. 410, "Flow of Fluid Through Valves, Fittings, and Pipe", 1976.
16. FPL Stress Report SP-041 (TR-5322-135), "Units 3 and 4 Book 1 of 4 Technical Report".
17. FPL Drawing 5613-P-766, Sheet 1 of 3, Rev. 5, "Turkey Point Nuclear Power Plant Unit 3".
18. FPL Drawing 5614-P-766, Sheet 1 of 3, Rev. 3, "Turkey Point Nuclear Power Plant Unit 4".
19. FPL Technical Report SI-13 TR-5322-15, Rev. 1, "Unit 3-RHR System".
20. FPL Technical Report SI-16 TR-5322-155, Rev. 1, "Unit 4 Book 1 Report and Book 2-BPC Stress Run".
21. FPL Document MN-3.11, "Piping Specification".
22. Bechtel Document P8-AT-AG, "Bechtel Welding Procedure Qualification Record PQR No. 47".
23. FPL Drawing 40038, Rev. 2, "10" Sch. 140 BW. Nozzle Reactor Coolant Piping".
24. FPL Document WPS-43, Sheet 2 of 3, Rev. 11, "Welding Procedure Specification".
25. ASME Boiler and Pressure Vessel Code, Section II, Part D - Properties, 2001 Edition with Addenda through 2003.
26. ASME Boiler and Pressure Vessel Code, Section XI, 2001 Edition with Addenda through 2003.
27. EPRI Report No. NP-5531, "Evaluation of High-Energy Pipe Rupture Experiments," January 1988.

28. EPRI Report NP-3596-SR, "PICEP: Pipe Crack Evaluation Computer Program," Rev. 1, July 1987.
29. P.E. Henry, "The two-Phase Critical Discharge of Initially Saturated or Sub-cooled Liquid," Nuclear Science and Engineering, Vol. 41, 1970.
30. EPRI Report NP-3395, "Calculation of Leak Rates Through Crack in Pipes and Tubes," December 1983.
31. Westinghouse Proprietary Document, "System Standard 1.3.X, Nuclear Steam Supply System Auxiliary Equipment Design Transients for All Standard Plants".
32. Westinghouse Proprietary Document, "System Standard 1.3.F, Nuclear Steam Supply System Reactor Coolant System Design Transients for Standard Plants with Model F Steam Generators".
33. Section XI Task Group for Piping Flaw Evaluation, ASME Code, "Evaluation of Flaws in Austenitic Steel Piping, " Journal of Pressure Vessel Technology, Vol. 108, August 1986.
34. FPL Drawing 5613-P-585, Sheet 1 of 1, Rev. 6, "Turkey Point Nuclear Power Plant Unit 3".
35. FPL Drawing 5613-P-586, Sheet 1 of 1, Rev. 6, "Turkey Point Nuclear Power Plant Unit 3".
36. FPL Drawing 5613-P-587, Sheet 2 of 2, Rev. 4, "Turkey Point Nuclear Power Plant Unit 3".
37. FPL Drawing 5613-P-669, Sheet 1 of 1, Rev. 5, "Turkey Point Nuclear Power Plant Unit 3".
38. FPL Drawing 5613-P-766, Sheet 2 of 3, Rev. 4, "Turkey Point Nuclear Power Plant Unit 3".
39. FPL Drawing 5614-P-509, Sheet 1 of 4, Rev. 9, "Turkey Point Nuclear Power Plant Unit 4".
40. FPL Drawing 5614-P-509, Sheet 3 of 4, Rev. 3, "Turkey Point Nuclear Power Plant Unit 4".
41. FPL Drawing 5614-P-509, Sheet 4 of 4, Rev. 3, "Turkey Point Nuclear Power Plant Unit 4".
42. FPL Drawing 5614-P-574, Sheet 1, Rev. 5, "Turkey Point Nuclear Power Plant Unit 4".

43. FPL Drawing 5614-P-766, Sheet 2 of 3, Rev. 2, "Turkey Point Nuclear Power Plant Unit 4".
44. (a) FPL Stress Report SP-13, 14, 15 (TR 5322-43) "Unit 3 Book 6 of 16-BPC Stress Run".
- (b) FPL Stress Report SP-13, 14, 15 (TR 5322-43) "Unit 3 Book 7 of 16- BPC Stress Run".
- (c) FPL Stress Report SP-13, 14, 15 (TR 5322-43) "Unit 3 Book 8 of 16- BPC Stress Run".
- (d) FPL Stress Report SP-13, 14, 15 (TR 5322-43) "Unit 3 Book 9 of 16- BPC Stress Run".
- (e) FPL Stress Report SP-13, 14, 15 (TR 5322-43) "Unit 3 Book 8 of 16- BPC Stress Run".
- (f) FPL Stress Report SP-13, 14, 15 (TR 5322-43) "Unit 3 Book 9 of 16- BPC Stress Run".
45. (a) FPL Stress Report SP-044 (TR 5322-126) "Unit 4 Book 6 of 7- BPC Stress Run".
- (b) FPL Stress Report SP-044 (TR 5322-126) "Unit 4 Book 7 of 7- BPC Stress Run".
46. FPL Stress Report SP-041 (Stress Problem 041), "FPL/FLA (Turkey point 3 and 4) Pressurizer Surge Nozzle Fatigue Calculations Due to Thermal Stratification Piping Loads – NRC Review".
47. FPL Stress Report SI-13 (TR 5322-15) "Unit 3 Book 2 of 2- BPC Stress Run."
48. FPL Stress Report SI-16 (TR 5322-155) "Unit 4 Book 2 of 2- BPC Stress Run."
49. **pc-CRACK**.
- a. **pc-CRACK** 4.1 CS, Version Control No. 4.1.0.0, Structural Integrity Associates, December 31, 2013.
- b. **pc-CRACK**TM for Windows, Version 3.1-98348, Structural Integrity Associates, 1998.
50. FPL Stress Report (TR 0537), "FPL/FLA (Turkey Point 3 and 4) Pressurizer Surge Nozzle Fatigue Calculation Due to Thermal Stratification Pipe Loads".
51. SI Report No. 1700109.402, (under Preparation) "*Evaluation of Fatigue of ASME Section III, Class 1 Components for Turkey Point Units 3 and 4 for Subsequent License Renewal*".

52. FPL Document EPU-PTN-10-0536, "FPL TURKEY POINT UNITS 3 & 4 EXTENDED POWER UPRATE (EPU) INFORMATION FOR LEAK BEFORE BREAK METHODOLOGY APPLIED TO RCL BRANCH PIPING".
53. ASME Code Case N-809, "Reference Fatigue Crack Growth Rate Curves for Austenitic Stainless Steels in Pressurized Water Reactor Environments Section XI, Division 1," Cases of the ASME Boiler and Pressure Vessel Code, June 23, 2015.
54. SI Corrective Action Report (CAR) No. 17-012, Revision 0, "Turkey Point LBB Evaluation, Calculation Package File No.: 0901350.304, Rev. 0, Calculation Title: Fatigue Crack Growth Evaluation," April 17, 2017.
55. Turkey Point Units 3 and 4 License Renewal Document, "Position Document to Address GSI-190 Issues Related to Fatigue Evaluation for Turkey Point Units 3 and 4", SI Report No. SIR-00-089. Rev. 0.



Structural Integrity Associates, Inc.®

CALCULATION PACKAGE

File No.: 0901350.304

Project No.: 1700109

Quality Program: ☒ Nuclear ☐ Commercial

PROJECT NAME:

Turkey Point 3 and 4 TLAA Support for SLR

CONTRACT NO.:

2000230248

CLIENT:




Florida Power & Light (FPL)

CLIENT:

Florida Power & Light (FPL)

CALCULATION TITLE:

Fatigue Crack Growth Evaluation

Document Revision	Affected Pages	Revision Description	Project Manager Approval Signature & Date	Preparer(s) & Checker(s) Signatures & Date
0	1 - 23 A1 – A24 Computer Files	Initial Issue	Art McSherry 4/15/10	Peihua Jing 4/15/10 Haiyang Qian 4/15/10
1	1 - 20 A1 – A52 Computer Files	Updated 60-year results in response to CAR 17-012. Extended evaluation to cover 80 years of operation and to use updated fatigue crack growth law.	Gary Stevens 7/10/17	Wilson Wong 7/10/17 DJ Shim 7/10/17
2	5, 6, 9, 11, 14	Addressed client editorial comments	 Gary Stevens 9/18/17	 Wilson Wong 9/18/17  DJ Shim 9/18/17

Contains Vendor Proprietary Information

Table of Contents

1.0	OBJECTIVE	4
2.0	METHODOLOGY	4
3.0	CALCULATIONS.....	5
3.1	Plant Design Transients	5
3.2	Stresses	7
3.2.1	<i>Internal Pressure</i>	8
3.2.2	<i>Thermal Expansion</i>	8
3.2.3	<i>Dead Weight</i>	9
3.2.4	<i>Residual Stress</i>	11
3.2.5	<i>Seismic Loads</i>	11
3.2.6	<i>Stress Ranges</i>	11
3.3	Allowable Flaw Size.....	14
3.4	Fatigue Crack Growth Analysis.....	14
3.4.1	<i>Fatigue Crack Growth Law Used for 60-Year Operation Calculations</i>	14
3.4.2	<i>Fatigue Crack Growth Law Used for 80-Year Operation Calculations</i>	15
3.4.3	<i>Part Through-Wall Crack Growth</i>	16
3.4.4	<i>Through-Wall Crack Growth</i>	16
4.0	RESULTS	17
5.0	REFERENCES	19
	APPENDIX A PC-CRACK OUTPUT	A-1

List of Tables

Table 3-1: Accumulator Line Operating Condition Transients.....	5
Table 3-2: RHR Line Operating Condition Transients.....	6
Table 3-3: Surge Line Operating Condition Transients	7
Table 3-4: Pipe Geometry Inputs.....	8
Table 3-5: Operating Conditions	8
Table 3-6: Piping Loads for Accumulator and RHR Lines	9
Table 3-7: Accumulator Line Maximum and Minimum Transient Stresses	10
Table 3-8: RHR Line Maximum and Minimum Transient Stresses.....	10
Table 3-9: Stress Ranges for Accumulator Line.....	12
Table 3-10: Stress Ranges for RHR Line	12
Table 3-11: Stress Ranges for Surge Line	13
Table 4-1: Fatigue Crack Growth Results	17

1.0 OBJECTIVE

This calculation package documents the analysis performed to study the fatigue crack growth of cracks in 5 auxiliary lines at the Turkey Point Nuclear Plant (PTN), Units 3 and 4 as part of the leak-before-break evaluation (LBB) of these lines. The auxiliary lines of interest are pipes attached to the primary reactor coolant loop (RCL) piping, shown as follows:

1. 10-inch diameter accumulator lines – 3 lines (one per RCL)
2. 12-inch pressurizer surge line – 1 line attached to “B” loop
3. 14-inch residual heat removal (RHR) line – 1 line attached to “C” loop in Unit 3 and “A” loop in Unit 4

The first objective of this analysis is to show that a postulated circumferential partial through-wall crack (PTWC) of ASME B&PV Code [1], IWB-3514 allowable depth for stainless steel (up to 12.5% of wall thickness) does not grow significantly between in-service inspection (ISI) intervals. The second purpose of this analysis is to demonstrate that if larger PTWCs exist they would tend to grow in the depth direction and through the pipe wall before extending significantly in length (circumferentially) to cause double guillotine break failure, thus exhibiting leak-before-break behavior. The third purpose of this analysis is to show that the through-wall crack is stable during an SSE event per NUREG-1061, Section 5.2 (g) [9].

In Revision 1 of the calculation, the previous fatigue crack growth evaluation for 60 years is updated to use the current version of the pc-CRACK software (**pc-CRACK 4.1** [8a]) and to correct for the errors documented in Corrective Action Report (CAR) 17-012 [15]. Also, fatigue crack growth for 80 years of operation is added to address Subsequent License Renewal (SLR) operation utilizing the updated ASME Code Case N-809 [6] fatigue crack growth rate.

2.0 METHODOLOGY

The fatigue crack growth calculations are performed with the following tasks:

- a. Calculate the total stresses range for each transient category including deadweight stresses.
- b. Use the ASME Section XI fatigue crack growth law [1] for austenitic stainless steels (for 60 years) and use the ASME Code Case N-809 [6] fatigue crack growth law (for 80 years) to perform crack growth analysis by applying the appropriate scaling factors to the reference K for the transient stresses.

Note that for Surge line, the stress range is given as design input, thus Step “a” is skipped.

3.0 CALCULATIONS

3.1 Plant Design Transients

Since the auxiliary lines at PTN were designed to the requirements of ANSI B31.1, no line specific transients are defined or analyzed in the design basis report. Hence, transient information from a generic Westinghouse plant is obtained to perform the crack growth evaluation. The plant transients affecting crack growth of the auxiliary lines of PTN Units 3 and 4, provided in References [2] and [3], are presented in Table 3-1 for the Accumulator Line and in Table 3-2 for the Residual Heat Removal Line.

In addition, the Surge Line experiences thermal stratification which results in a larger stress range, thus more fatigue growth during transients. A Westinghouse fatigue calculation [4] was conducted considering the thermal stratification during the transients. The definition of transients for crack growth, number of cycles, as well as the stress range for each transient are obtained from this calculation, and reproduced in Table 3-3.

Table 3-1: Accumulator Line Operating Condition Transients

Transient	Design Transients ⁽¹⁾	Occurrences ⁽²⁾	$\Delta P^{(3)}$ (psi)	ΔT (°F)
1	Inadvertent RCS Depressurization	20	1,117	490
2	Inadvertent Accumulator Blowdown	4	232	330
3	Post LOCA Operation	1	1,117	490
4	OBE	50 ⁽⁴⁾	0	0

Notes:

1. From Page 3-50 of Reference [2].
2. The above event counts reflect the 40-year design life, which is applicable to both 60 years and 80 years of operation per References [12 and 13].
3. Conservatively calculated as the pressure difference between the saturated steam pressure at high temperature and ambient pressure.
4. Assumed the same as in Surge Line [4].

Table 3-2: RHR Line Operating Condition Transients

Transient	Design Transients	Occurrences⁽¹⁾	ΔP (psi)	ΔT (°F)
1	Heat Up /Cooldown	200 each [Page 2-7]	1925 [Figure 3-2A,C]	437 [Figure 3-2B,D]
2	Unit Load/Unload at 15% Full power	500 each [Page 2-9]	0 [Figure 3-3]	9.6 [Figure 3-3]
3	Unit Load /Unload at 5% Full power	13,200 [Page 2-10]	68 [Figure 3-4A,D]	55 [Figure 3-4B,E]
4	Step Load Increase/Decrease of 10% Full power	2,000 each [Page 2-13]	109 [Figure 3-6A,D]	8.7 [Figure 3-6, B,E]
5	Reactor Trip with Cooldown and Safety Injection	10 [Page 2-26]	539 [Figure 3-15H]	139 [Figure 3-15J]
6	Primary Side Leakage Test	200 [Page 2-20]	800 [Page 2-20]	0 (Assumed)
7	OBE	50 ⁽²⁾	0	0

- Notes:
1. The above event counts reflect the 40-year design life, which is applicable to both 60 years and 80 years of operation per References [12 and 13].
 2. Assumed the same as in Surge Line [4].
 3. The Page numbers and Figure numbers in this table correspond to Reference [3].

Table 3-3: Surge Line Operating Condition Transients

Transient #	Design Transients	Occurrences ⁽¹⁾	Max Stress ⁽³⁾ (ksi)	Min Stress ⁽³⁾ (ksi)
1	Heatup	200 ⁽²⁾	10.158	-8.179
2	Unit Loading	13,200 ⁽²⁾	14.583	11.150
3	Step Load Increase and Decrease	4000	15.465	9.599
4	Large Step Load Decrease with Steam Dump	200	14.470	9.430
5	SS Fluctuation	3,150,000	12.232	10.895
6	Loss of Load	80	18.677	9.340
7	Loss of Power	40	17.259	9.449
8	Loss of Flow	80	14.286	9.299
9	Reactor Trip	400	15.963	2.654
10	Inadvertent Auxiliary Spray	10	15.045	11.108
11	OBE	50	15.735	3.972
12	Unit Unloading	13,200 ⁽²⁾	14.583 ⁽⁴⁾	11.150 ⁽⁴⁾
13	Cool Down	200 ⁽²⁾	10.158	-8.179
14	Turbine Roll Test	10	2.292	0.000
15	Hydrotest @ 3,107 psi	5	9.858	0.000
16	Leak Test @ 2,485 psi	50	8.145	0.000

- Notes:
1. The above event counts reflect the 40-year design life, which is applicable to both 60 years and 80 years of operation per References [12 and 13].
 2. Assumed the same as Accumulator Line [2].
 3. Stress values are obtained from Table 8 of Reference [4].
 4. Values are assumed the same as Unit Loading transient.

3.2 Stresses

Axial stresses in the auxiliary lines need to be determined since circumferential flaws are postulated for the LBB evaluation. For Surge Line, the stress range are documented in Reference [4] and given in Table 3-3. For Accumulator and RHR Lines, the axial stress due to the pressure, deadweight, thermal differentials for each of the transient as well as the seismic loads are calculated using the respective moments. Section 3.2.1 through Section 3.2.5 show the methodology of calculating stress range for Accumulator and RHR Lines. The thermal differentials for each transient of these lines are documented in References [2] and [3] and summarized in Table 3-1 and Table 3-2. The axial stresses due to each of the load categories are calculated by linear factorization as follows.

3.2.1 Internal Pressure

The axial stress due to operating pressure P_{oper} is calculated as

$$\sigma_p = \frac{P_{oper} D_i^2}{(D_o^2 - D_i^2)} \quad (3-1)$$

where, D_o is the outside diameter and D_i is the inside diameter of the pipe, obtained from Reference [5] and reproduced in Table 3-4.

Table 3-4: Pipe Geometry Inputs

	Accumulator Line	Surge Line ⁽¹⁾	RHR Line
OD, in	10.75	12.75	14.00
Thickness, in	1.00	1.125	1.25

Note: (1) The geometry on the Pipe side of Surge line is conservatively used.

The operating pressure for accumulator lines and RHR lines are obtained from Reference [5] and reproduced in Table 3-5.

Table 3-5: Operating Conditions

	Accumulator Line	Surge Line Pressurizer End	Surge Line Hot Leg End	RHR Line
Temperature, °F	555	653	610.9	610.9
Pressure, psig	2,485	2,235	2,235	2,235

For transients that have pressure different than the operating pressure, the axial stress due to pressure is factored by the ratio of the transient pressure range to the operating pressure range:

$$\sigma_p = \sigma_{max, oper} \frac{\Delta P}{\Delta P_{oper}} \quad (3-2)$$

The pressure range for the transients of Accumulator line and RHR line are obtained from References [2] and [3] and reproduced in Table 3-1 and Table 3-2 respectively.

3.2.2 Thermal Expansion

The axial stress due to thermal expansion moment can be calculated as:

$$\sigma_{TE, oper} = \frac{32 M D_o}{\pi (D_o^4 - D_i^4)} \quad (3-3)$$

where M is the thermal expansion Moment, D_o and D_i are the outside diameter and inside diameter of the pipe. Equation (3-3) is derived from the textbook solution of the axial stress due to moment [11]:

$$\sigma = \frac{M c}{I} \quad (3-4)$$

where $I = \frac{\pi(D_o^4 - D_i^4)}{64}$, and $c = D_o / 2$ [11].

Note that the maximum SRSS of thermal moments in x,y,z directions among all the loops in Unit 3 and Unit 4 are chosen, and the resultant moments are given in Table 3-6 for Accumulator Lines and RHR Lines.

For transients that have thermal expansion loads at a temperature other than operating temperature, the axial stress is calculated using Equation (3-3) factored by the ratio of the transient temperature range to the operating temperature range:

$$\sigma_{TE,trans} = \sigma_{TE,oper} \frac{\Delta T}{\Delta T_{oper}}, \quad (3-5)$$

where $\Delta T_{oper} = T_{oper} - 70$. The operating temperature for accumulator line and RHR line are obtained from Reference [5] and reproduced here in Table 3-5. The temperature range for the transients of Accumulator line and RHR line are obtained from References [2] and [3] and reproduced in Table 3-1 and Table 3-2, respectively.

Table 3-6: Piping Loads for Accumulator and RHR Lines

Components	Deadweight Moments (ft-lb)			Thermal Moments (ft-lb)			OBE Moments (ft-lb)		
	Mx	My	Mz	Mx	My	Mz	Mx	My	Mz
Accumulator Lines	2,847	5,545	25,236	38,919	33,733	26,644	40,607	38,813	17,688
RHR Lines	3,574	2,721	15,696	96,351	88,786	66,018	35,002	52,858	23,458

3.2.3 Dead Weight

The Deadweight moments are obtained as the maximum SRSS moments from Loads and Materials calculation package [5] and shown in Table 3-6. The axial stresses due to Deadweight moments are calculated as shown in Equation (3-3), where moment is the SRSS moments in x, y, z directions.

The calculated maximum and minimum axial stresses due to pressure, thermal, and dead weight for each of the plant transients are presented in Table 3-7 for Accumulator line and Table 3-8 for RHR Line.

Table 3-7: Accumulator Line Maximum and Minimum Transient Stresses

Transient	Maximum Stresses (ksi)				Minimum Stresses (ksi)			
	Pressure	Thermal	DW	Total	Pressure	Thermal	DW	Total
1	2.193	10.169	0.000	0.000	22.838	2.193	33.007	0.000
2	2.648	17.017	1.737	3.320	22.838	2.648	39.856	1.737
3	4.386	20.338	0.000	0.000	22.838	4.386	43.176	0.000
4	4.878	0.000	4.558	19.764 ⁽¹⁾	4.878	0.000	4.558	-0.891 ⁽¹⁾

Note: (1) The OBE stress (10.32 ksi) is added to maximum stress and subtracted from minimum stress.

Table 3-8: RHR Line Maximum and Minimum Transient Stresses

Transient	Maximum Stresses (ksi)				Minimum Stresses (ksi)			
	Pressure	Thermal	DW	Total	Pressure	Thermal	DW	Total
1	3.993	10.810	1.335	16.139	0.000	0.000	1.335	1.335
2	3.993	11.048	1.335	16.376	3.993	10.573	1.335	15.901
3	4.134	12.171	1.335	17.640	3.852	9.450	1.335	14.637
4	4.220	11.025	1.335	16.580	3.767	10.595	1.335	15.697
5	5.112	14.249	1.335	20.695	2.875	7.372	1.335	11.582
6	5.653	10.810	1.335	17.798	2.334	10.810	1.335	14.479
7	4.637	0	1.335	11.499 ⁽¹⁾	4.637	0.000	1.335	0.444 ⁽¹⁾

Note: (1) The OBE stress (5.53 ksi) is added to maximum stress and subtracted from minimum stress.

3.2.4 *Residual Stress*

For all the lines including the Surge line, the weld residual stress is conservatively represented by a pure through-wall bending stress equal to the yield stress of the pipe material at the operating temperature. Since Accumulator, RHR and Surge Lines are made of materials of similar type, the most conservative yield strength (S_y) was chosen for all three types of lines. Thus, $S_y = 18.28$ ksi of Type 316 stainless steel at 653°F [5] is used in the present analyses.

3.2.5 *Seismic Loads*

The number of OBE event occurrences are 50, obtained from Reference [4]. The OBE loads are obtained from Loads and Materials calculation package [5] and reproduced in Table 3-6 for use in part through-wall crack growth analyses. To show that a through-wall crack is stable during an SSE event per NUREG-1061, Section 5.2 (g) [9], 51 cycles of SSE loading obtained from Reference [14] (one SSE cycle assumed, along with 50 cycles of OBE).

3.2.6 *Stress Ranges*

The axial stress due to pressure, thermal, deadweight, seismic, and residual stresses determined above are combined to obtain the stress ranges corresponding to each of the transients identified in Tables 3-1 and Table 3-2 for the Accumulator line and RHR line.

For convenience, the stresses are separated based on their distribution across the thickness of the pipe. The pressure stresses are taken as uniform stresses whereas the stresses due to the other loads are assumed to vary linearly through the pipe wall.

The computed stress ranges for transients using Table 3-7 and Table 3-8 are presented in Table 3-9 and Table 3-10 for the Accumulator Line and RHR Line, respectively.

The stress range for the Surge Line is derived from Table 3-3. The maximum and minimum stresses in Table 3-3 are axial stress due to pressure and axial stresses due to deadweight, thermal, and seismic moment. The pressure stresses are taken as uniform stresses whereas the stresses due to the other loads are assumed to vary linearly through the pipe wall. For all the transients with no pressure information, the operating pressure of 2,250 psi is conservatively used to calculate the Maximum uniform stress. The computed stress ranges for transients using Table 3-3 are presented in Table 3-11 for the Surge Line.

Table 3-9: Stress Ranges for Accumulator Line

Transient	Cyclic Stresses (ksi)				DW + Residual (ksi)	Total Stress Ranges (ksi)			
	Maximum		Minimum			Maximum		Minimum	
	Uniform	Linear	Uniform	Linear		Uniform	Linear	Uniform	Linear
1	2.193	10.169	0.000	0.000	22.838	2.193	33.007	0.00	22.838
2	2.648	17.017	1.737	3.320	22.838	2.648	39.856	1.737	26.159
3	4.386	20.338	0.000	0.000	22.838	4.386	43.176	0.000	22.838
4	4.878	10.328	4.878	-10.328	22.838	4.878	33.166	4.878	12.511

Table 3-10: Stress Ranges for RHR Line

Transient	Cyclic Stresses (ksi)				DW + Residual (ksi)	Total Stress Ranges (ksi)			
	Maximum		Minimum			Maximum		Minimum	
	Uniform	Linear	Uniform	Linear		Uniform	Linear	Uniform	Linear
1	3.993	10.810	0.000	0.000	19.615	3.993	30.425	0	19.615
2	3.993	11.048	3.993	10.573	19.615	3.993	30.663	3.993	30.188
3	4.134	12.171	3.852	9.450	19.615	4.134	31.786	3.852	29.065
4	4.220	11.025	3.767	10.595	19.615	4.220	30.641	3.767	30.210
5	5.112	14.249	2.875	7.372	19.615	5.112	33.864	2.875	26.987
6	5.653	10.810	2.334	10.810	19.615	5.653	30.425	2.334	30.425
7	4.637	5.528	4.637	-5.528	19.615	4.6365	25.143	4.637	14.087

Table 3-11: Stress Ranges for Surge Line

Transient #	Total Stress Ranges (ksi)			
	Maximum		Minimum	
	Uniform ⁽¹⁾	Linear	Uniform	Linear
1	4.742	23.696	0.000	10.101
2	4.742	28.121	0.000	29.430
3	4.742	29.003	0.000	27.879
4	4.742	28.008	0.000	27.710
5	4.784 ⁽²⁾	25.728	4.700 ⁽²⁾	24.475
6	4.742	32.215	0.000	27.620
7	4.742	30.797	0.000	27.729
8	4.742	27.824	0.000	27.579
9	4.742	29.501	0.000	20.934
10	4.742	28.583	0.000	29.388
11	4.742	29.273	0.000	22.252
12	4.742	28.121	0.000	29.430
13	4.742	23.696	0.000	10.101
14	4.742	15.830	0.000	18.280
15	6.548 ⁽³⁾	21.590	0.000	18.280
16	5.237 ⁽⁴⁾	21.188	0.000	18.280

Note:

- (1) For all the transients with no pressure information, the operating pressure of 2,250 psi is conservatively used to calculate the Maximum uniform stress.
- (2) For Transient 5 (steady state fluctuation as shown in Table 3-3), a typical pressure ± 20 psi was added to 2,250 to calculate the maximum and minimum uniform stress
- (3) The pressure of 3,107 psi, as shown in Table 3-3, is used.
- (4) The pressure of 2,485 psi, as shown in Table 3-3, is used.

3.3 Allowable Flaw Size

At operating temperature, stainless steel material is expected to behave in a ductile manner. Hence, the net section plastic collapse methodology in Appendix C of ASME Code Section XI [1] can be used to determine the allowable flaw size. The load combination used for determining the allowable flaw size is pressure, deadweight, thermal and seismic loads. The flow stress, σ_f , for all three types of lines is conservatively assumed as 45.14 ksi – Type 316 at 653°F (Table 5 of Ref. [5]).

For the Accumulator Line, the total stress for this load combination is 19.02 ksi [14]. The stress ratio $(\sigma_m + \sigma_b) / \sigma_f = 0.42$. With an aspect ratio a/l of 0.1 and a thickness of 1.0 inch, starting with the maximum allowable flaw depth-to-thickness ratio of 0.75, the maximum possible flaw length is 7.5 inches. The ratio of this flaw length to the pipe circumference is 0.22. Using Table C-5310-3 Table C-5310-4 for emergency and faulted conditions, the allowable end-of-evaluation period flaw depth-to-thickness ratio is determined to be 0.75.

For the RHR Line, the total stress for this load combination is 24.73 ksi [14]. The stress ratio $(\sigma_m + \sigma_b) / \sigma_f = 0.55$. With an aspect ratio a/l of 0.1 and a thickness of 1.25 inch, starting with the maximum allowable flaw depth-to-thickness ratio of 0.75, the maximum possible flaw length is 9.34 inches. The ratio of this flaw length to the pipe circumference is 0.22. Using Table C-5310-3 Table C-5310-4 for emergency and faulted conditions, the allowable end-of-evaluation period flaw depth-to-thickness ratio is determined to be 0.70.

For the Surge Line, the total stress for this load combination is 17.38 ksi [13]. The stress ratio $(\sigma_m + \sigma_b) / \sigma_f = 0.39$. With an aspect ratio a/l of 0.1 and a thickness of 1.125 inch, starting with the maximum allowable flaw depth-to-thickness ratio of 0.75, the maximum possible flaw length is 8.44 inches. The ratio of this flaw length to the pipe circumference is 0.21. Using Table C-5310-3 Table C-5310-4 for emergency and faulted conditions, the allowable end-of-evaluation period flaw depth-to-thickness ratio is determined to be 0.75.

3.4 Fatigue Crack Growth Analysis

The fatigue crack growth analysis is performed for the number of cycles corresponding to the 40-year design plant life shown in Section 3.1. These cycles are applicable to both 60 years and 80 years of operation per References [12 and 13]. In the definition of the stress ranges, the stresses are cycled around the sum of deadweight and weld residual stresses, which are always in effect. For each enveloping transient category, the appropriate scaling factors (transient stress/reference stress) are input to obtain the actual K values for the fatigue crack growth.

3.4.1 *Fatigue Crack Growth Law Used for 60-Year Operation Calculations*

Crack growth in stainless steel for 60 years is calculated using the austenitic steel fatigue crack growth law in air from Article C-3210 of the ASME, Section XI [1], shown in Equation 3-6. Reference [7] indicates a factor of 2 may be applied to Equation 3-6 to account for a PWR environment. This is accounted for in **pc-CRACK 4.1** by doubling the number of cycles.

$$(da/dN)_{air} = C_0(\Delta K)^n, \text{ units of inch/cycle} \quad (3-6)$$

where:

$$\begin{aligned} da/dN &= \text{crack growth per cycle, } a \text{ is the crack depth, } N \text{ is the number of cycles} \\ C_0 &= C \cdot S \\ C &= 10^{-10.009 + 8.12 \times 10^{-4}T - 1.13 \times 10^{-6}T^2 + 1.02 \times 10^{-9}T^3} \\ S &= 1.0 \quad \text{when } R \leq 0 \\ &= 1.0 + 1.8R \quad \text{when } 0 < R \leq 0.79 \\ &= -43.35 + 57.97R \quad \text{when } 0.79 < R < 1.0 \\ T &= \text{metal temperature, } ^\circ\text{F (taken as the maximum during the transient)} \\ R &= \text{R-ratio} = (K_{min}/K_{max}) \\ \Delta K &= K_{max} - K_{min} = \text{range of stress intensity factor, ksi-in}^{0.5} \\ n &= 3.3 \text{ per Section XI, Appendix C [1]} \end{aligned}$$

Note that for negative R-ratios ($K_{min} < 0$ and $K_{max} > 0$), the “S” value is 1.0, which could lead to over conservative crack growth for the stainless steel weld. The max C_0 and thus most conservative growth rate is used for each transient considered.

3.4.2 Fatigue Crack Growth Law Used for 80-Year Operation Calculations

Crack growth in stainless steel for 80 years uses the updated FCG law for stainless steels and associated weld metals from ASME Code Case N-809 [6]:

$$da/dN = C_0 \cdot \Delta K^n, \text{ units of inch/cycle}$$

where:

$$\begin{aligned} C_0 &= \text{scaling parameter that accounts for the effect of loading rate and environment on fatigue crack growth rate} \\ &= C S_T S_R S_{ENV} \\ n &= \text{slope of the log (da/dN) versus log (ΔK) curve} = 2.25 \\ C &= \text{nominal fatigue crack growth rate constant} \\ &= 4.43 \times 10^{-7} \text{ for } \Delta K \geq \Delta K_{th} \\ &= 0 \text{ for } \Delta K < \Delta K_{th} \\ \Delta K &= \text{stress intensity factor range, ksi}\sqrt{\text{in}} \\ \Delta K_{th} &= 1.10 \text{ ksi}\sqrt{\text{in}} \\ S_T &= \text{parameter defining effect of temperature on FCG rate} \\ &= e^{-2516/T_K} \text{ for } 300^\circ\text{F} \leq T \leq 650^\circ\text{F} \\ &= 3.39 \times 10^5 e^{[-(2516/T_K) - 0.0301T_K]} \text{ for } 70^\circ\text{F} \leq T < 300^\circ\text{F} \\ T &= \text{metal temperature, } ^\circ\text{F} \\ S_R &= \text{parameter defining the effect of R-ratio on FCG rate} \\ &= 1.0 \text{ for } R < 0 \\ &= 1 + e^{8.02(R-0.748)} \text{ for } 0 \leq R < 1.0 \\ R &= K_{min}/K_{max} = \text{R ratio} \\ S_{ENV} &= \text{parameter defining the environmental effects on FCG rate} \end{aligned}$$

$$= T_R^{0.3}$$

$$T_R = \text{loading rise time, sec}$$

$$T_K = [(T-32)/1.8+273.15], \text{ K}$$

The metal temperature of 653°F is applied to calculate the crack growth rate. A conservative loading rise time of 15,000 seconds is applied to calculate the crack growth rate.

The crack growth rate changes based on the R-ratio. The da/dN for selected ΔK is calculated for different R-ratios and entered into **pc-CRACK 4.1** [8a] to calculate crack growth using Code Case N-809 FCG equation.

3.4.3 Part Through-Wall Crack Growth

The crack growth analysis is performed using the fracture mechanics software program **pc-CRACK 4.1** [8a]. Based on the guidelines of ASME Code Section XI, IWB-3514, an initial flaw size equal to the allowable depth of up to 12.5% of wall thickness is postulated. For the crack growth analysis, an aspect ratio a/l of 0.1 is conservatively assumed for the initial flaw, where 'a' is the flaw depth and 'l' is the flaw length.

The crack growth analysis performed by **pc-CRACK 4.1** requires that the allowable material fracture toughness, K_{Ic} , be input to stop the analysis when K_{Ic} is reached. A typical material K_{Ic} value of $135 \text{ ksi}\sqrt{\text{in}}$ for stainless steel is used for the purposes of the fatigue crack growth.

pc-CRACK 4.1 calculates K values for each pipe size for reference uniform tension and pure bending stresses of 1 ksi. The built-in crack model 309: Semi-Elliptical Circumferential Crack in Cylinder on the Inside Surface (Chapuliot) [8a] is used.

The stress intensity factors are determined for a conservative aspect ratio (a/l) of 0.1 and are shown in the output files in Appendix A.1 through A.6. Note that the pressure stresses are taken as uniform stresses whereas the stresses due to the other loads are assumed to vary linearly through the pipe wall.

3.4.4 Through-Wall Crack Growth

NUREG-1061, Section 5.2 (g) [9] requires that an evaluation be performed to show that the leakage flow size is stable during an SSE event. A simplified approach is to determine the crack growth of a through-wall leakage size flow to demonstrate stability. The initial through-wall flow is assumed to correspond to the leakage flow length for the most limiting location. A crack model in **pc-CRACK 3.1** [8b] assuming through-wall circumferential crack in a cylinder under tension and bending is used for the stress intensity K calculation.

For the Accumulator Line, the maximum $\sigma_m + \sigma_b$ is 19.02 ksi (Reference [14]), the bounding leakage flow size is 2.53 inch (Reference [10], with bending stress = 0 for 5gpm). The maximum $\sigma_m + \sigma_b$ is conservatively used as tension stress in the **pc-CRACK 3.1** input. The **pc-CRACK 3.1** output is shown in Appendix A.7. The resultant stress intensity factor K is $65.66 \text{ ksi}\sqrt{\text{in}}$.

Similarly, for the RHR Line, the maximum $\sigma_m + \sigma_b$ is 17.38 ksi (Reference [14]), the bounding leakage flow size is 3.12 inch (from Reference [10], with bending stress = 0 for 5gpm). The maximum $\sigma_m + \sigma_b$ is conservatively used as tension stress in the **pc-CRACK 3.1** input. The **pc-CRACK 3.1** output is shown in Appendix A.8. The resultant stress intensity factor K is $65.70 \text{ ksi}\sqrt{\text{in}}$.

Similarly, for the Surge Line, the maximum $\sigma_m + \sigma_b$ is 24.73 ksi (Reference [14]), the bounding leakage flow size is 3.30 inch (Reference [10], with bending stress = 0 for 5gpm). The maximum $\sigma_m + \sigma_b$ is conservatively used as tension stress in the **pc-CRACK 3.1** input. The **pc-CRACK 3.1** output is shown in Appendix A.9. The resultant stress intensity factor K is $101.77 \text{ ksi}\sqrt{\text{in}}$.

4.0 RESULTS

The results of the fatigue crack growth evaluations for both 60 years (using the Reference [1] crack growth law) and 80 years of operation (using the Reference [6] crack growth law) are summarized as follows:

Table 4-1: Fatigue Crack Growth Results

Auxiliary Line	Postulated Initial Flaw			60 Years (ASME Section XI)			80 Years (ASME CC N-809)		
	a/t	Depth a_i (in)	Half Length c_i (in)	a/t	Depth a_f (in)	Half Length c_f (in)	a/t	Depth a_f (in)	Half Length c_f (in)
Accumulator Line	12.50%	0.1250	0.6250	12.50%	0.1250	0.6250	12.50%	0.1250	0.6250
RHR Line	12.50%	0.1563	0.7815	12.50%	0.1563	0.7815	12.62%	0.1577	0.7817
Surge Line	12.50%	0.1406	0.7030	12.57%	0.1414	0.7031	20.10%	0.2261	0.7256

Considering the larger growth of 80 years using the crack growth law from ASME Code Case N-809, the results show that the postulated partial through wall crack ($a/t = 0.125$, $a/l = 0.1$) does not grow during the design plant life for the Accumulator Line. For the RHR Line, the postulated crack ($a/t = 0.125$, $a/l = 0.1$) grows only 0.0014 inch during the design plant life to a final a/t ratio of 0.1262. This final a/t ratio is less than the allowable ratio of 0.70 documented in Section 3.3. For the Surge Line, the postulated crack ($a/t = 0.125$, $a/l = 0.1$) grows 0.0855 inch during the design plant life to a final a/t ratio of 0.2010. This final a/t ratio is less than the allowable ratio of 0.75 documented in Section 3.3.

As shown in Table 4-1, for a partial through-wall crack in the RHR Line, the crack growth in the depth direction is 0.0014 inch and the crack growth in the length direction is 0.0004 inch. This is about 0.0009% of the 43.96 inch circumference length, and compared to the crack growth of 0.12% (12.50% to 12.62% in Table 4-1) in the depth direction, it is relatively small. For the Surge Line, the crack growth in the depth direction is 0.0855 inch and the crack growth in the length direction is 0.0452 inch. This is 0.113% of the 40.03 inch circumference length, and compared to the 7.6% (12.50% to 20.10%

in Table 4-1) in the depth direction, it is relatively small. Overall, for all the lines, the partial through-wall cracks tend to grow in the depth direction and through-wall before extending significantly in length (circumferentially) direction.

For 60 years for the Accumulator Line through wall crack, using a conservative R ratio (0.99) in the ASME Code Section XI crack growth curve for stainless steels in a water environment (Figure C-8410-1) gives a crack growth per cycle of 5.9×10^{-3} inches, whereas for 80 years the ASME Code Case N-809 crack growth curve gives 1.32×10^{-2} inches per cycle. For assumed 1 SSE and 50 OBE cycles, this translates into 0.301 inches for ASME Section XI crack growth law and 0.673 inches for Code Case N-809 crack growth law. This crack growth is insignificant compared to the total circumference of 33.77 inches.

Similarly, for 60 years for the RHR Line, using a conservative R ratio (0.99) in the ASME Code Section XI crack growth curve for stainless steels in a water environment (Figure C-8410-1), the crack growth per cycle is 5.9×10^{-3} inches, whereas for 80 years the ASME Code Case N-809 crack growth curve gives 1.33×10^{-2} inches per cycle. For assumed 1 SSE and 50 OBE cycles, this translates into 0.301 inches for ASME Section XI crack growth law and 0.678 inches for Code Case N-809 crack growth law. This crack growth is insignificant compared to the total circumference of 43.98 inches.

For 60 years for the Surge Line, using a conservative R ratio (0.99) in the ASME Code Section XI crack growth curve for stainless steels in a water environment (Figure C-8410-1), the crack growth per cycle is 2.49×10^{-2} inches, whereas for 80 years the ASME Code Case N-809 crack growth curve gives 3.55×10^{-2} inches per cycle. For assumed 1 SSE and 50 OBE cycles, this translates into 1.27 inches for ASME Section XI crack growth law and 1.81 inches for Code Case N-809 crack growth law. This crack growth is insignificant compared to the total circumference of 40.06 inches.

Thus for a through-wall crack, the crack growth in the length direction due to a seismic event is small compared to the total circumference and insignificant compared to the margin between the leakage-size crack size and the critical crack size.

Hence, the integrity of the auxiliary lines piping is not jeopardized between in-service inspections.

The **pc-CRACK** output files are presented in Appendix A.

5.0 REFERENCES

- 1) ASME Boiler and Pressure Vessel Code, Section XI, 2001 Edition with Addenda through 2003.
- 2) Westinghouse Proprietary Document, "System Standard 1.3.X, Nuclear Steam Supply System Auxiliary Equipment Design Transients for All Standard Plants"
- 3) Westinghouse Proprietary Document, "System Standard 1.3.F, Nuclear Steam Supply System Reactor Coolant System Design Transients for Standard Plants with Model F Steam Generators"
- 4) "FPL/FLA (Turkey Point 3 and 4) Pressurizer Surge Nozzle Fatigue Calculation Due to Thermal Stratification Pipe Loads", SI File No. 091350.205.
- 5) SI Calculation Package No. 0901350.301, "Loads and Material Properties for LBB Evaluation" (Please refer to the project revision log for the latest revision).
- 6) ASME Code Case N-809, "Reference Fatigue Crack Growth Rate Curves for Austenitic Stainless Steels in Pressurized Water Reactor Environments Section XI, Division 1," Cases of the ASME Boiler and Pressure Vessel Code, June 23, 2015.
- 7) Section XI Task Group for Piping Flaw Evaluation, ASME Code, "Evaluation of Flaws in Austenitic Steel Piping, " Journal of Pressure Vessel Technology, Vol. 108, August 1986.
- 8) **pc-CRACK**
 - a) **pc-CRACK** 4.1 CS, Version Control No. 4.1.0.0, Structural Integrity Associates, December 31, 2013.
 - b) **pc-CRACK™** for Windows, Version 3.1-98348, Structural Integrity Associates, 1998.
- 9) NUREG-1061, Volumes 1-5, "Report of the U. S. Nuclear Regulatory Commission Piping Review Committee," prepared by the Piping Review Committee, NRC, April 1985.
- 10) SI Calculation Package No. 0901350.302, "Leakage Calculation for LBB Evaluation" (Please refer to the project revision log for the latest revision).
- 11) "Roark's Formulas for Stress & Strain", Pages 67&94, Sixth Edition, by Warren C. Young, McGraw-Hill Inc., 1989.
- 12) SI Report No. 1700109.402, (currently under Preparation) "*Evaluation of Fatigue of ASME Section III, Class 1 Components for Turkey Point Units 3 and 4 for Subsequent License Renewal*".
- 13) Turkey Point Units 3 and 4 License Renewal Document, "Position Document to Address GSI-190 Issues Related to Fatigue Evaluation for Turkey Point Units 3 and 4", SI Report No. SIR-00-089. Rev 0.
- 14) SI Calculation Package No. 0901350.303, "Development of Bounding Analysis Curves for LBB Evaluation" (Please refer to the project revision log for the latest revision).

- 15) SI Corrective Action Report (CAR) No. 17-012, Revision 0, “Turkey Point LBB Evaluation, Calculation Package File No.: 0901350.304, Rev. 0, Calculation Title: Fatigue Crack Growth Evaluation,” April 17, 2017.

APPENDIX A

PC-CRACK OUTPUT

A.1 ACCUMULATOR LINE 60 YEARS

pc-CRACK 4.1 CS

Version Control No. 4.1.0.0

Structural Integrity Associates, Inc.
www.structint.com
pccrack@structint.com

Date: 05/18/2017 15:47

Input Data read from C:\Users\wwong\Documents\Projects\TurkeyPoint - 1700109\ACCL_60yr.pcf

Analysis Title: ACCL_60yr

Units Selected: US Customary
Linear Dimensions - inches
Stress - ksi
Load - kips
Temperature - deg F
Time - hours

Analysis Type: Crack Growth (LEFM)

Crack Growth Calculation Method - Cycle/Time Stepping
Maximum Number of Load Blocks = 1
Block Print Interval = 1

Crack Model: 309-Semi-Elliptical Circumferential Crack in Cylinder on the Inside Surface (Chapuliot)
Crack Depth, $a = 0.1250$
Half Crack Length, $c = 0.6250$
Wall Thickness, $t = 1.0000$
Inside Radius, $R_i = 4.3750$
Aspect ratio allowed to vary
Maximum $a/t = 0.8$
Crack Depth Print Increment for SIF Tabulation = 0.1
Maximum Aspect Ratio (c/a) for SIF Tabulation = 20
Aspect Ratio Increment for SIF Tabulation = 5

Total Load Cases: 2

Load Case 1: Uniform Stress
Type: Stress Coefficients Input by User

Coefficient C0 = 1.0000
Coefficient C1 = 0.0000
Coefficient C2 = 0.0000
Coefficient C3 = 0.0000

Load Case 2: Linear Stress
Type: Stress Coefficients Input by User

Coefficient C0 = 0.0000
Coefficient C1 = 1.0000
Coefficient C2 = 0.0000
Coefficient C3 = 0.0000

Total Load Sub-Blocks: 4

Load Sub-Block # 1

Load Sub-block Name: Group1
Maximum

Load Case Multiplier Load Case ID
 2.1930 Uniform Stress
 33.0070 Linear Stress

Minimum

Load Case Multiplier Load Case ID
 22.8380 Linear Stress

Growth Law: ASMEAusteniticAir

Cycles/Time: 40

Temperature: 653

Calc. Interval: 1

Print Interval: 20

Load Sub-Block # 2

Load Sub-block Name: Group2

Maximum

Load Case Multiplier Load Case ID
 2.6480 Uniform Stress
 39.8560 Linear Stress

Minimum

Load Case Multiplier Load Case ID
 1.7370 Uniform Stress
 26.1590 Linear Stress

Growth Law: ASMEAusteniticAir

Cycles/Time: 8

Temperature: 653

Calc. Interval: 1

Print Interval: 4

Load Sub-Block # 3

Load Sub-block Name: Group3

Maximum

Load Case Multiplier Load Case ID
 4.3860 Uniform Stress
 43.1760 Linear Stress

Minimum

Load Case Multiplier Load Case ID
 0.0000 Uniform Stress
 22.8380 Linear Stress

Growth Law: ASMEAusteniticAir

Cycles/Time: 2

Temperature: 653

Calc. Interval: 1

Print Interval: 1

Load Sub-Block # 4

Load Sub-block Name: Group4

Maximum

Load Case Multiplier Load Case ID
 4.8780 Uniform Stress
 33.1660 Linear Stress

Minimum

Load Case Multiplier Load Case ID
 4.8780 Uniform Stress
 12.5110 Linear Stress

Growth Law: ASMEAusteniticAir

Cycles/Time: 100

Temperature: 653

Calc. Interval: 1

Print Interval: 50

Material: 1

Sample Material 1: Only a sample

Austenitic Stainless Steel in Air environment

(U.S. Customary Units)

The Fatigue Crack Growth Rate (in/cycle) is given by:

$$da/dN = C_o * (\Delta K)^n$$

where

$$\Delta K = K_{max} - K_{min}$$

n = the slope of the log (da/dN) versus log (Delta K) = 3.3

C_o = a scaling constant

$$C_o = C * S$$

C is given by:

$$C = 10^{-10.009 + (8.12 * (10)^{-4} * T - (1.13 * (10)^{-6} * T^2) + (1.02 * (10)^{-9} * T^3)}$$

T is the metal temperature in deg F

S is a scaling parameter to account for R ratio and is given by:

$$S = 1.0 \quad \text{for } R \leq 0$$

$$= 1.0 + 1.8 * R \quad \text{for } 0 < R \leq 0.79$$

$$= -43.35 + 57.97 * R \quad \text{for } 0.79 < R < 1$$

where

$$R = K_{min} / K_{max}$$

No. of Data in the KIC Table = 1

Crack Depth	KIC
0.0000	135.0000

messages/Warnings:

Solution for Ri/t of 0.2 and 0.5 will be used

Number of Warnings in Inputs: 0

----- ANALYSIS RESULTS -----

STRESS INTENSITY FACTORS

Load Case # 1: Uniform Stress

----- Crack Dimensions -----						K at tips	
a	c	a/t	c/a	a	c		
c/a = 5.0000							
0.1250	0.6250	0.1250	5.0000	0.6576	0.3295		
0.2250	1.1250	0.2250	5.0000	0.9124	0.4544		
0.3250	1.6250	0.3250	5.0000	1.1574	0.5691		
0.4250	2.1250	0.4250	5.0000	1.4003	0.6801		
0.5250	2.6250	0.5250	5.0000	1.6661	0.7992		
0.6250	3.1250	0.6250	5.0000	1.9592	0.9250		
0.7250	3.6250	0.7250	5.0000	2.3325	1.0718		
c/a = 10.0000							
0.1250	1.2500	0.1250	10.0000	0.6918	0.2500		
0.2250	2.2500	0.2250	10.0000	0.9768	0.3439		

0.3250	3.2500	0.3250	10.0000	1.2642	0.4273
0.4250	4.2500	0.4250	10.0000	1.5608	0.5059
0.5250	5.2500	0.5250	10.0000	1.9026	0.5857
0.6250	6.2500	0.6250	10.0000	2.2888	0.6674
0.7250	7.2500	0.7250	10.0000	2.7905	0.7590

c/a = 15.0000

0.1250	1.8750	0.1250	15.0000	0.7025	0.2130
0.2250	3.3750	0.2250	15.0000	1.0002	0.2920
0.3250	4.8750	0.3250	15.0000	1.3065	0.3609
0.4250	6.3750	0.4250	15.0000	1.6279	0.4240
0.5250	7.8750	0.5250	15.0000	2.0067	0.4836
0.6250	9.3750	0.6250	15.0000	2.4302	0.5413
0.7250	10.8750	0.7250	15.0000	2.9588	0.5984

c/a = 20.0000

0.1250	2.5000	0.1250	20.0000	0.7076	0.1667
0.2250	4.5000	0.2250	20.0000	1.0094	0.2285
0.3250	6.5000	0.3250	20.0000	1.3200	0.2821
0.4250	8.5000	0.4250	20.0000	1.6464	0.3311
0.5250	10.5000	0.5250	20.0000	2.0311	0.3767
0.6250	12.5000	0.6250	20.0000	2.4621	0.4204
0.7250	14.5000	0.7250	20.0000	3.0024	0.4626

Load Case # 2: Linear Stress

----- Crack Dimensions ----- K at tips

a	c	a/t	c/a	a	c
c/a =	5.0000				

0.1250	0.6250	0.1250	5.0000	0.0504	4.509E-03
0.2250	1.1250	0.2250	5.0000	0.1241	0.0119
0.3250	1.6250	0.3250	5.0000	0.2226	0.0231
0.4250	2.1250	0.4250	5.0000	0.3448	0.0386
0.5250	2.6250	0.5250	5.0000	0.4956	0.0600
0.6250	3.1250	0.6250	5.0000	0.6799	0.0878
0.7250	3.6250	0.7250	5.0000	0.9217	0.1256

c/a = 10.0000

0.1250	1.2500	0.1250	10.0000	0.0524	2.236E-03
0.2250	2.2500	0.2250	10.0000	0.1307	6.020E-03
0.3250	3.2500	0.3250	10.0000	0.2377	0.0118
0.4250	4.2500	0.4250	10.0000	0.3739	0.0198
0.5250	5.2500	0.5250	10.0000	0.5474	0.0303
0.6250	6.2500	0.6250	10.0000	0.7644	0.0442
0.7250	7.2500	0.7250	10.0000	1.0561	0.0634

c/a = 15.0000

0.1250	1.8750	0.1250	15.0000	0.0531	1.410E-03
0.2250	3.3750	0.2250	15.0000	0.1330	3.790E-03
0.3250	4.8750	0.3250	15.0000	0.2437	7.355E-03
0.4250	6.3750	0.4250	15.0000	0.3861	0.0122
0.5250	7.8750	0.5250	15.0000	0.5704	0.0182
0.6250	9.3750	0.6250	15.0000	0.8016	0.0257
0.7250	10.8750	0.7250	15.0000	1.1081	0.0347

c/a = 20.0000

0.1250	2.5000	0.1250	20.0000	0.0534	1.045E-03
0.2250	4.5000	0.2250	20.0000	0.1341	2.809E-03
0.3250	6.5000	0.3250	20.0000	0.2460	5.438E-03
0.4250	8.5000	0.4250	20.0000	0.3902	8.957E-03
0.5250	10.5000	0.5250	20.0000	0.5771	0.0134
0.6250	12.5000	0.6250	20.0000	0.8118	0.0187

0.7250 14.5000 0.7250 20.0000 1.1243 0.0249

CRACK GROWTH ANALYSIS RESULTS

Total Cycles /Time	Subblock Cycles /Time	Kmax	Kmin	DaDn DeltaK a c	/DaDt a/t c/a	Crack Dimensions	
Blocks: 1							
20.0000	20.0000	3.1055	1.1509	1.9546	3.205E-09	0.1250	0.1250
		0.8714	0.1030	0.7684	1.071E-10	0.6250	5.0000
40.0000	40.0000	3.1055	1.1509	1.9546	3.205E-09	0.1250	0.1250
		0.8714	0.1030	0.7684	1.071E-10	0.6250	5.0000
44.0000	4.0000	3.7498	2.4605	1.2893	1.062E-09	0.1250	0.1250
		1.0522	0.6903	0.3619	1.605E-11	0.6250	5.0000
48.0000	8.0000	3.7498	2.4605	1.2893	1.062E-09	0.1250	0.1250
		1.0522	0.6903	0.3619	1.605E-11	0.6250	5.0000
49.0000	1.0000	5.0600	1.1509	3.9092	2.669E-08	0.1250	0.1250
		1.6398	0.1030	1.5368	9.678E-10	0.6250	5.0000
50.0000	2.0000	5.0601	1.1509	3.9092	2.669E-08	0.1250	0.1250
		1.6398	0.1030	1.5368	9.678E-10	0.6250	5.0000
100.0000	50.0000	4.8792	3.8383	1.0409	5.806E-10	0.1250	0.1250
		1.7568	1.6636	0.0931	9.637E-13	0.6250	5.0000
150.0000	100.0000	4.8792	3.8383	1.0409	5.806E-10	0.1250	0.1250
		1.7568	1.6636	0.0931	9.637E-13	0.6250	5.0000

Maximum number of blocks reached. The analysis terminated.

Number of Runtime Warnings: 0

*** End of pc-CRACK output ***

A.2 ACCUMULATOR LINE 80 YEARS

pc-CRACK 4.1 CS

Version Control No. 4.1.0.0

Structural Integrity Associates, Inc.
www.structint.com
pccrack@structint.com

Date: 05/18/2017 15:03

Input Data read from C:\Users\wwong\Documents\Projects\TurkeyPoint - 1700109\ACCL.pcf

Analysis Title: ACCL

Units Selected: US Customary
Linear Dimensions - inches
Stress - ksi
Load - kips
Temperature - deg F
Time - hours

Analysis Type: Crack Growth (LEFM)

Crack Growth Calculation Method - Cycle/Time Stepping
Maximum Number of Load Blocks = 1
Block Print Interval = 1

Crack Model: 309-Semi-Elliptical Circumferential Crack in Cylinder on the Inside Surface (Chapuliot)

Crack Depth, a = 0.1250
Half Crack Length, c = 0.6250
Wall Thickness, t = 1.0000
Inside Radius, R_i = 4.3750
Aspect ratio allowed to vary
Maximum a/t = 0.8
Crack Depth Print Increment for SIF Tabulation = 0.1
Maximum Aspect Ratio (c/a) for SIF Tabulation = 20
Aspect Ratio Increment for SIF Tabulation = 5

Total Load Cases: 2

Load Case 1: Uniform Stress
Type: Stress Coefficients Input by User

Coefficient C0 = 1.0000
Coefficient C1 = 0.0000
Coefficient C2 = 0.0000
Coefficient C3 = 0.0000

Load Case 2: Linear Stress
Type: Stress Coefficients Input by User

Coefficient C0 = 0.0000
Coefficient C1 = 1.0000
Coefficient C2 = 0.0000
Coefficient C3 = 0.0000

Total Load Sub-Blocks: 4

Load Sub-Block # 1

Load Sub-block Name: Group1
Maximum
Load Case Multiplier Load Case ID

2.1930 Uniform Stress
33.0070 Linear Stress

Minimum

Load Case Multiplier Load Case ID

22.8380 Linear Stress

Growth Law: TableDADN

Cycles/Time: 20

Calc. Interval: 1

Print Interval: 20

Load Sub-Block # 2

Load Sub-block Name: Group2

Maximum

Load Case Multiplier Load Case ID

2.6480 Uniform Stress

39.8560 Linear Stress

Minimum

Load Case Multiplier Load Case ID

1.7370 Uniform Stress

26.1590 Linear Stress

Growth Law: TableDADN

Cycles/Time: 4

Calc. Interval: 1

Print Interval: 4

Load Sub-Block # 3

Load Sub-block Name: Group3

Maximum

Load Case Multiplier Load Case ID

4.3860 Uniform Stress

43.1760 Linear Stress

Minimum

Load Case Multiplier Load Case ID

0.0000 Uniform Stress

22.8380 Linear Stress

Growth Law: TableDADN

Cycles/Time: 1

Calc. Interval: 1

Print Interval: 1

Load Sub-Block # 4

Load Sub-block Name: Group4

Maximum

Load Case Multiplier Load Case ID

4.8780 Uniform Stress

33.1660 Linear Stress

Minimum

Load Case Multiplier Load Case ID

4.8780 Uniform Stress

12.5110 Linear Stress

Growth Law: TableDADN

Cycles/Time: 50

Calc. Interval: 1

Print Interval: 50

Material: 1

Sample Material 1: Only a sample

Table(da/dn-DK)

No. of R ratios in the tables = 5

R Ratio = -100.0000

Delta K	da/dn
1.000E-03	2.410E-14
1.0000	2.410E-14
1.1000	1.680E-07
10.0000	2.410E-05
20.0000	1.150E-04
30.0000	2.850E-04
40.0000	5.450E-04
50.0000	9.000E-04
60.0000	1.360E-03
70.0000	1.920E-03
80.0000	2.590E-03
90.0000	3.380E-03
100.0000	4.280E-03

R Ratio = 0.1000

Delta K	da/dn
1.000E-03	2.420E-14
1.0000	2.420E-14
1.1000	1.690E-07
10.0000	2.420E-05
20.0000	1.150E-04
30.0000	2.870E-04
40.0000	5.480E-04
50.0000	9.050E-04
60.0000	1.360E-03
70.0000	1.930E-03
80.0000	2.610E-03
90.0000	3.400E-03
100.0000	4.300E-03

R Ratio = 0.5000

Delta K	da/dn
1.000E-03	2.740E-14
1.0000	2.740E-14
1.1000	1.910E-07
10.0000	2.740E-05
20.0000	1.300E-04
30.0000	3.240E-04
40.0000	6.190E-04
50.0000	1.020E-03
60.0000	1.540E-03
70.0000	2.180E-03
80.0000	2.950E-03
90.0000	3.840E-03
100.0000	4.870E-03

R Ratio = 0.7000

Delta K	da/dn
1.000E-03	4.050E-14
1.0000	4.050E-14
1.1000	2.820E-07
10.0000	4.050E-05
20.0000	1.920E-04
30.0000	4.790E-04
40.0000	9.150E-04
50.0000	1.510E-03
60.0000	2.280E-03
70.0000	3.220E-03
80.0000	4.350E-03
90.0000	5.680E-03
100.0000	7.190E-03

R Ratio = 1.0000

Delta K	da/dn
1.000E-03	2.060E-13
1.0000	2.060E-13
1.1000	1.430E-06
10.0000	2.060E-04
20.0000	9.780E-04
30.0000	2.440E-03
40.0000	4.650E-03
50.0000	7.690E-03
60.0000	0.0116
70.0000	0.0164
80.0000	0.0221
90.0000	0.0289
100.0000	0.0366

No. of Data in the KIC Table = 1

Crack Depth	KIC
0.0000	135.0000

messages/Warnings:

Solution for Ri/t of 0.2 and 0.5 will be used

Number of Warnings in Inputs: 0

----- ANALYSIS RESULTS -----

STRESS INTENSITY FACTORS

Load Case # 1: Uniform Stress

----- Crack Dimensions -----

K at tips

a	c	a/t	c/a	a	c
c/a =	5.0000				
0.1250	0.6250	0.1250	5.0000	0.6576	0.3295
0.2250	1.1250	0.2250	5.0000	0.9124	0.4544
0.3250	1.6250	0.3250	5.0000	1.1574	0.5691
0.4250	2.1250	0.4250	5.0000	1.4003	0.6801
0.5250	2.6250	0.5250	5.0000	1.6661	0.7992
0.6250	3.1250	0.6250	5.0000	1.9592	0.9250
0.7250	3.6250	0.7250	5.0000	2.3325	1.0718
c/a =	10.0000				
0.1250	1.2500	0.1250	10.0000	0.6918	0.2500
0.2250	2.2500	0.2250	10.0000	0.9768	0.3439
0.3250	3.2500	0.3250	10.0000	1.2642	0.4273
0.4250	4.2500	0.4250	10.0000	1.5608	0.5059
0.5250	5.2500	0.5250	10.0000	1.9026	0.5857
0.6250	6.2500	0.6250	10.0000	2.2888	0.6674
0.7250	7.2500	0.7250	10.0000	2.7905	0.7590
c/a =	15.0000				
0.1250	1.8750	0.1250	15.0000	0.7025	0.2130
0.2250	3.3750	0.2250	15.0000	1.0002	0.2920
0.3250	4.8750	0.3250	15.0000	1.3065	0.3609
0.4250	6.3750	0.4250	15.0000	1.6279	0.4240
0.5250	7.8750	0.5250	15.0000	2.0067	0.4836
0.6250	9.3750	0.6250	15.0000	2.4302	0.5413
0.7250	10.8750	0.7250	15.0000	2.9588	0.5984
c/a =	20.0000				
0.1250	2.5000	0.1250	20.0000	0.7076	0.1667

0.2250	4.5000	0.2250	20.0000	1.0094	0.2285
0.3250	6.5000	0.3250	20.0000	1.3200	0.2821
0.4250	8.5000	0.4250	20.0000	1.6464	0.3311
0.5250	10.5000	0.5250	20.0000	2.0311	0.3767
0.6250	12.5000	0.6250	20.0000	2.4621	0.4204
0.7250	14.5000	0.7250	20.0000	3.0024	0.4626

Load Case # 2: Linear Stress

----- Crack Dimensions -----				K at tips	
a	c	a/t	c/a	a	c
c/a = 5.0000					
0.1250	0.6250	0.1250	5.0000	0.0504	4.509E-03
0.2250	1.1250	0.2250	5.0000	0.1241	0.0119
0.3250	1.6250	0.3250	5.0000	0.2226	0.0231
0.4250	2.1250	0.4250	5.0000	0.3448	0.0386
0.5250	2.6250	0.5250	5.0000	0.4956	0.0600
0.6250	3.1250	0.6250	5.0000	0.6799	0.0878
0.7250	3.6250	0.7250	5.0000	0.9217	0.1256

c/a = 10.0000

0.1250	1.2500	0.1250	10.0000	0.0524	2.236E-03
0.2250	2.2500	0.2250	10.0000	0.1307	6.020E-03
0.3250	3.2500	0.3250	10.0000	0.2377	0.0118
0.4250	4.2500	0.4250	10.0000	0.3739	0.0198
0.5250	5.2500	0.5250	10.0000	0.5474	0.0303
0.6250	6.2500	0.6250	10.0000	0.7644	0.0442
0.7250	7.2500	0.7250	10.0000	1.0561	0.0634

c/a = 15.0000

0.1250	1.8750	0.1250	15.0000	0.0531	1.410E-03
0.2250	3.3750	0.2250	15.0000	0.1330	3.790E-03
0.3250	4.8750	0.3250	15.0000	0.2437	7.355E-03
0.4250	6.3750	0.4250	15.0000	0.3861	0.0122
0.5250	7.8750	0.5250	15.0000	0.5704	0.0182
0.6250	9.3750	0.6250	15.0000	0.8016	0.0257
0.7250	10.8750	0.7250	15.0000	1.1081	0.0347

c/a = 20.0000

0.1250	2.5000	0.1250	20.0000	0.0534	1.045E-03
0.2250	4.5000	0.2250	20.0000	0.1341	2.809E-03
0.3250	6.5000	0.3250	20.0000	0.2460	5.438E-03
0.4250	8.5000	0.4250	20.0000	0.3902	8.957E-03
0.5250	10.5000	0.5250	20.0000	0.5771	0.0134
0.6250	12.5000	0.6250	20.0000	0.8118	0.0187
0.7250	14.5000	0.7250	20.0000	1.1243	0.0249

CRACK GROWTH ANALYSIS RESULTS

Total Cycles /Time	Subblock Cycles /Time	Kmax	Kmin	DaDn DeltaK a c	/DaDt a/t c/a	Crack Dimensions	
Blocks:	1						
20.0000	20.0000	3.1058	1.1510	1.9547	6.692E-07	0.1250	0.1250
		0.8715	0.1030	0.7685	2.434E-14	0.6250	4.9995
24.0000	4.0000	3.7502	2.4608	1.2895	3.702E-07	0.1250	0.1250
		1.0523	0.6904	0.3620	3.717E-14	0.6250	4.9994
25.0000	1.0000	5.0606	1.1511	3.9095	3.045E-06	0.1250	0.1250
		1.6400	0.1030	1.5370	3.586E-07	0.6250	4.9993
75.0000	50.0000	4.8797	3.8386	1.0411	5.029E-11	0.1250	0.1250



1.7570 1.6639 0.0932 1.546E-13 0.6250 4.9993

Maximum number of blocks reached. The analysis terminated.

Number of Runtime Warnings: 0

*** End of pc-CRACK output ***

A.3 RHR LINE 60 YEARS

pc-CRACK 4.1 CS

Version Control No. 4.1.0.0

Structural Integrity Associates, Inc.
www.structint.com
pccrack@structint.com

Date: 05/18/2017 15:46

Input Data read from C:\Users\wwong\Documents\Projects\TurkeyPoint - 1700109\RHR_60yr.pcf

Analysis Title: RHR_60yr

Units Selected: US Customary
Linear Dimensions - inches
Stress - ksi
Load - kips
Temperature - deg F
Time - hours

Analysis Type: Crack Growth (LEFM)

Crack Growth Calculation Method - Cycle/Time Stepping
Maximum Number of Load Blocks = 1
Block Print Interval = 1

Crack Model: 309-Semi-Elliptical Circumferential Crack in Cylinder on the Inside Surface (Chapuliot)

Crack Depth, a = 0.1563
Half Crack Length, c = 0.7815
Wall Thickness, t = 1.2500
Inside Radius, R_i = 5.7500
Aspect ratio allowed to vary
Maximum a/t = 0.8
Crack Depth Print Increment for SIF Tabulation = 0.1
Maximum Aspect Ratio (c/a) for SIF Tabulation = 20
Aspect Ratio Increment for SIF Tabulation = 5

Total Load Cases: 2

Load Case 1: Uniform Stress
Type: Stress Coefficients Input by User

Coefficient C0 = 1.0000
Coefficient C1 = 0.0000
Coefficient C2 = 0.0000
Coefficient C3 = 0.0000

Load Case 2: Linear Stress
Type: Stress Coefficients Input by User

Coefficient C0 = 0.0000
Coefficient C1 = 1.0000
Coefficient C2 = 0.0000
Coefficient C3 = 0.0000

Total Load Sub-Blocks: 7

Load Sub-Block # 1

Load Sub-block Name: Group1
Maximum

Load Case Multiplier Load Case ID
 3.9930 Uniform Stress
 30.4250 Linear Stress
 Minimum
 Load Case Multiplier Load Case ID
 0.0000 Uniform Stress
 19.6150 Linear Stress
 Growth Law: ASMEAusteniticAir
 Cycles/Time: 800
 Temperature: 653
 Calc. Interval: 1
 Print Interval: 200

Load Sub-Block # 2

Load Sub-block Name: Group2
 Maximum
 Load Case Multiplier Load Case ID
 3.9930 Uniform Stress
 30.6630 Linear Stress
 Minimum
 Load Case Multiplier Load Case ID
 3.9930 Uniform Stress
 30.1880 Linear Stress
 Growth Law: ASMEAusteniticAir
 Cycles/Time: 2000
 Temperature: 653
 Calc. Interval: 1
 Print Interval: 500

Load Sub-Block # 3

Load Sub-block Name: Group3
 Maximum
 Load Case Multiplier Load Case ID
 4.1340 Uniform Stress
 31.7860 Linear Stress
 Minimum
 Load Case Multiplier Load Case ID
 3.8520 Uniform Stress
 29.0650 Linear Stress
 Growth Law: ASMEAusteniticAir
 Cycles/Time: 16400
 Temperature: 653
 Calc. Interval: 1
 Print Interval: 13200

Load Sub-Block # 4

Load Sub-block Name: Group4
 Maximum
 Load Case Multiplier Load Case ID
 4.2200 Uniform Stress
 30.6410 Linear Stress
 Minimum
 Load Case Multiplier Load Case ID
 3.7670 Uniform Stress
 30.2100 Linear Stress
 Growth Law: ASMEAusteniticAir
 Cycles/Time: 8000
 Temperature: 653
 Calc. Interval: 1
 Print Interval: 2000

Load Sub-Block # 5

Load Sub-block Name: Group5
 Maximum

Load Case Multiplier Load Case ID
 5.1120 Uniform Stress
 33.8640 Linear Stress

Minimum

Load Case Multiplier Load Case ID
 2.8750 Uniform Stress
 26.9870 Linear Stress

Growth Law: ASMEAusteniticAir

Cycles/Time: 20

Temperature: 653

Calc. Interval: 1

Print Interval: 10

Load Sub-Block # 6

Load Sub-block Name: Group6

Maximum

Load Case Multiplier Load Case ID
 5.6530 Uniform Stress
 30.4250 Linear Stress

Minimum

Load Case Multiplier Load Case ID
 2.3340 Uniform Stress
 30.4250 Linear Stress

Growth Law: ASMEAusteniticAir

Cycles/Time: 400

Temperature: 653

Calc. Interval: 1

Print Interval: 200

Load Sub-Block # 7

Load Sub-block Name: Group7

Maximum

Load Case Multiplier Load Case ID
 4.6365 Uniform Stress
 25.1430 Linear Stress

Minimum

Load Case Multiplier Load Case ID
 4.6365 Uniform Stress
 14.0870 Linear Stress

Growth Law: ASMEAusteniticAir

Cycles/Time: 100

Temperature: 653

Calc. Interval: 1

Print Interval: 50

Material: 1

Sample Material 1: Only a sample

Austenitic Stainless Steel in Air environment

(U.S. Customary Units)

The Fatigue Crack Growth Rate (in/cycle) is given by:

$$da/dN = Co * (\Delta K)^n$$

where

$\Delta K = K_{max} - K_{min}$

n = the slope of the log (da/dN) versus log (ΔK) = 3.3

Co = a scaling constant

$Co = C * S$

C is given by:

$$C = 10^{-10.009 + (8.12 \cdot (10)^{-4}) \cdot T - (1.13 \cdot (10)^{-6}) \cdot T^2 + (1.02 \cdot (10)^{-9}) \cdot T^3}$$

T is the metal temperature in deg F

S is a scaling parameter to account for R ratio and is given by:

$$\begin{aligned} S &= 1.0 && \text{for } R \leq 0 \\ &= 1.0 + 1.8 \cdot R && \text{for } 0 < R \leq 0.79 \\ &= -43.35 + 57.97 \cdot R && \text{for } 0.79 < R < 1 \end{aligned}$$

where

$$R = K_{min} / K_{max}$$

No. of Data in the KIC Table = 1

Crack Depth	KIC
0.0000	135.0000

messages/Warnings:

Solution for Ri/t of 0.2 and 0.5 will be used

Number of Warnings in Inputs: 0

----- ANALYSIS RESULTS -----

STRESS INTENSITY FACTORS

Load Case # 1: Uniform Stress

----- Crack Dimensions ----- K at tips

a	c	a/t	c/a	a	c
c/a = 5.0000					
0.1563	0.7815	0.1250	5.0000	0.7359	0.3686
0.2563	1.2815	0.2050	5.0000	0.9643	0.4814
0.3563	1.7815	0.2850	5.0000	1.1889	0.5872
0.4563	2.2815	0.3650	5.0000	1.4041	0.6867
0.5563	2.7815	0.4450	5.0000	1.6298	0.7894
0.6563	3.2815	0.5250	5.0000	1.8689	0.8969
0.7563	3.7815	0.6050	5.0000	2.1168	1.0063
0.8563	4.2815	0.6850	5.0000	2.4427	1.1365
0.9563	4.7815	0.7650	5.0000	2.7824	1.2705

c/a = 10.0000

0.1563	1.5630	0.1250	10.0000	0.7744	0.2796
0.2563	2.5630	0.2050	10.0000	1.0284	0.3648
0.3563	3.5630	0.2850	10.0000	1.2885	0.4421
0.4563	4.5630	0.3650	10.0000	1.5440	0.5138
0.5563	5.5630	0.4450	10.0000	1.8244	0.5848
0.6563	6.5630	0.5250	10.0000	2.1323	0.6565
0.7563	7.5630	0.6050	10.0000	2.4575	0.7281
0.8563	8.5630	0.6850	10.0000	2.9002	0.8090
0.9563	9.5630	0.7650	10.0000	3.3663	0.8910

c/a = 15.0000

0.1563	2.3445	0.1250	15.0000	0.7865	0.2382
0.2563	3.8445	0.2050	15.0000	1.0511	0.3102
0.3563	5.3445	0.2850	15.0000	1.3258	0.3740
0.4563	6.8445	0.3650	15.0000	1.5984	0.4325

0.5563	8.3445	0.4450	15.0000	1.9037	0.4878
0.6563	9.8445	0.5250	15.0000	2.2442	0.5409
0.7563	11.3445	0.6050	15.0000	2.6050	0.5926
0.8563	12.8445	0.6850	15.0000	3.0799	0.6442
0.9563	14.3445	0.7650	15.0000	3.5803	0.6952

c/a = 20.0000

0.1563	3.1260	0.1250	20.0000	0.7923	0.1864
0.2563	5.1260	0.2050	20.0000	1.0606	0.2427
0.3563	7.1260	0.2850	20.0000	1.3396	0.2924
0.4563	9.1260	0.3650	20.0000	1.6168	0.3379
0.5563	11.1260	0.4450	20.0000	1.9275	0.3806
0.6563	13.1260	0.5250	20.0000	2.2741	0.4212
0.7563	15.1260	0.6050	20.0000	2.6415	0.4605
0.8563	17.1260	0.6850	20.0000	3.1259	0.4989
0.9563	19.1260	0.7650	20.0000	3.6365	0.5366

Load Case # 2: Linear Stress

----- Crack Dimensions ----- K at tips

a	c	a/t	c/a	a	c
c/a =	5.0000				
0.1563	0.7815	0.1250	5.0000	0.0705	6.312E-03
0.2563	1.2815	0.2050	5.0000	0.1500	0.0141
0.3563	1.7815	0.2850	5.0000	0.2525	0.0255
0.4563	2.2815	0.3650	5.0000	0.3756	0.0404
0.5563	2.7815	0.4450	5.0000	0.5221	0.0598
0.6563	3.2815	0.5250	5.0000	0.6940	0.0844
0.7563	3.7815	0.6050	5.0000	0.8912	0.1144
0.8563	4.2815	0.6850	5.0000	1.1469	0.1541
0.9563	4.7815	0.7650	5.0000	1.4400	0.2011

c/a = 10.0000

0.1563	1.5630	0.1250	10.0000	0.0733	3.132E-03
0.2563	2.5630	0.2050	10.0000	0.1575	7.152E-03
0.3563	3.5630	0.2850	10.0000	0.2682	0.0130
0.4563	4.5630	0.3650	10.0000	0.4032	0.0207
0.5563	5.5630	0.4450	10.0000	0.5681	0.0305
0.6563	6.5630	0.5250	10.0000	0.7662	0.0427
0.7563	7.5630	0.6050	10.0000	0.9975	0.0575
0.8563	8.5630	0.6850	10.0000	1.3067	0.0776
0.9563	9.5630	0.7650	10.0000	1.6660	0.1013

c/a = 15.0000

0.1563	2.3445	0.1250	15.0000	0.0743	1.976E-03
0.2563	3.8445	0.2050	15.0000	0.1601	4.516E-03
0.3563	5.3445	0.2850	15.0000	0.2741	8.106E-03
0.4563	6.8445	0.3650	15.0000	0.4140	0.0128
0.5563	8.3445	0.4450	15.0000	0.5871	0.0186
0.6563	9.8445	0.5250	15.0000	0.7974	0.0255
0.7563	11.3445	0.6050	15.0000	1.0447	0.0337
0.8563	12.8445	0.6850	15.0000	1.3723	0.0433
0.9563	14.3445	0.7650	15.0000	1.7538	0.0542

c/a = 20.0000

0.1563	3.1260	0.1250	20.0000	0.0747	1.465E-03
0.2563	5.1260	0.2050	20.0000	0.1614	3.349E-03
0.3563	7.1260	0.2850	20.0000	0.2766	5.996E-03
0.4563	9.1260	0.3650	20.0000	0.4184	9.425E-03
0.5563	11.1260	0.4450	20.0000	0.5939	0.0136
0.6563	13.1260	0.5250	20.0000	0.8073	0.0187
0.7563	15.1260	0.6050	20.0000	1.0585	0.0246
0.8563	17.1260	0.6850	20.0000	1.3921	0.0312

0.9563 19.1260 0.7650 20.0000 1.7808 0.0387

CRACK GROWTH ANALYSIS RESULTS

Total Cycles /Time	Subblock Cycles /Time	Kmax	Kmin	DaDn		Crack Dimensions	
				DeltaK a c	/DaDt a/t c/a		
Blocks: 1							
200.0000	200.0000	5.0834	1.3827	3.7006	2.354E-08	0.1563	0.1250
	1.6639	0.1238	1.5401	9.930E-10	0.7815	4.9999	
400.0000	400.0000	5.0835	1.3828	3.7007	2.354E-08	0.1563	0.1250
	1.6640	0.1238	1.5402	9.931E-10	0.7815	4.9997	
600.0000	600.0000	5.0836	1.3829	3.7008	2.354E-08	0.1563	0.1251
	1.6640	0.1238	1.5402	9.932E-10	0.7815	4.9996	
800.0000	800.0000	5.0838	1.3829	3.7008	2.354E-08	0.1563	0.1251
	1.6641	0.1238	1.5403	9.933E-10	0.7815	4.9994	
1300.0000	500.0000	5.1005	5.0671	0.0335	4.065E-14	0.1563	0.1251
	1.6656	1.6626	2.999E-03	1.443E-17	0.7815	4.9994	
1800.0000	1000.0000	5.1005	5.0671	0.0335	4.065E-14	0.1563	0.1251
	1.6656	1.6626	2.999E-03	1.443E-17	0.7815	4.9994	
2300.0000	1500.0000	5.1005	5.0671	0.0335	4.065E-14	0.1563	0.1251
	1.6656	1.6626	2.999E-03	1.443E-17	0.7815	4.9994	
2800.0000	2000.0000	5.1005	5.0671	0.0335	4.065E-14	0.1563	0.1251
	1.6656	1.6626	2.999E-03	1.443E-17	0.7815	4.9994	
1.600E+04	1.320E+04	5.2835	4.8841	0.3994	1.043E-10	0.1563	0.1251
	1.7247	1.6036	0.1211	2.096E-12	0.7815	4.9994	
1.920E+04	1.640E+04	5.2835	4.8842	0.3994	1.043E-10	0.1563	0.1251
	1.7247	1.6036	0.1211	2.096E-12	0.7815	4.9993	
2.120E+04	2000.0000	5.2661	4.9023	0.3638	7.945E-11	0.1563	0.1251
	1.7492	1.5795	0.1697	5.439E-12	0.7815	4.9993	
2.320E+04	4000.0000	5.2661	4.9023	0.3638	7.945E-11	0.1563	0.1251
	1.7492	1.5795	0.1697	5.439E-12	0.7815	4.9993	
2.520E+04	6000.0000	5.2661	4.9023	0.3638	7.945E-11	0.1563	0.1251
	1.7492	1.5795	0.1697	5.439E-12	0.7815	4.9993	
2.720E+04	8000.0000	5.2661	4.9023	0.3638	7.945E-11	0.1563	0.1251
	1.7492	1.5795	0.1697	5.439E-12	0.7815	4.9993	
2.721E+04	10.0000	6.1498	4.0186	2.1312	5.566E-09	0.1563	0.1251
	2.0984	1.2303	0.8681	2.714E-10	0.7815	4.9993	
2.722E+04	20.0000	6.1498	4.0186	2.1312	5.566E-09	0.1563	0.1251
	2.0984	1.2303	0.8681	2.714E-10	0.7815	4.9993	
2.742E+04	200.0000	6.3056	3.8629	2.4427	8.436E-09	0.1563	0.1251
	2.2761	1.0526	1.2236	7.509E-10	0.7815	4.9993	
2.762E+04	400.0000	6.3056	3.8629	2.4427	8.436E-09	0.1563	0.1251
	2.2762	1.0526	1.2236	7.510E-10	0.7815	4.9992	
2.767E+04	50.0000	5.1851	4.4056	0.7795	5.466E-10	0.1563	0.1251
	1.8681	1.7982	0.0698	4.014E-13	0.7815	4.9992	
2.772E+04	100.0000	5.1851	4.4056	0.7795	5.466E-10	0.1563	0.1251
	1.8681	1.7982	0.0698	4.014E-13	0.7815	4.9992	

Maximum number of blocks reached. The analysis terminated.

Number of Runtime Warnings: 0

*** End of pc-CRACK output ***

A.4 RHR LINE 80 YEARS

pc-CRACK 4.1 CS

Version Control No. 4.1.0.0

Structural Integrity Associates, Inc.
www.structint.com
pccrack@structint.com

Date: 05/18/2017 14:15

Input Data read from C:\Users\wwong\Documents\Projects\TurkeyPoint - 1700109\RHR.pcf

Analysis Title: RHR

Units Selected: US Customary
Linear Dimensions - inches
Stress - ksi
Load - kips
Temperature - deg F
Time - hours

Analysis Type: Crack Growth (LEFM)

Crack Growth Calculation Method - Cycle/Time Stepping
Maximum Number of Load Blocks = 1
Block Print Interval = 1

Crack Model: 309-Semi-Elliptical Circumferential Crack in Cylinder on the Inside Surface (Chapuliot)
Crack Depth, $a = 0.1563$
Half Crack Length, $c = 0.7815$
Wall Thickness, $t = 1.2500$
Inside Radius, $R_i = 5.7500$
Aspect ratio allowed to vary
Maximum $a/t = 0.8$
Crack Depth Print Increment for SIF Tabulation = 0.1
Maximum Aspect Ratio (c/a) for SIF Tabulation = 20
Aspect Ratio Increment for SIF Tabulation = 5

Total Load Cases: 2

Load Case 1: Uniform Stress
Type: Stress Coefficients Input by User

Coefficient C0 = 1.0000
Coefficient C1 = 0.0000
Coefficient C2 = 0.0000
Coefficient C3 = 0.0000

Load Case 2: Linear Stress
Type: Stress Coefficients Input by User

Coefficient C0 = 0.0000
Coefficient C1 = 1.0000
Coefficient C2 = 0.0000
Coefficient C3 = 0.0000

Total Load Sub-Blocks: 7

Load Sub-Block # 1

Load Sub-block Name: Group1
Maximum

Load Case Multiplier Load Case ID
 3.9930 Uniform Stress
 30.4250 Linear Stress
 Minimum
 Load Case Multiplier Load Case ID
 0.0000 Uniform Stress
 19.6150 Linear Stress
 Growth Law: TableDADN
 Cycles/Time: 400
 Calc. Interval: 1
 Print Interval: 200

Load Sub-Block # 2

Load Sub-block Name: Group2
 Maximum
 Load Case Multiplier Load Case ID
 3.9930 Uniform Stress
 30.6630 Linear Stress
 Minimum
 Load Case Multiplier Load Case ID
 3.9930 Uniform Stress
 30.1880 Linear Stress
 Growth Law: TableDADN
 Cycles/Time: 1000
 Calc. Interval: 1
 Print Interval: 500

Load Sub-Block # 3

Load Sub-block Name: Group3
 Maximum
 Load Case Multiplier Load Case ID
 4.1340 Uniform Stress
 31.7860 Linear Stress
 Minimum
 Load Case Multiplier Load Case ID
 3.8520 Uniform Stress
 29.0650 Linear Stress
 Growth Law: TableDADN
 Cycles/Time: 13200
 Calc. Interval: 1
 Print Interval: 13200

Load Sub-Block # 4

Load Sub-block Name: Group4
 Maximum
 Load Case Multiplier Load Case ID
 4.2200 Uniform Stress
 30.6410 Linear Stress
 Minimum
 Load Case Multiplier Load Case ID
 3.7670 Uniform Stress
 30.2100 Linear Stress
 Growth Law: TableDADN
 Cycles/Time: 4000
 Calc. Interval: 1
 Print Interval: 2000

Load Sub-Block # 5

Load Sub-block Name: Group5
 Maximum
 Load Case Multiplier Load Case ID
 5.1120 Uniform Stress
 33.8640 Linear Stress
 Minimum

Load Case Multiplier Load Case ID
 2.8750 Uniform Stress
 26.9870 Linear Stress
 Growth Law: TableDADN
 Cycles/Time: 10
 Calc. Interval: 1
 Print Interval: 10

Load Sub-Block # 6

Load Sub-block Name: Group6
 Maximum
 Load Case Multiplier Load Case ID
 5.6530 Uniform Stress
 30.4250 Linear Stress
 Minimum
 Load Case Multiplier Load Case ID
 2.3340 Uniform Stress
 30.4250 Linear Stress
 Growth Law: TableDADN
 Cycles/Time: 200
 Calc. Interval: 1
 Print Interval: 200

Load Sub-Block # 7

Load Sub-block Name: Group7
 Maximum
 Load Case Multiplier Load Case ID
 4.6365 Uniform Stress
 25.1430 Linear Stress
 Minimum
 Load Case Multiplier Load Case ID
 4.6365 Uniform Stress
 14.0870 Linear Stress
 Growth Law: TableDADN
 Cycles/Time: 50
 Calc. Interval: 1
 Print Interval: 50

Material: 1
 Sample Material 1: Only a sample

Table(da/dn-DK)

No. of R ratios in the tables = 5

R Ratio = -100.0000

Delta K	da/dn
1.000E-03	2.410E-14
1.0000	2.410E-14
1.1000	1.680E-07
10.0000	2.410E-05
20.0000	1.150E-04
30.0000	2.850E-04
40.0000	5.450E-04
50.0000	9.000E-04
60.0000	1.360E-03
70.0000	1.920E-03
80.0000	2.590E-03
90.0000	3.380E-03
100.0000	4.280E-03

R Ratio = 0.1000

Delta K	da/dn
---------	-------

1.000E-03	2.420E-14
1.0000	2.420E-14
1.1000	1.690E-07
10.0000	2.420E-05
20.0000	1.150E-04
30.0000	2.870E-04
40.0000	5.480E-04
50.0000	9.050E-04
60.0000	1.360E-03
70.0000	1.930E-03
80.0000	2.610E-03
90.0000	3.400E-03
100.0000	4.300E-03

R Ratio = 0.5000

Delta K	da/dn
1.000E-03	2.740E-14
1.0000	2.740E-14
1.1000	1.910E-07
10.0000	2.740E-05
20.0000	1.300E-04
30.0000	3.240E-04
40.0000	6.190E-04
50.0000	1.020E-03
60.0000	1.540E-03
70.0000	2.180E-03
80.0000	2.950E-03
90.0000	3.840E-03
100.0000	4.870E-03

R Ratio = 0.7000

Delta K	da/dn
1.000E-03	4.050E-14
1.0000	4.050E-14
1.1000	2.820E-07
10.0000	4.050E-05
20.0000	1.920E-04
30.0000	4.790E-04
40.0000	9.150E-04
50.0000	1.510E-03
60.0000	2.280E-03
70.0000	3.220E-03
80.0000	4.350E-03
90.0000	5.680E-03
100.0000	7.190E-03

R Ratio = 1.0000

Delta K	da/dn
1.000E-03	2.060E-13
1.0000	2.060E-13
1.1000	1.430E-06
10.0000	2.060E-04
20.0000	9.780E-04
30.0000	2.440E-03
40.0000	4.650E-03
50.0000	7.690E-03
60.0000	0.0116
70.0000	0.0164
80.0000	0.0221
90.0000	0.0289
100.0000	0.0366

No. of Data in the KIC Table = 1

Crack Depth KIC

0.0000 135.0000

messages/Warnings:

Solution for Ri/t of 0.2 and 0.5 will be used

Number of Warnings in Inputs: 0

----- ANALYSIS RESULTS -----

STRESS INTENSITY FACTORS

Load Case # 1: Uniform Stress

----- Crack Dimensions -----				K at tips	
a	c	a/t	c/a	a	c
c/a = 5.0000					
0.1563	0.7815	0.1250	5.0000	0.7359	0.3686
0.2563	1.2815	0.2050	5.0000	0.9643	0.4814
0.3563	1.7815	0.2850	5.0000	1.1889	0.5872
0.4563	2.2815	0.3650	5.0000	1.4041	0.6867
0.5563	2.7815	0.4450	5.0000	1.6298	0.7894
0.6563	3.2815	0.5250	5.0000	1.8689	0.8969
0.7563	3.7815	0.6050	5.0000	2.1168	1.0063
0.8563	4.2815	0.6850	5.0000	2.4427	1.1365
0.9563	4.7815	0.7650	5.0000	2.7824	1.2705
c/a = 10.0000					
0.1563	1.5630	0.1250	10.0000	0.7744	0.2796
0.2563	2.5630	0.2050	10.0000	1.0284	0.3648
0.3563	3.5630	0.2850	10.0000	1.2885	0.4421
0.4563	4.5630	0.3650	10.0000	1.5440	0.5138
0.5563	5.5630	0.4450	10.0000	1.8244	0.5848
0.6563	6.5630	0.5250	10.0000	2.1323	0.6565
0.7563	7.5630	0.6050	10.0000	2.4575	0.7281
0.8563	8.5630	0.6850	10.0000	2.9002	0.8090
0.9563	9.5630	0.7650	10.0000	3.3663	0.8910
c/a = 15.0000					
0.1563	2.3445	0.1250	15.0000	0.7865	0.2382
0.2563	3.8445	0.2050	15.0000	1.0511	0.3102
0.3563	5.3445	0.2850	15.0000	1.3258	0.3740
0.4563	6.8445	0.3650	15.0000	1.5984	0.4325
0.5563	8.3445	0.4450	15.0000	1.9037	0.4878
0.6563	9.8445	0.5250	15.0000	2.2442	0.5409
0.7563	11.3445	0.6050	15.0000	2.6050	0.5926
0.8563	12.8445	0.6850	15.0000	3.0799	0.6442
0.9563	14.3445	0.7650	15.0000	3.5803	0.6952
c/a = 20.0000					
0.1563	3.1260	0.1250	20.0000	0.7923	0.1864
0.2563	5.1260	0.2050	20.0000	1.0606	0.2427
0.3563	7.1260	0.2850	20.0000	1.3396	0.2924
0.4563	9.1260	0.3650	20.0000	1.6168	0.3379
0.5563	11.1260	0.4450	20.0000	1.9275	0.3806
0.6563	13.1260	0.5250	20.0000	2.2741	0.4212
0.7563	15.1260	0.6050	20.0000	2.6415	0.4605
0.8563	17.1260	0.6850	20.0000	3.1259	0.4989
0.9563	19.1260	0.7650	20.0000	3.6365	0.5366

Load Case # 2: Linear Stress

----- Crack Dimensions ----- K at tips

a	c	a/t	c/a	a	c
c/a =	5.0000				
0.1563	0.7815	0.1250	5.0000	0.0705	6.312E-03
0.2563	1.2815	0.2050	5.0000	0.1500	0.0141
0.3563	1.7815	0.2850	5.0000	0.2525	0.0255
0.4563	2.2815	0.3650	5.0000	0.3756	0.0404
0.5563	2.7815	0.4450	5.0000	0.5221	0.0598
0.6563	3.2815	0.5250	5.0000	0.6940	0.0844
0.7563	3.7815	0.6050	5.0000	0.8912	0.1144
0.8563	4.2815	0.6850	5.0000	1.1469	0.1541
0.9563	4.7815	0.7650	5.0000	1.4400	0.2011

c/a =	10.0000				
0.1563	1.5630	0.1250	10.0000	0.0733	3.132E-03
0.2563	2.5630	0.2050	10.0000	0.1575	7.152E-03
0.3563	3.5630	0.2850	10.0000	0.2682	0.0130
0.4563	4.5630	0.3650	10.0000	0.4032	0.0207
0.5563	5.5630	0.4450	10.0000	0.5681	0.0305
0.6563	6.5630	0.5250	10.0000	0.7662	0.0427
0.7563	7.5630	0.6050	10.0000	0.9975	0.0575
0.8563	8.5630	0.6850	10.0000	1.3067	0.0776
0.9563	9.5630	0.7650	10.0000	1.6660	0.1013

c/a =	15.0000				
0.1563	2.3445	0.1250	15.0000	0.0743	1.976E-03
0.2563	3.8445	0.2050	15.0000	0.1601	4.516E-03
0.3563	5.3445	0.2850	15.0000	0.2741	8.106E-03
0.4563	6.8445	0.3650	15.0000	0.4140	0.0128
0.5563	8.3445	0.4450	15.0000	0.5871	0.0186
0.6563	9.8445	0.5250	15.0000	0.7974	0.0255
0.7563	11.3445	0.6050	15.0000	1.0447	0.0337
0.8563	12.8445	0.6850	15.0000	1.3723	0.0433
0.9563	14.3445	0.7650	15.0000	1.7538	0.0542

c/a =	20.0000				
0.1563	3.1260	0.1250	20.0000	0.0747	1.465E-03
0.2563	5.1260	0.2050	20.0000	0.1614	3.349E-03
0.3563	7.1260	0.2850	20.0000	0.2766	5.996E-03
0.4563	9.1260	0.3650	20.0000	0.4184	9.425E-03
0.5563	11.1260	0.4450	20.0000	0.5939	0.0136
0.6563	13.1260	0.5250	20.0000	0.8073	0.0187
0.7563	15.1260	0.6050	20.0000	1.0585	0.0246
0.8563	17.1260	0.6850	20.0000	1.3921	0.0312
0.9563	19.1260	0.7650	20.0000	1.7808	0.0387

CRACK GROWTH ANALYSIS RESULTS

Total Cycles /Time	Subblock Cycles /Time	Kmax	Kmin	DaDn DeltaK a c	/DaDt a/t c/a	Crack Dimensions	
Blocks: 1							
200.0000	200.0000	5.0984	1.3896	3.7088	2.742E-06	0.1568	0.1255
	1.6704	0.1249	1.5455	3.631E-07	0.7816	4.9830	
400.0000	400.0000	5.1137	1.3966	3.7171	2.757E-06	0.1574	0.1259
	1.6770	0.1260	1.5510	3.660E-07	0.7816	4.9661	
900.0000	500.0000	5.1307	5.0969	0.0338	1.988E-13	0.1574	0.1259
	1.6785	1.6755	3.052E-03	2.040E-13	0.7816	4.9661	
1400.0000	1000.0000	5.1307	5.0969	0.0338	1.988E-13	0.1574	0.1259
	1.6785	1.6755	3.052E-03	2.040E-13	0.7816	4.9661	
1.460E+04	1.320E+04	5.3148	4.9129	0.4019	1.367E-13	0.1574	0.1259

	1.7381	1.6160	0.1221	1.408E-13	0.7816	4.9661	
1.660E+04	2000.0000	5.2967	4.9316	0.3651	1.418E-13	0.1574	0.1259
	1.7626	1.5918	0.1708	1.218E-13	0.7816	4.9661	
1.860E+04	4000.0000	5.2967	4.9316	0.3651	1.418E-13	0.1574	0.1259
	1.7626	1.5918	0.1708	1.218E-13	0.7816	4.9661	
1.861E+04	10.0000	6.1850	4.0440	2.1410	1.153E-06	0.1574	0.1259
	2.1145	1.2402	0.8742	3.245E-14	0.7816	4.9657	
1.881E+04	200.0000	6.3484	3.8965	2.4519	1.447E-06	0.1577	0.1262
	2.2976	1.0640	1.2336	2.444E-07	0.7817	4.9569	
1.886E+04	50.0000	5.2204	4.4310	0.7894	9.075E-14	0.1577	0.1262
	1.8857	1.8143	0.0714	1.678E-13	0.7817	4.9569	

Maximum number of blocks reached. The analysis terminated.

Number of Runtime Warnings: 0

*** End of pc-CRACK output ***

A.5 SURGE LINE 60 YEARS

pc-CRACK 4.1 CS

Version Control No. 4.1.0.0

Structural Integrity Associates, Inc.
www.structint.com
pccrack@structint.com

Date: 05/18/2017 15:43

Input Data read from C:\Users\wwong\Documents\Projects\TurkeyPoint - 1700109\surge_60yr.pcf

Analysis Title: Surge_60yr

Units Selected: US Customary
Linear Dimensions - inches
Stress - ksi
Load - kips
Temperature - deg F
Time - hours

Analysis Type: Crack Growth (LEFM)

Crack Growth Calculation Method - Cycle/Time Stepping
Maximum Number of Load Blocks = 1
Block Print Interval = 1

Crack Model: 309-Semi-Elliptical Circumferential Crack in Cylinder on the Inside Surface (Chapuliot)

Crack Depth, a = 0.1406
Half Crack Length, c = 0.7030
Wall Thickness, t = 1.1250
Inside Radius, R_i = 5.2500
Aspect ratio allowed to vary
Maximum a/t = 0.8
Crack Depth Print Increment for SIF Tabulation = 0.1
Maximum Aspect Ratio (c/a) for SIF Tabulation = 20
Aspect Ratio Increment for SIF Tabulation = 5

Total Load Cases: 2

Load Case 1: Uniform Stress
Type: Stress Coefficients Input by User

Coefficient C0 = 1.0000
Coefficient C1 = 0.0000
Coefficient C2 = 0.0000
Coefficient C3 = 0.0000

Load Case 2: Linear Stress
Type: Stress Coefficients Input by User

Coefficient C0 = 0.0000
Coefficient C1 = 1.0000
Coefficient C2 = 0.0000
Coefficient C3 = 0.0000

Total Load Sub-Blocks: 16

Load Sub-Block # 1

Load Sub-block Name: Group1
Maximum
Load Case Multiplier Load Case ID
4.7420 Uniform Stress
23.6960 Linear Stress
Minimum
Load Case Multiplier Load Case ID
10.1010 Linear Stress
Growth Law: ASMEAusteniticAir
Cycles/Time: 400
Temperature: 653
Calc. Interval: 1
Print Interval: 200

Load Sub-Block # 2

Load Sub-block Name: Group2
Maximum
Load Case Multiplier Load Case ID
4.7420 Uniform Stress
28.1210 Linear Stress
Minimum
Load Case Multiplier Load Case ID
29.4300 Linear Stress
Growth Law: ASMEAusteniticAir
Cycles/Time: 16400
Temperature: 653
Calc. Interval: 1
Print Interval: 13200

Load Sub-Block # 3

Load Sub-block Name: Group3
Maximum
Load Case Multiplier Load Case ID
4.7420 Uniform Stress
29.0030 Linear Stress
Minimum
Load Case Multiplier Load Case ID
27.8790 Linear Stress
Growth Law: ASMEAusteniticAir
Cycles/Time: 8000
Temperature: 653
Calc. Interval: 1
Print Interval: 4000

Load Sub-Block # 4

Load Sub-block Name: Group4
Maximum
Load Case Multiplier Load Case ID
4.7420 Uniform Stress
28.0080 Linear Stress
Minimum
Load Case Multiplier Load Case ID
27.7100 Linear Stress
Growth Law: ASMEAusteniticAir
Cycles/Time: 400
Temperature: 653
Calc. Interval: 1
Print Interval: 200

Load Sub-Block # 5

Load Sub-block Name: Group5
Maximum
Load Case Multiplier Load Case ID
4.7840 Uniform Stress

25.7280 Linear Stress
 Minimum
 Load Case Multiplier Load Case ID
 4.7000 Uniform Stress
 24.4750 Linear Stress
 Growth Law: ASMEAusteniticAir
 Cycles/Time: 6300000
 Temperature: 653
 Calc. Interval: 1
 Print Interval: 65535

Load Sub-Block # 6

Load Sub-block Name: Group6
 Maximum
 Load Case Multiplier Load Case ID
 4.7420 Uniform Stress
 32.2150 Linear Stress
 Minimum
 Load Case Multiplier Load Case ID
 27.6200 Linear Stress
 Growth Law: ASMEAusteniticAir
 Cycles/Time: 160
 Temperature: 653
 Calc. Interval: 1
 Print Interval: 80

Load Sub-Block # 7

Load Sub-block Name: Group7
 Maximum
 Load Case Multiplier Load Case ID
 4.7420 Uniform Stress
 30.7970 Linear Stress
 Minimum
 Load Case Multiplier Load Case ID
 27.7290 Linear Stress
 Growth Law: ASMEAusteniticAir
 Cycles/Time: 80
 Temperature: 653
 Calc. Interval: 1
 Print Interval: 40

Load Sub-Block # 8

Load Sub-block Name: Group8
 Maximum
 Load Case Multiplier Load Case ID
 4.7420 Uniform Stress
 27.8240 Linear Stress
 Minimum
 Load Case Multiplier Load Case ID
 27.5790 Linear Stress
 Growth Law: ASMEAusteniticAir
 Cycles/Time: 160
 Temperature: 653
 Calc. Interval: 1
 Print Interval: 80

Load Sub-Block # 9

Load Sub-block Name: Group9
 Maximum
 Load Case Multiplier Load Case ID
 4.7420 Uniform Stress
 29.5010 Linear Stress
 Minimum
 Load Case Multiplier Load Case ID

20.9340 Linear Stress
Growth Law: ASMEAusteniticAir
Cycles/Time: 800
Temperature: 653
Calc. Interval: 1
Print Interval: 400

Load Sub-Block # 10

Load Sub-block Name: Group10
Maximum
Load Case Multiplier Load Case ID
4.7420 Uniform Stress
28.5830 Linear Stress
Minimum
Load Case Multiplier Load Case ID
29.3880 Linear Stress
Growth Law: ASMEAusteniticAir
Cycles/Time: 20
Temperature: 653
Calc. Interval: 1
Print Interval: 10

Load Sub-Block # 11

Load Sub-block Name: Group11
Maximum
Load Case Multiplier Load Case ID
4.7420 Uniform Stress
29.2730 Linear Stress
Minimum
Load Case Multiplier Load Case ID
22.2520 Linear Stress
Growth Law: ASMEAusteniticAir
Cycles/Time: 100
Temperature: 653
Calc. Interval: 1
Print Interval: 50

Load Sub-Block # 12

Load Sub-block Name: Group12
Maximum
Load Case Multiplier Load Case ID
4.7420 Uniform Stress
28.1210 Linear Stress
Minimum
Load Case Multiplier Load Case ID
29.4300 Linear Stress
Growth Law: ASMEAusteniticAir
Cycles/Time: 16400
Temperature: 653
Calc. Interval: 1
Print Interval: 13200

Load Sub-Block # 13

Load Sub-block Name: Group13
Maximum
Load Case Multiplier Load Case ID
4.7420 Uniform Stress
23.6960 Linear Stress
Minimum
Load Case Multiplier Load Case ID
10.1010 Linear Stress
Growth Law: ASMEAusteniticAir
Cycles/Time: 400
Temperature: 653

Calc. Interval: 1
Print Interval: 200

Load Sub-Block # 14

Load Sub-block Name: Group14
Maximum
Load Case Multiplier Load Case ID
4.7420 Uniform Stress
15.8300 Linear Stress
Minimum
Load Case Multiplier Load Case ID
18.2800 Linear Stress
Growth Law: ASMEAusteniticAir
Cycles/Time: 20
Temperature: 653
Calc. Interval: 1
Print Interval: 10

Load Sub-Block # 15

Load Sub-block Name: Group15
Maximum
Load Case Multiplier Load Case ID
6.5480 Uniform Stress
21.5900 Linear Stress
Minimum
Load Case Multiplier Load Case ID
18.2800 Linear Stress
Growth Law: ASMEAusteniticAir
Cycles/Time: 10
Temperature: 653
Calc. Interval: 1
Print Interval: 5

Load Sub-Block # 16

Load Sub-block Name: Group16
Maximum
Load Case Multiplier Load Case ID
5.2370 Uniform Stress
21.1880 Linear Stress
Minimum
Load Case Multiplier Load Case ID
18.2800 Linear Stress
Growth Law: ASMEAusteniticAir
Cycles/Time: 100
Temperature: 653
Calc. Interval: 1
Print Interval: 50

Material: 1
Sample Material 1: Only a sample

Austenitic Stainless Steel in Air environment

(U.S. Customary Units)

The Fatigue Crack Growth Rate (in/cycle) is given by:

$$da/dN = Co * (\Delta K)^n$$

where

$\Delta K = K_{max} - K_{min}$
n = the slope of the log (da/dN) versus log (ΔK) = 3.3
Co = a scaling constant

$$C_o = C * S$$

C is given by:

$$C = 10^{-10.009 + (8.12 * (10)^{-4}) * T - (1.13 * (10)^{-6}) * T^2 + (1.02 * (10)^{-9}) * T^3}$$

T is the metal temperature in deg F

S is a scaling parameter to account for R ratio and is given by:

$$S = 1.0 \quad \text{for } R \leq 0$$

$$= 1.0 + 1.8 * R \quad \text{for } 0 < R \leq 0.79$$

$$= -43.35 + 57.97 * R \quad \text{for } 0.79 < R < 1$$

where

$$R = K_{min} / K_{max}$$

No. of Data in the KIC Table = 1

Crack Depth	KIC
0.0000	135.0000

messages/Warnings:

Solution for Ri/t of 0.2 and 0.5 will be used

Number of Warnings in Inputs: 0

----- ANALYSIS RESULTS -----

STRESS INTENSITY FACTORS

Load Case # 1: Uniform Stress

----- Crack Dimensions ----- K at tips

a	c	a/t	c/a	a	c
c/a = 5.0000					
0.1406	0.7030	0.1250	5.0000	0.6981	0.3496
0.2406	1.2030	0.2139	5.0000	0.9394	0.4683
0.3406	1.7030	0.3028	5.0000	1.1743	0.5787
0.4406	2.2030	0.3916	5.0000	1.4001	0.6825
0.5406	2.7030	0.4805	5.0000	1.6479	0.7948
0.6406	3.2030	0.5694	5.0000	1.9023	0.9087
0.7406	3.7030	0.6583	5.0000	2.2139	1.0377
0.8406	4.2030	0.7472	5.0000	2.5672	1.1779
c/a = 10.0000					
0.1406	1.4060	0.1250	10.0000	0.7347	0.2653
0.2406	2.4060	0.2139	10.0000	1.0038	0.3546
0.3406	3.4060	0.3028	10.0000	1.2769	0.4350
0.4406	4.4060	0.3916	10.0000	1.5462	0.5095
0.5406	5.4060	0.4805	10.0000	1.8603	0.5854
0.6406	6.4060	0.5694	10.0000	2.1907	0.6607
0.7406	7.4060	0.6583	10.0000	2.6105	0.7421
0.8406	8.4060	0.7472	10.0000	3.0960	0.8281
c/a = 15.0000					
0.1406	2.1090	0.1250	15.0000	0.7461	0.2260
0.2406	3.6090	0.2139	15.0000	1.0267	0.3013

0.3406	5.1090	0.3028	15.0000	1.3154	0.3675
0.4406	6.6090	0.3916	15.0000	1.6028	0.4281
0.5406	8.1090	0.4805	15.0000	1.9478	0.4854
0.6406	9.6090	0.5694	15.0000	2.3142	0.5405
0.7406	11.1090	0.6583	15.0000	2.7708	0.5950
0.8406	12.6090	0.7472	15.0000	3.2945	0.6490

c/a = 20.0000

0.1406	2.8120	0.1250	20.0000	0.7517	0.1768
0.2406	4.8120	0.2139	20.0000	1.0363	0.2357
0.3406	6.8120	0.3028	20.0000	1.3296	0.2872
0.4406	8.8120	0.3916	20.0000	1.6222	0.3344
0.5406	10.8120	0.4805	20.0000	1.9735	0.3783
0.6406	12.8120	0.5694	20.0000	2.3467	0.4204
0.7406	14.8120	0.6583	20.0000	2.8122	0.4613
0.8406	16.8120	0.7472	20.0000	3.3462	0.5013

Load Case # 2: Linear Stress

----- Crack Dimensions ----- K at tips

a c a/t c/a a c
c/a = 5.0000

0.1406	0.7030	0.1250	5.0000	0.0601	5.386E-03
0.2406	1.2030	0.2139	5.0000	0.1369	0.0130
0.3406	1.7030	0.3028	5.0000	0.2375	0.0243
0.4406	2.2030	0.3916	5.0000	0.3595	0.0394
0.5406	2.7030	0.4805	5.0000	0.5087	0.0600
0.6406	3.2030	0.5694	5.0000	0.6829	0.0858
0.7406	3.7030	0.6583	5.0000	0.9031	0.1198
0.8406	4.2030	0.7472	5.0000	1.1709	0.1625

c/a = 10.0000

0.1406	1.4060	0.1250	10.0000	0.0626	2.673E-03
0.2406	2.4060	0.2139	10.0000	0.1439	6.589E-03
0.3406	3.4060	0.3028	10.0000	0.2528	0.0124
0.4406	4.4060	0.3916	10.0000	0.3873	0.0202
0.5406	5.4060	0.4805	10.0000	0.5571	0.0305
0.6406	6.4060	0.5694	10.0000	0.7595	0.0432
0.7406	7.4060	0.6583	10.0000	1.0234	0.0602
0.8406	8.4060	0.7472	10.0000	1.3513	0.0817

c/a = 15.0000

0.1406	2.1090	0.1250	15.0000	0.0634	1.686E-03
0.2406	3.6090	0.2139	15.0000	0.1464	4.154E-03
0.3406	5.1090	0.3028	15.0000	0.2586	7.727E-03
0.4406	6.6090	0.3916	15.0000	0.3982	0.0124
0.5406	8.1090	0.4805	15.0000	0.5774	0.0184
0.6406	9.6090	0.5694	15.0000	0.7931	0.0256
0.7406	11.1090	0.6583	15.0000	1.0739	0.0341
0.8406	12.6090	0.7472	15.0000	1.4228	0.0442

c/a = 20.0000

0.1406	2.8120	0.1250	20.0000	0.0638	1.251E-03
0.2406	4.8120	0.2139	20.0000	0.1476	3.080E-03
0.3406	6.8120	0.3028	20.0000	0.2611	5.712E-03
0.4406	8.8120	0.3916	20.0000	0.4026	9.175E-03
0.5406	10.8120	0.4805	20.0000	0.5844	0.0135
0.6406	12.8120	0.5694	20.0000	0.8035	0.0187
0.7406	14.8120	0.6583	20.0000	1.0892	0.0247
0.8406	16.8120	0.7472	20.0000	1.4445	0.0316

CRACK GROWTH ANALYSIS RESULTS

Total Cycles /Time	Subblock Cycles /Time	Kmax	Kmin	DaDn		Crack Dimensions	
				DeltaK a c	/DaDt a/t c/a		
Blocks:	1						
200.0000	200.0000	4.7359	0.6076	4.1283	2.791E-08	0.1406	0.1250
	1.7857	0.0544	1.7313	1.359E-09	0.7030	4.9998	
400.0000	400.0000	4.7360	0.6076	4.1284	2.791E-08	0.1406	0.1250
	1.7858	0.0544	1.7314	1.359E-09	0.7030	4.9996	
1.360E+04	1.320E+04	5.0082	1.7743	3.2339	1.659E-08	0.1408	0.1252
	1.8127	0.1592	1.6535	1.282E-09	0.7030	4.9920	
1.680E+04	1.640E+04	5.0097	1.7753	3.2344	1.660E-08	0.1409	0.1252
	1.8134	0.1593	1.6541	1.284E-09	0.7030	4.9901	
2.080E+04	4000.0000	5.0650	1.6830	3.3819	1.876E-08	0.1410	0.1253
	1.8192	0.1511	1.6681	1.310E-09	0.7030	4.9875	
2.480E+04	8000.0000	5.0671	1.6843	3.3828	1.878E-08	0.1410	0.1254
	1.8203	0.1514	1.6689	1.312E-09	0.7030	4.9849	
2.500E+04	200.0000	5.0071	1.6742	3.3329	1.792E-08	0.1410	0.1254
	1.8149	0.1504	1.6645	1.300E-09	0.7030	4.9848	
2.520E+04	400.0000	5.0072	1.6742	3.3329	1.792E-08	0.1410	0.1254
	1.8150	0.1505	1.6645	1.300E-09	0.7030	4.9846	
9.074E+04	6.554E+04	4.8988	4.7643	0.1344	3.650E-12	0.1410	0.1254
	1.8173	1.7811	0.0363	4.997E-14	0.7030	4.9846	
1.563E+05	1.311E+05	4.8988	4.7643	0.1344	3.650E-12	0.1410	0.1254
	1.8173	1.7811	0.0363	4.997E-14	0.7030	4.9846	
2.218E+05	1.966E+05	4.8988	4.7643	0.1344	3.650E-12	0.1410	0.1254
	1.8173	1.7811	0.0363	4.997E-14	0.7030	4.9846	
2.873E+05	2.621E+05	4.8988	4.7644	0.1344	3.650E-12	0.1410	0.1254
	1.8173	1.7811	0.0363	4.997E-14	0.7030	4.9846	
3.529E+05	3.277E+05	4.8988	4.7644	0.1344	3.650E-12	0.1410	0.1254
	1.8173	1.7811	0.0363	4.997E-14	0.7030	4.9846	
4.184E+05	3.932E+05	4.8988	4.7644	0.1344	3.650E-12	0.1410	0.1254
	1.8173	1.7811	0.0363	4.997E-14	0.7030	4.9846	
4.839E+05	4.587E+05	4.8988	4.7644	0.1344	3.650E-12	0.1410	0.1254
	1.8173	1.7811	0.0363	4.997E-14	0.7030	4.9846	
5.495E+05	5.243E+05	4.8988	4.7644	0.1344	3.650E-12	0.1410	0.1254
	1.8173	1.7811	0.0363	4.997E-14	0.7030	4.9846	
6.150E+05	5.898E+05	4.8988	4.7644	0.1344	3.650E-12	0.1410	0.1254
	1.8174	1.7811	0.0363	4.997E-14	0.7030	4.9846	
6.806E+05	6.554E+05	4.8988	4.7644	0.1344	3.650E-12	0.1410	0.1254
	1.8174	1.7811	0.0363	4.997E-14	0.7030	4.9845	
7.461E+05	7.209E+05	4.8988	4.7644	0.1344	3.651E-12	0.1410	0.1254
	1.8174	1.7811	0.0363	4.997E-14	0.7030	4.9845	
8.116E+05	7.864E+05	4.8988	4.7644	0.1344	3.651E-12	0.1410	0.1254
	1.8174	1.7811	0.0363	4.997E-14	0.7030	4.9845	
8.772E+05	8.520E+05	4.8988	4.7644	0.1344	3.651E-12	0.1410	0.1254
	1.8174	1.7811	0.0363	4.997E-14	0.7030	4.9845	
9.427E+05	9.175E+05	4.8988	4.7644	0.1344	3.651E-12	0.1410	0.1254
	1.8174	1.7811	0.0363	4.997E-14	0.7030	4.9845	
1.008E+06	9.830E+05	4.8989	4.7644	0.1344	3.651E-12	0.1410	0.1254
	1.8174	1.7811	0.0363	4.997E-14	0.7030	4.9845	
1.074E+06	1.049E+06	4.8989	4.7644	0.1344	3.651E-12	0.1410	0.1254
	1.8174	1.7811	0.0363	4.997E-14	0.7030	4.9845	
1.139E+06	1.114E+06	4.8989	4.7644	0.1344	3.651E-12	0.1410	0.1254
	1.8174	1.7811	0.0363	4.997E-14	0.7030	4.9845	
1.205E+06	1.180E+06	4.8989	4.7644	0.1344	3.651E-12	0.1410	0.1254
	1.8174	1.7811	0.0363	4.997E-14	0.7030	4.9845	
1.270E+06	1.245E+06	4.8989	4.7644	0.1344	3.651E-12	0.1410	0.1254
	1.8174	1.7811	0.0363	4.997E-14	0.7030	4.9845	
1.336E+06	1.311E+06	4.8989	4.7645	0.1344	3.651E-12	0.1410	0.1254
	1.8174	1.7811	0.0363	4.997E-14	0.7030	4.9845	
1.401E+06	1.376E+06	4.8989	4.7645	0.1344	3.651E-12	0.1410	0.1254
	1.8174	1.7811	0.0363	4.997E-14	0.7030	4.9844	
1.467E+06	1.442E+06	4.8989	4.7645	0.1344	3.651E-12	0.1410	0.1254
	1.8174	1.7811	0.0363	4.997E-14	0.7030	4.9844	

1.533E+06	1.507E+06	4.8989	4.7645	0.1344	3.651E-12	0.1410	0.1254
	1.8174	1.7811	0.0363	4.997E-14	0.7030	4.9844	
1.598E+06	1.573E+06	4.8989	4.7645	0.1344	3.651E-12	0.1410	0.1254
	1.8174	1.7811	0.0363	4.997E-14	0.7030	4.9844	
1.664E+06	1.638E+06	4.8989	4.7645	0.1344	3.651E-12	0.1410	0.1254
	1.8174	1.7811	0.0363	4.997E-14	0.7030	4.9844	
1.729E+06	1.704E+06	4.8989	4.7645	0.1344	3.651E-12	0.1410	0.1254
	1.8174	1.7811	0.0363	4.997E-14	0.7030	4.9844	
1.795E+06	1.769E+06	4.8989	4.7645	0.1344	3.651E-12	0.1410	0.1254
	1.8174	1.7811	0.0363	4.998E-14	0.7030	4.9844	
1.860E+06	1.835E+06	4.8989	4.7645	0.1344	3.651E-12	0.1410	0.1254
	1.8174	1.7812	0.0363	4.998E-14	0.7030	4.9844	
1.926E+06	1.901E+06	4.8989	4.7645	0.1344	3.651E-12	0.1410	0.1254
	1.8174	1.7812	0.0363	4.998E-14	0.7030	4.9844	
1.991E+06	1.966E+06	4.8989	4.7645	0.1344	3.651E-12	0.1410	0.1254
	1.8174	1.7812	0.0363	4.998E-14	0.7030	4.9844	
2.057E+06	2.032E+06	4.8990	4.7645	0.1344	3.651E-12	0.1410	0.1254
	1.8174	1.7812	0.0363	4.998E-14	0.7030	4.9844	
2.122E+06	2.097E+06	4.8990	4.7645	0.1344	3.651E-12	0.1410	0.1254
	1.8174	1.7812	0.0363	4.998E-14	0.7030	4.9844	
2.188E+06	2.163E+06	4.8990	4.7645	0.1344	3.651E-12	0.1410	0.1254
	1.8174	1.7812	0.0363	4.998E-14	0.7030	4.9843	
2.253E+06	2.228E+06	4.8990	4.7645	0.1344	3.651E-12	0.1410	0.1254
	1.8174	1.7812	0.0363	4.998E-14	0.7030	4.9843	
2.319E+06	2.294E+06	4.8990	4.7645	0.1344	3.651E-12	0.1410	0.1254
	1.8174	1.7812	0.0363	4.998E-14	0.7030	4.9843	
2.384E+06	2.359E+06	4.8990	4.7645	0.1344	3.651E-12	0.1410	0.1254
	1.8174	1.7812	0.0363	4.998E-14	0.7030	4.9843	
2.450E+06	2.425E+06	4.8990	4.7646	0.1344	3.651E-12	0.1410	0.1254
	1.8174	1.7812	0.0363	4.998E-14	0.7030	4.9843	
2.516E+06	2.490E+06	4.8990	4.7646	0.1344	3.651E-12	0.1410	0.1254
	1.8174	1.7812	0.0363	4.998E-14	0.7030	4.9843	
2.581E+06	2.556E+06	4.8990	4.7646	0.1344	3.651E-12	0.1410	0.1254
	1.8175	1.7812	0.0363	4.998E-14	0.7030	4.9843	
2.647E+06	2.621E+06	4.8990	4.7646	0.1344	3.651E-12	0.1410	0.1254
	1.8175	1.7812	0.0363	4.998E-14	0.7030	4.9843	
2.712E+06	2.687E+06	4.8990	4.7646	0.1344	3.651E-12	0.1410	0.1254
	1.8175	1.7812	0.0363	4.998E-14	0.7030	4.9843	
2.778E+06	2.752E+06	4.8990	4.7646	0.1344	3.651E-12	0.1411	0.1254
	1.8175	1.7812	0.0363	4.998E-14	0.7030	4.9843	
2.843E+06	2.818E+06	4.8990	4.7646	0.1344	3.651E-12	0.1411	0.1254
	1.8175	1.7812	0.0363	4.998E-14	0.7030	4.9843	
2.909E+06	2.884E+06	4.8990	4.7646	0.1344	3.651E-12	0.1411	0.1254
	1.8175	1.7812	0.0363	4.998E-14	0.7030	4.9843	
2.974E+06	2.949E+06	4.8990	4.7646	0.1344	3.651E-12	0.1411	0.1254
	1.8175	1.7812	0.0363	4.998E-14	0.7030	4.9842	
3.040E+06	3.015E+06	4.8990	4.7646	0.1344	3.651E-12	0.1411	0.1254
	1.8175	1.7812	0.0363	4.998E-14	0.7030	4.9842	
3.105E+06	3.080E+06	4.8990	4.7646	0.1344	3.651E-12	0.1411	0.1254
	1.8175	1.7812	0.0363	4.998E-14	0.7030	4.9842	
3.171E+06	3.146E+06	4.8991	4.7646	0.1344	3.651E-12	0.1411	0.1254
	1.8175	1.7812	0.0363	4.998E-14	0.7030	4.9842	
3.236E+06	3.211E+06	4.8991	4.7646	0.1344	3.651E-12	0.1411	0.1254
	1.8175	1.7812	0.0363	4.998E-14	0.7030	4.9842	
3.302E+06	3.277E+06	4.8991	4.7646	0.1344	3.651E-12	0.1411	0.1254
	1.8175	1.7812	0.0363	4.998E-14	0.7030	4.9842	
3.367E+06	3.342E+06	4.8991	4.7646	0.1344	3.651E-12	0.1411	0.1254
	1.8175	1.7812	0.0363	4.998E-14	0.7030	4.9842	
3.433E+06	3.408E+06	4.8991	4.7646	0.1344	3.651E-12	0.1411	0.1254
	1.8175	1.7812	0.0363	4.998E-14	0.7030	4.9842	
3.499E+06	3.473E+06	4.8991	4.7646	0.1344	3.651E-12	0.1411	0.1254
	1.8175	1.7812	0.0363	4.998E-14	0.7030	4.9842	
3.564E+06	3.539E+06	4.8991	4.7647	0.1344	3.651E-12	0.1411	0.1254
	1.8175	1.7812	0.0363	4.998E-14	0.7030	4.9842	
3.630E+06	3.604E+06	4.8991	4.7647	0.1344	3.651E-12	0.1411	0.1254
	1.8175	1.7812	0.0363	4.998E-14	0.7030	4.9842	
3.695E+06	3.670E+06	4.8991	4.7647	0.1344	3.651E-12	0.1411	0.1254
	1.8175	1.7812	0.0363	4.999E-14	0.7030	4.9842	

3.761E+06	3.735E+06	4.8991	4.7647	0.1344	3.651E-12	0.1411	0.1254
	1.8175	1.7812	0.0363	4.999E-14	0.7030	4.9841	
3.826E+06	3.801E+06	4.8991	4.7647	0.1344	3.651E-12	0.1411	0.1254
	1.8175	1.7812	0.0363	4.999E-14	0.7030	4.9841	
3.892E+06	3.867E+06	4.8991	4.7647	0.1344	3.651E-12	0.1411	0.1254
	1.8175	1.7813	0.0363	4.999E-14	0.7030	4.9841	
3.957E+06	3.932E+06	4.8991	4.7647	0.1344	3.651E-12	0.1411	0.1254
	1.8175	1.7813	0.0363	4.999E-14	0.7030	4.9841	
4.023E+06	3.998E+06	4.8991	4.7647	0.1344	3.652E-12	0.1411	0.1254
	1.8175	1.7813	0.0363	4.999E-14	0.7030	4.9841	
4.088E+06	4.063E+06	4.8991	4.7647	0.1344	3.652E-12	0.1411	0.1254
	1.8175	1.7813	0.0363	4.999E-14	0.7030	4.9841	
4.154E+06	4.129E+06	4.8991	4.7647	0.1344	3.652E-12	0.1411	0.1254
	1.8175	1.7813	0.0363	4.999E-14	0.7030	4.9841	
4.219E+06	4.194E+06	4.8992	4.7647	0.1344	3.652E-12	0.1411	0.1254
	1.8175	1.7813	0.0363	4.999E-14	0.7030	4.9841	
4.285E+06	4.260E+06	4.8992	4.7647	0.1344	3.652E-12	0.1411	0.1254
	1.8175	1.7813	0.0363	4.999E-14	0.7030	4.9841	
4.351E+06	4.325E+06	4.8992	4.7647	0.1344	3.652E-12	0.1411	0.1254
	1.8175	1.7813	0.0363	4.999E-14	0.7030	4.9841	
4.416E+06	4.391E+06	4.8992	4.7647	0.1344	3.652E-12	0.1411	0.1254
	1.8175	1.7813	0.0363	4.999E-14	0.7030	4.9841	
4.482E+06	4.456E+06	4.8992	4.7647	0.1344	3.652E-12	0.1411	0.1254
	1.8175	1.7813	0.0363	4.999E-14	0.7030	4.9841	
4.547E+06	4.522E+06	4.8992	4.7647	0.1344	3.652E-12	0.1411	0.1254
	1.8176	1.7813	0.0363	4.999E-14	0.7030	4.9840	
4.613E+06	4.587E+06	4.8992	4.7648	0.1344	3.652E-12	0.1411	0.1254
	1.8176	1.7813	0.0363	4.999E-14	0.7030	4.9840	
4.678E+06	4.653E+06	4.8992	4.7648	0.1344	3.652E-12	0.1411	0.1254
	1.8176	1.7813	0.0363	4.999E-14	0.7030	4.9840	
4.744E+06	4.719E+06	4.8992	4.7648	0.1344	3.652E-12	0.1411	0.1254
	1.8176	1.7813	0.0363	4.999E-14	0.7030	4.9840	
4.809E+06	4.784E+06	4.8992	4.7648	0.1344	3.652E-12	0.1411	0.1254
	1.8176	1.7813	0.0363	4.999E-14	0.7030	4.9840	
4.875E+06	4.850E+06	4.8992	4.7648	0.1344	3.652E-12	0.1411	0.1254
	1.8176	1.7813	0.0363	4.999E-14	0.7030	4.9840	
4.940E+06	4.915E+06	4.8992	4.7648	0.1344	3.652E-12	0.1411	0.1254
	1.8176	1.7813	0.0363	4.999E-14	0.7030	4.9840	
5.006E+06	4.981E+06	4.8992	4.7648	0.1344	3.652E-12	0.1411	0.1254
	1.8176	1.7813	0.0363	4.999E-14	0.7030	4.9840	
5.071E+06	5.046E+06	4.8992	4.7648	0.1344	3.652E-12	0.1411	0.1254
	1.8176	1.7813	0.0363	4.999E-14	0.7030	4.9840	
5.137E+06	5.112E+06	4.8992	4.7648	0.1344	3.652E-12	0.1411	0.1254
	1.8176	1.7813	0.0363	4.999E-14	0.7030	4.9840	
5.202E+06	5.177E+06	4.8992	4.7648	0.1344	3.652E-12	0.1411	0.1254
	1.8176	1.7813	0.0363	4.999E-14	0.7030	4.9840	
5.268E+06	5.243E+06	4.8993	4.7648	0.1344	3.652E-12	0.1411	0.1254
	1.8176	1.7813	0.0363	4.999E-14	0.7030	4.9840	
5.334E+06	5.308E+06	4.8993	4.7648	0.1344	3.652E-12	0.1411	0.1254
	1.8176	1.7813	0.0363	4.999E-14	0.7030	4.9839	
5.399E+06	5.374E+06	4.8993	4.7648	0.1344	3.652E-12	0.1411	0.1254
	1.8176	1.7813	0.0363	4.999E-14	0.7030	4.9839	
5.465E+06	5.439E+06	4.8993	4.7648	0.1344	3.652E-12	0.1411	0.1254
	1.8176	1.7813	0.0363	4.999E-14	0.7030	4.9839	
5.530E+06	5.505E+06	4.8993	4.7648	0.1344	3.652E-12	0.1411	0.1254
	1.8176	1.7813	0.0363	4.999E-14	0.7030	4.9839	
5.596E+06	5.570E+06	4.8993	4.7648	0.1344	3.652E-12	0.1411	0.1254
	1.8176	1.7813	0.0363	5.000E-14	0.7030	4.9839	
5.661E+06	5.636E+06	4.8993	4.7648	0.1344	3.652E-12	0.1411	0.1254
	1.8176	1.7813	0.0363	5.000E-14	0.7030	4.9839	
5.727E+06	5.702E+06	4.8993	4.7649	0.1344	3.652E-12	0.1411	0.1254
	1.8176	1.7813	0.0363	5.000E-14	0.7030	4.9839	
5.792E+06	5.767E+06	4.8993	4.7649	0.1344	3.652E-12	0.1411	0.1254
	1.8176	1.7813	0.0363	5.000E-14	0.7030	4.9839	
5.858E+06	5.833E+06	4.8993	4.7649	0.1344	3.652E-12	0.1411	0.1254
	1.8176	1.7813	0.0363	5.000E-14	0.7030	4.9839	
5.923E+06	5.898E+06	4.8993	4.7649	0.1344	3.652E-12	0.1411	0.1254
	1.8176	1.7814	0.0363	5.000E-14	0.7030	4.9839	

5.989E+06	5.964E+06	4.8993	4.7649	0.1344	3.652E-12	0.1411	0.1254
	1.8176	1.7814	0.0363	5.000E-14	0.7030	4.9839	
6.054E+06	6.029E+06	4.8993	4.7649	0.1344	3.652E-12	0.1411	0.1254
	1.8176	1.7814	0.0363	5.000E-14	0.7030	4.9839	
6.120E+06	6.095E+06	4.8993	4.7649	0.1344	3.652E-12	0.1411	0.1254
	1.8176	1.7814	0.0363	5.000E-14	0.7030	4.9838	
6.185E+06	6.160E+06	4.8993	4.7649	0.1344	3.652E-12	0.1411	0.1254
	1.8176	1.7814	0.0363	5.000E-14	0.7030	4.9838	
6.251E+06	6.226E+06	4.8993	4.7649	0.1344	3.652E-12	0.1411	0.1254
	1.8176	1.7814	0.0363	5.000E-14	0.7030	4.9838	
6.317E+06	6.291E+06	4.8994	4.7649	0.1344	3.652E-12	0.1411	0.1254
	1.8176	1.7814	0.0363	5.000E-14	0.7030	4.9838	
6.325E+06	6.300E+06	4.8994	4.7649	0.1344	3.652E-12	0.1411	0.1254
	1.8176	1.7814	0.0363	5.000E-14	0.7030	4.9838	
6.325E+06	80.0000	5.2621	1.6692	3.5929	2.252E-08	0.1411	0.1254
	1.8382	0.1500	1.6881	1.360E-09	0.7030	4.9838	
6.325E+06	160.0000	5.2621	1.6692	3.5929	2.252E-08	0.1411	0.1254
	1.8382	0.1500	1.6882	1.360E-09	0.7030	4.9837	
6.325E+06	40.0000	5.1765	1.6758	3.5006	2.082E-08	0.1411	0.1254
	1.8305	0.1506	1.6799	1.339E-09	0.7030	4.9837	
6.325E+06	80.0000	5.1765	1.6759	3.5006	2.082E-08	0.1411	0.1254
	1.8305	0.1506	1.6799	1.339E-09	0.7030	4.9836	
6.326E+06	80.0000	4.9968	1.6668	3.3300	1.785E-08	0.1411	0.1254
	1.8144	0.1498	1.6646	1.300E-09	0.7030	4.9836	
6.326E+06	160.0000	4.9969	1.6668	3.3300	1.785E-08	0.1411	0.1254
	1.8144	0.1498	1.6646	1.300E-09	0.7030	4.9835	
6.326E+06	400.0000	5.0985	1.2654	3.8332	2.568E-08	0.1411	0.1254
	1.8237	0.1137	1.7099	1.375E-09	0.7030	4.9832	
6.326E+06	800.0000	5.0988	1.2655	3.8333	2.568E-08	0.1411	0.1254
	1.8238	0.1138	1.7100	1.376E-09	0.7030	4.9828	
6.326E+06	10.0000	5.0433	1.7766	3.2668	1.711E-08	0.1411	0.1254
	1.8188	0.1597	1.6591	1.296E-09	0.7030	4.9828	
6.326E+06	20.0000	5.0433	1.7766	3.2668	1.711E-08	0.1411	0.1254
	1.8188	0.1597	1.6591	1.296E-09	0.7030	4.9828	
6.326E+06	50.0000	5.0851	1.3452	3.7399	2.415E-08	0.1411	0.1254
	1.8226	0.1209	1.7017	1.362E-09	0.7030	4.9828	
6.327E+06	100.0000	5.0851	1.3452	3.7399	2.415E-08	0.1411	0.1254
	1.8226	0.1209	1.7017	1.362E-09	0.7030	4.9827	
6.340E+06	1.320E+04	5.0215	1.7831	3.2384	1.668E-08	0.1413	0.1256
	1.8194	0.1606	1.6588	1.297E-09	0.7031	4.9751	
6.343E+06	1.640E+04	5.0230	1.7841	3.2389	1.669E-08	0.1414	0.1257
	1.8201	0.1607	1.6594	1.298E-09	0.7031	4.9732	
6.343E+06	200.0000	4.7548	0.6124	4.1425	2.824E-08	0.1414	0.1257
	1.7960	0.0552	1.7409	1.385E-09	0.7031	4.9730	
6.343E+06	400.0000	4.7550	0.6124	4.1426	2.825E-08	0.1414	0.1257
	1.7961	0.0552	1.7409	1.385E-09	0.7031	4.9728	
6.343E+06	10.0000	4.2781	1.1083	3.1698	1.390E-08	0.1414	0.1257
	1.7532	0.0999	1.6533	1.220E-09	0.7031	4.9728	
6.343E+06	20.0000	4.2781	1.1083	3.1698	1.390E-08	0.1414	0.1257
	1.7532	0.0999	1.6533	1.220E-09	0.7031	4.9728	
6.343E+06	5.0000	5.8911	1.1083	4.7828	4.932E-08	0.1414	0.1257
	2.4194	0.0999	2.3195	3.634E-09	0.7031	4.9728	
6.343E+06	10.0000	5.8911	1.1083	4.7828	4.932E-08	0.1414	0.1257
	2.4194	0.0999	2.3195	3.634E-09	0.7031	4.9728	
6.343E+06	50.0000	4.9494	1.1083	3.8411	2.507E-08	0.1414	0.1257
	1.9564	0.0999	1.8566	1.771E-09	0.7031	4.9728	
6.343E+06	100.0000	4.9494	1.1083	3.8411	2.507E-08	0.1414	0.1257
	1.9564	0.0999	1.8566	1.771E-09	0.7031	4.9727	

Maximum number of blocks reached. The analysis terminated.

Number of Runtime Warnings: 0

*** End of pc-CRACK output ***

A.6 SURGE LINE 80 YEARS

pc-CRACK 4.1 CS

Version Control No. 4.1.0.0

Structural Integrity Associates, Inc.
www.structint.com
pccrack@structint.com

Date: 05/18/2017 15:04

Input Data read from C:\Users\wwong\Documents\Projects\TurkeyPoint - 1700109\surge.pcf

Analysis Title: Surge

Units Selected: US Customary
Linear Dimensions - inches
Stress - ksi
Load - kips
Temperature - deg F
Time - hours

Analysis Type: Crack Growth (LEFM)

Crack Growth Calculation Method - Cycle/Time Stepping
Maximum Number of Load Blocks = 1
Block Print Interval = 1

Crack Model: 309-Semi-Elliptical Circumferential Crack in Cylinder on the Inside Surface (Chapuliot)
Crack Depth, a = 0.1406
Half Crack Length, c = 0.7030
Wall Thickness, t = 1.1250
Inside Radius, R_i = 5.2500
Aspect ratio allowed to vary
Maximum a/t = 0.8
Crack Depth Print Increment for SIF Tabulation = 0.1
Maximum Aspect Ratio (c/a) for SIF Tabulation = 20
Aspect Ratio Increment for SIF Tabulation = 5

Total Load Cases: 2

Load Case 1: Uniform Stress
Type: Stress Coefficients Input by User

Coefficient C0 = 1.0000
Coefficient C1 = 0.0000
Coefficient C2 = 0.0000
Coefficient C3 = 0.0000

Load Case 2: Linear Stress
Type: Stress Coefficients Input by User

Coefficient C0 = 0.0000
Coefficient C1 = 1.0000
Coefficient C2 = 0.0000
Coefficient C3 = 0.0000

Total Load Sub-Blocks: 16

Load Sub-Block # 1

Load Sub-block Name: Group1
Maximum
Load Case Multiplier Load Case ID
4.7420 Uniform Stress
23.6960 Linear Stress
Minimum
Load Case Multiplier Load Case ID
10.1010 Linear Stress
Growth Law: TableDADN
Cycles/Time: 200
Calc. Interval: 1
Print Interval: 200

Load Sub-Block # 2

Load Sub-block Name: Group2
Maximum
Load Case Multiplier Load Case ID
4.7420 Uniform Stress
28.1210 Linear Stress
Minimum
Load Case Multiplier Load Case ID
29.4300 Linear Stress
Growth Law: TableDADN
Cycles/Time: 13200
Calc. Interval: 1
Print Interval: 13200

Load Sub-Block # 3

Load Sub-block Name: Group3
Maximum
Load Case Multiplier Load Case ID
4.7420 Uniform Stress
29.0030 Linear Stress
Minimum
Load Case Multiplier Load Case ID
27.8790 Linear Stress
Growth Law: TableDADN
Cycles/Time: 4000
Calc. Interval: 1
Print Interval: 4000

Load Sub-Block # 4

Load Sub-block Name: Group4
Maximum
Load Case Multiplier Load Case ID
4.7420 Uniform Stress
28.0080 Linear Stress
Minimum
Load Case Multiplier Load Case ID
27.7100 Linear Stress
Growth Law: TableDADN
Cycles/Time: 200
Calc. Interval: 1
Print Interval: 200

Load Sub-Block # 5

Load Sub-block Name: Group5
Maximum
Load Case Multiplier Load Case ID
4.7840 Uniform Stress
25.7280 Linear Stress
Minimum
Load Case Multiplier Load Case ID

4.7000 Uniform Stress
24.4750 Linear Stress

Growth Law: TableDADN

Cycles/Time: 3150000

Calc. Interval: 1

Print Interval: 65535

Load Sub-Block # 6

Load Sub-block Name: Group6

Maximum

Load Case Multiplier Load Case ID

4.7420 Uniform Stress

32.2150 Linear Stress

Minimum

Load Case Multiplier Load Case ID

27.6200 Linear Stress

Growth Law: TableDADN

Cycles/Time: 80

Calc. Interval: 1

Print Interval: 80

Load Sub-Block # 7

Load Sub-block Name: Group7

Maximum

Load Case Multiplier Load Case ID

4.7420 Uniform Stress

30.7970 Linear Stress

Minimum

Load Case Multiplier Load Case ID

27.7290 Linear Stress

Growth Law: TableDADN

Cycles/Time: 40

Calc. Interval: 1

Print Interval: 40

Load Sub-Block # 8

Load Sub-block Name: Group8

Maximum

Load Case Multiplier Load Case ID

4.7420 Uniform Stress

27.8240 Linear Stress

Minimum

Load Case Multiplier Load Case ID

27.5790 Linear Stress

Growth Law: TableDADN

Cycles/Time: 80

Calc. Interval: 1

Print Interval: 80

Load Sub-Block # 9

Load Sub-block Name: Group9

Maximum

Load Case Multiplier Load Case ID

4.7420 Uniform Stress

29.5010 Linear Stress

Minimum

Load Case Multiplier Load Case ID

20.9340 Linear Stress

Growth Law: TableDADN

Cycles/Time: 400

Calc. Interval: 1

Print Interval: 400

Load Sub-Block # 10

Load Sub-block Name: Group10
Maximum
Load Case Multiplier Load Case ID
4.7420 Uniform Stress
28.5830 Linear Stress
Minimum
Load Case Multiplier Load Case ID
29.3880 Linear Stress
Growth Law: TableDADN
Cycles/Time: 10
Calc. Interval: 1
Print Interval: 10

Load Sub-Block # 11

Load Sub-block Name: Group11
Maximum
Load Case Multiplier Load Case ID
4.7420 Uniform Stress
29.2730 Linear Stress
Minimum
Load Case Multiplier Load Case ID
22.2520 Linear Stress
Growth Law: TableDADN
Cycles/Time: 50
Calc. Interval: 1
Print Interval: 50

Load Sub-Block # 12

Load Sub-block Name: Group12
Maximum
Load Case Multiplier Load Case ID
4.7420 Uniform Stress
28.1210 Linear Stress
Minimum
Load Case Multiplier Load Case ID
29.4300 Linear Stress
Growth Law: TableDADN
Cycles/Time: 13200
Calc. Interval: 1
Print Interval: 13200

Load Sub-Block # 13

Load Sub-block Name: Group13
Maximum
Load Case Multiplier Load Case ID
4.7420 Uniform Stress
23.6960 Linear Stress
Minimum
Load Case Multiplier Load Case ID
10.1010 Linear Stress
Growth Law: TableDADN
Cycles/Time: 200
Calc. Interval: 1
Print Interval: 200

Load Sub-Block # 14

Load Sub-block Name: Group14
Maximum
Load Case Multiplier Load Case ID
4.7420 Uniform Stress
15.8300 Linear Stress
Minimum
Load Case Multiplier Load Case ID

18.2800 Linear Stress
 Growth Law: TableDADN
 Cycles/Time: 10
 Calc. Interval: 1
 Print Interval: 10

Load Sub-Block # 15

Load Sub-block Name: Group15
 Maximum
 Load Case Multiplier Load Case ID
 6.5480 Uniform Stress
 21.5900 Linear Stress
 Minimum
 Load Case Multiplier Load Case ID
 18.2800 Linear Stress
 Growth Law: TableDADN
 Cycles/Time: 5
 Calc. Interval: 1
 Print Interval: 5

Load Sub-Block # 16

Load Sub-block Name: Group16
 Maximum
 Load Case Multiplier Load Case ID
 5.2370 Uniform Stress
 21.1880 Linear Stress
 Minimum
 Load Case Multiplier Load Case ID
 18.2800 Linear Stress
 Growth Law: TableDADN
 Cycles/Time: 50
 Calc. Interval: 1
 Print Interval: 50

Material: 1
 Sample Material 1: Only a sample

Table(da/dn-DK)

No. of R ratios in the tables = 5

R Ratio = -100.0000

Delta K	da/dn
1.000E-03	2.410E-14
1.0000	2.410E-14
1.1000	1.680E-07
10.0000	2.410E-05
20.0000	1.150E-04
30.0000	2.850E-04
40.0000	5.450E-04
50.0000	9.000E-04
60.0000	1.360E-03
70.0000	1.920E-03
80.0000	2.590E-03
90.0000	3.380E-03
100.0000	4.280E-03

R Ratio = 0.1000

Delta K	da/dn
1.000E-03	2.420E-14
1.0000	2.420E-14
1.1000	1.690E-07
10.0000	2.420E-05

20.0000	1.150E-04
30.0000	2.870E-04
40.0000	5.480E-04
50.0000	9.050E-04
60.0000	1.360E-03
70.0000	1.930E-03
80.0000	2.610E-03
90.0000	3.400E-03
100.0000	4.300E-03

R Ratio = 0.5000

Delta K	da/dn
1.000E-03	2.740E-14
1.0000	2.740E-14
1.1000	1.910E-07
10.0000	2.740E-05
20.0000	1.300E-04
30.0000	3.240E-04
40.0000	6.190E-04
50.0000	1.020E-03
60.0000	1.540E-03
70.0000	2.180E-03
80.0000	2.950E-03
90.0000	3.840E-03
100.0000	4.870E-03

R Ratio = 0.7000

Delta K	da/dn
1.000E-03	4.050E-14
1.0000	4.050E-14
1.1000	2.820E-07
10.0000	4.050E-05
20.0000	1.920E-04
30.0000	4.790E-04
40.0000	9.150E-04
50.0000	1.510E-03
60.0000	2.280E-03
70.0000	3.220E-03
80.0000	4.350E-03
90.0000	5.680E-03
100.0000	7.190E-03

R Ratio = 1.0000

Delta K	da/dn
1.000E-03	2.060E-13
1.0000	2.060E-13
1.1000	1.430E-06
10.0000	2.060E-04
20.0000	9.780E-04
30.0000	2.440E-03
40.0000	4.650E-03
50.0000	7.690E-03
60.0000	0.0116
70.0000	0.0164
80.0000	0.0221
90.0000	0.0289
100.0000	0.0366

No. of Data in the KIC Table = 1

Crack Depth	KIC
0.0000	135.0000

messages/Warnings:
Solution for Ri/t of 0.2 and 0.5 will be used

Number of Warnings in Inputs: 0

----- ANALYSIS RESULTS -----

STRESS INTENSITY FACTORS

Load Case # 1: Uniform Stress

----- Crack Dimensions -----

K at tips

a	c	a/t	c/a	a	c
c/a =	5.0000				
0.1406	0.7030	0.1250	5.0000	0.6981	0.3496
0.2406	1.2030	0.2139	5.0000	0.9394	0.4683
0.3406	1.7030	0.3028	5.0000	1.1743	0.5787
0.4406	2.2030	0.3916	5.0000	1.4001	0.6825
0.5406	2.7030	0.4805	5.0000	1.6479	0.7948
0.6406	3.2030	0.5694	5.0000	1.9023	0.9087
0.7406	3.7030	0.6583	5.0000	2.2139	1.0377
0.8406	4.2030	0.7472	5.0000	2.5672	1.1779

c/a = 10.0000

0.1406	1.4060	0.1250	10.0000	0.7347	0.2653
0.2406	2.4060	0.2139	10.0000	1.0038	0.3546
0.3406	3.4060	0.3028	10.0000	1.2769	0.4350
0.4406	4.4060	0.3916	10.0000	1.5462	0.5095
0.5406	5.4060	0.4805	10.0000	1.8603	0.5854
0.6406	6.4060	0.5694	10.0000	2.1907	0.6607
0.7406	7.4060	0.6583	10.0000	2.6105	0.7421
0.8406	8.4060	0.7472	10.0000	3.0960	0.8281

c/a = 15.0000

0.1406	2.1090	0.1250	15.0000	0.7461	0.2260
0.2406	3.6090	0.2139	15.0000	1.0267	0.3013
0.3406	5.1090	0.3028	15.0000	1.3154	0.3675
0.4406	6.6090	0.3916	15.0000	1.6028	0.4281
0.5406	8.1090	0.4805	15.0000	1.9478	0.4854
0.6406	9.6090	0.5694	15.0000	2.3142	0.5405
0.7406	11.1090	0.6583	15.0000	2.7708	0.5950
0.8406	12.6090	0.7472	15.0000	3.2945	0.6490

c/a = 20.0000

0.1406	2.8120	0.1250	20.0000	0.7517	0.1768
0.2406	4.8120	0.2139	20.0000	1.0363	0.2357
0.3406	6.8120	0.3028	20.0000	1.3296	0.2872
0.4406	8.8120	0.3916	20.0000	1.6222	0.3344
0.5406	10.8120	0.4805	20.0000	1.9735	0.3783
0.6406	12.8120	0.5694	20.0000	2.3467	0.4204
0.7406	14.8120	0.6583	20.0000	2.8122	0.4613
0.8406	16.8120	0.7472	20.0000	3.3462	0.5013

Load Case # 2: Linear Stress

----- Crack Dimensions -----

K at tips

a	c	a/t	c/a	a	c
c/a =	5.0000				
0.1406	0.7030	0.1250	5.0000	0.0601	5.386E-03
0.2406	1.2030	0.2139	5.0000	0.1369	0.0130
0.3406	1.7030	0.3028	5.0000	0.2375	0.0243
0.4406	2.2030	0.3916	5.0000	0.3595	0.0394
0.5406	2.7030	0.4805	5.0000	0.5087	0.0600

0.6406	3.2030	0.5694	5.0000	0.6829	0.0858
0.7406	3.7030	0.6583	5.0000	0.9031	0.1198
0.8406	4.2030	0.7472	5.0000	1.1709	0.1625

c/a = 10.0000

0.1406	1.4060	0.1250	10.0000	0.0626	2.673E-03
0.2406	2.4060	0.2139	10.0000	0.1439	6.589E-03
0.3406	3.4060	0.3028	10.0000	0.2528	0.0124
0.4406	4.4060	0.3916	10.0000	0.3873	0.0202
0.5406	5.4060	0.4805	10.0000	0.5571	0.0305
0.6406	6.4060	0.5694	10.0000	0.7595	0.0432
0.7406	7.4060	0.6583	10.0000	1.0234	0.0602
0.8406	8.4060	0.7472	10.0000	1.3513	0.0817

c/a = 15.0000

0.1406	2.1090	0.1250	15.0000	0.0634	1.686E-03
0.2406	3.6090	0.2139	15.0000	0.1464	4.154E-03
0.3406	5.1090	0.3028	15.0000	0.2586	7.727E-03
0.4406	6.6090	0.3916	15.0000	0.3982	0.0124
0.5406	8.1090	0.4805	15.0000	0.5774	0.0184
0.6406	9.6090	0.5694	15.0000	0.7931	0.0256
0.7406	11.1090	0.6583	15.0000	1.0739	0.0341
0.8406	12.6090	0.7472	15.0000	1.4228	0.0442

c/a = 20.0000

0.1406	2.8120	0.1250	20.0000	0.0638	1.251E-03
0.2406	4.8120	0.2139	20.0000	0.1476	3.080E-03
0.3406	6.8120	0.3028	20.0000	0.2611	5.712E-03
0.4406	8.8120	0.3916	20.0000	0.4026	9.175E-03
0.5406	10.8120	0.4805	20.0000	0.5844	0.0135
0.6406	12.8120	0.5694	20.0000	0.8035	0.0187
0.7406	14.8120	0.6583	20.0000	1.0892	0.0247
0.8406	16.8120	0.7472	20.0000	1.4445	0.0316

CRACK GROWTH ANALYSIS RESULTS

Total Cycles /Time	Subblock Cycles /Time	Kmax	Kmin	DaDn		Crack Dimensions	
				DeltaK	/DaDt		
				a c	a/t c/a		
Blocks: 1							
200.0000	200.0000	4.7522	0.6117	4.1405	3.361E-06	0.1413	0.1256
	1.7946	0.0551	1.7395	4.737E-07	0.7031	4.9770	
1.340E+04	1.320E+04	5.8383	2.3483	3.4900	2.489E-06	0.1713	0.1523
	2.2510	0.2613	1.9897	6.441E-07	0.7100	4.1441	
1.740E+04	4000.0000	6.2262	2.4395	3.7867	2.981E-06	0.1829	0.1626
	2.4187	0.2884	2.1303	7.517E-07	0.7129	3.8981	
1.760E+04	200.0000	6.1546	2.4355	3.7191	2.866E-06	0.1834	0.1631
	2.4152	0.2885	2.1267	7.489E-07	0.7130	3.8867	
8.314E+04	6.554E+04	5.9870	5.8114	0.1755	1.758E-13	0.1834	0.1631
	2.4103	2.3596	0.0507	1.839E-13	0.7130	3.8867	
1.487E+05	1.311E+05	5.9870	5.8114	0.1755	1.758E-13	0.1834	0.1631
	2.4103	2.3596	0.0507	1.839E-13	0.7130	3.8867	
2.142E+05	1.966E+05	5.9870	5.8114	0.1755	1.758E-13	0.1834	0.1631
	2.4103	2.3596	0.0507	1.839E-13	0.7130	3.8867	
2.797E+05	2.621E+05	5.9870	5.8114	0.1755	1.758E-13	0.1834	0.1631
	2.4103	2.3596	0.0507	1.839E-13	0.7130	3.8867	
3.453E+05	3.277E+05	5.9870	5.8114	0.1755	1.758E-13	0.1834	0.1631
	2.4103	2.3596	0.0507	1.839E-13	0.7130	3.8867	
4.108E+05	3.932E+05	5.9870	5.8114	0.1755	1.758E-13	0.1834	0.1631
	2.4103	2.3596	0.0507	1.839E-13	0.7130	3.8867	
4.763E+05	4.587E+05	5.9870	5.8114	0.1755	1.758E-13	0.1834	0.1631

	2.4103	2.3596	0.0507	1.839E-13	0.7130	3.8867	
5.419E+05	5.243E+05	5.9870	5.8114	0.1755	1.758E-13	0.1834	0.1631
	2.4103	2.3596	0.0507	1.839E-13	0.7130	3.8867	
6.074E+05	5.898E+05	5.9870	5.8114	0.1755	1.758E-13	0.1834	0.1631
	2.4103	2.3596	0.0507	1.839E-13	0.7130	3.8867	
6.730E+05	6.554E+05	5.9870	5.8114	0.1755	1.758E-13	0.1834	0.1631
	2.4103	2.3596	0.0507	1.839E-13	0.7130	3.8867	
7.385E+05	7.209E+05	5.9870	5.8114	0.1755	1.758E-13	0.1834	0.1631
	2.4103	2.3596	0.0507	1.839E-13	0.7130	3.8867	
8.040E+05	7.864E+05	5.9870	5.8114	0.1755	1.758E-13	0.1834	0.1631
	2.4103	2.3596	0.0507	1.839E-13	0.7130	3.8867	
8.696E+05	8.520E+05	5.9870	5.8114	0.1755	1.758E-13	0.1834	0.1631
	2.4103	2.3596	0.0507	1.839E-13	0.7130	3.8867	
9.351E+05	9.175E+05	5.9870	5.8114	0.1755	1.758E-13	0.1834	0.1631
	2.4103	2.3596	0.0507	1.839E-13	0.7130	3.8867	
1.001E+06	9.830E+05	5.9870	5.8114	0.1755	1.758E-13	0.1834	0.1631
	2.4103	2.3596	0.0507	1.839E-13	0.7130	3.8867	
1.066E+06	1.049E+06	5.9870	5.8114	0.1755	1.758E-13	0.1834	0.1631
	2.4103	2.3596	0.0507	1.839E-13	0.7130	3.8867	
1.132E+06	1.114E+06	5.9870	5.8114	0.1755	1.758E-13	0.1834	0.1631
	2.4103	2.3596	0.0507	1.839E-13	0.7130	3.8867	
1.197E+06	1.180E+06	5.9870	5.8114	0.1755	1.758E-13	0.1834	0.1631
	2.4103	2.3596	0.0507	1.839E-13	0.7130	3.8867	
1.263E+06	1.245E+06	5.9870	5.8114	0.1755	1.758E-13	0.1834	0.1631
	2.4103	2.3596	0.0507	1.839E-13	0.7130	3.8867	
1.328E+06	1.311E+06	5.9870	5.8114	0.1755	1.758E-13	0.1834	0.1631
	2.4103	2.3596	0.0507	1.839E-13	0.7130	3.8867	
1.394E+06	1.376E+06	5.9870	5.8114	0.1755	1.758E-13	0.1834	0.1631
	2.4103	2.3596	0.0507	1.839E-13	0.7130	3.8867	
1.459E+06	1.442E+06	5.9870	5.8114	0.1755	1.758E-13	0.1834	0.1631
	2.4103	2.3596	0.0507	1.839E-13	0.7130	3.8867	
1.525E+06	1.507E+06	5.9870	5.8114	0.1755	1.758E-13	0.1834	0.1631
	2.4103	2.3596	0.0507	1.839E-13	0.7130	3.8867	
1.590E+06	1.573E+06	5.9870	5.8114	0.1755	1.758E-13	0.1834	0.1631
	2.4103	2.3596	0.0507	1.839E-13	0.7130	3.8867	
1.656E+06	1.638E+06	5.9870	5.8114	0.1755	1.758E-13	0.1834	0.1631
	2.4103	2.3596	0.0507	1.839E-13	0.7130	3.8867	
1.722E+06	1.704E+06	5.9870	5.8114	0.1755	1.758E-13	0.1834	0.1631
	2.4103	2.3596	0.0507	1.839E-13	0.7130	3.8867	
1.787E+06	1.769E+06	5.9870	5.8114	0.1755	1.758E-13	0.1834	0.1631
	2.4103	2.3596	0.0507	1.839E-13	0.7130	3.8867	
1.853E+06	1.835E+06	5.9870	5.8114	0.1755	1.758E-13	0.1834	0.1631
	2.4103	2.3596	0.0507	1.839E-13	0.7130	3.8867	
1.918E+06	1.901E+06	5.9870	5.8114	0.1755	1.758E-13	0.1834	0.1631
	2.4103	2.3596	0.0507	1.839E-13	0.7130	3.8867	
1.984E+06	1.966E+06	5.9870	5.8114	0.1755	1.758E-13	0.1834	0.1631
	2.4103	2.3596	0.0507	1.839E-13	0.7130	3.8867	
2.049E+06	2.032E+06	5.9870	5.8114	0.1755	1.758E-13	0.1834	0.1631
	2.4103	2.3596	0.0507	1.839E-13	0.7130	3.8867	
2.115E+06	2.097E+06	5.9870	5.8114	0.1755	1.758E-13	0.1834	0.1631
	2.4103	2.3596	0.0507	1.839E-13	0.7130	3.8867	
2.180E+06	2.163E+06	5.9870	5.8114	0.1755	1.758E-13	0.1834	0.1631
	2.4103	2.3596	0.0507	1.839E-13	0.7130	3.8867	
2.246E+06	2.228E+06	5.9870	5.8114	0.1755	1.758E-13	0.1834	0.1631
	2.4103	2.3596	0.0507	1.839E-13	0.7130	3.8867	
2.311E+06	2.294E+06	5.9870	5.8114	0.1755	1.758E-13	0.1834	0.1631
	2.4103	2.3596	0.0507	1.839E-13	0.7130	3.8867	
2.377E+06	2.359E+06	5.9870	5.8114	0.1755	1.758E-13	0.1834	0.1631
	2.4103	2.3596	0.0507	1.839E-13	0.7130	3.8867	
2.442E+06	2.425E+06	5.9870	5.8114	0.1755	1.758E-13	0.1834	0.1631
	2.4103	2.3596	0.0507	1.839E-13	0.7130	3.8867	
2.508E+06	2.490E+06	5.9870	5.8114	0.1755	1.758E-13	0.1834	0.1631
	2.4103	2.3596	0.0507	1.839E-13	0.7130	3.8867	
2.573E+06	2.556E+06	5.9870	5.8114	0.1755	1.758E-13	0.1834	0.1631
	2.4103	2.3596	0.0507	1.839E-13	0.7130	3.8867	
2.639E+06	2.621E+06	5.9870	5.8114	0.1755	1.758E-13	0.1834	0.1631
	2.4103	2.3596	0.0507	1.839E-13	0.7130	3.8867	
2.705E+06	2.687E+06	5.9870	5.8114	0.1755	1.758E-13	0.1834	0.1631

	2.4103	2.3596	0.0507	1.839E-13	0.7130	3.8867	
2.770E+06	2.752E+06	5.9870	5.8114	0.1755	1.758E-13	0.1834	0.1631
	2.4103	2.3596	0.0507	1.839E-13	0.7130	3.8867	
2.836E+06	2.818E+06	5.9870	5.8114	0.1755	1.758E-13	0.1834	0.1631
	2.4103	2.3596	0.0507	1.839E-13	0.7130	3.8867	
2.901E+06	2.884E+06	5.9870	5.8114	0.1755	1.758E-13	0.1834	0.1631
	2.4103	2.3596	0.0507	1.839E-13	0.7130	3.8867	
2.967E+06	2.949E+06	5.9870	5.8114	0.1755	1.758E-13	0.1834	0.1631
	2.4103	2.3596	0.0507	1.839E-13	0.7130	3.8867	
3.032E+06	3.015E+06	5.9870	5.8114	0.1755	1.758E-13	0.1834	0.1631
	2.4103	2.3596	0.0507	1.839E-13	0.7130	3.8867	
3.098E+06	3.080E+06	5.9870	5.8114	0.1755	1.758E-13	0.1834	0.1631
	2.4103	2.3596	0.0507	1.839E-13	0.7130	3.8867	
3.163E+06	3.146E+06	5.9870	5.8114	0.1755	1.758E-13	0.1834	0.1631
	2.4103	2.3596	0.0507	1.839E-13	0.7130	3.8867	
3.168E+06	3.150E+06	5.9870	5.8114	0.1755	1.758E-13	0.1834	0.1631
	2.4103	2.3596	0.0507	1.839E-13	0.7130	3.8867	
3.168E+06	80.0000	6.5328	2.4329	4.0999	3.544E-06	0.1837	0.1633
	2.4625	0.2885	2.1740	7.863E-07	0.7131	3.8811	
3.168E+06	40.0000	6.4117	2.4450	3.9667	3.299E-06	0.1839	0.1634
	2.4493	0.2901	2.1592	7.746E-07	0.7131	3.8785	
3.168E+06	80.0000	6.1557	2.4361	3.7196	2.867E-06	0.1841	0.1636
	2.4209	0.2893	2.1317	7.528E-07	0.7132	3.8740	
3.168E+06	400.0000	6.3506	1.8730	4.4776	4.219E-06	0.1858	0.1651
	2.4588	0.2238	2.2350	8.324E-07	0.7135	3.8408	
3.168E+06	10.0000	6.2693	2.6300	3.6393	2.750E-06	0.1858	0.1652
	2.4493	0.3143	2.1350	7.576E-07	0.7135	3.8402	
3.168E+06	50.0000	6.3365	1.9943	4.3422	3.961E-06	0.1860	0.1653
	2.4591	0.2385	2.2206	8.204E-07	0.7136	3.8364	
3.181E+06	1.320E+04	7.2721	3.4363	3.8358	3.146E-06	0.2244	0.1995
	2.9151	0.4679	2.4472	1.040E-06	0.7253	3.2319	
3.182E+06	200.0000	6.7878	1.1893	5.5985	6.719E-06	0.2258	0.2007
	2.8613	0.1627	2.6986	1.272E-06	0.7255	3.2138	
3.182E+06	10.0000	5.8622	2.1528	3.7095	2.825E-06	0.2258	0.2007
	2.7350	0.2945	2.4404	1.017E-06	0.7256	3.2135	
3.182E+06	5.0000	8.0641	2.1532	5.9109	7.811E-06	0.2258	0.2007
	3.7728	0.2946	3.4782	2.251E-06	0.7256	3.2130	
3.182E+06	50.0000	6.9172	2.1566	4.7607	4.867E-06	0.2261	0.2010
	3.0838	0.2953	2.7885	1.369E-06	0.7256	3.2098	

Maximum number of blocks reached. The analysis terminated.

Number of Runtime Warnings: 0

*** End of pc-CRACK output ***

A.7 ACCUMULATOR LINE THROUGH-WALL CRACK STRESS INTENSITY CALCULATION

tm
 pc-CRACK for Windows
 Version 3.1-98348
 (C) Copyright '84 - '98
 Structural Integrity Associates, Inc.
 3315 Almaden Expressway, Suite 24
 San Jose, CA 95118-1557
 Voice: 408-978-8200
 Fax: 408-978-8964
 E-mail: pccrack@structint.com

Linear Elastic Fracture Mechanics

Date: Wed Apr 14 21:22:15 2010
 Input Data and Results File: ACCL_TH.LFM

Title: Accumulator Line through wall crack stress intensity

Load Cases:

Case ID	Stress Coefficients				
	C0	C1	C2	C3	Type
tension	19.02	0	0	0	Coeff

-----Through Wall Stresses for Load Cases With Stress Coeff-----

Wall Depth	Case tension
---------------	-----------------

0.0000	19.02
0.2530	19.02
0.5060	19.02
0.7590	19.02
1.0120	19.02
1.2650	19.02
1.5180	19.02
1.7710	19.02
2.0240	19.02
2.2770	19.02
2.5300	19.02

Crack Model: Through-Wall Circ. Crack in Cylinder Under Tension And Bending

Crack Parameters:

Wall thickness: 1.0000

Outside diameter: 10.7500

Half crack length: 2.5300

Poisson ratio: 0.3000

Tension: $C_0 = P / (2 \cdot \pi \cdot R_m \cdot t)$

Max. bending: $C_1 = M / (\pi \cdot t \cdot R_m \cdot R_m)$

All other stress coefficients are neglected.

-----Stress Intensity Factor-----

Crack Size	Case tension
---------------	-----------------

0.0506	7.58399
0.1012	10.7281
0.1518	13.1448
0.2024	15.1874
0.2530	16.9932
0.3036	18.6326
0.3542	20.148
0.4048	21.5668

0.4554	22.9085
0.5060	24.187
0.5566	25.4134
0.6072	26.5958
0.6578	27.7413
0.7084	28.8553
0.7590	29.9424
0.8096	31.0067
0.8602	32.0514
0.9108	33.0795
0.9614	34.0936
1.0120	35.096
1.0626	36.0886
1.1132	37.0733
1.1638	38.0516
1.2144	39.0252
1.2650	39.9954
1.3156	40.9634
1.3662	41.9304
1.4168	42.8974
1.4674	43.8655
1.5180	44.8356
1.5686	45.8085
1.6192	46.7852
1.6698	47.7663
1.7204	48.7526
1.7710	49.7448
1.8216	50.7435
1.8722	51.7494
1.9228	52.7631
1.9734	53.7852
2.0240	54.8161
2.0746	55.8564
2.1252	56.9067
2.1758	57.9673
2.2264	59.0389
2.2770	60.1217
2.3276	61.2163
2.3782	62.323
2.4288	63.4424
2.4794	64.5468
2.5300	65.6637

End of pc-CRACK Output

A.8 RHR LINE THROUGH-WALL CRACK STRESS INTENSITY CALCULATION

tm
 pc-CRACK for Windows
 Version 3.1-98348
 (C) Copyright '84 - '98
 Structural Integrity Associates, Inc.
 3315 Almaden Expressway, Suite 24
 San Jose, CA 95118-1557
 Voice: 408-978-8200
 Fax: 408-978-8964
 E-mail: pccrack@structint.com

Linear Elastic Fracture Mechanics

Date: Wed Apr 14 21:21:35 2010
 Input Data and Results File: RHR_TH.LFM

Title: RHR Line through wall crack growth

Load Cases:

Case ID	Stress Coefficients				Type
	C0	C1	C2	C3	
tension	17.38	0	0	0	Coeff

-----Through Wall Stresses for Load Cases With Stress Coeff-----

Wall Depth	Case tension
---------------	-----------------

0.0000	17.38
0.3120	17.38
0.6240	17.38
0.9360	17.38
1.2480	17.38
1.5600	17.38
1.8720	17.38
2.1840	17.38
2.4960	17.38
2.8080	17.38
3.1200	17.38

Crack Model: Through-Wall Circ. Crack in Cylinder Under Tension And Bending

Crack Parameters:

Wall thickness: 1.2500

Outside diameter: 14.0000

Half crack length: 3.1200

Poisson ratio: 0.3000

Tension: $C_0 = P / (2 \cdot \pi \cdot R_m \cdot t)$

Max. bending: $C_1 = M / (\pi \cdot t \cdot R_m \cdot R_m)$

All other stress coefficients are neglected.

-----Stress Intensity Factor-----

Crack Size	Case tension
---------------	-----------------

0.0624	7.69576
0.1248	10.886
0.1872	13.3379
0.2496	15.4099
0.3120	17.2411
0.3744	18.9032
0.4368	20.4389
0.4992	21.8763

0.5616	23.2347
0.6240	24.5286
0.6864	25.7689
0.7488	26.9641
0.8112	28.121
0.8736	29.2453
0.9360	30.3416
0.9984	31.4139
1.0608	32.4656
1.1232	33.4997
1.1856	34.5186
1.2480	35.5247
1.3104	36.52
1.3728	37.5063
1.4352	38.4852
1.4976	39.4582
1.5600	40.4267
1.6224	41.3919
1.6848	42.355
1.7472	43.317
1.8096	44.2789
1.8720	45.2416
1.9344	46.206
1.9968	47.1728
2.0592	48.1429
2.1216	49.117
2.1840	50.0957
2.2464	51.0797
2.3088	52.0695
2.3712	53.0659
2.4336	54.0692
2.4960	55.0801
2.5584	56.099
2.6208	57.1265
2.6832	58.1629
2.7456	59.2088
2.8080	60.2646
2.8704	61.3307
2.9328	62.4074
2.9952	63.4952
3.0576	64.5944
3.1200	65.6977

End of pc-CRACK Output

A.9 SURGE LINE THROUGH-WALL CRACK STRESS INTENSITY CALCULATION

tm
 pc-CRACK for Windows
 Version 3.1-98348
 (C) Copyright '84 - '98
 Structural Integrity Associates, Inc.
 3315 Almaden Expressway, Suite 24
 San Jose, CA 95118-1557
 Voice: 408-978-8200
 Fax: 408-978-8964
 E-mail: pccrack@structint.com

Linear Elastic Fracture Mechanics

Date: Wed Apr 14 21:20:14 2010
 Input Data and Results File: SURGE_TH.LFM
 Title: SURGE Line through wall crack growth
 Load Cases:

Case ID	Stress Coefficients C0	C1	C2	C3	Type
tension	24.73	0	0	0	Coeff

-----Through Wall Stresses for Load Cases With Stress Coeff-----
 Wall Case
 Depth tension

0.0000	24.73
0.3300	24.73
0.6600	24.73
0.9900	24.73
1.3200	24.73
1.6500	24.73
1.9800	24.73
2.3100	24.73
2.6400	24.73
2.9700	24.73
3.3000	24.73

Crack Model: Through-Wall Circ. Crack in Cylinder Under Tension And Bending

Crack Parameters:
 Wall thickness: 1.1250
 Outside diameter: 12.7500
 Half crack length: 3.3000
 Poisson ratio: 0.3000
 Tension: $C_0 = P / (2 \cdot \pi \cdot R_m \cdot t)$
 Max. bending: $C_1 = M / (\pi \cdot t \cdot R_m \cdot R_m)$
 All other stress coefficients are neglected.

-----Stress Intensity Factor-----
 Crack Case
 Size tension

0.0660	11.2621
0.1320	15.9321
0.1980	19.5234
0.2640	22.5608
0.3300	25.2483
0.3960	27.6912
0.4620	29.9521
0.5280	32.0723
0.5940	34.0806
0.6600	35.9982
0.7260	37.8413

0.7920	39.6225
0.8580	41.3522
0.9240	43.0387
0.9900	44.689
1.0560	46.3092
1.1220	47.9043
1.1880	49.4788
1.2540	51.0368
1.3200	52.5815
1.3860	54.1163
1.4520	55.6438
1.5180	57.1666
1.5840	58.6871
1.6500	60.2074
1.7160	61.7294
1.7820	63.2549
1.8480	64.7857
1.9140	66.3232
1.9800	67.8691
2.0460	69.4245
2.1120	70.991
2.1780	72.5696
2.2440	74.1615
2.3100	75.7679
2.3760	77.3898
2.4420	79.0281
2.5080	80.6839
2.5740	82.358
2.6400	84.0514
2.7060	85.7647
2.7720	87.499
2.8380	89.2371
2.9040	90.9721
2.9700	92.7252
3.0360	94.4966
3.1020	96.2866
3.1680	98.0955
3.2340	99.9235
3.3000	101.771

End of pc-CRACK Output

Enclosure 4
Non-proprietary Reference Documents
and
Redacted Versions of Proprietary
Reference Documents
(Public Version)
Attachment 13

PWROG-17033- NP, Revision 0

Update for Subsequent License Renewal:

**WCAP-13045, Compliance to ASME Code Case N-481 of the Primary
Loop Pump Casings of Westinghouse Type Nuclear Steam Supply
Systems, October 2017**

(34 Total Pages, including cover sheets)



PWROG-17033-NP
Revision 0

WESTINGHOUSE NON-PROPRIETARY CLASS 3

Update for Subsequent License Renewal: WCAP-13045, “Compliance to ASME Code Case N-481 of the Primary Loop Pump Casings of Westinghouse Type Nuclear Steam Supply Systems”

Materials Committee

PA-MSC-1498, Revision 0

October 2017

PWROG-17033-NP
Revision 0

Update for Subsequent License Renewal: WCAP-13045, “Compliance to ASME Code Case N-481 of the Primary Loop Pump Casings of Westinghouse Type Nuclear Steam Supply Systems”

PA-MSC-1498, Revision 0
October 2017

Author: Anees Udyawar*
Structural Design and Analysis III

Reviewer: Alexandria Carolan*
Structural Design and Analysis III

Approved: Lynn Patterson*, Manager
Structural Design and Analysis III

James Molkenthin*, Program Director
PWR Owners Group PMO

*Electronically approved records are authenticated in the electronic document management system.

Westinghouse Electric Company LLC
1000 Westinghouse Drive
Cranberry Township, PA 16066, USA

© 2017 Westinghouse Electric Company LLC
All Rights Reserved

ACKNOWLEDGEMENTS

This report was developed and funded by the PWR Owners Group under the leadership of the participating utility representatives of the Materials Committee.

LEGAL NOTICE

This report was prepared as an account of work performed by Westinghouse Electric Company LLC. Neither Westinghouse Electric Company LLC, nor any person acting on its behalf:

1. Makes any warranty or representation, express or implied including the warranties of fitness for a particular purpose or merchantability, with respect to the accuracy, completeness, or usefulness of the information contained in this report, or that the use of any information, apparatus, method, or process disclosed in this report may not infringe privately owned rights; or
2. Assumes any liabilities with respect to the use of, or for damages resulting from the use of, any information, apparatus, method, or process disclosed in this report.

COPYRIGHT NOTICE

This report has been prepared by Westinghouse Electric Company LLC and bears a Westinghouse Electric Company copyright notice. Information in this report is the property of and contains copyright material owned by Westinghouse Electric Company LLC and/or its affiliates, subcontractors and/or suppliers. It is transmitted to you in confidence and trust, and you agree to treat this document and the material contained therein in strict accordance with the terms and conditions of the agreement under which it was provided to you. Any unauthorized use of this document is prohibited.

As a participating member of this task, you are permitted to make the number of copies of the information contained in this report that are necessary for your internal use in connection with your implementation of the report results for your plant(s) in your normal conduct of business. Should implementation of this report involve a third party, you are permitted to make the number of copies of the information contained in this report that are necessary for the third party's use in supporting your implementation at your plant(s) in your normal conduct of business if you have received the prior, written consent of Westinghouse Electric Company LLC to transmit this information to a third party or parties. All copies made by you must include the copyright notice in all instances and the proprietary notice if the original was identified as proprietary.

DISTRIBUTION NOTICE

This report was prepared for the PWR Owners Group. This Distribution Notice is intended to establish guidance for access to this information. This report (including proprietary and non-proprietary versions) is not to be provided to any individual or organization outside of the PWR Owners Group program participants without prior written approval of the PWR Owners Group Program Management Office. However, prior written approval is not required for program participants to provide copies of Class 3 Non-Proprietary reports to third parties that are supporting implementation at their plant, and for submittals to the NRC.

PWR Owners Group
United States Member Participation* for PA-MSC-1498, Revision 0

Utility Member	Plant Site(s)	Participant	
		Yes	No
Ameren Missouri	Callaway (W)		X
American Electric Power	D.C. Cook 1 & 2 (W)	X	
Arizona Public Service	Palo Verde Units 1, 2, & 3 (CE)		X
Dominion Connecticut	Millstone 2 (CE)		X
	Millstone 3 (W)	X	
Dominion VA	North Anna 1 & 2 (W)	X	
	Surry 1 & 2 (W)	X	
Duke Energy Carolinas	Catawba 1 & 2 (W)	X	
	McGuire 1 & 2 (W)	X	
	Oconee 1, 2, & 3 (B&W)	X	
Duke Energy Progress	Robinson 2 (W)	X	
	Shearon Harris (W)	X	
Entergy Palisades	Palisades (CE)		X
Entergy Nuclear Northeast	Indian Point 2 & 3 (W)		X
Entergy Operations South	Arkansas 1 (B&W)		X
	Arkansas 2 (CE)		X
	Waterford 3 (CE)		X
Exelon Generation Co. LLC	Braidwood 1 & 2 (W)	X	
	Byron 1 & 2 (W)	X	
	TMI 1 (B&W)		X
	Calvert Cliffs 1 & 2 (CE)		X
	Ginna (W)		X
FirstEnergy Nuclear Operating Co.	Beaver Valley 1 & 2 (W)		X
	Davis-Besse (B&W)		X
Florida Power & Light \ NextEra	St. Lucie 1 & 2 (CE)		X
	Turkey Point 3 & 4 (W)	X	
	Seabrook (W)		X
	Pt. Beach 1 & 2 (W)	X	
Luminant Power	Comanche Peak 1 & 2 (W)		X

PWR Owners Group
United States Member Participation* for PA-MSC-1498, Revision 0

Utility Member	Plant Site(s)	Participant	
		Yes	No
Omaha Public Power District	Fort Calhoun (CE)		X
Pacific Gas & Electric	Diablo Canyon 1 & 2 (W)		X
PSEG – Nuclear	Salem 1 & 2 (W)		X
South Carolina Electric & Gas	V.C. Summer (W)	X	
So. Texas Project Nuclear Operating Co.	South Texas Project 1 & 2 (W)		X
Southern Nuclear Operating Co.	Farley 1 & 2 (W)	X	
	Vogtle 1 & 2 (W)	X	
Tennessee Valley Authority	Sequoyah 1 & 2 (W)		X
	Watts Bar 1 & 2 (W)		X
Wolf Creek Nuclear Operating Co.	Wolf Creek (W)		X
Xcel Energy	Prairie Island 1 & 2 (W)	X	

* **Project participants as of the date the final deliverable was completed. On occasion, additional members will join a project. Please contact the PWR Owners Group Program Management Office to verify participation before sending this document to participants not listed above.**

PWR Owners Group
International Member Participation* for PA-MSC-1498, Revision 0

Utility Member	Plant Site(s)	Participant	
		Yes	No
Asociación Nuclear Ascó-Vandellòs	Asco 1 & 2 (W)		X
	Vandellos 2 (W)		X
Axpo AG	Beznau 1 & 2 (W)		X
Centrales Nucleares Almaraz-Trillo	Almaraz 1 & 2 (W)		X
EDF Energy	Sizewell B (W)		X
Electrabel	Doel 1, 2 & 4 (W)		X
	Tihange 1 & 3 (W)		X
Electricite de France	58 Units		X
Elektricitets Produktiemaatschappij Zuid-Nederland	Borssele 1 (Siemens)		X
Eletronuclear-Elektrobras	Angra 1 (W)		X
Emirates Nuclear Energy Corporation	Barakah 1 & 2		X
Eskom	Koeberg 1 & 2 (W)		X
Hokkaido	Tomari 1, 2 & 3 (MHI)		X
Japan Atomic Power Company	Tsuruga 2 (MHI)		X
Kansai Electric Co., LTD	Mihama 3 (W)		X
	Ohj 1, 2, 3 & 4 (W & MHI)		X
	Takahama 1, 2, 3 & 4 (W & MHI)		X
Korea Hydro & Nuclear Power Corp.	Kori 1, 2, 3 & 4 (W)		X
	Hanbit 1 & 2 (W)		X
	Hanbit 3, 4, 5 & 6 (CE)		X
	Hanul 3, 4, 5 & 6 (CE)		X
Kyushu	Genkai 2, 3 & 4 (MHI)		X
	Sendai 1 & 2 (MHI)		X
Nuklearna Elektrarna KRSKO	Krsko (W)		X
Ringhals AB	Ringhals 2, 3 & 4 (W)		X
Shikoku	Ikata 1, 2 & 3 (MHI)		X
Taiwan Power Co.	Maanshan 1 & 2 (W)		X

* Project participants as of the date the final deliverable was completed. On occasion, additional members will join a project. Please contact the PWR Owners Group Program Management Office to verify participation before sending this document to participants not listed above.

TABLE OF CONTENTS

1	BACKGROUND AND PURPOSE	1-1
1.1	OPERATING EXPERIENCE AND APPLICATION OF LATEST FRACTURE TOUGHNESS DATABASE	1-3
2	STABILITY ANALYSIS AND FRACTURE TOUGHNESS	2-1
2.1	FRACTURE TOUGHNESS DETERMINED IN WCAP-13045	2-1
2.2	FRACTURE TOUGHNESS BASED ON NUREG/CR-4513, REVISION 2	2-3
3	FATIGUE CRACK GROWTH ANALYSIS	3-1
4	CONCLUSIONS	4-1
5	REFERENCES	5-1
	APPENDIX A: ASME SECTION XI CODE CASE N-481	A-1
	APPENDIX B: ASME SECTION XI CODE IMPLEMENTATION OF N-481	B-1
	APPENDIX C: CAST AUSTENITIC STAINLESS STEEL (CASS) PRESENTATION AT ASME CODE MEETING	C-1

1 BACKGROUND AND PURPOSE

The purpose of this report is to provide continued justification of the fracture mechanics integrity evaluation in WCAP-13045 [1], "Compliance to ASME Code Case N-481 of the Primary Loop Pump Casings of Westinghouse Type Nuclear Steam Supply Systems," for application to Subsequent License Renewal (SLR), 80 years of design life. The fracture mechanics assessment for SLR provided in this report will allow plants to continue performing visual inspections, in lieu of volumetric inspections, for pump casings as incorporated in the ASME Section XI code.

Table IWB-2500-1, Examination Categories of Section XI of the ASME Boiler and Pressure Vessel Code [2] previously mandated periodic volumetric inspections of the welds of the primary loop pump casings of nuclear power plants. Since these inspections are costly in terms of dollars and radiation exposure, the ASME Code body approved a code case, N-481 [3] in March 1990 (see Appendix A of this report), to provide an alternative to the volumetric inspection requirement. The NRC accepted the Code Case N-481 in Regulatory Guide 1.147, "Inservice Inspection Code Case Acceptability ASME Section XI Division 1," in April 1992.

Given that most pump casings are heavy-wall cast stainless steel, a volumetric inspection of the full thickness of the welds using the ultrasonic test method from the outside diameter surface is impractical due to the severe attenuation associated with the large grain structures. A volumetric inspection of the full thickness of the welds would require unconventional approaches (inside diameter and outside diameter ultrasonic testing or radiographic testing) that require access to the internal side of the pump casing.

ASME Code Case N-481 [3] allowed the replacement of volumetric examination of primary loop pump casings with a safety and serviceability fracture mechanics based integrity evaluation supplemented by specific visual inspections. WCAP-13045 [1] presents the integrity evaluation that was performed to demonstrate compliance with ASME Code Case N-481.

Since the time WCAP-13045 [1] was published (in September 1991), the ASME code tables have been updated to be consistent with the guidance of Code Case N-481 in mandating visual inspections of the primary loop pump casings. In March 2004, the code case was annulled by ASME, and the information in the code case was implemented into the 2008 addenda of ASME Section XI – see Appendices B and C. However, the technical basis of the WCAP-13045 report was based on experience with evaluations performed for an assumed 40 year life. Due to the Subsequent License Renewal (SLR) program to extend a plants service life to 80 years, the integrity evaluations in WCAP-13045 need to be reviewed and confirmed to be applicable for 80 years of service. The fracture mechanics integrity assessment in this report, as well as the requirements of Code Case N-481 (now incorporated into the ASME Section XI Code) will be reaffirmed to demonstrate that the visual inspections for pump casings continue to remain valid for an 80 year life.

WCAP-13045 [1] presents the fracture mechanics based integrity evaluation for cast austenitic stainless steel pump casing as required by Code Case N-481 [3]. The evaluations completed in WCAP-13045 are applicable to Westinghouse-designed main coolant pumps. There are eight

different models of pumps in Westinghouse type pressurized water reactors (PWR), Models 63, 70, 93, 93A, 93A-1, 93D, 100A, and 100D. Models 63, 70, 93 and 93D all have a tangent outlet nozzle. Models 93A and 93A-1 have outlet nozzles that are radially orientated. Models 100A and 100D are similar to the general shape of Model 93 but with a radially oriented outlet nozzle like Model 93A. Models 93, 93A and 93A-1 are the most common among Westinghouse type PWRs, making up around 90% of the total on a domestic plant basis.

In WCAP-13045, a model representative of each of the outlet nozzle configurations was chosen for a 3D finite element stress analysis and fracture evaluation (the inlet nozzles are reasonably axisymmetric with the pump casing proper). The representative models chosen were the Model 93A (radial outlet nozzle) and Model 93 (tangential outlet nozzle). The material of the pump casings are fabricated from SA-351 CF8 except for three plants pumps which were fabricated from SA-351 CF8M. The SA-351 CF8M and CF8 are known to be susceptible to thermal aging.

In WCAP-13045, thermal aging of the cast austenitic stainless steel pump casings (CF8M and CF8) was addressed using end of life fracture toughness values for all Westinghouse design pump casings. The fracture toughness criteria were established using the lowest toughness for each pump component. This report will justify the continued use of the end of life fracture toughness values determined in WCAP-13045 for 80 years of service.

The fracture toughness is used in WCAP-13045 as part of the elastic plastic fracture mechanics (EPFM) analysis based on the J-integral approach; therefore, it is necessary to reconfirm the fracture toughness values for an 80 year evaluation, and demonstrate that the EPFM analysis continues to remain valid for 80 years. The J-integral evaluation also used bounding loads that covered a wide range of pump casing nozzle loads from the different plant designs. Hence, this report will discuss the reconfirmation of the toughness properties rather than the applied loads, since the applied loadings in the J-integral analysis considered in WCAP-13045 will not be impacted by license extension to 80 years. Note that the fracture toughness properties based on the CF8M (high molybdenum content) material is more susceptible (limiting) to thermal aging than CF8 materials. Therefore, the CF8M material is used in the fracture mechanics assessment herein; as a result, the conclusions for CF8M fracture toughness determined in this report will apply for the CF8 material as well.

Fatigue crack growth evaluations were also determined in WCAP-13045 for the high stress outlet nozzle crotch regions. Various crack sizes were considered, and based on the evaluation it was demonstrated that the fatigue crack growth was small. The discussion in this report will also justify that the fatigue crack growth evaluations considered in WCAP-13045 are still applicable for the 80 year design life.

Thus, as part of PA-MS-C-1498 [4] scope which will be investigated in this report, the following two items are reviewed to confirm the continued applicability of WCAP-13045 [1] for 80 years of service.

1. Confirm that the fracture toughness (J_{Ic} – J at crack initiation and J_{max} – J at maximum crack extension) used in WCAP-13045 [1] and the associated tearing modulus (T_{mat}) for the stability analysis remains applicable for 80 years of service. The postulated 1/4T flaw

size used in the stability analysis is compared with the final flaw size due to fatigue crack growth.

2. Confirm that the generic fatigue crack growth (FCG) analysis performed in WCAP-13045 remains applicable for 80 years of service, specifically the stresses, stress intensity factor (SIF) equations, transient definitions and cycles, and the FCG rate.

The stability calculations in WCAP-13045 are reviewed based on the applicability of the fracture toughness for SLR in Section 2 of this report, while the fatigue crack growth analysis is reviewed based on for FCG rates, stresses, and transient definitions and cycles in Section 3. The final conclusions of this report are provided in Section 4, with all cited references provided in Section 5.

Appendix A of this report also provides the ASME Section XI Code Case N-481, for reference, which was approved and published in March 1990, and later annulled in March 2004, as the requirements of the code case were incorporated in the 2008 addenda of the ASME Section XI IWB-2500 (see Appendices B and C).

1.1 OPERATING EXPERIENCE AND APPLICATION OF LATEST FRACTURE TOUGHNESS DATABASE

The primary reactor coolant loop pump casings in Westinghouse type primary water reactor designs have an operating history that demonstrates the inherent flaw tolerance and structural stability of the pump casings. Based on industry information, there have been no detectable service induced flaws nor discernable degradation of the cast austenitic stainless steel (CASS) pump casings and welds in the PWR operating history.

The fracture mechanics evaluation herein also considers the latest fracture toughness correlations that have been developed for the cast austenitic stainless steel pump casings. The end of life fracture toughness properties for the pump casing materials are determined based on NUREG/CR-4513, Revision 2, "Estimation of Fracture Toughness of Cast Stainless Steels during Thermal Aging in LWR systems," by Omesh Chopra, published in May 2016 [11].

Revision 2 of NUREG/CR-4513 provides a large database for CASS material and thermal aging, and builds on the work performed in 1994 for Revision 1 of NUREG/CR-4513. In 1994, the Argonne National Laboratory (ANL) completed an extensive research program in assessing the extent of thermal aging of cast stainless steel materials [11]. The ANL research program measured mechanical properties of cast stainless steel materials after they had been heated in controlled ovens for long periods of time. ANL compiled a data base, both from data within ANL and from international sources, of about 85 compositions of cast stainless steel exposed to a temperature range of 290-400°C (550-750°F) for up to 58,000 hours (6.5 years). In 2015 the work done by ANL was augmented, and the fracture toughness database for CASS materials was aged to 100,000 hours at 290-350°C (554-633°F). The methodology for estimating fracture properties has been extended to cover CASS materials with a ferrite content of up to 40%. From

this database (NUREG/CR-4513, Revision 2), ANL developed lower bound correlations for estimating the extent of thermal aging of cast stainless steel [11].

ANL developed the fracture toughness estimation procedures by correlating data in the database conservatively. After developing the correlations, ANL validated the estimation procedures by comparing the estimated fracture toughness with the measured value for several cast stainless steel plant components removed from actual plant service. The procedure developed by ANL in [11] was considered herein for the end of life fracture toughness values in this report. The ANL research program was sponsored and the procedure was accepted by the NRC.

This document contains Westinghouse Electric Company LLC proprietary information and data which has been identified by brackets. Coding (a,c,e) associated with the brackets sets forth the basis on which the information is considered proprietary. These code letters are listed with their meanings in BMS-LGL-84 [13].

2 STABILITY ANALYSIS AND FRACTURE TOUGHNESS

2.1 FRACTURE TOUGHNESS DETERMINED IN WCAP-13045

The fracture mechanics integrity evaluation is based on the Elastic Plastic Fracture Mechanics (EPFM) methodology as discussed in Sections 10 and 11 of WCAP-13045 [1]. The EPFM is determined for a postulated 1/4T (1/4 thickness) flaw size with a six-to-one (6:1) aspect ratio. This particular flaw size is consistent with the guidelines of Code Case N-481 Part (d)(5). The location of the postulated 1/4T flaws are either at highest stressed region, regions of significant stress concentrations, or locations in welds not affected by discontinuities such as nozzles. Additional discussion on flaw postulation is provided in Section 9 of WCAP-13045.

The criterion for establishing stability is based on the fracture toughness of the pump casings, as well as the tearing modulus, T , as described in Section 10.4 of WCAP-13045 and shown below:

A crack is stable if either

- 1) $J_{\text{applied}} < J_{\text{Ic}}$ or if
- 2) $J_{\text{applied}} > J_{\text{Ic}}$ then $T_{\text{applied}} < T_{\text{material}}$ and $J_{\text{applied}} \leq J_{\text{maximum}}$

The applied toughness (J_{applied} or J_{app}) and applied tearing modulus (T_{applied} or T_{app}) are calculated based on the EPRI handbook methodology [10], based on various combinations of loading parameters and material properties for the various pump designs as discussed in WCAP-13045. The J_{app} and T_{app} are not going to be impacted by the extension of design life to 80 years; however, the fracture toughness material parameters such as the crack initiation toughness (J_{Ic}), which is based on a J-integral resistance curve, the maximum fracture toughness (J_{maximum} or J_{max}), and the tearing modulus (T_{material} or T_{mat}) need be reviewed to confirm that these parameters will not be impacted by a life extension to 80 years.

The end of service fracture toughness (J_{Ic} , T_{mat} , and J_{max}) of the pump casings are calculated in Section 5 of WCAP-13045 [1]. The lower bound toughness criteria selected from among all the pump casing (and welds) models (Models 63, 70, 93, 93A, 93A-1, 93D, 100A, and 100D) are given in Table 5-1 of WCAP-13045. The minimum fracture toughness values based on the most limiting SA-351 CF8M component from Table 5-1 of WCAP-13045 are shown in Table 1 below for consideration in this report. The fracture toughness properties for CF8M from WCAP-13045 will envelop the CF8 material, as thermal aging is more limiting for CF8M materials as compared to CF8.

Table 1: End-of-Service Fracture Toughness from WCAP-13045 (Table 5-1) [1]

Material	J_{Ic} (in-lb/in ²)	T_{mat} (dimensionless)	J_{max} (in-lb/in ²)
Model 93 SA-351 CF8M	[] ^{a,c,e}	[] ^{a,c,e}	[] ^{a,c,e}
<u>Chemistry:</u> [] ^{a,c,e}			

Note: The values J_{Ic} , T_{mat} , and J_{max} shown for the CF8M material above are listed in Table 5-1 and on page A-30 of WCAP-13045.

The fracture toughness data in Table 1 (from Table 5-1 of WCAP-13045) is based on the chemistry data from Appendix A (pg A-30) of WCAP-13045. Based on the chemistry of the limiting heat of cast austenitic stainless steel (i.e., Silicon (Si), Chromium (Cr), Molybdenum (Mo), Nickel (Ni), Carbon (C), Manganese (Mn), and Nitrogen (N) in percent weight, and percent delta ferrite), the fracture toughness is calculated per the discussion provided in WCAP-10931 [5], Slama [6], and WCAP-10456 [7].

Based on the results from Slama [6] and WCAP-10456 [7], the minimum (saturated) fracture toughness properties were obtained after only []^{a,c,e}

Therefore, the fracture toughness properties shown in Table 1 (per Table 5-1 of WCAP-13045) are already at the full-aged saturated condition material values, and are therefore applicable for 80 years of service life since the resulting minimum (saturated) properties are reached by []^{a,c,e}

Therefore, the EPFM stability analysis and conclusions in WCAP-13045 [1], based on the saturated fracture toughness values in Table 1, continue to remain applicable for the subsequent license renewal application.

For a confirmatory analysis, the minimum fracture toughness values based on Table 5-1 of WCAP-13045 (as shown in Table 1) are also compared with the latest fracture toughness correlations for thermal aging of cast austenitic stainless steel CF8M material per NUREG/CR-4513, Revision 2 [11], see Section 2.2 below. This comparison will provide further evidence and confirmation that the fracture toughness values in WCAP-13045 [1] are bounding and applicable for the 80 year design life.

2.2 FRACTURE TOUGHNESS BASED ON NUREG/CR-4513, REVISION 2

In this section of the report, a confirmatory calculation is performed to determine the J_{IC} , T_{mat} and J_{max} based on the NUREG/CR-4513 Revision 2 [11] for the most limiting CF8M pump casing material, using the limiting heat specific chemistry values provided in Table 1 (based originally from WCAP-13045). NUREG/CR-4513 provides the latest industry guidelines/correlations for the calculation of fracture toughness values for CF8M. The fracture toughness values calculated per NUREG/CR-4513 will be compared to the values determined in Table 1, from WCAP-13045. This comparison in fracture toughness values will demonstrate if the toughness properties from WCAP-13045 continue to remain bounding and acceptable for 80 years. Note that the impact of thermal aging on CF8 fracture toughness properties is less than that for CF8M; hence the evaluation herein is only considered for CF8M since this material type will envelop the fracture toughness values for CF8.

The following methodology and equations are taken from NUREG/CR-4513, Revision 2 [11] and applicable for CF8M type material. The calculated fracture toughness values based on [11] are shown in Table 2.

$$Cr_{eq} = Cr + 1.21(Mo) + 0.48(Si) - 4.99 = (\text{Chromium equivalent})$$

$$Ni_{eq} = (Ni) + 0.11(Mn) - 0.0086(Mn)^2 + 18.4(N) + 24.5(C) + 2.77 = (\text{Nickel equivalent})$$

$$\delta_c = 100.3(Cr_{eq} / Ni_{eq})^2 - 170.72(Cr_{eq} / Ni_{eq}) + 74.22 = (\text{Ferrite Content})$$

where the elements are in percent weight and δ_c is ferrite in percent volume.

The saturation room temperature (RT) impact energies of the cast stainless steel materials are determined from the chemical composition.

For CF8M steel with < 10% Ni, the saturation value of RT impact energy Cv_{sat} (J/cm²) is the lower value determined from

$$\log_{10} Cv_{sat} = 0.27 + 2.81 \exp(-0.022\phi)$$

where the material parameter ϕ is expressed as

$$\phi = \delta_c (Ni + Si + Mn)^2 (C + 0.4N) / 5.0$$

and from

$$\log_{10} Cv_{sat} = 7.28 - 0.011\delta_c - 0.185Cr - 0.369Mo - 0.451Si - 0.007Ni - 4.71(C + 0.4N)$$

For CF8M steel with $\geq 10\%$ Ni, the saturation value of RT impact energy Cv_{sat} (J/cm²) is the lower value determined from

$$\log_{10} Cv_{sat} = 0.84 + 2.54 \exp(-0.047\phi)$$

where the material parameter ϕ is expressed as

$$\phi = \delta_c (Ni + Si + Mn)^2 (C + 0.4N) / 5.0$$

and from

$$\log_{10} Cv_{sat} = 7.28 - 0.011\delta_c - 0.185Cr - 0.369Mo - 0.451Si - 0.007Ni - 4.71(C + 0.4N)$$

The saturation J-R curve at RT, for static-cast CF8M steel is given by

$$J_d = 1.44 (Cv_{sat})^{1.35} (\Delta a)^n \text{ for } Cv_{sat} < 35 \text{ J/cm}^2$$

$$J_d = 16 (Cv_{sat})^{0.67} (\Delta a)^n \text{ for } Cv_{sat} \geq 35 \text{ J/cm}^2$$

$$n = 0.20 + 0.08 \log_{10} (Cv_{sat})$$

where J_d is the “deformation J” in kJ/m^2 and Δa is the crack extension in mm.

The saturation J-R curve at 290-320°C (554-608°F), for static-cast CF8M steel is given by

$$J_d = 5.5 (Cv_{sat})^{0.98} (\Delta a)^n \text{ for } Cv_{sat} < 46 \text{ J/cm}^2$$

$$J_d = 49 (Cv_{sat})^{0.41} (\Delta a)^n \text{ for } Cv_{sat} \geq 46 \text{ J/cm}^2$$

$$n = 0.19 + 0.07 \log_{10} (Cv_{sat})$$

where J_d is the “deformation J” in kJ/m^2 and Δa is the crack extension in mm.

[
 $J^{a,c,e}$ The tearing modulus, $T_{material}$ is calculated by $T = dJ/da * E/\sigma_f^2$, where dJ/da is the slope of the J-R curve, E is elastic modulus, and σ_f is the flow strength (average of the yield strength and ultimate strength). Using the NUREG/CR-4513, Revision 2 [11] methodology the fracture toughness properties are given in Table 2. Based on NUREG/CR-4513, Revision 2, the fracture toughness correlations used for the full aged condition is applicable for plants operating at and beyond 15 EFPY (Effective Full Power Years) for the CF8M materials. Currently, PWR pumps in the fleet are operating well beyond the 15 EFPY service life; therefore, the use of the fracture toughness correlations described above is applicable for the fully aged or saturated conditions.

Therefore, the fracture toughness values based on the original methodology in WCAP-13045 is limiting (see Table 1) as compared to the fracture toughness properties based on NUREG/CR-4513 (see Table 2). Hence, by calculating the latest industry correlation for fracture toughness values for aged cast austenitic stainless steel from NUREG/CR-4513, it can be demonstrated that the aged toughness values in Table 1 (from Table 5-1 of WCAP-13045) are still bounding and limiting for subsequent license renewal (80 years).

Table 2: NUREG/CR-4513 [11] Fully-Aged (Saturated) Fracture Toughness

Material	J_{Ic} (in-lb/in ²)	T_{mat} (dimensionless)	J_{max} (in-lb/in ²)
Model 93 SA-351 CF8M	[] ^{a,c,e}	[] ^{a,c,e}	[] ^{a,c,e}
<p><u>Chemistry (per Table 1):</u> []^{a,c,e}</p> <p>ASME Code properties are used for E (modulus of elasticity) = 25.6×10^6 psi and Yield Strength = 19,350 psi. Ultimate strength = 67,000 psi per Table 6-3 of WCAP-13045, which is close approximation to ASME code values. Values are for the cold leg temperature, approximately 550°F.</p>			

3 FATIGUE CRACK GROWTH ANALYSIS

Two fatigue crack growth analyses were originally performed in Section 12 of WCAP-13045 [1], one for a postulated crack in the highest stressed outlet nozzle knuckle of the Model 93A pump casing and the other in the highest stressed outlet nozzle knuckle of the Model 93 pump casing. The FCG analysis of the Model 93A pump was performed prior to the publication of the stainless steel FCG law in the ASME Section XI Code; therefore, the FCG law in [Equation 1] from [9] was initially considered in WCAP-13045. However, the FCG analysis for Model 93A was calculated based on [Equation 2] which was an updated version of [Equation 1] for stainless steel in water environment. [Equation 1] in WCAP-13045 was provided for information purposes and is also reproduced below as well:

$$\frac{da}{dN} = 5.4 \times 10^{-12} (K_{eff})^{4.48} \quad (\text{inches/cycle}) \quad [\text{Equation 1}]$$

$$K_{eff} = K_{max}(1-R)^{0.5}$$

$$R = K_{min}/K_{max} \quad K_{max} \text{ and } K_{min} \text{ is in units of ksi } \sqrt{\text{in}}$$

The FCG law used for the Model 93 postulated flaw was based on Figure C-3210-1 of Article C-3000 of Section XI of the ASME Code (1989 Edition) and analytically described in [1] as shown below:

$$\frac{da}{dN} = C F S E (\Delta K)^{3.30} \quad (\text{inches/cycle}) \quad [\text{Equation 2}]$$

where $C = 2.42 \times 10^{-20}$, $F = 1$ for temperatures below 800°F, $S = R$ ratio correction (see Equations 3's 'S' definition below), $R =$ ratio of the minimum stress intensity factor (SIF) to the maximum SIF, $\Delta K =$ range of stress intensity factors (psi $\sqrt{\text{in}}$), and $E = 2$ based on stainless steel in water [8].

The current NRC approved 2007 edition with 2008 addenda of ASME Section XI Appendix C fatigue crack growth for stainless steel is shown below. A factor of 2 is applied to the da/dN rate to account for environmental effects of a postulated flaw in water as described in [8]:

$$\frac{da}{dN} = 2 * C_o S (\Delta K_I)^{3.3} \quad (\text{inches/cycle}) \quad [\text{Equation 3}]$$

$$\text{where } C_o = 10^{-10.009 + 8.12 \times 10^{-4} T - 1.13 \times 10^{-6} T^2 + 1.02 \times 10^{-9} T^3}$$

$$T = \text{Temperature } (^{\circ}\text{F}) = 550^{\circ}\text{F} \text{ (see Table 11-1 and Table 11-6 of [1])}$$

$$S = 1.0 \text{ for } R \leq 0, S = 1 + 1.8R \text{ when } 0 < R < 0.79, \text{ and } S = -43.35 + 57.97R \text{ when } 0.79 < R < 1$$

$$\Delta K_I \text{ is in units of ksi } \sqrt{\text{in}}, R = K_{min}/K_{max}$$

There are no significant differences between the current stainless steel FCG rate in water, [Equation 3] and the FCG rate used in WCAP-13045 [1], [Equation 2] for the Model 93

postulated flaws. The difference between the current stainless steel FCG rate in water [Equation 3] and the FCG rate considered in WCAP-13045, [Equation 1] for the Model 93A postulated flaw is also insignificant. The FCG results for the Model 93A postulated flaws in WCAP-13045 were actually based on [Equation 2], and [Equation 1] is provided in WCAP-13045 for historical reasons. Therefore, the existing FCG rates in Section 12 of WCAP-13045 are acceptable based on current industry standards for fatigue crack growth for stainless steel material in a water environment.

Other inputs required for an FCG analysis are the stress intensity factors, stresses, transient cycles and transient definitions. The stress intensity factor (SIF) correlations used for the FCG analysis in WCAP-13045 are consistent with the current correlations provided in ASME Section XI Appendix A. The transient stresses used in the fatigue crack growth are generic and encompass the various pump designs; furthermore, these stresses have not changed for the subsequent license renewal period (80 years). The number of predicted cycles for 80 years of service are assumed to be bounded by the transient cycles considered in Table 12-2 of WCAP-13045; moreover, the transient definitions are also not expected to change over the 80 year design life. Therefore, the generic transient description and number of cycles in Table 12-2 of WCAP-13045 [1] are assumed to envelop the transient conditions for 80 years of service.

Plants considering 80 years life extension count cycles and typically comply with original design basis cycles for 40 years; therefore, there will be no significant increases in the number of cycles for 80 years. For a confirmatory evaluation, the FCG cycles for 40 years were doubled for 80 years to account for any large differences in the transient cycles, and it was demonstrated that the final flaw size would still be less than the stability flaw size for this region; see more discussion below.

The calculated FCG for four flaw sizes in the outlet nozzle knuckle region of the Model 93A pump casing are given in Table 12-1 of WCAP-13045, and for three flaw sizes in Table 12-3 for the outlet nozzle knuckle region of the Model 93 pump casing. One of the flaw size cases for FCG was for an initial flaw depth of 0.3"; this particular flaw depth was the maximum acceptable flaw size in the Acceptance Standards in Table IWB-3518-2 (for pressure retaining welds in pump casings) up to the 2007 Edition of the ASME Section XI code (see more details in Appendix B and Reference 12). The flaw depth of 0.3" is still the maximum acceptable flaw size in the Acceptance Standards Table IWB-3519.2-2 (for pump casings) in later editions of the ASME Section XI Code. Therefore the flaw depth of 0.3" was an important flaw size case to consider in WCAP-13045 for flaw tolerance evaluation, and any actual as-found flaws larger than this depth would need to be evaluated based on fracture mechanics. The other FCG postulated flaw size cases in WCAP-13045 were provided as sensitivity studies to demonstrate that the flaws do not grow significantly over time.

Based on the fatigue crack growth analyses per Tables 12-1 and 12-3 of WCAP-13045, the flaw depth of 0.3" grows to a maximum value of []^{a,c,e} over 40 years of service. If all other inputs for an FCG analysis (stress intensity factors, stress, transient cycles and transient definitions) are bounded by or are similar to the inputs of WCAP-13045, then the fatigue crack growths for 80 years are expected to be similar to or less than the crack growth in Table 12-1 and Table 12-3 of WCAP-13045 for 40 years. Moreover, even if the transient cycles for 40 years

is doubled for the SLR evaluations (80 years) to account for any large differences in the transient cycles, then the final flaw size would continue to be less than the minimum stability flaw size of 1/4T flaw depth ([]^{a,c,e} as per Table 11-6 of WCAP-13045), associated with the location of the highest stressed region. Therefore, the FCG analysis provided in Section 12 of WCAP-13045 continues to remain valid for the 80 year SLR programs.

4 CONCLUSIONS

The objective of this report is to review the main coolant loop pump casing fracture mechanics integrity evaluations and the fatigue crack growth analysis performed in WCAP-13045 [1], and reaffirm its applicability for 80 years of service.

Section 2.1 discussed the most limiting pump casing CF8M fracture toughness and the tearing modulus used in the WCAP-13045 J-integral stability evaluations (EPFM). The WCAP-13045 fracture toughness determinations continue to remain applicable for 80 years of service because the fracture toughness parameters are at full-aged saturated conditions so any additional aging past 40 years does not have an impact on the fracture toughness parameters. Section 2.2 compared the minimum fracture toughness from WCAP-13045 with the latest industry toughness correlations from NUREG/CR-4513, Revision 2 [11]. Based on the conclusions in Section 2.2, it is demonstrated that the fracture toughness in WCAP-13045 are less than (more conservative and limiting) the toughness values in NUREG/CR-4513. Therefore, as compared with the current industry standards, the fracture toughness values in WCAP-13045 continue to remain limiting and applicable for 80 years of operation. Thus, the EPFM analysis for pump casings performed in WCAP-13045 is still valid for 80 years since the minimum fracture toughness used in the stability analysis is confirmed to be applicable for 80 years of service life.

A qualitative assessment for the fatigue crack growth evaluation was performed in Section 3 of this report for the pump casings. It was determined that the current FCG rate for stainless steel in water environment based on ASME Section XI as compared to the rates used in WCAP-13045 are comparable and there will be insignificant impact on the crack growth analysis. Furthermore, the stresses used in the FCG analysis are generic and envelop the various pump designs; furthermore these stresses do not change for the SLR program. The stress intensity factor used in the FCG analysis are consistent with the current industry standards for similar FCG evaluations. The transient definitions in the FCG analysis are also not expected to change over the design life, and the cycles used in the WCAP-13045 are assumed to bound the predicted 80 year transient cycles. Lastly, there is sufficient margin between the final crack growth and the flaw size used for stability, so even if the 40 year transient cycles are doubled for the SLR (80 years), the final flaw size would continue to be less than the stability flaw size, $1/4T$ flaw depth, for the stability analysis of WCAP-13045.

In conclusion, the fracture mechanics integrity evaluation in WCAP-13045 [1] for pump casings, continues to remain applicable for the Subsequent License Renewal, 80 years of design life. The fracture mechanics assessment for SLR in this report allow plants to continue performing visual inspections, in lieu of volumetric inspections, for pump casings as incorporated in the ASME Section XI code.

5 REFERENCES

- 1) Westinghouse Document, WCAP-13045, "Compliance to ASME Code Case N-481 of the Primary Loop Pump Casings of Westinghouse Type Nuclear Steam Supply System," September 1991.
- 2) ASME Boiler and Pressure Vessel Code, Section XI, "Rules for Inservice Inspection of Nuclear Power Plant Components."
- 3) Code Case N-481, "Alternative Examination Requirements for Cast Austenitic Pump Casings," Section XI, Division 1, Approval Date: March 5, 1990.
- 4) PWROG Project Authorization, PA-MS-C-1498, Revision 0, "Update for Subsequent License Renewal: WCAP-13045, 'Compliance to ASME Code Case N-481 of the Primary Loop Pump Casings of Westinghouse Type Nuclear Steam Supply Systems'."
- 5) Westinghouse Document, WCAP-10931, Revision 1, "Toughness Criteria for Thermally Aged Cast Stainless Steel," July 1986.
- 6) Slama, G., Petrequin, P., Masson, S. H. and Mager, T. R., "Effect of Aging on Mechanical Properties of Austenitic Stainless Steel Casting Welds," presented at SMIRT 7 Post Conference Seminar 6 – Assuring Structural Integrity of Steel Reactor Pressure Boundary Components, August 29/30, 1983, Monterey, CA.
- 7) Westinghouse Document, WCAP-10456, "The Effects of Thermal Aging on Structural Integrity of Cast Stainless Steel Piping for Westinghouse Nuclear Steam Supply Systems," November 1983.
- 8) "Evaluation of Flaws in Austenitic Steel Piping," Trans. ASME, Journal of Pressure Vessel Technology, Vol. 108, pp. 352-366, 1986.
- 9) Bamford, W. H., "Fatigue Crack Growth of Stainless Steel Piping in a Pressurized Water Reactor Environment," Trans ASME, Journal of Pressure Vessel Technology, February 1979.
- 10) Kumar, V., German, M. D. and Shih, C. P., "An Engineering Approach for Elastic-Plastic Fracture Analysis," EPRI Report NP-1931, Project 1237-1, Electric Power Research Institute, July 1981.
- 11) O. K. Chopra, "Estimation of Fracture Toughness of Cast Stainless Steels During Thermal Aging in LWR Systems," NUREG/CR-4513, Revision 2, U.S. Nuclear Regulatory Commission, Washington, D.C., May 2016.
- 12) Presentation by Warren Bamford at ASME Code Meeting Working Group on Operating Plant Criteria, "CASS Examination Limitations History for WGOPC," August 2016, Washington D.C. [See Appendix C]
- 13) BMS-LGL-84, Revision 0.00, "Protection of Proprietary Information Regarding Submittals to the USNRC including Safety Analysis Reports for Commercial Nuclear Power Plants," Effective Date: April 15, 2017.

APPENDIX A: ASME SECTION XI CODE CASE N-481

a,c,e

APPENDIX B: ASME SECTION XI CODE IMPLEMENTATION OF N-481

In the 2008 Addenda of ASME Section XI, the Code implemented Code Case N-481 and removed the requirements of performing examination of pressure retaining welds in pump casings (ASME Section XI IWB-2500, Examination Category B-L-1); see below excerpt from Reference 12 (full presentation provided in Appendix C). Pump casings (ASME Section XI IWB-2500, Examination Category B-L-2) are only required to be inspected visually, VT-3, when the pump is disassembled for maintenance or repair.

a,c,e

APPENDIX C: CAST AUSTENITIC STAINLESS STEEL (CASS) PRESENTATION AT ASME CODE MEETING

Provided in this appendix is the Reference 12 presentation made by Warren Bamford at the ASME Section XI Code Meeting at Washington D.C. This presentation provides a discussion on the history of Code Case N-481 and its implementation in the ASME Code Section XI inspection guidelines.

a,c,e

[

]

a,c,e

[

]

a,c,e

[

]

a,c,e

[

]

a,c,e

[

]

a,c,e

[

]

a,c,e

[

]

a,c,e

[

]

a,c,e

[

]

a,c,e

[

]

a,c,e

[

]

a,c,e

[

]

a,c,e

[

]

a,c,e

[

]

a,c,e

[

]

a,c,e

[

]

a,c,e

[

]

a,c,e

[

]

a,c,e